Chiou and Youngs PEER-NGA Empirical Ground Motion Model for the Average Horizontal Component of Peak Acceleration and Pseudo-Spectral Acceleration for Spectral Periods of 0.01 to 10 Seconds

Interim Report for USGS Review

June 14, 2006
(Revised Editorially July 10,2006)

by

Brian S.-J. Chiou
California Department of Transportation
Sacramento, California

and

Robert R. Youngs
Geomatrix Consultants
Oakland, California

Chiou and Youngs PEER-NGA Empirical Ground Motion Model for the Average Horizontal Component of Peak Acceleration and Pseudo-Spectral Acceleration for Spectral Periods of 0.01 to 10 Seconds
June 14, 2006

INTRODUCTION

This document describes an empirically-based ground motion model for the average horizontal component of ground motion developed as part of the PEER-NGA study. The model is developed for peak ground acceleration and 5%-damped pseudo-spectral accelerations at spectral periods from 0.01 to 10 seconds (spectral frequencies of 100 Hz to 0.1 Hz, respectively). An accompanying FORTRAN routine (CY2006.for) is provided to compute the ground motion estimates given the appropriate input parameters.

EMPRIRICAL DATABASE

DATA SELECTION

The database used in this study was the PEER NGA Flatfile Version 7.2. This database contained 3,551 recordings from 173 earthquakes. The ground motion model was developed to represent the following conditions:

1. Shallow crustal earthquakes in active tectonic regions, principally California.
2. Free field ground motions.
3. Average randomly oriented component.
4. Explicit incorporation of local soil conditions.

These conditions were used to select an appropriate data set from the PEER-NGA Flatfile.

Table 1 lists the earthquakes that were removed because they do not meet the first condition. Most of these earthquakes occurred in the oceanic crust of the Gorda plate. Ground motions from earthquakes occurring in the Gorda plate have been found to be more consistent with ground motions from Benioff zone (subduction intraslab) earthquakes than shallow crustal earthquakes (Geomatrix, 1995). Four earthquakes from Taiwan were excluded because they occurred offshore in a potentially similar environment and because of the uncertainty in their location. The four northwest China earthquakes were excluded because of their large depths ($\geq$20 km) and the very limited data about the events and their recordings. Data from the 1979 St Elias earthquake were excluded because this earthquake is interpreted to have occurred on a subduction zone interface. Data from the 1992 Cape Mendocino earthquakes were included. The favored interpretation is that this event occurred on reverse faults in the overriding continental crust near to but not on the subduction zone interface. Data from the 1985 Nahanni and 1992 Roermond, Netherlands earthquakes were included. These earthquakes are interpreted to have occurred at the boundary of stable continental regions (SCR) with active tectonic regions.

The remaining earthquakes are from a variety of active tectonic regions, as indicated in Table 2. Several investigators have shown that ground motion relationships based on California

data are consistent with strong motion data in other active tectonic regions (e.g. Italy – Sabetta and Pugliese, 1996; the Mediterranean basin – Ambraseys et al., 1996; Japan – Fukushima and Tanaka, 1990). It has also been common to include ground motions from earthquakes such as Gazli, 1976, and Tabas, 1978, in developing ground motion models for application in California (e.g. Abrahamson and Silva, 1997, Campbell, 1997, Sadigh et al. 1997). In this study we start with the hypothesis that the ground motions from these separate active tectonic regions are similar and can be combined. We examine this hypothesis during model development.

Table 1: Excluded Earthquakes

EQID	EQNAME	Comment
0003	Humbolt Bay	Gorda plate
0005	Northwest Calif-01	Gorda plate
0007	Northwest Calif-02	Gorda plate
0008	Northern Calif-01	Gorda plate
0011	Northwest Calif-03	Gorda plate
0013	Northern Calif-02	Gorda plate
0017	Northern Calif-03	Gorda plate
0022	Northern Calif-04	Gorda plate
0026	Northern Calif-05	Gorda plate
0035	Northern Calif-07	Gorda plate
0067	Trinidad	Gorda plate
0071	Taiwan SMART1(5)	Deep offshore event
0084	Trinidad offshore	Gorda plate
0086	Taiwan SMART1(25)	Deep offshore event
0093	Pelekanada, Greece	Deep event
0095	Taiwan SMART1(33)	Deep offshore event
0109	Taiwan SMART1(45)	Offshore event
0142	St Elias, Alaska	Subduction interface event
0153	Northwest China-01	Poorly known event
0154	Northwest China-02	Poorly known event of moderate depth
0155	Northwest China-03	Poorly known event of moderate depth
0156	Northwest China-04	Poorly known event of moderate depth

To meet the second condition, recordings made in large buildings and at depth were removed. These are indicted by the "Geomatrix" C1 site codes of 'C', 'D', 'E', 'F', 'G', and 'H' (non-abutment sites). The exclusion of basement and large building/massive foundation recordings eliminates several additional earthquakes, notably the 1935 Helena records and a number from Imperial Valley recorded at the old Imperial Valley Irrigation District site. We included records from sites that have been characterized as having topographic effects (e.g. Tarzana Cedar Hill Nursery, Pacoima Dam left abutment) and dam abutments in general. Our rational for including these records is that the effect of topography has not been systematically studied for all of the records in the database and many of the other recording stations may have topographic enhancement or suppression of ground motions. Therefore, topographic effects are considered to be part of the variability introduced into ground motions by travel path and site effects.

The third condition is represented by specifying the ground motion component to be the orientation-independent ground motion measure GMRotI50 defined by Boore et al. (2006). Use of this ground motion measure eliminates recordings for which only a single horizontal component was obtained. The notable effect of imposing this condition is the elimination of the Cholame-Shandon Array #2 recording from the 1966 Parkfield earthquake.

The ground motion model developed in this study explicitly accounts for site conditions. Therefore, recordings from sites for which there is no available information of the local soil conditions were excluded. These data were limited to a few recordings from earthquakes in Greece and Turkey.

The regional distribution of the selected recordings is listed in Table 2

Table 2: Regional Distribution of Selected Recordings

Active Region	Number of Earthquakes	Number of Recordings
Alaska	3	57
Armenia	1	1
California	81	1311
Canada	1	3
Georgia	1	5
Greece	8	13
Idaho	2	5
Iran	2	14
Israel	1	1
Italy	8	43
Japan	1	22
the Netherlands	1	3
New Zealand	4	5
Nicaragua	2	2
Russia	1	1
San Salvador	1	2
Taiwan	6	1753
Turkey	7	56
Totals	**131**	**3297**

Figure 1 shows the magnitude-distance distribution of the selected recordings. As in most recent developments of empirical ground motion models for application in California, recordings from other regions serve the primary roll in providing data at large (**M** > 7) magnitudes.

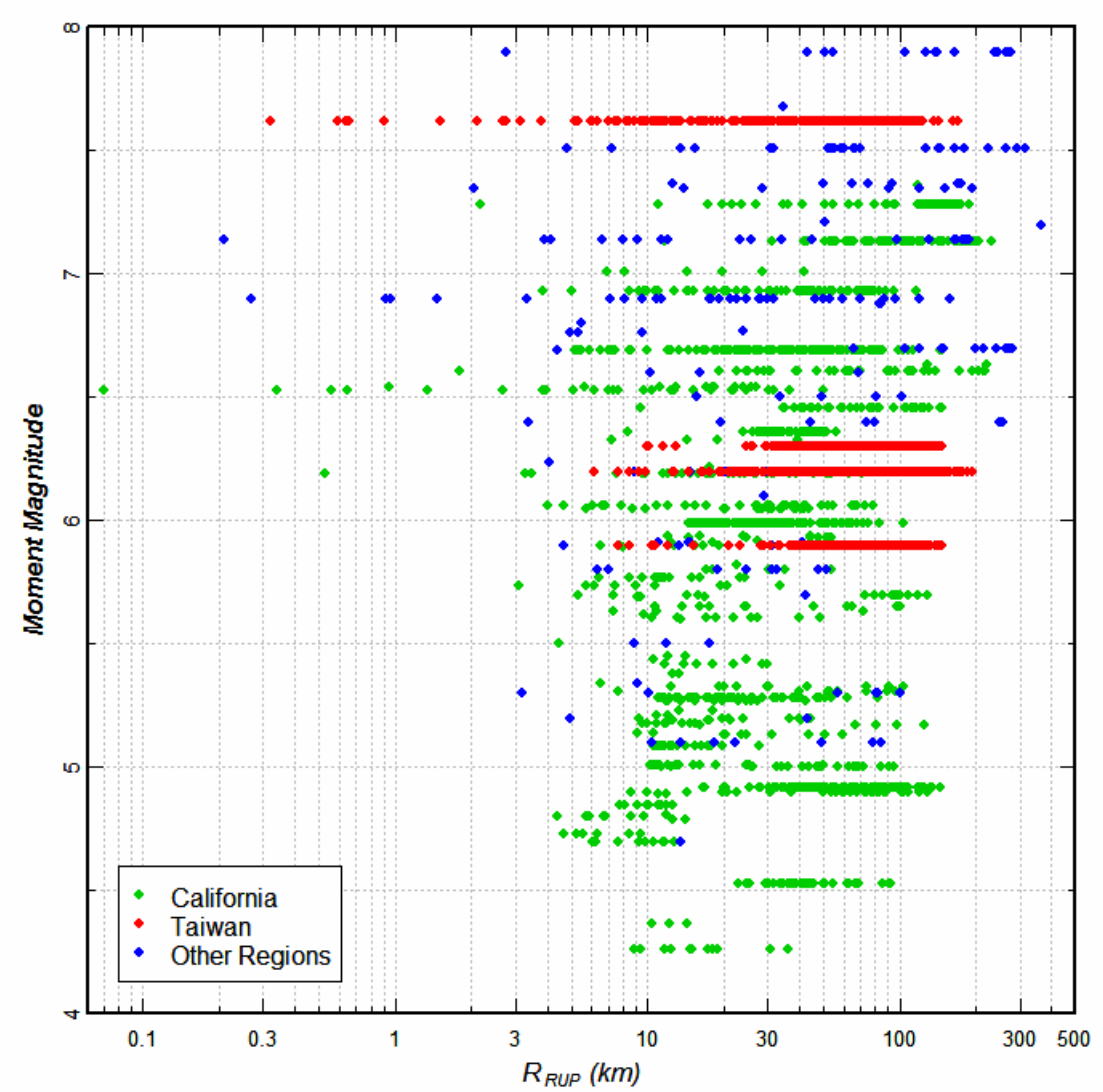

Figure 1: Magnitude-distance-region distribution of selected recordings.

Figure 2 shows the values of peak acceleration and 1.0-sec pseudo spectral acceleration for the selected recordings plotted versus rupture distance, R_{RUP}.

During the PEER-NGA project, the issue was raised concerning the use of data from aftershocks. We have included data from aftershocks but have allowed for the possibility that there may be systematic differences in the ground motion amplitudes produced by main shocks and aftershocks. Our reason for including the data is that they provide additional information to constrain the soil amplification model parameters.

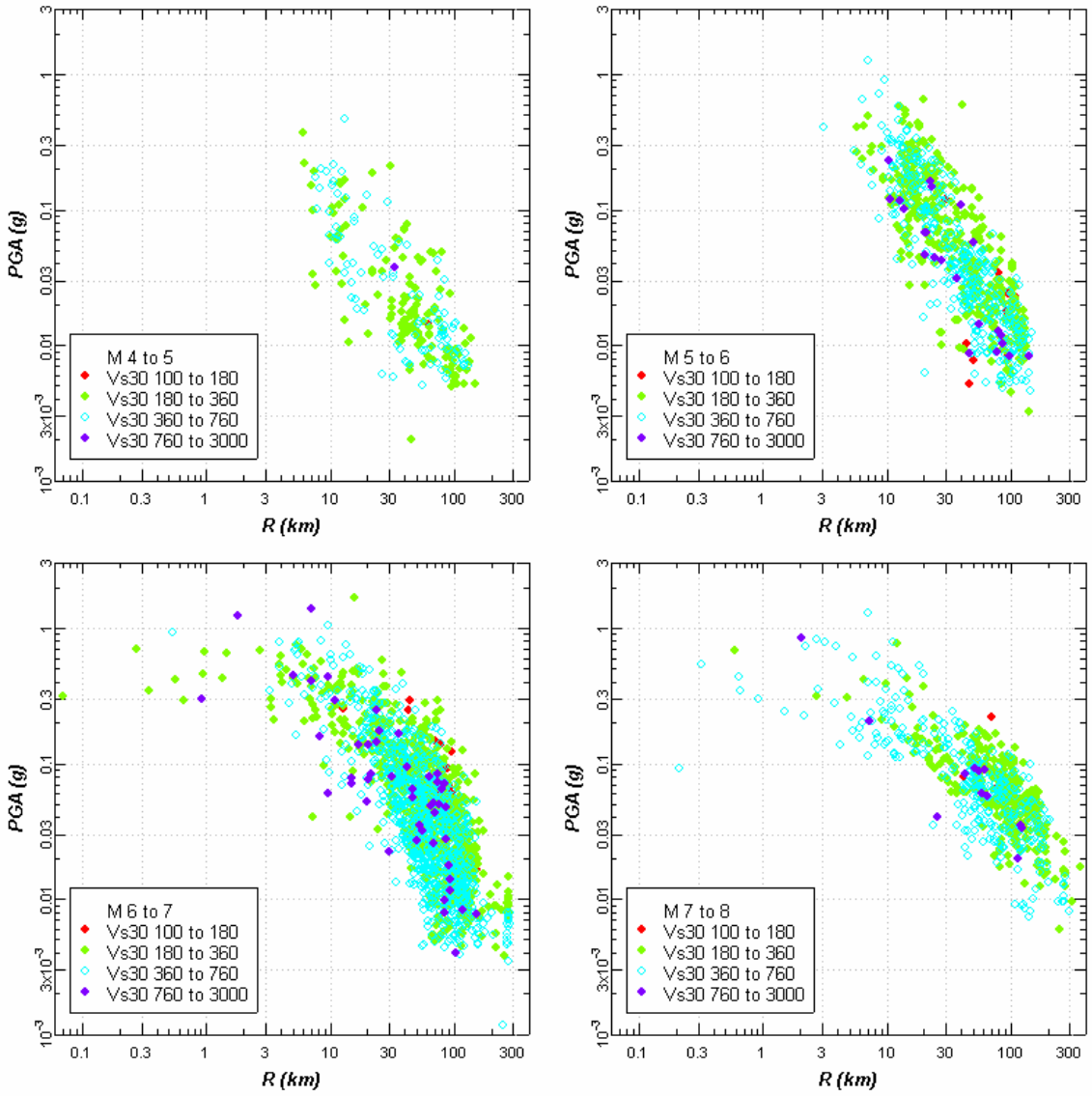

Figure 2: Empirical ground motion data used in developing the ground motion model (1 of 2).

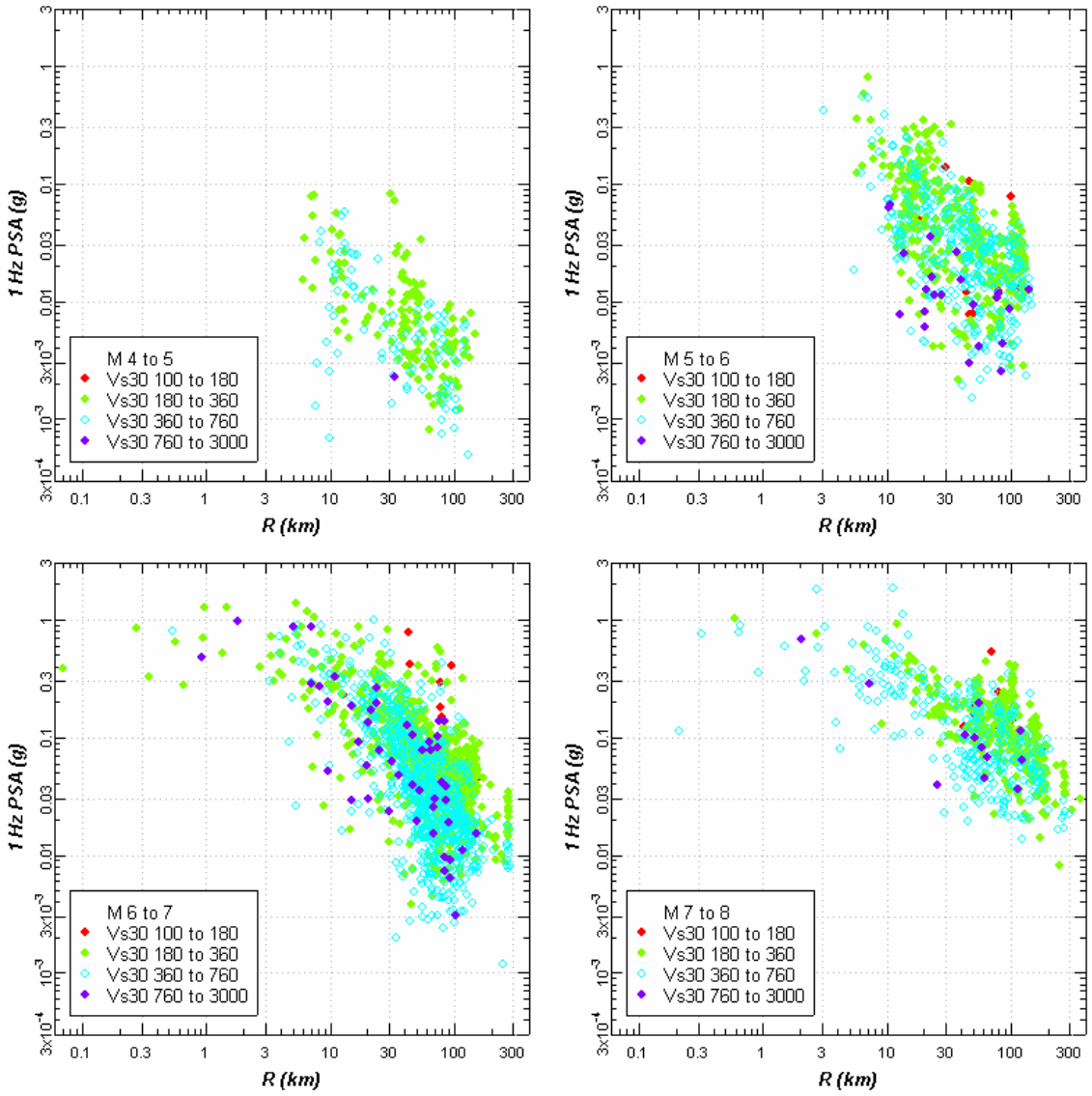

Figure 2: Empirical ground motion data used in developing the ground motion model (2 of 2).

MISSING DATA

The PEER-NGA database contains missing metadata for many of the recordings. The missing data of importance to the ground motion model developed in this study are the following: faulting mechanisms and fault dips for smaller earthquakes; rupture distances for those earthquakes without published rupture models, and for many sites, the average shear wave velocity, V_{S30}, and sediment depth defined as the depth to shear wave velocities of 1 and 2.5 km/s, $Z_{1.0}$ and $Z_{2.5}$, respectively. The missing values for these parameters were imputed (estimated) as follows.

Rupture Depth, Strike, Dip, and Rake: The PEER-NGA database contains 41 earthquakes with missing parameters defining the characteristics of the earthquake rupture. These earthquakes are listed in Table 3 along with estimated values for the missing parameters. The missing values were estimated from other associated events such as the main shock or other aftershocks, or from the tectonic environment. For those earthquakes unassociated with other events, fault dips were assigned based on known or inferred mechanisms as follows, 90º for strike-slip, 40º for reverse (based on average value reported by Sibson and Xie, 1998), and 55º for normal (generic value for normal faults and close to the average of 54º for the normal mechanisms with known dips in the PEER-NGA data base). Where fault strike could not be inferred, it was assumed to be random. The comments in Table 3 indicated the basis for each estimate.

Table 3: Inferred Mechanisms, Hypocenter Depths and Fault Dips

EQID	Earthquake	M	Inferred Mechanism[1,2]	Inferred Depth[1]	Inferred Strike[1]	Inferred Dip[1]	Comments
0002	Helena, Montana-02	6	SS	6	268	75	Values assumed equal to event 0001
0003	Humbolt Bay	5.8	SS	10	Random	90	Strike-slip mechanism and nominal depth of 10 km assumed for offshore Gorda plate earthquakes
0004	Imperial Valley-01	5	SS			90	Strike-slip assumed for Imperial Valley earthquakes
0005	Northwest Calif-01	5.5	SS	10	Random	90	Strike-slip mechanism and nominal depth of 10 km assumed for offshore Gorda plate earthquakes
0007	Northwest Calif-02	6.6	SS	10	Random	90	Strike-slip mechanism and nominal depth of 10 km assumed for offshore Gorda plate earthquakes
0008	Northern Calif-01	6.4	SS	10	Random	90	Strike-slip mechanism and nominal depth of 10 km assumed for offshore Gorda plate earthquakes
0009	Borrego	6.5		8	Random		Assumed similar to event 0028
0010	Imperial Valley-03	5.6		9.5			Average depth of other Imperial Valley earthquakes
0011	Northwest Calif-03	5.8	SS	10	Random	90	Strike-slip mechanism and nominal depth of 10 km assumed for offshore Gorda plate earthquakes
0013	Northern Calif-02	5.2	SS	10	Random	90	Strike-slip mechanism and nominal depth of 10 km assumed for offshore Gorda plate earthquakes
0014	Southern California	6	SS	10	Random	90	Assumed similar to event 25
0015	Imperial Valley-04	5.5	SS	9.5	Random	90	Strike-slip assumed for Imperial Valley earthquakes, depth average of similar events
0016	Central Calif-01	5.3	SS	7.4	Random	90	Assumed SS similar to other Hollister earthquakes and depth taken as average of values for events 0034 and 0098
0017	Northern Calif-03	6.5	SS	10	Random	90	Strike-slip mechanism and nominal depth of 10 km assumed for offshore Gorda plate earthquakes
0018	Imperial Valley-05	5.4	SS	9.5	Random	90	Strike-slip assumed for Imperial Valley earthquakes, depth average of similar events
0021	Central Calif-02	5	SS	7.4	Random	90	Assumed SS similar to other Hollister earthquakes and depth taken as average of values for events 0034 and 0098
0022	Northern Calif-04	5.7	SS	10	Random	90	Strike-slip mechanism and nominal depth of 10 km assumed for offshore Gorda plate earthquakes
0023	Hollister-01	5.6	SS	7.4	Random	90	Assumed SS similar to other Hollister earthquakes and depth

Table 3: Inferred Mechanisms, Hypocenter Depths and Fault Dips

EQID	Earthquake	M	Inferred Mechanism[1,2]	Inferred Depth[1]	Inferred Strike[1]	Inferred Dip[1]	Comments
							taken as average of values for events 0034 and 0098
0024	Hollister-02	5.5	SS	7.4	Random	90	Assumed SS similar to other Hollister earthquakes and depth taken as average of values for events 0034 and 0098
0026	Northern Calif-05	5.6		10			Nominal depth of 10 km assumed for offshore Gorda plate earthquakes
0027	Northern Calif-06	5.2	SS	7.4	Random	90	Assumed SS similar to other Hollister earthquakes and depth taken as average of values for events 0034 and 0098
0032	Managua, Nicaragua-02	5.2	SS		40	80	Values assumed equal to event 0031
0034	Hollister-03	5.14			Random		
0042	Fruili, Italy-03	5.5	RV		233	16	Average of values for events 0040 and 0043
0044	Izmir, Turkey	5.3	NM		Random	55	Mechanism based on environment
0060	Mammoth Lakes-05	5.7	SS		16	60	Average of values for events 0058-0065 in sequence
0065	Mammoth Lakes-09	4.85	SS		Random	67.5	Average for other SS Mammoth earthquakes
0066	Almiros, Greece	5.2	NM		Random	55	Assumed normal based on environment
0070	Irpinia, Italy-03	4.7	NM		Random	65	Assumed normal similar to events 0068 and 0069, dip average for those events
0089	New Zealand-01	5.5	NM		Random	55	Assumed normal based on environment
0092	Veroia, Greece	5.3	NM		Random	55	Assumed normal based on environment
0093	Pelekanada, Greece	5	NM		Random	55	Assumed normal based on environment
0095	Taiwan SMART1(33)	5.8	NM		Random	61.5	Average for focal mechanism planes
0104	Chalfant Valley-03	5.65	SS		Random	90	Assumed SS similar to events 0102 and 0103
0106	Kalamata, Greece-01	6.2	NM		Random	55	Assumed normal based on environment
0107	Kalamata, Greece-02	5.4	NM		Random	55	Assumed normal based on environment
0112	New Zealand-03	5.8	NM		Random	55	Assumed normal based on environment
0124	New Zealand-04	5.7	NM		Random	55	Assumed normal based on environment
0132	Kozani, Greece-03	5.3	NM		Random	42	Assumed normal based on environment
0147	Northridge-02	6.05	RV		Random	40	Assumed mechanism similar to main shock event 127 and other aftershocks
0148	Northridge-03	5.2	RV		Random	40	Assumed mechanism similar to main shock event 127 and other aftershocks

[1] Values not listed are know for specific event
[2] SS – strike-slip, RV – reverse, NM – normal faulting

Rupture Distances and Source-Site Geometry: One hundred and ten of the 173 earthquakes in the PEER-NGA database do not have associated finite fault models that can be used to compute the standard closest distance to rupture measures (e.g. rupture distance R_{RUP} and Joyner-Boore distance, R_{JB}) and the source-site geometry parameters such as hanging wall and foot wall positions and the source-site angle θ_{SITE}. Use of hypocentral distance, R_{HYP}, and epicentral distance, R_{EPI}, for R_{RUP} and R_{JB}, respectively, introduces a bias in the values as in most situations $R_{RUP} < R_{HYP}$ and $R_{JB} > R_{EPI}$, event for small events. The various geometry and distance measures for these earthquakes were estimated by simulating earthquake ruptures using the earthquake size and known or inferred information on the hypocentral depth, fault strike, fault dip, and rupture mechanism. Appendix B describes the simulation process. Figure 3 shows the ratios of R_{JB}/R_{EPI} and R_{RUP}/R_{HYP} for the 702 recordings from the 110 earthquakes and indicates the magnitude of the bias that could be introduced by using R_{EPI} for R_{JB} and R_{HYP} for R_{RUP}. The analysis also provided estimates of the depth to the top of rupture, Z_{TOR}, and rupture width, W, for these earthquakes.

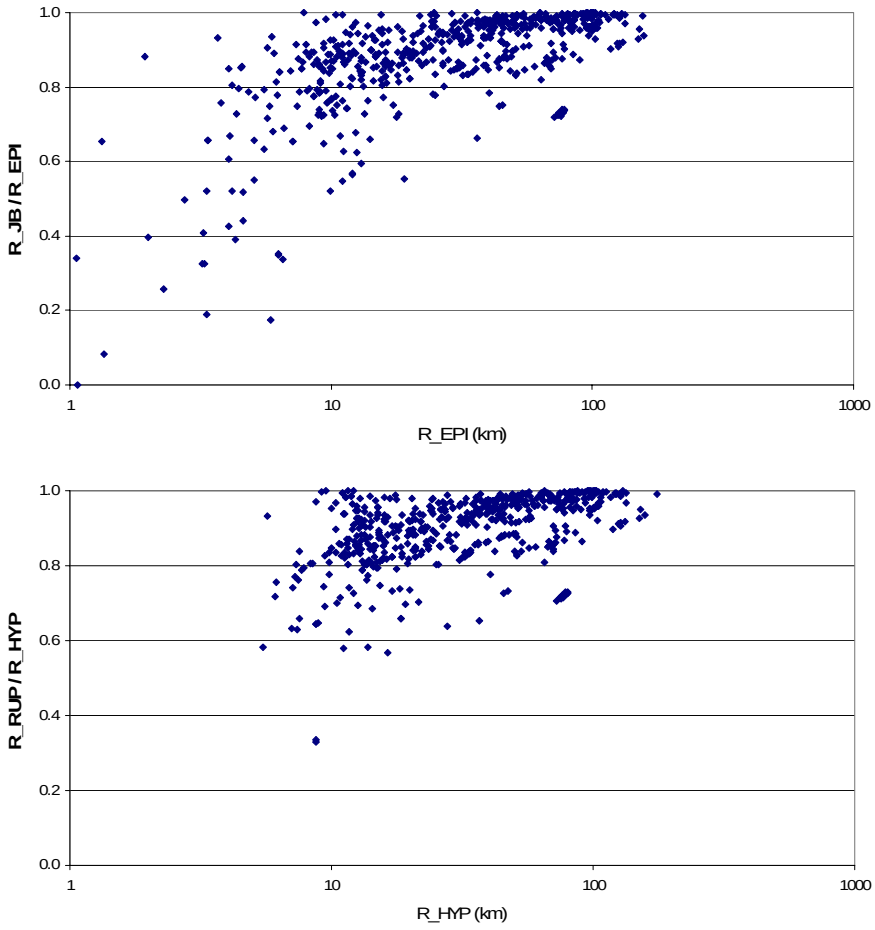

Figure 3: Ratio of estimated values of R_{JB} and R_{RUP} to R_{EPI} and R_{HYP} for recordings from earthquakes without finite fault models in the PEER-NGA database.

Site Average Shear Wave Velocity: Approximately two-thirds of the recordings in the PEER-NGA database were obtained at sites without measured values of shear wave velocity. As part of the database compilation, empirical correlations between surface geology and the average shear wave velocity in the top 30 meters, V_{S30} were developed (ref: PEER-NGA database report). These relationships together with assessments of the surface geology from geologic maps and site descriptions were used to estimate values of V_{S30} at the sites without measured velocities. Figures 3 and 4 show the distribution of the measured (solid circles) and estimated (open circles) values of V_{S30} versus magnitude and distance for the records selected for use from the PEER-NGA database. Also indicated on the figures are the divisions of the NEHRP site categories A through E.

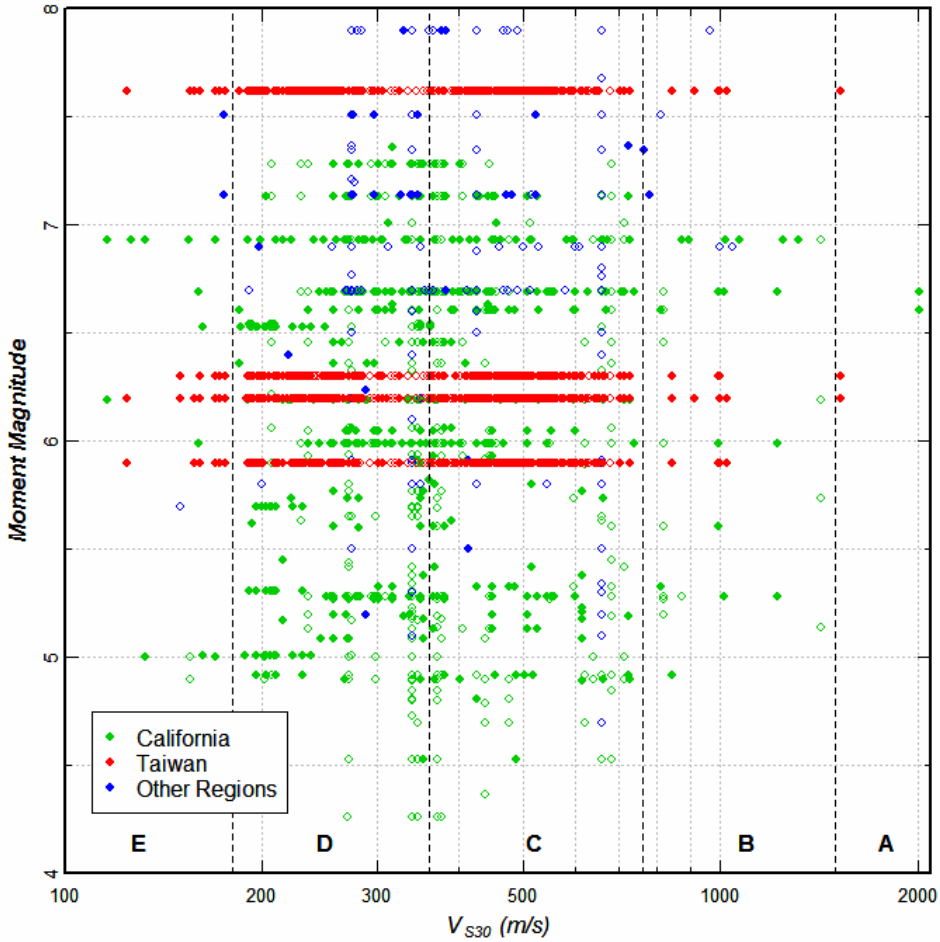

Figure 4: V_{S30}-magnitude-region distribution of selected recordings. Closed symbols indicated measured values, open symbols indicate inferred values. NEHRP site classes are indicated along the bottom edge.

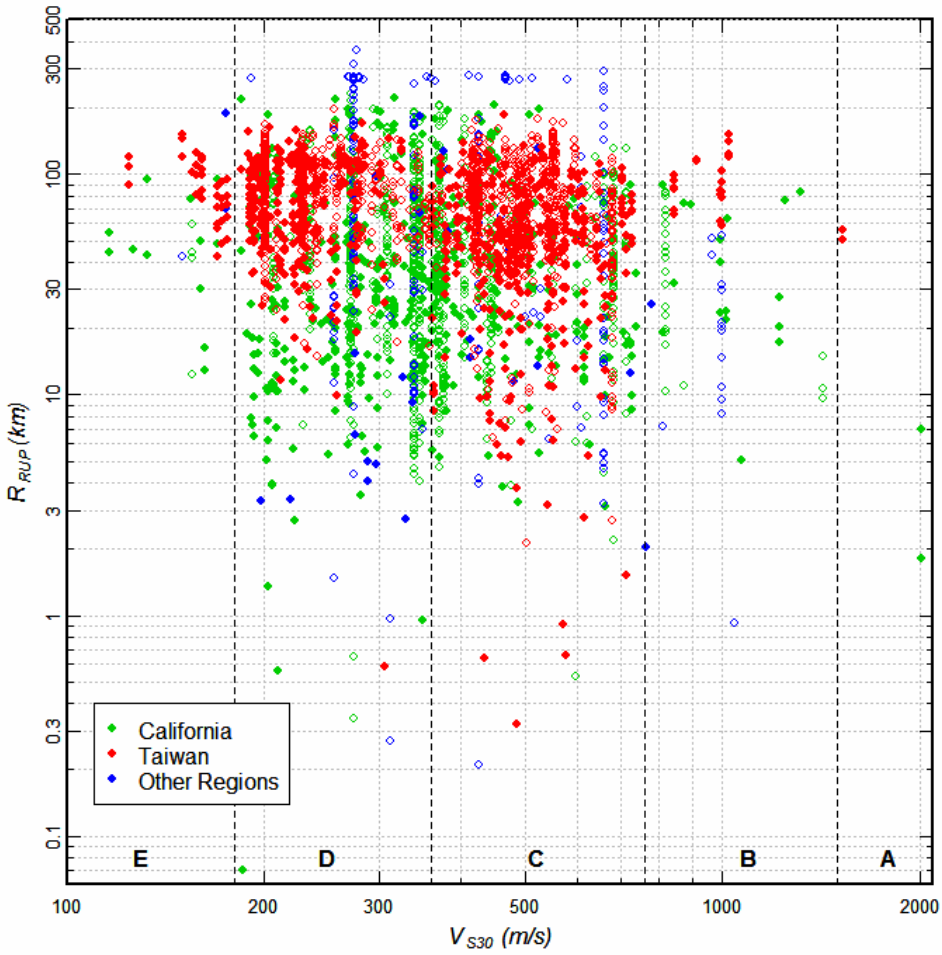

Figure 5: V_{S30}-distance-region distribution of selected recordings. Closed symbols indicated measured values, open symbols indicate inferred values. NEHRP site classes are indicated along the bottom edge.

Additional analysis was performed as part of this study to improve the correlation between surface geology and V*S30* for the Taiwan sites. This analysis is described in Appendix C. Additional velocity measurements and incorporation of elevation as a predictor variable were used to refine the V*S30* estimates for the Taiwan sites.

The data distributions plotted on Figures 4 and 5 indicate that the PEER-NGA database is primarily a soil/soft rock database.

Sediment Thickness: The thickness of the near-surface sediments is represented by the depths to shear eave velocity horizons of 1.0, 1.5, and 2.5 km/s. These data are only available in the PEER-NGA database for sites within the Southern California Earthquake Center 3-D basin model (Magistrale et al., 2000, 200?) and for sites in the San Francisco Bay area (J. Boatwright, personal communication, 2005?). Figure 6 shows the relationship between V_{S30} and $Z_{1.0}$ and between V_{S30} and $Z_{2.5}$. The dashed line shows the relationship used to infer missing values of $Z_{1.0}$.

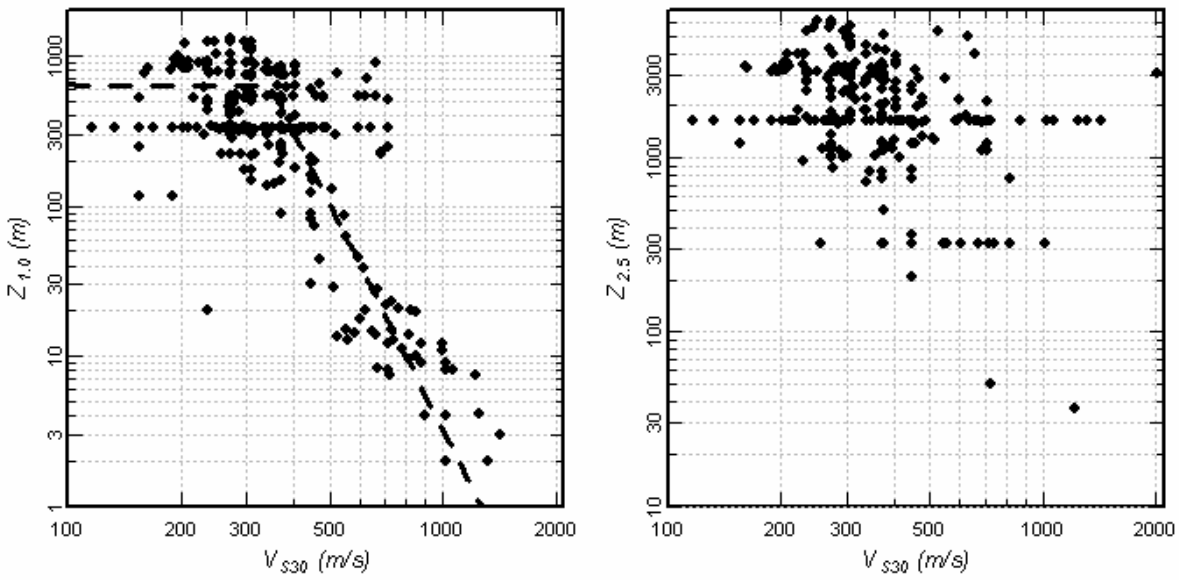

Figure 6: Relationship between V_{S30} and $Z_{1.0}$ and $Z_{2.5}$ for sites contained in the PEER-NGA database. Dashed line on plot for $Z_{1.0}$ was used to infer missing values.

SUPPLEMENTAL EMPRIRICAL DATA

The PEER-NGA strong motion data were supplemented with ground motion data from the California TriNet system. Time histories recorded at broad band stations for events 0163, 0167, and 0170 were provided by Dave Boore (personal communication, 2005). Peak acceleration values and estimates of site conditions for many other events were supplied by Jack Boatwright (2005, 2006 personal communication) and were obtained from the TriNet website. Appendix D describes the development of metadata and processing of these strong motion values. The data were used to provide additional guidance on function forms and provide additional constraints on parameters of the ground motion model.

MODEL FORMULATION

All ground motion models, empirical or theoretical/numerical, attempt to capture three basic aspects of ground motion estimation, the effect of the amount of energy radiated at the source, the effect of attenuation of seismic waves along the path due to geometric spreading and energy absorption, and the effect of local modification of the seismic waves by the near-surface materials. The empirical ground motion model developed in this study attempts to capture these elements using (relatively) simple algebraic expressions to represent the average behavior observed in the empirical strong motion data. The form of these expressions was guided by trends in the data, simple seismological models, past experience, and examination of the results of 1-D and 3-D ground motion simulations conducted as part of the PEER-NGA project.

Seismic Source Scaling

Effect of Earthquake Size: The simplest and most commonly used measure for correlating the amount of energy released in an earthquake with the resulting amplitudes of ground motions is the earthquake magnitude, defined in the PEER-NGA database in terms of moment magnitude **M**. Most empirical ground motion models have used a polynomial function for scaling the log of ground motions y with magnitude of the form

$$\ln(y) \propto C_2(T) \times \mathbf{M} + C_3(T) \times (m_C - \mathbf{M})^n \qquad (1)$$

where coefficients C_3 and possibly C_2 vary with spectral period T, the exponent n is typically in the range of 2 to 3, and the value of m_C is independent of T.

We have introduced an alternative form for magnitude scaling that reflects the results obtained using seismological models for the form of the earthquake source spectrum. Figure 7 shows response spectra computed using the stochastic ground motion model (e.g. Boore 2003) with two source spectra models, a Brune (1970, 1971) source with a stress parameter of 70 bars and the Atkinson and Silva (1997) empirical source spectra model for California earthquakes. Both forms of source spectra display similar trends in magnitude scaling. For high frequency motions (> ~ 10 Hz), the magnitude scaling of ln(y) is approximately linear at a relatively flat slope in the magnitude range of $5 \leq \mathbf{M} \leq 8.5$. The slope of the curves reflects the scaling of the source spectrum above the corner frequency. For very low frequency motions (< ~0.3 Hz) the magnitude scaling in the range of $5 \leq \mathbf{M} \leq 7$ is again approximately linear, but at a much larger slope than for high frequency motions, reflecting scaling of the source spectrum below the corner frequency.

At intermediate spectral frequencies, there is a transition in the scaling of ln(y) with magnitude from low-frequency scaling at low magnitudes to high-frequency scaling at large magnitudes. This transition occurs over the magnitude range where the corner frequency of the source spectrum is near the spectral frequency of the ground motion. As the spectral frequency of the ground motions decreases, the magnitude range for this transition shifts to larger magnitudes, reflecting the decrease in corner frequency with increasing magnitude.

The shape of the magnitude scaling curves shown in Figure 7 is modeled by the expression:

$$\ln(y) \propto C_2 \times \mathbf{M} + \frac{1}{C_n(T)}(C_2 - C_3) \times \ln\left[1 + \exp\left\{C_n(T) \times (C_{\mathbf{M}}(T) - \mathbf{M})\right\}\right] \quad (2)$$

In Equation (2) parameter C_2 is the slope of the magnitude scaling relationship above the corner frequency, C_3 is the slope of the magnitude scaling relationship below the corner frequency. Parameter C_n controls the magnitude range over which the transition from C_2 scaling to C_3 scaling occurs. Parameter $C_{\mathbf{M}}$ is the magnitude at the midpoint of this transition and its value varies with the spectral period of the ground motion parameter y. The function form of Equation (2) was tested by fitting a set of ground motion response spectra simulated using the program SMSIM (Boore, 2005) and the Atkinson and Silva (2000) stochastic ground motion. Figure 8 shows the magnitude scaling obtained from the simulated ground motions. As indicated on the figure, the functional form of Equation (2) can provide a close fit to the simulations.

Figure 9 shows peak acceleration data in the distance range of 30 to 50 km and the VS30 range of 300 to 400 m/s from the PEER-NGA database and from the TriNet data (Appendix D). These values were fit using three alternative scaling relationships. The quadratic form of Equation (1) uses an exponent n of 2. The Sadigh et al. (1997) form of Equation (1) uses n equal to 2.5 and m_C equal to 8.5. In the magnitude scaling defined by Equation (2), parameter C_3 represents scaling of ground motion spectra below the corner frequency where the source spectra are directly proportional to seismic moment, M_0. Because $\mathbf{M} \propto \frac{2}{3}M_0$, theoretically, C_3 should equal $1.5 \times \ln(10)$ or 3.45 and the fit of Equation (2) to the data shown on Figure 9 used this value of C_3. Parameter C2 represents the scaling of the source spectra above the corner frequency. The source spectral model defined by Atkinson and Silva (2000) produces scaling of $\ln(y) \propto 1.06\mathbf{M}$. As described in the next section, in the Sadigh et al. (1997) form of Equation (1), parameter C_2 also represents the magnitude scaling of the source spectra at distances unaffected by extended-source effects and in the Sadigh et al. (1997) values of C_2 were 1.0 to 1.1. The fit of the Sadigh et al. (1997) form of Equation (1) to the data on Figure 9 also produced C_2 equal to 1.0. In fitting Equation (2) to the data on Figure 9, C_2 was constrained to be 1.06, the value obtained from the magnitude scaling of source spectra above the corner frequency defined by Atkinson and Silva (2000). All three forms provide essentially equally good fits to the data. We prefer the scaling form of Equation (2) because we believe that it better represents our current concept of the variation in earthquake source spectra with earthquake magnitude.

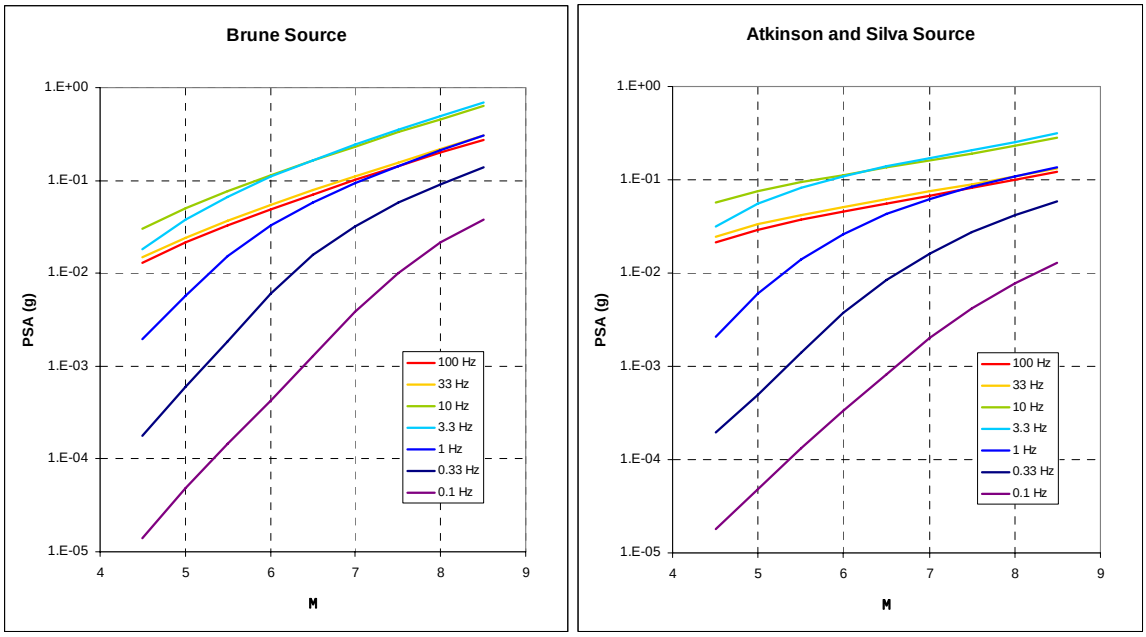

Figure 7: Response spectra at a distance of 30 km computed using the stochastic ground motion model and two source spectra, a Brune (1970, 1971) source with a 70 bar stress parameter and the Atkinson and Silva (1997) source model for California earthquakes. Western US crustal amplification (e.g. Boore and Joyner, 1997) is applied in computing the spectra.

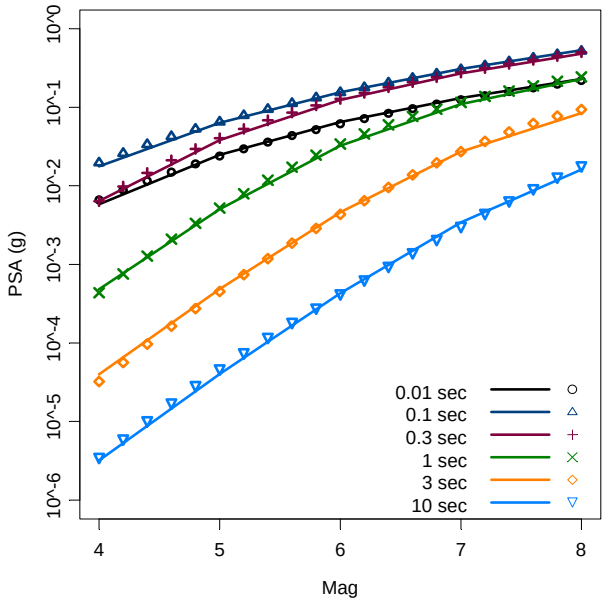

Figure 8: Magnitude scaling predicted by the seismic source model of Atkinson and Silva (2000) (points) and the result of fitting Equation (2) to the data (lines).

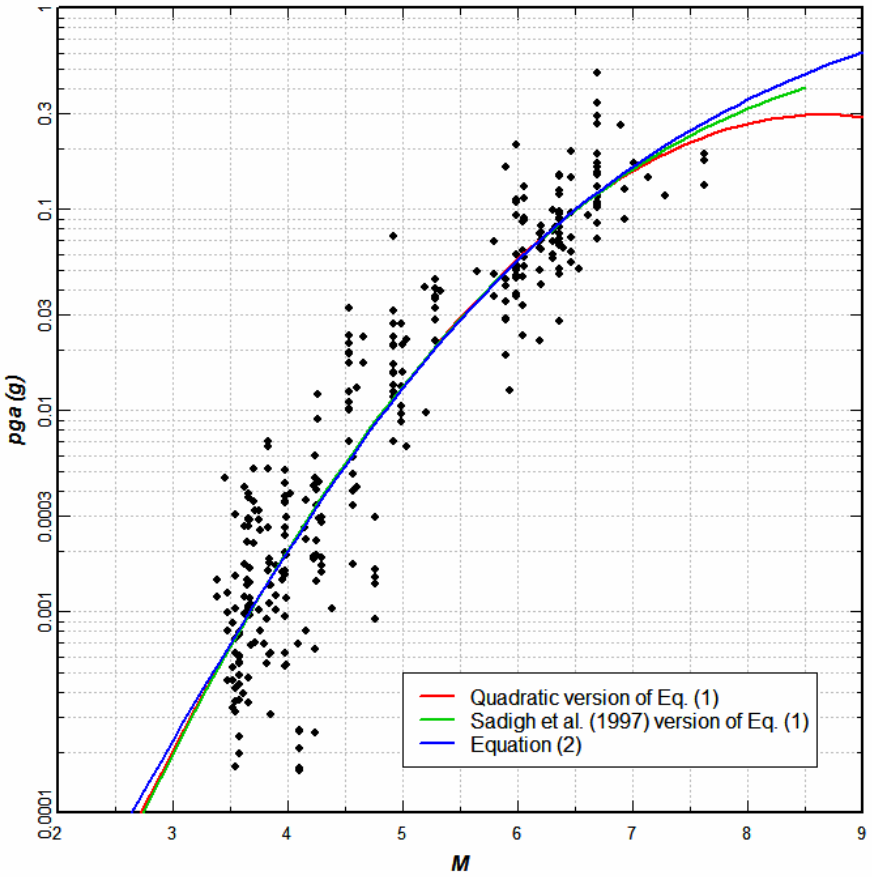

Figure 9: Peak acceleration data from the PEER-NGA database and from TriNet (Appendix D) for the distance range $30 \leq R_{RUP} \leq 50$ and the velocity range $300 \leq V_{S30} \leq 400$ fit by alternative function forms of magnitude scaling.

Other Source Effects: Most recent empirical ground motion models include a scaling term that reflects alternative rupture styles. Typically it has been found that reverse faulting earthquakes produce larger high frequency motions than strike-slip earthquakes. In some of these empirical models the difference between strike-slip and reverse earthquakes diminishes as the spectral period increases, with the motion from strike-slip earthquakes becoming larger for period motions (e.g. Abrahamson and Silva, 1997; Campbell and Bozorgnia, 2003; Ambraseys et al, 2005). Chiou et al. (2000) showed that when the geometric hanging wall effect was removed from ground motion residuals by using the R_{RMS} distance measure, reverse-faulting earthquake still produced statistically significant higher motions than strike-slip earthquakes. Some empirical models have shown that normal-faulting/extension regime earthquakes produce lower ground motions than strike-slip earthquakes (e.g. Spudich et al., 1999, Ambraseys et al. 2005) while others have included normal-faulting and strike-slip together in a single class (e.g. Abrahamson and Silva, 1997; Silva et al., 1997; Campbell and Bozorgnia, 2003). The potential effect of style of faulting will be examined by including dummy variables F_{RV} and F_{NM} in the regression model. These parameters take on a value of 1.0 for earthquake ruptures with rake angles, λ, in the appropriate range and 0 otherwise.

Other source parameters that will be examined include depth to top of rupture Z_{TOR}, aspect ratio, AR, and static stress drop, $\Delta\sigma_S$.

PATH SCALING

Near-Source Distance Scaling: The scaling or attenuation of ground motion amplitude with distance from the earthquake rupture involves a number of issues. Foremost of interest for engineering application in active tectonic regions is the effect of extended sources that leads to magnitude-dependent attenuation rates at least within the distance range of 0 to 100 km. The consequence of this effect is what has been termed near-source saturation – less magnitude scaling at small source-site distances than at large source-site distances. There are four functional forms that have been used to model this effect in empirical ground motion models. These forms are shown on Figure 10 in terms of recent applications. The form that has been used for many years by Ross Sadigh and also by Ken Campbell is defined by Equation (3):

$$\ln(y) \propto C_2\mathbf{M} + C_4 \times \ln\left[R + c(\mathbf{M})\right]$$
$$c(\mathbf{M}) = C_5 \exp\left\{C_6\mathbf{M}\right\} \tag{3}$$

In this form, magnitude-dependence is introduced by making parameter c a function of magnitude. Campbell (1993) introduced a modified version of Equation (3):

$$\ln(y) \propto C_2\mathbf{M} + C_4 \times \ln\left[\sqrt{R^2 + c(\mathbf{M})^2}\right]$$
$$c(\mathbf{M}) = C_5 \exp\left\{C_6\mathbf{M}\right\} \tag{4}$$

Campbell and Bozorgnia (2003) further modified Equation (4) to introduce a quadratic magnitude term in defining $c(\mathbf{M})$.

The forms defined by Equations (3) and (4) introduce magnitude dependence through the parameter $c(\mathbf{M})$. An alternative approach is to incorporate magnitude-dependence in the "slope" term. Idriss (1991) introduced the form

$$\ln(y) \propto C_2\mathbf{M} + (C_4 + C_5\mathbf{M}) \times \ln\left[R + c\right] \tag{5}$$

Abrahamson and Silva (1997) introduced a modified version of (5):

$$\ln(y) \propto C_2\mathbf{M} + (C_4 + C_5\mathbf{M}) \times \ln\left[\sqrt{R^2 + c^2}\right] \tag{6}$$

The attenuation behavior of the four models shown on Figure 10 can be illustrated by plotting the attenuation rate, defined as $\partial \ln(y) / \partial \ln(R)$, versus distance. Figure 11 shows the results. For those models that use the term $\ln\left[\sqrt{R^2 + c^2}\right]$, the rate of attenuation approaches the value of the parameter C_4 or C_4+$C_5\mathbf{M}$ at relatively short distances, allowing an interpretation of its value as an estimate of the rate of geometric spreading. For those models that use the term $\ln\left[R + c\right]$, the attenuation rate approaches the value of C_4 or

C_4+C_5**M** slowly and the value of the parameter cannot be interpreted as an estimate of the rate of geometric spreading at distances less that 50 km.

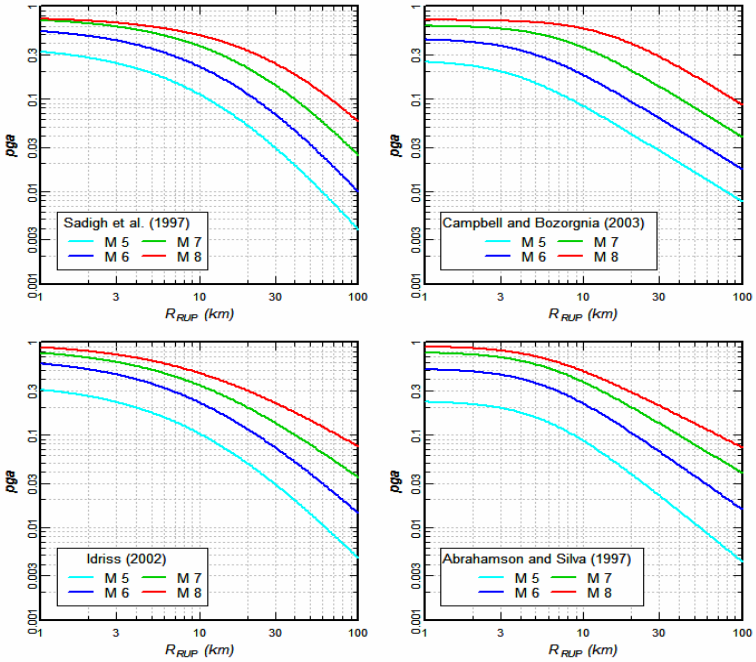

Figure 10: Illustration functional forms used to capture magnitude-dependence of distance attenuation for distances less than 100 km. All plots are for rupture distance to a vertical strike-slip fault rupturing the surface and the values for Campbell and Bozorgnia (2003) were computed using a minimum R_{SEIS} of 3 km.

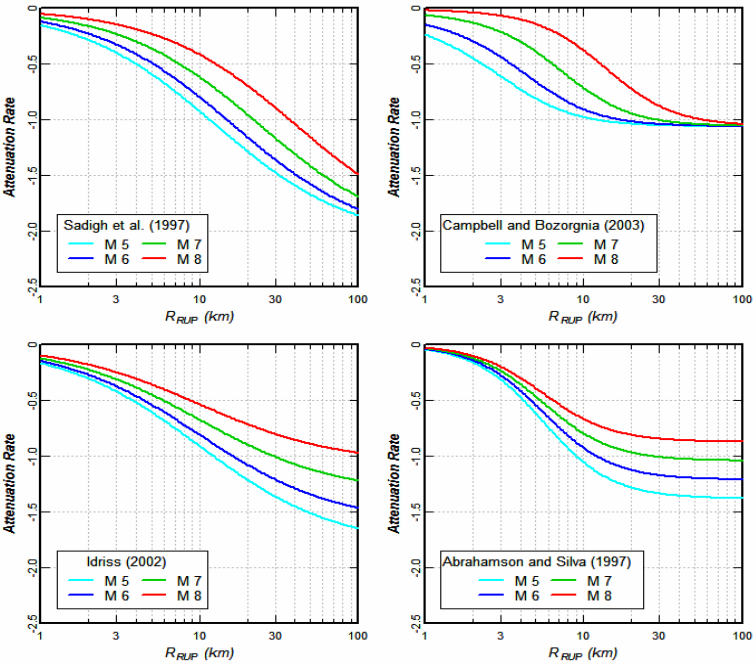

Figure 11: Plots of the instantaneous slope of the attenuation curve for the four ground motion models shown in Figure 10. The attenuation rate is defined as $\partial \ln(pga) / \partial \ln(R)$.

The different forms of distance scaling defined by Equations (3) through (6) also result in differences in the variation in the scaling of ground motions with magnitude at different distances. Figure 12 shows the magnitude scaling, defined as $\partial \ln(y) / \partial \mathbf{M}$, for the four ground motion models shown in Figure 10. The steps in the values of $\partial \ln(y) / \partial \mathbf{M}$ occur where there are changes in the model parameters for different magnitude ranges. The distance attenuation functional forms that use a magnitude-dependent slope, Equations (5) and (6) produce continued increases in magnitude scaling with increasing distance. Those that use a magnitude-dependent near-source adjustment term, c(M), result in a gradual approach to distance-independent magnitude scaling.

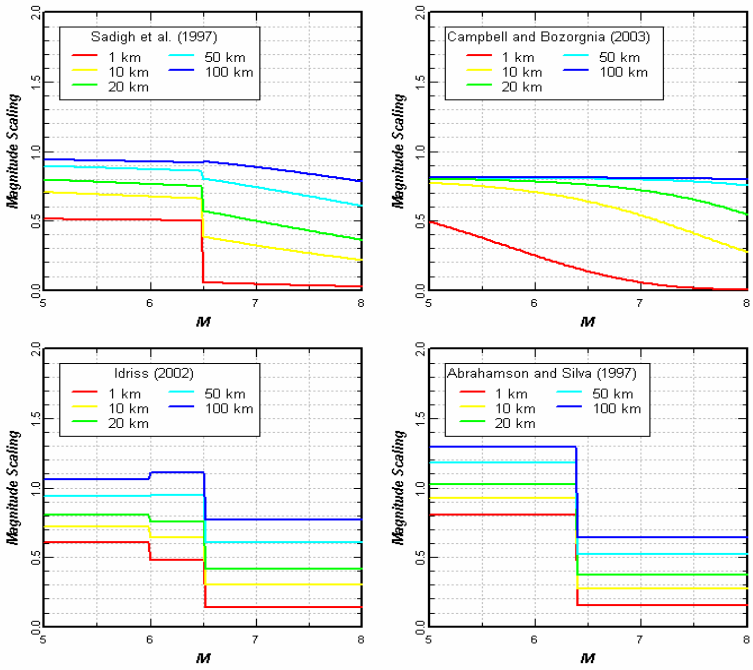

Figure 12: Plots of magnitude scaling at a range of distances produced by the form of the attenuation curve for the four ground motion models shown in Figure 10. Magnitude scaling is defined as $\partial \ln(pga) / \partial \mathbf{M}$.

We examined the alternative forms and their fit to the PEER-NGA data and came to the conclusion that they all would work equally well given the data distribution. Discrimination among them would require a great deal more data at distances less than 10 km. The relationships we are to develop are required to cover the distance range of 0 to 200 km. We based our selection of the functional form on the behavior over the full magnitude range. The data show magnitude-dependence in the rate of attenuation at all distances. However, we believe that the mechanisms that cause this behavior may be different at different distances. At distances less than ~50 km, magnitude-dependence is due to the effect of extended sources. This effect can be modeled by all of the form. However, at large distances, >100 km, we think that another effect may be causing magnitude-dependence in the attenuation of response spectral ordinates – the interaction of Q with the differences in source Fourier spectra as a function of magnitude. This concept is explored below. The magnitude-dependence at large distances may also be modeled by the various functional forms. We prefer to use a model form that allows for separation of the effect of magnitude at small and at large distances, and therefore select the form defined by Equation (3). This form

allows the interpretation of the coefficient C_2 as the asymptotic value of magnitude scaling at large distances from the source. This same argument should make us favor the functional form of Equation (4) over that of Equation (3) in that with the function form of Equation (4) the coefficient C_4 can be interpreted as the geometric spreading at distances greater than about $2\times c(\mathbf{M})$. We experimented extensively with this form, but ultimately decided not to use it because we judged that it resulted in too little distance scaling over the distance range of 0 to 10 km for large-magnitude earthquakes.

Previous implementations of the functional form of Equation (3) (e.g. Sadigh et al., 1997) have typically specified different parameters for large and small magnitude earthquakes. This results in a step function for the magnitude scaling, as illustrated in the upper left-hand plot of Figure 12. We prefer to have a smooth transition in the magnitude scaling over the full magnitude range. This was accomplished by using the relationship:

$$c(\mathbf{M}) = C_5 \cosh\{C_6 \max(\mathbf{M} - 3,0)\} \tag{7}$$

The use of Equation (7) has the property that $c(\mathbf{M})$ varies smoothly from a constant at small magnitudes to $c(\mathbf{M}) \propto \exp(C_6\mathbf{M})$ at large magnitudes.

<u>Path Scaling at Large Distances</u>: Many studies of the attenuation of ground motion Fourier amplitudes with distance have indicated that there is a change in the rate of geometric spreading from approximately proportional to $1/R$ at short distances to $1/\sqrt{R}$ at large distances, with this transition occurring in the range of 40 to 70 km. This change has been interpreted to be the combination of the effects of post-critical reflections from the lower crust and transition from direct body wave to *Lg* wave spreading (e.g. Atkinson and Mereu, 1992). Models of the decay of Fourier spectra with distance in California have found or assumed that the geometric spreading is proportional to $1/\sqrt{R}$ for distances greater than 40 km (Raoof et al., 1999; Erickson et al., 2004) and this form of geometric spreading was used by Atkinson and Silva (2000) to model strong ground motions. Earlier, Atkinson and Silva (1997) used a tri-linear form of attenuation similar to that defined by Atkinson and Mereu (1992), but indicated that a bi-linear form would also work.

We explored this effect by modeling the broadband data assembled for three small (**M** 4.3 to 4.9) Southern California earthquakes (Anza, Yorba Linda, and Big Bear City, events 0163, 0167, and 0170, respectively). These data were fit with three functional forms, a 1-slope model:

$$\begin{aligned} &\ln(y) = C_1 + C_2 F_{BBC} + C_3 F_{YL} + C_4 \ln(R_0) + \gamma R + \phi_1 \ln(V_{S30}/400) \\ &R_0 = \sqrt{R^2 + 6^2} \end{aligned} \tag{8}$$

a 2-slope model with the second slope ½ of the first:

$$\begin{aligned} &\ln(y) = C_1 + C_2 F_{BBC} + C_3 F_{YL} + C_4 \{\ln(R_1) + \ln(R_2)/2\} + \gamma R + \phi_1 \ln(V_{S30}/400) \\ &R_0 = \sqrt{R^2 + 6^2}, R_1 = \min(R_0, C_8), R_2 = \max(1, R_0/C_8) \end{aligned} \tag{9}$$

and a 2-slope model with the second slope fixed at -0.5:

$$\ln(y) = C_1 + C_2 F_{BBC} + C_3 F_{YL} + C_4 \ln(R_1) - 0.5 \ln(R_2) + \gamma R + \phi_1 \ln(V_{S30} / 400)$$
$$R_0 = \sqrt{R^2 + 6^2}\,, R_1 = \min(R_0, C_8), R_2 = \max(1, R_0 / C_8) \quad (10)$$

This study was performed before our final decision on the function form for distance attenuation near the source but alternative forms were found to produce similar results. The data cannot determine *h* (insufficient data at small distances) so it was fixed at 6. Dummy variables F_{BBC} and F_{YL} were used for the intercepts rather than magnitude scaling with random effects. There is sufficient data for each event (~200 records) that the random effect should equal the mean residual and the magnitude range is small (4.33 to 4.92). The analysis was conducted for spectral periods in the range of 0.01 to 5 seconds. Examination of the recordings (Appendix D) indicated that they could be used without processing to periods at least as long as 5 seconds.

Figure 13 shows the results of fitting Equations 8 and 9 to the data. At all spectral periods, the 2-slope models produced slightly smaller standard errors that the single slope model. The location for the break in slope varied between 40 and 60 km. In addition, use of the single-slope model produces unrealistic positive values of the anelastic attenuation term γ for longer period motions, a fact also noted by Atkinson and Silva (1997).

The TRI-Net *pga* data from many of the better-recorded small magnitude earthquakes display the change in attenuation rate slope. Tests of the PEER-NGA data also show that a two-slope model is statistically significant with a slope break also in the range of 45 to 60 km. Examination of the 1-D rock numerical simulation data also indicate that two-slope model provides a good fit with a beak in slope at about 60 km.

Based on the above considerations, we adopted the concept of a change in the rate of attenuation occurring at a distances of approximately 50 km from the source. The appropriate value of the attenuation rate at distances beyond this point cannot be readily determined from the data because it is highly correlated with the assessment of the anelastic attenuation term γ, as had been noted by many previous investigators (e.g. Atkinson, 1989; Frankel et al., 1990). Therefore, we assume that the rate of attenuation can be modeled by a slope of -0.5 and will let the anelastic attenuation term γ account for departures from this value.

The anelastic attenuation parameter γ is likely to have some degree of magnitude dependence. Boatwright et al. (2003) found magnitude-dependence in the anelastic attenuation term from their study of *pga* and *pgv* from northern California ShakeMap data, with increasing magnitude producing smaller absolute values of γ (less energy absorption). In addition, stochastic simulations of ground motions using a magnitude-independent *Q* model will produce magnitude-dependence in the resulting anelastic attenuation term γ fit to response spectra ordinates (e.g. Campbell, 2003). This effect was also noted by us in fitting ground motions using the Atkinson and Silva (2000) ground motion model. The effect is likely due to the shift to lower frequencies driving the damped oscillator response (and driving *pga*, Boatwright et al., 2003) as the size of the earthquake increases and lower frequency motions typically display lower values of *Q*.

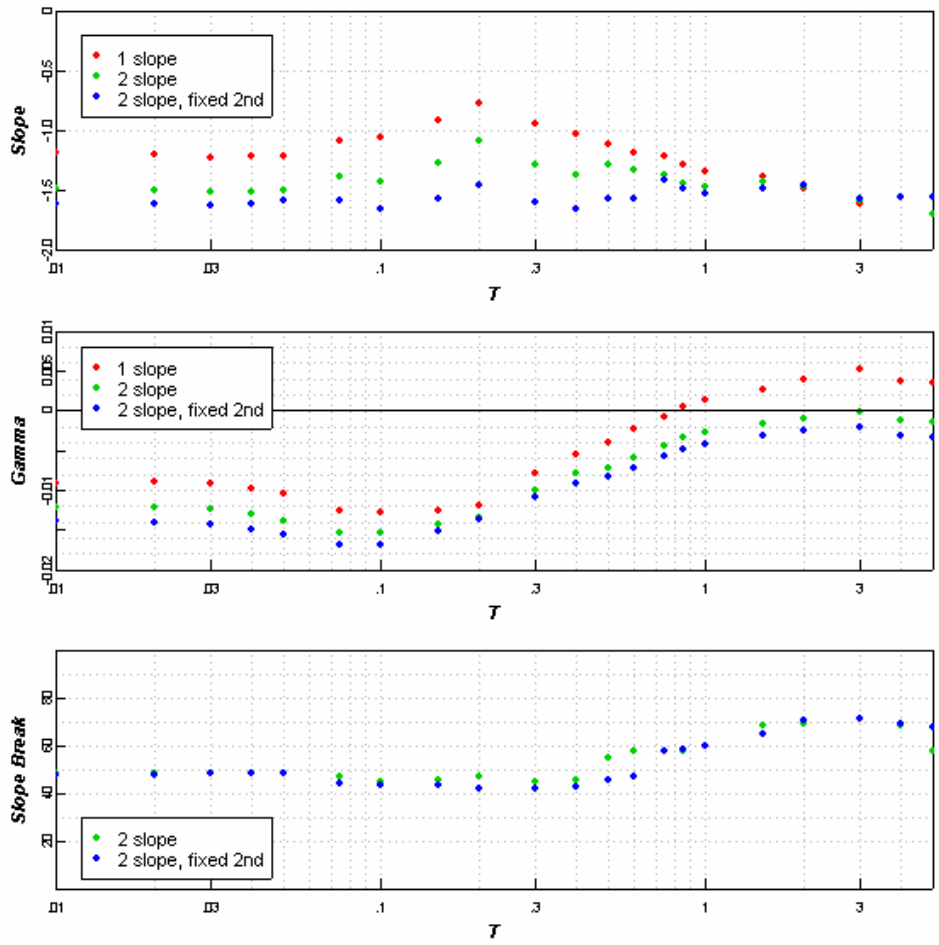

Figure 13: Coefficients resulting from fits of Equations (8), (9), and (10) to the broad band data for earthquakes 0163, 0167, and 0170. *T* is spectral period in seconds.

The form of Equation (10) has a sharp break in the slope of the attenuation curve. This form appears to work well for individual earthquakes. However, the ground motion model developed in this study is intended to apply over all of California and includes data from a number of active tectonic regions. Therefore, Equation (10) was modified to introduce a smooth transition from near-source to far-source attenuation rates. The selected form for the distance attenuation function for the ground motion model developed in this study is:

$$\ln(y) \propto C_4 \ln\left[R_{RUP} + C_5 \cosh\left\{C_6 \max(\mathbf{M} - 3{,}0)\right\}\right] + (-0.5 - C_4) \ln\sqrt{R_{RUP}^2 + R_B^2} + \gamma(\mathbf{M}) \qquad (11)$$

This form incorporates magnitude-dependent extended source effects, potentially magnitude-dependent wave propagation effects on responds spectra at large distances and a smooth transition from dominance of ground motions by direct waves at small distances to dominance by *Lg* waves at large distances.

<u>Source-Site Geometry Effects</u>: Analyses of ground motions from thrust earthquakes by Somerville and Abrahamson (1995) and Abrahamson and Somerville (1996) proposed the so called "hanging wall" effect in which ground motions are enhanced in the hanging wall of

thrust earthquakes. The effect was attributed to the inability of the R_{RUP} distance measure to capture the general proximity of a hanging wall site to rupture on the fault plane dipping beneath it. Chiou et al. (2000) performed extensive analyses of empirical and numerical modeling data for dipping fault ruptures and reached the same conclusion. They were able to remove the effect by using a root-mean-squared distance measure, R_{RMS}.

The hanging wall effect is seen in the PEER-NGA data. Figure 14 shows intra-event residuals for data from dip-slip earthquakes (both reverse/thrust and normal) plotted versus horizontal distance from a point above the top of the fault rupture. The dashed line is a locally-weighted least-squares fit to the residual. It shows an upward warp in the region where the hanging wall effect is expected to be present. The effect is also seen in the 1-D rock ground motion simulations conducted for the PEER-NGA project (Somerville et al., 2006).

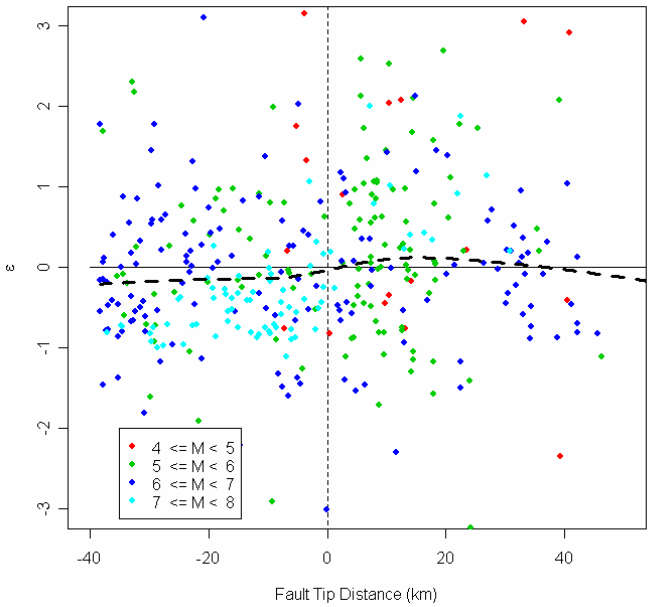

Figure 14: Intra-event residual for sites in the hanging wall (positive fault tip distance) and footwall (negative fault tip distance) from dip-slip earthquakes. Black dashed line is a locally-weighted least-squares (lowess) fit to the residuals.

Abrahamson and Silva (1997) included the hanging wall effect in their empirical ground motion model as a distance-dependent term with an abrupt switch from no effect to full effect as one crosses into the hanging wall region, defined as sites with a source-site angle, θ_{SITE}, between 60º and 120º. Boore et al. (1997) conclude that their use of R_{JB} implicitly accounts for the hanging wall effect in that all site directly above the rupture have $R_{JB} = 0$. Campbell and Bozorgnia (2003) introduces a smooth variation in the hanging wall effect by tapering the effect from a maximum at $R_{JB} = 0$ to zero for $R_{JB} > 5$ km while using R_{SEIS} as the primary distance measure for assessing ground motion amplitudes.

We have extended the concept proposed by Campbell and Bozorgnia (2003) by defining the hanging wall effect to be proportional to the factor $[1 - R_{JB} / R_{RUP}]$. Figures 15 through 17 illustrate the behavior of this function. Figure 15 shows a map view of a fault rupture with

the top of rupture located at x = 0 and the fault dipping downward towards positive x. Figure 16 show the variation of the factor $[1 - R_{JB} / R_{RUP}]$ with location along three lines for the case when the top of rupture at x=0 is at the ground surface. Line 1 runs from negative values in the foot wall to positive values in the hanging wall. In the foot wall, $R_{JB} = R_{RUP}$ and the hanging wall effect is zero. Thus the function acts as a switch equivalent to other formulations that only apply the effect on the hanging wall side of the fault. Lines 2 and 3 show the variation of $[1 - R_{JB} / R_{RUP}]$ as one moves away from the rupture along strike. Line 2 is located near the top of the rupture and line 3 near the bottom. The function $[1 - R_{JB} / R_{RUP}]$ decays much more rapidly for Line 2 than for Line 3. Most of Line 2 lies outside of the area typically defined as subject to the hanging wall effect while much of Line 3 for small values of y lines within the hanging wall area. The term $[1 - R_{JB} / R_{RUP}]$ provides for a smooth transition in the level of the hanging wall effect throughout the along strike region.

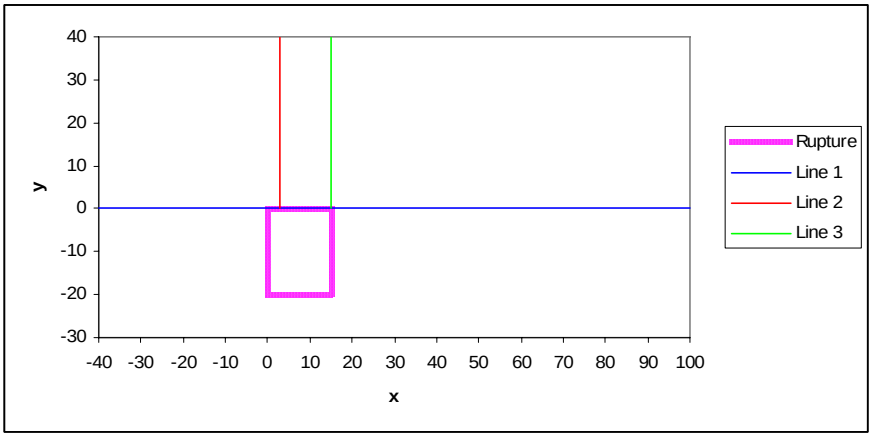

Figure 15: Map view of example fault rupture.

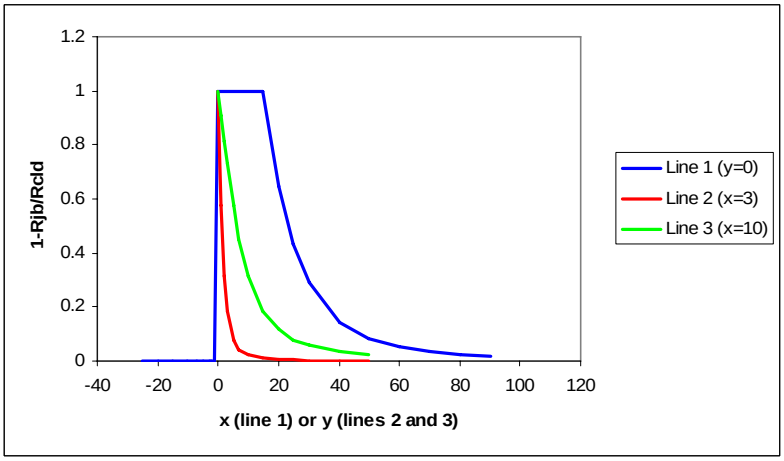

Figure 16: Variation of the term $[1 - R_{JB} / R_{RUP}]$ with location for the three lines shown on Figure 15. Top of rupture is at the ground surface at x=0.

Figure 17 shows the variation of the term $[1 - R_{JB} / R_{RUP}]$ for the case when the top of rupture is located at a depth of 5 km. Now, the hanging wall effect extends into the footwall side of

the rupture, although this region is mostly to the hanging wall side of a projection of the rupture to the surface (i.e. on the hanging wall of the fault, but the foot wall side of the rupture). It seams reasonable that there should be some increased motion in this area for a buried fault.

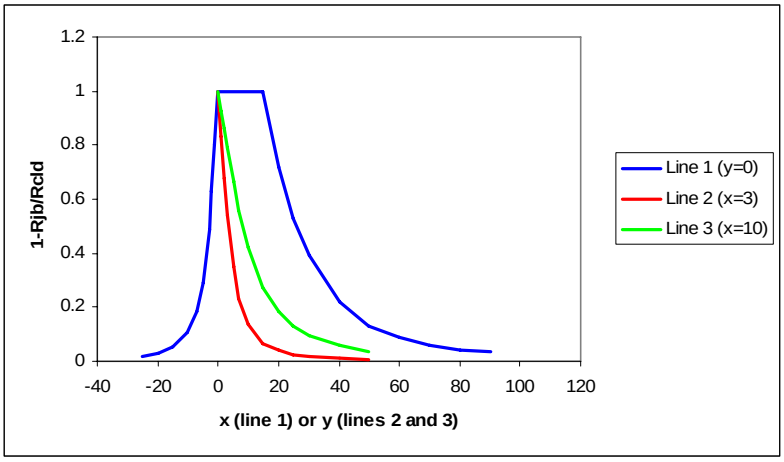

Figure 17: Variation of the term $[1 - R_{JB} / R_{RUP}]$ with location for the three lines shown on Figure 15. Top of rupture is at a depth of 5 km at x=0.

The effectiveness of the term $[1 - R_{JB} / R_{RUP}]$ to capture the hanging wall effect was tested by fitting the selected PEER-NGA data for peak acceleration with a regression model without a hanging wall term. The residuals were found to be correlated with $[1 - R_{JB} / R_{RUP}]$ with a p-value of 0.0024. Exploratory analysis indicated that the model $[1 - R_{JB} / R_{RUP}]^n$ with n equal to 2 and ½ produced poorer fits to the data (larger standard error) than a linear model (n= 1). No significant difference between normal and reverse faulting data was found (p value of 0.63 for adding a normal fault difference in the correlation). The behavior of the residuals with respect to $[1 - R_{JB} / R_{RUP}]$ was checked by separately fitting the data on the hanging wall, $60^o \le \theta_{SITE} \le 120^o$, and footwall, $-60^o \le \theta_{SITE} \le -120^o$ sides of the rupture, excluding sites directly above the rupture (R_{JB}=0). Figure 18 shows the residuals and linear fits with respect to$[1 - R_{JB} / R_{RUP}]$ constrained to go through 0 at $[1 - R_{JB} / R_{RUP}]$=0. The solid lines show the mean trend and the dashed lines the 90% confidence interval for the mean. The residuals on the hanging wall and footwall side of the ruptures have essentially identical trends.

Previous empirical models (Abrahamson and Silva, 1997; Campbell and Bozorgnia, 2003) have limited the hanging wall effect to faults with dip angles, δ, less than 70º. Assuming the hanging wall effect is a geometric effect, one might expect that it might correlate with δ. Figure 19 shows residuals for sites on the hanging wall of reverse faults (R_{JB} = 0) plotted versus δ. The data indicate increasing motion with decreasing δ. The trend was modeled with linear functions with 90º - δ, $\cos(\delta)$ and $\cos^2(\delta)$. All three functions show a significant trend with the residuals, with $\cos^2(\delta)$ providing a slightly better fit than the other two models. Similar results were found including data from sites with $[1 - R_{JB} / R_{RUP}] > 0.8$ and for data from sites with $R_{JB} < 5$ km.

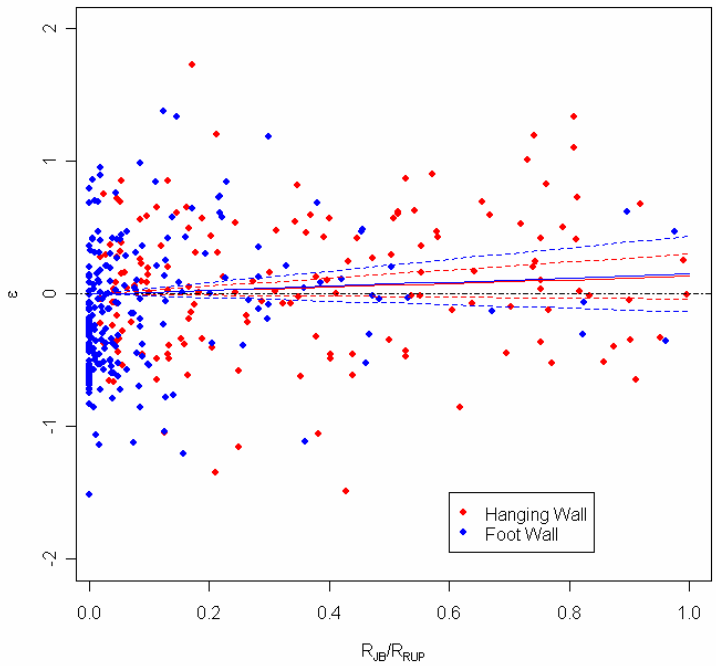

Figure 18: Intra-event residuals for dip-slip earthquake for a model without a hanging wall term. The residuals were fit with a linear regression line constrained to pass through 0 at $[1 - R_{JB} / R_{RUP}] = 0$. Solid line shows the mean trend and the dashed lines indicate the 90% confidence interval for the mean.

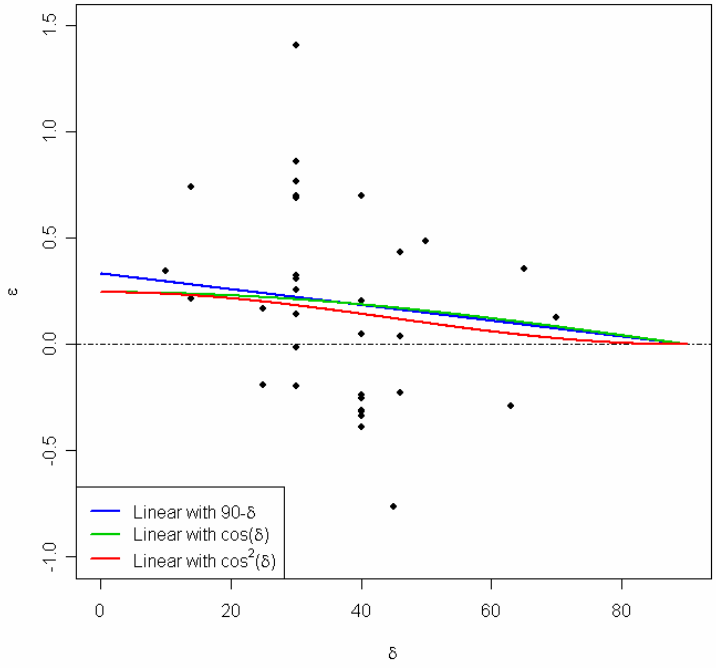

Figure 19: Intra-event residuals from fitting a model without a hanging wall term for sites with R_{JB} = 0 and F_{HW} = 1 plotted against fault dip, δ.

Although, the term $[1 - R_{JB} / R_{RUP}]$ appears to model well the hanging wall effect, there are two additional aspects it does not capture. Assuming that the hanging wall effect is a

geometric effect, we expect that smaller overall ruptures would produce less effect than larger rupture, given the same values of R_{JB} and R_{RUP}. Previous implementations of the hanging wall effect in empirical models have reduced the effect to 0 for magnitudes less than **M** 6. Similarly, as the same size rupture is moved to deeper depths, we would also expect the hanging wall effect to be reduced. Both smaller rupture sizes and greater depths would tend to move make R_{RMS} closer to R_{RUP}, and thus, according to the analysis of Chiou et al. (2000), reduce the hanging wall effect.

We propose a geometric factor, $HW^* = 2\psi/\pi$, to represent the combined effect of rupture size and rupture depth. The factor is illustrated on Figure 20. The angle ψ represents the half-angle of the exposure of the surface to the fault plane and is a function of the rupture width, W, and the rupture depth, Z_{TOR}. Using the geometry of the fault rupture, HW^* is computed by the relationship:

$$HW^* = \frac{2}{\tau} tan^{-1}\left(\frac{W\,cos(\delta)}{2(Z_{TOR}+\zeta)}\right) \tag{12}$$

The factor ζ is included to remove singularities in the calculation and to limit the hanging wall effect for small magnitudes at shallow depths. Figure 21 show the variation of HW^* with **M** and Z_{TOR} with ζ set equal to 1 km. The function introduces a decrease in the hanging wall effect with increasing rupture depth that is magnitude-dependent.

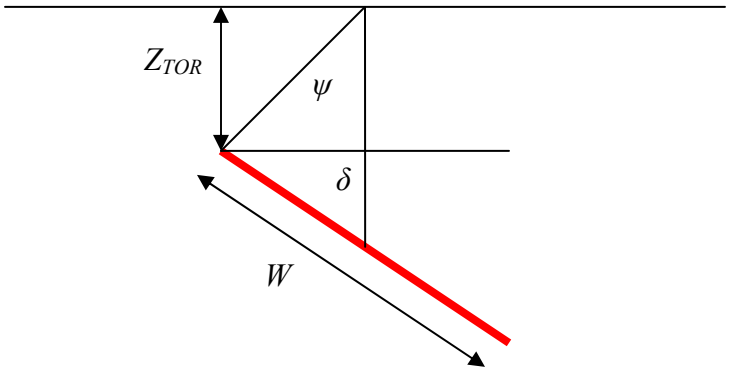

Figure 20: Illustration of the hanging wall geometric factor HW^*.

Figure 22 shows that HW^* correlates with both magnitude and Z_{TOR} for the data selected for use in this study.

One additional aspect of the hanging wall effect needs to be addressed. The function $[1 - R_{JB} / R_{RUP}]$ produces the same level of hanging wall effect at locations on top of the rupture. However, the numerical modeling results presented in Chiou et al. (2000) and those conducted for the PEER-NGA project (Somerville et al., 2006) show the hanging wall effect tapering to zero at the fault tip for faults with surface rupture. We model this effect by multiplying the hanging wall term by $\tanh(0.5R_{RUP})$.

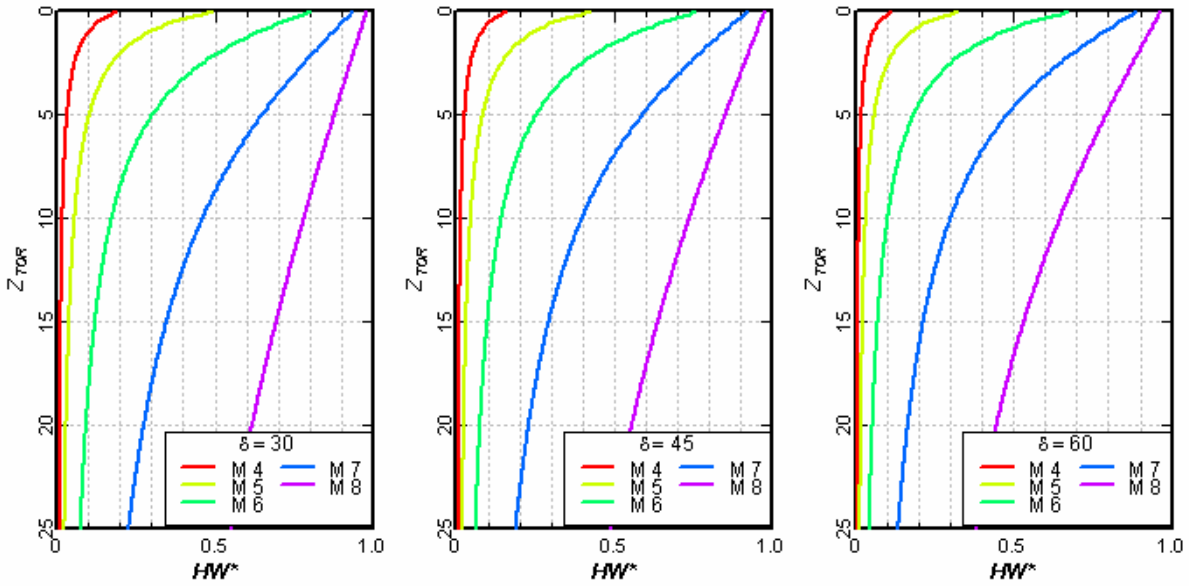

Figure 21: Variation of *HW** with magnitude, depth to top of rupture for $\zeta = 1$ km and a range of fault dips.

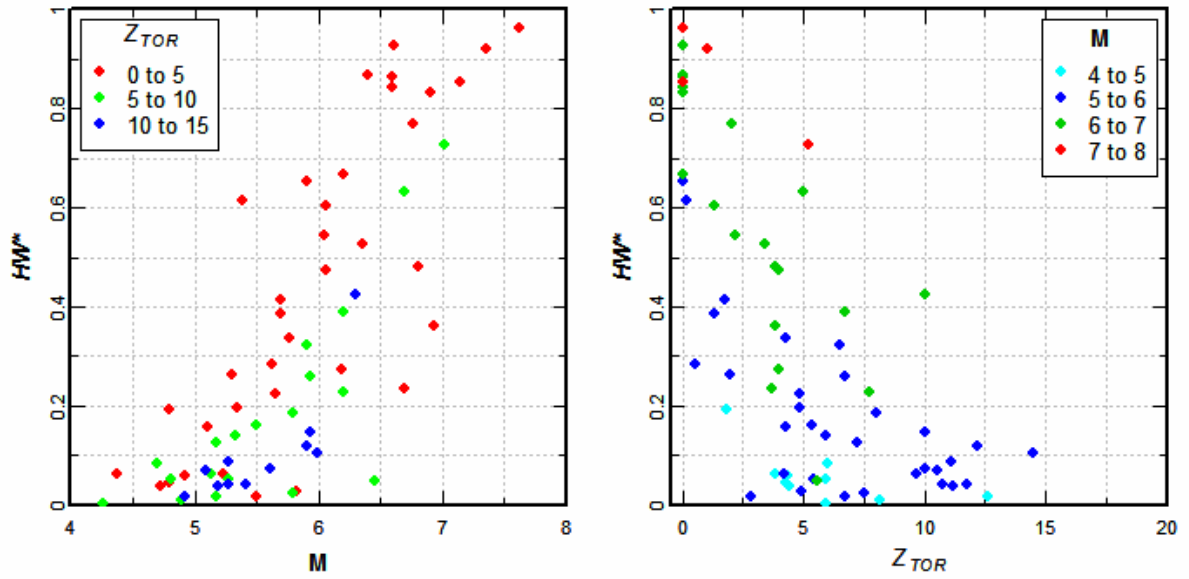

Figure 22: Correlation of *HW** with magnitude and depth to top of rupture for the earthquakes in the PEER-NGA database selected for use in this study.

The complete hanging wall function is given by:

$$f_{HW} = \tanh(0.5R_{RUP}) \times \cos^2(\delta) \times \frac{2}{\pi} \tan^{-1}\left(\frac{W\cos(\delta)}{2(Z_{TOR}+1)}\right) \times \left[1 - \frac{R_{JB}}{R_{RUP}+0.001}\right] \qquad (13)$$

The factor of 0.001 is added in the denominator of R_{JB}/R_{RUP} to prevent a singularity at R_{RUP}=0. We admit that the formulation is defined somewhat arbitrarily. However, we think that it serves the function of reducing the hanging wall effect with decreasing magnitude and

with increasing rupture depth. The data in the PEER-NGA data set are insufficient to test if Equation (13) performs better than piece-wise linear functions of R_{RUP}, **M** and Z_{TOR}.

SITE EFFECTS

Near-Surface Geology: The incorporation of the effects of near-surface geology or site classification has gone through an evolution in the past 10 years. At the beginning of this period, ground motion models typically contained a scaling parameter based on site classification (e.g. Boore et al., 1993), or presented different models for "rock" and "soil" sites (e.g. Campbell, 1993; Sadigh et al. 1997). Classification of recording sites into rock or soil sites varied among investigators. Boore et al. (1997) introduced the explicit use of the average shear wave velocity in the upper 30 meters, V_{S30}, in the ground motion model. Abrahamson and Silva (1997) building on an earlier model by Youngs (1993) introduced the explicit modeling of non-linear site effects in the ground motion model. The model we have developed for incorporating near-surface geology combines these concepts.

$$\ln(y_{site}) = \ln(y_{ref}) + f_{Site}(V_{S30}, y_{ref}) \tag{14}$$

The parameter y_{ref} is the ground motion on the reference site condition derived from the source and path scaling models described in the previous section. The reference site shear wave velocity was chosen to be 1130 m/sec because of the initial use of site response data to develop the functional form (Silva, 2004) and because it is expected that there will not be significant nonlinear site response at this velocity. As indicated on Figures 4 and 5, there are very few data with values of V_{S30} greater than 1100 m/sec. The reference motion is defined to be the spectral acceleration at the spectral period of interest for two reasons. Bazzurro and Cornell (2004) indicate that the spectral acceleration at spectral period T is "the single most helpful parameter" for the prediction of site amplification at that period. In addition, the estimation of the coefficients of the ground motion model is performed using random (mixed) effects regression in which the reference motion includes the random event term representing the deviation of the average ground motions from a given earthquake from the global population mean. Use of the reference spectral acceleration at period T to estimate surface ground motions at the same period eliminates the need to include the correlation in the random effects between those at period T and those at another period, such as *pga* at "zero" period.

The function form for the site response model f_{Site} with $y_{ref} = SA_{1130}$ is given by:

$$f_{Site}(V_{S30}, T, SA_{1130}) = a(V_{S30}, T) + b(V_{S30}, T) \ln\left[\frac{SA_{1130}(T) + c(T)}{c(T)}\right]$$

where

$$a(V_{S30}, T) = \phi_1 \ln\left[\frac{V_{S30}}{1130}\right] \tag{15}$$

$$b(Vs30, T) = \phi_2(T) \exp\{\phi_3(T) \times (V_{S30} - 360)\}$$

$$c(T) = \phi_4(T)$$

The interpretation of the parameters *a*, *b*, and *c* is illustrated in Figure 23. Parameter *a* represents the linear site response that occurs at small level of reference site motion. It is modeled as a linear function of $\ln[V_{S30}]$ consistent with previous representations (e.g. Boore et al., 1997). Parameter *c* represents the ground motion level in the middle of the transition from linear to nonlinear behavior. Parameter *b* represents the nonlinear behavior in terms of a linear decrease in the natural log of site amplification, f_S, with increasing amplitude of the reference motion. In general, a stronger nonlinearity in soil response corresponds to a more negative value for *b* (stronger dependence on SA_{1130}). It is expected that the degree of nonlinearity is a function of the stiffness of the site soils and is represented by making *b* a function of V_{S30}.

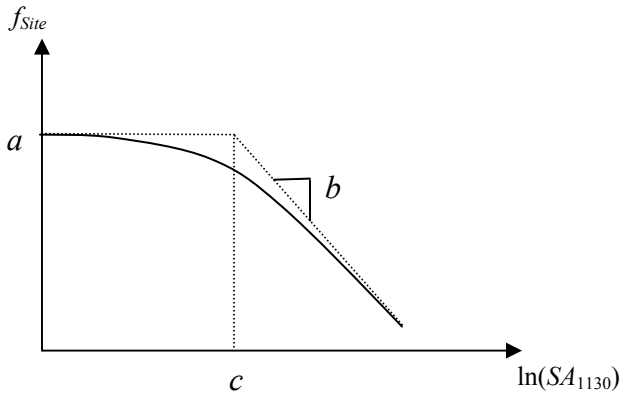

Figure 23: Soil amplification function

The ability of Equation (15) to represent nonlinear site response is illustrated in Figures 24 and 25. Figure 24 shows site amplification factors for *pga* derived from Silva's (2004) simulations. Two soil property models were used by Silva (2004), the EPRI (1993) set of soil modulus and damping relationships and the less nonlinear set Peninsular Range set developed by Silva et al. (1996). The solid lines shown on the figure are the result of fitting Equation (15) to the combined amplification factors for the two soil model sets and indicate that the function form can well represent the behavior implied by nonlinear (equivalent-linear) site response. Figure 25 shows the values of parameters *a* and *b* derived from the results of Silva (2004). The dashed lines show that the function forms for *a* and *b* in Equation (15) provide a good match to the site response results.

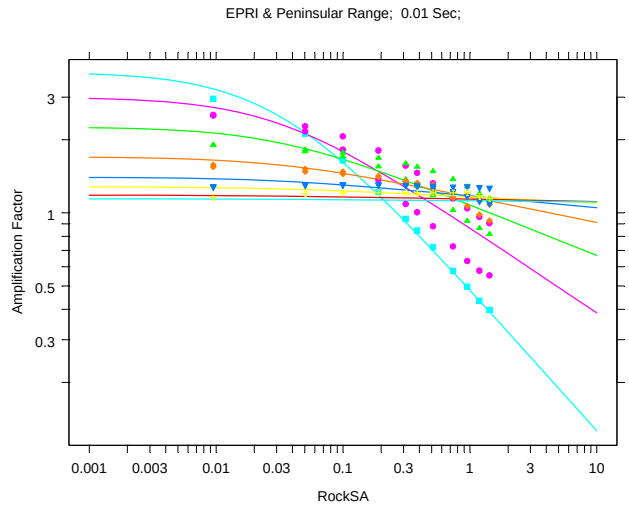

Figure 24: Soil amplification as a function of ground motion level from 1-D equivalent linear site response analyses (Silva, 2004). Colors denote VS30 as follows: light blue - 150m/s, magenta - 270m/s, green - 400m/s, red - 560m/s, and blue - 750m/s.

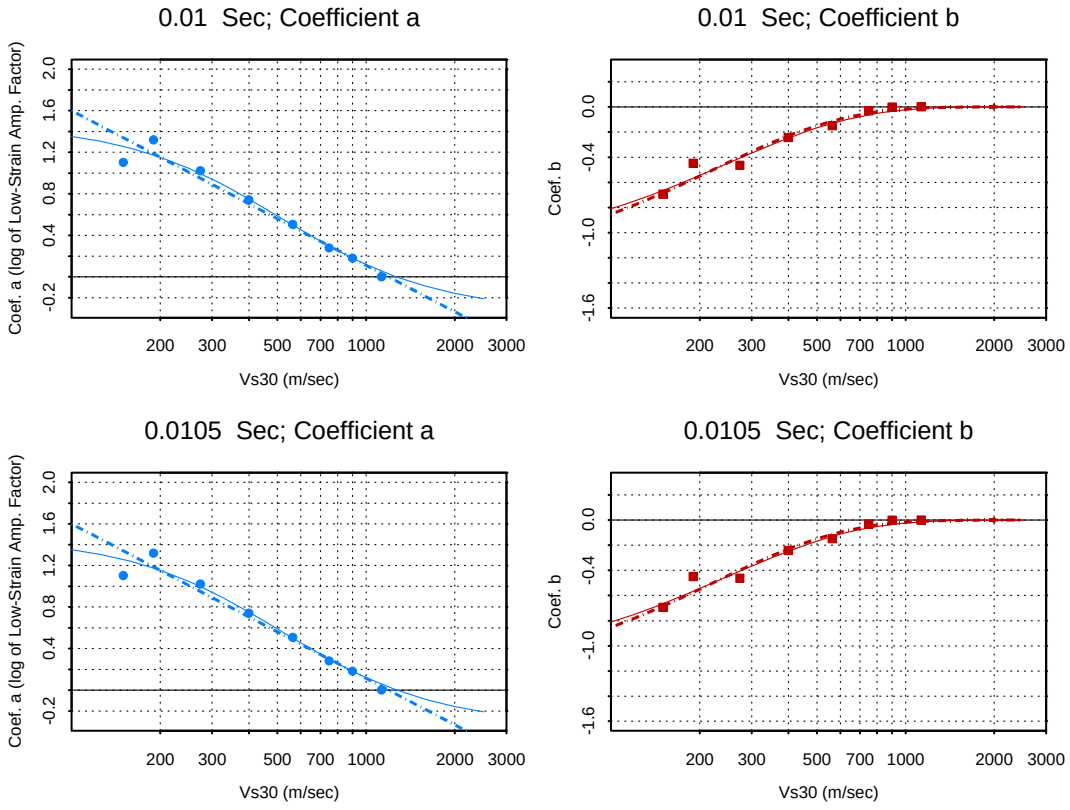

Figure 25: Fit of models for coefficients *a* and *b* to the 1-D site response results from Silva (2004). The dashed lines represent fits using the functional forms in Equation 15.

Choi and Stewart (2005) developed a model for the dependence of nonlinear site amplification on V_{S30} and the level of input rock motion. Figure 26 compares the variation of the parameter *b* computed from their models with results obtained from fitting Equation (15)

to the PEER-NGA *pga* data selected for use in this study. The functional form of Equation (15) provides a good match to the general behavior of the models developed by Choi and Stewart (2003).

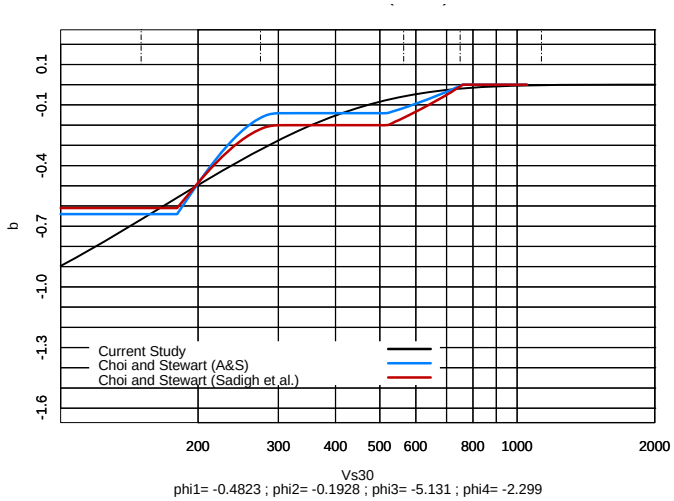

Figure 26: Comparison of parameter *b* dependence on V_{S30} obtained by Choi and Stewart (2003) (blue curve – Abrahamson and Silva, 1997, reference motions, red – Sadigh et al., 1997, reference motions) with the trend obtained in this study from the PEER-NGA data (black line).

Basin Depth: As discussed in Campbell (1997), a number of investigators have indicated the importance influence of sediment/basin depth on site ground motions and the parameter has been included in several of the models developed by Ken Campbell (e.g. Campbell, 1997). Day et al. (2006) developed a model for site amplification as a function of the depth to shear wave velocities of 1.0, 1.5, and 2.5 km/s ($Z_{1.0}$, $Z_{1.5}$, and $Z_{2.5}$, respectively) based on 3-D ground motion simulations using the SCEC 3-D velocity model (Magistrale et al., 2000). We have found that Day et al.'s model compares well with site amplifications observed in the broad band data for earthquakes 0163, 0167, and 0170. The model developed by Day et al. (2006) represents site amplification solely in terms of the sediment depth. As shown on Figure 6, there is a high degree of correlation between V_{S30} and $Z_{1.0}$ or $Z_{2.5}$. Our preliminary analysis indicates that it is very difficult to separate the effect of these two parameters at low frequencies. Use of the Day et al. (2006) model results would require accounting for removal of portion of the site amplification represented by the function f_S defined above. In addition, values of $Z_{1.0}$ or $Z_{2.5}$ are not readily available on a global basis. Therefore, we have developed the base model without including sediment thickness. We have computed residuals with respect to this model as a function of $Z_{1.0}$ and $Z_{2.5}$ and intend to develop ground motion adjustments that can be performed if these parameters are known for a site.

MODEL PARAMETER DEVELOPMENT

The general form of the ground motion model used to assess the model parameters is shown in Equation (16):

$$ln\left[y_{Surface}\right] = ln[\,y_{1130}\,] + f_{Site} + \sigma \cdot z_{ij}$$

$$ln[\,y_{1130}\,] = c_1 + f_{Source} + f_{Path} + f_{HW} + \tau \cdot z_i$$

$$f_{Source} = c_2(\mathbf{M} - 6) + \left(\frac{c_2 - c_3}{c_n}\right) \times ln\left[1 + exp\{c_n(c_{\mathbf{M}} - \mathbf{M})\}\right] + c_{1a}F_{RV} + c_{1b}F_{NM} + c_7(Z_{TOR} - 4)$$

$$f_{Path} = c_4\, ln\left[R_{RUP} + c_5\, cosh\{c_6\, max(\mathbf{M} - c_{HM}, 0)\}\right] + (c_{4a} - c_4) \times ln\left[\sqrt{R_{RUP}^2 + c_{RB}^2}\right] + \left[c_{\gamma 1} + c_{\gamma 2} / cosh\{max(\mathbf{M} - c_{\gamma 3}, 0\}\right] \times R_{RUP}$$

$$f_{HW} = c_9\, cos^2(\delta) \times tanh(R_{RUP}/2) \times \frac{tan^{-1}\left\{\frac{W\, cos(\delta)}{2(Z_{TOR}+1)}\right\}}{\pi/2} \times \left\{1 - \frac{R_{JB}}{R_{RUP} + 0.001}\right\}$$

$$f_{Site} = \phi_1\, min\left\{ln\left[\frac{V_{S30}}{1130}\right], 0\right\} + b_{Site}\, ln\left[\frac{exp\{ln[\,y_{1130}\,]\} + \phi_4}{\phi_4}\right]$$

$$b_{Site} = \phi_2 \times \left[exp\{\phi_3(min(V_{S30}, 1130) - 360)\} - exp\,\phi_3(1130 - 360)\right] \qquad (16)$$

The parameter y_{1130} is the ground motion on the reference site condition (V_{S30} = 1130 m/sec). Its level is based on the source scaling function f_{Source}, the path scaling function, f_{Path}, the hanging wall function f_{HW}, and a random effect $\tau\, z_i$ that is modeled as a Gaussian random variate with inter-event standard deviation τ. The log of the ground motion at a site is the sum of the log of the reference motion and a nonlinear amplification, f_{Site}, that is a function of V_{S30} and the level of the reference motion. The ground motions at the site also include a random Gaussian variate with intra-event standard deviation σ. The inter-event component of randomness in included when computing the site amplification. Also note that the site amplification function uses the reference motion for the same spectral period. The additional parameters in Equation (16) are: R_{RUP} , closest distance to the rupture plane (km); R_{JB} , Joyner-Boore distance to the rupture plane (km); δ , rupture dip; W , rupture width (km); Z_{TOR} , depth to top of rupture (km); F_{RV} , reverse faulting factor equal to 1 for $30^o \le \lambda \le 150^o$, and 0 otherwise; F_{NM} , normal faulting factor equal to 1 for $-120^o \le \lambda \le -60^o$, 0 otherwise; λ , slip rake angle; V_{S30} , average shear wave velocity for top 30 m (m/s). Note, f_{HW} applies to all faulting styles.

The model parameters were obtained by fitting the model to the selected PEER-NGA data using the nonlinear mixed effects method *nlme* implemented in the statistical packages S-Plus and **R**. The process used to obtain these parameters is described below.

EFFECT OF DATA TRUNCATION

The initial analyses of the PEER-NGA data suggested that the anelastic attenuation term γ in Equation (11) was 50-percent larger in absolute value for earthquakes from Taiwan than for earthquakes in California or the other active tectonic regions represented in the selected database (Table 2). For *pga* the estimated values of γ were approximately -0.006 for California earthquakes and approximately -0.009 for Taiwan earthquakes. This would imply that Q for Taiwan was significantly lower than Q for California or the other regions. However, review of the literature failed to produce studies that confirmed this result. The comparison of Q estimates was made more difficult by the varying assumptions about geometric spreading made by the various investigators. In addition, the estimates of γ obtained from the broadband data for the three southern California earthquakes 0163, 0167 and 0170 were in the range of -0.012 to -0.014 (Figure 13).

These results led us to consideration of the effects of missing response data on the estimation of ground motion model parameters. There are two forms of missing response data treated in the literature: censoring and truncation. Censoring occurs when a known set of instruments is triggered, but the response is only known to be below $y_{truncation}$. In this case, the number of censored observations and predictor variables for these observations (e.g. **M**, R_{RUP}, *and VS30*) are known for the censored sample. Truncation occurs when the observed sample is truncated at some response level $y_{truncation}$ such that no responses are reported below this level. The number of missing values and values of the predictor variables for these observations are unknown. The two forms of missing response variables lead to different forms of the sample likelihood function in fitting models by maximum likelihood.

Censoring/truncation of the strong motion database occur due to the occurrence of ground motions below the trigger threshold for the recording instruments and from the selective processing of recordings favoring those with larger amplitudes. Censoring/truncation occurs also from record processing as frequency bands with low signal/noise ratios are filtered out of the process records. Although the number of possible recordings in a given earthquake is knowable, some instruments may have malfunctioned and there is not a complete accounting of the possible instruments available. Therefore, the truncation model is considered the most appropriate condition.

Some evidence of truncation of the data is seen in Figure 2, but it is more apparent when examining individual earthquakes. An obvious case is shown in Figure 27 for the three small southern California earthquakes analyzed previously. The left hand plot shows the 660 *pga* values for the three earthquakes obtained from the broad band recordings and the right hand plot shows the 119 *pga* values for the processed records that are in the PEER-NGA database for these earthquakes. Approximate truncation levels are indicated by the dashed horizontal lines. The curves indicate fits to the data using truncated regression techniques with random effects as follows.

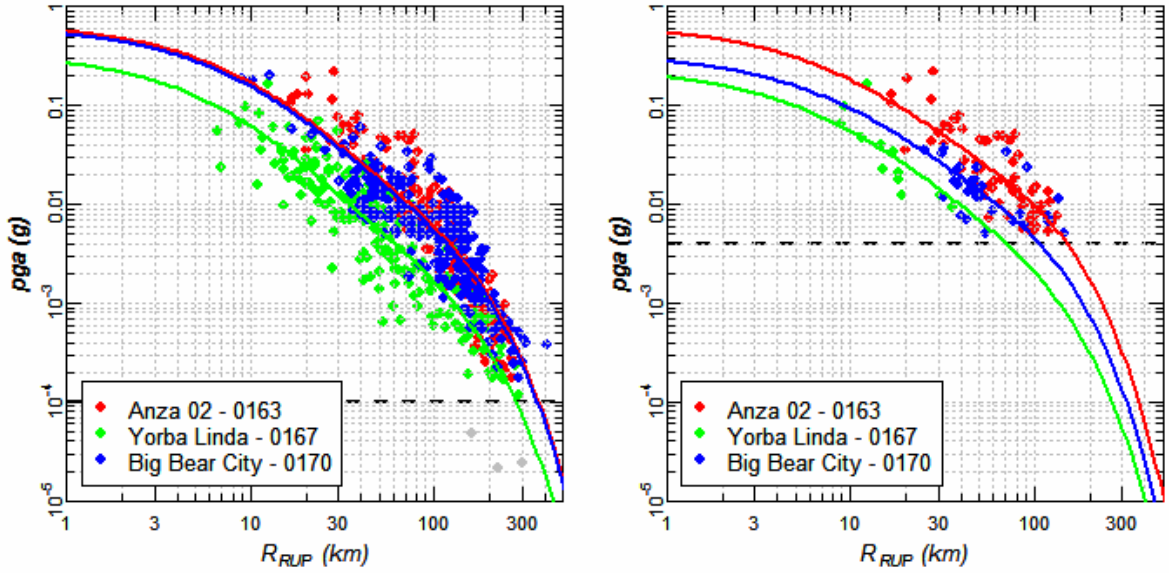

Figure 27: Example of data truncation. Left hand plot shows broad-band peak acceleration data for three small southern California earthquakes and right hand plot shows PEER-NGA data for the same events. Curves show truncated regression fits to the combined data with the truncation level indicated by the horizontal dashed line.

The sample likelihood and log likelihood functions for a regression model without random effects in which the responses have been truncated below a level $y_{\text{truncation}}$ are given by:

$$L = \prod_i \frac{\varphi_N(y_i|\mathbf{x}_i,\boldsymbol{\beta})}{1-\Phi_N(Z_{trunc}|x_i,\boldsymbol{\beta})}$$
$$\ln(L) = \sum_i \left[-\ln(\sigma^2)/2 - \{\ln(y_i)-\mu(\mathbf{x}_i,\boldsymbol{\beta})\}^2/2\sigma^2\right] - \sum_i \ln\left[1-\Phi_N(y_{truncation}|\mathbf{x}_i,\boldsymbol{\beta})\right] \quad (17)$$

In Equation (17) φ_N and Φ_N are the normal density and cumulative normal functions, $\mathbf{x}_i$ is the vector of predictor variables for the i^{th} observation and $\boldsymbol{\beta}$ is the vector of model coefficients. Application of this to the analysis of ground motion data has been performed by Toro (1981) and more recently by Bragato (2004). We have extended the concept of truncation to the mixed effects model. Using the formulation of Brillinger and Preisler (1984), the sample likelihood function is:

$$L = \prod_i \int \left[\frac{1}{\sqrt{2\pi}} \exp\{-z_i^2/2\} \cdot \prod_j \left(\frac{1}{\sigma\sqrt{2\pi}} \frac{\exp\{-(y_{ij}-\mu_{ij}(\theta)-\tau\cdot z_i)^2/2\sigma^2\}}{\left[1-\Phi(y_{truncation}|\mu_{ij}(\theta)+\tau\cdot z_i,\sigma)\right]} \right) \right] dz \quad (18)$$

In Equation (18), the index i refers to the individual earthquakes and the index j refers to the separate observations for the i^{th} earthquake. The term $\left[1-\Phi(y_{truncation}|\mu_{ij}(\theta)+\tau\cdot z_i,\sigma)\right]$ normalizes the probability for the y_{ij}^{th} observation by dividing by 1 minus the probability distribution tail below the truncation limit $y_{truncation}$. The random effect for the i^{th} earthquake, $\tau\cdot z_i$, appears in both the error term for the ij^{th} observation and in the density normalization

term $\left[1-\Phi(y_{truncation}\left|\mu_{ij}(\theta)+\tau\cdot z_i,\sigma\right)\right]$. Maximum likelihood solutions to Equation (18) were performed using numerical integration and the general optimization routine *optim* in R.

The data shown in Figure 27 were fit by maximum likelihood using Equation (18) and a ground motion model in which all the parameters were fixed except γ and the random effect for each event. The truncation levels for each case are indicated on the figure. For this example, γ = -0.013 was obtained from the fit to the full data set and γ = -0.015 was obtained from the fit to the PEER-NGA data for these three events.

To further evaluate the potential impact of data truncation on the model development, we developed extended *pga* data sets for 10 additional California earthquakes. These extended data sets are described in Appendix D and the earthquakes are listed in Table 4. Additional *pga* data for Northridge (EQID 0127) were supplied by Vladimir Graizer (personal communication, 2006). The remaining data were obtained from the TriNet/ShakeMap webpages. Only the High Broadband data were used. The PEER-NGA set of earthquakes was supplemented by data from the Feb 2, 2000 Loma Linda; Dec 23, 2003 San Simeon; and the Sept 28, 2004 Parkfield earthquake. In addition, an extended data set was developed for the 1995 Kobe earthquake using the data presented in Fukushima et al. (2000).

For each of these earthquakes, estimates of γ were made using truncated regression and a ground motion model with fixed values of the other parameters. To remove the influence of hanging wall effects, hanging wall and footwall sites were removed. Estimates of γ were obtained using just the PEER-NGA data and using the extended data and these are listed in Table 4 along with the number of recordings used in each analysis. Figure 28 shows examples of the results for four of the earthquakes. For the Northridge earthquake, similar estimates of γ were obtained from the PEER-NGA and extended data set. However, for the other three earthquakes shown on Figure 28, the estimate of γ obtained from the PEER-NGA data set were approximately 2/3 of the values obtained from the extended data sets. As indicated by the results in Table 4, the values of γ computed using only PEER-NGA data are typically smaller than obtained from the extended data. The few cases where the PEER-NGA data produced larger (and often unrealistic) values of γ are for earthquakes with very limited samples in the PEER-NGA database (e.g. San Juan Bautista, Mohawk Valley). Truncated regression analyses performed using the combined PEER-NGA data for these earthquakes also produce smaller value for γ than analysis using the combined extended data sets.

As a short-term solution to this problem, we decided to develop the ground motion model using the PEER-NGA data truncated at a maximum distance of 70 km. This distance was selected by visual inspection as the point where, on average, data truncation may begin to affect the distribution of recordings in the PEER-NGA data base. The regression analyses were performed using a model for γ determined from the combined extended data sets for California earthquakes. Figure 29 shows the values of γ for the earthquakes listed in Table 4. The results indicate that γ decreases in absolute value with increasing magnitude, similar to results reported by others from analysis of empirical data (e.g. Campbell, 1993) and stochastic ground motion simulations (e.g. Campbell, 2003).

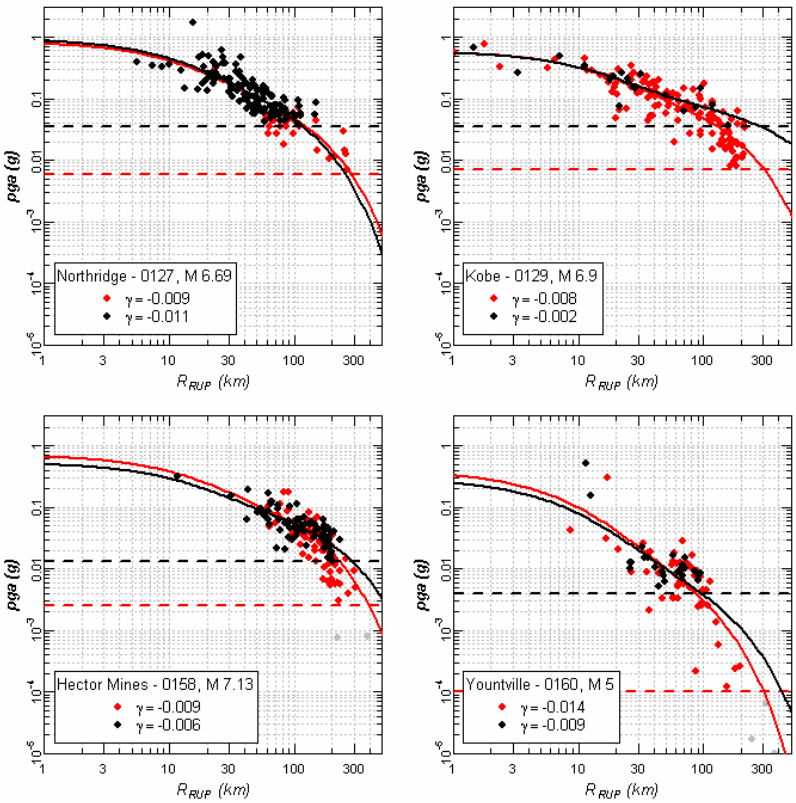

Figure 28: Comparison of fits to expanded data sets (red plus black points) and PEER-NGA data only (black points) for individual earthquakes using truncated regression. Truncation levels are indicated by the horizontal dashed lines for the enhanced (red) and PEER-NGA only (black) data sets. Only neutral site were used for reverse faulting earthquakes.

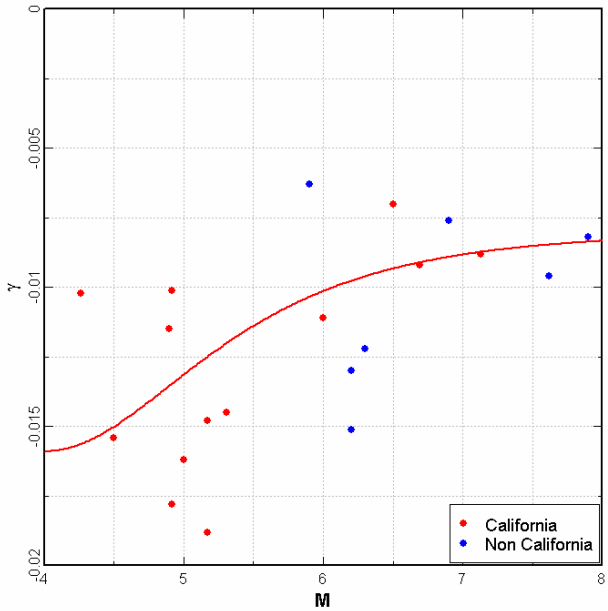

Figure 29: Estimates of γ from analysis of the extended data sets (Table 4). Red curve shows the model developed by a fit to the combined California earthquake data set.

Table 4: Estimate of Anelastic Attenuation Parameter γ For Individual Earthquakes

EQID	Earthquake	M	PEER-NGA Data Set		Expanded Data Set		Region
			γ	Number of Recordings	γ	Number of Recordings	
0127	Northridge	6.69	-0.0108	122	-0.0092	154	California
0129	Kobe	6.9	-0.0020	22	-0.0076	157	Japan
0137	Chi-Chi	7.62	-0.0096	305			Taiwan
0157	San Juan Bautista	5.17	-0.0392	2	-0.0188	23	California
0158	Hector Mines	7.13	-0.0056	82	-0.0088	163	California
0160	Yountville	5	-0.0088	24	-0.0162	76	California
0162	Mohawk Val, Portola	5.17	-0.0191	6	-0.0148	36	California
0163	Anza-02	4.92	-0.0164	72	-0.0178	193	California
0165	CA/Baja Border Area	5.31	-0.0433	9	-0.0145	142	California
0166	Gilroy	4.9	-0.0054	34	-0.0115	136	California
0167	Yorba Linda	4.265	-0.0851	12	-0.0102	207	California
0169	Denali	7.9	-0.0082	23			Alaska
0170	Big Bear City	4.92	-0.0004	35	-0.0101	262	California
0171	Chi-Chi, Taiwan-02	5.9	-0.0063	277			Taiwan
0172	Chi-Chi, Taiwan-03	6.2	-0.0151	225			Taiwan
0173	Chi-Chi, Taiwan-04	6.2	-0.0130	241			Taiwan
0174	Chi-Chi, Taiwan-05	6.2	-0.0130	310			Taiwan
0175	Chi-Chi, Taiwan-06	6.3	-0.0122	260			Taiwan
	Loma Linda	4.5			-0.0154	93	California
	Parkfield	6			-0.0111	308	California
	San Simeon	6.5			-0.0070	225	California

The combined extended data from the 13 California earthquakes was fit by a function form that produce a smooth transition from the value γ at magnitudes less than 5 to values at larger magnitudes. A continued linear decrease in the absolute value of γ was judged to not be appropriate based on analyses of simulated motions using the Atkinson and Silva (2000) model and because the value of γ computed for the **M** 7.9 Denali earthquake was similar to the values obtained for the larger California earthquakes in the range of **M** 6.5 to 7.1. Analyses of individual smaller magnitude earthquakes in the TriNet data set (Appendix D) did not indicate a continued decrease in γ. The resulting relationship is:

$$\gamma(pga)_{California} = -0.00804 - 0.00785 / \cosh\{\max(\mathbf{M} - 4,0)\} \qquad (19)$$

This relationship is plotted on Figure 29. The limited data for earthquakes from other regions (Kobe, Japan; Denali, Alaska; Chi-Chi main shock and aftershocks, Taiwan) are generally consistent with this relationship. The data indicate that the value of γ for Taiwan may be slightly greater than that for California, but the difference is much less than the 50-percent larger values obtained from the initial regressions using the full PEER-NGA data base.

We believe that our short-term solution should provide an appropriate model for California earthquake ground motions. The model parameters will be based on strong motion data

recorded within 70 km of earthquake ruptures, the region of primary concern for application of the model. We also believe that the model properly represents the attenuation of ground motion at larger distances in California. The issue we have raised points out the need to systematically collect and process all recordings from large earthquakes if there is interest in correctly modeling the attenuation of ground motions at large distances.

Equation (19) provides a relationship for γ for *pga*. The relationships for other spectral periods was constructed by using the period-dependence of γ computed from analysis of the broadband data from the three small southern California earthquakes and scaling the values by the relative difference in γ at *pga*, that is:

$$\gamma(T)_{California} = \gamma(T)_{Anza-YL-BBC} \times \frac{\gamma(pga)_{California}}{\gamma(pga)_{Anza-YL-BBC}} \tag{20}$$

Figure 30 compares the model developed for γ with values obtained from direct regression of the PEER-NGA data without imposing any distance truncation and without using truncated regression. The variation of γ with spectral period T is similar.

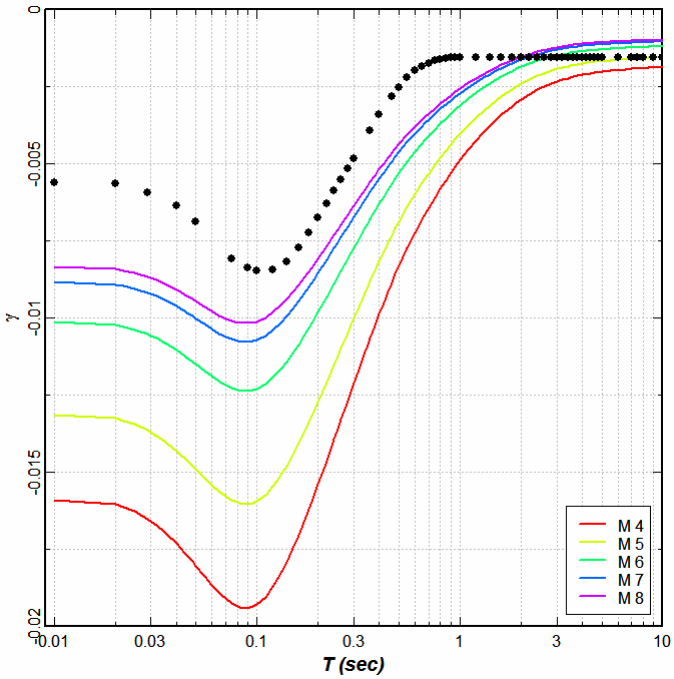

Figure 30: Comparison of the model developed for γ (Equations 19 and 20) versus values of γ obtained from regression without truncation (black points) of the PEER-NGA data set.

MODELING STEPS

The parameters of the ground motion model were developed through an iterative process that involved performing regressions for the entire spectral period range with some parts of the model fixed, examining the trend of remaining parameters with spectral period, developing smoothing models for these parameters with period, and then repeating the analysis to examine the variation of the remaining parameters. The major steps in the development of the parameters are summarized below. All analyses were performed using the PEER-NGA

data truncated at a maximum distance of R_{RUP} = 70 km. In addition, the magnitude scaling parameters c_2 and c_3 were fixed at 1.06 and 3.45 for all analyses and in the final model. As discussed in the model development section, c_3 = 3.45 represents scaling of low-frequency amplitudes proportional to seismic moment. Parameter c_2 was fixed at 1.06, the value derived from the Atkinson and Silva (2006) seismic source model. All previous applications of the general function form used by Ross Sadigh have yielded far-source high-frequency magnitude scaling coefficients that are consistent with this value. Preliminary analysis of the PEER-NGA data also produced values near 1.06. Parameter c_4 was examined by analyses of PEER-NGA data and TriNet data. It was concluded that a range of values for c_4 would provide satisfactory fits to the data with adjustments to the rate of attenuation occurring through changes of parameters c_5 and c_6. The change in attenuation rate with distance was set to occur at c_{RB} = 50 km. A value near 50 km was consistently found in all preliminary analyses.

After extensive exploratory analysis of the data, we concluded that the PEER-NGA dataset does not sample a sufficiently wide range of motion and Vs30 to allow the simultaneous estimation of all 3 nonlinear soil parameters ($\varphi_{2,}$ $\varphi_{3,}$, and φ_4) We thus decided to fix φ_4 through other supporting information. Both our preliminary analysis of the PEER-NGA data and our analysis of the simulated soil amplification factors from Silva (2004) suggested that φ_4 is about 0.1g in the case of *pga*. The empirical study of Choi and Stewart (2005) also indicate 0.1g is a viable value for φ_4. We thus fix *pga*'s φ_4 at 0.1g. To fix φ_4 of other periods, we anchor the rock spectral shape of M6.5 at 10 km (Silva et a. Add referrecne) at *0.1g pga*. The remaining two nonlinear parameters will adjust to the fixed value of φ_4 and they are more than sufficient to capture the nonlinear soil behavior existing in the PEER-NGA dataset.

In the preliminary analyses it was found that the data exhibited a statistically significant dependence on source depth parameterized as the depth to top of rupture, Z_{TOR} and that aftershocks showed a stronger dependence on depths than main shocks. Also, the data indicated that the style of faulting effects were weaker for aftershocks than for main shocks. Therefore, the analyses were performed with separate depth dependence and style of faulting effects for main shocks and aftershocks.

First Phase:

Step 1: The first phase of the analysis used only data from neutral sites. Sites with the hanging wall/foot wall flags set to 'fw' or 'hw' in the PEER-NGA database were removed. This simplification was performed to examine other portions of the model without interaction with the hanging wall function f_{HW}. In particular, regression with the full model showed high correlation between estimates of the hanging wall parameters and the parameters for style of faulting and soil nonlinearity. Using a simple model for the reference motion (without style of faulting, depth of rupture, and variable magnitude scaling) the parameters of the non-linear soil model (φ_2 and φ_3) were obtained from fits to the NGA data. At longer periods when the soil response becomes nearly linear, estimates of the nonlinear soil parameter φ_3 fluctuated wildly and had very large errors of estimation. Therefore parameter φ_3 for periods longer than 1.0 seconds were fixed to produce a smooth transition to linear behavior at spectral periods near 1.0 sec and greater.

Step 2: Using the smoothed values of φ_3, regression analyses were performed to examine the variation of c_n and $c_{\mathbf{M}}$ with period. Parameter c_n was then smoothed and parameter $c_{\mathbf{M}}$ re-estimated, then smoothed.

Step 3: The next step was to assess parameters c_5 and c_6 which control the shape of the distance attenuation near the source. With the smoothed values of c_n and $c_{\mathbf{M}}$ from step 2, the variation of c_5 and c_6 with period was examined. Parameter c_5 was smoothed, parameter c_6 re-estimated, then smoothed. It should be noted that the variation of c_5 and c_6 with period and a constant value of c_4 accomplishes a similar effect to the variation of c_4 with period for fixed c_5 and c_6 in Sadigh et al. (1997).

Step 4: The final step in the first phase of the analysis was reassessment of the nonlinear soil model parameters. With the above model parameters fixed, parameters of φ_2 and φ_3 were re-estimated from the data. Parameter φ_3 was then smoothed, φ_2 re-estimated, then smoothed.

Second Phase:

Step 5: In the second phase of parameter development, the hanging wall and footwall data were included and the hanging wall functional form for f_{HW} was added to the model. Initially, the inclusion of the hanging wall data resulting in reverse and strike slip faulting having the same amplitudes ($c_{1a} \sim 0$). However, it was discovered that this result was largely due to data from the Chi-Chi main shock. When the Chi-Chi main shock was removed, c_{1a} increased to approximately 0.1 and the amplitude of the hanging wall coefficient c_9 was reduced. There is a large degree of coupling between these parameters. The value of c_{1a} is marginally statistically significant (t-values slightly greater than 2). The analysis by Chiou et al. (2000) found that when the geometric hanging wall effect was removed by using R_{RMS}, a style of faulting effect remained with reverse faulting earthquakes producing larger ground motions than strike-slip earthquakes. On this basis, we have assumed that there is a style of faulting effect for reverse faults. The value of parameter c_{1a} was estimated without the Chi-Chi main shock data.

The style of faulting effect for normal faults, c_{1b} was found to be statistically significant only when normal faulting flag F_{NM} was restricted to be 1 for rake angles in the range $-120^\circ \leq \lambda \leq -60^\circ$, that is normal-oblique earthquakes have the same level of ground motions as strike-slip earthquakes. Parameter c_{1b} is also only marginally significant with t-values slightly greater than 2.

Parameter c_{1a} was found to decrease with increasing spectral period, becoming 0 at a period of 1.0 seconds and then decreasing to about -0.1 at long periods. This is consisted with the trends observed in previous empirical models (e.g. Abrahamson and Silva, 1997; Campbell and Bozorgnia, 2003; the soil model of Sadigh et al., 1997). At high frequency, this is consistent with an interpretation of higher stress drops (stress parameters) for reverse faulting earthquakes than for strike-slip earthquakes. However, the negative values of c_{1a} at long periods is not consistent with this concept, indicating that other factors may also be influencing the difference between the motions produced by the two styles of faulting. For normal faulting, the value of c_{1b} was approximately -0.25 and decreased in absolute value as the spectral period decreased. For spectral periods greater than about 1.0 second, the value of c_{1b} becomes very uncertain. If one speculates that the negative value of c_{1a} for reverse

faulting earthquakes at long periods is due to more compact dip-slip earthquakes being less efficient at producing long period motions than long strike-slip earthquakes, then perhaps the values of c_{1a} and c_{1b} should be similar in this period range. We have made this assumption in developing the period dependence of c_{1b}.

Step 6: With c_{1a} and c_{1b} fixed, the period variation of the hanging wall scaling factor, c_9 was defined. The smoothed value of c_9 decreases to 0 at long periods.

Step 7: The next step was completion of the soil amplification model, f_{Site}. The variation of φ_2 and φ_3, with period was re-evaluated holding the previously smoothed parameters of the model fixed. This assessment resulted in modifications to φ_2 that indicated slightly more nonlinearity. These parameters were then smoothed and φ_1, the linear scaling term, was recomputed and smoothed.

Step 8: The next step was to fix the remaining parameter for main shocks, the dependence on the depth to top of rupture defined by parameter c_7. This parameter was found to decay to zero as the spectral period increases, consistent with the concept that it represents an increase in dynamic stress drop or the "stress parameter" with increasing depth of rupture.

Step 9: The remaining parameters in the ground motion model for main shock motions are the intercept term c_1 and the variance terms τ and σ. Because all of the other model parameters have been fixed, the aftershock data can now be removed from the analysis. The resulting effect on the intercept term c_1 is negligible (less than 0.01 percent) and produces a slight reduction in the inter-event variability τ.

The estimated values of c_1 exhibited noticeable steps at periods of 0.8, 4, and 8 seconds, as shown in Figure 31. These steps occur at periods where there are large reductions in the number of usable data, defined by the minimum usable frequency, as shown on Figure 32. The derivative of c_1 with respect to spectral period was computed numerically. These values, shown on Figure 33, show peaks that usually coincide with a sudden drop in the number of usable data (Figure 32). These observations suggest that the estimated values of c_1 may be biased by the systematic removal of weaker motion, which would tend to leave larger ground motion amplitudes in the remaining data. We therefore took the following steps to smooth parameter c_1. We first estimated the bias due to data drop out at 0.8, 1.1, and 1.6 seconds. The bias is taken as the increase in the c_1 estimate when the dataset is replaced by the reduced set for the next longer spectral period. Secondly, at periods longer than 1.6 second, we impose a constant slope of -1.4 (the horizontal dotted line Figure 33), matching the trend in the data. As a result, the large-magnitude spectra do not reach constant displacement scaling at periods up to 10 seconds, the limit of our model. The resulting values for c_1 are shown by the red curve in Figure 21.

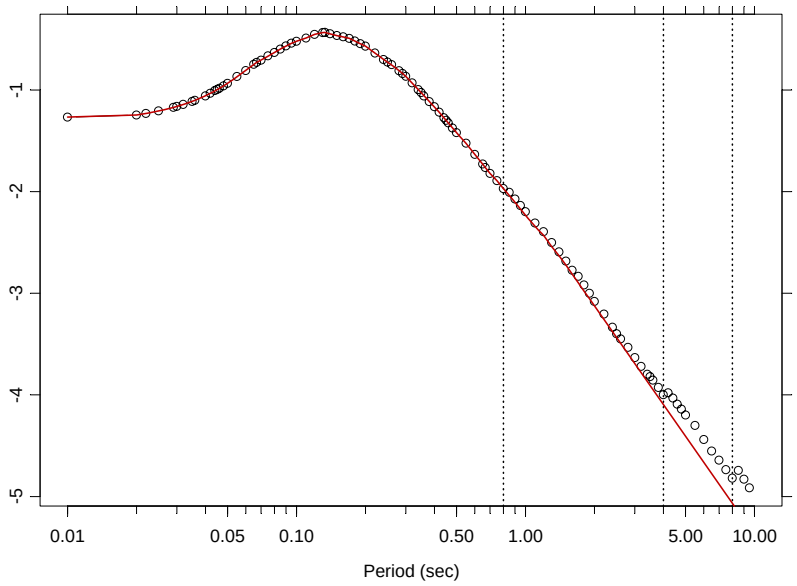

Figure 31: Variation of parameter c_1 with spectral period.

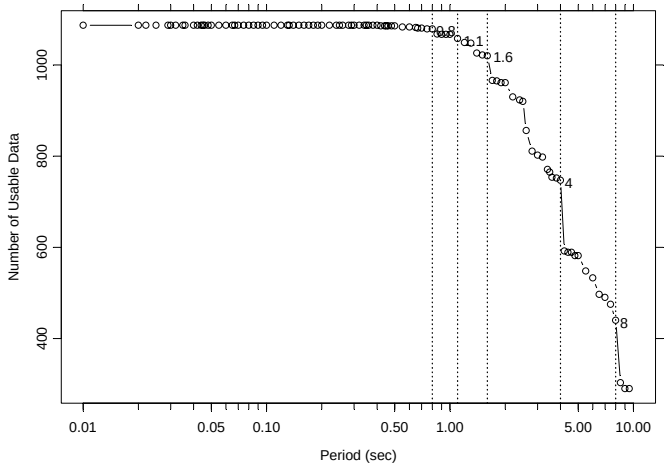

Figure 32: Variation of number of usable recordings as a function of spectral period.

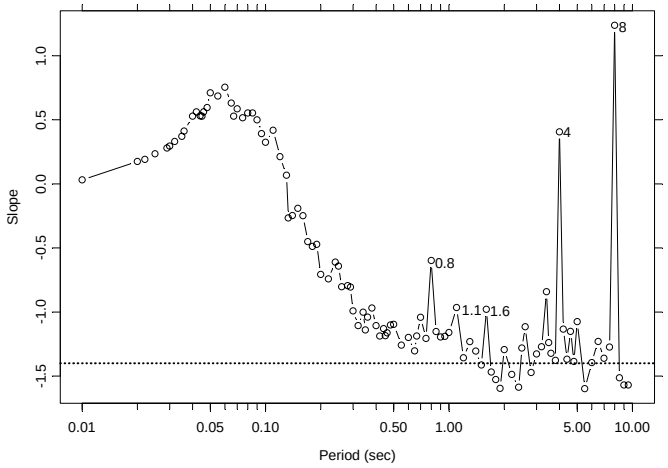

Figure 33: Variation of the derivative of parameter c_1 with respect to spectral period.

FINAL MODEL FORMULATION

The final model formulation is given by the relationships:

$$\begin{aligned}\ln\left(SA_{1130ij}\right) &= \mathrm{c}_1 + \mathrm{c}_{1a}F_{RVi} + c_{1b}F_{NMi} + \mathrm{c}_7\left(Z_{TORi} - 4\right) \\ &+ \mathrm{c}_2\left(\mathbf{M}_i - 6\right) + \frac{\mathrm{c}_2 - \mathrm{c}_3}{\mathrm{c}_n}\ln\left(1 + e^{\mathrm{c}_n\left(\mathrm{c}_M - \mathbf{M}_i\right)}\right) \\ &+ \mathrm{c}_4\ln\left(R_{RUPij} + \mathrm{c}_5\cosh\left(\mathrm{c}_6\left(\mathbf{M}_i - \mathrm{c}_{HM}, 0\right)_{\max}\right)\right) \\ &+ \left(\mathrm{c}_{4a} - c_4\right)\ln\left(\sqrt{R^2{}_{RUPij} + \mathrm{c}_{RB}{}^2}\right) \\ &+ \left\{\mathrm{c}_{\gamma 1} + \frac{\mathrm{c}_{\gamma 2}}{\cosh\left(\left(\mathbf{M}_i - \mathrm{c}_{\gamma 3}, 0\right)_{\max}\right)}\right\}\cdot R_{RUPij} \\ &+ \mathrm{c}_9\cdot\cos^2\delta_i\cdot\tanh\left(\frac{R_{RUPij}}{2}\right)\tan^{-1}\left(\frac{W_i\cos\delta_i}{2\left(Z_{TORi}+1\right)}\right)\frac{1}{\pi/2}\left\{1 - \frac{R_{JBij}}{R_{RUPij} + 0.001}\right\} \\ &+ \tau\cdot z_i\end{aligned} \tag{21a}$$

$$\begin{aligned}\ln\left(SA_{ij}\right) &= \ln\left(SA_{1130ij}\right) \\ &+ \phi_1\cdot\left(\ln\left(\frac{V_{S30ij}}{1130}\right), 0\right)_{\min} \\ &+ \phi_2\cdot\left\{e^{\phi_3\left(\left(V_{S30ij}, 1130\right)_{\min} - 360\right)} - e^{\phi_3\left(1130 - 360\right)}\right\}\cdot\ln\left(\frac{SA_{1130ij} + \phi_4}{\phi_4}\right) \\ &+ \sigma\cdot z_{ij}\end{aligned} \tag{21b}$$

The predictor variables for this model are:

R_{RUP} = closest distance to the rupture plane (km)
R_{JB} = Joyner-Boore distance to the rupture plane (km)
δ = rupture dip
W = rupture width (km)
Z_{TOR} = depth to top of rupture (km)
F_{RV} = 1 for $30^\circ \leq \lambda \leq 150^\circ$, 0 otherwise (combined reverse and reverse-oblique)
F_{NM} = 1 for $-120^\circ \leq \lambda \leq -60^\circ$, 0 otherwise (only normal earthquakes, normal-oblique considered to be the same as strike-slip.
λ = rake angle
V_{S30} = Average shear wave velocity for top 30 m (m/s)
τ = inter-event standard error
σ = intra-event standard error

The coefficients of Equations (21a) and (21b) are listed in Table 5.

Table 5: Coefficients of Chiou and Youngs (2006) Empirical Ground Motion Model for the Average Horizontal Component

Period (sec)	c_1	c_{1a}	c_{1b}	c_2	c_3	c_n	c_M	C_4	c_{4a}	c_{RB}	c_5	c_6	c_{HM}	c_7	c_9	$c_{\gamma 1}$	$c_{\gamma 2}$	$c_{\gamma 3}$	φ_1	φ_2	φ_3	φ_4	τ	σ
0.010	-1.2686	0.1000	-0.2554	1.060	3.450	2.996	4.184	-2.10	-0.50	50.	6.1600	0.4893	3.0	0.0512	1.0480	-0.008040	-0.007850	4.0	-0.482300	-0.192800	-0.005911	0.100359	0.3024	0.4720
0.020	-1.2474	0.1000	-0.2554	1.060	3.450	3.292	4.188	-2.10	-0.50	50.	6.1580	0.4893	3.0	0.0512	1.0830	-0.008113	-0.007921	4.0	-0.472300	-0.189500	-0.005864	0.103066	0.3034	0.4736
0.022	-1.2308	0.1000	-0.2554	1.060	3.450	3.352	4.183	-2.10	-0.50	50.	6.1580	0.4893	3.0	0.0512	1.0990	-0.008155	-0.007962	4.0	-0.469100	-0.190900	-0.005817	0.104269	0.3089	0.4747
0.025	-1.2064	0.1000	-0.2554	1.060	3.450	3.429	4.173	-2.10	-0.50	50.	6.1590	0.4893	3.0	0.0512	1.1250	-0.008230	-0.008035	4.0	-0.463900	-0.194100	-0.005730	0.106074	0.3151	0.4769
0.029	-1.1716	0.1000	-0.2554	1.060	3.450	3.501	4.159	-2.10	-0.50	50.	6.1600	0.4893	3.0	0.0512	1.1570	-0.008351	-0.008154	4.0	-0.456600	-0.200600	-0.005578	0.109583	0.3235	0.4815
0.030	-1.1622	0.1000	-0.2554	1.060	3.450	3.514	4.156	-2.10	-0.50	50.	6.1600	0.4893	3.0	0.0511	1.1650	-0.008387	-0.008189	4.0	-0.454800	-0.202600	-0.005533	0.110415	0.3257	0.4822
0.032	-1.1432	0.1000	-0.2554	1.060	3.450	3.533	4.148	-2.10	-0.50	50.	6.1600	0.4893	3.0	0.0511	1.1770	-0.008454	-0.008255	4.0	-0.451300	-0.207100	-0.005451	0.112089	0.3303	0.4835
0.035	-1.1136	0.1000	-0.2554	1.060	3.450	3.551	4.138	-2.10	-0.50	50.	6.1600	0.4893	3.0	0.0510	1.1940	-0.008564	-0.008362	4.0	-0.446300	-0.214400	-0.005316	0.114716	0.3339	0.4865
0.036	-1.1032	0.1000	-0.2554	1.060	3.450	3.555	4.135	-2.10	-0.50	50.	6.1600	0.4893	3.0	0.0509	1.1990	-0.008599	-0.008396	4.0	-0.444700	-0.216900	-0.005274	0.115598	0.3346	0.4879
0.040	-1.0598	0.1000	-0.2554	1.060	3.450	3.563	4.123	-2.10	-0.50	50.	6.1600	0.4893	3.0	0.0508	1.2150	-0.008754	-0.008547	4.0	-0.438500	-0.227500	-0.005087	0.120311	0.3384	0.4925
0.042	-1.0341	0.1000	-0.2554	1.060	3.450	3.563	4.117	-2.10	-0.50	50.	6.1600	0.4893	3.0	0.0507	1.2210	-0.008833	-0.008624	4.0	-0.435700	-0.232900	-0.005002	0.122617	0.3432	0.4945
0.044	-1.0080	0.1000	-0.2554	1.060	3.450	3.561	4.112	-2.10	-0.50	50.	6.1600	0.4893	3.0	0.0506	1.2270	-0.008906	-0.008696	4.0	-0.433100	-0.238300	-0.004917	0.125023	0.3468	0.4957
0.045	-0.9961	0.1000	-0.2554	1.060	3.450	3.559	4.110	-2.10	-0.50	50.	6.1600	0.4893	3.0	0.0506	1.2290	-0.008945	-0.008734	4.0	-0.431800	-0.241000	-0.004873	0.126226	0.3476	0.4962
0.046	-0.9845	0.1000	-0.2554	1.060	3.450	3.557	4.108	-2.10	-0.50	50.	6.1600	0.4893	3.0	0.0505	1.2320	-0.008984	-0.008771	4.0	-0.430600	-0.243700	-0.004834	0.127429	0.3493	0.4968
0.048	-0.9606	0.1000	-0.2554	1.060	3.450	3.553	4.104	-2.10	-0.50	50.	6.1600	0.4893	3.0	0.0505	1.2350	-0.009050	-0.008836	4.0	-0.428400	-0.249100	-0.004758	0.129935	0.3551	0.4985
0.050	-0.9363	0.1000	-0.2554	1.060	3.450	3.547	4.101	-2.10	-0.50	50.	6.1600	0.4893	3.0	0.0504	1.2380	-0.009121	-0.008906	4.0	-0.426300	-0.254400	-0.004682	0.132442	0.3634	0.4989
0.055	-0.8686	0.1000	-0.2554	1.060	3.450	3.531	4.094	-2.10	-0.50	50.	6.1600	0.4893	3.0	0.0502	1.2440	-0.009288	-0.009068	4.0	-0.422200	-0.267100	-0.004517	0.138858	0.3856	0.4998
0.060	-0.8090	0.1000	-0.2554	1.060	3.450	3.513	4.089	-2.10	-0.50	50.	6.1570	0.4893	3.0	0.0500	1.2480	-0.009433	-0.009210	4.0	-0.419500	-0.278900	-0.004374	0.145375	0.3913	0.5029
0.065	-0.7487	0.1000	-0.2554	1.060	3.450	3.493	4.087	-2.10	-0.50	50.	6.1510	0.4893	3.0	0.0499	1.2490	-0.009561	-0.009335	4.0	-0.418300	-0.289500	-0.004266	0.151892	0.4036	0.5027
0.067	-0.7296	0.1000	-0.2554	1.060	3.450	3.484	4.086	-2.10	-0.50	50.	6.1490	0.4892	3.0	0.0498	1.2500	-0.009603	-0.009376	4.0	-0.418200	-0.293400	-0.004228	0.153998	0.4092	0.5012
0.070	-0.7065	0.1000	-0.2554	1.060	3.450	3.471	4.086	-2.10	-0.50	50.	6.1450	0.4890	3.0	0.0497	1.2500	-0.009656	-0.009428	4.0	-0.418500	-0.298700	-0.004182	0.158309	0.4065	0.5036
0.075	-0.6661	0.1000	-0.2554	1.060	3.450	3.448	4.086	-2.10	-0.50	50.	6.1370	0.4886	3.0	0.0495	1.2490	-0.009733	-0.009503	4.0	-0.419900	-0.306600	-0.004120	0.164525	0.4101	0.5043
0.080	-0.6329	0.1000	-0.2554	1.060	3.450	3.423	4.087	-2.10	-0.50	50.	6.1280	0.4882	3.0	0.0494	1.2480	-0.009782	-0.009550	4.0	-0.422600	-0.313200	-0.004079	0.170540	0.4120	0.5068
0.085	-0.5993	0.1000	-0.2554	1.060	3.450	3.397	4.090	-2.10	-0.50	50.	6.1180	0.4878	3.0	0.0492	1.2450	-0.009808	-0.009577	4.0	-0.426300	-0.318700	-0.004058	0.176355	0.4131	0.5091
0.090	-0.5678	0.1000	-0.2554	1.060	3.450	3.369	4.094	-2.10	-0.50	50.	6.1070	0.4872	3.0	0.0491	1.2430	-0.009809	-0.009577	4.0	-0.431000	-0.323100	-0.004050	0.181769	0.4200	0.5092
0.095	-0.5408	0.1000	-0.2554	1.060	3.450	3.341	4.099	-2.10	-0.50	50.	6.0940	0.4867	3.0	0.0490	1.2390	-0.009788	-0.009557	4.0	-0.436300	-0.326600	-0.004058	0.186983	0.4243	0.5084
0.100	-0.5207	0.1000	-0.2554	1.060	3.450	3.312	4.103	-2.10	-0.50	50.	6.0820	0.4861	3.0	0.0488	1.2350	-0.009753	-0.009522	4.0	-0.442100	-0.329300	-0.004075	0.191795	0.4230	0.5104
0.110	-0.4899	0.1000	-0.2554	1.060	3.450	3.255	4.114	-2.10	-0.50	50.	6.0550	0.4849	3.0	0.0486	1.2260	-0.009627	-0.009400	4.0	-0.454800	-0.332800	-0.004136	0.200518	0.4126	0.5125
0.120	-0.4535	0.1000	-0.2554	1.060	3.450	3.199	4.128	-2.10	-0.50	50.	6.0280	0.4835	3.0	0.0484	1.2150	-0.009460	-0.009236	4.0	-0.467900	-0.334300	-0.004228	0.207736	0.4243	0.5148
0.130	-0.4365	0.1000	-0.2554	1.060	3.450	3.145	4.142	-2.10	-0.50	50.	6.0000	0.4822	3.0	0.0482	1.2040	-0.009269	-0.009050	4.0	-0.481100	-0.334300	-0.004348	0.213752	0.4088	0.5150
0.133	-0.4350	0.1000	-0.2554	1.060	3.450	3.129	4.146	-2.10	-0.50	50.	5.9920	0.4818	3.0	0.0482	1.2010	-0.009205	-0.008988	4.0	-0.485000	-0.334100	-0.004383	0.215456	0.4055	0.5141
0.140	-0.4487	0.1000	-0.2554	1.060	3.450	3.093	4.156	-2.10	-0.50	50.	5.9720	0.4810	3.0	0.0481	1.1930	-0.009054	-0.008840	4.0	-0.493900	-0.333300	-0.004476	0.218464	0.4012	0.5109
0.150	-0.4658	0.1000	-0.2554	1.060	3.450	3.044	4.172	-2.10	-0.50	50.	5.9460	0.4797	3.0	0.0479	1.1820	-0.008832	-0.008623	4.0	-0.506100	-0.331400	-0.004617	0.222073	0.3929	0.5096
0.160	-0.4782	0.1000	-0.2543	1.060	3.450	2.997	4.187	-2.10	-0.50	50.	5.9200	0.4784	3.0	0.0477	1.1700	-0.008610	-0.008406	4.0	-0.517600	-0.328800	-0.004762	0.224580	0.3778	0.5111
0.170	-0.4933	0.1000	-0.2527	1.060	3.450	2.952	4.202	-2.10	-0.50	50.	5.8960	0.4772	3.0	0.0476	1.1590	-0.008398	-0.008199	4.0	-0.528300	-0.325700	-0.004903	0.226284	0.3652	0.5117
0.180	-0.5191	0.1000	-0.2511	1.060	3.450	2.910	4.217	-2.10	-0.50	50.	5.8730	0.4760	3.0	0.0474	1.1470	-0.008183	-0.007989	4.0	-0.538500	-0.322400	-0.005047	0.227086	0.3526	0.5168
0.190	-0.5455	0.1000	-0.2495	1.060	3.450	2.870	4.232	-2.10	-0.50	50.	5.8510	0.4749	3.0	0.0473	1.1360	-0.007976	-0.007787	4.0	-0.547900	-0.318600	-0.005185	0.227187	0.3380	0.5182
0.200	-0.5698	0.1000	-0.2478	1.060	3.450	2.831	4.248	-2.10	-0.50	50.	5.8300	0.4739	3.0	0.0471	1.1240	-0.007776	-0.007592	4.0	-0.556800	-0.314700	-0.005316	0.226685	0.3234	0.5154
0.220	-0.6372	0.1000	-0.2442	1.060	3.450	2.760	4.276	-2.10	-0.50	50.	5.7930	0.4721	3.0	0.0468	1.1020	-0.007397	-0.007222	4.0	-0.573100	-0.306000	-0.005572	0.224279	0.3189	0.5110
0.240	-0.7017	0.1000	-0.2405	1.060	3.450	2.692	4.304	-2.10	-0.50	50.	5.7580	0.4707	3.0	0.0466	1.0810	-0.007044	-0.006878	4.0	-0.587700	-0.296700	-0.005799	0.220469	0.3087	0.5123
0.250	-0.7267	0.1000	-0.2385	1.060	3.450	2.658	4.318	-2.10	-0.50	50.	5.7420	0.4700	3.0	0.0464	1.0700	-0.006877	-0.006714	4.0	-0.594400	-0.291900	-0.005905	0.218013	0.3075	0.5129
0.260	-0.7519	0.1000	-0.2366	1.060	3.450	2.626	4.332	-2.10	-0.50	50.	5.7260	0.4694	3.0	0.0463	1.0590	-0.006715	-0.006556	4.0	-0.600800	-0.286800	-0.006006	0.215557	0.3018	0.5159
0.280	-0.8115	0.1000	-0.2327	1.060	3.450	2.564	4.358	-2.10	-0.50	50.	5.6950	0.4682	3.0	0.0460	1.0390	-0.006408	-0.006257	4.0	-0.612800	-0.276500	-0.006195	0.209942	0.2871	0.5256
0.290	-0.8394	0.1000	-0.2308	1.060	3.450	2.533	4.371	-2.10	-0.50	50.	5.6800	0.4676	3.0	0.0459	1.0290	-0.006263	-0.006115	4.0	-0.618500	-0.271300	-0.006289	0.207035	0.2876	0.5303
0.300	-0.8667	0.1000	-0.2288	1.060	3.450	2.505	4.384	-2.10	-0.50	50.	5.6650	0.4671	3.0	0.0458	1.0190	-0.006123	-0.005979	4.0	-0.623800	-0.266000	-0.006371	0.204027	0.2902	0.5343
0.320	-0.9306	0.1000	-0.2250	1.060	3.450	2.449	4.409	-2.10	-0.50	50.	5.6360	0.4660	3.0	0.0455	1.0000	-0.005859	-0.005720	4.0	-0.633900	-0.255400	-0.006532	0.197811	0.2836	0.5426
0.340	-0.9978	0.1000	-0.2211	1.060	3.450	2.397	4.432	-2.10	-0.50	50.	5.6080	0.4649	3.0	0.0453	0.9813	-0.005614	-0.005481	4.0	-0.643200	-0.244900	-0.006678	0.191494	0.2879	0.5429
0.350	-1.0268	0.1000	-0.2192	1.060	3.450	2.372	4.444	-2.10	-0.50	50.	5.5950	0.4644	3.0	0.0452	0.9722	-0.005497	-0.005368	4.0	-0.647600	-0.239600	-0.006745	0.188386	0.2931	0.5428
0.360	-1.0589	0.1000	-0.2173	1.060	3.450	2.348	4.456	-2.10	-0.50	50.	5.5810	0.4639	3.0	0.0450	0.9632	-0.005386	-0.005259	4.0	-0.651800	-0.234400	-0.006812	0.185278	0.2959	0.5408
0.380	-1.1152	0.0994	-0.2135	1.060	3.450	2.303	4.477	-2.10	-0.50	50.	5.5550	0.4629	3.0	0.0448	0.9458	-0.005175	-0.005053	4.0	-0.659900	-0.224000	-0.006943	0.179163	0.3009	0.5370
0.400	-1.1649	0.0987	-0.2098	1.060	3.450	2.261	4.498	-2.10	-0.50	50.	5.5310	0.4619	3.0	0.0445	0.9288	-0.004980	-0.004862	4.0	-0.667500	-0.213900	-0.007055	0.173147	0.3088	0.5373
0.420	-1.2189	0.0978	-0.2061	1.060	3.450	2.222	4.517	-2.10	-0.50	50.	5.5070	0.4609	3.0	0.0442	0.9123	-0.004799	-0.004686	4.0	-0.674600	-0.203900	-0.007162	0.167332	0.3175	0.5390
0.440	-1.2742	0.0967	-0.2025	1.060	3.450	2.185	4.536	-2.10	-0.50	50.	5.4840	0.4601	3.0	0.0439	0.8963	-0.004632	-0.004522	4.0	-0.681300	-0.194300	-0.007263	0.161718	0.3232	0.5395
0.450	-1.2996	0.0960	-0.2007	1.060	3.450	2.167	4.545	-2.10	-0.50	50.	5.4730	0.4597	3.0	0.0437	0.8885	-0.004552	-0.004445	4.0	-0.684500	-0.189600	-0.007314	0.159011	0.3215	0.5397
0.460	-1.3257	0.0951	-0.1990	1.060	3.450	2.150	4.554	-2.10	-0.50	50.	5.4630	0.4593	3.0	0.0436	0.8809	-0.004477	-0.004371	4.0	-0.687600	-0.185000	-0.007365	0.156304	0.3173	0.5398
0.480	-1.3752	0.0931	-0.1955	1.060	3.450	2.118	4.571	-2.10	-0.50	50.	5.4440	0.4586	3.0	0.0432	0.8658	-0.004332	-0.004230	4.0	-0.693700	-0.176100	-0.007447	0.151090	0.3063	0.5419
0.500	-1.4201	0.0906	-0.1920	1.060	3.450	2.087	4.588	-2.10	-0.50	50.	5.4250	0.4578	3.0	0.0429	0.8513	-0.004199	-0.004100	4.0	-0.699500	-0.167600	-0.007529	0.146177	0.3038	0.5461
0.550	-1.5247	0.0828	-0.1839	1.060	3.450	2.017	4.627	-2.10	-0.50	50.	5.3820	0.4564	3.0	0.0421	0.8167	-0.003903	-0.003811	4.0	-0.712800	-0.148000	-0.007712	0.134547	0.3095	0.5511
0.600	-1.6343	0.0744	-0.1768	1.060	3.450	1.957	4.663	-2.10	-0.50	50.	5.3440	0.4553	3.0	0.0412	0.7846	-0.003652	-0.003565	4.0	-0.724800	-0.131100	-0.007868	0.124221	0.3170	0.5614
0.650	-1.7303	0.0652	-0.1705	1.060	3.450	1.904	4.696	-2.10	-0.50	50.	5.3110	0.4544	3.0	0.0404	0.7542	-0.003435	-0.003354	4.0	-0.735700	-0.116400	-0.008003	0.114997	0.3205	0.5638

Table 5: Coefficients of Chiou and Youngs (2006) Empirical Ground Motion Model for the Average Horizontal Component

Period (sec)	c_1	c_{1a}	c_{1b}	c_2	c_3	c_n	c_M	C_4	c_{4a}	c_{RB}	c_5	c_6	c_{HM}	c_7	c_9	$c_{\gamma 1}$	$c_{\gamma 2}$	$c_{\gamma 3}$	φ_1	φ_2	φ_3	φ_4	τ	σ
0.667	-1.7640	0.0617	-0.1686	1.060	3.450	1.887	4.707	-2.10	-0.50	50.	5.3010	0.4541	3.0	0.0401	0.7443	-0.003368	-0.003288	4.0	-0.739300	-0.112000	-0.008043	0.112190	0.3224	0.5652
0.700	-1.8214	0.0547	-0.1651	1.060	3.450	1.855	4.728	-2.10	-0.50	50.	5.2820	0.4536	3.0	0.0395	0.7256	-0.003246	-0.003169	4.0	-0.745800	-0.103900	-0.008115	0.106776	0.3203	0.5661
0.750	-1.8933	0.0435	-0.1603	1.060	3.450	1.812	4.757	-2.10	-0.50	50.	5.2560	0.4530	3.0	0.0387	0.6982	-0.003078	-0.003005	4.0	-0.755100	-0.093100	-0.008213	0.099377	0.3029	0.5641
0.800	-1.9712	0.0323	-0.1562	1.060	3.450	1.773	4.785	-2.10	-0.50	50.	5.2330	0.4525	3.0	0.0379	0.6721	-0.002929	-0.002860	4.0	-0.763700	-0.083770	-0.008304	0.092739	0.3086	0.5621
0.850	-2.0411	0.0214	-0.1525	1.060	3.450	1.737	4.811	-2.10	-0.50	50.	5.2110	0.4521	3.0	0.0372	0.6471	-0.002795	-0.002729	4.0	-0.771800	-0.075640	-0.008379	0.086744	0.2934	0.5605
0.900	-2.1069	0.0112	-0.1491	1.060	3.450	1.704	4.836	-2.10	-0.50	50.	5.1920	0.4517	3.0	0.0364	0.6229	-0.002674	-0.002611	4.0	-0.779300	-0.068540	-0.008438	0.081330	0.2999	0.5578
0.950	-2.1716	0.0018	-0.1461	1.060	3.450	1.675	4.860	-2.10	-0.50	50.	5.1730	0.4513	3.0	0.0357	0.5996	-0.002564	-0.002504	4.0	-0.786400	-0.062260	-0.008497	0.076427	0.3106	0.5540
1.000	-2.2326	-0.0068	-0.1433	1.060	3.450	1.648	4.882	-2.10	-0.50	50.	5.1550	0.4511	3.0	0.0350	0.5771	-0.002464	-0.002406	4.0	-0.793100	-0.056690	-0.008548	0.071956	0.3165	0.5477
1.100	-2.3433	-0.0210	-0.1384	1.060	3.450	1.605	4.925	-2.10	-0.50	50.	5.1230	0.4508	3.0	0.0336	0.5346	-0.002287	-0.002233	4.0	-0.805400	-0.047240	-0.008626	0.064146	0.3421	0.5442
1.200	-2.4313	-0.0328	-0.1342	1.060	3.450	1.572	4.964	-2.10	-0.50	50.	5.0960	0.4506	3.0	0.0322	0.4951	-0.002138	-0.002087	4.0	-0.816500	-0.039500	-0.008695	0.057579	0.3510	0.5381
1.300	-2.5399	-0.0432	-0.1306	1.060	3.450	1.546	5.001	-2.10	-0.50	50.	5.0720	0.4505	3.0	0.0308	0.4584	-0.002010	-0.001962	4.0	-0.826500	-0.033080	-0.008747	0.051984	0.3494	0.5383
1.400	-2.6311	-0.0525	-0.1274	1.060	3.450	1.526	5.037	-2.10	-0.50	50.	5.0520	0.4505	3.0	0.0294	0.4244	-0.001898	-0.001854	4.0	-0.835900	-0.027680	-0.008791	0.047192	0.3469	0.5374
1.500	-2.7212	-0.0602	-0.1247	1.060	3.450	1.511	5.070	-2.10	-0.50	50.	5.0370	0.4504	3.0	0.0280	0.3930	-0.001802	-0.001759	4.0	-0.844400	-0.023140	-0.008818	0.043041	0.3513	0.5379
1.600	-2.8125	-0.0661	-0.1221	1.060	3.450	1.498	5.102	-2.10	-0.50	50.	5.0240	0.4504	3.0	0.0266	0.3639	-0.001717	-0.001677	4.0	-0.852300	-0.019290	-0.008835	0.039412	0.3591	0.5440
1.700	-2.8974	-0.0707	-0.1199	1.060	3.450	1.489	5.133	-2.10	-0.50	50.	5.0160	0.4503	3.0	0.0253	0.3369	-0.001643	-0.001604	4.0	-0.859500	-0.016030	-0.008862	0.036234	0.3655	0.5447
1.800	-2.9774	-0.0746	-0.1177	1.060	3.450	1.481	5.162	-2.10	-0.50	50.	5.0100	0.4503	3.0	0.0240	0.3120	-0.001578	-0.001540	4.0	-0.866400	-0.013270	-0.008871	0.033426	0.3735	0.5440
1.900	-3.0531	-0.0784	-0.1158	1.060	3.450	1.474	5.191	-2.10	-0.50	50.	5.0060	0.4503	3.0	0.0226	0.2889	-0.001519	-0.001483	4.0	-0.872700	-0.010920	-0.008880	0.030940	0.3810	0.5413
2.000	-3.1249	-0.0821	-0.1140	1.060	3.450	1.470	5.217	-2.10	-0.50	50.	5.0030	0.4503	3.0	0.0214	0.2675	-0.001467	-0.001433	4.0	-0.878600	-0.008925	-0.008880	0.028714	0.3818	0.5439
2.200	-3.2583	-0.0886	-0.1107	1.060	3.450	1.463	5.269	-2.10	-0.50	50.	5.0000	0.4502	3.0	0.0188	0.2294	-0.001381	-0.001348	4.0	-0.889100	-0.005808	-0.008888	0.024924	0.3764	0.5460
2.400	-3.3802	-0.0932	-0.1080	1.060	3.450	1.458	5.317	-2.10	-0.50	50.	5.0000	0.4502	3.0	0.0165	0.1965	-0.001311	-0.001280	4.0	-0.898100	-0.003580	-0.008888	0.021826	0.3889	0.5442
2.500	-3.4373	-0.0948	-0.1067	1.060	3.450	1.456	5.339	-2.10	-0.50	50.	5.0000	0.4502	3.0	0.0154	0.1818	-0.001281	-0.001251	4.0	-0.902100	-0.002728	-0.008888	0.020553	0.3896	0.5431
2.600	-3.4922	-0.0961	-0.1056	1.060	3.450	1.456	5.361	-2.10	-0.50	50.	5.0000	0.4502	3.0	0.0143	0.1680	-0.001255	-0.001225	4.0	-0.905700	-0.002017	-0.008888	0.019270	0.4008	0.5381
2.800	-3.5960	-0.0982	-0.1036	1.060	3.450	1.455	5.401	-2.10	-0.50	50.	5.0000	0.4501	3.0	0.0124	0.1431	-0.001209	-0.001181	4.0	-0.912200	-0.000930	-0.008888	0.017114	0.4099	0.5321
3.000	-3.6926	-0.0999	-0.1019	1.060	3.450	1.456	5.439	-2.10	-0.50	50.	5.0000	0.4501	3.0	0.0106	0.1210	-0.001172	-0.001145	4.0	-0.917300	-0.000190	-0.008888	0.015300	0.4045	0.5397
3.200	-3.7829	-0.1000	-0.1006	1.060	3.450	1.457	5.474	-2.10	-0.50	50.	5.0000	0.4501	3.0	0.0090	0.1016	-0.001142	-0.001115	4.0	-0.921500	0.000000	-0.008888	0.013745	0.4127	0.5480
3.400	-3.8678	-0.1000	-0.1000	1.060	3.450	1.458	5.507	-2.10	-0.50	50.	5.0000	0.4501	3.0	0.0076	0.0846	-0.001117	-0.001091	4.0	-0.924600	0.000000	-0.008880	0.012402	0.4195	0.5524
3.500	-3.9084	-0.1000	-0.1000	1.060	3.450	1.459	5.523	-2.10	-0.50	50.	5.0000	0.4501	3.0	0.0069	0.0769	-0.001106	-0.001080	4.0	-0.925900	0.000000	-0.008880	0.011821	0.4162	0.5532
3.600	-3.9478	-0.1000	-0.1000	1.060	3.450	1.461	5.538	-2.10	-0.50	50.	5.0000	0.4501	3.0	0.0063	0.0698	-0.001096	-0.001071	4.0	-0.926800	0.000000	-0.008880	0.011239	0.4158	0.5549
3.800	-4.0235	-0.1000	-0.1000	1.060	3.450	1.463	5.569	-2.10	-0.50	50.	5.0000	0.4500	3.0	0.0052	0.0569	-0.001079	-0.001054	4.0	-0.928200	0.000000	-0.008880	0.010226	0.4215	0.5547
4.000	-4.0953	-0.1000	-0.1000	1.060	3.450	1.465	5.598	-2.10	-0.50	50.	5.0000	0.4500	3.0	0.0041	0.0459	-0.001065	-0.001040	4.0	-0.928600	0.000000	-0.008880	0.009334	0.4287	0.5563
4.200	-4.1636	-0.1000	-0.1000	1.060	3.450	1.468	5.625	-2.10	-0.50	50.	5.0000	0.4500	3.0	0.0033	0.0364	-0.001052	-0.001027	4.0	-0.928100	0.000000	-0.008880	0.008552	0.4648	0.5521
4.400	-4.2288	-0.1000	-0.1000	1.060	3.450	1.470	5.652	-2.10	-0.50	50.	5.0000	0.4500	3.0	0.0025	0.0283	-0.001042	-0.001017	4.0	-0.926900	0.000000	-0.008880	0.007850	0.4520	0.5609
4.600	-4.2910	-0.1000	-0.1000	1.060	3.450	1.473	5.678	-2.10	-0.50	50.	5.0000	0.4500	3.0	0.0019	0.0213	-0.001032	-0.001007	4.0	-0.924900	0.000000	-0.008880	0.007229	0.4443	0.5709
4.800	-4.3506	-0.1000	-0.1000	1.060	3.450	1.475	5.703	-2.10	-0.50	50.	5.0000	0.4500	3.0	0.0014	0.0154	-0.001024	-0.001000	4.0	-0.922200	0.000000	-0.008880	0.006677	0.4466	0.5782
5.000	-4.4077	-0.1000	-0.1000	1.060	3.450	1.478	5.728	-2.10	-0.50	50.	5.0000	0.4500	3.0	0.0010	0.0104	-0.001016	-0.000992	4.0	-0.918800	0.000000	-0.008880	0.006176	0.4405	0.5837
5.500	-4.5412	-0.1000	-0.1000	1.060	3.450	1.483	5.786	-2.10	-0.50	50.	5.0000	0.4500	3.0	0.0002	0.0012	-0.000999	-0.000976	4.0	-0.907500	0.000000	-0.008880	0.005133	0.4379	0.5894
6.000	-4.6630	-0.1000	-0.1000	1.060	3.450	1.488	5.840	-2.10	-0.50	50.	5.0000	0.4500	3.0	0.0000	0.0000	-0.000987	-0.000964	4.0	-0.892900	0.000000	-0.008880	0.004311	0.4245	0.5997
6.500	-4.7750	-0.1000	-0.1000	1.060	3.450	1.492	5.892	-2.10	-0.50	50.	5.0000	0.4500	3.0	0.0000	0.0000	-0.000977	-0.000954	4.0	-0.875800	0.000000	-0.008880	0.003659	0.4414	0.6110
7.000	-4.8788	-0.1000	-0.1000	1.060	3.450	1.496	5.942	-2.10	-0.50	50.	5.0000	0.4500	3.0	0.0000	0.0000	-0.000968	-0.000945	4.0	-0.856900	0.000000	-0.008880	0.003128	0.4585	0.6038
7.500	-4.9754	-0.1000	-0.1000	1.060	3.450	1.498	5.989	-2.10	-0.50	50.	5.0000	0.4500	3.0	0.0000	0.0000	-0.000961	-0.000938	4.0	-0.837000	0.000000	-0.008880	0.002697	0.4888	0.6048
8.000	-5.0657	-0.1000	-0.1000	1.060	3.450	1.499	6.034	-2.10	-0.50	50.	5.0000	0.4500	3.0	0.0000	0.0000	-0.000955	-0.000933	4.0	-0.816500	0.000000	-0.008880	0.002346	0.5105	0.6156
8.500	-5.1506	-0.1000	-0.1000	1.060	3.450	1.500	6.077	-2.10	-0.50	50.	5.0000	0.4500	3.0	0.0000	0.0000	-0.000950	-0.000927	4.0	-0.795900	0.000000	-0.008880	0.002045	0.3588	0.6110
9.000	-5.2306	-0.1000	-0.1000	1.060	3.450	1.501	6.117	-2.10	-0.50	50.	5.0000	0.4500	3.0	0.0000	0.0000	-0.000945	-0.000923	4.0	-0.775700	0.000000	-0.008880	0.001795	0.3597	0.6264
9.500	-5.3063	-0.1000	-0.1000	1.060	3.450	1.501	6.156	-2.10	-0.50	50.	5.0000	0.4500	3.0	0.0000	0.0000	-0.000941	-0.000919	4.0	-0.756000	0.000000	-0.008880	0.001584	0.3528	0.6357
10.000	-5.3820	-0.1000	-0.1000	1.060	3.450	1.502	6.193	-2.10	-0.50	50.	5.0000	0.4500	3.0	0.0000	0.0000	-0.000937	-0.000914	4.0	-0.737200	0.000000	-0.008880	0.001404	0.2934	0.6445

MODEL RESULTS

Inter-Event Residuals: Figure 34 shows the random intercept values c_1 for the main shocks. The horizontal lines define the population means. The difference between the individual values and the population mean define the inter-event residuals. The residuals do not exhibit a trend with magnitude. The values for California and non-California earthquakes do not show any trends with respect to the population mean, indicating that both sets of earthquakes are consistent with the model. The inter-event term for the Chi-Chi main shock is approximately $1.5\times\tau$ below the population mean for *pga* (0.01 sec spectral acceleration), and becomes positive for periods of 1.0 seconds and greater. These results indicate that the data from the other active tectonic regions are consistent with ground motions from California earthquakes.

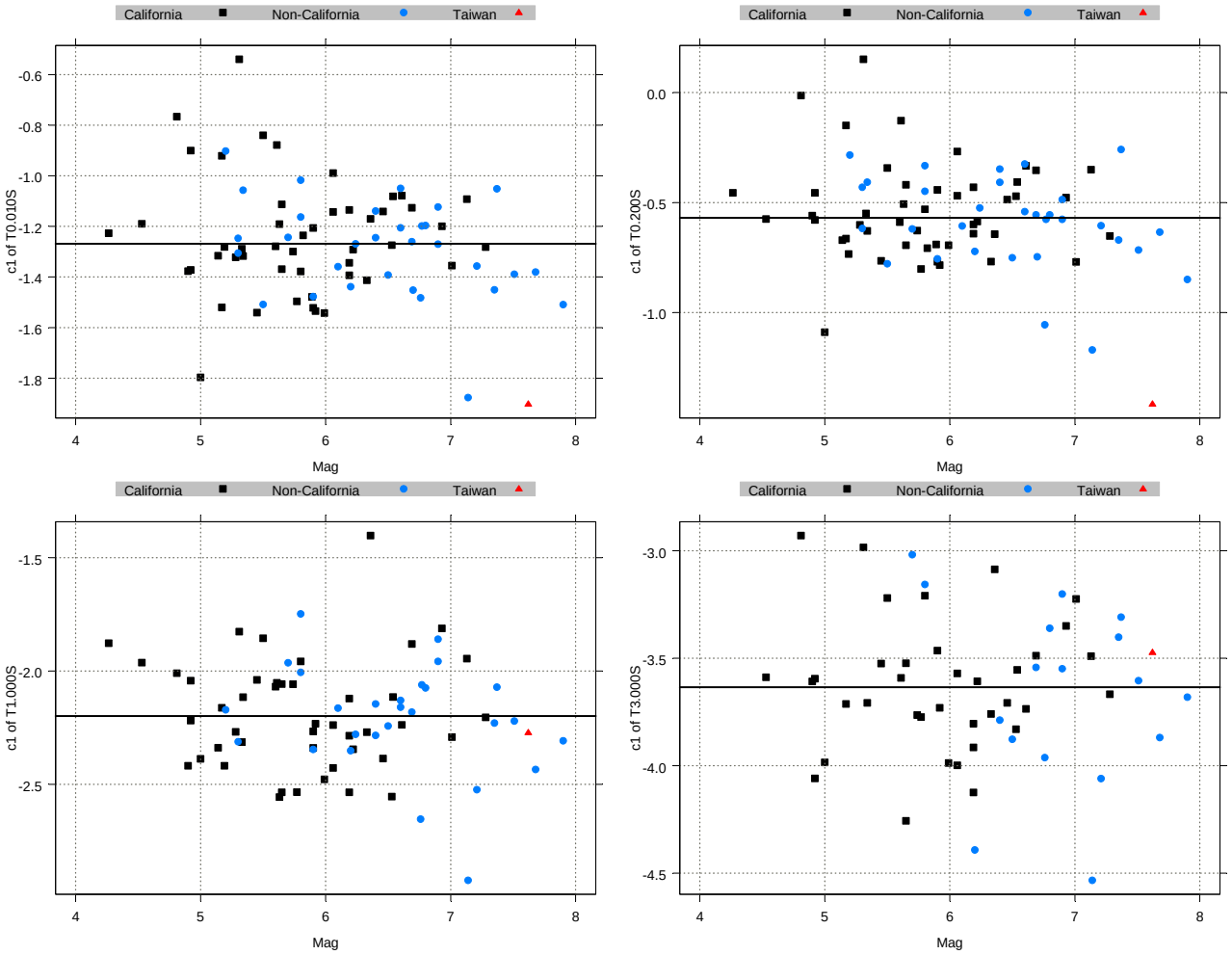

Figure 34: Inter-event values of the intercept c_1 for spectral periods of 0.01 sec (*pga*), 0.1, 1.0 and 3.0 seconds. The horizontal line denotes the population mean. Difference between population mean and individual value represents inter-event residual.

Intra-Event Residuals: Figure 35a through 35d show the intra-event residuals plotted versus magnitude and R_{RUP} for spectral periods of 0.01 (*pga*), 0.2, 1.0 and 3.0 seconds respectively. The distribution of residuals is further subdivided into comparisons with respect to R_{RUP} for California,

non-California, and Taiwan earthquakes, versus R_{RUP} for a range of magnitude intervals. The residuals do not exhibit any trends with respect to magnitude or distance.

Figures 36a through 36d show the intra-event residuals plotted versus V_{S30} both as a composite plot and for individual ranges of reference ground motion amplitude. Again, the residuals do not exhibit any systematic trends. Note that the soil model assumes that there is no deamplification of ground motions below the reference ground motion level of SA_{1130} for sites with V_{S30} greater that 1130 m/sec. Although there is very little data in the PEER-NGA data base for sites with V_{S30} greater that 1130 m/sec, the limited data, if anything, suggest a slight upward trend in the residuals. The site amplification model developed here does not account for the effect of the lower kappa expected for hard rock sites which would tend to lead to increases in high frequency ground motions.

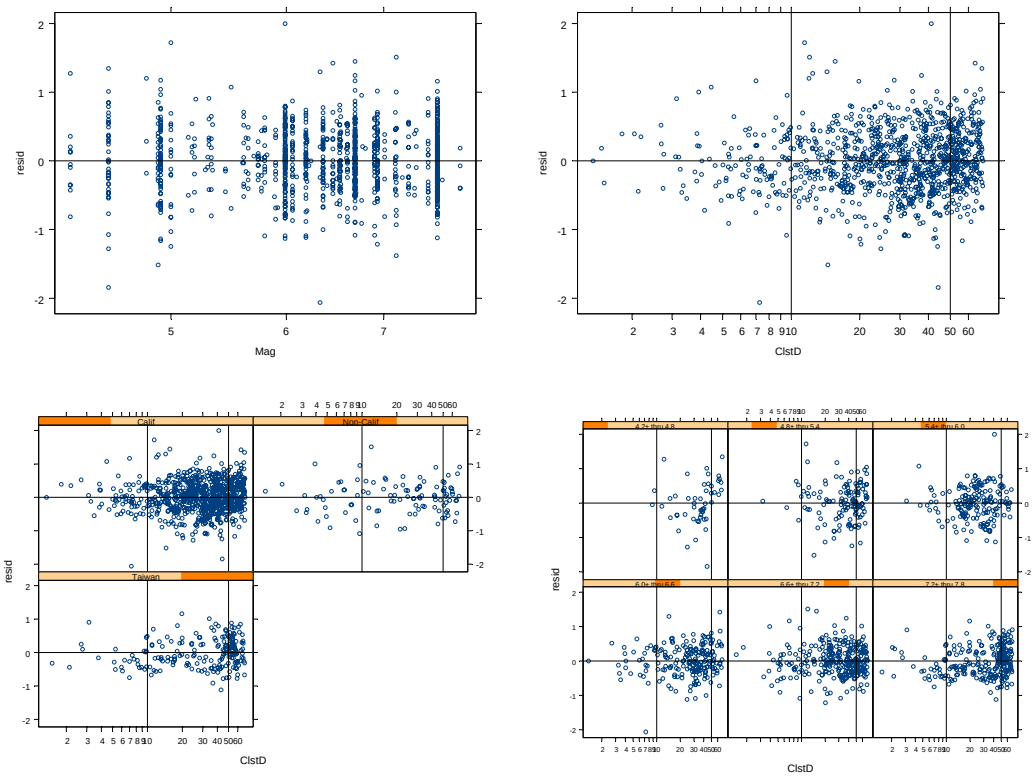

Figure 35a: Intra-event residuals for spectral period of 0.01 seconds (*pga*).

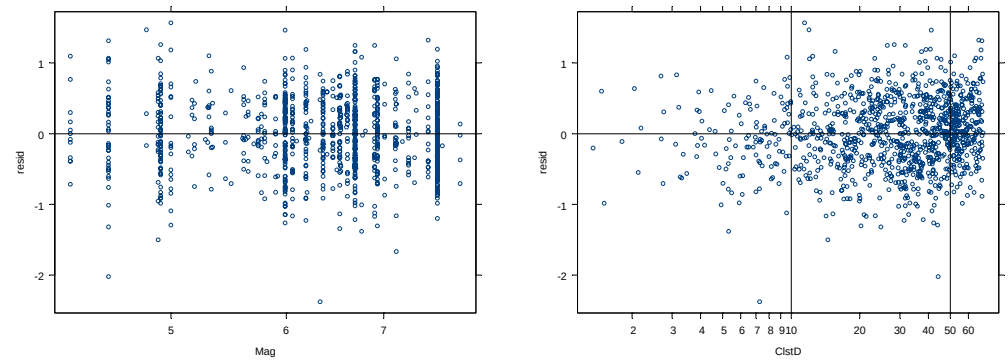

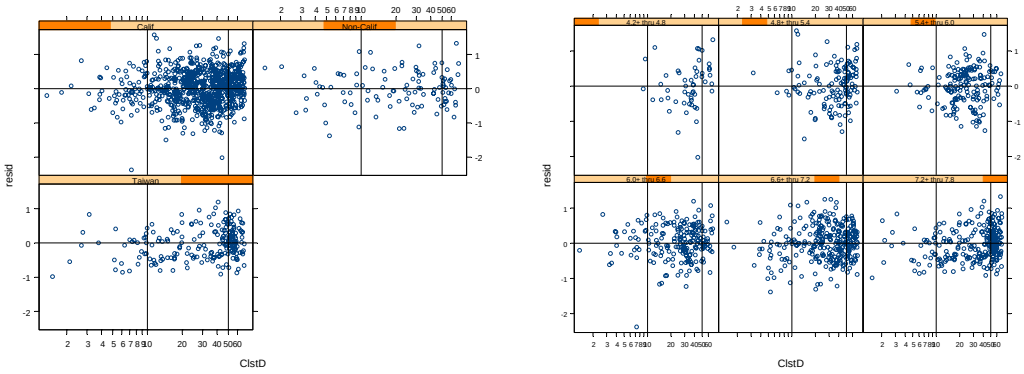

Figure 35b: Intra-event residuals for spectral period of 0.2 seconds.

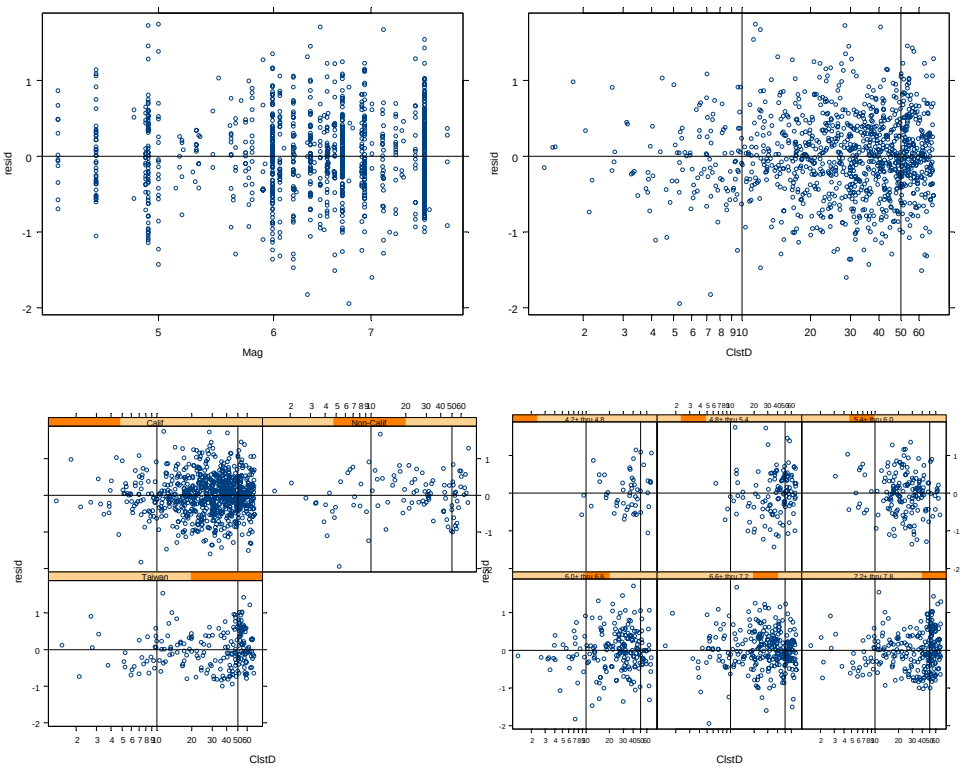

Figure 35c: Intra-event residuals for spectral period of 1.0 seconds.

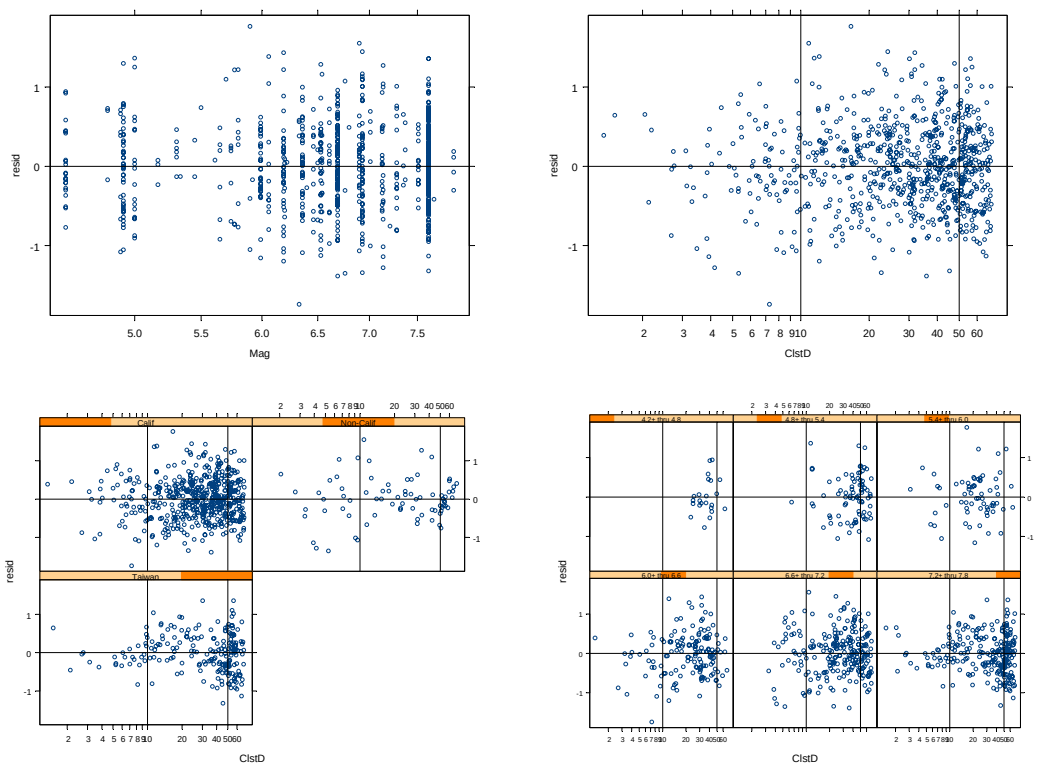

Figure 35d: Intra-event residuals for spectral period of 3.0 seconds.

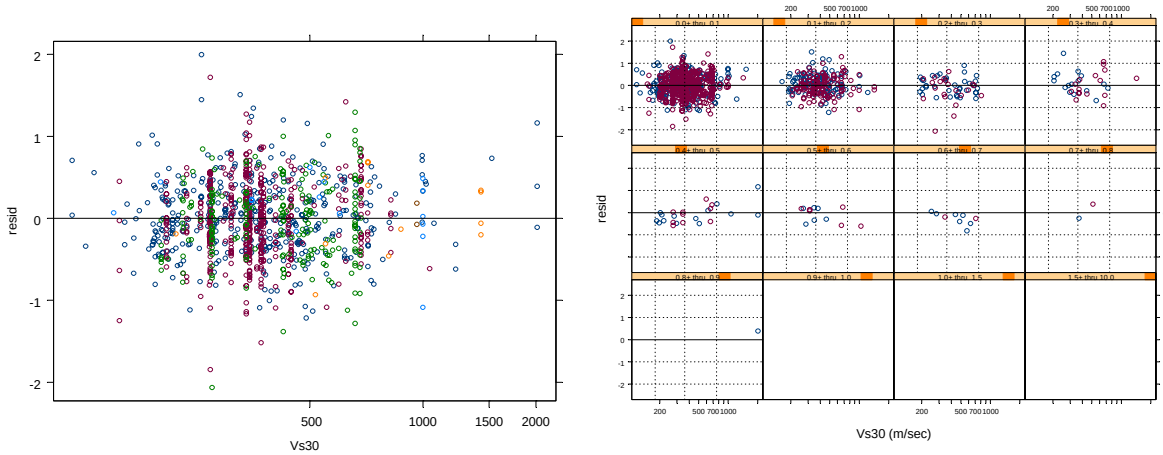

Figure 36a: Intra-event residuals versus V_{S30} for spectral period of 0.01 seconds (*pga*).

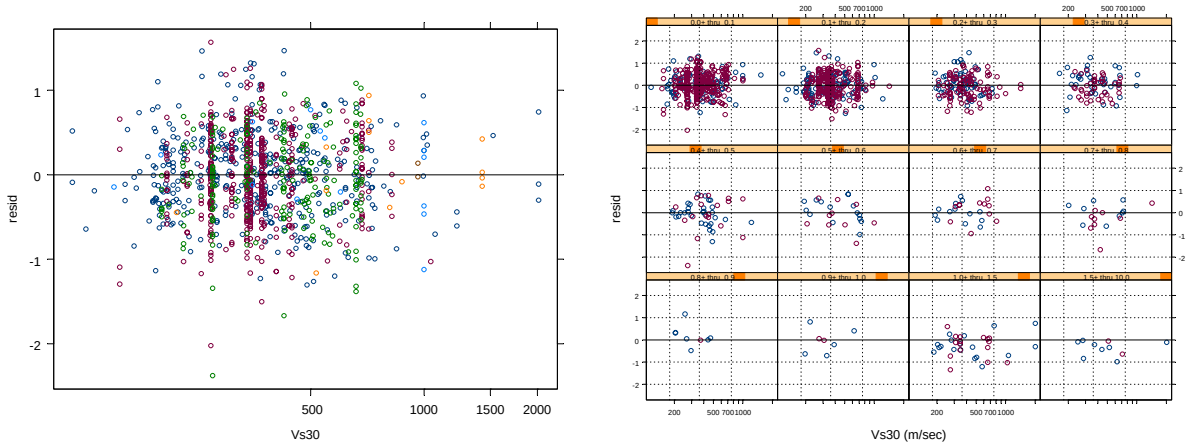

Figure 36b: Intra-event residuals versus V_{S30} for spectral period of 0.2 seconds.

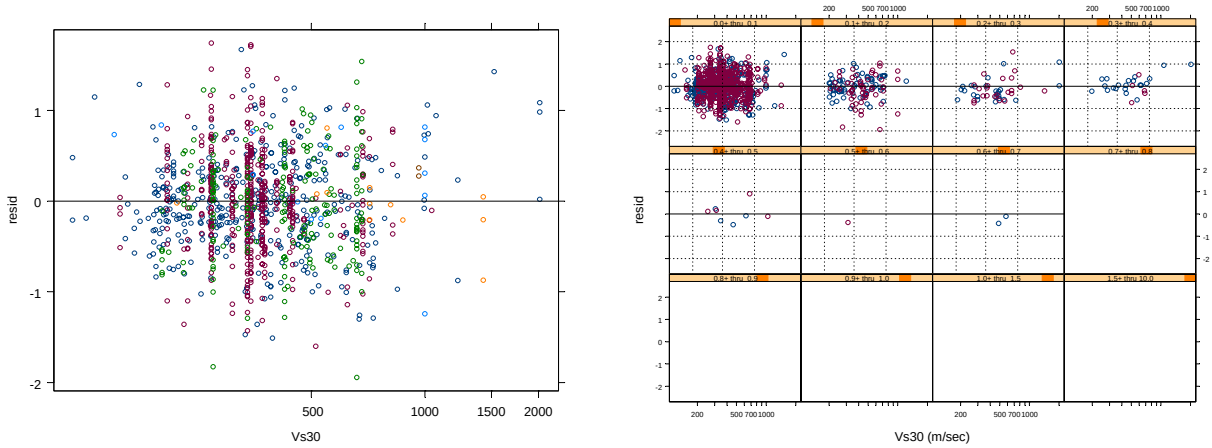

Figure 36b: Intra-event residuals versus V_{S30} for spectral period of 1.0 seconds.

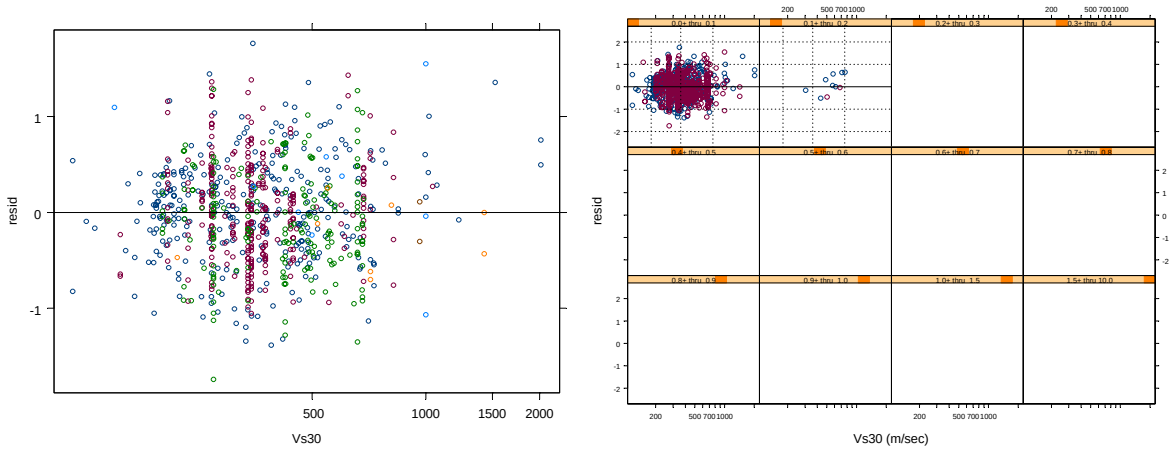

Figure 36d: Intra-event residuals versus V_{S30} for spectral period of 3.0 seconds.

Figures 37a though 37d show the intra-event residual plotted versus $Z_{1.0}$ for those sites for which the depth to V_S of 1.0 km/sec is available in the PEER-NGA data base. Two plots are

shown on each figure. The depths for southern California sites in the PEER-NGA data base, as well as the modeling performed by Day et al. (2006), are based on the SCEC Version 2 3-D velocity model (Magistrale et al., 2000). The SCES web site contains an updated Version 4 velocity model for southern California. The major change between Version 2 and Version 4 is in the velocity gradient at shallow depths, with the depths to V_S of 1.0 km/s in the Version 4 model being systematically 60 percent of the depths in the Version 2 model. The depths to V_S of 2.5 km/s is similar in Version 2 and Version 4 of the SCEC models. At this time, we are not prepared to propose a model for the effect of sediment depth because of the uncertainty in the $Z_{1.0}$ depths for the southern California sites. We think that $Z_{1.0}$ is a more practical parameter to use than $Z_{2.5}$ because it is more likely to be available to a user based on site data.

The residuals do indicate that large sediment depths lead to larger ground motions. The residuals also indicate that very thin sediment depths lead to smaller long period motions (Figures 37c and 37d).

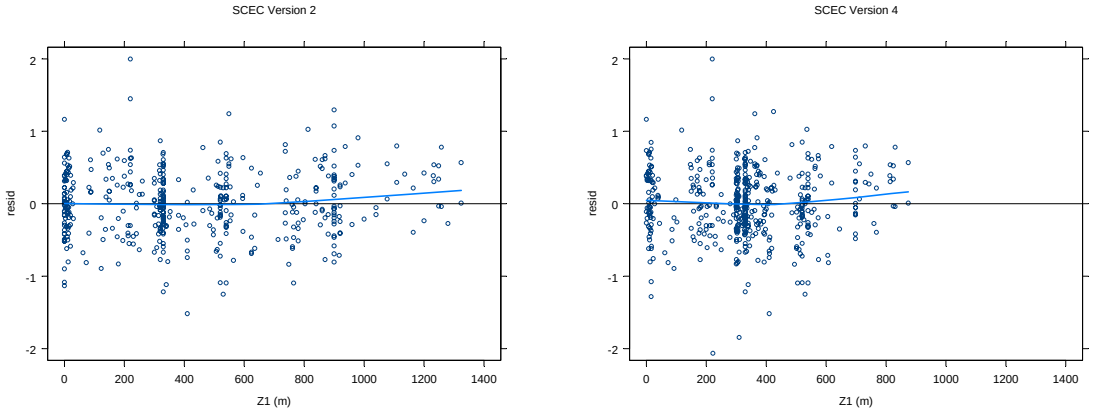

Figure 37a: Intra-event residuals versus $Z_{1.0}$ for spectral period of 0.01 seconds (*pga*). Plot on left shows sites with velocities based on SCEC Version 2 3-D velocity model and plot on right shows sites with velocities based on SCEC Version 4 3-D velocity model.

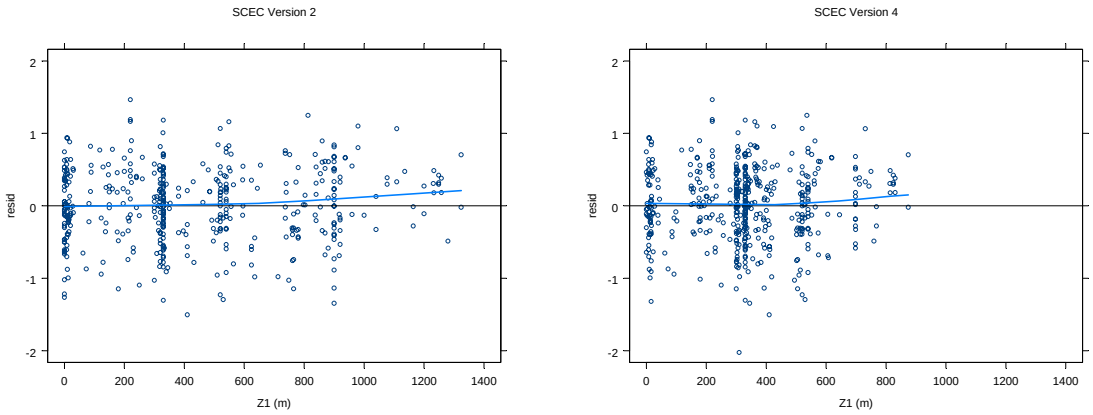

Figure 37b: Intra-event residuals versus $Z_{1.0}$ for spectral period of 0.2 seconds. Plot on left shows sites with velocities based on SCEC Version 2 3-D velocity model and plot on right shows sites with velocities based on SCEC Version 4 3-D velocity model.

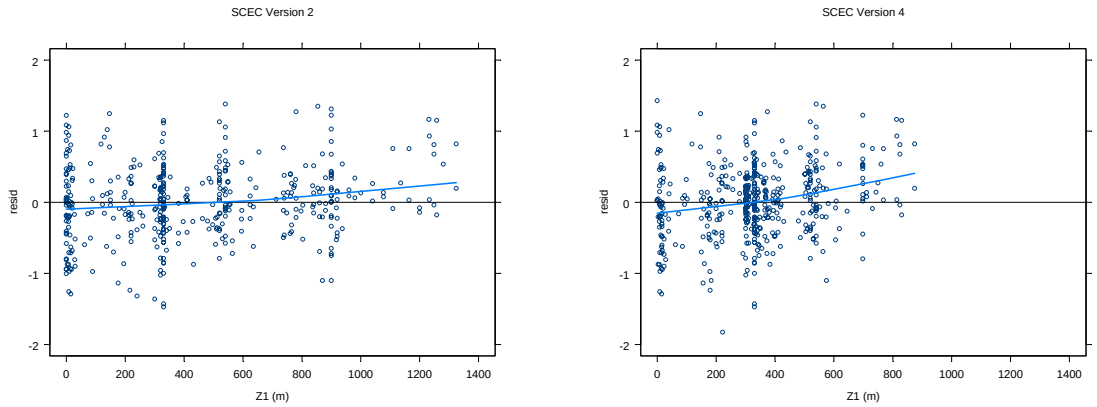

Figure 37c: Intra-event residuals versus $Z_{1.0}$ for spectral period of 1.0 seconds. Plot on left shows sites with velocities based on SCEC Version 2 3-D velocity model and plot on right shows sites with velocities based on SCEC Version 4 3-D velocity model.

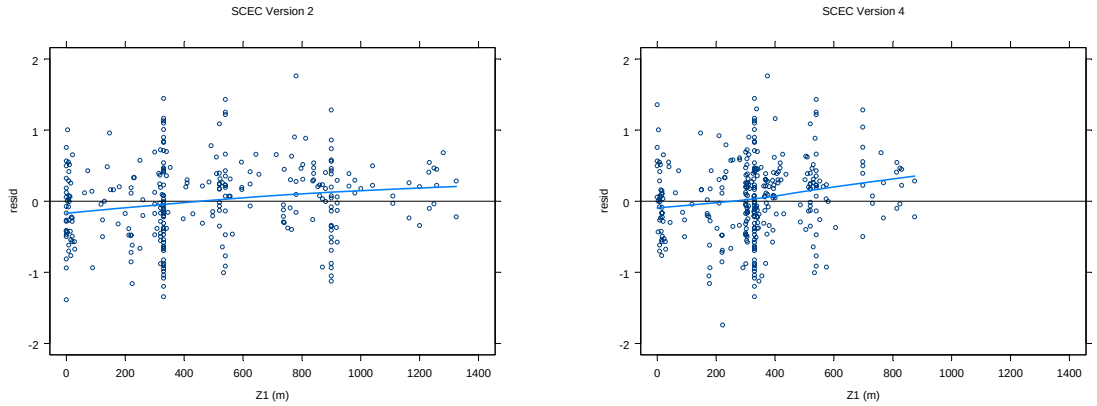

Figure 37d: Intra-event residuals versus $Z_{1.0}$ for spectral period of 3.0 seconds. Plot on left shows sites with velocities based on SCEC Version 2 3-D velocity model and plot on right shows sites with velocities based on SCEC Version 4 3-D velocity model.

Comparisons with Data for Individual Earthquakes: Appendix E contains plots showing the model fit to the data for individual earthquakes. The predicted ground motions in these plots include the inter-event random effect.

Nonlinear Soil Model: Figures 37a through 37b compare the site amplifications versus V_{S30} and ground motion amplitude predicted by the nonlinear soil model developed as part of this ground motion model with the site amplifications computed by Silva (2004) using equivalent linear site response analyses and by Choi and Stewart (2003) using empirical ground motion data. The soil model developed in this study compares well with the site response results computed by Silva (2004) for spectral periods of 0.01, 0.2, and 1.0 seconds and shows greater amplification at a spectral period of 3.0 seconds. The model compares well to Choi and Stewart's results at spectral periods of 0.01 and 1.0 seconds, is more nonlinear at a spectral period of 0.2 seconds, and shows greater amplification a period of 3.0 seconds.

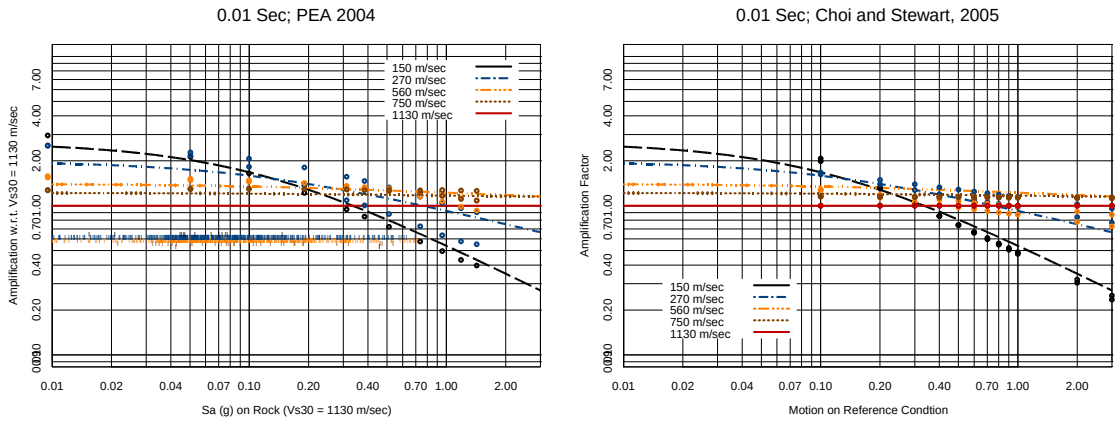

Figure 38a: Nonlinear site amplification predicted by ground motion model developed in this study compared to those computed by Silva (2004) – on left, and Choi and Stewart – on right, for spectral period of 0.01 seconds (*pga*).

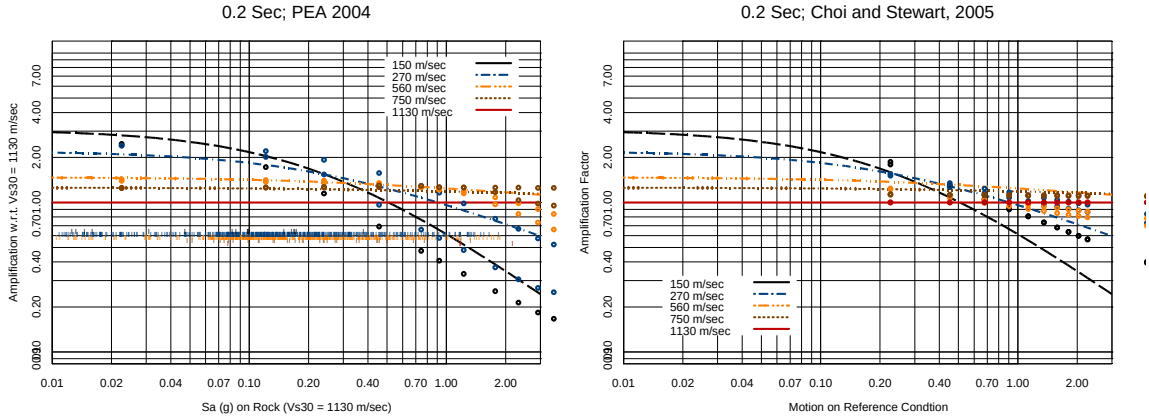

Figure 38b: Nonlinear site amplification predicted by ground motion model developed in this study compared to those computed by Silva (2004) – on left, and Choi and Stewart – on right, for spectral period of 0.2 seconds.

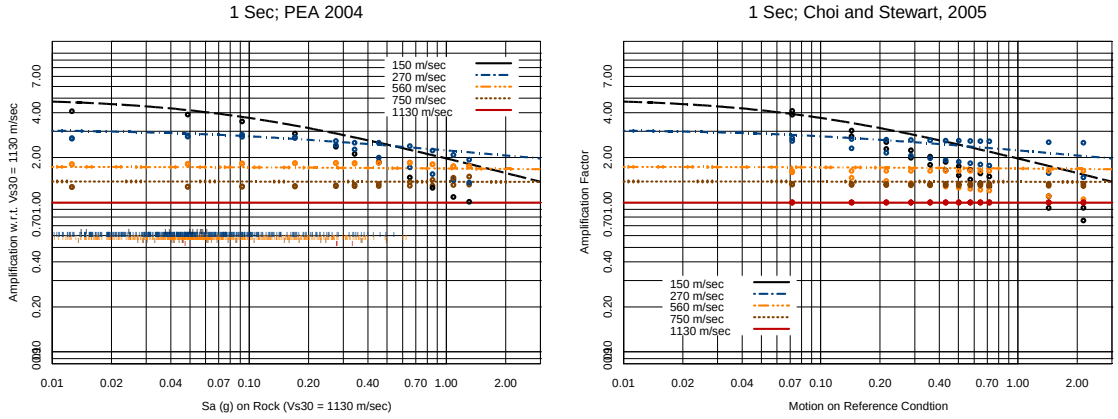

Figure 38c: Nonlinear site amplification predicted by ground motion model developed in this study compared to those computed by Silva (2004) – on left, and Choi and Stewart – on right, for spectral period of 1.0 seconds.

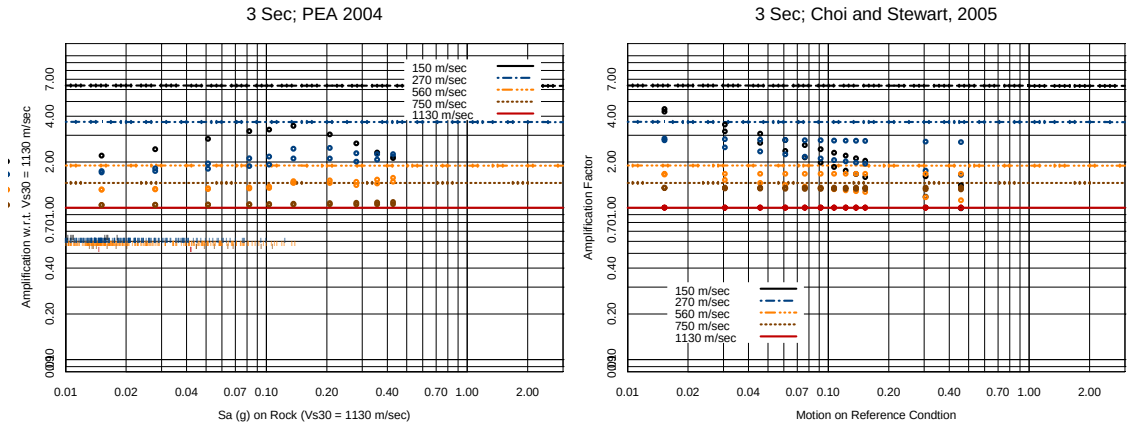

Figure 38d: Nonlinear site amplification predicted by ground motion model developed in this study compared to those computed by Silva (2004) – on left, and Choi and Stewart – on right, for spectral period of 3.0 seconds.

<u>Comparison with Previous Model</u>: Figures 39 and 40 compare the response spectra predicted by the ground motion model developed in this study with response spectra predicted by the models developed by Sadigh et al. (1997). The comparisons require an assessment of V_{S30} representative of the Sadigh et al. (1997) relationships. For soil, we have used a value of 310 m/s, the velocity suggested by Boore et al. (1997) as representative of generic soil. For generic rock, Boore et al. (1997) suggested a value of 620 m/s. However, we think that this may be higher than the average for the data used by Sadigh et al. (1997), which included recordings from many site that are now classified as NEHRP C. Therefore, we selected a velocity of 520 m/s for purpose of making the comparisons. Figures 41, 42, 43, and 44 provide comparisons of the magnitude and distance scaling for the two models. The model developed in this study produces ground motion estimates than are in general similar to those obtained using the Sadigh et al. (199&) model. The new model tends to produce lower ground motions in the distance range of 10 to 50 km and larger ground motions at larger distances. The models are more similar for soil than for rock, which is to be expected given that the majority of ground motion data is recorded on soil sites.

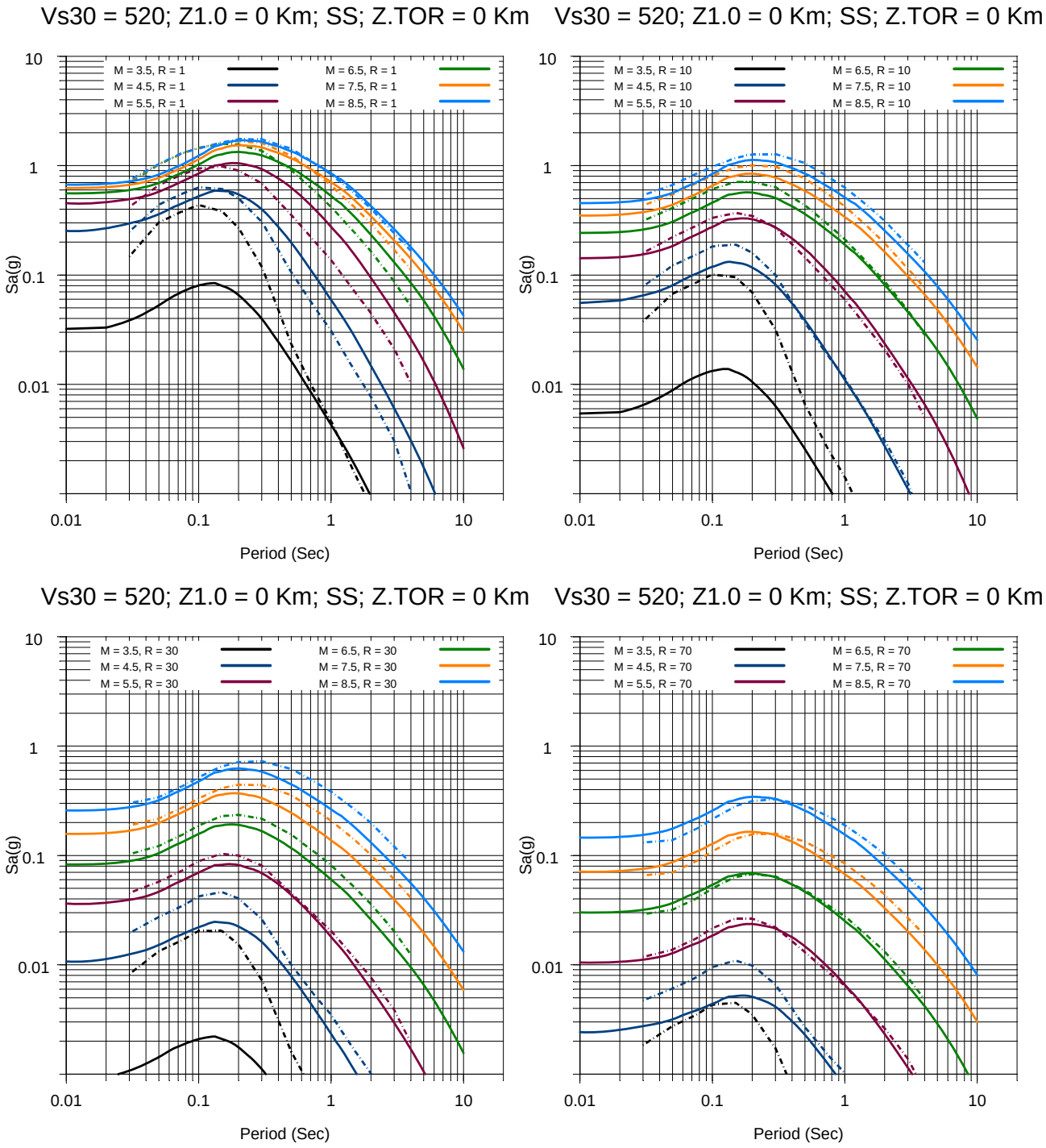

Figure 39: Comparison of median response spectra predicted by the model developed in this study (solid curves) and predicted by Sadigh et al. (1997) (dashed curves) for soft rock. A V_{S30} of 520 m/s was used to represent the average conditions for Sadigh et al.'s (1997) rock model.

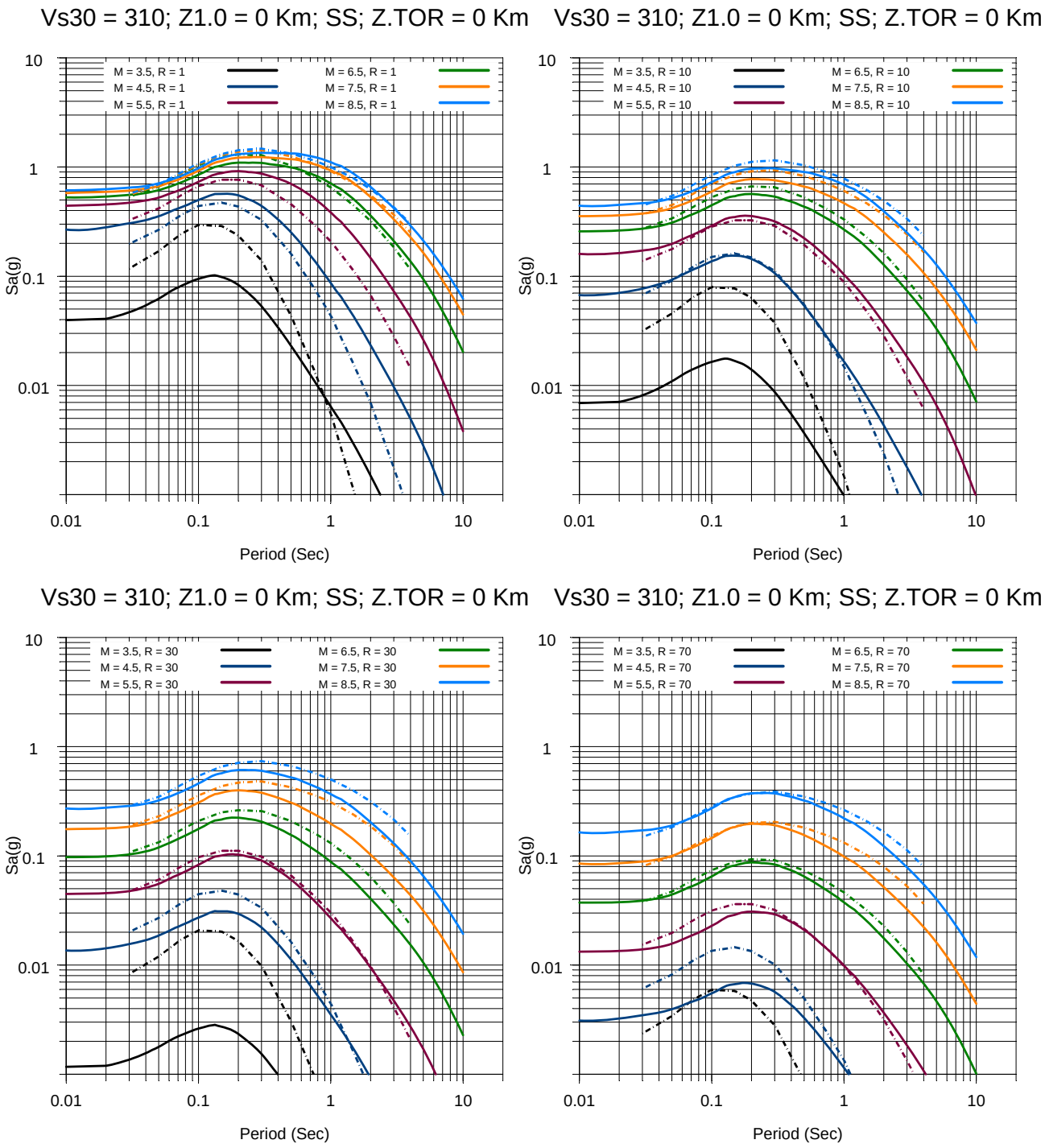

Figure 40: Comparison of median response spectra predicted by the model developed in this study (solid curves) and predicted by Sadigh et al. (1997) (dashed curves) for firm soil. A V_{S30} of 310 m/s was used to represent the average conditions for Sadigh et al.'s (1997) soil model.

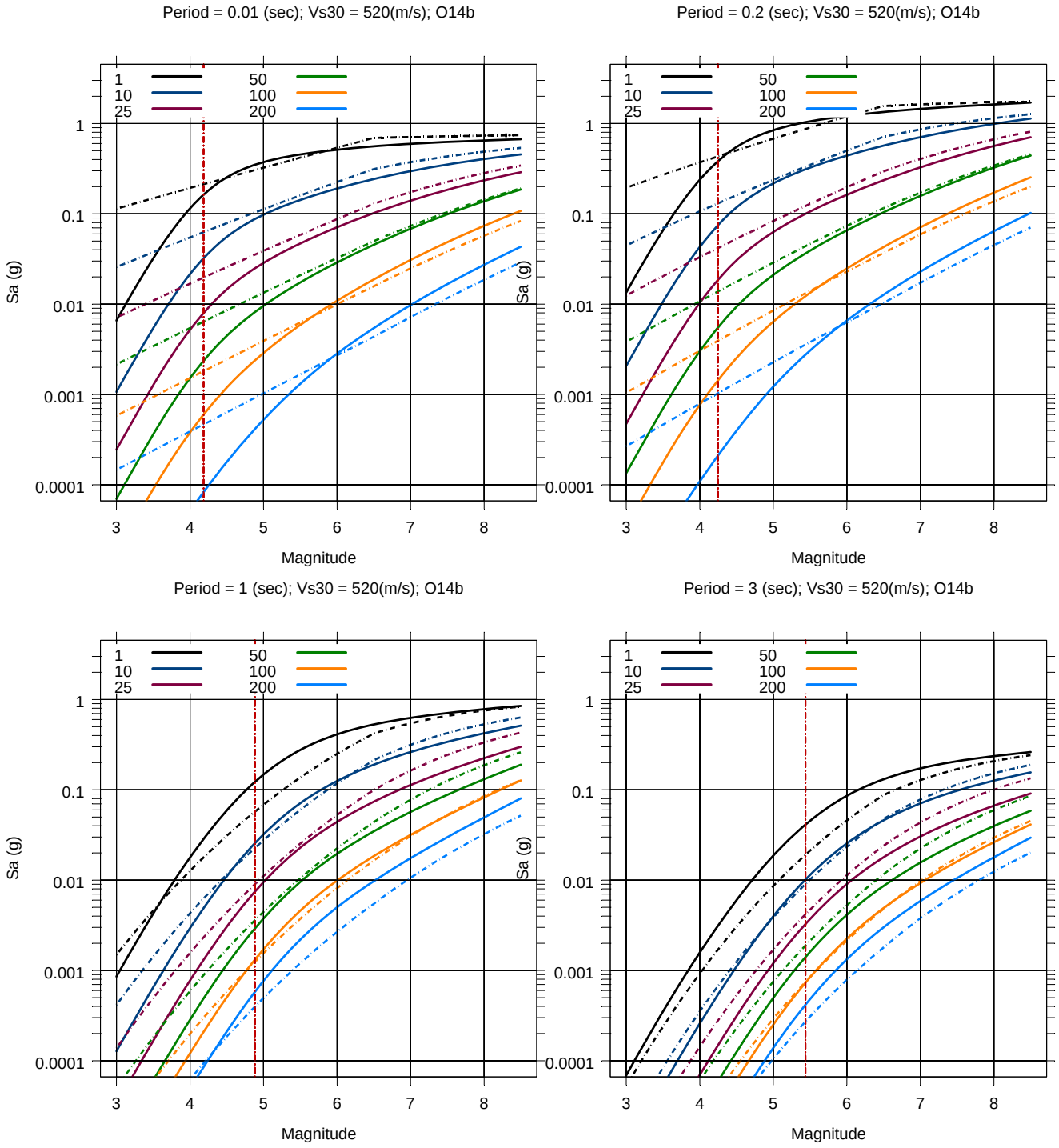

Figure 41: Comparison of magnitude scaling predicted by the model developed in this study (solid curves) and predicted by Sadigh et al. (1997) (dashed curves) for soft rock. A V_{S30} of 520 m/s was used to represent the average conditions for Sadigh et al.'s (1997) rock model.

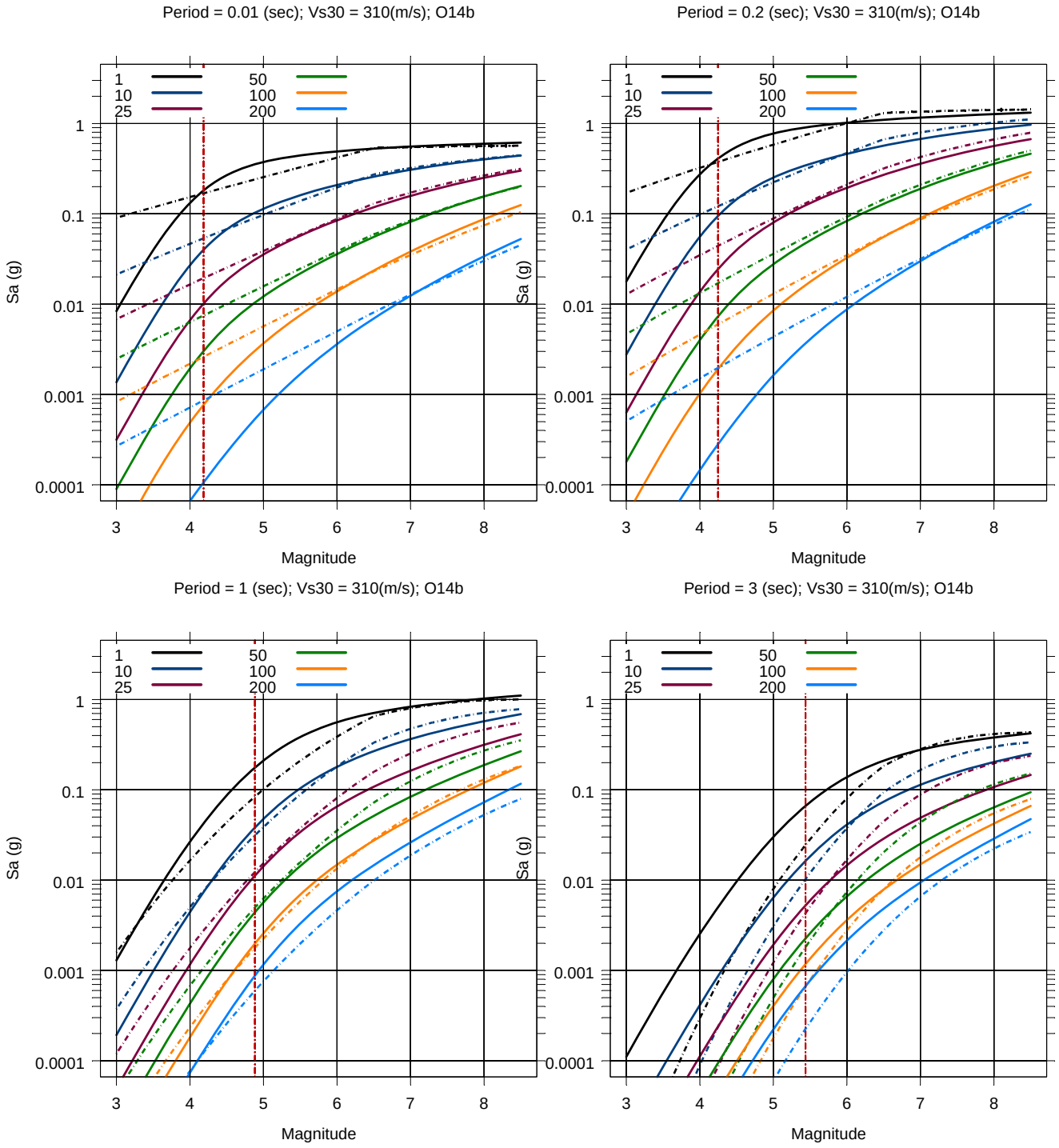

Figure 42: Comparison of magnitude scaling predicted by the model developed in this study (solid curves) and predicted by Sadigh et al. (1997) (dashed curves) for soil. A V_{S30} of 310 m/s was used to represent the average conditions for Sadigh et al.'s (1997) soil model.

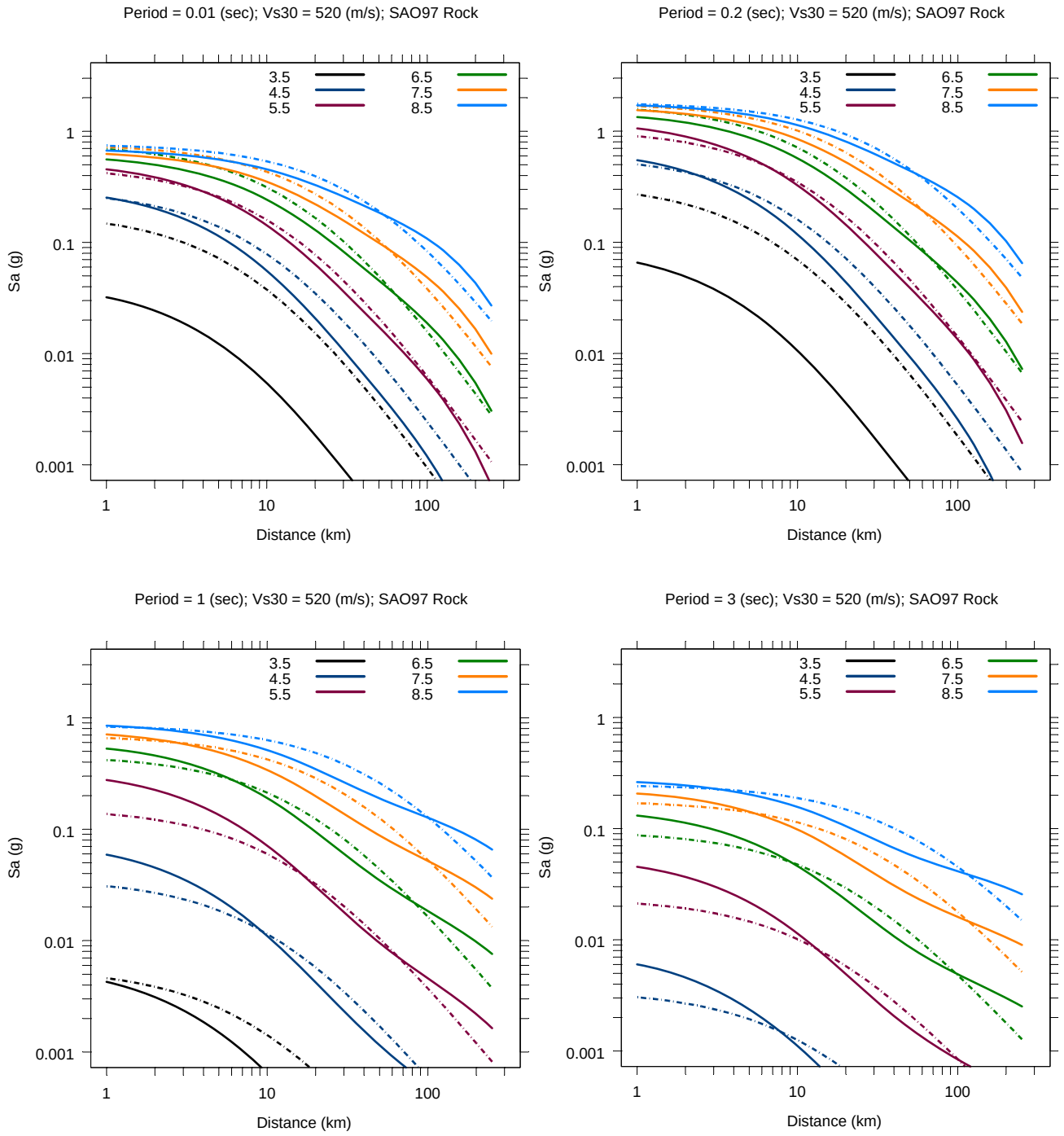

Figure 43: Comparison of distance scaling predicted by the model developed in this study (solid curves) and predicted by Sadigh et al. (1997) (dashed curves) for soft rock. A V_{S30} of 520 m/s was used to represent the average conditions for Sadigh et al.'s (1997) rock model.

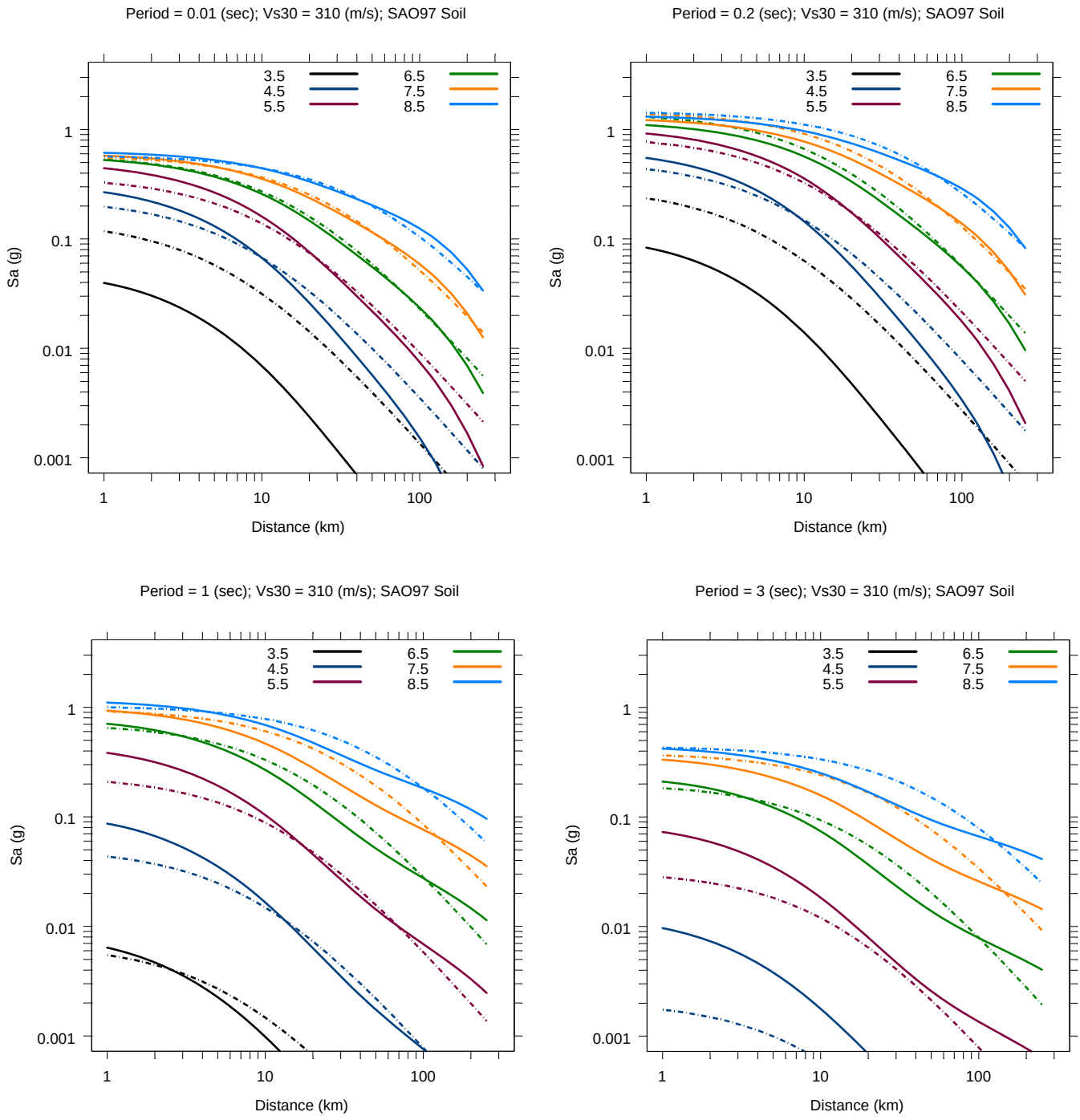

Figure 44: Comparison of distance scaling predicted by the model developed in this study (solid curves) and predicted by Sadigh et al. (1997) (dashed curves) for soil. A V_{S30} of 310 m/s was used to represent the average conditions for Sadigh et al.'s (1997) soil model.

<u>Comparison with Data at Distances > 70 km</u>: Figure 45 shows intra-event residuals for the two large California earthquakes that are in both the PEER-NGA data set and the extended TriNet data set. The residuals were computed using the event terms determined fro the regression of the PEER-NGA data for $R_{RUP} \leq 70$ km. The model fit to the data for $R_{RUP} \leq 70$ km does a reasonable job of predicting the ground motions at larger distances when extrapolated using the model for γ given in Equation (19).

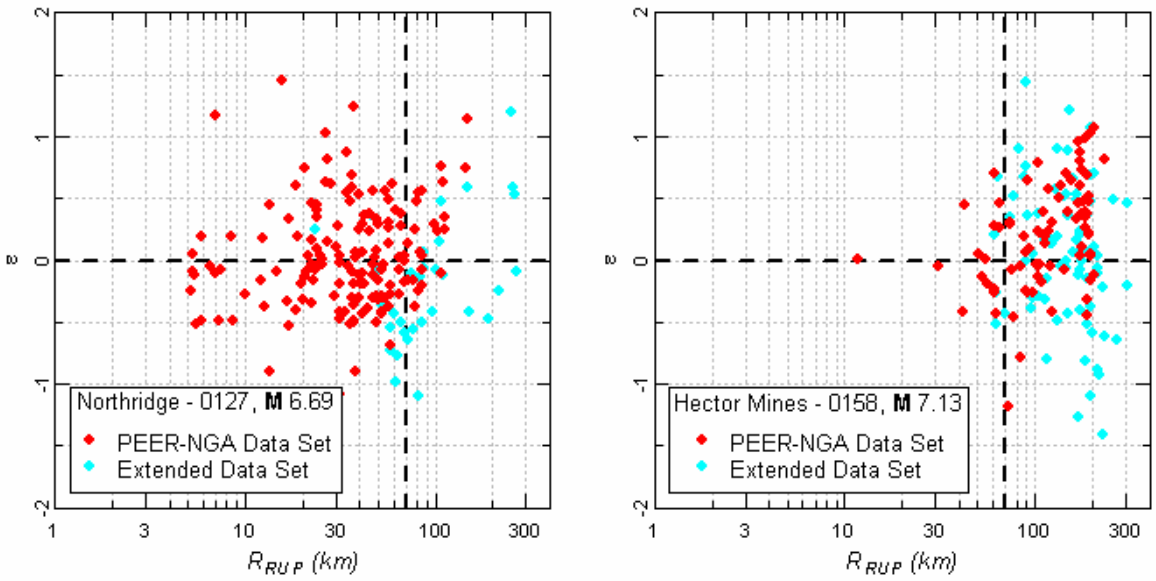

Figure 45: Intra-event residuals for the Northridge and Hector Mines *pga* data from the PEER-NGA and extended data sets. The residuals were computed using the event term for each earthquake determined in the overall regression of the PEER-NGA data for $R_{RUP} \leq 70$ km.

EXAMPLE CALCULATIONS

FORTRAN routine CY2006.FOR and the accompanying coefficients table file CY2006.C are provided to implement the model developed in this study. Example input and output files are provided for four scenarios: **M** 5 and **M** 7 strike-slip earthquakes and **M** 5 and **M** 7 reverse faulting earthquakes. The required input variables are indicated by the header record in the example input files. Note the routine reads a value for the source-site angle θ_{SITE}, but it is not presently used in the model. The routine accepts its main input and writes the output to the console. After invoking at the command prompt, the routine asks for the coefficient file and then loops over prompts for the input and output files.

Table 6 list the computed values of ground motion for the four example scenarios for spectral periods of 0.01, 0.2, 1.0, 3.0 seconds.

Table 6: Example Calculations

Period (sec)	***M***	R_{RUP}	V_{S30}	R_{JB}	*Width (km)*	F_{RV}	F_{NM}	Z_{TOR}	δ	SA_{1130} (g)	SA (g)
M 5 Strike Slip											
0.01	5	5	760	5	2.98	0	0	5	90	0.176143	0.209829
0.01	5	10	760	10	2.98	0	0	5	90	0.090143	0.108028
0.01	5	15	760	15	2.98	0	0	5	90	0.054094	0.065046
0.01	5	30	760	30	2.98	0	0	5	90	0.019356	0.023371
0.01	5	50	760	50	2.98	0	0	5	90	0.008551	0.010340
0.01	5	100	760	100	2.98	0	0	5	90	0.002559	0.003097
0.01	5	200	760	200	2.98	0	0	5	90	0.000469	0.000567
0.2	5	5	760	5	2.98	0	0	5	90	0.381812	0.461236
0.2	5	10	760	10	2.98	0	0	5	90	0.190465	0.232906
0.2	5	15	760	15	2.98	0	0	5	90	0.112706	0.138741
0.2	5	30	760	30	2.98	0	0	5	90	0.039643	0.049184
0.2	5	50	760	50	2.98	0	0	5	90	0.017440	0.021698
0.2	5	100	760	100	2.98	0	0	5	90	0.005271	0.006569
0.2	5	200	760	200	2.98	0	0	5	90	0.001001	0.001249
1	5	5	760	5	2.98	0	0	5	90	0.042062	0.057565
1	5	10	760	10	2.98	0	0	5	90	0.020717	0.028364
1	5	15	760	15	2.98	0	0	5	90	0.012403	0.016984
1	5	30	760	30	2.98	0	0	5	90	0.004750	0.006505
1	5	50	760	50	2.98	0	0	5	90	0.002427	0.003324
1	5	100	760	100	2.98	0	0	5	90	0.001108	0.001518
1	5	200	760	200	2.98	0	0	5	90	0.000495	0.000678
3	5	5	760	5	2.98	0	0	5	90	0.004184	0.006020
3	5	10	760	10	2.98	0	0	5	90	0.002059	0.002962
3	5	15	760	15	2.98	0	0	5	90	0.001238	0.001781
3	5	30	760	30	2.98	0	0	5	90	0.000485	0.000698
3	5	50	760	50	2.98	0	0	5	90	0.000257	0.000370
3	5	100	760	100	2.98	0	0	5	90	0.000130	0.000187
3	5	200	760	200	2.98	0	0	5	90	0.000072	0.000103
M 5 Reverse											
0.01	5	5	760	0	2.98	1	0	5	45	0.206129	0.245144
0.01	5	10	760	7.03	2.98	1	0	5	45	0.101354	0.121352
0.01	5	15	760	13.21	2.98	1	0	5	45	0.060198	0.072341
0.01	5	30	760	29.15	2.98	1	0	5	45	0.021427	0.025864
0.01	5	50	760	49.49	2.98	1	0	5	45	0.009456	0.011433
0.01	5	100	760	99.75	2.98	1	0	5	45	0.002828	0.003423
0.01	5	200	760	199.87	2.98	1	0	5	45	0.000518	0.000627
0.2	5	5	760	0	2.98	1	0	5	45	0.448670	0.540181
0.2	5	10	760	7.03	2.98	1	0	5	45	0.214421	0.261728

Table 6: Example Calculations

Period (sec)	***M***	R_{RUP}	V_{S30}	R_{JB}	*Width (km)*	F_{RV}	F_{NM}	Z_{TOR}	δ	SA_{1130} (g)	SA (g)
0.2	5	15	760	13.21	2.98	1	0	5	45	0.125488	0.154291
0.2	5	30	760	29.15	2.98	1	0	5	45	0.043890	0.054425
0.2	5	50	760	49.49	2.98	1	0	5	45	0.019286	0.023989
0.2	5	100	760	99.75	2.98	1	0	5	45	0.005826	0.007261
0.2	5	200	760	199.87	2.98	1	0	5	45	0.001107	0.001380
1	5	5	760	0	2.98	1	0	5	45	0.043114	0.059003
1	5	10	760	7.03	2.98	1	0	5	45	0.020773	0.028440
1	5	15	760	13.21	2.98	1	0	5	45	0.012366	0.016933
1	5	30	760	29.15	2.98	1	0	5	45	0.004722	0.006467
1	5	50	760	49.49	2.98	1	0	5	45	0.002411	0.003302
1	5	100	760	99.75	2.98	1	0	5	45	0.001101	0.001508
1	5	200	760	199.87	2.98	1	0	5	45	0.000492	0.000674
3	5	5	760	0	2.98	1	0	5	45	0.003811	0.005484
3	5	10	760	7.03	2.98	1	0	5	45	0.001867	0.002686
3	5	15	760	13.21	2.98	1	0	5	45	0.001121	0.001613
3	5	30	760	29.15	2.98	1	0	5	45	0.000439	0.000632
3	5	50	760	49.49	2.98	1	0	5	45	0.000233	0.000335
3	5	100	760	99.75	2.98	1	0	5	45	0.000118	0.000169
3	5	200	760	199.87	2.98	1	0	5	45	0.000065	0.000093
M 7 Strike Slip											
0.01	7	1	760	1	15	0	0	0	90	0.463402	0.545734
0.01	7	3	760	3	15	0	0	0	90	0.383809	0.453108
0.01	7	5	760	5	15	0	0	0	90	0.322935	0.382068
0.01	7	10	760	10	15	0	0	0	90	0.222043	0.263855
0.01	7	15	760	15	15	0	0	0	90	0.162970	0.194290
0.01	7	30	760	30	15	0	0	0	90	0.083725	0.100392
0.01	7	50	760	50	15	0	0	0	90	0.048374	0.058203
0.01	7	100	760	100	15	0	0	0	90	0.021465	0.025910
0.01	7	200	760	200	15	0	0	0	90	0.006741	0.008153
0.2	7	1	760	1	15	0	0	0	90	1.191088	1.400097
0.2	7	3	760	3	15	0	0	0	90	0.968443	1.144679
0.2	7	5	760	5	15	0	0	0	90	0.802274	0.952864
0.2	7	10	760	10	15	0	0	0	90	0.535453	0.642152
0.2	7	15	760	15	15	0	0	0	90	0.384799	0.464770
0.2	7	30	760	30	15	0	0	0	90	0.190554	0.233014
0.2	7	50	760	50	15	0	0	0	90	0.107702	0.132645
0.2	7	100	760	100	15	0	0	0	90	0.047088	0.058369
0.2	7	200	760	200	15	0	0	0	90	0.014938	0.018591
1	7	1	760	1	15	0	0	0	90	0.346583	0.473229
1	7	3	760	3	15	0	0	0	90	0.273912	0.374131
1	7	5	760	5	15	0	0	0	90	0.222119	0.303475
1	7	10	760	10	15	0	0	0	90	0.143489	0.196153
1	7	15	760	15	15	0	0	0	90	0.101703	0.139083
1	7	30	760	30	15	0	0	0	90	0.050992	0.069777
1	7	50	760	50	15	0	0	0	90	0.030852	0.042231
1	7	100	760	100	15	0	0	0	90	0.017184	0.023528
1	7	200	760	200	15	0	0	0	90	0.009468	0.012965
3	7	1	760	1	15	0	0	0	90	0.084565	0.121676
3	7	3	760	3	15	0	0	0	90	0.066542	0.095744
3	7	5	760	5	15	0	0	0	90	0.053799	0.077408
3	7	10	760	10	15	0	0	0	90	0.034632	0.049830
3	7	15	760	15	15	0	0	0	90	0.024545	0.035316
3	7	30	760	30	15	0	0	0	90	0.012419	0.017870
3	7	50	760	50	15	0	0	0	90	0.007672	0.011039
3	7	100	760	100	15	0	0	0	90	0.004553	0.006551
3	7	200	760	200	15	0	0	0	90	0.002877	0.004140
M 7 Reverse											

Table 6: Example Calculations

Period (sec)	***M***	R_{RUP}	V_{S30}	R_{JB}	*Width (km)*	F_{RV}	F_{NM}	Z_{TOR}	δ	SA_{1130} (g)	SA (g)
0.01	7	1	760	0	21.21	1	0	0	45	0.639258	0.749553
0.01	7	3	760	0	21.21	1	0	0	45	0.654854	0.767582
0.01	7	5	760	0	21.21	1	0	0	45	0.572953	0.672824
0.01	7	10	760	0	21.21	1	0	0	45	0.396471	0.467862
0.01	7	15	760	6.21	21.21	1	0	0	45	0.238586	0.283285
0.01	7	30	760	25.98	21.21	1	0	0	45	0.098676	0.118171
0.01	7	50	760	47.70	21.21	1	0	0	45	0.054655	0.065717
0.01	7	100	760	98.87	21.21	1	0	0	45	0.023852	0.028781
0.01	7	200	760	199.44	21.21	1	0	0	45	0.007460	0.009022
0.2	7	1	760	0	21.21	1	0	0	45	1.669724	1.944378
0.2	7	3	760	0	21.21	1	0	0	45	1.705223	1.984528
0.2	7	5	760	0	21.21	1	0	0	45	1.473110	1.721495
0.2	7	10	760	0	21.21	1	0	0	45	0.989930	1.169403
0.2	7	15	760	6.21	21.21	1	0	0	45	0.574944	0.688389
0.2	7	30	760	25.98	21.21	1	0	0	45	0.225632	0.275190
0.2	7	50	760	47.70	21.21	1	0	0	45	0.121882	0.149907
0.2	7	100	760	98.87	21.21	1	0	0	45	0.052344	0.064845
0.2	7	200	760	199.44	21.21	1	0	0	45	0.016533	0.020572
1	7	1	760	0	21.21	1	0	0	45	0.388935	0.530966
1	7	3	760	0	21.21	1	0	0	45	0.345553	0.471825
1	7	5	760	0	21.21	1	0	0	45	0.286310	0.391039
1	7	10	760	0	21.21	1	0	0	45	0.185606	0.253648
1	7	15	760	6.21	21.21	1	0	0	45	0.117929	0.161248
1	7	30	760	25.98	21.21	1	0	0	45	0.052472	0.071801
1	7	50	760	47.70	21.21	1	0	0	45	0.031018	0.042458
1	7	100	760	98.87	21.21	1	0	0	45	0.017119	0.023439
1	7	200	760	199.44	21.21	1	0	0	45	0.009411	0.012887
3	7	1	760	0	21.21	1	0	0	45	0.078509	0.112963
3	7	3	760	0	21.21	1	0	0	45	0.063312	0.091096
3	7	5	760	0	21.21	1	0	0	45	0.051419	0.073984
3	7	10	760	0	21.21	1	0	0	45	0.033124	0.047661
3	7	15	760	6.21	21.21	1	0	0	45	0.022944	0.033013
3	7	30	760	25.98	21.21	1	0	0	45	0.011322	0.016291
3	7	50	760	47.70	21.21	1	0	0	45	0.006960	0.010015
3	7	100	760	98.87	21.21	1	0	0	45	0.004123	0.005932
3	7	200	760	199.44	21.21	1	0	0	45	0.002604	0.003747

MODEL APPLICABILITY

The model developed in this study is considered to be applicable for estimation pseudo spectral accelerations (5% damping) for earthquakes in active tectonic regions in which the following conditions apply:

$4 \leq \mathbf{M} \leq 8.5$ for strike-slip earthquakes
$4 \leq \mathbf{M} \leq 8.0$ for reverse and normal faulting earthquakes
$0 \leq R_{RUP} \leq 200$ km
$150 \leq V_{S30} \leq 1500$.

The model was developed using the anelastic attenuation parameter γ constrained by data from California earthquakes. For application in other regions where distances greater than about 50 km are a major contributor to the hazard, the adjustments to the γ parameter may be warranted and can be performed using the hybrid approach developed by Campbell (2003).

In making such adjustments, we would stress the need for the user to obtain estimates of Q for the two regions that are based on consistent geometric spreading models. The site response portion of the ground motion model was constructed to force all ground motions to be the same for V_{S30} greater than 1130 m/s. As the rock velocity increases we expect the shallow crustal damping (i.e. "kappa") to decrease, resulting in increases in high frequency motions. Data for such sites are not present in the PEER-NGA data base and this effect is not captured in our model. The model was developed using recordings from earthquakes with a maximum depth to top of rupture of 15 km and a maximum hypocentral depth of 19 km. The model predicts a linear increase in ln(*psa*) with increasing Z_{TOR} over this range. Application of the model in regions with very thick crust (e.g. >> 20 km) is an extrapolation outside of the range of data used to develop the model parameters.

REFERENCES

Abrahamson, N.A., and Silva, W.J., 1997, Empirical response spectral attenuation relations for shallow crustal earthquakes, *Seismological Research Letters*, v. 68, p. 94-127.

Abrahamson, N.A., and P.G. Somerville, 1996, Effects of the hanging wall and footwall on the ground motions recorded during the Northridge earthquake, *Bulletin of the Seismological Society of America*, v.86, p. S93-S99.

Ambraseys, N.N, Simpson, K.A., and Bommer, J.J, 1996, Prediction of horizontal response spectra in Europe, *Earthquake Engineering and Structural Dynamics*, v. 25, p. 371-400.

Ambraseys, N.N., J Douglas, S.K. Sarma1, and P.M. Smit, 2005, Equations for the estimation of strong ground motions from shallow crustal earthquakes using data from Europe and the Middle East: horizontal peak ground acceleration and spectral acceleration, *Bulletin of Earthquake Engineering*, v 3, p. 1-35.

Atkinson, G.M., 1989, Attenuation of the Lg phase and site response for the Eastern Canada Telemetered Network, *Seismological Research Letters*, v.60, n. 2, p. 59-69.

Atkinson, G.M. and R. Mereu, 1992, The shape of ground motion attenuation curves in southeastern Canada, *Bulletin of the Seismological Society of America*, v.82, p. 2014-2031.

Atkinson, G.M. and W. Silva, 1997, An empirical study of earthquake source spectra for California earthquakes, *Bulletin of the Seismological Society of America*, v.87, p. 97-113.

Atkinson, G.M. and W. Silva, 2000, Stochastic modeling of California ground motions, *Bulletin of the Seismological Society of America*, v.90, p. 255-274.

Bazzurro, P. and C.A. Cornell, 2004, Ground-motion amplification in nonlinear soil sites with uncertain properties, *Bulletin of the Seismological Society of America*, v.94, p. 2090-2109.

Boatwright, J., H. Bundock, J. Luetgert, L. Seekins, L. Gee, and P. Lombard, 2003, The dependence of PGA and PGV on distance and magnitude inferred from northern California ShakeMap data, *Bulletin of the Seismological Society of America*, v. 93, p. 2043-2055.

Boore, D.M., 2003, Simulation of ground motion using the stochastic method, *Pure and Applied Geophysics*, v. 160, p. 635-676.

Boore, D.M., 2005, SMSIM – Fortran programs for simulating ground motions from earthquakes: Version 2.3-A revision of OFR 96-80-A: U.S. Geological Survey Open File Report 00-509, 15 August, 55 p.

Boore, D.M. and W.B. Joyner, 1997, Site amplification for generic rock sites, *Bulletin of the Seismological Society of America*, v.87, p. 327-341.

Boore, D.M., W.B, Joyner, and T.E. Fumal, 1993, Estimation of response spectra and peak accelerations from western North American earthquakes: an interim report, *U.S. Geological Survey Open-File Report 93-509*, 72 p.

Boore, D.M., W.B, Joyner, and T.E. Fumal, 1997, Equations for estimating horizontal response spectra and peak acceleration from western North American earthquakes–A summary of recent work, *Seismological Research Letters*, v. 68, p. 128-153.

Boore, D.M., J. Watson-Lamprey, and N.A. Abrahamson, 2006 (in press), Orientation-independent measures of ground motion, *Bulletin of the Seismological Society of America*, v. 96, in press.

Bragato, P.L., 2004, Regression analysis with truncated samples and its application to ground-motion attenuation studies, Bulletin of the Seismological Society of America, v. 94, p. 1369-1378.

Brillinger, D.R., and H.K. Preisler, 1984, An exploratory analysis of the Joyner-Boore attenuation data, *Bulletin of the Seismological Society of America*, v. 74, p. 1441-1450.

Brune, J., 1970, Tectonic stress and the spectra of seismic shear waves from earthquakes, *Journal of Geophysical Research*, v. 75, p. 4997-5009.

Brune, J., 1971, Correction, *Journal of Geophysical Research*, v. 76, p. 5002.

Campbell, K.W., 1993, Empirical prediction of near-source ground motion from large earthquakes, *Proceedings International Workshop on Earthquake Hazards and Large Dams in the Himalaya, January 15-16, New Deli India*.

Campbell, K.W., 1997, Empirical near-source attenuation relationships for horizontal and vertical components of peak ground acceleration, peak ground velocity, and pseudo-absolute acceleration response spectra, *Seismological Research Letters*, v. 68, p. 154-179.

Campbell, K., 2003, Prediction of strong ground motion using the hybrid empirical method and its use in the development of ground motion (attenuation) relations in eastern North America, *Bulletin of the Seismological Society of America*, v. 93, p. 1012-1033.

Campbell, K.W., and Y. Bozorgnia, 2003, Updated near-source ground-motion (attenuation) relations for the horizontal and vertical components of peak ground acceleration and acceleration response spectra, *Bulletin of the Seismological Society of America*, v.93, p. 314-331.

Chiou, S.-J., F.I. Makdisi, and R.R. Youngs, 2000, Style-of-faulting and footwall/hanging wall effects on strong ground motion, FY 1995 NEHRP Award Number 1434-95-G-2614, final report, 21 p.

Choi, Y., and J.P. Stewart, 2003, nonlinear site amplification as function of 30 m shear wave velocity, *Earthquake Spectra*, v. 21, p. 1-30.

Day, S.M., J. Bielak, D. Dreger, R. Graves, S. Larson, K.B. Olsen, A. Pitarka, and L. Ramirez-Guzman, 2006, Numerical simulation of basin effects on long-period ground motion, *Proceedings of the 8th National Conference on Earthquake Engineering*, April 18-22, San Francisco, California, USA, paper No. 1857.

EPRI, 1993, Guidelines for determining design basis ground motions, Electric Power Research Institute Report EPRI TR-102293, Vol. 1.

Erickson, D., D.E. McNamara, and H.M. Benz, 2004, Frequency-dependent *Lg Q* within the continental United States, *Bulletin of the Seismological Society of America*, v.94, p. 1630-1643.

Frankel, A., A. McGarr, J. Bicknell, J. Mori, L. Seeber, and E. Cranswick, 1990, Attenuation of high-frequency shear waves in the crust, measurements from New York State, South Africa, and southern California, *Journal of Geophysical Research*, v. 95, p. 17,441-17,457.

Fukushima, Y., and T. Tanaka, 1990, A new attenuation relation for peak horizontal acceleration of strong earthquake ground motion in Japan, *Bulletin of the Seismological Society of America*, v. 80, p. 757-783.

Fukushima, Y., K. Irikura, T. Uetake, and H. Matsumoto, 2000, Characteristics of observed peak amplitude for strong ground motion from the 1995 Hyogoken Nanbu (Kobe) earthquake, *Bulletin of the Seismological Society of America*, v. 90, p. 545-565.

Geomatrix, 1995, Seismic design mapping State of Oregon: Report prepared for the Oregon Department of Transportation, Personal Services Contract 11688, Geomatrix Consultants Project No. 2442, January.

Idriss, I.M., 1991, Procedures for selecting earthquake ground motions at rock sites, *National Institute of Standards and Technology*, Report No. NIST GCR 93-625.

Idriss, I.M., (2002) Personal Communication.

Magistrale, H., S.M. Day, R. Clayton, and R.W. Graves, 2000, The SCEC southern California reference three-dimensional seismic velocity model version 2, Bulletin of the Seismological Society of America, v. 90, p. S65-S76.

Mai, P.M., P. Spudich, and J. Boatwright, 2005, Hypocenter locations in finite-source rupture models, Bulletin of the Seismological Society of America, v. 95, p. 965-980.

Raoof, M., R. Herrmann, and L. Malagnini, 1999, Attenuation and excitation of three-component ground motion in southern California, *Bulletin of the Seismological Society of America*, v.89, p. 888-902.

Sabetta, F., and Pugliese, A., 1996, Estimation of response spectra and simulation of nonstationary earthquake ground motions, *Bulletin of the Seismological Society of America*, v. 86, p. 337-352.

Sadigh, K., Chang, C.-Y., Egan, J.A., Makdisi, F.I., and Youngs, R.R., 1997, Attenuation relationships for shallow crustal earthquakes based on California strong motion data, *Seismological Research Letters*, v. 68, no. 1, p. 180-189.

Sibson, R. H., and Xie, G., 1998, Dip range for intracontinental reverse fault ruptures: Truth not stranger than friction, *Bulletin of the Seismological Society of America*, v. 88, p. 1014-1022.

Silva, W.C., Abrahamson, N., Toro, G., and Costantino, C., 1996, Description and validation of the stochastic ground motion model: Report submitted to Brookhaven National Laboratory, Associated Universities, Inc., New York (available at www.pacificengineering.org).

Somerville, P.G., and N.A. Abrahamson, 1995, Prediction of ground motions for thrust earthquakes, Report to the California Strong Motion Instrumentation Program (CSMIP).

Somerville, P., N. Collins, R. Graves, A. Pitarka, W. Silva, and Y. Zeng, 2006, Simulation of ground motion scaling characteristics for the NGA-E project, *Proceedings of the 8th National*

Conference on Earthquake Engineering, April 18-22, San Francisco, California, USA, paper No. 1789.

Spudich, P., W.B. Joyner, A.G. Lindh, D.M. Boore, B.M. Margaris, and J.B. Fletcher, SEA99: a revised ground motion prediction relation for use in extensional tectonic regimes, *Bulletin of the Seismological Society of America*, v. 89, p. 1156-1170.

Silva, W., 2004, Site response simulations for the PEER-NGA project, Draft report to the Pacific Earthquake Engineering Research Center, with updated results in 2005.

Toro G.R., 1981, Biases in seismic ground motion prediction, Ph. D. Thesis, Dept. of Civil Eng., Massachusetts Inst. of Technology, 133 p.

Wells, D.L., and Coppersmith, K.J., 1994, New empirical relationships among magnitude, rupture length, rupture width, rupture area, and surface displacement, *Bulletin of the Seismological Society of America*, v. 84, p. 974-1002.

Youngs, R.R., 1993, Soil amplification and vertical to horizontal ratios for analysis of strong motion data from active tectonic regions, Appendix 2C in Guidelines for Determining Design Basis Ground Motions, Vol. 2: Appendices for Ground Motion Estimation, EPRI Report TR-102293.

Appendix A
Recordings from PEER-NGA Flatfile Version 7.2 Used in Developing Chiou and Youngs 2006 Empirical Ground Motion Model

RSN	EQID	Earthquake	M	Station No,	Station
12	0012	Kern County	7.36	24303	LA - Hollywood Stor FF
23	0020	San Francisco	5.28	1117	Golden Gate Park
28	0025	Parkfield	6.19	1016	Cholame - Shandon Array #12
30	0025	Parkfield	6.19	1014	Cholame - Shandon Array #5
31	0025	Parkfield	6.19	1015	Cholame - Shandon Array #8
33	0025	Parkfield	6.19	1438	Temblor pre-1969
37	0028	Borrego Mtn	6.63	24303	LA - Hollywood Stor FF
40	0028	Borrego Mtn	6.63	280	San Onofre - So Cal Edison
41	0029	Lytle Creek	5.33	24278	Castaic - Old Ridge Route
42	0029	Lytle Creek	5.33	112	Cedar Springs Pumphouse
43	0029	Lytle Creek	5.33	111	Cedar Springs, Allen Ranch
44	0029	Lytle Creek	5.33	113	Colton - So Cal Edison
45	0029	Lytle Creek	5.33	620	Devil's Canyon
46	0029	Lytle Creek	5.33	24303	LA - Hollywood Stor FF
47	0029	Lytle Creek	5.33	24271	Lake Hughes #1
48	0029	Lytle Creek	5.33	278	Puddingstone Dam (Abutment)
49	0029	Lytle Creek	5.33	104	Santa Anita Dam
50	0029	Lytle Creek	5.33	290	Wrightwood - 6074 Park Dr
51	0030	San Fernando	6.61	411	2516 Via Tejon PV
52	0030	San Fernando	6.61	103	Anza Post Office
54	0030	San Fernando	6.61	105	Borrego Springs Fire Sta
55	0030	San Fernando	6.61	1	Buena Vista - Taft
56	0030	San Fernando	6.61	108	Carbon Canyon Dam
57	0030	San Fernando	6.61	24278	Castaic - Old Ridge Route
58	0030	San Fernando	6.61	112	Cedar Springs Pumphouse
59	0030	San Fernando	6.61	111	Cedar Springs, Allen Ranch
60	0030	San Fernando	6.61	1013	Cholame - Shandon Array #2
61	0030	San Fernando	6.61	1015	Cholame - Shandon Array #8
62	0030	San Fernando	6.61	113	Colton - So Cal Edison
63	0030	San Fernando	6.61	121	Fairmont Dam
64	0030	San Fernando	6.61	998	Fort Tejon
65	0030	San Fernando	6.61	994	Gormon - Oso Pump Plant
66	0030	San Fernando	6.61	12331	Hemet Fire Station
67	0030	San Fernando	6.61	1035	Isabella Dam (Aux Abut)
68	0030	San Fernando	6.61	24303	LA - Hollywood Stor FF
70	0030	San Fernando	6.61	24271	Lake Hughes #1
71	0030	San Fernando	6.61	128	Lake Hughes #12
72	0030	San Fernando	6.61	126	Lake Hughes #4
73	0030	San Fernando	6.61	127	Lake Hughes #9
74	0030	San Fernando	6.61	1041	Maricopa Array #1
75	0030	San Fernando	6.61	1042	Maricopa Array #2
76	0030	San Fernando	6.61	1043	Maricopa Array #3
77	0030	San Fernando	6.61	279	Pacoima Dam (upper left abut)
78	0030	San Fernando	6.61	262	Palmdale Fire Station
81	0030	San Fernando	6.61	269	Pearblossom Pump
82	0030	San Fernando	6.61	272	Port Hueneme
83	0030	San Fernando	6.61	278	Puddingstone Dam (Abutment)
84	0030	San Fernando	6.61	314	San Diego Gas & Electric
85	0030	San Fernando	6.61	465	San Juan Capistrano
86	0030	San Fernando	6.61	280	San Onofre - So Cal Edison
87	0030	San Fernando	6.61	104	Santa Anita Dam
88	0030	San Fernando	6.61	285	Santa Felita Dam (Outlet)
89	0030	San Fernando	6.61	1027	Tehachapi Pump
91	0030	San Fernando	6.61	287	Upland - San Antonio Dam
92	0030	San Fernando	6.61	1102	Wheeler Ridge - Ground
93	0030	San Fernando	6.61	289	Whittier Narrows Dam
94	0030	San Fernando	6.61	290	Wrightwood - 6074 Park Dr
95	0031	Managua, Nicaragua-01	6.24	3501	Managua, ESSO
96	0032	Managua, Nicaragua-02	5.2	3501	Managua, ESSO
97	0033	Point Mugu	5.65	272	Port Hueneme
98	0034	Hollister-03	5.14	47379	Gilroy Array #1
100	0034	Hollister-03	5.14	47126	San Juan Bautista, 24 Polk St
106	0036	Oroville-01	5.89	1051	Oroville Seismograph Station

RSN	EQID	Earthquake	M	Station No,	Station
107	0037	Oroville-02	4.79	1545	Oroville Airport
108	0037	Oroville-02	4.79	1546	Up & Down Cafe (OR1)
109	0038	Oroville-04	4.37	1544	Medical Center
110	0038	Oroville-04	4.37	1545	Oroville Airport
111	0038	Oroville-04	4.37	1546	Up & Down Cafe (OR1)
112	0039	Oroville-03	4.7	1542	Broadbeck Residence
113	0039	Oroville-03	4.7	1543	DWR Garage
114	0039	Oroville-03	4.7	1550	Duffy Residence (OR5)
115	0039	Oroville-03	4.7	1493	Johnson Ranch
116	0039	Oroville-03	4.7	1496	Nelson Ranch (OR7)
117	0039	Oroville-03	4.7	1545	Oroville Airport
118	0039	Oroville-03	4.7	1549	Pacific Heights Rd (OR4)
119	0039	Oroville-03	4.7	1551	Summit Ave (OR6)
120	0039	Oroville-03	4.7	1546	Up & Down Cafe (OR1)
121	0040	Friuli, Italy-01	6.5	8002	Barcis
122	0040	Friuli, Italy-01	6.5	8004	Codroipo
123	0040	Friuli, Italy-01	6.5	8005	Conegliano
124	0040	Friuli, Italy-01	6.5	8007	Feltre
125	0040	Friuli, Italy-01	6.5	8012	Tolmezzo
126	0041	Gazli, USSR	6.8	9201	Karakyr
127	0042	Fruili, Italy-03	5.5	8023	Buia
128	0042	Fruili, Italy-03	5.5	8014	Forgaria Cornino
129	0042	Fruili, Italy-03	5.5	8022	San Rocco
130	0043	Friuli, Italy-02	5.91	8023	Buia
131	0043	Friuli, Italy-02	5.91	8004	Codroipo
132	0043	Friuli, Italy-02	5.91	8014	Forgaria Cornino
133	0043	Friuli, Italy-02	5.91	8022	San Rocco
134	0044	Izmir, Turkey	5.3	99999	Izmir
135	0045	Santa Barbara	5.92	106	Cachuma Dam Toe
137	0046	Tabas, Iran	7.35	69	Bajestan
138	0046	Tabas, Iran	7.35	70	Boshrooyeh
139	0046	Tabas, Iran	7.35	9102	Dayhook
140	0046	Tabas, Iran	7.35	71	Ferdows
141	0046	Tabas, Iran	7.35	72	Kashmar
142	0046	Tabas, Iran	7.35	73	Sedeh
143	0046	Tabas, Iran	7.35	9101	Tabas
144	0047	Dursunbey, Turkey	5.34	99999	Dursunbey
145	0048	Coyote Lake	5.74	57217	Coyote Lake Dam (SW Abut)
146	0048	Coyote Lake	5.74	47379	Gilroy Array #1
147	0048	Coyote Lake	5.74	47380	Gilroy Array #2
148	0048	Coyote Lake	5.74	47381	Gilroy Array #3
149	0048	Coyote Lake	5.74	57382	Gilroy Array #4
150	0048	Coyote Lake	5.74	57383	Gilroy Array #6
151	0048	Coyote Lake	5.74	57191	Halls Valley
152	0048	Coyote Lake	5.74	47315	SJB Overpass, Bent 3 g.l.
153	0048	Coyote Lake	5.74	47315	SJB Overpass, Bent 5 g.l.
154	0048	Coyote Lake	5.74	47126	San Juan Bautista, 24 Polk St
155	0049	Norcia, Italy	5.9	99999	Bevagna
156	0049	Norcia, Italy	5.9	99999	Cascia
157	0049	Norcia, Italy	5.9	99999	Spoleto
158	0050	Imperial Valley-06	6.53	6616	Aeropuerto Mexicali
159	0050	Imperial Valley-06	6.53	6618	Agrarias
160	0050	Imperial Valley-06	6.53	5054	Bonds Corner
161	0050	Imperial Valley-06	6.53	5060	Brawley Airport
162	0050	Imperial Valley-06	6.53	5053	Calexico Fire Station
163	0050	Imperial Valley-06	6.53	5061	Calipatria Fire Station
164	0050	Imperial Valley-06	6.53	6604	Cerro Prieto
165	0050	Imperial Valley-06	6.53	6621	Chihuahua
166	0050	Imperial Valley-06	6.53	5066	Coachella Canal #4
167	0050	Imperial Valley-06	6.53	6622	Compuertas
169	0050	Imperial Valley-06	6.53	6605	Delta
170	0050	Imperial Valley-06	6.53	01136	EC County Center FF
171	0050	Imperial Valley-06	6.53	1336	EC Meloland Overpass FF
172	0050	Imperial Valley-06	6.53	5056	El Centro Array #1
173	0050	Imperial Valley-06	6.53	412	El Centro Array #10
174	0050	Imperial Valley-06	6.53	5058	El Centro Array #11
175	0050	Imperial Valley-06	6.53	931	El Centro Array #12
176	0050	Imperial Valley-06	6.53	5059	El Centro Array #13
178	0050	Imperial Valley-06	6.53	5057	El Centro Array #3

RSN	EQID	Earthquake	M	Station No,	Station
179	0050	Imperial Valley-06	6.53	955	El Centro Array #4
180	0050	Imperial Valley-06	6.53	952	El Centro Array #5
181	0050	Imperial Valley-06	6.53	5158	El Centro Array #6
182	0050	Imperial Valley-06	6.53	5028	El Centro Array #7
183	0050	Imperial Valley-06	6.53	958	El Centro Array #8
184	0050	Imperial Valley-06	6.53	5165	El Centro Differential Array
185	0050	Imperial Valley-06	6.53	5055	Holtville Post Office
186	0050	Imperial Valley-06	6.53	11023	Niland Fire Station
187	0050	Imperial Valley-06	6.53	5051	Parachute Test Site
188	0050	Imperial Valley-06	6.53	5052	Plaster City
189	0050	Imperial Valley-06	6.53	6619	SAHOP Casa Flores
190	0050	Imperial Valley-06	6.53	286	Superstition Mtn Camera
191	0050	Imperial Valley-06	6.53	6610	Victoria
192	0050	Imperial Valley-06	6.53	11369	Westmorland Fire Sta
193	0051	Imperial Valley-07	5.01	5054	Bonds Corner
194	0051	Imperial Valley-07	5.01	5060	Brawley Airport
195	0051	Imperial Valley-07	5.01	5053	Calexico Fire Station
196	0051	Imperial Valley-07	5.01	6605	Delta
197	0051	Imperial Valley-07	5.01	5056	El Centro Array #1
198	0051	Imperial Valley-07	5.01	412	El Centro Array #10
199	0051	Imperial Valley-07	5.01	5058	El Centro Array #11
200	0051	Imperial Valley-07	5.01	5115	El Centro Array #2
201	0051	Imperial Valley-07	5.01	5057	El Centro Array #3
202	0051	Imperial Valley-07	5.01	955	El Centro Array #4
203	0051	Imperial Valley-07	5.01	952	El Centro Array #5
204	0051	Imperial Valley-07	5.01	5158	El Centro Array #6
205	0051	Imperial Valley-07	5.01	5028	El Centro Array #7
206	0051	Imperial Valley-07	5.01	958	El Centro Array #8
207	0051	Imperial Valley-07	5.01	5165	El Centro Differential Array
208	0051	Imperial Valley-07	5.01	5055	Holtville Post Office
209	0052	Imperial Valley-08	5.62	11369	Westmorland Fire Sta
210	0053	Livermore-01	5.8	58219	APEEL 3E Hayward CSUH
212	0053	Livermore-01	5.8	1265	Del Valle Dam (Toe)
213	0053	Livermore-01	5.8	57064	Fremont - Mission San Jose
214	0053	Livermore-01	5.8	57187	San Ramon - Eastman Kodak
215	0053	Livermore-01	5.8	57134	San Ramon Fire Station
216	0053	Livermore-01	5.8	57063	Tracy - Sewage Treatm Plant
217	0054	Livermore-02	5.42	58219	APEEL 3E Hayward CSUH
219	0054	Livermore-02	5.42	1265	Del Valle Dam (Toe)
220	0054	Livermore-02	5.42	57064	Fremont - Mission San Jose
221	0054	Livermore-02	5.42	57T01	Livermore - Fagundas Ranch
222	0054	Livermore-02	5.42	57T02	Livermore - Morgan Terr Park
223	0054	Livermore-02	5.42	57187	San Ramon - Eastman Kodak
224	0054	Livermore-02	5.42	57134	San Ramon Fire Station
225	0055	Anza (Horse Canyon)-01	5.19	5044	Anza - Pinyon Flat
226	0055	Anza (Horse Canyon)-01	5.19	5045	Anza - Terwilliger Valley
227	0055	Anza (Horse Canyon)-01	5.19	5160	Anza Fire Station
228	0055	Anza (Horse Canyon)-01	5.19	5049	Borrego Air Ranch
229	0055	Anza (Horse Canyon)-01	5.19	5047	Rancho De Anza
230	0056	Mammoth Lakes-01	6.06	54099	Convict Creek
231	0056	Mammoth Lakes-01	6.06	54214	Long Valley Dam (Upr L Abut)
232	0056	Mammoth Lakes-01	6.06	54301	Mammoth Lakes H. S.
233	0057	Mammoth Lakes-02	5.69	54099	Convict Creek
234	0057	Mammoth Lakes-02	5.69	54214	Long Valley Dam (Upr L Abut)
235	0057	Mammoth Lakes-02	5.69	54301	Mammoth Lakes H. S.
236	0058	Mammoth Lakes-03	5.91	54099	Convict Creek
237	0058	Mammoth Lakes-03	5.91	54214	Long Valley Dam (Downst)
238	0058	Mammoth Lakes-03	5.91	54214	Long Valley Dam (L Abut)
239	0058	Mammoth Lakes-03	5.91	54214	Long Valley Dam (Upr L Abut)
240	0059	Mammoth Lakes-04	5.7	54099	Convict Creek
241	0059	Mammoth Lakes-04	5.7	54214	Long Valley Dam (Downst)
242	0059	Mammoth Lakes-04	5.7	54214	Long Valley Dam (L Abut)
243	0059	Mammoth Lakes-04	5.7	54214	Long Valley Dam (Upr L Abut)
244	0060	Mammoth Lakes-05	5.7	54099	Convict Creek
245	0060	Mammoth Lakes-05	5.7	54214	Long Valley Dam (Upr L Abut)
246	0061	Mammoth Lakes-06	5.94	54100	Benton
247	0061	Mammoth Lakes-06	5.94	54424	Bishop - Paradise Lodge
248	0061	Mammoth Lakes-06	5.94	54099	Convict Creek
249	0061	Mammoth Lakes-06	5.94	43	Fish & Game (FIS)

RSN	EQID	Earthquake	M	Station No,	Station
250	0061	Mammoth Lakes-06	5.94	54214	Long Valley Dam (Upr L Abut)
251	0062	Mammoth Lakes-07	4.73	43	Fish & Game (FIS)
252	0062	Mammoth Lakes-07	4.73	3	Green Church
253	0062	Mammoth Lakes-07	4.73	35	Long Valley Fire Sta
254	0062	Mammoth Lakes-07	4.73	36	Mammoth Elem School
255	0062	Mammoth Lakes-07	4.73	34	USC Cash Baugh Ranch
256	0062	Mammoth Lakes-07	4.73	37	USC McGee Creek Inn
257	0063	Mammoth Lakes-08	4.8	41	Cashbaugh (CBR)
258	0063	Mammoth Lakes-08	4.8	42	Convict Lakes (CON)
259	0063	Mammoth Lakes-08	4.8	43	Fish & Game (FIS)
261	0063	Mammoth Lakes-08	4.8	35	Long Valley Fire Sta
262	0063	Mammoth Lakes-08	4.8	36	Mammoth Elem School
263	0063	Mammoth Lakes-08	4.8	40	USC Convict Lakes
264	0063	Mammoth Lakes-08	4.8	37	USC McGee Creek Inn
265	0064	Victoria, Mexico	6.33	6604	Cerro Prieto
266	0064	Victoria, Mexico	6.33	6621	Chihuahua
268	0064	Victoria, Mexico	6.33	6619	SAHOP Casa Flores
269	0064	Victoria, Mexico	6.33	6624	Victoria Hospital Sotano
270	0065	Mammoth Lakes-09	4.85	42	Convict Lakes (CON)
271	0065	Mammoth Lakes-09	4.85	43	Fish & Game (FIS)
272	0065	Mammoth Lakes-09	4.85	3	Green Church
273	0065	Mammoth Lakes-09	4.85	44	Hot Creek (HCF)
274	0065	Mammoth Lakes-09	4.85	35	Long Valley Fire Sta
275	0065	Mammoth Lakes-09	4.85	36	Mammoth Elem School
276	0065	Mammoth Lakes-09	4.85	45	McGee Creek (MGE)
277	0065	Mammoth Lakes-09	4.85	40	USC Convict Lakes
278	0065	Mammoth Lakes-09	4.85	52	USC McGee Creek
283	0068	Irpinia, Italy-01	6.9	99999	Arienzo
284	0068	Irpinia, Italy-01	6.9	99999	Auletta
285	0068	Irpinia, Italy-01	6.9	99999	Bagnoli Irpinio
286	0068	Irpinia, Italy-01	6.9	99999	Bisaccia
287	0068	Irpinia, Italy-01	6.9	99999	Bovino
288	0068	Irpinia, Italy-01	6.9	99999	Brienza
289	0068	Irpinia, Italy-01	6.9	99999	Calitri
290	0068	Irpinia, Italy-01	6.9	99999	Mercato San Severino
291	0068	Irpinia, Italy-01	6.9	99999	Rionero In Vulture
292	0068	Irpinia, Italy-01	6.9	99999	Sturno
293	0068	Irpinia, Italy-01	6.9	99999	Torre Del Greco
294	0068	Irpinia, Italy-01	6.9	99999	Tricarico
295	0069	Irpinia, Italy-02	6.2	99999	Auletta
296	0069	Irpinia, Italy-02	6.2	99999	Bagnoli Irpinio
297	0069	Irpinia, Italy-02	6.2	99999	Bisaccia
298	0069	Irpinia, Italy-02	6.2	99999	Bovino
299	0069	Irpinia, Italy-02	6.2	99999	Brienza
300	0069	Irpinia, Italy-02	6.2	99999	Calitri
301	0069	Irpinia, Italy-02	6.2	99999	Mercato San Severino
302	0069	Irpinia, Italy-02	6.2	99999	Rionero In Vulture
303	0069	Irpinia, Italy-02	6.2	99999	Sturno
304	0069	Irpinia, Italy-02	6.2	99999	Tricarico
305	0070	Irpinia, Italy-03	4.7	99999	Conza (Base)
313	0072	Corinth, Greece	6.6	99999	Corinth
314	0073	Westmorland	5.9	5060	Brawley Airport
315	0073	Westmorland	5.9	11023	Niland Fire Station
316	0073	Westmorland	5.9	5051	Parachute Test Site
317	0073	Westmorland	5.9	5062	Salton Sea Wildlife Refuge
318	0073	Westmorland	5.9	286	Superstition Mtn Camera
319	0073	Westmorland	5.9	11369	Westmorland Fire Sta
320	0074	Mammoth Lakes-10	5.34	54099	Convict Creek
321	0075	Mammoth Lakes-11	5.31	54099	Convict Creek
322	0076	Coalinga-01	6.36	46314	Cantua Creek School
323	0076	Coalinga-01	6.36	36229	Parkfield - Cholame 12W
324	0076	Coalinga-01	6.36	36452	Parkfield - Cholame 1E
325	0076	Coalinga-01	6.36	36230	Parkfield - Cholame 2E
326	0076	Coalinga-01	6.36	36228	Parkfield - Cholame 2WA
327	0076	Coalinga-01	6.36	36450	Parkfield - Cholame 3E
328	0076	Coalinga-01	6.36	36410	Parkfield - Cholame 3W
329	0076	Coalinga-01	6.36	36412	Parkfield - Cholame 4AW
330	0076	Coalinga-01	6.36	36411	Parkfield - Cholame 4W
331	0076	Coalinga-01	6.36	36227	Parkfield - Cholame 5W

RSN	EQID	Earthquake	M	Station No,	Station
332	0076	Coalinga-01	6.36	36451	Parkfield - Cholame 6W
333	0076	Coalinga-01	6.36	36226	Parkfield - Cholame 8W
334	0076	Coalinga-01	6.36	36407	Parkfield - Fault Zone 1
335	0076	Coalinga-01	6.36	36444	Parkfield - Fault Zone 10
336	0076	Coalinga-01	6.36	36453	Parkfield - Fault Zone 11
337	0076	Coalinga-01	6.36	36138	Parkfield - Fault Zone 12
338	0076	Coalinga-01	6.36	36456	Parkfield - Fault Zone 14
339	0076	Coalinga-01	6.36	36445	Parkfield - Fault Zone 15
340	0076	Coalinga-01	6.36	36457	Parkfield - Fault Zone 16
341	0076	Coalinga-01	6.36	36413	Parkfield - Fault Zone 2
342	0076	Coalinga-01	6.36	36408	Parkfield - Fault Zone 3
343	0076	Coalinga-01	6.36	36414	Parkfield - Fault Zone 4
344	0076	Coalinga-01	6.36	36454	Parkfield - Fault Zone 6
345	0076	Coalinga-01	6.36	36431	Parkfield - Fault Zone 7
346	0076	Coalinga-01	6.36	36449	Parkfield - Fault Zone 8
347	0076	Coalinga-01	6.36	36443	Parkfield - Fault Zone 9
348	0076	Coalinga-01	6.36	36415	Parkfield - Gold Hill 1W
349	0076	Coalinga-01	6.36	36421	Parkfield - Gold Hill 2E
350	0076	Coalinga-01	6.36	36416	Parkfield - Gold Hill 2W
351	0076	Coalinga-01	6.36	36439	Parkfield - Gold Hill 3E
352	0076	Coalinga-01	6.36	36420	Parkfield - Gold Hill 3W
353	0076	Coalinga-01	6.36	36433	Parkfield - Gold Hill 4W
354	0076	Coalinga-01	6.36	36434	Parkfield - Gold Hill 5W
355	0076	Coalinga-01	6.36	36432	Parkfield - Gold Hill 6W
356	0076	Coalinga-01	6.36	36422	Parkfield - Stone Corral 2E
357	0076	Coalinga-01	6.36	36437	Parkfield - Stone Corral 3E
358	0076	Coalinga-01	6.36	36438	Parkfield - Stone Corral 4E
359	0076	Coalinga-01	6.36	36455	Parkfield - Vineyard Cany 1E
360	0076	Coalinga-01	6.36	36448	Parkfield - Vineyard Cany 1W
362	0076	Coalinga-01	6.36	36447	Parkfield - Vineyard Cany 2W
363	0076	Coalinga-01	6.36	36176	Parkfield - Vineyard Cany 3W
364	0076	Coalinga-01	6.36	36446	Parkfield - Vineyard Cany 4W
366	0076	Coalinga-01	6.36	36441	Parkfield - Vineyard Cany 6W
368	0076	Coalinga-01	6.36	1162	Pleasant Valley P.P. - yard
369	0076	Coalinga-01	6.36	46175	Slack Canyon
370	0077	Coalinga-02	5.09	4	ALP (temp)
371	0077	Coalinga-02	5.09	46T05	Anticline Ridge - Palmer Ave
372	0077	Coalinga-02	5.09	1607	Anticline Ridge Free-Field
373	0077	Coalinga-02	5.09	1607	Anticline Ridge Pad
374	0077	Coalinga-02	5.09	1606	Burnett Construction
375	0077	Coalinga-02	5.09	46617	Coalinga-14th & Elm (Old CHP)
376	0077	Coalinga-02	5.09	46T07	Harris Ranch - Hdqtrs (temp)
377	0077	Coalinga-02	5.09	5	LLN (temp)
379	0077	Coalinga-02	5.09	1604	Oil City
380	0077	Coalinga-02	5.09	46T06	Oil Fields - Skunk Hollow
381	0077	Coalinga-02	5.09	1608	Oil Fields Fire Station
382	0077	Coalinga-02	5.09	1609	Palmer Ave
383	0077	Coalinga-02	5.09	1162	Pleasant Valley P.P. - yard
384	0077	Coalinga-02	5.09	7	SGT (temp)
385	0077	Coalinga-02	5.09	8	SUB (temp)
386	0077	Coalinga-02	5.09	1605	Skunk Hollow
387	0077	Coalinga-02	5.09	47T03	Sulphur Baths (temp)
388	0077	Coalinga-02	5.09	9	TRA (temp)
389	0077	Coalinga-02	5.09	10	VEW (temp)
390	0077	Coalinga-02	5.09	11	YUB (temp)
391	0078	Coalinga-03	5.38	1606	Burnett Construction
392	0078	Coalinga-03	5.38	46617	Coalinga-14th & Elm (Old CHP)
393	0078	Coalinga-03	5.38	47T03	Sulphur Baths (temp)
394	0079	Coalinga-04	5.18	1607	Anticline Ridge Free-Field
395	0079	Coalinga-04	5.18	1607	Anticline Ridge Pad
396	0079	Coalinga-04	5.18	1606	Burnett Construction
397	0079	Coalinga-04	5.18	46617	Coalinga-14th & Elm (Old CHP)
398	0079	Coalinga-04	5.18	1604	Oil City
399	0079	Coalinga-04	5.18	1608	Oil Fields Fire Station - FF
400	0079	Coalinga-04	5.18	1608	Oil Fields Fire Station - Pad
401	0079	Coalinga-04	5.18	1609	Palmer Ave
402	0079	Coalinga-04	5.18	1605	Skunk Hollow
403	0079	Coalinga-04	5.18	47T03	Sulphur Baths (temp)
404	0079	Coalinga-04	5.18	1651	Transmitter Hill

RSN	EQID	Earthquake	M	Station No,	Station
405	0080	Coalinga-05	5.77	1606	Burnett Construction
406	0080	Coalinga-05	5.77	46617	Coalinga-14th & Elm (Old CHP)
407	0080	Coalinga-05	5.77	1604	Oil City
408	0080	Coalinga-05	5.77	1608	Oil Fields Fire Station - FF
409	0080	Coalinga-05	5.77	1608	Oil Fields Fire Station - Pad
410	0080	Coalinga-05	5.77	1609	Palmer Ave
411	0080	Coalinga-05	5.77	1162	Pleasant Valley P.P. - FF
412	0080	Coalinga-05	5.77	1162	Pleasant Valley P.P. - yard
413	0080	Coalinga-05	5.77	1605	Skunk Hollow
414	0080	Coalinga-05	5.77	47T03	Sulphur Baths (temp)
415	0080	Coalinga-05	5.77	1651	Transmitter Hill
416	0081	Coalinga-06	4.89	46617	Coalinga-14th & Elm (Old CHP)
417	0081	Coalinga-06	4.89	47T03	Sulphur Baths (temp)
418	0082	Coalinga-07	5.21	46617	Coalinga-14th & Elm (Old CHP)
419	0082	Coalinga-07	5.21	47T03	Sulphur Baths (temp)
420	0083	Ierissos, Greece	6.7	99999	Ierissos
423	0085	Coalinga-08	5.23	46617	Coalinga-14th & Elm (Old CHP)
424	0085	Coalinga-08	5.23	47T03	Sulphur Baths (temp)
437	0087	Borah Peak, ID-01	6.88	99999	CPP-610
439	0087	Borah Peak, ID-01	6.88	99999	TAN-719
442	0088	Borah Peak, ID-02	5.1	99999	BOR
443	0088	Borah Peak, ID-02	5.1	99999	CEM
444	0088	Borah Peak, ID-02	5.1	99999	HAU
445	0089	New Zealand-01	5.5	081A	Turangi Telephone Exchange
446	0090	Morgan Hill	6.19	58376	APEEL 1E - Hayward
447	0090	Morgan Hill	6.19	57066	Agnews State Hospital
448	0090	Morgan Hill	6.19	1652	Anderson Dam (Downstream)
449	0090	Morgan Hill	6.19	47125	Capitola
450	0090	Morgan Hill	6.19	57007	Corralitos
451	0090	Morgan Hill	6.19	57217	Coyote Lake Dam (SW Abut)
452	0090	Morgan Hill	6.19	58375	Foster City - APEEL 1
453	0090	Morgan Hill	6.19	57064	Fremont - Mission San Jose
454	0090	Morgan Hill	6.19	47006	Gilroy - Gavilan Coll.
455	0090	Morgan Hill	6.19	47379	Gilroy Array #1
456	0090	Morgan Hill	6.19	47380	Gilroy Array #2
457	0090	Morgan Hill	6.19	47381	Gilroy Array #3
458	0090	Morgan Hill	6.19	57382	Gilroy Array #4
459	0090	Morgan Hill	6.19	57383	Gilroy Array #6
460	0090	Morgan Hill	6.19	57425	Gilroy Array #7
461	0090	Morgan Hill	6.19	57191	Halls Valley
463	0090	Morgan Hill	6.19	1656	Hollister Diff Array #1
464	0090	Morgan Hill	6.19	1656	Hollister Diff Array #3
465	0090	Morgan Hill	6.19	1656	Hollister Diff Array #4
466	0090	Morgan Hill	6.19	1656	Hollister Diff Array #5
467	0090	Morgan Hill	6.19	1656	Hollister Diff. Array
468	0090	Morgan Hill	6.19	56012	Los Banos
469	0090	Morgan Hill	6.19	58223	SF Intern. Airport
470	0090	Morgan Hill	6.19	47126	San Juan Bautista, 24 Polk St
471	0090	Morgan Hill	6.19	1655	San Justo Dam (L Abut)
472	0090	Morgan Hill	6.19	1655	San Justo Dam (R Abut)
476	0090	Morgan Hill	6.19	58135	UCSC Lick Observatory
477	0091	Lazio-Abruzzo, Italy	5.8	99999	Atina
478	0091	Lazio-Abruzzo, Italy	5.8	99999	Garigliano-Centrale Nucleare
479	0091	Lazio-Abruzzo, Italy	5.8	99999	Isernia-Sant'Agapito
480	0091	Lazio-Abruzzo, Italy	5.8	99999	Pontecorvo
481	0091	Lazio-Abruzzo, Italy	5.8	99999	Roccamonfina
485	0094	Bishop (Rnd Val)	5.82	1661	McGee Creek - Surface
494	0096	Drama, Greece	5.2	99999	Kavala
495	0097	Nahanni, Canada	6.76	6097	Site 1
496	0097	Nahanni, Canada	6.76	6098	Site 2
497	0097	Nahanni, Canada	6.76	6099	Site 3
498	0098	Hollister-04	5.45	1656	Hollister Diff Array #1
499	0098	Hollister-04	5.45	1656	Hollister Diff Array #3
501	0098	Hollister-04	5.45	47189	SAGO South - Surface
502	0099	Mt. Lewis	5.6	57191	Halls Valley
511	0101	N. Palm Springs	6.06	5224	Anza - Red Mountain
512	0101	N. Palm Springs	6.06	5231	Anza - Tule Canyon
513	0101	N. Palm Springs	6.06	5160	Anza Fire Station
514	0101	N. Palm Springs	6.06	5073	Cabazon

RSN	EQID	Earthquake	M	Station No,	Station
515	0101	N. Palm Springs	6.06	754	Colton Interchange - Vault
516	0101	N. Palm Springs	6.06	5157	Cranston Forest Station
517	0101	N. Palm Springs	6.06	12149	Desert Hot Springs
518	0101	N. Palm Springs	6.06	5069	Fun Valley
519	0101	N. Palm Springs	6.06	12331	Hemet Fire Station
520	0101	N. Palm Springs	6.06	23321	Hesperia
521	0101	N. Palm Springs	6.06	5043	Hurkey Creek Park
522	0101	N. Palm Springs	6.06	5067	Indio
523	0101	N. Palm Springs	6.06	12026	Indio - Coachella Canal
524	0101	N. Palm Springs	6.06	22170	Joshua Tree
525	0101	N. Palm Springs	6.06	707	Lake Mathews Dike Toe
526	0101	N. Palm Springs	6.06	22T13	Landers Fire Station
527	0101	N. Palm Springs	6.06	5071	Morongo Valley
528	0101	N. Palm Springs	6.06	13198	Murrieta Hot Springs
529	0101	N. Palm Springs	6.06	5070	North Palm Springs
530	0101	N. Palm Springs	6.06	12025	Palm Springs Airport
531	0101	N. Palm Springs	6.06	12168	Puerta La Cruz
532	0101	N. Palm Springs	6.06	23497	Rancho Cucamonga - FF
533	0101	N. Palm Springs	6.06	13123	Riverside Airport
534	0101	N. Palm Springs	6.06	12204	San Jacinto - Soboba
535	0101	N. Palm Springs	6.06	12202	San Jacinto - Valley Cemetary
536	0101	N. Palm Springs	6.06	5230	Santa Rosa Mountain
537	0101	N. Palm Springs	6.06	12206	Silent Valley - Poppet Flat
538	0101	N. Palm Springs	6.06	5038	Sunnymead
539	0101	N. Palm Springs	6.06	13172	Temecula - 6th & Mercedes
540	0101	N. Palm Springs	6.06	5072	Whitewater Trout Farm
541	0101	N. Palm Springs	6.06	13199	Winchester Bergman Ran
542	0101	N. Palm Springs	6.06	13201	Winchester Page Bros R
543	0102	Chalfant Valley-01	5.77	54100	Benton
544	0102	Chalfant Valley-01	5.77	54171	Bishop - LADWP South St
545	0102	Chalfant Valley-01	5.77	54424	Bishop - Paradise Lodge
546	0102	Chalfant Valley-01	5.77	54T03	Lake Crowley - Shehorn Res.
547	0102	Chalfant Valley-01	5.77	54428	Zack Brothers Ranch
548	0103	Chalfant Valley-02	6.19	54100	Benton
549	0103	Chalfant Valley-02	6.19	54171	Bishop - LADWP South St
550	0103	Chalfant Valley-02	6.19	54424	Bishop - Paradise Lodge
551	0103	Chalfant Valley-02	6.19	54099	Convict Creek
552	0103	Chalfant Valley-02	6.19	54T03	Lake Crowley - Shehorn Res.
553	0103	Chalfant Valley-02	6.19	54214	Long Valley Dam (Downst)
554	0103	Chalfant Valley-02	6.19	54214	Long Valley Dam (L Abut)
555	0103	Chalfant Valley-02	6.19	54T04	Mammoth Lakes Sheriff Subst.
556	0103	Chalfant Valley-02	6.19	1661	McGee Creek - Surface
557	0103	Chalfant Valley-02	6.19	54101	Tinemaha Res. Free Field
558	0103	Chalfant Valley-02	6.19	54428	Zack Brothers Ranch
559	0104	Chalfant Valley-03	5.65	54171	Bishop - LADWP South St
560	0104	Chalfant Valley-03	5.65	54424	Bishop - Paradise Lodge
561	0104	Chalfant Valley-03	5.65	54428	Zack Brothers Ranch
562	0105	Chalfant Valley-04	5.44	54171	Bishop - LADWP South St
563	0105	Chalfant Valley-04	5.44	54428	Zack Brothers Ranch
568	0108	San Salvador	5.8	99999	Geotech Investig Center
569	0108	San Salvador	5.8	99999	National Geografical Inst
585	0110	Baja California	5.5	6604	Cerro Prieto
586	0111	New Zealand-02	6.6	113A	Maraenui Primary School
587	0111	New Zealand-02	6.6	99999	Matahina Dam
588	0112	New Zealand-03	5.8	99999	Matahina Dam
589	0113	Whittier Narrows-01	5.99	24461	Alhambra - Fremont School
590	0113	Whittier Narrows-01	5.99	24402	Altadena - Eaton Canyon
591	0113	Whittier Narrows-01	5.99	90088	Anaheim - W Ball Rd
592	0113	Whittier Narrows-01	5.99	90093	Arcadia - Campus Dr
593	0113	Whittier Narrows-01	5.99	24087	Arleta - Nordhoff Fire Sta
594	0113	Whittier Narrows-01	5.99	90069	Baldwin Park - N Holly
595	0113	Whittier Narrows-01	5.99	90094	Bell Gardens - Jaboneria
596	0113	Whittier Narrows-01	5.99	90014	Beverly Hills - 12520 Mulhol
597	0113	Whittier Narrows-01	5.99	90013	Beverly Hills - 14145 Mulhol
598	0113	Whittier Narrows-01	5.99	90061	Big Tujunga, Angeles Nat F
600	0113	Whittier Narrows-01	5.99	951	Brea Dam (Downstream)
601	0113	Whittier Narrows-01	5.99	951	Brea Dam (L Abut)
602	0113	Whittier Narrows-01	5.99	90012	Burbank - N Buena Vista
603	0113	Whittier Narrows-01	5.99	90052	Calabasas - N Las Virg

RSN	EQID	Earthquake	M	Station No,	Station
604	0113	Whittier Narrows-01	5.99	90053	Canoga Park - Topanga Can
605	0113	Whittier Narrows-01	5.99	90057	Canyon Country - W Lost Cany
606	0113	Whittier Narrows-01	5.99	108	Carbon Canyon Dam
607	0113	Whittier Narrows-01	5.99	90040	Carson - Catskill Ave
608	0113	Whittier Narrows-01	5.99	90081	Carson - Water St
609	0113	Whittier Narrows-01	5.99	24277	Castaic - Hasley Canyon
610	0113	Whittier Narrows-01	5.99	24278	Castaic - Old Ridge Route
611	0113	Whittier Narrows-01	5.99	90078	Compton - Castlegate St
612	0113	Whittier Narrows-01	5.99	90068	Covina - S Grand Ave
613	0113	Whittier Narrows-01	5.99	90070	Covina - W Badillo
614	0113	Whittier Narrows-01	5.99	90079	Downey - Birchdale
615	0113	Whittier Narrows-01	5.99	14368	Downey - Co Maint Bldg
616	0113	Whittier Narrows-01	5.99	90066	El Monte - Fairview Av
617	0113	Whittier Narrows-01	5.99	13122	Featherly Park - Maint
618	0113	Whittier Narrows-01	5.99	90002	Fountain Valley - Euclid
619	0113	Whittier Narrows-01	5.99	709	Garvey Res. - Control Bldg
620	0113	Whittier Narrows-01	5.99	90063	Glendale - Las Palmas
621	0113	Whittier Narrows-01	5.99	90065	Glendora - N Oakbank
622	0113	Whittier Narrows-01	5.99	90073	Hacienda Heights - Colima
623	0113	Whittier Narrows-01	5.99	12331	Hemet Fire Station
624	0113	Whittier Narrows-01	5.99	13197	Huntington Beach - Lake St
625	0113	Whittier Narrows-01	5.99	14196	Inglewood - Union Oil
626	0113	Whittier Narrows-01	5.99	14403	LA - 116th St School
627	0113	Whittier Narrows-01	5.99	24157	LA - Baldwin Hills
628	0113	Whittier Narrows-01	5.99	90054	LA - Centinela St
629	0113	Whittier Narrows-01	5.99	24389	LA - Century City CC North
630	0113	Whittier Narrows-01	5.99	24390	LA - Century City CC South
631	0113	Whittier Narrows-01	5.99	90015	LA - Chalon Rd
632	0113	Whittier Narrows-01	5.99	90033	LA - Cypress Ave
634	0113	Whittier Narrows-01	5.99	90034	LA - Fletcher Dr
635	0113	Whittier Narrows-01	5.99	24303	LA - Hollywood Stor FF
636	0113	Whittier Narrows-01	5.99	90016	LA - N Faring Rd
637	0113	Whittier Narrows-01	5.99	90032	LA - N Figueroa St
638	0113	Whittier Narrows-01	5.99	90021	LA - N Westmoreland
639	0113	Whittier Narrows-01	5.99	24400	LA - Obregon Park
640	0113	Whittier Narrows-01	5.99	90022	LA - S Grand Ave
641	0113	Whittier Narrows-01	5.99	90091	LA - Saturn St
642	0113	Whittier Narrows-01	5.99	90023	LA - W 70th St
643	0113	Whittier Narrows-01	5.99	90017	LA - Wonderland Ave
644	0113	Whittier Narrows-01	5.99	14395	LB - Harbor Admin FF
645	0113	Whittier Narrows-01	5.99	90080	LB - Orange Ave
646	0113	Whittier Narrows-01	5.99	14242	LB - Rancho Los Cerritos
647	0113	Whittier Narrows-01	5.99	14241	LB - Recreation Park
648	0113	Whittier Narrows-01	5.99	90060	La Crescenta - New York
649	0113	Whittier Narrows-01	5.99	90074	La Habra - Briarcliff
650	0113	Whittier Narrows-01	5.99	90072	La Puente - Rimgrove Av
651	0113	Whittier Narrows-01	5.99	24271	Lake Hughes #1
652	0113	Whittier Narrows-01	5.99	90084	Lakewood - Del Amo Blvd
653	0113	Whittier Narrows-01	5.99	24526	Lancaster - Med Off FF
654	0113	Whittier Narrows-01	5.99	90045	Lawndale - Osage Ave
655	0113	Whittier Narrows-01	5.99	24055	Leona Valley #5 - Ritter
656	0113	Whittier Narrows-01	5.99	24309	Leona Valley #6
657	0113	Whittier Narrows-01	5.99	90050	Malibu - Las Flores Canyon
658	0113	Whittier Narrows-01	5.99	24396	Malibu - Point Dume Sch
659	0113	Whittier Narrows-01	5.99	90051	Malibu - W Pacific Cst Hwy
661	0113	Whittier Narrows-01	5.99	90062	Mill Creek, Angeles Nat For
662	0113	Whittier Narrows-01	5.99	24283	Moorpark - Fire Sta
663	0113	Whittier Narrows-01	5.99	24399	Mt Wilson - CIT Seis Sta
664	0113	Whittier Narrows-01	5.99	90009	N Hollywood - Coldwater Can
665	0113	Whittier Narrows-01	5.99	24279	Newhall - Fire Sta
666	0113	Whittier Narrows-01	5.99	90056	Newhall - W Pico Canyon Rd.
667	0113	Whittier Narrows-01	5.99	90003	Northridge - 17645 Saticoy St
668	0113	Whittier Narrows-01	5.99	634	Norwalk - Imp Hwy, S Grnd
669	0113	Whittier Narrows-01	5.99	697	Orange Co. Reservoir
670	0113	Whittier Narrows-01	5.99	90049	Pacific Palisades - Sunset
671	0113	Whittier Narrows-01	5.99	24088	Pacoima Kagel Canyon
672	0113	Whittier Narrows-01	5.99	90005	Pacoima Kagel Canyon USC
673	0113	Whittier Narrows-01	5.99	90007	Panorama City - Roscoe
674	0113	Whittier Narrows-01	5.99	80046	Pasadena - Brown Gym

RSN	EQID	Earthquake	M	Station No,	Station
677	0113	Whittier Narrows-01	5.99	80047	Pasadena - CIT Calif Blvd
678	0113	Whittier Narrows-01	5.99	80051	Pasadena - CIT Indust. Rel
681	0113	Whittier Narrows-01	5.99	80048	Pasadena - CIT Lura St
683	0113	Whittier Narrows-01	5.99	90095	Pasadena - Old House Rd
684	0113	Whittier Narrows-01	5.99	90047	Playa Del Rey - Saran
685	0113	Whittier Narrows-01	5.99	23525	Pomona - 4th & Locust FF
686	0113	Whittier Narrows-01	5.99	23497	Rancho Cucamonga - FF
687	0113	Whittier Narrows-01	5.99	90044	Rancho Palos Verdes - Luconia
688	0113	Whittier Narrows-01	5.99	13123	Riverside Airport
689	0113	Whittier Narrows-01	5.99	24274	Rosamond - Goode Ranch
690	0113	Whittier Narrows-01	5.99	90019	San Gabriel - E Grand Ave
691	0113	Whittier Narrows-01	5.99	24401	San Marino - SW Academy
692	0113	Whittier Narrows-01	5.99	90077	Santa Fe Springs - E.Joslin
693	0113	Whittier Narrows-01	5.99	90048	Santa Monica - Second St
694	0113	Whittier Narrows-01	5.99	90010	Studio City - Coldwater Can
695	0113	Whittier Narrows-01	5.99	90006	Sun Valley - Roscoe Blvd
696	0113	Whittier Narrows-01	5.99	90008	Sun Valley - Sunland
697	0113	Whittier Narrows-01	5.99	90058	Sunland - Mt Gleason Ave
698	0113	Whittier Narrows-01	5.99	24514	Sylmar - Olive View Med FF
699	0113	Whittier Narrows-01	5.99	90001	Sylmar - Sayre St
700	0113	Whittier Narrows-01	5.99	24436	Tarzana - Cedar Hill
701	0113	Whittier Narrows-01	5.99	90082	Terminal Island - S Seaside
702	0113	Whittier Narrows-01	5.99	90038	Torrance - W 226th St
703	0113	Whittier Narrows-01	5.99	24047	Vasquez Rocks Park
704	0113	Whittier Narrows-01	5.99	90090	Villa Park - Serrano Ave
705	0113	Whittier Narrows-01	5.99	90071	West Covina - S Orange Ave
706	0113	Whittier Narrows-01	5.99	289	Whittier Narrows Dam upstream
707	0114	Whittier Narrows-02	5.27	24461	Alhambra - Fremont School
708	0114	Whittier Narrows-02	5.27	24402	Altadena - Eaton Canyon
709	0114	Whittier Narrows-02	5.27	14368	Downey - Co Maint Bldg
710	0114	Whittier Narrows-02	5.27	14196	Inglewood - Union Oil
711	0114	Whittier Narrows-02	5.27	14403	LA - 116th St School
712	0114	Whittier Narrows-02	5.27	24157	LA - Baldwin Hills
713	0114	Whittier Narrows-02	5.27	24303	LA - Hollywood Stor FF
714	0114	Whittier Narrows-02	5.27	24400	LA - Obregon Park
715	0114	Whittier Narrows-02	5.27	24399	Mt Wilson - CIT Seis Sta
716	0114	Whittier Narrows-02	5.27	24401	San Marino - SW Academy
717	0114	Whittier Narrows-02	5.27	24436	Tarzana - Cedar Hill
718	0115	Superstition Hills-01	6.22	5210	Wildlife Liquef. Array
719	0116	Superstition Hills-02	6.54	5060	Brawley Airport
720	0116	Superstition Hills-02	6.54	5061	Calipatria Fire Station
721	0116	Superstition Hills-02	6.54	1335	El Centro Imp. Co. Cent
722	0116	Superstition Hills-02	6.54	9401	Kornbloom Road (temp)
723	0116	Superstition Hills-02	6.54	5051	Parachute Test Site
724	0116	Superstition Hills-02	6.54	5052	Plaster City
725	0116	Superstition Hills-02	6.54	9400	Poe Road (temp)
726	0116	Superstition Hills-02	6.54	5062	Salton Sea Wildlife Refuge
727	0116	Superstition Hills-02	6.54	286	Superstition Mtn Camera
728	0116	Superstition Hills-02	6.54	11369	Westmorland Fire Sta
729	0116	Superstition Hills-02	6.54	5210	Wildlife Liquef. Array
730	0117	Spitak, Armenia	6.77	12	Gukasian
731	0118	Loma Prieta	6.93	58373	APEEL 10 - Skyline
732	0118	Loma Prieta	6.93	1002	APEEL 2 - Redwood City
733	0118	Loma Prieta	6.93	58393	APEEL 2E Hayward Muir Sch
734	0118	Loma Prieta	6.93	58219	APEEL 3E Hayward CSUH
735	0118	Loma Prieta	6.93	58378	APEEL 7 - Pulgas
736	0118	Loma Prieta	6.93	1161	APEEL 9 - Crystal Springs Res
737	0118	Loma Prieta	6.93	57066	Agnews State Hospital
738	0118	Loma Prieta	6.93	99999	Alameda Naval Air Stn Hanger
739	0118	Loma Prieta	6.93	1652	Anderson Dam (Downstream)
740	0118	Loma Prieta	6.93	1652	Anderson Dam (L Abut)
741	0118	Loma Prieta	6.93	13	BRAN
742	0118	Loma Prieta	6.93	1210	Bear Valley #1, Fire Station
743	0118	Loma Prieta	6.93	1479	Bear Valley #10, Webb Residence
744	0118	Loma Prieta	6.93	1481	Bear Valley #12, Williams Ranch
745	0118	Loma Prieta	6.93	1483	Bear Valley #14, Upper Butts Rn
746	0118	Loma Prieta	6.93	1474	Bear Valley #5, Callens Ranch
747	0118	Loma Prieta	6.93	1476	Bear Valley #7, Pinnacles
749	0118	Loma Prieta	6.93	1005	Berkeley - Strawberry Canyon

RSN	EQID	Earthquake	M	Station No,	Station
750	0118	Loma Prieta	6.93	58471	Berkeley LBL
751	0118	Loma Prieta	6.93	1687	Calaveras Reservoir
752	0118	Loma Prieta	6.93	47125	Capitola
753	0118	Loma Prieta	6.93	57007	Corralitos
754	0118	Loma Prieta	6.93	57504	Coyote Lake Dam (Downst)
755	0118	Loma Prieta	6.93	57217	Coyote Lake Dam (SW Abut)
756	0118	Loma Prieta	6.93	1689	Dublin - Fire Station
757	0118	Loma Prieta	6.93	58664	Dumbarton Bridge West End FF
758	0118	Loma Prieta	6.93	1662	Emeryville - 6363 Christie
759	0118	Loma Prieta	6.93	58375	Foster City - APEEL 1
760	0118	Loma Prieta	6.93	1515	Foster City - Menhaden Court
761	0118	Loma Prieta	6.93	1686	Fremont - Emerson Court
762	0118	Loma Prieta	6.93	57064	Fremont - Mission San Jose
763	0118	Loma Prieta	6.93	47006	Gilroy - Gavilan Coll.
764	0118	Loma Prieta	6.93	57476	Gilroy - Historic Bldg.
765	0118	Loma Prieta	6.93	47379	Gilroy Array #1
766	0118	Loma Prieta	6.93	47380	Gilroy Array #2
767	0118	Loma Prieta	6.93	47381	Gilroy Array #3
768	0118	Loma Prieta	6.93	57382	Gilroy Array #4
769	0118	Loma Prieta	6.93	57383	Gilroy Array #6
770	0118	Loma Prieta	6.93	57425	Gilroy Array #7
771	0118	Loma Prieta	6.93	1678	Golden Gate Bridge
772	0118	Loma Prieta	6.93	57191	Halls Valley
773	0118	Loma Prieta	6.93	58498	Hayward - BART Sta
776	0118	Loma Prieta	6.93	47524	Hollister - South & Pine
778	0118	Loma Prieta	6.93	1656	Hollister Diff. Array
779	0118	Loma Prieta	6.93	16	LGPC
780	0118	Loma Prieta	6.93	1590	Larkspur Ferry Terminal (FF)
781	0118	Loma Prieta	6.93	58233	Lower Crystal Springs Dam dwnst
782	0118	Loma Prieta	6.93	47377	Monterey City Hall
783	0118	Loma Prieta	6.93	58472	Oakland - Outer Harbor Wharf
784	0118	Loma Prieta	6.93	58224	Oakland - Title & Trust
785	0118	Loma Prieta	6.93	68003	Olema - Point Reyes Station
786	0118	Loma Prieta	6.93	58264	Palo Alto - 1900 Embarc.
787	0118	Loma Prieta	6.93	1601	Palo Alto - SLAC Lab
788	0118	Loma Prieta	6.93	58338	Piedmont Jr High
789	0118	Loma Prieta	6.93	58043	Point Bonita
790	0118	Loma Prieta	6.93	58505	Richmond City Hall
791	0118	Loma Prieta	6.93	47189	SAGO South - Surface
792	0118	Loma Prieta	6.93	1675	SF - 1295 Shafter
794	0118	Loma Prieta	6.93	58130	SF - Diamond Heights
795	0118	Loma Prieta	6.93	58131	SF - Pacific Heights
796	0118	Loma Prieta	6.93	58222	SF - Presidio
797	0118	Loma Prieta	6.93	58151	SF - Rincon Hill
798	0118	Loma Prieta	6.93	58133	SF - Telegraph Hill
799	0118	Loma Prieta	6.93	58223	SF Intern. Airport
800	0118	Loma Prieta	6.93	47179	Salinas - John & Work
801	0118	Loma Prieta	6.93	57563	San Jose - Santa Teresa Hills
802	0118	Loma Prieta	6.93	58065	Saratoga - Aloha Ave
803	0118	Loma Prieta	6.93	58235	Saratoga - W Valley Coll.
804	0118	Loma Prieta	6.93	58539	So. San Francisco, Sierra Pt.
806	0118	Loma Prieta	6.93	1695	Sunnyvale - Colton Ave.
807	0118	Loma Prieta	6.93	1688	Sunol - Forest Fire Station
808	0118	Loma Prieta	6.93	58117	Treasure Island
809	0118	Loma Prieta	6.93	15	UCSC
810	0118	Loma Prieta	6.93	58135	UCSC Lick Observatory
811	0118	Loma Prieta	6.93	14	WAHO
812	0118	Loma Prieta	6.93	58127	Woodside
813	0118	Loma Prieta	6.93	58163	Yerba Buena Island
3548	0118	Loma Prieta	6.93	57180	Los Gatos - Lexington Dam
815	0119	Griva, Greece	6.1	99999	Kilkis
816	0120	Georgia, USSR	6.2	18	Ambralauri
817	0120	Georgia, USSR	6.2	21	Baz
818	0120	Georgia, USSR	6.2	19	Iri
819	0120	Georgia, USSR	6.2	20	Oni
820	0120	Georgia, USSR	6.2	22	Zem
821	0121	Erzican, Turkey	6.69	95	Erzincan
822	0122	Roermond, Netherlands	5.3	99999	GSH
823	0122	Roermond, Netherlands	5.3	99999	OLF

RSN	EQID	Earthquake	M	Station No,	Station
824	0122	Roermond, Netherlands	5.3	99999	WBS
825	0123	Cape Mendocino	7.01	89005	Cape Mendocino
826	0123	Cape Mendocino	7.01	89509	Eureka - Myrtle & West
827	0123	Cape Mendocino	7.01	89486	Fortuna - Fortuna Blvd
828	0123	Cape Mendocino	7.01	89156	Petrolia
829	0123	Cape Mendocino	7.01	89324	Rio Dell Overpass - FF
830	0123	Cape Mendocino	7.01	89530	Shelter Cove Airport
831	0124	New Zealand-04	5.7	930A	Edgecumbe Substation Electric
832	0125	Landers	7.28	21081	Amboy
833	0125	Landers	7.28	90088	Anaheim - W Ball Rd
834	0125	Landers	7.28	90099	Arcadia - Arcadia Av
835	0125	Landers	7.28	90093	Arcadia - Campus Dr
836	0125	Landers	7.28	32075	Baker Fire Station
837	0125	Landers	7.28	90069	Baldwin Park - N Holly
838	0125	Landers	7.28	23559	Barstow
839	0125	Landers	7.28	90094	Bell Gardens - Jaboneria
840	0125	Landers	7.28	90061	Big Tujunga, Angeles Nat F
841	0125	Landers	7.28	33083	Boron Fire Station
842	0125	Landers	7.28	90087	Brea - S Flower Av
843	0125	Landers	7.28	90086	Buena Park - La Palma
844	0125	Landers	7.28	90012	Burbank - N Buena Vista
845	0125	Landers	7.28	90052	Calabasas - N Las Virg
846	0125	Landers	7.28	90004	Chatsworth - Devonshire
847	0125	Landers	7.28	90078	Compton - Castlegate St
848	0125	Landers	7.28	23	Coolwater
849	0125	Landers	7.28	90070	Covina - W Badillo
850	0125	Landers	7.28	12149	Desert Hot Springs
851	0125	Landers	7.28	14368	Downey - Co Maint Bldg
852	0125	Landers	7.28	90067	Duarte - Mel Canyon Rd.
853	0125	Landers	7.28	90066	El Monte - Fairview Av
854	0125	Landers	7.28	13122	Featherly Park - Maint
855	0125	Landers	7.28	24577	Fort Irwin
856	0125	Landers	7.28	90002	Fountain Valley - Euclid
857	0125	Landers	7.28	90063	Glendale - Las Palmas
858	0125	Landers	7.28	90065	Glendora - N Oakbank
859	0125	Landers	7.28	90073	Hacienda Heights - Colima
860	0125	Landers	7.28	12331	Hemet Fire Station
861	0125	Landers	7.28	90083	Huntington Bch - Waikiki
862	0125	Landers	7.28	12026	Indio - Coachella Canal
863	0125	Landers	7.28	14196	Inglewood - Union Oil
864	0125	Landers	7.28	22170	Joshua Tree
865	0125	Landers	7.28	14403	LA - 116th St School
867	0125	Landers	7.28	90034	LA - Fletcher Dr
868	0125	Landers	7.28	90032	LA - N Figueroa St
869	0125	Landers	7.28	90021	LA - N Westmoreland
870	0125	Landers	7.28	24400	LA - Obregon Park
871	0125	Landers	7.28	90022	LA - S Grand Ave
872	0125	Landers	7.28	90020	LA - W 15th St
873	0125	Landers	7.28	90023	LA - W 70th St
874	0125	Landers	7.28	90080	LB - Orange Ave
875	0125	Landers	7.28	90060	La Crescenta - New York
876	0125	Landers	7.28	90074	La Habra - Briarcliff
877	0125	Landers	7.28	90072	La Puente - Rimgrove Av
878	0125	Landers	7.28	90084	Lakewood - Del Amo Blvd
879	0125	Landers	7.28	24	Lucerne
880	0125	Landers	7.28	100	Mission Creek Fault
881	0125	Landers	7.28	5071	Morongo Valley
882	0125	Landers	7.28	5070	North Palm Springs
883	0125	Landers	7.28	90003	Northridge - 17645 Saticoy St
884	0125	Landers	7.28	12025	Palm Springs Airport
885	0125	Landers	7.28	23525	Pomona - 4th & Locust FF
886	0125	Landers	7.28	12168	Puerta La Cruz
887	0125	Landers	7.28	13123	Riverside Airport
888	0125	Landers	7.28	23542	San Bernardino - E & Hospitality
889	0125	Landers	7.28	90019	San Gabriel - E Grand Ave
890	0125	Landers	7.28	90077	Santa Fe Springs - E.Joslin
891	0125	Landers	7.28	12206	Silent Valley - Poppet Flat
892	0125	Landers	7.28	90006	Sun Valley - Roscoe Blvd
893	0125	Landers	7.28	90008	Sun Valley - Sunland

RSN	EQID	Earthquake	M	Station No,	Station
894	0125	Landers	7.28	90058	Sunland - Mt Gleason Ave
895	0125	Landers	7.28	24436	Tarzana - Cedar Hill
896	0125	Landers	7.28	90089	Tustin - E Sycamore
897	0125	Landers	7.28	22161	Twentynine Palms
898	0125	Landers	7.28	90090	Villa Park - Serrano Ave
899	0125	Landers	7.28	90071	West Covina - S Orange Ave
900	0125	Landers	7.28	22074	Yermo Fire Station
901	0126	Big Bear-01	6.46	22561	Big Bear Lake - Civic Center
902	0126	Big Bear-01	6.46	12149	Desert Hot Springs
903	0126	Big Bear-01	6.46	12626	Desert Shores
904	0126	Big Bear-01	6.46	24575	Elizabeth Lake
905	0126	Big Bear-01	6.46	13122	Featherly Park - Maint
906	0126	Big Bear-01	6.46	12331	Hemet Fire Station
907	0126	Big Bear-01	6.46	23583	Hesperia - 4th & Palm
908	0126	Big Bear-01	6.46	12026	Indio - Coachella Canal
909	0126	Big Bear-01	6.46	12543	Indio - Riverside Co Fair Grnds
910	0126	Big Bear-01	6.46	22170	Joshua Tree
912	0126	Big Bear-01	6.46	24592	LA - City Terrace
913	0126	Big Bear-01	6.46	24611	LA - Temple & Hope
914	0126	Big Bear-01	6.46	24605	LA - Univ. Hospital
915	0126	Big Bear-01	6.46	12624	Lake Cachulla
916	0126	Big Bear-01	6.46	11625	Mecca - CVWD Yard
917	0126	Big Bear-01	6.46	23572	Mt Baldy - Elementary Sch
918	0126	Big Bear-01	6.46	13160	Newport Bch - Irvine Ave. F.S
919	0126	Big Bear-01	6.46	11591	North Shore - Durmid
920	0126	Big Bear-01	6.46	11613	North Shore - Salton Sea Pk HQ
921	0126	Big Bear-01	6.46	12025	Palm Springs Airport
922	0126	Big Bear-01	6.46	23584	Pear Blossom - Pallet Creek
923	0126	Big Bear-01	6.46	23597	Phelan - Wilson Ranch
924	0126	Big Bear-01	6.46	12168	Puerta La Cruz
925	0126	Big Bear-01	6.46	23598	Rancho Cucamonga - Deer Can
926	0126	Big Bear-01	6.46	23497	Rancho Cucamonga - FF
927	0126	Big Bear-01	6.46	13123	Riverside Airport
928	0126	Big Bear-01	6.46	12636	Sage - Fire Station
929	0126	Big Bear-01	6.46	11628	Salton City
931	0126	Big Bear-01	6.46	23542	San Bernardino - E & Hospitality
932	0126	Big Bear-01	6.46	12202	San Jacinto - Valley Cemetary
933	0126	Big Bear-01	6.46	14578	Seal Beach - Office Bldg
934	0126	Big Bear-01	6.46	12206	Silent Valley - Poppet Flat
935	0126	Big Bear-01	6.46	12630	Snow Creek
936	0126	Big Bear-01	6.46	24436	Tarzana - Cedar Hill A
937	0126	Big Bear-01	6.46	13172	Temecula - 6th & Mercedes
938	0126	Big Bear-01	6.46	13199	Winchester Bergman Ran
939	0126	Big Bear-01	6.46	23573	Wrightwood - Nielson Ranch
940	0126	Big Bear-01	6.46	23574	Wrightwood - Swarthout
941	0126	Big Bear-01	6.46	22074	Yermo Fire Station
942	0127	Northridge-01	6.69	24461	Alhambra - Fremont School
943	0127	Northridge-01	6.69	25169	Anacapa Island
944	0127	Northridge-01	6.69	90088	Anaheim - W Ball Rd
945	0127	Northridge-01	6.69	24576	Anaverde Valley - City R
946	0127	Northridge-01	6.69	24310	Antelope Buttes
947	0127	Northridge-01	6.69	90099	Arcadia - Arcadia Av
948	0127	Northridge-01	6.69	90093	Arcadia - Campus Dr
949	0127	Northridge-01	6.69	24087	Arleta - Nordhoff Fire Sta
950	0127	Northridge-01	6.69	90069	Baldwin Park - N Holly
951	0127	Northridge-01	6.69	90094	Bell Gardens - Jaboneria
952	0127	Northridge-01	6.69	90014	Beverly Hills - 12520 Mulhol
953	0127	Northridge-01	6.69	90013	Beverly Hills - 14145 Mulhol
954	0127	Northridge-01	6.69	90061	Big Tujunga, Angeles Nat F
955	0127	Northridge-01	6.69	90087	Brea - S Flower Av
956	0127	Northridge-01	6.69	90086	Buena Park - La Palma
957	0127	Northridge-01	6.69	90059	Burbank - Howard Rd.
958	0127	Northridge-01	6.69	25282	Camarillo
959	0127	Northridge-01	6.69	90053	Canoga Park - Topanga Can
960	0127	Northridge-01	6.69	90057	Canyon Country - W Lost Cany
961	0127	Northridge-01	6.69	90040	Carson - Catskill Ave
962	0127	Northridge-01	6.69	90081	Carson - Water St
963	0127	Northridge-01	6.69	24278	Castaic - Old Ridge Route
964	0127	Northridge-01	6.69	90078	Compton - Castlegate St

RSN	EQID	Earthquake	M	Station No,	Station
965	0127	Northridge-01	6.69	90068	Covina - S Grand Ave
966	0127	Northridge-01	6.69	90070	Covina - W Badillo
967	0127	Northridge-01	6.69	90079	Downey - Birchdale
968	0127	Northridge-01	6.69	14368	Downey - Co Maint Bldg
969	0127	Northridge-01	6.69	90067	Duarte - Mel Canyon Rd.
970	0127	Northridge-01	6.69	90066	El Monte - Fairview Av
971	0127	Northridge-01	6.69	24575	Elizabeth Lake
972	0127	Northridge-01	6.69	13122	Featherly Park - Maint
973	0127	Northridge-01	6.69	90085	Garden Grove - Santa Rita
974	0127	Northridge-01	6.69	90063	Glendale - Las Palmas
975	0127	Northridge-01	6.69	90065	Glendora - N Oakbank
976	0127	Northridge-01	6.69	90073	Hacienda Heights - Colima
977	0127	Northridge-01	6.69	13660	Hemet - Ryan Airfield
978	0127	Northridge-01	6.69	90018	Hollywood - Willoughby Ave
979	0127	Northridge-01	6.69	90083	Huntington Bch - Waikiki
980	0127	Northridge-01	6.69	13197	Huntington Beach - Lake St
981	0127	Northridge-01	6.69	14196	Inglewood - Union Oil
983	0127	Northridge-01	6.69	655	Jensen Filter Plant Generator
984	0127	Northridge-01	6.69	14403	LA - 116th St School
985	0127	Northridge-01	6.69	24157	LA - Baldwin Hills
986	0127	Northridge-01	6.69	638	LA - Brentwood VA Hospital
987	0127	Northridge-01	6.69	90054	LA - Centinela St
988	0127	Northridge-01	6.69	24389	LA - Century City CC North
989	0127	Northridge-01	6.69	90015	LA - Chalon Rd
990	0127	Northridge-01	6.69	24592	LA - City Terrace
991	0127	Northridge-01	6.69	90033	LA - Cypress Ave
993	0127	Northridge-01	6.69	90034	LA - Fletcher Dr
994	0127	Northridge-01	6.69	141	LA - Griffith Park Observatory
995	0127	Northridge-01	6.69	24303	LA - Hollywood Stor FF
996	0127	Northridge-01	6.69	90016	LA - N Faring Rd
997	0127	Northridge-01	6.69	90032	LA - N Figueroa St
998	0127	Northridge-01	6.69	90021	LA - N Westmoreland
999	0127	Northridge-01	6.69	24400	LA - Obregon Park
1000	0127	Northridge-01	6.69	24612	LA - Pico & Sentous
1001	0127	Northridge-01	6.69	90022	LA - S Grand Ave
1003	0127	Northridge-01	6.69	90091	LA - Saturn St
1004	0127	Northridge-01	6.69	637	LA - Sepulveda VA Hospital
1005	0127	Northridge-01	6.69	24611	LA - Temple & Hope
1006	0127	Northridge-01	6.69	24688	LA - UCLA Grounds
1007	0127	Northridge-01	6.69	24605	LA - Univ. Hospital
1008	0127	Northridge-01	6.69	90020	LA - W 15th St
1009	0127	Northridge-01	6.69	5082	LA - Wadsworth VA Hospital North
1010	0127	Northridge-01	6.69	5082	LA - Wadsworth VA Hospital South
1011	0127	Northridge-01	6.69	90017	LA - Wonderland Ave
1012	0127	Northridge-01	6.69	99999	LA 00
1013	0127	Northridge-01	6.69	0	LA Dam
1014	0127	Northridge-01	6.69	14560	LB - City Hall
1015	0127	Northridge-01	6.69	14242	LB - Rancho Los Cerritos
1016	0127	Northridge-01	6.69	90060	La Crescenta - New York
1017	0127	Northridge-01	6.69	90074	La Habra - Briarcliff
1018	0127	Northridge-01	6.69	90072	La Puente - Rimgrove Av
1019	0127	Northridge-01	6.69	24271	Lake Hughes #1
1020	0127	Northridge-01	6.69	24607	Lake Hughes #12A
1021	0127	Northridge-01	6.69	24469	Lake Hughes #4 - Camp Mend
1022	0127	Northridge-01	6.69	24523	Lake Hughes #4B - Camp Mend
1023	0127	Northridge-01	6.69	127	Lake Hughes #9
1024	0127	Northridge-01	6.69	90084	Lakewood - Del Amo Blvd
1025	0127	Northridge-01	6.69	24475	Lancaster - Fox Airfield Grnd
1026	0127	Northridge-01	6.69	90045	Lawndale - Osage Ave
1027	0127	Northridge-01	6.69	24305	Leona Valley #1
1028	0127	Northridge-01	6.69	24306	Leona Valley #2
1029	0127	Northridge-01	6.69	24307	Leona Valley #3
1030	0127	Northridge-01	6.69	24308	Leona Valley #4
1031	0127	Northridge-01	6.69	24055	Leona Valley #5 - Ritter
1032	0127	Northridge-01	6.69	24309	Leona Valley #6
1033	0127	Northridge-01	6.69	23595	Littlerock - Brainard Can
1034	0127	Northridge-01	6.69	24396	Malibu - Point Dume Sch
1035	0127	Northridge-01	6.69	90046	Manhattan Beach - Manhattan
1036	0127	Northridge-01	6.69	34093	Mojave - Hwys 14 & 58

RSN	EQID	Earthquake	M	Station No,	Station
1037	0127	Northridge-01	6.69	34237	Mojave - Oak Creek Canyon
1038	0127	Northridge-01	6.69	90011	Montebello - Bluff Rd.
1039	0127	Northridge-01	6.69	24283	Moorpark - Fire Sta
1040	0127	Northridge-01	6.69	23572	Mt Baldy - Elementary Sch
1041	0127	Northridge-01	6.69	24399	Mt Wilson - CIT Seis Sta
1042	0127	Northridge-01	6.69	90009	N Hollywood - Coldwater Can
1043	0127	Northridge-01	6.69	24586	Neenach - Sacatara Ck
1044	0127	Northridge-01	6.69	24279	Newhall - Fire Sta
1045	0127	Northridge-01	6.69	90056	Newhall - W Pico Canyon Rd.
1046	0127	Northridge-01	6.69	13160	Newport Bch - Irvine Ave. F.S
1047	0127	Northridge-01	6.69	13610	Newport Bch - Newp & Coast
1048	0127	Northridge-01	6.69	90003	Northridge - 17645 Saticoy St
1049	0127	Northridge-01	6.69	90049	Pacific Palisades - Sunset
1050	0127	Northridge-01	6.69	24207	Pacoima Dam (downstr)
1051	0127	Northridge-01	6.69	24207	Pacoima Dam (upper left)
1052	0127	Northridge-01	6.69	24088	Pacoima Kagel Canyon
1053	0127	Northridge-01	6.69	24521	Palmdale - Hwy 14 & Palmdale
1054	0127	Northridge-01	6.69	99999	Pardee - SCE
1055	0127	Northridge-01	6.69	90095	Pasadena - N Sierra Madre
1056	0127	Northridge-01	6.69	23597	Phelan - Wilson Ranch
1057	0127	Northridge-01	6.69	90047	Playa Del Rey - Saran
1058	0127	Northridge-01	6.69	25148	Point Mugu - Laguna Peak
1059	0127	Northridge-01	6.69	25281	Port Hueneme - Naval Lab.
1060	0127	Northridge-01	6.69	23598	Rancho Cucamonga - Deer Can
1061	0127	Northridge-01	6.69	14404	Rancho Palos Verdes - Hawth
1062	0127	Northridge-01	6.69	90044	Rancho Palos Verdes - Luconia
1063	0127	Northridge-01	6.69	77	Rinaldi Receiving Sta
1064	0127	Northridge-01	6.69	13123	Riverside Airport
1065	0127	Northridge-01	6.69	14405	Rolling Hills Est-Rancho Vista
1066	0127	Northridge-01	6.69	24092	Rosamond - Airport
1067	0127	Northridge-01	6.69	23672	San Bernardino - CSUSB Gr
1068	0127	Northridge-01	6.69	5245	San Bernardino - Co Service Bldg - Freefield
1069	0127	Northridge-01	6.69	23542	San Bernardino - E & Hospitality
1070	0127	Northridge-01	6.69	90019	San Gabriel - E Grand Ave
1071	0127	Northridge-01	6.69	12673	San Jacinto - CDF Fire Sta
1072	0127	Northridge-01	6.69	24401	San Marino - SW Academy
1073	0127	Northridge-01	6.69	14159	San Pedro - Palos Verdes
1074	0127	Northridge-01	6.69	24644	Sandberg - Bald Mtn
1075	0127	Northridge-01	6.69	25091	Santa Barbara - UCSB Goleta
1076	0127	Northridge-01	6.69	90077	Santa Fe Springs - E.Joslin
1077	0127	Northridge-01	6.69	24538	Santa Monica City Hall
1078	0127	Northridge-01	6.69	5108	Santa Susana Ground
1079	0127	Northridge-01	6.69	14578	Seal Beach - Office Bldg
1080	0127	Northridge-01	6.69	90055	Simi Valley - Katherine Rd
1082	0127	Northridge-01	6.69	90006	Sun Valley - Roscoe Blvd
1083	0127	Northridge-01	6.69	90058	Sunland - Mt Gleason Ave
1084	0127	Northridge-01	6.69	74	Sylmar - Converter Sta
1085	0127	Northridge-01	6.69	75	Sylmar - Converter Sta East
1086	0127	Northridge-01	6.69	24514	Sylmar - Olive View Med FF
1087	0127	Northridge-01	6.69	24436	Tarzana - Cedar Hill A
1088	0127	Northridge-01	6.69	90082	Terminal Island - S Seaside
1089	0127	Northridge-01	6.69	5081	Topanga - Fire Sta
1090	0127	Northridge-01	6.69	90089	Tustin - E Sycamore
1091	0127	Northridge-01	6.69	24047	Vasquez Rocks Park
1092	0127	Northridge-01	6.69	25340	Ventura - Harbor & California
1093	0127	Northridge-01	6.69	90090	Villa Park - Serrano Ave
1094	0127	Northridge-01	6.69	90071	West Covina - S Orange Ave
1095	0127	Northridge-01	6.69	90075	Whittier - S. Alta Dr
1096	0127	Northridge-01	6.69	23590	Wrightwood - Jackson Flat
1097	0127	Northridge-01	6.69	23573	Wrightwood - Nielson Ranch
1098	0127	Northridge-01	6.69	23574	Wrightwood - Swarthout
3549	0127	Northridge-01	6.69	5080	Monte Nido Fire Station
3550	0127	Northridge-01	6.69	5229	Loma Linda
3551	0127	Northridge-01	6.69	5229	Loma Linda
1099	0128	Double Springs	5.9	65398	Woodfords
1100	0129	Kobe, Japan	6.9	99999	Abeno

RSN	EQID	Earthquake	M	Station No,	Station
1101	0129	Kobe, Japan	6.9	99999	Amagasaki
1102	0129	Kobe, Japan	6.9	99999	Chihaya
1103	0129	Kobe, Japan	6.9	99999	FUK
1104	0129	Kobe, Japan	6.9	99999	Fukushima
1105	0129	Kobe, Japan	6.9	99999	HIK
1106	0129	Kobe, Japan	6.9	99999	KJMA
1107	0129	Kobe, Japan	6.9	99999	Kakogawa
1108	0129	Kobe, Japan	6.9	99999	Kobe University
1109	0129	Kobe, Japan	6.9	99999	MZH
1110	0129	Kobe, Japan	6.9	99999	Morigawachi
1111	0129	Kobe, Japan	6.9	99999	Nishi-Akashi
1112	0129	Kobe, Japan	6.9	99999	OKA
1113	0129	Kobe, Japan	6.9	99999	OSAJ
1114	0129	Kobe, Japan	6.9	99999	Port Island (0 m)
1115	0129	Kobe, Japan	6.9	99999	Sakai
1116	0129	Kobe, Japan	6.9	99999	Shin-Osaka
1117	0129	Kobe, Japan	6.9	99999	TOT
1118	0129	Kobe, Japan	6.9	99999	Tadoka
1119	0129	Kobe, Japan	6.9	99999	Takarazuka
1120	0129	Kobe, Japan	6.9	99999	Takatori
1121	0129	Kobe, Japan	6.9	99999	Yae
1123	0130	Kozani, Greece-01	6.4	99999	Florina
1124	0130	Kozani, Greece-01	6.4	99999	Kardista
1126	0130	Kozani, Greece-01	6.4	99999	Kozani
1129	0131	Kozani, Greece-02	5.1	99999	Chromio Anapsiktirio
1130	0131	Kozani, Greece-02	5.1	99999	Grevena
1131	0132	Kozani, Greece-03	5.3	99999	Chromio Anapsiktirio
1132	0132	Kozani, Greece-03	5.3	99999	Grevena
1133	0133	Kozani, Greece-04	5.1	99999	Grevena
1135	0133	Kozani, Greece-04	5.1	99999	Karpero
1136	0134	Dinar, Turkey	6.4	99999	Balikesir
1139	0134	Dinar, Turkey	6.4	99999	Cardak
1141	0134	Dinar, Turkey	6.4	99999	Dinar
1142	0134	Dinar, Turkey	6.4	99999	Izmir Trigger #1
1145	0135	Gulf of Aqaba	7.2	99999	Hadera
1147	0136	Kocaeli, Turkey	7.51	99999	Ambarli
1148	0136	Kocaeli, Turkey	7.51	99999	Arcelik
1149	0136	Kocaeli, Turkey	7.51	99999	Atakoy
1151	0136	Kocaeli, Turkey	7.51	99999	Balikesir
1152	0136	Kocaeli, Turkey	7.51	99999	Bornova
1153	0136	Kocaeli, Turkey	7.51	99999	Botas
1154	0136	Kocaeli, Turkey	7.51	99999	Bursa Sivil
1155	0136	Kocaeli, Turkey	7.51	99999	Bursa Tofas
1156	0136	Kocaeli, Turkey	7.51	99999	Canakkale
1157	0136	Kocaeli, Turkey	7.51	99999	Cekmece
1158	0136	Kocaeli, Turkey	7.51	99999	Duzce
1159	0136	Kocaeli, Turkey	7.51	99999	Eregli
1160	0136	Kocaeli, Turkey	7.51	99999	Fatih
1162	0136	Kocaeli, Turkey	7.51	99999	Goynuk
1163	0136	Kocaeli, Turkey	7.51	99999	Hava Alani
1164	0136	Kocaeli, Turkey	7.51	99999	Istanbul
1165	0136	Kocaeli, Turkey	7.51	99999	Izmit
1166	0136	Kocaeli, Turkey	7.51	99999	Iznik
1167	0136	Kocaeli, Turkey	7.51	99999	Kutahya
1168	0136	Kocaeli, Turkey	7.51	99999	Manisa
1169	0136	Kocaeli, Turkey	7.51	99999	Maslak
1170	0136	Kocaeli, Turkey	7.51	99999	Mecidiyekoy
1172	0136	Kocaeli, Turkey	7.51	99999	Tekirdag
1175	0136	Kocaeli, Turkey	7.51	99999	Usak
1176	0136	Kocaeli, Turkey	7.51	99999	Yarimca
1177	0136	Kocaeli, Turkey	7.51	99999	Zeytinburnu
1180	0137	Chi-Chi, Taiwan	7.62	99999	CHY002
1181	0137	Chi-Chi, Taiwan	7.62	99999	CHY004
1182	0137	Chi-Chi, Taiwan	7.62	99999	CHY006
1183	0137	Chi-Chi, Taiwan	7.62	99999	CHY008
1184	0137	Chi-Chi, Taiwan	7.62	99999	CHY010
1185	0137	Chi-Chi, Taiwan	7.62	99999	CHY012
1186	0137	Chi-Chi, Taiwan	7.62	99999	CHY014
1187	0137	Chi-Chi, Taiwan	7.62	99999	CHY015

RSN	EQID	Earthquake	M	Station No,	Station
1188	0137	Chi-Chi, Taiwan	7.62	99999	CHY016
1189	0137	Chi-Chi, Taiwan	7.62	99999	CHY017
1190	0137	Chi-Chi, Taiwan	7.62	99999	CHY019
1191	0137	Chi-Chi, Taiwan	7.62	99999	CHY022
1192	0137	Chi-Chi, Taiwan	7.62	99999	CHY023
1193	0137	Chi-Chi, Taiwan	7.62	99999	CHY024
1194	0137	Chi-Chi, Taiwan	7.62	99999	CHY025
1195	0137	Chi-Chi, Taiwan	7.62	99999	CHY026
1196	0137	Chi-Chi, Taiwan	7.62	99999	CHY027
1197	0137	Chi-Chi, Taiwan	7.62	99999	CHY028
1198	0137	Chi-Chi, Taiwan	7.62	99999	CHY029
1199	0137	Chi-Chi, Taiwan	7.62	99999	CHY032
1200	0137	Chi-Chi, Taiwan	7.62	99999	CHY033
1201	0137	Chi-Chi, Taiwan	7.62	99999	CHY034
1202	0137	Chi-Chi, Taiwan	7.62	99999	CHY035
1203	0137	Chi-Chi, Taiwan	7.62	99999	CHY036
1204	0137	Chi-Chi, Taiwan	7.62	99999	CHY039
1205	0137	Chi-Chi, Taiwan	7.62	99999	CHY041
1206	0137	Chi-Chi, Taiwan	7.62	99999	CHY042
1207	0137	Chi-Chi, Taiwan	7.62	99999	CHY044
1208	0137	Chi-Chi, Taiwan	7.62	99999	CHY046
1209	0137	Chi-Chi, Taiwan	7.62	99999	CHY047
1210	0137	Chi-Chi, Taiwan	7.62	99999	CHY050
1211	0137	Chi-Chi, Taiwan	7.62	99999	CHY052
1212	0137	Chi-Chi, Taiwan	7.62	99999	CHY054
1213	0137	Chi-Chi, Taiwan	7.62	99999	CHY055
1214	0137	Chi-Chi, Taiwan	7.62	99999	CHY057
1215	0137	Chi-Chi, Taiwan	7.62	99999	CHY058
1216	0137	Chi-Chi, Taiwan	7.62	99999	CHY059
1217	0137	Chi-Chi, Taiwan	7.62	99999	CHY060
1218	0137	Chi-Chi, Taiwan	7.62	99999	CHY061
1220	0137	Chi-Chi, Taiwan	7.62	99999	CHY063
1221	0137	Chi-Chi, Taiwan	7.62	99999	CHY065
1222	0137	Chi-Chi, Taiwan	7.62	99999	CHY066
1223	0137	Chi-Chi, Taiwan	7.62	99999	CHY067
1224	0137	Chi-Chi, Taiwan	7.62	99999	CHY069
1225	0137	Chi-Chi, Taiwan	7.62	99999	CHY070
1226	0137	Chi-Chi, Taiwan	7.62	99999	CHY071
1227	0137	Chi-Chi, Taiwan	7.62	99999	CHY074
1228	0137	Chi-Chi, Taiwan	7.62	99999	CHY076
1229	0137	Chi-Chi, Taiwan	7.62	99999	CHY078
1230	0137	Chi-Chi, Taiwan	7.62	99999	CHY079
1231	0137	Chi-Chi, Taiwan	7.62	99999	CHY080
1232	0137	Chi-Chi, Taiwan	7.62	99999	CHY081
1233	0137	Chi-Chi, Taiwan	7.62	99999	CHY082
1234	0137	Chi-Chi, Taiwan	7.62	99999	CHY086
1235	0137	Chi-Chi, Taiwan	7.62	99999	CHY087
1236	0137	Chi-Chi, Taiwan	7.62	99999	CHY088
1237	0137	Chi-Chi, Taiwan	7.62	99999	CHY090
1238	0137	Chi-Chi, Taiwan	7.62	99999	CHY092
1239	0137	Chi-Chi, Taiwan	7.62	99999	CHY093
1240	0137	Chi-Chi, Taiwan	7.62	99999	CHY094
1241	0137	Chi-Chi, Taiwan	7.62	99999	CHY096
1242	0137	Chi-Chi, Taiwan	7.62	99999	CHY099
1243	0137	Chi-Chi, Taiwan	7.62	99999	CHY100
1244	0137	Chi-Chi, Taiwan	7.62	99999	CHY101
1245	0137	Chi-Chi, Taiwan	7.62	99999	CHY102
1246	0137	Chi-Chi, Taiwan	7.62	99999	CHY104
1247	0137	Chi-Chi, Taiwan	7.62	99999	CHY107
1248	0137	Chi-Chi, Taiwan	7.62	9999917	CHY109
1250	0137	Chi-Chi, Taiwan	7.62	99999	CHY116
1256	0137	Chi-Chi, Taiwan	7.62	99999	HWA002
1257	0137	Chi-Chi, Taiwan	7.62	99999	HWA003
1258	0137	Chi-Chi, Taiwan	7.62	99999	HWA005
1259	0137	Chi-Chi, Taiwan	7.62	99999	HWA006
1260	0137	Chi-Chi, Taiwan	7.62	99999	HWA007
1261	0137	Chi-Chi, Taiwan	7.62	99999	HWA009
1262	0137	Chi-Chi, Taiwan	7.62	99999	HWA011
1263	0137	Chi-Chi, Taiwan	7.62	99999	HWA012

RSN	EQID	Earthquake	M	Station No,	Station
1264	0137	Chi-Chi, Taiwan	7.62	99999	HWA013
1265	0137	Chi-Chi, Taiwan	7.62	99999	HWA014
1266	0137	Chi-Chi, Taiwan	7.62	99999	HWA015
1267	0137	Chi-Chi, Taiwan	7.62	99999	HWA016
1268	0137	Chi-Chi, Taiwan	7.62	99999	HWA017
1269	0137	Chi-Chi, Taiwan	7.62	99999	HWA019
1270	0137	Chi-Chi, Taiwan	7.62	99999	HWA020
1271	0137	Chi-Chi, Taiwan	7.62	99999	HWA022
1272	0137	Chi-Chi, Taiwan	7.62	99999	HWA023
1273	0137	Chi-Chi, Taiwan	7.62	99999	HWA024
1274	0137	Chi-Chi, Taiwan	7.62	99999	HWA025
1275	0137	Chi-Chi, Taiwan	7.62	99999	HWA026
1276	0137	Chi-Chi, Taiwan	7.62	99999	HWA027
1277	0137	Chi-Chi, Taiwan	7.62	99999	HWA028
1278	0137	Chi-Chi, Taiwan	7.62	99999	HWA029
1279	0137	Chi-Chi, Taiwan	7.62	99999	HWA030
1280	0137	Chi-Chi, Taiwan	7.62	99999	HWA031
1281	0137	Chi-Chi, Taiwan	7.62	99999	HWA032
1282	0137	Chi-Chi, Taiwan	7.62	99999	HWA033
1283	0137	Chi-Chi, Taiwan	7.62	99999	HWA034
1284	0137	Chi-Chi, Taiwan	7.62	99999	HWA035
1285	0137	Chi-Chi, Taiwan	7.62	99999	HWA036
1286	0137	Chi-Chi, Taiwan	7.62	99999	HWA037
1287	0137	Chi-Chi, Taiwan	7.62	99999	HWA038
1288	0137	Chi-Chi, Taiwan	7.62	99999	HWA039
1289	0137	Chi-Chi, Taiwan	7.62	99999	HWA041
1290	0137	Chi-Chi, Taiwan	7.62	99999	HWA043
1291	0137	Chi-Chi, Taiwan	7.62	99999	HWA044
1292	0137	Chi-Chi, Taiwan	7.62	99999	HWA045
1293	0137	Chi-Chi, Taiwan	7.62	99999	HWA046
1294	0137	Chi-Chi, Taiwan	7.62	99999	HWA048
1295	0137	Chi-Chi, Taiwan	7.62	99999	HWA049
1296	0137	Chi-Chi, Taiwan	7.62	99999	HWA050
1297	0137	Chi-Chi, Taiwan	7.62	99999	HWA051
1300	0137	Chi-Chi, Taiwan	7.62	99999	HWA055
1301	0137	Chi-Chi, Taiwan	7.62	99999	HWA056
1302	0137	Chi-Chi, Taiwan	7.62	99999	HWA057
1303	0137	Chi-Chi, Taiwan	7.62	99999	HWA058
1304	0137	Chi-Chi, Taiwan	7.62	99999	HWA059
1305	0137	Chi-Chi, Taiwan	7.62	99999	HWA060
1307	0137	Chi-Chi, Taiwan	7.62	99999	ILA001
1308	0137	Chi-Chi, Taiwan	7.62	99999	ILA002
1309	0137	Chi-Chi, Taiwan	7.62	99999	ILA003
1310	0137	Chi-Chi, Taiwan	7.62	99999	ILA004
1311	0137	Chi-Chi, Taiwan	7.62	99999	ILA005
1312	0137	Chi-Chi, Taiwan	7.62	99999	ILA006
1313	0137	Chi-Chi, Taiwan	7.62	99999	ILA007
1314	0137	Chi-Chi, Taiwan	7.62	99999	ILA008
1315	0137	Chi-Chi, Taiwan	7.62	99999	ILA010
1316	0137	Chi-Chi, Taiwan	7.62	99999	ILA012
1317	0137	Chi-Chi, Taiwan	7.62	99999	ILA013
1318	0137	Chi-Chi, Taiwan	7.62	99999	ILA014
1319	0137	Chi-Chi, Taiwan	7.62	99999	ILA015
1320	0137	Chi-Chi, Taiwan	7.62	99999	ILA016
1321	0137	Chi-Chi, Taiwan	7.62	99999	ILA021
1322	0137	Chi-Chi, Taiwan	7.62	99999	ILA024
1323	0137	Chi-Chi, Taiwan	7.62	9999917	ILA027
1324	0137	Chi-Chi, Taiwan	7.62	99999	ILA030
1325	0137	Chi-Chi, Taiwan	7.62	99999	ILA031
1326	0137	Chi-Chi, Taiwan	7.62	9999917	ILA032
1327	0137	Chi-Chi, Taiwan	7.62	9999917	ILA035
1328	0137	Chi-Chi, Taiwan	7.62	99999	ILA036
1329	0137	Chi-Chi, Taiwan	7.62	99999	ILA037
1330	0137	Chi-Chi, Taiwan	7.62	9999917	ILA039
1331	0137	Chi-Chi, Taiwan	7.62	99999	ILA041
1332	0137	Chi-Chi, Taiwan	7.62	99999	ILA042
1333	0137	Chi-Chi, Taiwan	7.62	9999917	ILA043
1334	0137	Chi-Chi, Taiwan	7.62	99999	ILA044
1335	0137	Chi-Chi, Taiwan	7.62	99999	ILA046

RSN	EQID	Earthquake	M	Station No,	Station
1336	0137	Chi-Chi, Taiwan	7.62	99999	ILA048
1337	0137	Chi-Chi, Taiwan	7.62	99999	ILA049
1338	0137	Chi-Chi, Taiwan	7.62	99999	ILA050
1339	0137	Chi-Chi, Taiwan	7.62	99999	ILA051
1340	0137	Chi-Chi, Taiwan	7.62	99999	ILA052
1341	0137	Chi-Chi, Taiwan	7.62	99999	ILA054
1342	0137	Chi-Chi, Taiwan	7.62	99999	ILA055
1343	0137	Chi-Chi, Taiwan	7.62	99999	ILA056
1344	0137	Chi-Chi, Taiwan	7.62	99999	ILA059
1345	0137	Chi-Chi, Taiwan	7.62	99999	ILA061
1346	0137	Chi-Chi, Taiwan	7.62	99999	ILA062
1347	0137	Chi-Chi, Taiwan	7.62	99999	ILA063
1348	0137	Chi-Chi, Taiwan	7.62	99999	ILA064
1349	0137	Chi-Chi, Taiwan	7.62	99999	ILA066
1350	0137	Chi-Chi, Taiwan	7.62	99999	ILA067
1351	0137	Chi-Chi, Taiwan	7.62	99999	KAU001
1352	0137	Chi-Chi, Taiwan	7.62	99999	KAU003
1353	0137	Chi-Chi, Taiwan	7.62	99999	KAU006
1354	0137	Chi-Chi, Taiwan	7.62	99999	KAU007
1355	0137	Chi-Chi, Taiwan	7.62	99999	KAU008
1356	0137	Chi-Chi, Taiwan	7.62	99999	KAU010
1357	0137	Chi-Chi, Taiwan	7.62	99999	KAU011
1358	0137	Chi-Chi, Taiwan	7.62	99999	KAU012
1359	0137	Chi-Chi, Taiwan	7.62	99999	KAU015
1360	0137	Chi-Chi, Taiwan	7.62	99999	KAU018
1361	0137	Chi-Chi, Taiwan	7.62	99999	KAU020
1362	0137	Chi-Chi, Taiwan	7.62	99999	KAU022
1363	0137	Chi-Chi, Taiwan	7.62	99999	KAU030
1364	0137	Chi-Chi, Taiwan	7.62	99999	KAU032
1365	0137	Chi-Chi, Taiwan	7.62	99999	KAU033
1367	0137	Chi-Chi, Taiwan	7.62	99999	KAU037
1368	0137	Chi-Chi, Taiwan	7.62	99999	KAU038
1373	0137	Chi-Chi, Taiwan	7.62	99999	KAU044
1374	0137	Chi-Chi, Taiwan	7.62	99999	KAU046
1375	0137	Chi-Chi, Taiwan	7.62	99999	KAU047
1376	0137	Chi-Chi, Taiwan	7.62	99999	KAU048
1377	0137	Chi-Chi, Taiwan	7.62	99999	KAU050
1380	0137	Chi-Chi, Taiwan	7.62	99999	KAU054
1381	0137	Chi-Chi, Taiwan	7.62	99999	KAU057
1382	0137	Chi-Chi, Taiwan	7.62	99999	KAU058
1383	0137	Chi-Chi, Taiwan	7.62	99999	KAU062
1384	0137	Chi-Chi, Taiwan	7.62	99999	KAU063
1385	0137	Chi-Chi, Taiwan	7.62	99999	KAU064
1386	0137	Chi-Chi, Taiwan	7.62	99999	KAU066
1387	0137	Chi-Chi, Taiwan	7.62	99999	KAU069
1388	0137	Chi-Chi, Taiwan	7.62	99999	KAU073
1389	0137	Chi-Chi, Taiwan	7.62	99999	KAU074
1390	0137	Chi-Chi, Taiwan	7.62	99999	KAU075
1391	0137	Chi-Chi, Taiwan	7.62	99999	KAU077
1392	0137	Chi-Chi, Taiwan	7.62	99999	KAU078
1393	0137	Chi-Chi, Taiwan	7.62	99999	KAU081
1394	0137	Chi-Chi, Taiwan	7.62	99999	KAU082
1395	0137	Chi-Chi, Taiwan	7.62	99999	KAU083
1396	0137	Chi-Chi, Taiwan	7.62	99999	KAU085
1397	0137	Chi-Chi, Taiwan	7.62	99999	KAU086
1398	0137	Chi-Chi, Taiwan	7.62	99999	KAU087
1399	0137	Chi-Chi, Taiwan	7.62	99999	KAU088
1400	0137	Chi-Chi, Taiwan	7.62	9999917	NCU
1409	0137	Chi-Chi, Taiwan	7.62	9999917	TAP
1410	0137	Chi-Chi, Taiwan	7.62	99999	TAP003
1411	0137	Chi-Chi, Taiwan	7.62	99999	TAP005
1412	0137	Chi-Chi, Taiwan	7.62	99999	TAP006
1413	0137	Chi-Chi, Taiwan	7.62	99999	TAP007
1414	0137	Chi-Chi, Taiwan	7.62	99999	TAP008
1415	0137	Chi-Chi, Taiwan	7.62	99999	TAP010
1416	0137	Chi-Chi, Taiwan	7.62	99999	TAP012
1417	0137	Chi-Chi, Taiwan	7.62	99999	TAP013
1418	0137	Chi-Chi, Taiwan	7.62	99999	TAP014
1419	0137	Chi-Chi, Taiwan	7.62	99999	TAP017

RSN	EQID	Earthquake	M	Station No,	Station
1420	0137	Chi-Chi, Taiwan	7.62	99999	TAP020
1421	0137	Chi-Chi, Taiwan	7.62	99999	TAP021
1422	0137	Chi-Chi, Taiwan	7.62	99999	TAP024
1423	0137	Chi-Chi, Taiwan	7.62	99999	TAP026
1424	0137	Chi-Chi, Taiwan	7.62	99999	TAP028
1425	0137	Chi-Chi, Taiwan	7.62	99999	TAP032
1426	0137	Chi-Chi, Taiwan	7.62	99999	TAP034
1427	0137	Chi-Chi, Taiwan	7.62	99999	TAP035
1428	0137	Chi-Chi, Taiwan	7.62	99999	TAP036
1429	0137	Chi-Chi, Taiwan	7.62	99999	TAP041
1430	0137	Chi-Chi, Taiwan	7.62	99999	TAP042
1431	0137	Chi-Chi, Taiwan	7.62	99999	TAP043
1432	0137	Chi-Chi, Taiwan	7.62	99999	TAP046
1433	0137	Chi-Chi, Taiwan	7.62	99999	TAP047
1434	0137	Chi-Chi, Taiwan	7.62	99999	TAP049
1435	0137	Chi-Chi, Taiwan	7.62	99999	TAP051
1436	0137	Chi-Chi, Taiwan	7.62	99999	TAP052
1437	0137	Chi-Chi, Taiwan	7.62	99999	TAP053
1438	0137	Chi-Chi, Taiwan	7.62	99999	TAP059
1439	0137	Chi-Chi, Taiwan	7.62	99999	TAP060
1440	0137	Chi-Chi, Taiwan	7.62	99999	TAP065
1442	0137	Chi-Chi, Taiwan	7.62	99999	TAP067
1443	0137	Chi-Chi, Taiwan	7.62	99999	TAP069
1444	0137	Chi-Chi, Taiwan	7.62	99999	TAP072
1445	0137	Chi-Chi, Taiwan	7.62	99999	TAP075
1446	0137	Chi-Chi, Taiwan	7.62	99999	TAP077
1447	0137	Chi-Chi, Taiwan	7.62	99999	TAP078
1448	0137	Chi-Chi, Taiwan	7.62	99999	TAP079
1449	0137	Chi-Chi, Taiwan	7.62	99999	TAP081
1450	0137	Chi-Chi, Taiwan	7.62	99999	TAP083
1451	0137	Chi-Chi, Taiwan	7.62	99999	TAP084
1452	0137	Chi-Chi, Taiwan	7.62	99999	TAP086
1453	0137	Chi-Chi, Taiwan	7.62	99999	TAP087
1454	0137	Chi-Chi, Taiwan	7.62	99999	TAP090
1455	0137	Chi-Chi, Taiwan	7.62	99999	TAP094
1456	0137	Chi-Chi, Taiwan	7.62	99999	TAP095
1457	0137	Chi-Chi, Taiwan	7.62	99999	TAP097
1458	0137	Chi-Chi, Taiwan	7.62	99999	TAP098
1459	0137	Chi-Chi, Taiwan	7.62	99999	TAP100
1463	0137	Chi-Chi, Taiwan	7.62	99999	TCU003
1464	0137	Chi-Chi, Taiwan	7.62	99999	TCU006
1465	0137	Chi-Chi, Taiwan	7.62	99999	TCU007
1466	0137	Chi-Chi, Taiwan	7.62	99999	TCU008
1468	0137	Chi-Chi, Taiwan	7.62	99999	TCU010
1470	0137	Chi-Chi, Taiwan	7.62	99999	TCU014
1471	0137	Chi-Chi, Taiwan	7.62	99999	TCU015
1472	0137	Chi-Chi, Taiwan	7.62	99999	TCU017
1473	0137	Chi-Chi, Taiwan	7.62	99999	TCU018
1475	0137	Chi-Chi, Taiwan	7.62	99999	TCU026
1476	0137	Chi-Chi, Taiwan	7.62	99999	TCU029
1477	0137	Chi-Chi, Taiwan	7.62	99999	TCU031
1478	0137	Chi-Chi, Taiwan	7.62	99999	TCU033
1479	0137	Chi-Chi, Taiwan	7.62	99999	TCU034
1480	0137	Chi-Chi, Taiwan	7.62	99999	TCU036
1481	0137	Chi-Chi, Taiwan	7.62	99999	TCU038
1482	0137	Chi-Chi, Taiwan	7.62	99999	TCU039
1483	0137	Chi-Chi, Taiwan	7.62	99999	TCU040
1484	0137	Chi-Chi, Taiwan	7.62	99999	TCU042
1486	0137	Chi-Chi, Taiwan	7.62	99999	TCU046
1488	0137	Chi-Chi, Taiwan	7.62	99999	TCU048
1489	0137	Chi-Chi, Taiwan	7.62	99999	TCU049
1490	0137	Chi-Chi, Taiwan	7.62	99999	TCU050
1491	0137	Chi-Chi, Taiwan	7.62	99999	TCU051
1492	0137	Chi-Chi, Taiwan	7.62	99999	TCU052
1493	0137	Chi-Chi, Taiwan	7.62	99999	TCU053
1494	0137	Chi-Chi, Taiwan	7.62	99999	TCU054
1495	0137	Chi-Chi, Taiwan	7.62	99999	TCU055
1496	0137	Chi-Chi, Taiwan	7.62	99999	TCU056
1497	0137	Chi-Chi, Taiwan	7.62	99999	TCU057

RSN	EQID	Earthquake	M	Station No,	Station
1498	0137	Chi-Chi, Taiwan	7.62	99999	TCU059
1499	0137	Chi-Chi, Taiwan	7.62	99999	TCU060
1500	0137	Chi-Chi, Taiwan	7.62	99999	TCU061
1501	0137	Chi-Chi, Taiwan	7.62	99999	TCU063
1502	0137	Chi-Chi, Taiwan	7.62	99999	TCU064
1503	0137	Chi-Chi, Taiwan	7.62	99999	TCU065
1504	0137	Chi-Chi, Taiwan	7.62	99999	TCU067
1505	0137	Chi-Chi, Taiwan	7.62	99999	TCU068
1506	0137	Chi-Chi, Taiwan	7.62	99999	TCU070
1507	0137	Chi-Chi, Taiwan	7.62	99999	TCU071
1508	0137	Chi-Chi, Taiwan	7.62	99999	TCU072
1509	0137	Chi-Chi, Taiwan	7.62	99999	TCU074
1510	0137	Chi-Chi, Taiwan	7.62	99999	TCU075
1511	0137	Chi-Chi, Taiwan	7.62	99999	TCU076
1512	0137	Chi-Chi, Taiwan	7.62	99999	TCU078
1513	0137	Chi-Chi, Taiwan	7.62	99999	TCU079
1515	0137	Chi-Chi, Taiwan	7.62	99999	TCU082
1516	0137	Chi-Chi, Taiwan	7.62	99999	TCU083
1517	0137	Chi-Chi, Taiwan	7.62	99999	TCU084
1518	0137	Chi-Chi, Taiwan	7.62	99999	TCU085
1519	0137	Chi-Chi, Taiwan	7.62	99999	TCU087
1520	0137	Chi-Chi, Taiwan	7.62	99999	TCU088
1521	0137	Chi-Chi, Taiwan	7.62	99999	TCU089
1522	0137	Chi-Chi, Taiwan	7.62	99999	TCU092
1523	0137	Chi-Chi, Taiwan	7.62	99999	TCU094
1525	0137	Chi-Chi, Taiwan	7.62	99999	TCU096
1526	0137	Chi-Chi, Taiwan	7.62	99999	TCU098
1527	0137	Chi-Chi, Taiwan	7.62	99999	TCU100
1528	0137	Chi-Chi, Taiwan	7.62	99999	TCU101
1529	0137	Chi-Chi, Taiwan	7.62	99999	TCU102
1530	0137	Chi-Chi, Taiwan	7.62	99999	TCU103
1531	0137	Chi-Chi, Taiwan	7.62	99999	TCU104
1532	0137	Chi-Chi, Taiwan	7.62	99999	TCU105
1533	0137	Chi-Chi, Taiwan	7.62	99999	TCU106
1534	0137	Chi-Chi, Taiwan	7.62	99999	TCU107
1535	0137	Chi-Chi, Taiwan	7.62	99999	TCU109
1536	0137	Chi-Chi, Taiwan	7.62	99999	TCU110
1537	0137	Chi-Chi, Taiwan	7.62	99999	TCU111
1538	0137	Chi-Chi, Taiwan	7.62	99999	TCU112
1539	0137	Chi-Chi, Taiwan	7.62	99999	TCU113
1540	0137	Chi-Chi, Taiwan	7.62	99999	TCU115
1541	0137	Chi-Chi, Taiwan	7.62	99999	TCU116
1542	0137	Chi-Chi, Taiwan	7.62	99999	TCU117
1543	0137	Chi-Chi, Taiwan	7.62	99999	TCU118
1544	0137	Chi-Chi, Taiwan	7.62	99999	TCU119
1545	0137	Chi-Chi, Taiwan	7.62	99999	TCU120
1546	0137	Chi-Chi, Taiwan	7.62	99999	TCU122
1547	0137	Chi-Chi, Taiwan	7.62	99999	TCU123
1548	0137	Chi-Chi, Taiwan	7.62	99999	TCU128
1550	0137	Chi-Chi, Taiwan	7.62	99999	TCU136
1551	0137	Chi-Chi, Taiwan	7.62	99999	TCU138
1552	0137	Chi-Chi, Taiwan	7.62	99999	TCU140
1553	0137	Chi-Chi, Taiwan	7.62	99999	TCU141
1554	0137	Chi-Chi, Taiwan	7.62	99999	TCU145
1555	0137	Chi-Chi, Taiwan	7.62	99999	TCU147
1557	0137	Chi-Chi, Taiwan	7.62	99999	TTN001
1558	0137	Chi-Chi, Taiwan	7.62	99999	TTN002
1559	0137	Chi-Chi, Taiwan	7.62	99999	TTN003
1560	0137	Chi-Chi, Taiwan	7.62	99999	TTN004
1561	0137	Chi-Chi, Taiwan	7.62	99999	TTN005
1562	0137	Chi-Chi, Taiwan	7.62	99999	TTN006
1563	0137	Chi-Chi, Taiwan	7.62	99999	TTN007
1564	0137	Chi-Chi, Taiwan	7.62	99999	TTN008
1565	0137	Chi-Chi, Taiwan	7.62	99999	TTN009
1566	0137	Chi-Chi, Taiwan	7.62	99999	TTN010
1567	0137	Chi-Chi, Taiwan	7.62	99999	TTN012
1568	0137	Chi-Chi, Taiwan	7.62	99999	TTN013
1569	0137	Chi-Chi, Taiwan	7.62	99999	TTN014
1570	0137	Chi-Chi, Taiwan	7.62	99999	TTN015

RSN	EQID	Earthquake	M	Station No,	Station
1572	0137	Chi-Chi, Taiwan	7.62	99999	TTN018
1573	0137	Chi-Chi, Taiwan	7.62	99999	TTN020
1574	0137	Chi-Chi, Taiwan	7.62	99999	TTN022
1575	0137	Chi-Chi, Taiwan	7.62	99999	TTN023
1576	0137	Chi-Chi, Taiwan	7.62	99999	TTN024
1577	0137	Chi-Chi, Taiwan	7.62	99999	TTN025
1578	0137	Chi-Chi, Taiwan	7.62	99999	TTN026
1579	0137	Chi-Chi, Taiwan	7.62	99999	TTN027
1580	0137	Chi-Chi, Taiwan	7.62	99999	TTN028
1581	0137	Chi-Chi, Taiwan	7.62	99999	TTN031
1582	0137	Chi-Chi, Taiwan	7.62	99999	TTN032
1583	0137	Chi-Chi, Taiwan	7.62	99999	TTN033
1584	0137	Chi-Chi, Taiwan	7.62	99999	TTN036
1585	0137	Chi-Chi, Taiwan	7.62	99999	TTN040
1586	0137	Chi-Chi, Taiwan	7.62	99999	TTN041
1587	0137	Chi-Chi, Taiwan	7.62	99999	TTN042
1588	0137	Chi-Chi, Taiwan	7.62	99999	TTN044
1589	0137	Chi-Chi, Taiwan	7.62	99999	TTN045
1590	0137	Chi-Chi, Taiwan	7.62	99999	TTN046
1592	0137	Chi-Chi, Taiwan	7.62	99999	TTN048
1593	0137	Chi-Chi, Taiwan	7.62	99999	TTN050
1594	0137	Chi-Chi, Taiwan	7.62	99999	TTN051
1599	0138	Duzce, Turkey	7.14	99999	Ambarli
1600	0138	Duzce, Turkey	7.14	99999	Arcelik
1601	0138	Duzce, Turkey	7.14	99999	Aslan R.
1602	0138	Duzce, Turkey	7.14	99999	Bolu
1603	0138	Duzce, Turkey	7.14	99999	Bursa Tofas
1604	0138	Duzce, Turkey	7.14	99999	Cekmece
1605	0138	Duzce, Turkey	7.14	99999	Duzce
1606	0138	Duzce, Turkey	7.14	99999	Fatih
1608	0138	Duzce, Turkey	7.14	99999	Hava Alani
1609	0138	Duzce, Turkey	7.14	99999	Kocamustafapaba Tomb
1610	0138	Duzce, Turkey	7.14	99999	Kutahya
1611	0138	Duzce, Turkey	7.14	1058	Lamont 1058
1612	0138	Duzce, Turkey	7.14	1059	Lamont 1059
1613	0138	Duzce, Turkey	7.14	1060	Lamont 1060
1614	0138	Duzce, Turkey	7.14	1061	Lamont 1061
1615	0138	Duzce, Turkey	7.14	1062	Lamont 1062
1616	0138	Duzce, Turkey	7.14	362	Lamont 362
1617	0138	Duzce, Turkey	7.14	375	Lamont 375
1618	0138	Duzce, Turkey	7.14	531	Lamont 531
1619	0138	Duzce, Turkey	7.14	99999	Mudurnu
1620	0138	Duzce, Turkey	7.14	99999	Sakarya
1621	0138	Duzce, Turkey	7.14	99999	Yarimca
1622	0139	Stone Canyon	4.81	1210	Bear Valley #1, Fire Station
1623	0139	Stone Canyon	4.81	1211	Melendy Ranch
1624	0139	Stone Canyon	4.81	1343	Stone Canyon Geophys Obs
1626	0140	Sitka, Alaska	7.68	2714	Sitka Observatory
1627	0141	Caldiran, Turkey	7.21	37	Maku
1630	0143	Upland	5.63	99999	Ocean Floor SEMS III
1631	0143	Upland	5.63	23525	Pomona - 4th & Locust FF
1632	0143	Upland	5.63	23497	Rancho Cucamonga - FF
1633	0144	Manjil, Iran	7.37	99999	Abbar
1634	0144	Manjil, Iran	7.37	99999	Abhar
1636	0144	Manjil, Iran	7.37	99999	Qazvin
1637	0144	Manjil, Iran	7.37	99999	Rudsar
1638	0144	Manjil, Iran	7.37	99999	Tehran - Building & Housing
1639	0144	Manjil, Iran	7.37	99999	Tehran - Sarif University
1640	0144	Manjil, Iran	7.37	99999	Tonekabun
1641	0145	Sierra Madre	5.61	24402	Altadena - Eaton Canyon
1642	0145	Sierra Madre	5.61	23210	Cogswell Dam - Right Abutment
1643	0145	Sierra Madre	5.61	24592	LA - City Terrace
1644	0145	Sierra Madre	5.61	24400	LA - Obregon Park
1645	0145	Sierra Madre	5.61	24399	Mt Wilson - CIT Seis Sta
1646	0145	Sierra Madre	5.61	5296	Pasadena - USGS/NSMP Office
1647	0145	Sierra Madre	5.61	24401	San Marino - SW Academy
1648	0145	Sierra Madre	5.61	24436	Tarzana - Cedar Hill A
1649	0145	Sierra Madre	5.61	24047	Vasquez Rocks Park
1650	0147	Northridge-02	6.05	24576	Anaverde Valley - City R

RSN	EQID	Earthquake	M	Station No,	Station
1651	0147	Northridge-02	6.05	24087	Arleta - Nordhoff Fire Sta
1652	0147	Northridge-02	6.05	24278	Castaic - Old Ridge Route
1653	0147	Northridge-02	6.05	14368	Downey - Co Maint Bldg
1654	0147	Northridge-02	6.05	24575	Elizabeth Lake
1655	0147	Northridge-02	6.05	14196	Inglewood - Union Oil
1656	0147	Northridge-02	6.05	14403	LA - 116th St School
1657	0147	Northridge-02	6.05	24157	LA - Baldwin Hills
1658	0147	Northridge-02	6.05	24389	LA - Century City CC North
1659	0147	Northridge-02	6.05	24592	LA - City Terrace
1660	0147	Northridge-02	6.05	24303	LA - Hollywood Stor FF
1661	0147	Northridge-02	6.05	24400	LA - Obregon Park
1662	0147	Northridge-02	6.05	24611	LA - Temple & Hope
1663	0147	Northridge-02	6.05	24605	LA - Univ. Hospital
1664	0147	Northridge-02	6.05	24607	Lake Hughes #12A
1665	0147	Northridge-02	6.05	24279	Newhall - Fire Sta
1666	0147	Northridge-02	6.05	24088	Pacoima Kagel Canyon
1667	0147	Northridge-02	6.05	24521	Palmdale - Hwy 14 & Palmdale
1668	0148	Northridge-03	5.2	24278	Castaic - Old Ridge Route
1669	0148	Northridge-03	5.2	24575	Elizabeth Lake
1670	0148	Northridge-03	5.2	24279	Newhall - Fire Sta
1671	0148	Northridge-03	5.2	24088	Pacoima Kagel Canyon
1672	0148	Northridge-03	5.2	24644	Sandberg - Bald Mtn
1673	0148	Northridge-03	5.2	24538	Santa Monica City Hall
1674	0148	Northridge-03	5.2	24436	Tarzana - Cedar Hill A
1675	0149	Northridge-04	5.93	24576	Anaverde Valley - City R
1676	0149	Northridge-04	5.93	24278	Castaic - Old Ridge Route
1677	0149	Northridge-04	5.93	24575	Elizabeth Lake
1678	0149	Northridge-04	5.93	24592	LA - City Terrace
1679	0149	Northridge-04	5.93	24611	LA - Temple & Hope
1680	0149	Northridge-04	5.93	24605	LA - Univ. Hospital
1681	0149	Northridge-04	5.93	24283	Moorpark - Fire Sta
1682	0150	Northridge-05	5.13	24576	Anaverde Valley - City R
1683	0150	Northridge-05	5.13	24278	Castaic - Old Ridge Route
1684	0150	Northridge-05	5.13	24575	Elizabeth Lake
1686	0150	Northridge-05	5.13	655	Jensen Filter Plant Generator
1687	0150	Northridge-05	5.13	24592	LA - City Terrace
1688	0150	Northridge-05	5.13	24283	Moorpark - Fire Sta
1689	0150	Northridge-05	5.13	24088	Pacoima Kagel Canyon
1690	0150	Northridge-05	5.13	24763	Sylmar - County Hospital Grounds
1691	0151	Northridge-06	5.28	25169	Anacapa Island
1692	0151	Northridge-06	5.28	24576	Anaverde Valley - City R
1693	0151	Northridge-06	5.28	24087	Arleta - Nordhoff Fire Sta
1694	0151	Northridge-06	5.28	90014	Beverly Hills - 12520 Mulhol
1695	0151	Northridge-06	5.28	90061	Big Tujunga, Angeles Nat F
1696	0151	Northridge-06	5.28	90059	Burbank - Howard Rd.
1697	0151	Northridge-06	5.28	90012	Burbank - N Buena Vista
1698	0151	Northridge-06	5.28	90052	Calabasas - N Las Virg
1699	0151	Northridge-06	5.28	24278	Castaic - Old Ridge Route
1700	0151	Northridge-06	5.28	24575	Elizabeth Lake
1701	0151	Northridge-06	5.28	90018	Hollywood - Willoughby Ave
1702	0151	Northridge-06	5.28	14196	Inglewood - Union Oil
1704	0151	Northridge-06	5.28	655	Jensen Filter Plant Generator
1705	0151	Northridge-06	5.28	14403	LA - 116th St School
1706	0151	Northridge-06	5.28	24157	LA - Baldwin Hills
1707	0151	Northridge-06	5.28	24389	LA - Century City CC North
1708	0151	Northridge-06	5.28	24592	LA - City Terrace
1709	0151	Northridge-06	5.28	141	LA - Griffith Park Observatory
1710	0151	Northridge-06	5.28	24303	LA - Hollywood Stor FF
1711	0151	Northridge-06	5.28	90016	LA - N Faring Rd
1712	0151	Northridge-06	5.28	24611	LA - Temple & Hope
1713	0151	Northridge-06	5.28	24605	LA - Univ. Hospital
1714	0151	Northridge-06	5.28	90023	LA - W 70th St
1715	0151	Northridge-06	5.28	90017	LA - Wonderland Ave
1716	0151	Northridge-06	5.28	90060	La Crescenta - New York
1717	0151	Northridge-06	5.28	24607	Lake Hughes #12A
1718	0151	Northridge-06	5.28	23595	Littlerock - Brainard Can
1719	0151	Northridge-06	5.28	24396	Malibu - Point Dume Sch
1720	0151	Northridge-06	5.28	90062	Mill Creek, Angeles Nat For
1721	0151	Northridge-06	5.28	24279	Newhall - Fire Sta

RSN	EQID	Earthquake	M	Station No,	Station
1722	0151	Northridge-06	5.28	90003	Northridge - 17645 Saticoy St
1723	0151	Northridge-06	5.28	24088	Pacoima Kagel Canyon
1724	0151	Northridge-06	5.28	24521	Palmdale - Hwy 14 & Palmdale
1725	0151	Northridge-06	5.28	90007	Panorama City - Roscoe
1726	0151	Northridge-06	5.28	5296	Pasadena - USGS/NSMP Office
1727	0151	Northridge-06	5.28	23598	Rancho Cucamonga - Deer Can
1728	0151	Northridge-06	5.28	77	Rinaldi Receiving Sta
1729	0151	Northridge-06	5.28	24401	San Marino - SW Academy
1730	0151	Northridge-06	5.28	24538	Santa Monica City Hall
1731	0151	Northridge-06	5.28	14578	Seal Beach - Office Bldg
1732	0151	Northridge-06	5.28	90055	Simi Valley - Katherine Rd
1733	0151	Northridge-06	5.28	90006	Sun Valley - Roscoe Blvd
1734	0151	Northridge-06	5.28	90008	Sun Valley - Sunland
1735	0151	Northridge-06	5.28	90058	Sunland - Mt Gleason Ave
1736	0151	Northridge-06	5.28	74	Sylmar - Converter Sta
1737	0151	Northridge-06	5.28	75	Sylmar - Converter Sta East
1738	0151	Northridge-06	5.28	90001	Sylmar - Sayre St
1739	0151	Northridge-06	5.28	24436	Tarzana - Cedar Hill A
1740	0152	Little Skull Mtn,NV	5.65	99999	Station #1-Lathrop Wells
1741	0152	Little Skull Mtn,NV	5.65	99999	Station #2-NTS Control Pt. 1
1742	0152	Little Skull Mtn,NV	5.65	99999	Station #3-Beaty
1743	0152	Little Skull Mtn,NV	5.65	99999	Station #4-Pahrump 2
1744	0152	Little Skull Mtn,NV	5.65	99999	Station #5-Pahrump 1
1745	0152	Little Skull Mtn,NV	5.65	99999	Station #6-Las Vegas Calico Basin
1746	0152	Little Skull Mtn,NV	5.65	99999	Station #7-Las Vegas Ann Road
1747	0152	Little Skull Mtn,NV	5.65	99999	Station #8-Death Valley Scotties Castle
1758	0157	San Juan Bautista	5.17	1656	Hollister Diff. Array
1759	0158	Hector Mine	7.13	5239	12440 Imperial Hwy, North Grn
1761	0158	Hector Mine	7.13	24402	Altadena - Eaton Canyon
1762	0158	Hector Mine	7.13	21081	Amboy
1763	0158	Hector Mine	7.13	5044	Anza - Pinyon Flat
1764	0158	Hector Mine	7.13	5222	Anza - Tripp Flats Training
1765	0158	Hector Mine	7.13	24087	Arleta - Nordhoff Fire Sta
1766	0158	Hector Mine	7.13	32075	Baker Fire Station
1767	0158	Hector Mine	7.13	12674	Banning - Twin Pines Road
1768	0158	Hector Mine	7.13	23559	Barstow
1769	0158	Hector Mine	7.13	5402	Beverly Hills Pac Bell Bsmt
1770	0158	Hector Mine	7.13	22791	Big Bear Lake - Fire Station
1771	0158	Hector Mine	7.13	5271	Bombay Beach Fire Station
1772	0158	Hector Mine	7.13	5398	Burbank Airport
1773	0158	Hector Mine	7.13	5073	Cabazon
1775	0158	Hector Mine	7.13	24278	Castaic - Old Ridge Route
1776	0158	Hector Mine	7.13	12149	Desert Hot Springs
1777	0158	Hector Mine	7.13	5265	Devore - Devore Water Company
1778	0158	Hector Mine	7.13	14368	Downey - Co Maint Bldg
1779	0158	Hector Mine	7.13	412	El Centro Array #10
1780	0158	Hector Mine	7.13	13122	Featherly Park - Maint
1781	0158	Hector Mine	7.13	5401	Fillmore Pac Bell
1782	0158	Hector Mine	7.13	5075	Forest Falls Post Office
1783	0158	Hector Mine	7.13	24577	Fort Irwin
1784	0158	Hector Mine	7.13	11684	Frink
1785	0158	Hector Mine	7.13	5069	Fun Valley
1786	0158	Hector Mine	7.13	22T04	Heart Bar State Park
1787	0158	Hector Mine	7.13	99999	Hector
1788	0158	Hector Mine	7.13	12331	Hemet Fire Station
1789	0158	Hector Mine	7.13	23583	Hesperia - 4th & Palm
1790	0158	Hector Mine	7.13	13197	Huntington Beach - Lake St
1791	0158	Hector Mine	7.13	12026	Indio - Coachella Canal
1792	0158	Hector Mine	7.13	12543	Indio - Riverside Co Fair Grnds
1793	0158	Hector Mine	7.13	655	Jensen Filter Plant Generator
1794	0158	Hector Mine	7.13	22170	Joshua Tree
1795	0158	Hector Mine	7.13	12647	Joshua Tree N.M. - Keys View
1796	0158	Hector Mine	7.13	14403	LA - 116th St School
1797	0158	Hector Mine	7.13	24592	LA - City Terrace
1798	0158	Hector Mine	7.13	14787	LA - MLK Hospital Grounds
1799	0158	Hector Mine	7.13	24400	LA - Obregon Park
1800	0158	Hector Mine	7.13	24612	LA - Pico & Sentous
1801	0158	Hector Mine	7.13	24611	LA - Temple & Hope
1802	0158	Hector Mine	7.13	5399	LAX Fire Station

RSN	EQID	Earthquake	M	Station No,	Station
1803	0158	Hector Mine	7.13	14560	LB - City Hall
1804	0158	Hector Mine	7.13	5408	La Canada - Wald Residence
1805	0158	Hector Mine	7.13	24271	Lake Hughes #1
1806	0158	Hector Mine	7.13	5029	Leona Valley - Fire Station #1
1807	0158	Hector Mine	7.13	5030	Little Rock Post Office
1808	0158	Hector Mine	7.13	5396	Los Angeles - Acosta Residence
1809	0158	Hector Mine	7.13	5409	Lytle Creek Fire Station
1810	0158	Hector Mine	7.13	11625	Mecca - CVWD Yard
1811	0158	Hector Mine	7.13	5162	Mentone Fire Station #9
1812	0158	Hector Mine	7.13	5076	Mill Creek Ranger Station
1813	0158	Hector Mine	7.13	5071	Morongo Valley
1814	0158	Hector Mine	7.13	24279	Newhall - Fire Sta
1815	0158	Hector Mine	7.13	13160	Newport Bch - Irvine Ave. F.S
1816	0158	Hector Mine	7.13	5295	North Palm Springs Fire Sta #36
1817	0158	Hector Mine	7.13	11591	North Shore - Durmid
1818	0158	Hector Mine	7.13	24088	Pacoima Kagel Canyon
1819	0158	Hector Mine	7.13	262	Palmdale Fire Station
1820	0158	Hector Mine	7.13	24691	Pasadena - Fair Oaks & Walnut
1821	0158	Hector Mine	7.13	23525	Pomona - 4th & Locust FF
1822	0158	Hector Mine	7.13	13123	Riverside Airport
1823	0158	Hector Mine	7.13	11628	Salton City
1824	0158	Hector Mine	7.13	5331	San Bernardino - Del Rosa Wk Sta
1825	0158	Hector Mine	7.13	23542	San Bernardino - E & Hospitality
1826	0158	Hector Mine	7.13	5339	San Bernardino - Fire Sta. #10
1827	0158	Hector Mine	7.13	5337	San Bernardino - Fire Sta. #4
1828	0158	Hector Mine	7.13	5330	San Bernardino - Fire Sta. #9
1829	0158	Hector Mine	7.13	5328	San Bernardino - Mont. Mem Pk
1830	0158	Hector Mine	7.13	5371	San Bernardino - N Verdemont Sch
1831	0158	Hector Mine	7.13	12204	San Jacinto - Soboba
1832	0158	Hector Mine	7.13	5300	Seven Oaks Dam Project Office
1833	0158	Hector Mine	7.13	12630	Snow Creek
1834	0158	Hector Mine	7.13	24763	Sylmar - County Hospital Grounds
1835	0158	Hector Mine	7.13	13172	Temecula - 6th & Mercedes
1836	0158	Hector Mine	7.13	22161	Twentynine Palms
1837	0158	Hector Mine	7.13	5031	Valyermo Forest Fire Station
1838	0158	Hector Mine	7.13	5072	Whitewater Trout Farm
1839	0158	Hector Mine	7.13	14840	Whittier - Scott & Whittier
1840	0158	Hector Mine	7.13	289	Whittier Narrows Dam downstream
1841	0158	Hector Mine	7.13	23573	Wrightwood - Nielson Ranch
1842	0158	Hector Mine	7.13	5282	Wrightwood Post Office
1843	0160	Yountville	5	1002	APEEL 2 - Redwood City
1844	0160	Yountville	5	1756	Alameda - Oakland Airport FS #4
1845	0160	Yountville	5	1755	Alameda Fire Station #1
1846	0160	Yountville	5	1760	Benicia Fire Station #1
1847	0160	Yountville	5	1690	Danville Fire Station
1848	0160	Yountville	5	1689	Dublin - Fire Station
1849	0160	Yountville	5	1737	El Cerrito - Mira Vista Country
1850	0160	Yountville	5	1753	Foster City - Bowditch School
1851	0160	Yountville	5	1678	Golden Gate Bridge
1852	0160	Yountville	5	1590	Larkspur Ferry Terminal (FF)
1853	0160	Yountville	5	1765	Napa Fire Station #3
1854	0160	Yountville	5	1762	Novato Fire Station #1
1855	0160	Yountville	5	1751	Novato Fire Station #4
1856	0160	Yountville	5	1743	Petaluma Fire Station
1857	0160	Yountville	5	1768	Petaluma Fire Station #1
1858	0160	Yountville	5	1691	Pleasant Hill Fire Station #2
1859	0160	Yountville	5	1785	Pleasanton Fire Station #1
1860	0160	Yountville	5	1749	Richmond - Point Molate
1861	0160	Yountville	5	1722	Richmond Rod & Gun Club
1862	0160	Yountville	5	1735	San Francisco - 9th Circuit Crt
1863	0160	Yountville	5	1774	San Francisco - Fire Station #2
1865	0160	Yountville	5	1767	Santa Rosa Fire Station #1
1866	0160	Yountville	5	1761	Sonoma Fire Station #1
1867	0160	Yountville	5	1759	Vallejo Fire Station #1
1868	0161	Big Bear-02	4.53	23788	Colton - Hospital Complex FF
1869	0161	Big Bear-02	4.53	5341	Colton - Kaiser Medical Clinic
1870	0161	Big Bear-02	4.53	5265	Devore - Devore Water Company
1871	0161	Big Bear-02	4.53	5075	Forest Falls Post Office
1872	0161	Big Bear-02	4.53	23957	Helendale - Helendale & Vista

RSN	EQID	Earthquake	M	Station No,	Station
1873	0161	Big Bear-02	4.53	12331	Hemet Fire Station
1874	0161	Big Bear-02	4.53	23583	Hesperia - 4th & Palm
1875	0161	Big Bear-02	4.53	5161	Highland Fire Station
1876	0161	Big Bear-02	4.53	13924	Homeland - Hwy 74 & Sultanas
1877	0161	Big Bear-02	4.53	5294	Indio - Jackson Road
1878	0161	Big Bear-02	4.53	12904	Indio - Monroe & Carreon
1879	0161	Big Bear-02	4.53	22959	Landers - Hwy 247 & Jesse
1881	0161	Big Bear-02	4.53	5409	Lytle Creek Fire Station
1882	0161	Big Bear-02	4.53	5162	Mentone Fire Station #9
1883	0161	Big Bear-02	4.53	5076	Mill Creek Ranger Station
1884	0161	Big Bear-02	4.53	13927	Moreno Valley - Alessandro&More
1885	0161	Big Bear-02	4.53	13925	Moreno Valley - Indian & Kennedy
1886	0161	Big Bear-02	4.53	5071	Morongo Valley
1887	0161	Big Bear-02	4.53	5295	North Palm Springs Fire Sta #36
1888	0161	Big Bear-02	4.53	23958	Pinon Hills - Hwy 138 & Mtn Road
1889	0161	Big Bear-02	4.53	5037	Reche Canyon - Olive Dell Ranch
1890	0161	Big Bear-02	4.53	13915	Riverside - I215 & 3rd
1891	0161	Big Bear-02	4.53	5331	San Bernardino - Del Rosa Wk Sta
1892	0161	Big Bear-02	4.53	23542	San Bernardino - E & Hospitality
1893	0161	Big Bear-02	4.53	5339	San Bernardino - Fire Sta. #10
1894	0161	Big Bear-02	4.53	5329	San Bernardino - Fire Sta. #11
1895	0161	Big Bear-02	4.53	5337	San Bernardino - Fire Sta. #4
1896	0161	Big Bear-02	4.53	5327	San Bernardino - Fire Sta. #7
1897	0161	Big Bear-02	4.53	5330	San Bernardino - Fire Sta. #9
1898	0161	Big Bear-02	4.53	5373	San Bernardino - Lincoln School
1899	0161	Big Bear-02	4.53	23898	San Bernardino - Medical Center
1900	0161	Big Bear-02	4.53	5328	San Bernardino - Mont. Mem Pk
1901	0161	Big Bear-02	4.53	23780	San Bernardino - Mtn Vw & Clstr
1902	0161	Big Bear-02	4.53	5336	San Bernardino - Serrano School
1903	0161	Big Bear-02	4.53	5300	Seven Oaks Dam Downstream Surf.
1904	0161	Big Bear-02	4.53	5300	Seven Oaks Dam Right Abt.
1905	0161	Big Bear-02	4.53	13930	Sun City - I215 & McCall Blvd
1906	0161	Big Bear-02	4.53	5031	Valyermo Forest Fire Station
1907	0161	Big Bear-02	4.53	5072	Whitewater Trout Farm
1908	0161	Big Bear-02	4.53	5282	Wrightwood Post Office
1909	0161	Big Bear-02	4.53	22074	Yermo Fire Station
1910	0161	Big Bear-02	4.53	23920	Yucaipa Valley - Calimesa & Cnty
1911	0162	Mohawk Val, Portola	5.17	2019	Carson City - Nevada Com College
1912	0162	Mohawk Val, Portola	5.17	1133	Martis Creek Dam (Dwn Stream)
1913	0162	Mohawk Val, Portola	5.17	1133	Martis Creek Dam (Left Abtmnt)
1914	0162	Mohawk Val, Portola	5.17	1133	Martis Creek Dam (Right Abtmnt)
1915	0162	Mohawk Val, Portola	5.17	2023	Reno - Sierra Pacific Power Co
1916	0162	Mohawk Val, Portola	5.17	2018	Silver Springs Fire Station
1917	0163	Anza-02	4.92	02467	Alpine Fire Station
1918	0163	Anza-02	4.92	5044	Anza - Pinyon Flat
1919	0163	Anza-02	4.92	5222	Anza - Tripp Flats Training
1920	0163	Anza-02	4.92	5160	Anza Fire Station
1921	0163	Anza-02	4.92	12919	Beaumont - 6th & Maple
1922	0163	Anza-02	4.92	22791	Big Bear Lake - Fire Station
1923	0163	Anza-02	4.92	5220	Borrego Springs - Scripps Clinic
1924	0163	Anza-02	4.92	5073	Cabazon
1925	0163	Anza-02	4.92	5053	Calexico Fire Station
1926	0163	Anza-02	4.92	13096	Canyon Lake Vacation Dr&San Joaq
1927	0163	Anza-02	4.92	12076	Coachella - 6th & Palm
1928	0163	Anza-02	4.92	13099	Corona - 6th & Smith
1929	0163	Anza-02	4.92	13098	Corona - Hwy 91 & McKinley
1930	0163	Anza-02	4.92	464	El Centro - Meadows Union School
1931	0163	Anza-02	4.92	412	El Centro Array #10
1932	0163	Anza-02	4.92	5058	El Centro Array #11
1933	0163	Anza-02	4.92	5028	El Centro Array #7
1934	0163	Anza-02	4.92	5069	Fun Valley
1935	0163	Anza-02	4.92	12923	Hemet - Acacia & Stanford
1936	0163	Anza-02	4.92	13093	Hemet - Cawston & Devonshire
1937	0163	Anza-02	4.92	12331	Hemet Fire Station
1938	0163	Anza-02	4.92	5161	Highland Fire Station
1940	0163	Anza-02	4.92	13924	Homeland - Hwy 74 & Sultanas
1941	0163	Anza-02	4.92	5043	Hurkey Creek Park
1942	0163	Anza-02	4.92	12116	Idyllwild - Hwy 243 & Pine Crest
1943	0163	Anza-02	4.92	5232	Idyllwild - Keenwild Fire Sta.

RSN	EQID	Earthquake	M	Station No,	Station
1944	0163	Anza-02	4.92	5372	Idyllwild - Kenworthy Fire Sta.
1945	0163	Anza-02	4.92	12966	Indian Wells - Hwy111 & El Dorad
1946	0163	Anza-02	4.92	5294	Indio - Jackson Road
1947	0163	Anza-02	4.92	22170	Joshua Tree
1948	0163	Anza-02	4.92	12951	La Quinta - Bermudas & Durango
1949	0163	Anza-02	4.92	13922	Lake Elsinore - Graham & Poe
1950	0163	Anza-02	4.92	5270	Mecca Fire Station
1951	0163	Anza-02	4.92	13929	Menifee Valley - Murrieta&Scott
1952	0163	Anza-02	4.92	5076	Mill Creek Ranger Station
1953	0163	Anza-02	4.92	23091	Mira Loma - Mission&San Sevaine
1954	0163	Anza-02	4.92	13927	Moreno Valley - Alessandro&More
1955	0163	Anza-02	4.92	13925	Moreno Valley - Indian & Kennedy
1956	0163	Anza-02	4.92	13080	Moreno Valley - Sunny Mead & Vil
1957	0163	Anza-02	4.92	5071	Morongo Valley
1958	0163	Anza-02	4.92	5223	Mountain Center - Pine Mtn Rnch
1959	0163	Anza-02	4.92	11023	Niland Fire Station
1960	0163	Anza-02	4.92	5295	North Palm Springs Fire Sta #36
1961	0163	Anza-02	4.92	13095	Nuevo - 11th & McKinley
1962	0163	Anza-02	4.92	5375	Ocotillo Wells - Veh. Rec. Area
1963	0163	Anza-02	4.92	12952	Palm Desert - Country Club & Por
1964	0163	Anza-02	4.92	13928	Perris - San Jacinto & C Street
1965	0163	Anza-02	4.92	03449	Poway - City Hall Grounds
1966	0163	Anza-02	4.92	12092	Radec - Sage & Cottonwood School
1967	0163	Anza-02	4.92	12953	Rancho Mirage - G Ford & B Hope
1968	0163	Anza-02	4.92	5037	Reche Canyon - Olive Dell Ranch
1969	0163	Anza-02	4.92	13913	Riverside - Hole & La Sierra
1970	0163	Anza-02	4.92	13079	Riverside - Hwy 91 & Van Buren
1971	0163	Anza-02	4.92	13921	Riverside - Limonite & Downey
1972	0163	Anza-02	4.92	13916	Riverside - Van Buren&Trautwein
1973	0163	Anza-02	4.92	13123	Riverside Airport
1974	0163	Anza-02	4.92	12636	Sage - Fire Station
1975	0163	Anza-02	4.92	5331	San Bernardino - Del Rosa Wk Sta
1976	0163	Anza-02	4.92	5339	San Bernardino - Fire Sta. #10
1977	0163	Anza-02	4.92	5329	San Bernardino - Fire Sta. #11
1978	0163	Anza-02	4.92	5337	San Bernardino - Fire Sta. #4
1979	0163	Anza-02	4.92	5327	San Bernardino - Fire Sta. #7
1980	0163	Anza-02	4.92	5373	San Bernardino - Lincoln School
1981	0163	Anza-02	4.92	5328	San Bernardino - Mont. Mem Pk
1982	0163	Anza-02	4.92	5336	San Bernardino - Serrano School
1983	0163	Anza-02	4.92	5289	San Jacinto - MWD West Portal
1984	0163	Anza-02	4.92	12102	San Jacinto CDF Fire Station 25
1985	0163	Anza-02	4.92	5300	Seven Oaks Dam Downstream Surf.
1986	0163	Anza-02	4.92	13930	Sun City - I215 & McCall Blvd
1987	0163	Anza-02	4.92	13172	Temecula - 6th & Mercedes
1988	0163	Anza-02	4.92	22954	Twentynine Palms - Two Miles&Alp
1989	0163	Anza-02	4.92	5072	Whitewater Trout Farm
1990	0164	Gulf of California	5.7	5054	Bonds Corner
1991	0164	Gulf of California	5.7	5053	Calexico Fire Station
1992	0164	Gulf of California	5.7	5061	Calipatria Fire Station
1993	0164	Gulf of California	5.7	464	El Centro - Meadows Union School
1994	0164	Gulf of California	5.7	412	El Centro Array #10
1995	0164	Gulf of California	5.7	5058	El Centro Array #11
1996	0164	Gulf of California	5.7	5028	El Centro Array #7
1998	0164	Gulf of California	5.7	5055	Holtville Post Office
1999	0164	Gulf of California	5.7	5272	Imperial Valley - Midway Well
2000	0164	Gulf of California	5.7	5052	Plaster City
2001	0164	Gulf of California	5.7	5273	Seeley School
2002	0165	CA/Baja Border Area	5.31	5060	Brawley Airport
2003	0165	CA/Baja Border Area	5.31	5053	Calexico Fire Station
2004	0165	CA/Baja Border Area	5.31	5061	Calipatria Fire Station
2005	0165	CA/Baja Border Area	5.31	464	El Centro - Meadows Union School
2006	0165	CA/Baja Border Area	5.31	412	El Centro Array #10
2007	0165	CA/Baja Border Area	5.31	5058	El Centro Array #11
2008	0165	CA/Baja Border Area	5.31	5028	El Centro Array #7
2009	0165	CA/Baja Border Area	5.31	5055	Holtville Post Office
2010	0165	CA/Baja Border Area	5.31	5062	Salton Sea Wildlife Refuge
2011	0166	Gilroy	4.9	1756	Alameda - Oakland Airport FS #4
2012	0166	Gilroy	4.9	1755	Alameda Fire Station #1
2013	0166	Gilroy	4.9	47729	Big Sur - Hwy 1 & Pfeiffer Cyn

RSN	EQID	Earthquake	M	Station No,	Station
2014	0166	Gilroy	4.9	1720	Cupertino - Sunnyvale Rod & Gun
2015	0166	Gilroy	4.9	1689	Dublin - Fire Station
2016	0166	Gilroy	4.9	1753	Foster City - Bowditch School
2017	0166	Gilroy	4.9	1750	Fremont - Coyote Hills Park
2018	0166	Gilroy	4.9	57064	Fremont - Mission San Jose
2019	0166	Gilroy	4.9	47006	Gilroy - Gavilan Coll.
2020	0166	Gilroy	4.9	47381	Gilroy Array #3
2021	0166	Gilroy	4.9	57383	Gilroy Array #6
2022	0166	Gilroy	4.9	1678	Golden Gate Bridge
2023	0166	Gilroy	4.9	1754	Hayward Fire - Station #1
2024	0166	Gilroy	4.9	1797	Hollister - Airport Bldg #3
2026	0166	Gilroy	4.9	47524	Hollister - South & Pine
2027	0166	Gilroy	4.9	1697	Los Gatos - Los Altos Rod & Gun
2028	0166	Gilroy	4.9	1784	Menlo Park - USGS Bldg #11 Shop
2029	0166	Gilroy	4.9	1745	Menlo Park - USGS Bldg #15 FF
2030	0166	Gilroy	4.9	1758	Morgan Hill - El Toro Fire Sta
2031	0166	Gilroy	4.9	1787	Palo Alto - Fire Station #7 SLAC
2032	0166	Gilroy	4.9	1749	Richmond - Point Molate
2033	0166	Gilroy	4.9	47762	Salinas - County Hospital Gnds
2034	0166	Gilroy	4.9	1675	San Francisco - Fire Station #17
2036	0166	Gilroy	4.9	57600	San Jose - Emory & Bellrose
2037	0166	Gilroy	4.9	57604	San Jose - S Clara Co Bldg Grnd
2038	0166	Gilroy	4.9	1742	San Jose - Weather Station
2039	0166	Gilroy	4.9	47126	San Juan Bautista, 24 Polk St
2040	0166	Gilroy	4.9	57748	Santa Clara - Hwy 237/Alviso OVP
2041	0166	Gilroy	4.9	48906	Santa Cruz - Co Office Bldg Gnds
2042	0166	Gilroy	4.9	1695	Sunnyvale - Colton Ave.
2043	0166	Gilroy	4.9	1688	Sunol - Forest Fire Station
2044	0166	Gilroy	4.9	1684	Sunol - Ohlone Wilderness Reg Pk
2045	0166	Gilroy	4.9	1739	Union City - Masonic Home
2046	0166	Gilroy	4.9	1752	Woodside - Filoli Visitor Center
2047	0167	Yorba Linda	4.265	13066	Anaheim - Brookhurst & Crescent
2048	0167	Yorba Linda	4.265	13068	Anaheim - Hwy 91 & Weir Cyn Rd
2049	0167	Yorba Linda	4.265	13849	Anaheim - Lakeview & Riverdale
2050	0167	Yorba Linda	4.265	13873	Brea - Central Ave Caltrans Yard
2051	0167	Yorba Linda	4.265	24941	City of Commerce - Whittier &
2052	0167	Yorba Linda	4.265	13099	Corona - 6th & Smith
2053	0167	Yorba Linda	4.265	13100	Corona - Green River & Cyn Crest
2054	0167	Yorba Linda	4.265	13878	Fullerton - CSU Fullerton Grnds
2055	0167	Yorba Linda	4.265	13880	Fullerton - Hermosa & Harbor
2056	0167	Yorba Linda	4.265	13879	Fullerton - Valencia&Brookhurst
2057	0167	Yorba Linda	4.265	13881	La Habra - La Habra&Monte Vista
2058	0167	Yorba Linda	4.265	13079	Riverside - Hwy 91 & Van Buren
2060	0168	Nenana Mountain, Alaska	6.7	8036	Anchorage - DOI Off. of Aircraft
2061	0168	Nenana Mountain, Alaska	6.7	8024	Anchorage - Dowl Eng Warehouse
2062	0168	Nenana Mountain, Alaska	6.7	K202	Anchorage - K2-02
2063	0168	Nenana Mountain, Alaska	6.7	K203	Anchorage - K2-03
2064	0168	Nenana Mountain, Alaska	6.7	K204	Anchorage - K2-04
2065	0168	Nenana Mountain, Alaska	6.7	K205	Anchorage - K2-05
2066	0168	Nenana Mountain, Alaska	6.7	K206	Anchorage - K2-06
2067	0168	Nenana Mountain, Alaska	6.7	K207	Anchorage - K2-07
2068	0168	Nenana Mountain, Alaska	6.7	K208	Anchorage - K2-08
2069	0168	Nenana Mountain, Alaska	6.7	K209	Anchorage - K2-09
2070	0168	Nenana Mountain, Alaska	6.7	K210	Anchorage - K2-10
2071	0168	Nenana Mountain, Alaska	6.7	K211	Anchorage - K2-11
2072	0168	Nenana Mountain, Alaska	6.7	K212	Anchorage - K2-12
2073	0168	Nenana Mountain, Alaska	6.7	K213	Anchorage - K2-13
2074	0168	Nenana Mountain, Alaska	6.7	K214	Anchorage - K2-14
2075	0168	Nenana Mountain, Alaska	6.7	K215	Anchorage - K2-15
2076	0168	Nenana Mountain, Alaska	6.7	K216	Anchorage - K2-16
2077	0168	Nenana Mountain, Alaska	6.7	K217	Anchorage - K2-17
2078	0168	Nenana Mountain, Alaska	6.7	K218	Anchorage - K2-18
2079	0168	Nenana Mountain, Alaska	6.7	K219	Anchorage - K2-19
2081	0168	Nenana Mountain, Alaska	6.7	K221	Anchorage - K2-21
2082	0168	Nenana Mountain, Alaska	6.7	K222	Anchorage - K2-22
2083	0168	Nenana Mountain, Alaska	6.7	8037	Anchorage - NOAA Weather Fac.
2084	0168	Nenana Mountain, Alaska	6.7	8038	Anchorage - New Fire Station #1
2085	0168	Nenana Mountain, Alaska	6.7	8039	Anchorage - New Fire Station #7
2086	0168	Nenana Mountain, Alaska	6.7	8030	Anchorage - Police Headquarters

RSN	EQID	Earthquake	M	Station No,	Station
2087	0168	Nenana Mountain, Alaska	6.7	8027	Anchorage - State Fish & Game
2088	0168	Nenana Mountain, Alaska	6.7	8007	Anchorage International Airport
2089	0168	Nenana Mountain, Alaska	6.7	FA02	Fairbanks - Ester Fire Station
2090	0168	Nenana Mountain, Alaska	6.7	2797	Fairbanks - Geophysic. Obs, CIGO
2091	0168	Nenana Mountain, Alaska	6.7	ps07	TAPS Pump Station #07
2092	0168	Nenana Mountain, Alaska	6.7	ps08	TAPS Pump Station #08
2093	0168	Nenana Mountain, Alaska	6.7	ps09	TAPS Pump Station #09
2095	0169	Denali, Alaska	7.9	8036	Anchorage - DOI Off. of Aircraft
2096	0169	Denali, Alaska	7.9	8024	Anchorage - Dowl Eng Warehouse
2097	0169	Denali, Alaska	7.9	K202	Anchorage - K2-02
2098	0169	Denali, Alaska	7.9	K203	Anchorage - K2-03
2099	0169	Denali, Alaska	7.9	K204	Anchorage - K2-04
2100	0169	Denali, Alaska	7.9	K205	Anchorage - K2-05
2101	0169	Denali, Alaska	7.9	K206	Anchorage - K2-06
2102	0169	Denali, Alaska	7.9	8037	Anchorage - NOAA Weather Fac.
2103	0169	Denali, Alaska	7.9	8038	Anchorage - New Fire Station #1
2104	0169	Denali, Alaska	7.9	8039	Anchorage - New Fire Station #7
2105	0169	Denali, Alaska	7.9	8030	Anchorage - Police Headquarters
2106	0169	Denali, Alaska	7.9	8027	Anchorage - State Fish & Game
2107	0169	Denali, Alaska	7.9	Carl	Carlo (temp)
2108	0169	Denali, Alaska	7.9	8019	Eagle River - AK Geologic Mat
2109	0169	Denali, Alaska	7.9	FA02	Fairbanks - Ester Fire Station
2110	0169	Denali, Alaska	7.9	2797	Fairbanks - Geophysic. Obs, CIGO
2111	0169	Denali, Alaska	7.9	R109	R109 (temp)
2112	0169	Denali, Alaska	7.9	ps08	TAPS Pump Station #08
2113	0169	Denali, Alaska	7.9	ps09	TAPS Pump Station #09
2114	0169	Denali, Alaska	7.9	ps10	TAPS Pump Station #10
2115	0169	Denali, Alaska	7.9	ps11	TAPS Pump Station #11
2116	0169	Denali, Alaska	7.9	ps12	TAPS Pump Station #12
2118	0169	Denali, Alaska	7.9	2723	Valdez - Valdez Dock Company
2119	0170	Big Bear City	4.92	5222	Anza - Tripp Flats Training
2120	0170	Big Bear City	4.92	5073	Cabazon
2121	0170	Big Bear City	4.92	5341	Colton - Kaiser Medical Clinic
2122	0170	Big Bear City	4.92	5265	Devore - Devore Water Company
2123	0170	Big Bear City	4.92	5075	Forest Falls Post Office
2124	0170	Big Bear City	4.92	5161	Highland Fire Station
2125	0170	Big Bear City	4.92	5294	Indio - Jackson Road
2126	0170	Big Bear City	4.92	5029	Leona Valley - Fire Station #1
2128	0170	Big Bear City	4.92	5396	Los Angeles - Acosta Residence
2129	0170	Big Bear City	4.92	5162	Mentone Fire Station #9
2130	0170	Big Bear City	4.92	5076	Mill Creek Ranger Station
2131	0170	Big Bear City	4.92	5071	Morongo Valley
2132	0170	Big Bear City	4.92	5295	North Palm Springs Fire Sta #36
2133	0170	Big Bear City	4.92	262	Palmdale Fire Station
2134	0170	Big Bear City	4.92	5032	Paradise Springs - Camp Office
2135	0170	Big Bear City	4.92	5296	Pasadena - USGS/NSMP Office
2137	0170	Big Bear City	4.92	5245	San Bernardino - Co Service Bldg - Freefield
2138	0170	Big Bear City	4.92	5331	San Bernardino - Del Rosa Wk Sta
2139	0170	Big Bear City	4.92	5339	San Bernardino - Fire Sta. #10
2140	0170	Big Bear City	4.92	5329	San Bernardino - Fire Sta. #11
2141	0170	Big Bear City	4.92	5337	San Bernardino - Fire Sta. #4
2142	0170	Big Bear City	4.92	5327	San Bernardino - Fire Sta. #7
2143	0170	Big Bear City	4.92	5330	San Bernardino - Fire Sta. #9
2144	0170	Big Bear City	4.92	5373	San Bernardino - Lincoln School
2145	0170	Big Bear City	4.92	5328	San Bernardino - Mont. Mem Pk
2146	0170	Big Bear City	4.92	5371	San Bernardino - N Verdemont Sch
2147	0170	Big Bear City	4.92	5336	San Bernardino - Serrano School
2148	0170	Big Bear City	4.92	5036	San Bernardino - Sycamore FS
2149	0170	Big Bear City	4.92	5300	Seven Oaks Dam Downstream Surf.
2150	0170	Big Bear City	4.92	5300	Seven Oaks Dam Right Abt.
2151	0170	Big Bear City	4.92	5435	Sky Valley - Fire Station #56
2152	0170	Big Bear City	4.92	5423	Sylmar - Fire Station #91
2153	0170	Big Bear City	4.92	5031	Valyermo Forest Fire Station
2154	0170	Big Bear City	4.92	5072	Whitewater Trout Farm
2155	0170	Big Bear City	4.92	5282	Wrightwood Post Office
2156	0171	Chi-Chi, Taiwan-02	5.9	99999	CHY017
2157	0171	Chi-Chi, Taiwan-02	5.9	99999	CHY019
2158	0171	Chi-Chi, Taiwan-02	5.9	99999	CHY022

RSN	EQID	Earthquake	M	Station No,	Station
2159	0171	Chi-Chi, Taiwan-02	5.9	99999	CHY024
2160	0171	Chi-Chi, Taiwan-02	5.9	99999	CHY025
2161	0171	Chi-Chi, Taiwan-02	5.9	99999	CHY026
2162	0171	Chi-Chi, Taiwan-02	5.9	99999	CHY027
2163	0171	Chi-Chi, Taiwan-02	5.9	99999	CHY028
2164	0171	Chi-Chi, Taiwan-02	5.9	99999	CHY029
2165	0171	Chi-Chi, Taiwan-02	5.9	99999	CHY032
2166	0171	Chi-Chi, Taiwan-02	5.9	99999	CHY033
2167	0171	Chi-Chi, Taiwan-02	5.9	99999	CHY034
2168	0171	Chi-Chi, Taiwan-02	5.9	99999	CHY035
2169	0171	Chi-Chi, Taiwan-02	5.9	99999	CHY036
2170	0171	Chi-Chi, Taiwan-02	5.9	99999	CHY039
2171	0171	Chi-Chi, Taiwan-02	5.9	99999	CHY041
2172	0171	Chi-Chi, Taiwan-02	5.9	99999	CHY042
2173	0171	Chi-Chi, Taiwan-02	5.9	99999	CHY044
2174	0171	Chi-Chi, Taiwan-02	5.9	99999	CHY046
2175	0171	Chi-Chi, Taiwan-02	5.9	99999	CHY047
2176	0171	Chi-Chi, Taiwan-02	5.9	99999	CHY050
2177	0171	Chi-Chi, Taiwan-02	5.9	99999	CHY052
2178	0171	Chi-Chi, Taiwan-02	5.9	99999	CHY054
2179	0171	Chi-Chi, Taiwan-02	5.9	99999	CHY055
2180	0171	Chi-Chi, Taiwan-02	5.9	99999	CHY056
2181	0171	Chi-Chi, Taiwan-02	5.9	99999	CHY057
2182	0171	Chi-Chi, Taiwan-02	5.9	99999	CHY058
2183	0171	Chi-Chi, Taiwan-02	5.9	99999	CHY060
2184	0171	Chi-Chi, Taiwan-02	5.9	99999	CHY061
2185	0171	Chi-Chi, Taiwan-02	5.9	99999	CHY062
2186	0171	Chi-Chi, Taiwan-02	5.9	99999	CHY063
2187	0171	Chi-Chi, Taiwan-02	5.9	99999	CHY065
2188	0171	Chi-Chi, Taiwan-02	5.9	99999	CHY067
2189	0171	Chi-Chi, Taiwan-02	5.9	99999	CHY071
2190	0171	Chi-Chi, Taiwan-02	5.9	99999	CHY074
2191	0171	Chi-Chi, Taiwan-02	5.9	99999	CHY075
2192	0171	Chi-Chi, Taiwan-02	5.9	99999	CHY076
2193	0171	Chi-Chi, Taiwan-02	5.9	99999	CHY078
2194	0171	Chi-Chi, Taiwan-02	5.9	99999	CHY079
2195	0171	Chi-Chi, Taiwan-02	5.9	99999	CHY080
2196	0171	Chi-Chi, Taiwan-02	5.9	99999	CHY081
2197	0171	Chi-Chi, Taiwan-02	5.9	99999	CHY082
2198	0171	Chi-Chi, Taiwan-02	5.9	99999	CHY086
2199	0171	Chi-Chi, Taiwan-02	5.9	99999	CHY088
2200	0171	Chi-Chi, Taiwan-02	5.9	99999	CHY090
2201	0171	Chi-Chi, Taiwan-02	5.9	99999	CHY092
2202	0171	Chi-Chi, Taiwan-02	5.9	99999	CHY093
2203	0171	Chi-Chi, Taiwan-02	5.9	99999	CHY094
2204	0171	Chi-Chi, Taiwan-02	5.9	99999	CHY099
2205	0171	Chi-Chi, Taiwan-02	5.9	99999	CHY100
2206	0171	Chi-Chi, Taiwan-02	5.9	99999	CHY101
2207	0171	Chi-Chi, Taiwan-02	5.9	99999	CHY102
2208	0171	Chi-Chi, Taiwan-02	5.9	99999	CHY104
2209	0171	Chi-Chi, Taiwan-02	5.9	99999	CHY107
2210	0171	Chi-Chi, Taiwan-02	5.9	99999	CHY111
2211	0171	Chi-Chi, Taiwan-02	5.9	99999	CHY112
2212	0171	Chi-Chi, Taiwan-02	5.9	99999	CHY114
2213	0171	Chi-Chi, Taiwan-02	5.9	99999	CHY115
2214	0171	Chi-Chi, Taiwan-02	5.9	99999	CHY116
2215	0171	Chi-Chi, Taiwan-02	5.9	99999	HWA002
2216	0171	Chi-Chi, Taiwan-02	5.9	99999	HWA005
2217	0171	Chi-Chi, Taiwan-02	5.9	99999	HWA006
2218	0171	Chi-Chi, Taiwan-02	5.9	99999	HWA007
2219	0171	Chi-Chi, Taiwan-02	5.9	99999	HWA009
2220	0171	Chi-Chi, Taiwan-02	5.9	99999	HWA011
2221	0171	Chi-Chi, Taiwan-02	5.9	99999	HWA012
2222	0171	Chi-Chi, Taiwan-02	5.9	99999	HWA013
2223	0171	Chi-Chi, Taiwan-02	5.9	99999	HWA014
2224	0171	Chi-Chi, Taiwan-02	5.9	99999	HWA015
2225	0171	Chi-Chi, Taiwan-02	5.9	99999	HWA016
2226	0171	Chi-Chi, Taiwan-02	5.9	99999	HWA017
2227	0171	Chi-Chi, Taiwan-02	5.9	99999	HWA019

RSN	EQID	Earthquake	M	Station No,	Station
2228	0171	Chi-Chi, Taiwan-02	5.9	99999	HWA020
2229	0171	Chi-Chi, Taiwan-02	5.9	99999	HWA022
2230	0171	Chi-Chi, Taiwan-02	5.9	99999	HWA023
2231	0171	Chi-Chi, Taiwan-02	5.9	99999	HWA024
2232	0171	Chi-Chi, Taiwan-02	5.9	99999	HWA025
2233	0171	Chi-Chi, Taiwan-02	5.9	99999	HWA026
2234	0171	Chi-Chi, Taiwan-02	5.9	99999	HWA027
2235	0171	Chi-Chi, Taiwan-02	5.9	99999	HWA028
2236	0171	Chi-Chi, Taiwan-02	5.9	99999	HWA029
2237	0171	Chi-Chi, Taiwan-02	5.9	99999	HWA030
2238	0171	Chi-Chi, Taiwan-02	5.9	99999	HWA031
2239	0171	Chi-Chi, Taiwan-02	5.9	99999	HWA032
2240	0171	Chi-Chi, Taiwan-02	5.9	99999	HWA033
2241	0171	Chi-Chi, Taiwan-02	5.9	99999	HWA034
2242	0171	Chi-Chi, Taiwan-02	5.9	99999	HWA035
2243	0171	Chi-Chi, Taiwan-02	5.9	99999	HWA036
2244	0171	Chi-Chi, Taiwan-02	5.9	99999	HWA037
2245	0171	Chi-Chi, Taiwan-02	5.9	99999	HWA038
2246	0171	Chi-Chi, Taiwan-02	5.9	99999	HWA039
2247	0171	Chi-Chi, Taiwan-02	5.9	99999	HWA041
2248	0171	Chi-Chi, Taiwan-02	5.9	99999	HWA043
2249	0171	Chi-Chi, Taiwan-02	5.9	99999	HWA044
2250	0171	Chi-Chi, Taiwan-02	5.9	99999	HWA045
2251	0171	Chi-Chi, Taiwan-02	5.9	99999	HWA046
2252	0171	Chi-Chi, Taiwan-02	5.9	99999	HWA048
2253	0171	Chi-Chi, Taiwan-02	5.9	99999	HWA049
2254	0171	Chi-Chi, Taiwan-02	5.9	99999	HWA050
2255	0171	Chi-Chi, Taiwan-02	5.9	99999	HWA051
2256	0171	Chi-Chi, Taiwan-02	5.9	99999	HWA055
2257	0171	Chi-Chi, Taiwan-02	5.9	99999	HWA056
2258	0171	Chi-Chi, Taiwan-02	5.9	99999	HWA057
2259	0171	Chi-Chi, Taiwan-02	5.9	99999	HWA058
2260	0171	Chi-Chi, Taiwan-02	5.9	99999	HWA059
2261	0171	Chi-Chi, Taiwan-02	5.9	99999	HWA060
2263	0171	Chi-Chi, Taiwan-02	5.9	99999	ILA001
2264	0171	Chi-Chi, Taiwan-02	5.9	99999	ILA002
2265	0171	Chi-Chi, Taiwan-02	5.9	99999	ILA003
2266	0171	Chi-Chi, Taiwan-02	5.9	99999	ILA004
2267	0171	Chi-Chi, Taiwan-02	5.9	99999	ILA005
2268	0171	Chi-Chi, Taiwan-02	5.9	99999	ILA006
2269	0171	Chi-Chi, Taiwan-02	5.9	99999	ILA007
2270	0171	Chi-Chi, Taiwan-02	5.9	99999	ILA008
2271	0171	Chi-Chi, Taiwan-02	5.9	99999	ILA010
2272	0171	Chi-Chi, Taiwan-02	5.9	99999	ILA012
2273	0171	Chi-Chi, Taiwan-02	5.9	99999	ILA013
2274	0171	Chi-Chi, Taiwan-02	5.9	99999	ILA014
2275	0171	Chi-Chi, Taiwan-02	5.9	99999	ILA015
2276	0171	Chi-Chi, Taiwan-02	5.9	99999	ILA016
2277	0171	Chi-Chi, Taiwan-02	5.9	99999	ILA021
2278	0171	Chi-Chi, Taiwan-02	5.9	99999	ILA024
2279	0171	Chi-Chi, Taiwan-02	5.9	99999	ILA030
2280	0171	Chi-Chi, Taiwan-02	5.9	99999	ILA031
2281	0171	Chi-Chi, Taiwan-02	5.9	99999	ILA037
2282	0171	Chi-Chi, Taiwan-02	5.9	99999	ILA041
2283	0171	Chi-Chi, Taiwan-02	5.9	99999	ILA042
2284	0171	Chi-Chi, Taiwan-02	5.9	99999	ILA044
2285	0171	Chi-Chi, Taiwan-02	5.9	99999	ILA046
2286	0171	Chi-Chi, Taiwan-02	5.9	99999	ILA048
2287	0171	Chi-Chi, Taiwan-02	5.9	99999	ILA049
2288	0171	Chi-Chi, Taiwan-02	5.9	99999	ILA050
2289	0171	Chi-Chi, Taiwan-02	5.9	99999	ILA051
2290	0171	Chi-Chi, Taiwan-02	5.9	99999	ILA052
2291	0171	Chi-Chi, Taiwan-02	5.9	99999	ILA055
2292	0171	Chi-Chi, Taiwan-02	5.9	99999	ILA056
2293	0171	Chi-Chi, Taiwan-02	5.9	99999	ILA059
2294	0171	Chi-Chi, Taiwan-02	5.9	99999	ILA061
2295	0171	Chi-Chi, Taiwan-02	5.9	99999	ILA062
2296	0171	Chi-Chi, Taiwan-02	5.9	99999	ILA063
2297	0171	Chi-Chi, Taiwan-02	5.9	99999	ILA064

RSN	EQID	Earthquake	M	Station No,	Station
2298	0171	Chi-Chi, Taiwan-02	5.9	99999	ILA066
2299	0171	Chi-Chi, Taiwan-02	5.9	99999	ILA067
2300	0171	Chi-Chi, Taiwan-02	5.9	99999	KAU001
2301	0171	Chi-Chi, Taiwan-02	5.9	99999	KAU010
2302	0171	Chi-Chi, Taiwan-02	5.9	99999	KAU020
2303	0171	Chi-Chi, Taiwan-02	5.9	99999	KAU050
2304	0171	Chi-Chi, Taiwan-02	5.9	99999	KAU054
2305	0171	Chi-Chi, Taiwan-02	5.9	99999	KAU069
2306	0171	Chi-Chi, Taiwan-02	5.9	99999	KAU078
2307	0171	Chi-Chi, Taiwan-02	5.9	99999	KAU085
2308	0171	Chi-Chi, Taiwan-02	5.9	99999	TAP003
2309	0171	Chi-Chi, Taiwan-02	5.9	99999	TAP005
2310	0171	Chi-Chi, Taiwan-02	5.9	99999	TAP007
2311	0171	Chi-Chi, Taiwan-02	5.9	99999	TAP008
2312	0171	Chi-Chi, Taiwan-02	5.9	99999	TAP010
2313	0171	Chi-Chi, Taiwan-02	5.9	99999	TAP013
2314	0171	Chi-Chi, Taiwan-02	5.9	99999	TAP014
2315	0171	Chi-Chi, Taiwan-02	5.9	99999	TAP017
2316	0171	Chi-Chi, Taiwan-02	5.9	99999	TAP020
2317	0171	Chi-Chi, Taiwan-02	5.9	99999	TAP021
2318	0171	Chi-Chi, Taiwan-02	5.9	99999	TAP024
2319	0171	Chi-Chi, Taiwan-02	5.9	99999	TAP026
2320	0171	Chi-Chi, Taiwan-02	5.9	99999	TAP028
2321	0171	Chi-Chi, Taiwan-02	5.9	99999	TAP032
2322	0171	Chi-Chi, Taiwan-02	5.9	99999	TAP033
2323	0171	Chi-Chi, Taiwan-02	5.9	99999	TAP034
2324	0171	Chi-Chi, Taiwan-02	5.9	99999	TAP035
2325	0171	Chi-Chi, Taiwan-02	5.9	99999	TAP041
2326	0171	Chi-Chi, Taiwan-02	5.9	99999	TAP042
2327	0171	Chi-Chi, Taiwan-02	5.9	99999	TAP043
2328	0171	Chi-Chi, Taiwan-02	5.9	99999	TAP046
2329	0171	Chi-Chi, Taiwan-02	5.9	99999	TAP049
2330	0171	Chi-Chi, Taiwan-02	5.9	99999	TAP051
2331	0171	Chi-Chi, Taiwan-02	5.9	99999	TAP052
2332	0171	Chi-Chi, Taiwan-02	5.9	99999	TAP053
2334	0171	Chi-Chi, Taiwan-02	5.9	99999	TAP067
2335	0171	Chi-Chi, Taiwan-02	5.9	99999	TAP075
2336	0171	Chi-Chi, Taiwan-02	5.9	99999	TAP077
2337	0171	Chi-Chi, Taiwan-02	5.9	99999	TAP078
2338	0171	Chi-Chi, Taiwan-02	5.9	99999	TAP079
2339	0171	Chi-Chi, Taiwan-02	5.9	99999	TAP086
2340	0171	Chi-Chi, Taiwan-02	5.9	99999	TAP087
2341	0171	Chi-Chi, Taiwan-02	5.9	99999	TAP088
2342	0171	Chi-Chi, Taiwan-02	5.9	99999	TAP089
2343	0171	Chi-Chi, Taiwan-02	5.9	99999	TAP090
2344	0171	Chi-Chi, Taiwan-02	5.9	99999	TAP094
2345	0171	Chi-Chi, Taiwan-02	5.9	99999	TAP095
2346	0171	Chi-Chi, Taiwan-02	5.9	99999	TAP098
2347	0171	Chi-Chi, Taiwan-02	5.9	99999	TAP100
2349	0171	Chi-Chi, Taiwan-02	5.9	99999	TAP104
2350	0171	Chi-Chi, Taiwan-02	5.9	99999	TCU003
2351	0171	Chi-Chi, Taiwan-02	5.9	99999	TCU006
2352	0171	Chi-Chi, Taiwan-02	5.9	99999	TCU007
2353	0171	Chi-Chi, Taiwan-02	5.9	99999	TCU008
2354	0171	Chi-Chi, Taiwan-02	5.9	99999	TCU010
2355	0171	Chi-Chi, Taiwan-02	5.9	99999	TCU014
2356	0171	Chi-Chi, Taiwan-02	5.9	99999	TCU026
2357	0171	Chi-Chi, Taiwan-02	5.9	99999	TCU029
2358	0171	Chi-Chi, Taiwan-02	5.9	99999	TCU031
2359	0171	Chi-Chi, Taiwan-02	5.9	99999	TCU033
2360	0171	Chi-Chi, Taiwan-02	5.9	99999	TCU034
2361	0171	Chi-Chi, Taiwan-02	5.9	99999	TCU035
2362	0171	Chi-Chi, Taiwan-02	5.9	99999	TCU036
2363	0171	Chi-Chi, Taiwan-02	5.9	99999	TCU038
2364	0171	Chi-Chi, Taiwan-02	5.9	99999	TCU039
2365	0171	Chi-Chi, Taiwan-02	5.9	99999	TCU040
2366	0171	Chi-Chi, Taiwan-02	5.9	99999	TCU042
2367	0171	Chi-Chi, Taiwan-02	5.9	99999	TCU045
2368	0171	Chi-Chi, Taiwan-02	5.9	99999	TCU046

RSN	EQID	Earthquake	M	Station No,	Station
2369	0171	Chi-Chi, Taiwan-02	5.9	99999	TCU048
2370	0171	Chi-Chi, Taiwan-02	5.9	99999	TCU050
2371	0171	Chi-Chi, Taiwan-02	5.9	99999	TCU051
2372	0171	Chi-Chi, Taiwan-02	5.9	99999	TCU052
2373	0171	Chi-Chi, Taiwan-02	5.9	99999	TCU053
2374	0171	Chi-Chi, Taiwan-02	5.9	99999	TCU054
2375	0171	Chi-Chi, Taiwan-02	5.9	99999	TCU055
2376	0171	Chi-Chi, Taiwan-02	5.9	99999	TCU056
2377	0171	Chi-Chi, Taiwan-02	5.9	99999	TCU057
2378	0171	Chi-Chi, Taiwan-02	5.9	99999	TCU059
2379	0171	Chi-Chi, Taiwan-02	5.9	99999	TCU060
2380	0171	Chi-Chi, Taiwan-02	5.9	99999	TCU061
2381	0171	Chi-Chi, Taiwan-02	5.9	99999	TCU063
2382	0171	Chi-Chi, Taiwan-02	5.9	99999	TCU065
2383	0171	Chi-Chi, Taiwan-02	5.9	99999	TCU067
2384	0171	Chi-Chi, Taiwan-02	5.9	99999	TCU068
2385	0171	Chi-Chi, Taiwan-02	5.9	99999	TCU071
2386	0171	Chi-Chi, Taiwan-02	5.9	99999	TCU073
2387	0171	Chi-Chi, Taiwan-02	5.9	99999	TCU074
2388	0171	Chi-Chi, Taiwan-02	5.9	99999	TCU075
2389	0171	Chi-Chi, Taiwan-02	5.9	99999	TCU076
2390	0171	Chi-Chi, Taiwan-02	5.9	99999	TCU078
2391	0171	Chi-Chi, Taiwan-02	5.9	99999	TCU079
2393	0171	Chi-Chi, Taiwan-02	5.9	99999	TCU082
2394	0171	Chi-Chi, Taiwan-02	5.9	99999	TCU083
2395	0171	Chi-Chi, Taiwan-02	5.9	99999	TCU084
2396	0171	Chi-Chi, Taiwan-02	5.9	99999	TCU085
2397	0171	Chi-Chi, Taiwan-02	5.9	99999	TCU087
2398	0171	Chi-Chi, Taiwan-02	5.9	99999	TCU088
2399	0171	Chi-Chi, Taiwan-02	5.9	99999	TCU089
2400	0171	Chi-Chi, Taiwan-02	5.9	99999	TCU092
2401	0171	Chi-Chi, Taiwan-02	5.9	99999	TCU094
2402	0171	Chi-Chi, Taiwan-02	5.9	99999	TCU098
2403	0171	Chi-Chi, Taiwan-02	5.9	99999	TCU100
2404	0171	Chi-Chi, Taiwan-02	5.9	99999	TCU103
2405	0171	Chi-Chi, Taiwan-02	5.9	99999	TCU104
2406	0171	Chi-Chi, Taiwan-02	5.9	99999	TCU105
2407	0171	Chi-Chi, Taiwan-02	5.9	99999	TCU106
2408	0171	Chi-Chi, Taiwan-02	5.9	99999	TCU107
2409	0171	Chi-Chi, Taiwan-02	5.9	99999	TCU109
2410	0171	Chi-Chi, Taiwan-02	5.9	99999	TCU110
2411	0171	Chi-Chi, Taiwan-02	5.9	99999	TCU111
2412	0171	Chi-Chi, Taiwan-02	5.9	99999	TCU112
2413	0171	Chi-Chi, Taiwan-02	5.9	99999	TCU113
2414	0171	Chi-Chi, Taiwan-02	5.9	99999	TCU115
2415	0171	Chi-Chi, Taiwan-02	5.9	99999	TCU116
2416	0171	Chi-Chi, Taiwan-02	5.9	99999	TCU117
2417	0171	Chi-Chi, Taiwan-02	5.9	99999	TCU118
2418	0171	Chi-Chi, Taiwan-02	5.9	99999	TCU119
2419	0171	Chi-Chi, Taiwan-02	5.9	99999	TCU120
2420	0171	Chi-Chi, Taiwan-02	5.9	99999	TCU122
2421	0171	Chi-Chi, Taiwan-02	5.9	99999	TCU123
2422	0171	Chi-Chi, Taiwan-02	5.9	99999	TCU128
2423	0171	Chi-Chi, Taiwan-02	5.9	9999936	TCU129
2424	0171	Chi-Chi, Taiwan-02	5.9	99999	TCU131
2425	0171	Chi-Chi, Taiwan-02	5.9	99999	TCU136
2426	0171	Chi-Chi, Taiwan-02	5.9	99999	TCU137
2427	0171	Chi-Chi, Taiwan-02	5.9	99999	TCU138
2428	0171	Chi-Chi, Taiwan-02	5.9	99999	TCU140
2429	0171	Chi-Chi, Taiwan-02	5.9	99999	TCU141
2430	0171	Chi-Chi, Taiwan-02	5.9	99999	TCU145
2431	0171	Chi-Chi, Taiwan-02	5.9	99999	TCU147
2432	0171	Chi-Chi, Taiwan-02	5.9	99999	TTN001
2433	0171	Chi-Chi, Taiwan-02	5.9	99999	TTN004
2434	0171	Chi-Chi, Taiwan-02	5.9	99999	TTN014
2435	0171	Chi-Chi, Taiwan-02	5.9	99999	TTN020
2436	0171	Chi-Chi, Taiwan-02	5.9	99999	TTN022
2437	0171	Chi-Chi, Taiwan-02	5.9	99999	TTN023
2438	0171	Chi-Chi, Taiwan-02	5.9	99999	TTN024

RSN	EQID	Earthquake	M	Station No,	Station
2439	0171	Chi-Chi, Taiwan-02	5.9	99999	TTN025
2440	0171	Chi-Chi, Taiwan-02	5.9	99999	TTN026
2441	0171	Chi-Chi, Taiwan-02	5.9	99999	TTN027
2442	0171	Chi-Chi, Taiwan-02	5.9	99999	TTN031
2443	0171	Chi-Chi, Taiwan-02	5.9	99999	TTN032
2444	0171	Chi-Chi, Taiwan-02	5.9	99999	TTN033
2445	0171	Chi-Chi, Taiwan-02	5.9	99999	TTN040
2446	0171	Chi-Chi, Taiwan-02	5.9	99999	TTN041
2447	0171	Chi-Chi, Taiwan-02	5.9	99999	TTN042
2448	0171	Chi-Chi, Taiwan-02	5.9	99999	TTN044
2449	0171	Chi-Chi, Taiwan-02	5.9	99999	TTN045
2450	0171	Chi-Chi, Taiwan-02	5.9	99999	TTN046
2451	0171	Chi-Chi, Taiwan-02	5.9	99999	TTN051
2452	0172	Chi-Chi, Taiwan-03	6.2	99999	CHY015
2453	0172	Chi-Chi, Taiwan-03	6.2	99999	CHY016
2454	0172	Chi-Chi, Taiwan-03	6.2	99999	CHY017
2455	0172	Chi-Chi, Taiwan-03	6.2	99999	CHY019
2456	0172	Chi-Chi, Taiwan-03	6.2	99999	CHY022
2457	0172	Chi-Chi, Taiwan-03	6.2	99999	CHY024
2458	0172	Chi-Chi, Taiwan-03	6.2	99999	CHY025
2459	0172	Chi-Chi, Taiwan-03	6.2	99999	CHY026
2460	0172	Chi-Chi, Taiwan-03	6.2	99999	CHY027
2461	0172	Chi-Chi, Taiwan-03	6.2	99999	CHY028
2462	0172	Chi-Chi, Taiwan-03	6.2	99999	CHY029
2463	0172	Chi-Chi, Taiwan-03	6.2	99999	CHY032
2464	0172	Chi-Chi, Taiwan-03	6.2	99999	CHY033
2465	0172	Chi-Chi, Taiwan-03	6.2	99999	CHY034
2466	0172	Chi-Chi, Taiwan-03	6.2	99999	CHY035
2467	0172	Chi-Chi, Taiwan-03	6.2	99999	CHY036
2468	0172	Chi-Chi, Taiwan-03	6.2	99999	CHY039
2469	0172	Chi-Chi, Taiwan-03	6.2	99999	CHY041
2470	0172	Chi-Chi, Taiwan-03	6.2	99999	CHY042
2471	0172	Chi-Chi, Taiwan-03	6.2	99999	CHY044
2472	0172	Chi-Chi, Taiwan-03	6.2	99999	CHY046
2473	0172	Chi-Chi, Taiwan-03	6.2	99999	CHY047
2474	0172	Chi-Chi, Taiwan-03	6.2	99999	CHY050
2475	0172	Chi-Chi, Taiwan-03	6.2	99999	CHY052
2476	0172	Chi-Chi, Taiwan-03	6.2	99999	CHY054
2477	0172	Chi-Chi, Taiwan-03	6.2	99999	CHY055
2478	0172	Chi-Chi, Taiwan-03	6.2	99999	CHY056
2479	0172	Chi-Chi, Taiwan-03	6.2	99999	CHY057
2480	0172	Chi-Chi, Taiwan-03	6.2	99999	CHY058
2481	0172	Chi-Chi, Taiwan-03	6.2	99999	CHY060
2482	0172	Chi-Chi, Taiwan-03	6.2	99999	CHY061
2483	0172	Chi-Chi, Taiwan-03	6.2	99999	CHY062
2484	0172	Chi-Chi, Taiwan-03	6.2	99999	CHY063
2485	0172	Chi-Chi, Taiwan-03	6.2	99999	CHY065
2486	0172	Chi-Chi, Taiwan-03	6.2	99999	CHY066
2487	0172	Chi-Chi, Taiwan-03	6.2	99999	CHY067
2488	0172	Chi-Chi, Taiwan-03	6.2	99999	CHY069
2489	0172	Chi-Chi, Taiwan-03	6.2	99999	CHY070
2490	0172	Chi-Chi, Taiwan-03	6.2	99999	CHY074
2491	0172	Chi-Chi, Taiwan-03	6.2	99999	CHY075
2492	0172	Chi-Chi, Taiwan-03	6.2	99999	CHY076
2493	0172	Chi-Chi, Taiwan-03	6.2	99999	CHY078
2494	0172	Chi-Chi, Taiwan-03	6.2	99999	CHY079
2495	0172	Chi-Chi, Taiwan-03	6.2	99999	CHY080
2496	0172	Chi-Chi, Taiwan-03	6.2	99999	CHY081
2497	0172	Chi-Chi, Taiwan-03	6.2	99999	CHY082
2498	0172	Chi-Chi, Taiwan-03	6.2	99999	CHY086
2499	0172	Chi-Chi, Taiwan-03	6.2	99999	CHY087
2500	0172	Chi-Chi, Taiwan-03	6.2	99999	CHY088
2501	0172	Chi-Chi, Taiwan-03	6.2	99999	CHY090
2502	0172	Chi-Chi, Taiwan-03	6.2	99999	CHY093
2503	0172	Chi-Chi, Taiwan-03	6.2	99999	CHY094
2504	0172	Chi-Chi, Taiwan-03	6.2	99999	CHY096
2505	0172	Chi-Chi, Taiwan-03	6.2	99999	CHY099
2506	0172	Chi-Chi, Taiwan-03	6.2	99999	CHY100
2507	0172	Chi-Chi, Taiwan-03	6.2	99999	CHY101

RSN	EQID	Earthquake	M	Station No,	Station
2508	0172	Chi-Chi, Taiwan-03	6.2	99999	CHY102
2509	0172	Chi-Chi, Taiwan-03	6.2	99999	CHY104
2510	0172	Chi-Chi, Taiwan-03	6.2	99999	CHY107
2511	0172	Chi-Chi, Taiwan-03	6.2	99999	CHY114
2512	0172	Chi-Chi, Taiwan-03	6.2	99999	CHY115
2513	0172	Chi-Chi, Taiwan-03	6.2	99999	CHY116
2514	0172	Chi-Chi, Taiwan-03	6.2	99999	HWA002
2515	0172	Chi-Chi, Taiwan-03	6.2	99999	HWA005
2516	0172	Chi-Chi, Taiwan-03	6.2	99999	HWA006
2517	0172	Chi-Chi, Taiwan-03	6.2	99999	HWA009
2518	0172	Chi-Chi, Taiwan-03	6.2	99999	HWA011
2519	0172	Chi-Chi, Taiwan-03	6.2	99999	HWA012
2520	0172	Chi-Chi, Taiwan-03	6.2	99999	HWA013
2521	0172	Chi-Chi, Taiwan-03	6.2	99999	HWA014
2522	0172	Chi-Chi, Taiwan-03	6.2	99999	HWA015
2523	0172	Chi-Chi, Taiwan-03	6.2	99999	HWA016
2524	0172	Chi-Chi, Taiwan-03	6.2	99999	HWA017
2525	0172	Chi-Chi, Taiwan-03	6.2	99999	HWA019
2526	0172	Chi-Chi, Taiwan-03	6.2	99999	HWA020
2527	0172	Chi-Chi, Taiwan-03	6.2	99999	HWA022
2528	0172	Chi-Chi, Taiwan-03	6.2	99999	HWA024
2529	0172	Chi-Chi, Taiwan-03	6.2	99999	HWA025
2530	0172	Chi-Chi, Taiwan-03	6.2	99999	HWA027
2531	0172	Chi-Chi, Taiwan-03	6.2	99999	HWA028
2532	0172	Chi-Chi, Taiwan-03	6.2	99999	HWA029
2533	0172	Chi-Chi, Taiwan-03	6.2	99999	HWA030
2534	0172	Chi-Chi, Taiwan-03	6.2	99999	HWA031
2535	0172	Chi-Chi, Taiwan-03	6.2	99999	HWA032
2536	0172	Chi-Chi, Taiwan-03	6.2	99999	HWA033
2537	0172	Chi-Chi, Taiwan-03	6.2	99999	HWA034
2538	0172	Chi-Chi, Taiwan-03	6.2	99999	HWA035
2539	0172	Chi-Chi, Taiwan-03	6.2	99999	HWA036
2540	0172	Chi-Chi, Taiwan-03	6.2	99999	HWA037
2541	0172	Chi-Chi, Taiwan-03	6.2	99999	HWA038
2542	0172	Chi-Chi, Taiwan-03	6.2	99999	HWA039
2543	0172	Chi-Chi, Taiwan-03	6.2	99999	HWA041
2544	0172	Chi-Chi, Taiwan-03	6.2	99999	HWA043
2545	0172	Chi-Chi, Taiwan-03	6.2	99999	HWA044
2546	0172	Chi-Chi, Taiwan-03	6.2	99999	HWA045
2547	0172	Chi-Chi, Taiwan-03	6.2	99999	HWA046
2548	0172	Chi-Chi, Taiwan-03	6.2	99999	HWA048
2549	0172	Chi-Chi, Taiwan-03	6.2	99999	HWA049
2550	0172	Chi-Chi, Taiwan-03	6.2	99999	HWA050
2551	0172	Chi-Chi, Taiwan-03	6.2	99999	HWA051
2552	0172	Chi-Chi, Taiwan-03	6.2	99999	HWA056
2553	0172	Chi-Chi, Taiwan-03	6.2	99999	HWA057
2554	0172	Chi-Chi, Taiwan-03	6.2	99999	HWA058
2555	0172	Chi-Chi, Taiwan-03	6.2	99999	HWA059
2557	0172	Chi-Chi, Taiwan-03	6.2	99999	ILA006
2558	0172	Chi-Chi, Taiwan-03	6.2	99999	ILA007
2559	0172	Chi-Chi, Taiwan-03	6.2	99999	ILA013
2560	0172	Chi-Chi, Taiwan-03	6.2	99999	ILA037
2561	0172	Chi-Chi, Taiwan-03	6.2	99999	ILA044
2562	0172	Chi-Chi, Taiwan-03	6.2	99999	ILA048
2563	0172	Chi-Chi, Taiwan-03	6.2	99999	ILA062
2564	0172	Chi-Chi, Taiwan-03	6.2	99999	ILA064
2565	0172	Chi-Chi, Taiwan-03	6.2	99999	ILA066
2566	0172	Chi-Chi, Taiwan-03	6.2	99999	ILA067
2567	0172	Chi-Chi, Taiwan-03	6.2	99999	KAU001
2568	0172	Chi-Chi, Taiwan-03	6.2	99999	KAU010
2569	0172	Chi-Chi, Taiwan-03	6.2	99999	KAU012
2570	0172	Chi-Chi, Taiwan-03	6.2	99999	KAU018
2571	0172	Chi-Chi, Taiwan-03	6.2	99999	KAU020
2572	0172	Chi-Chi, Taiwan-03	6.2	99999	KAU022
2573	0172	Chi-Chi, Taiwan-03	6.2	99999	KAU050
2574	0172	Chi-Chi, Taiwan-03	6.2	99999	KAU054
2575	0172	Chi-Chi, Taiwan-03	6.2	99999	KAU063
2576	0172	Chi-Chi, Taiwan-03	6.2	99999	KAU064
2577	0172	Chi-Chi, Taiwan-03	6.2	99999	KAU066

RSN	EQID	Earthquake	M	Station No,	Station
2578	0172	Chi-Chi, Taiwan-03	6.2	99999	KAU069
2579	0172	Chi-Chi, Taiwan-03	6.2	99999	KAU074
2580	0172	Chi-Chi, Taiwan-03	6.2	99999	KAU077
2581	0172	Chi-Chi, Taiwan-03	6.2	99999	KAU078
2582	0172	Chi-Chi, Taiwan-03	6.2	99999	KAU085
2583	0172	Chi-Chi, Taiwan-03	6.2	99999	KAU088
2584	0172	Chi-Chi, Taiwan-03	6.2	99999	TAP034
2585	0172	Chi-Chi, Taiwan-03	6.2	99999	TAP053
2586	0172	Chi-Chi, Taiwan-03	6.2	99999	TCU006
2587	0172	Chi-Chi, Taiwan-03	6.2	99999	TCU015
2588	0172	Chi-Chi, Taiwan-03	6.2	99999	TCU017
2589	0172	Chi-Chi, Taiwan-03	6.2	99999	TCU026
2590	0172	Chi-Chi, Taiwan-03	6.2	99999	TCU029
2591	0172	Chi-Chi, Taiwan-03	6.2	99999	TCU031
2592	0172	Chi-Chi, Taiwan-03	6.2	99999	TCU032
2593	0172	Chi-Chi, Taiwan-03	6.2	99999	TCU033
2594	0172	Chi-Chi, Taiwan-03	6.2	99999	TCU034
2595	0172	Chi-Chi, Taiwan-03	6.2	99999	TCU035
2596	0172	Chi-Chi, Taiwan-03	6.2	99999	TCU036
2597	0172	Chi-Chi, Taiwan-03	6.2	99999	TCU038
2598	0172	Chi-Chi, Taiwan-03	6.2	99999	TCU039
2599	0172	Chi-Chi, Taiwan-03	6.2	99999	TCU040
2600	0172	Chi-Chi, Taiwan-03	6.2	99999	TCU042
2601	0172	Chi-Chi, Taiwan-03	6.2	99999	TCU045
2602	0172	Chi-Chi, Taiwan-03	6.2	99999	TCU046
2603	0172	Chi-Chi, Taiwan-03	6.2	99999	TCU047
2604	0172	Chi-Chi, Taiwan-03	6.2	99999	TCU048
2605	0172	Chi-Chi, Taiwan-03	6.2	99999	TCU049
2606	0172	Chi-Chi, Taiwan-03	6.2	99999	TCU050
2607	0172	Chi-Chi, Taiwan-03	6.2	99999	TCU051
2608	0172	Chi-Chi, Taiwan-03	6.2	99999	TCU052
2609	0172	Chi-Chi, Taiwan-03	6.2	99999	TCU053
2610	0172	Chi-Chi, Taiwan-03	6.2	99999	TCU054
2611	0172	Chi-Chi, Taiwan-03	6.2	99999	TCU056
2612	0172	Chi-Chi, Taiwan-03	6.2	99999	TCU057
2613	0172	Chi-Chi, Taiwan-03	6.2	99999	TCU059
2614	0172	Chi-Chi, Taiwan-03	6.2	99999	TCU060
2615	0172	Chi-Chi, Taiwan-03	6.2	99999	TCU061
2616	0172	Chi-Chi, Taiwan-03	6.2	99999	TCU063
2617	0172	Chi-Chi, Taiwan-03	6.2	99999	TCU064
2618	0172	Chi-Chi, Taiwan-03	6.2	99999	TCU065
2619	0172	Chi-Chi, Taiwan-03	6.2	99999	TCU067
2620	0172	Chi-Chi, Taiwan-03	6.2	99999	TCU068
2621	0172	Chi-Chi, Taiwan-03	6.2	99999	TCU070
2622	0172	Chi-Chi, Taiwan-03	6.2	99999	TCU071
2623	0172	Chi-Chi, Taiwan-03	6.2	99999	TCU072
2624	0172	Chi-Chi, Taiwan-03	6.2	99999	TCU073
2625	0172	Chi-Chi, Taiwan-03	6.2	99999	TCU074
2626	0172	Chi-Chi, Taiwan-03	6.2	99999	TCU075
2627	0172	Chi-Chi, Taiwan-03	6.2	99999	TCU076
2628	0172	Chi-Chi, Taiwan-03	6.2	99999	TCU078
2629	0172	Chi-Chi, Taiwan-03	6.2	99999	TCU079
2631	0172	Chi-Chi, Taiwan-03	6.2	99999	TCU082
2632	0172	Chi-Chi, Taiwan-03	6.2	99999	TCU084
2633	0172	Chi-Chi, Taiwan-03	6.2	99999	TCU085
2634	0172	Chi-Chi, Taiwan-03	6.2	99999	TCU087
2635	0172	Chi-Chi, Taiwan-03	6.2	99999	TCU089
2636	0172	Chi-Chi, Taiwan-03	6.2	99999	TCU094
2637	0172	Chi-Chi, Taiwan-03	6.2	99999	TCU095
2638	0172	Chi-Chi, Taiwan-03	6.2	99999	TCU098
2639	0172	Chi-Chi, Taiwan-03	6.2	99999	TCU100
2640	0172	Chi-Chi, Taiwan-03	6.2	99999	TCU102
2641	0172	Chi-Chi, Taiwan-03	6.2	99999	TCU103
2642	0172	Chi-Chi, Taiwan-03	6.2	99999	TCU104
2643	0172	Chi-Chi, Taiwan-03	6.2	99999	TCU105
2644	0172	Chi-Chi, Taiwan-03	6.2	99999	TCU106
2645	0172	Chi-Chi, Taiwan-03	6.2	99999	TCU107
2646	0172	Chi-Chi, Taiwan-03	6.2	99999	TCU109
2647	0172	Chi-Chi, Taiwan-03	6.2	99999	TCU112

RSN	EQID	Earthquake	M	Station No,	Station
2648	0172	Chi-Chi, Taiwan-03	6.2	99999	TCU113
2649	0172	Chi-Chi, Taiwan-03	6.2	99999	TCU115
2650	0172	Chi-Chi, Taiwan-03	6.2	99999	TCU116
2651	0172	Chi-Chi, Taiwan-03	6.2	99999	TCU117
2652	0172	Chi-Chi, Taiwan-03	6.2	99999	TCU118
2653	0172	Chi-Chi, Taiwan-03	6.2	99999	TCU119
2654	0172	Chi-Chi, Taiwan-03	6.2	99999	TCU120
2655	0172	Chi-Chi, Taiwan-03	6.2	99999	TCU122
2656	0172	Chi-Chi, Taiwan-03	6.2	99999	TCU123
2657	0172	Chi-Chi, Taiwan-03	6.2	99999	TCU128
2658	0172	Chi-Chi, Taiwan-03	6.2	9999936	TCU129
2659	0172	Chi-Chi, Taiwan-03	6.2	99999	TCU131
2660	0172	Chi-Chi, Taiwan-03	6.2	99999	TCU136
2661	0172	Chi-Chi, Taiwan-03	6.2	99999	TCU138
2662	0172	Chi-Chi, Taiwan-03	6.2	99999	TCU140
2663	0172	Chi-Chi, Taiwan-03	6.2	99999	TCU141
2664	0172	Chi-Chi, Taiwan-03	6.2	99999	TCU145
2665	0172	Chi-Chi, Taiwan-03	6.2	99999	TCU147
2666	0172	Chi-Chi, Taiwan-03	6.2	99999	TTN001
2667	0172	Chi-Chi, Taiwan-03	6.2	99999	TTN003
2668	0172	Chi-Chi, Taiwan-03	6.2	99999	TTN004
2669	0172	Chi-Chi, Taiwan-03	6.2	99999	TTN009
2670	0172	Chi-Chi, Taiwan-03	6.2	99999	TTN010
2671	0172	Chi-Chi, Taiwan-03	6.2	99999	TTN012
2672	0172	Chi-Chi, Taiwan-03	6.2	99999	TTN014
2673	0172	Chi-Chi, Taiwan-03	6.2	99999	TTN018
2674	0172	Chi-Chi, Taiwan-03	6.2	99999	TTN020
2675	0172	Chi-Chi, Taiwan-03	6.2	99999	TTN022
2676	0172	Chi-Chi, Taiwan-03	6.2	99999	TTN024
2677	0172	Chi-Chi, Taiwan-03	6.2	99999	TTN025
2678	0172	Chi-Chi, Taiwan-03	6.2	99999	TTN026
2679	0172	Chi-Chi, Taiwan-03	6.2	99999	TTN027
2680	0172	Chi-Chi, Taiwan-03	6.2	99999	TTN028
2681	0172	Chi-Chi, Taiwan-03	6.2	99999	TTN031
2682	0172	Chi-Chi, Taiwan-03	6.2	99999	TTN032
2683	0172	Chi-Chi, Taiwan-03	6.2	99999	TTN033
2684	0172	Chi-Chi, Taiwan-03	6.2	99999	TTN036
2685	0172	Chi-Chi, Taiwan-03	6.2	99999	TTN040
2686	0172	Chi-Chi, Taiwan-03	6.2	99999	TTN041
2687	0172	Chi-Chi, Taiwan-03	6.2	99999	TTN042
2688	0172	Chi-Chi, Taiwan-03	6.2	99999	TTN044
2689	0172	Chi-Chi, Taiwan-03	6.2	99999	TTN045
2690	0172	Chi-Chi, Taiwan-03	6.2	99999	TTN046
2691	0172	Chi-Chi, Taiwan-03	6.2	99999	TTN048
2692	0172	Chi-Chi, Taiwan-03	6.2	99999	TTN050
2693	0172	Chi-Chi, Taiwan-03	6.2	99999	TTN051
2694	0173	Chi-Chi, Taiwan-04	6.2	99999	CHY015
2695	0173	Chi-Chi, Taiwan-04	6.2	99999	CHY016
2696	0173	Chi-Chi, Taiwan-04	6.2	99999	CHY017
2697	0173	Chi-Chi, Taiwan-04	6.2	99999	CHY019
2698	0173	Chi-Chi, Taiwan-04	6.2	99999	CHY022
2699	0173	Chi-Chi, Taiwan-04	6.2	99999	CHY024
2700	0173	Chi-Chi, Taiwan-04	6.2	99999	CHY025
2701	0173	Chi-Chi, Taiwan-04	6.2	99999	CHY026
2702	0173	Chi-Chi, Taiwan-04	6.2	99999	CHY027
2703	0173	Chi-Chi, Taiwan-04	6.2	99999	CHY028
2704	0173	Chi-Chi, Taiwan-04	6.2	99999	CHY029
2705	0173	Chi-Chi, Taiwan-04	6.2	99999	CHY030
2706	0173	Chi-Chi, Taiwan-04	6.2	99999	CHY032
2707	0173	Chi-Chi, Taiwan-04	6.2	99999	CHY033
2708	0173	Chi-Chi, Taiwan-04	6.2	99999	CHY034
2709	0173	Chi-Chi, Taiwan-04	6.2	99999	CHY035
2710	0173	Chi-Chi, Taiwan-04	6.2	99999	CHY036
2711	0173	Chi-Chi, Taiwan-04	6.2	99999	CHY039
2712	0173	Chi-Chi, Taiwan-04	6.2	99999	CHY042
2713	0173	Chi-Chi, Taiwan-04	6.2	99999	CHY044
2714	0173	Chi-Chi, Taiwan-04	6.2	99999	CHY046
2715	0173	Chi-Chi, Taiwan-04	6.2	99999	CHY047
2716	0173	Chi-Chi, Taiwan-04	6.2	99999	CHY050

RSN	EQID	Earthquake	M	Station No,	Station
2717	0173	Chi-Chi, Taiwan-04	6.2	99999	CHY052
2718	0173	Chi-Chi, Taiwan-04	6.2	99999	CHY054
2719	0173	Chi-Chi, Taiwan-04	6.2	99999	CHY055
2720	0173	Chi-Chi, Taiwan-04	6.2	99999	CHY056
2721	0173	Chi-Chi, Taiwan-04	6.2	99999	CHY057
2722	0173	Chi-Chi, Taiwan-04	6.2	99999	CHY058
2723	0173	Chi-Chi, Taiwan-04	6.2	99999	CHY059
2724	0173	Chi-Chi, Taiwan-04	6.2	99999	CHY060
2725	0173	Chi-Chi, Taiwan-04	6.2	99999	CHY061
2726	0173	Chi-Chi, Taiwan-04	6.2	99999	CHY062
2727	0173	Chi-Chi, Taiwan-04	6.2	99999	CHY063
2728	0173	Chi-Chi, Taiwan-04	6.2	99999	CHY065
2729	0173	Chi-Chi, Taiwan-04	6.2	99999	CHY066
2730	0173	Chi-Chi, Taiwan-04	6.2	99999	CHY067
2731	0173	Chi-Chi, Taiwan-04	6.2	99999	CHY069
2732	0173	Chi-Chi, Taiwan-04	6.2	99999	CHY070
2733	0173	Chi-Chi, Taiwan-04	6.2	99999	CHY071
2734	0173	Chi-Chi, Taiwan-04	6.2	99999	CHY074
2735	0173	Chi-Chi, Taiwan-04	6.2	99999	CHY075
2736	0173	Chi-Chi, Taiwan-04	6.2	99999	CHY076
2737	0173	Chi-Chi, Taiwan-04	6.2	99999	CHY078
2738	0173	Chi-Chi, Taiwan-04	6.2	99999	CHY079
2739	0173	Chi-Chi, Taiwan-04	6.2	99999	CHY080
2740	0173	Chi-Chi, Taiwan-04	6.2	99999	CHY081
2741	0173	Chi-Chi, Taiwan-04	6.2	99999	CHY082
2742	0173	Chi-Chi, Taiwan-04	6.2	99999	CHY086
2743	0173	Chi-Chi, Taiwan-04	6.2	99999	CHY087
2744	0173	Chi-Chi, Taiwan-04	6.2	99999	CHY088
2745	0173	Chi-Chi, Taiwan-04	6.2	99999	CHY090
2746	0173	Chi-Chi, Taiwan-04	6.2	99999	CHY092
2747	0173	Chi-Chi, Taiwan-04	6.2	99999	CHY093
2748	0173	Chi-Chi, Taiwan-04	6.2	99999	CHY094
2749	0173	Chi-Chi, Taiwan-04	6.2	99999	CHY096
2750	0173	Chi-Chi, Taiwan-04	6.2	99999	CHY099
2751	0173	Chi-Chi, Taiwan-04	6.2	99999	CHY100
2752	0173	Chi-Chi, Taiwan-04	6.2	99999	CHY101
2753	0173	Chi-Chi, Taiwan-04	6.2	99999	CHY102
2754	0173	Chi-Chi, Taiwan-04	6.2	99999	CHY104
2755	0173	Chi-Chi, Taiwan-04	6.2	99999	CHY107
2756	0173	Chi-Chi, Taiwan-04	6.2	99999	CHY114
2757	0173	Chi-Chi, Taiwan-04	6.2	99999	CHY115
2758	0173	Chi-Chi, Taiwan-04	6.2	99999	CHY116
2759	0173	Chi-Chi, Taiwan-04	6.2	99999	HWA002
2760	0173	Chi-Chi, Taiwan-04	6.2	99999	HWA005
2761	0173	Chi-Chi, Taiwan-04	6.2	99999	HWA006
2762	0173	Chi-Chi, Taiwan-04	6.2	99999	HWA007
2763	0173	Chi-Chi, Taiwan-04	6.2	99999	HWA009
2764	0173	Chi-Chi, Taiwan-04	6.2	99999	HWA011
2765	0173	Chi-Chi, Taiwan-04	6.2	99999	HWA013
2766	0173	Chi-Chi, Taiwan-04	6.2	99999	HWA014
2767	0173	Chi-Chi, Taiwan-04	6.2	99999	HWA015
2768	0173	Chi-Chi, Taiwan-04	6.2	99999	HWA016
2769	0173	Chi-Chi, Taiwan-04	6.2	99999	HWA017
2770	0173	Chi-Chi, Taiwan-04	6.2	99999	HWA019
2771	0173	Chi-Chi, Taiwan-04	6.2	99999	HWA020
2772	0173	Chi-Chi, Taiwan-04	6.2	99999	HWA024
2773	0173	Chi-Chi, Taiwan-04	6.2	99999	HWA025
2774	0173	Chi-Chi, Taiwan-04	6.2	99999	HWA026
2775	0173	Chi-Chi, Taiwan-04	6.2	99999	HWA027
2776	0173	Chi-Chi, Taiwan-04	6.2	99999	HWA028
2777	0173	Chi-Chi, Taiwan-04	6.2	99999	HWA029
2778	0173	Chi-Chi, Taiwan-04	6.2	99999	HWA030
2779	0173	Chi-Chi, Taiwan-04	6.2	99999	HWA031
2780	0173	Chi-Chi, Taiwan-04	6.2	99999	HWA032
2781	0173	Chi-Chi, Taiwan-04	6.2	99999	HWA033
2782	0173	Chi-Chi, Taiwan-04	6.2	99999	HWA034
2783	0173	Chi-Chi, Taiwan-04	6.2	99999	HWA035
2784	0173	Chi-Chi, Taiwan-04	6.2	99999	HWA036
2785	0173	Chi-Chi, Taiwan-04	6.2	99999	HWA037

RSN	EQID	Earthquake	M	Station No,	Station
2786	0173	Chi-Chi, Taiwan-04	6.2	99999	HWA038
2787	0173	Chi-Chi, Taiwan-04	6.2	99999	HWA039
2788	0173	Chi-Chi, Taiwan-04	6.2	99999	HWA041
2789	0173	Chi-Chi, Taiwan-04	6.2	99999	HWA043
2790	0173	Chi-Chi, Taiwan-04	6.2	99999	HWA044
2791	0173	Chi-Chi, Taiwan-04	6.2	99999	HWA045
2792	0173	Chi-Chi, Taiwan-04	6.2	99999	HWA046
2793	0173	Chi-Chi, Taiwan-04	6.2	99999	HWA048
2794	0173	Chi-Chi, Taiwan-04	6.2	99999	HWA049
2795	0173	Chi-Chi, Taiwan-04	6.2	99999	HWA050
2796	0173	Chi-Chi, Taiwan-04	6.2	99999	HWA051
2797	0173	Chi-Chi, Taiwan-04	6.2	99999	HWA055
2798	0173	Chi-Chi, Taiwan-04	6.2	99999	HWA056
2799	0173	Chi-Chi, Taiwan-04	6.2	99999	HWA057
2800	0173	Chi-Chi, Taiwan-04	6.2	99999	HWA058
2801	0173	Chi-Chi, Taiwan-04	6.2	99999	HWA059
2803	0173	Chi-Chi, Taiwan-04	6.2	99999	ILA067
2804	0173	Chi-Chi, Taiwan-04	6.2	99999	KAU001
2805	0173	Chi-Chi, Taiwan-04	6.2	99999	KAU003
2806	0173	Chi-Chi, Taiwan-04	6.2	99999	KAU006
2807	0173	Chi-Chi, Taiwan-04	6.2	99999	KAU007
2808	0173	Chi-Chi, Taiwan-04	6.2	99999	KAU008
2809	0173	Chi-Chi, Taiwan-04	6.2	99999	KAU012
2810	0173	Chi-Chi, Taiwan-04	6.2	99999	KAU015
2811	0173	Chi-Chi, Taiwan-04	6.2	99999	KAU017
2812	0173	Chi-Chi, Taiwan-04	6.2	99999	KAU018
2813	0173	Chi-Chi, Taiwan-04	6.2	99999	KAU020
2814	0173	Chi-Chi, Taiwan-04	6.2	99999	KAU022
2815	0173	Chi-Chi, Taiwan-04	6.2	99999	KAU032
2816	0173	Chi-Chi, Taiwan-04	6.2	99999	KAU037
2817	0173	Chi-Chi, Taiwan-04	6.2	99999	KAU038
2818	0173	Chi-Chi, Taiwan-04	6.2	99999	KAU045
2819	0173	Chi-Chi, Taiwan-04	6.2	99999	KAU048
2820	0173	Chi-Chi, Taiwan-04	6.2	99999	KAU050
2821	0173	Chi-Chi, Taiwan-04	6.2	99999	KAU054
2822	0173	Chi-Chi, Taiwan-04	6.2	99999	KAU055
2823	0173	Chi-Chi, Taiwan-04	6.2	99999	KAU058
2824	0173	Chi-Chi, Taiwan-04	6.2	99999	KAU062
2825	0173	Chi-Chi, Taiwan-04	6.2	99999	KAU063
2826	0173	Chi-Chi, Taiwan-04	6.2	99999	KAU064
2827	0173	Chi-Chi, Taiwan-04	6.2	99999	KAU066
2828	0173	Chi-Chi, Taiwan-04	6.2	99999	KAU069
2829	0173	Chi-Chi, Taiwan-04	6.2	99999	KAU073
2830	0173	Chi-Chi, Taiwan-04	6.2	99999	KAU074
2831	0173	Chi-Chi, Taiwan-04	6.2	99999	KAU075
2832	0173	Chi-Chi, Taiwan-04	6.2	99999	KAU077
2833	0173	Chi-Chi, Taiwan-04	6.2	99999	KAU078
2834	0173	Chi-Chi, Taiwan-04	6.2	99999	KAU081
2835	0173	Chi-Chi, Taiwan-04	6.2	99999	KAU083
2836	0173	Chi-Chi, Taiwan-04	6.2	99999	KAU085
2837	0173	Chi-Chi, Taiwan-04	6.2	99999	KAU087
2838	0173	Chi-Chi, Taiwan-04	6.2	99999	KAU088
2839	0173	Chi-Chi, Taiwan-04	6.2	99999	KAU089
2840	0173	Chi-Chi, Taiwan-04	6.2	99999	TAP026
2841	0173	Chi-Chi, Taiwan-04	6.2	99999	TAP088
2842	0173	Chi-Chi, Taiwan-04	6.2	99999	TCU017
2843	0173	Chi-Chi, Taiwan-04	6.2	99999	TCU026
2844	0173	Chi-Chi, Taiwan-04	6.2	99999	TCU029
2845	0173	Chi-Chi, Taiwan-04	6.2	99999	TCU031
2846	0173	Chi-Chi, Taiwan-04	6.2	99999	TCU033
2847	0173	Chi-Chi, Taiwan-04	6.2	99999	TCU035
2848	0173	Chi-Chi, Taiwan-04	6.2	99999	TCU036
2849	0173	Chi-Chi, Taiwan-04	6.2	99999	TCU038
2850	0173	Chi-Chi, Taiwan-04	6.2	99999	TCU039
2851	0173	Chi-Chi, Taiwan-04	6.2	99999	TCU040
2852	0173	Chi-Chi, Taiwan-04	6.2	99999	TCU042
2853	0173	Chi-Chi, Taiwan-04	6.2	99999	TCU046
2854	0173	Chi-Chi, Taiwan-04	6.2	99999	TCU048
2855	0173	Chi-Chi, Taiwan-04	6.2	99999	TCU049

RSN	EQID	Earthquake	M	Station No,	Station
2856	0173	Chi-Chi, Taiwan-04	6.2	99999	TCU050
2857	0173	Chi-Chi, Taiwan-04	6.2	99999	TCU051
2858	0173	Chi-Chi, Taiwan-04	6.2	99999	TCU052
2859	0173	Chi-Chi, Taiwan-04	6.2	99999	TCU053
2860	0173	Chi-Chi, Taiwan-04	6.2	99999	TCU054
2861	0173	Chi-Chi, Taiwan-04	6.2	99999	TCU056
2862	0173	Chi-Chi, Taiwan-04	6.2	99999	TCU057
2863	0173	Chi-Chi, Taiwan-04	6.2	99999	TCU059
2864	0173	Chi-Chi, Taiwan-04	6.2	99999	TCU060
2865	0173	Chi-Chi, Taiwan-04	6.2	99999	TCU061
2866	0173	Chi-Chi, Taiwan-04	6.2	99999	TCU064
2867	0173	Chi-Chi, Taiwan-04	6.2	99999	TCU067
2868	0173	Chi-Chi, Taiwan-04	6.2	99999	TCU068
2869	0173	Chi-Chi, Taiwan-04	6.2	99999	TCU070
2870	0173	Chi-Chi, Taiwan-04	6.2	99999	TCU082
2871	0173	Chi-Chi, Taiwan-04	6.2	99999	TCU084
2872	0173	Chi-Chi, Taiwan-04	6.2	99999	TCU087
2873	0173	Chi-Chi, Taiwan-04	6.2	99999	TCU089
2874	0173	Chi-Chi, Taiwan-04	6.2	99999	TCU095
2875	0173	Chi-Chi, Taiwan-04	6.2	99999	TCU098
2876	0173	Chi-Chi, Taiwan-04	6.2	99999	TCU100
2877	0173	Chi-Chi, Taiwan-04	6.2	99999	TCU102
2878	0173	Chi-Chi, Taiwan-04	6.2	99999	TCU103
2879	0173	Chi-Chi, Taiwan-04	6.2	99999	TCU104
2880	0173	Chi-Chi, Taiwan-04	6.2	99999	TCU105
2881	0173	Chi-Chi, Taiwan-04	6.2	99999	TCU106
2882	0173	Chi-Chi, Taiwan-04	6.2	99999	TCU107
2883	0173	Chi-Chi, Taiwan-04	6.2	99999	TCU109
2884	0173	Chi-Chi, Taiwan-04	6.2	99999	TCU110
2885	0173	Chi-Chi, Taiwan-04	6.2	99999	TCU112
2886	0173	Chi-Chi, Taiwan-04	6.2	99999	TCU113
2887	0173	Chi-Chi, Taiwan-04	6.2	99999	TCU115
2888	0173	Chi-Chi, Taiwan-04	6.2	99999	TCU116
2889	0173	Chi-Chi, Taiwan-04	6.2	99999	TCU117
2890	0173	Chi-Chi, Taiwan-04	6.2	99999	TCU118
2891	0173	Chi-Chi, Taiwan-04	6.2	99999	TCU119
2892	0173	Chi-Chi, Taiwan-04	6.2	99999	TCU120
2893	0173	Chi-Chi, Taiwan-04	6.2	99999	TCU122
2894	0173	Chi-Chi, Taiwan-04	6.2	99999	TCU123
2895	0173	Chi-Chi, Taiwan-04	6.2	99999	TCU131
2896	0173	Chi-Chi, Taiwan-04	6.2	99999	TCU136
2897	0173	Chi-Chi, Taiwan-04	6.2	99999	TCU138
2898	0173	Chi-Chi, Taiwan-04	6.2	99999	TCU140
2899	0173	Chi-Chi, Taiwan-04	6.2	99999	TCU141
2900	0173	Chi-Chi, Taiwan-04	6.2	99999	TCU145
2901	0173	Chi-Chi, Taiwan-04	6.2	99999	TTN001
2902	0173	Chi-Chi, Taiwan-04	6.2	99999	TTN002
2903	0173	Chi-Chi, Taiwan-04	6.2	99999	TTN003
2904	0173	Chi-Chi, Taiwan-04	6.2	99999	TTN004
2905	0173	Chi-Chi, Taiwan-04	6.2	99999	TTN005
2906	0173	Chi-Chi, Taiwan-04	6.2	99999	TTN006
2907	0173	Chi-Chi, Taiwan-04	6.2	99999	TTN007
2908	0173	Chi-Chi, Taiwan-04	6.2	99999	TTN008
2909	0173	Chi-Chi, Taiwan-04	6.2	99999	TTN009
2910	0173	Chi-Chi, Taiwan-04	6.2	99999	TTN010
2911	0173	Chi-Chi, Taiwan-04	6.2	99999	TTN012
2912	0173	Chi-Chi, Taiwan-04	6.2	99999	TTN014
2913	0173	Chi-Chi, Taiwan-04	6.2	99999	TTN015
2914	0173	Chi-Chi, Taiwan-04	6.2	99999	TTN018
2915	0173	Chi-Chi, Taiwan-04	6.2	99999	TTN020
2916	0173	Chi-Chi, Taiwan-04	6.2	99999	TTN022
2917	0173	Chi-Chi, Taiwan-04	6.2	99999	TTN023
2918	0173	Chi-Chi, Taiwan-04	6.2	99999	TTN024
2919	0173	Chi-Chi, Taiwan-04	6.2	99999	TTN025
2920	0173	Chi-Chi, Taiwan-04	6.2	99999	TTN026
2921	0173	Chi-Chi, Taiwan-04	6.2	99999	TTN027
2922	0173	Chi-Chi, Taiwan-04	6.2	99999	TTN028
2923	0173	Chi-Chi, Taiwan-04	6.2	99999	TTN031
2924	0173	Chi-Chi, Taiwan-04	6.2	99999	TTN032

RSN	EQID	Earthquake	M	Station No,	Station
2925	0173	Chi-Chi, Taiwan-04	6.2	99999	TTN033
2926	0173	Chi-Chi, Taiwan-04	6.2	99999	TTN036
2927	0173	Chi-Chi, Taiwan-04	6.2	99999	TTN040
2928	0173	Chi-Chi, Taiwan-04	6.2	99999	TTN041
2929	0173	Chi-Chi, Taiwan-04	6.2	99999	TTN042
2930	0173	Chi-Chi, Taiwan-04	6.2	99999	TTN044
2931	0173	Chi-Chi, Taiwan-04	6.2	99999	TTN045
2932	0173	Chi-Chi, Taiwan-04	6.2	99999	TTN046
2933	0173	Chi-Chi, Taiwan-04	6.2	99999	TTN048
2934	0173	Chi-Chi, Taiwan-04	6.2	99999	TTN050
2935	0173	Chi-Chi, Taiwan-04	6.2	99999	TTN051
2936	0174	Chi-Chi, Taiwan-05	6.2	99999	CHY014
2937	0174	Chi-Chi, Taiwan-05	6.2	99999	CHY015
2938	0174	Chi-Chi, Taiwan-05	6.2	99999	CHY016
2939	0174	Chi-Chi, Taiwan-05	6.2	99999	CHY017
2940	0174	Chi-Chi, Taiwan-05	6.2	99999	CHY019
2941	0174	Chi-Chi, Taiwan-05	6.2	99999	CHY022
2942	0174	Chi-Chi, Taiwan-05	6.2	99999	CHY024
2943	0174	Chi-Chi, Taiwan-05	6.2	99999	CHY025
2944	0174	Chi-Chi, Taiwan-05	6.2	99999	CHY026
2945	0174	Chi-Chi, Taiwan-05	6.2	99999	CHY027
2946	0174	Chi-Chi, Taiwan-05	6.2	99999	CHY029
2947	0174	Chi-Chi, Taiwan-05	6.2	99999	CHY030
2948	0174	Chi-Chi, Taiwan-05	6.2	99999	CHY032
2949	0174	Chi-Chi, Taiwan-05	6.2	99999	CHY033
2950	0174	Chi-Chi, Taiwan-05	6.2	99999	CHY035
2951	0174	Chi-Chi, Taiwan-05	6.2	99999	CHY039
2952	0174	Chi-Chi, Taiwan-05	6.2	99999	CHY042
2953	0174	Chi-Chi, Taiwan-05	6.2	99999	CHY044
2954	0174	Chi-Chi, Taiwan-05	6.2	99999	CHY046
2955	0174	Chi-Chi, Taiwan-05	6.2	99999	CHY047
2956	0174	Chi-Chi, Taiwan-05	6.2	99999	CHY050
2957	0174	Chi-Chi, Taiwan-05	6.2	99999	CHY052
2958	0174	Chi-Chi, Taiwan-05	6.2	99999	CHY054
2959	0174	Chi-Chi, Taiwan-05	6.2	99999	CHY055
2960	0174	Chi-Chi, Taiwan-05	6.2	99999	CHY056
2961	0174	Chi-Chi, Taiwan-05	6.2	99999	CHY057
2962	0174	Chi-Chi, Taiwan-05	6.2	99999	CHY058
2963	0174	Chi-Chi, Taiwan-05	6.2	99999	CHY059
2964	0174	Chi-Chi, Taiwan-05	6.2	99999	CHY060
2965	0174	Chi-Chi, Taiwan-05	6.2	99999	CHY061
2966	0174	Chi-Chi, Taiwan-05	6.2	99999	CHY062
2967	0174	Chi-Chi, Taiwan-05	6.2	99999	CHY063
2968	0174	Chi-Chi, Taiwan-05	6.2	99999	CHY065
2969	0174	Chi-Chi, Taiwan-05	6.2	99999	CHY066
2970	0174	Chi-Chi, Taiwan-05	6.2	99999	CHY067
2971	0174	Chi-Chi, Taiwan-05	6.2	99999	CHY069
2972	0174	Chi-Chi, Taiwan-05	6.2	99999	CHY070
2973	0174	Chi-Chi, Taiwan-05	6.2	99999	CHY071
2974	0174	Chi-Chi, Taiwan-05	6.2	99999	CHY075
2975	0174	Chi-Chi, Taiwan-05	6.2	99999	CHY076
2976	0174	Chi-Chi, Taiwan-05	6.2	99999	CHY078
2977	0174	Chi-Chi, Taiwan-05	6.2	99999	CHY079
2978	0174	Chi-Chi, Taiwan-05	6.2	99999	CHY081
2979	0174	Chi-Chi, Taiwan-05	6.2	99999	CHY082
2980	0174	Chi-Chi, Taiwan-05	6.2	99999	CHY086
2981	0174	Chi-Chi, Taiwan-05	6.2	99999	CHY087
2982	0174	Chi-Chi, Taiwan-05	6.2	99999	CHY088
2983	0174	Chi-Chi, Taiwan-05	6.2	99999	CHY090
2984	0174	Chi-Chi, Taiwan-05	6.2	99999	CHY093
2985	0174	Chi-Chi, Taiwan-05	6.2	99999	CHY094
2986	0174	Chi-Chi, Taiwan-05	6.2	99999	CHY096
2987	0174	Chi-Chi, Taiwan-05	6.2	99999	CHY099
2988	0174	Chi-Chi, Taiwan-05	6.2	99999	CHY100
2989	0174	Chi-Chi, Taiwan-05	6.2	99999	CHY102
2990	0174	Chi-Chi, Taiwan-05	6.2	99999	CHY107
2991	0174	Chi-Chi, Taiwan-05	6.2	99999	CHY111
2992	0174	Chi-Chi, Taiwan-05	6.2	99999	CHY114
2993	0174	Chi-Chi, Taiwan-05	6.2	99999	CHY115

RSN	EQID	Earthquake	M	Station No,	Station
2994	0174	Chi-Chi, Taiwan-05	6.2	99999	CHY116
2995	0174	Chi-Chi, Taiwan-05	6.2	99999	HWA002
2996	0174	Chi-Chi, Taiwan-05	6.2	99999	HWA003
2997	0174	Chi-Chi, Taiwan-05	6.2	99999	HWA005
2998	0174	Chi-Chi, Taiwan-05	6.2	99999	HWA007
2999	0174	Chi-Chi, Taiwan-05	6.2	99999	HWA009
3000	0174	Chi-Chi, Taiwan-05	6.2	99999	HWA011
3001	0174	Chi-Chi, Taiwan-05	6.2	99999	HWA012
3002	0174	Chi-Chi, Taiwan-05	6.2	99999	HWA013
3003	0174	Chi-Chi, Taiwan-05	6.2	99999	HWA014
3004	0174	Chi-Chi, Taiwan-05	6.2	99999	HWA015
3005	0174	Chi-Chi, Taiwan-05	6.2	99999	HWA016
3006	0174	Chi-Chi, Taiwan-05	6.2	99999	HWA017
3007	0174	Chi-Chi, Taiwan-05	6.2	99999	HWA019
3008	0174	Chi-Chi, Taiwan-05	6.2	99999	HWA020
3009	0174	Chi-Chi, Taiwan-05	6.2	99999	HWA022
3010	0174	Chi-Chi, Taiwan-05	6.2	99999	HWA023
3011	0174	Chi-Chi, Taiwan-05	6.2	99999	HWA024
3012	0174	Chi-Chi, Taiwan-05	6.2	99999	HWA025
3013	0174	Chi-Chi, Taiwan-05	6.2	99999	HWA026
3014	0174	Chi-Chi, Taiwan-05	6.2	99999	HWA027
3015	0174	Chi-Chi, Taiwan-05	6.2	99999	HWA028
3016	0174	Chi-Chi, Taiwan-05	6.2	99999	HWA029
3017	0174	Chi-Chi, Taiwan-05	6.2	99999	HWA030
3018	0174	Chi-Chi, Taiwan-05	6.2	99999	HWA031
3019	0174	Chi-Chi, Taiwan-05	6.2	99999	HWA032
3020	0174	Chi-Chi, Taiwan-05	6.2	99999	HWA033
3021	0174	Chi-Chi, Taiwan-05	6.2	99999	HWA034
3022	0174	Chi-Chi, Taiwan-05	6.2	99999	HWA035
3023	0174	Chi-Chi, Taiwan-05	6.2	99999	HWA036
3024	0174	Chi-Chi, Taiwan-05	6.2	99999	HWA037
3025	0174	Chi-Chi, Taiwan-05	6.2	99999	HWA038
3026	0174	Chi-Chi, Taiwan-05	6.2	99999	HWA039
3027	0174	Chi-Chi, Taiwan-05	6.2	99999	HWA041
3028	0174	Chi-Chi, Taiwan-05	6.2	99999	HWA043
3029	0174	Chi-Chi, Taiwan-05	6.2	99999	HWA044
3030	0174	Chi-Chi, Taiwan-05	6.2	99999	HWA045
3031	0174	Chi-Chi, Taiwan-05	6.2	99999	HWA046
3032	0174	Chi-Chi, Taiwan-05	6.2	99999	HWA048
3033	0174	Chi-Chi, Taiwan-05	6.2	99999	HWA049
3034	0174	Chi-Chi, Taiwan-05	6.2	99999	HWA050
3035	0174	Chi-Chi, Taiwan-05	6.2	99999	HWA051
3036	0174	Chi-Chi, Taiwan-05	6.2	99999	HWA056
3037	0174	Chi-Chi, Taiwan-05	6.2	99999	HWA057
3038	0174	Chi-Chi, Taiwan-05	6.2	99999	HWA058
3039	0174	Chi-Chi, Taiwan-05	6.2	99999	HWA059
3040	0174	Chi-Chi, Taiwan-05	6.2	99999	HWA060
3042	0174	Chi-Chi, Taiwan-05	6.2	99999	ILA001
3043	0174	Chi-Chi, Taiwan-05	6.2	99999	ILA002
3044	0174	Chi-Chi, Taiwan-05	6.2	99999	ILA004
3045	0174	Chi-Chi, Taiwan-05	6.2	99999	ILA005
3046	0174	Chi-Chi, Taiwan-05	6.2	99999	ILA006
3047	0174	Chi-Chi, Taiwan-05	6.2	99999	ILA007
3048	0174	Chi-Chi, Taiwan-05	6.2	99999	ILA008
3049	0174	Chi-Chi, Taiwan-05	6.2	99999	ILA010
3050	0174	Chi-Chi, Taiwan-05	6.2	99999	ILA012
3051	0174	Chi-Chi, Taiwan-05	6.2	99999	ILA013
3052	0174	Chi-Chi, Taiwan-05	6.2	99999	ILA014
3053	0174	Chi-Chi, Taiwan-05	6.2	99999	ILA015
3054	0174	Chi-Chi, Taiwan-05	6.2	99999	ILA016
3055	0174	Chi-Chi, Taiwan-05	6.2	99999	ILA021
3056	0174	Chi-Chi, Taiwan-05	6.2	99999	ILA024
3057	0174	Chi-Chi, Taiwan-05	6.2	99999	ILA030
3058	0174	Chi-Chi, Taiwan-05	6.2	99999	ILA031
3059	0174	Chi-Chi, Taiwan-05	6.2	99999	ILA037
3060	0174	Chi-Chi, Taiwan-05	6.2	99999	ILA041
3061	0174	Chi-Chi, Taiwan-05	6.2	99999	ILA042
3062	0174	Chi-Chi, Taiwan-05	6.2	99999	ILA044
3063	0174	Chi-Chi, Taiwan-05	6.2	99999	ILA048

RSN	EQID	Earthquake	M	Station No,	Station
3064	0174	Chi-Chi, Taiwan-05	6.2	99999	ILA049
3065	0174	Chi-Chi, Taiwan-05	6.2	99999	ILA051
3066	0174	Chi-Chi, Taiwan-05	6.2	99999	ILA052
3067	0174	Chi-Chi, Taiwan-05	6.2	99999	ILA054
3068	0174	Chi-Chi, Taiwan-05	6.2	99999	ILA055
3069	0174	Chi-Chi, Taiwan-05	6.2	99999	ILA056
3070	0174	Chi-Chi, Taiwan-05	6.2	99999	ILA059
3071	0174	Chi-Chi, Taiwan-05	6.2	99999	ILA061
3072	0174	Chi-Chi, Taiwan-05	6.2	99999	ILA062
3073	0174	Chi-Chi, Taiwan-05	6.2	99999	ILA064
3074	0174	Chi-Chi, Taiwan-05	6.2	99999	ILA066
3075	0174	Chi-Chi, Taiwan-05	6.2	99999	KAU001
3076	0174	Chi-Chi, Taiwan-05	6.2	99999	KAU007
3077	0174	Chi-Chi, Taiwan-05	6.2	99999	KAU012
3078	0174	Chi-Chi, Taiwan-05	6.2	99999	KAU015
3079	0174	Chi-Chi, Taiwan-05	6.2	99999	KAU018
3080	0174	Chi-Chi, Taiwan-05	6.2	99999	KAU020
3081	0174	Chi-Chi, Taiwan-05	6.2	99999	KAU022
3082	0174	Chi-Chi, Taiwan-05	6.2	99999	KAU030
3083	0174	Chi-Chi, Taiwan-05	6.2	99999	KAU032
3084	0174	Chi-Chi, Taiwan-05	6.2	99999	KAU033
3085	0174	Chi-Chi, Taiwan-05	6.2	99999	KAU035
3086	0174	Chi-Chi, Taiwan-05	6.2	99999	KAU036
3087	0174	Chi-Chi, Taiwan-05	6.2	99999	KAU037
3088	0174	Chi-Chi, Taiwan-05	6.2	99999	KAU038
3089	0174	Chi-Chi, Taiwan-05	6.2	99999	KAU039
3090	0174	Chi-Chi, Taiwan-05	6.2	99999	KAU040
3091	0174	Chi-Chi, Taiwan-05	6.2	99999	KAU045
3092	0174	Chi-Chi, Taiwan-05	6.2	99999	KAU048
3093	0174	Chi-Chi, Taiwan-05	6.2	99999	KAU050
3094	0174	Chi-Chi, Taiwan-05	6.2	99999	KAU051
3095	0174	Chi-Chi, Taiwan-05	6.2	99999	KAU054
3096	0174	Chi-Chi, Taiwan-05	6.2	99999	KAU056
3097	0174	Chi-Chi, Taiwan-05	6.2	99999	KAU057
3098	0174	Chi-Chi, Taiwan-05	6.2	99999	KAU058
3099	0174	Chi-Chi, Taiwan-05	6.2	99999	KAU062
3100	0174	Chi-Chi, Taiwan-05	6.2	99999	KAU063
3101	0174	Chi-Chi, Taiwan-05	6.2	99999	KAU064
3102	0174	Chi-Chi, Taiwan-05	6.2	99999	KAU066
3103	0174	Chi-Chi, Taiwan-05	6.2	99999	KAU069
3104	0174	Chi-Chi, Taiwan-05	6.2	99999	KAU073
3105	0174	Chi-Chi, Taiwan-05	6.2	99999	KAU074
3106	0174	Chi-Chi, Taiwan-05	6.2	99999	KAU075
3107	0174	Chi-Chi, Taiwan-05	6.2	99999	KAU077
3108	0174	Chi-Chi, Taiwan-05	6.2	99999	KAU078
3109	0174	Chi-Chi, Taiwan-05	6.2	99999	KAU081
3110	0174	Chi-Chi, Taiwan-05	6.2	99999	KAU083
3111	0174	Chi-Chi, Taiwan-05	6.2	99999	KAU085
3112	0174	Chi-Chi, Taiwan-05	6.2	99999	KAU087
3113	0174	Chi-Chi, Taiwan-05	6.2	99999	KAU088
3114	0174	Chi-Chi, Taiwan-05	6.2	99999	KAU089
3115	0174	Chi-Chi, Taiwan-05	6.2	99999	TAP010
3116	0174	Chi-Chi, Taiwan-05	6.2	99999	TAP013
3117	0174	Chi-Chi, Taiwan-05	6.2	99999	TAP021
3118	0174	Chi-Chi, Taiwan-05	6.2	99999	TAP026
3119	0174	Chi-Chi, Taiwan-05	6.2	99999	TAP028
3120	0174	Chi-Chi, Taiwan-05	6.2	99999	TAP032
3121	0174	Chi-Chi, Taiwan-05	6.2	99999	TAP033
3122	0174	Chi-Chi, Taiwan-05	6.2	99999	TAP034
3123	0174	Chi-Chi, Taiwan-05	6.2	99999	TAP035
3124	0174	Chi-Chi, Taiwan-05	6.2	99999	TAP036
3125	0174	Chi-Chi, Taiwan-05	6.2	99999	TAP041
3126	0174	Chi-Chi, Taiwan-05	6.2	99999	TAP042
3127	0174	Chi-Chi, Taiwan-05	6.2	99999	TAP043
3128	0174	Chi-Chi, Taiwan-05	6.2	99999	TAP049
3129	0174	Chi-Chi, Taiwan-05	6.2	99999	TAP051
3130	0174	Chi-Chi, Taiwan-05	6.2	99999	TAP052
3131	0174	Chi-Chi, Taiwan-05	6.2	99999	TAP053
3132	0174	Chi-Chi, Taiwan-05	6.2	99999	TAP059

RSN	EQID	Earthquake	M	Station No,	Station
3133	0174	Chi-Chi, Taiwan-05	6.2	99999	TAP060
3135	0174	Chi-Chi, Taiwan-05	6.2	99999	TAP067
3136	0174	Chi-Chi, Taiwan-05	6.2	99999	TAP069
3137	0174	Chi-Chi, Taiwan-05	6.2	99999	TAP072
3138	0174	Chi-Chi, Taiwan-05	6.2	99999	TAP075
3139	0174	Chi-Chi, Taiwan-05	6.2	99999	TAP077
3140	0174	Chi-Chi, Taiwan-05	6.2	99999	TAP078
3141	0174	Chi-Chi, Taiwan-05	6.2	99999	TAP079
3142	0174	Chi-Chi, Taiwan-05	6.2	99999	TAP081
3143	0174	Chi-Chi, Taiwan-05	6.2	99999	TAP083
3144	0174	Chi-Chi, Taiwan-05	6.2	99999	TAP084
3145	0174	Chi-Chi, Taiwan-05	6.2	99999	TAP086
3146	0174	Chi-Chi, Taiwan-05	6.2	99999	TAP087
3147	0174	Chi-Chi, Taiwan-05	6.2	99999	TAP088
3148	0174	Chi-Chi, Taiwan-05	6.2	99999	TAP090
3149	0174	Chi-Chi, Taiwan-05	6.2	99999	TAP091
3150	0174	Chi-Chi, Taiwan-05	6.2	99999	TAP094
3151	0174	Chi-Chi, Taiwan-05	6.2	99999	TAP095
3152	0174	Chi-Chi, Taiwan-05	6.2	99999	TAP097
3153	0174	Chi-Chi, Taiwan-05	6.2	99999	TAP098
3154	0174	Chi-Chi, Taiwan-05	6.2	99999	TAP100
3156	0174	Chi-Chi, Taiwan-05	6.2	99999	TCU005
3157	0174	Chi-Chi, Taiwan-05	6.2	99999	TCU006
3158	0174	Chi-Chi, Taiwan-05	6.2	99999	TCU007
3159	0174	Chi-Chi, Taiwan-05	6.2	99999	TCU008
3160	0174	Chi-Chi, Taiwan-05	6.2	99999	TCU014
3161	0174	Chi-Chi, Taiwan-05	6.2	99999	TCU018
3162	0174	Chi-Chi, Taiwan-05	6.2	99999	TCU026
3163	0174	Chi-Chi, Taiwan-05	6.2	99999	TCU029
3164	0174	Chi-Chi, Taiwan-05	6.2	99999	TCU031
3165	0174	Chi-Chi, Taiwan-05	6.2	99999	TCU033
3166	0174	Chi-Chi, Taiwan-05	6.2	99999	TCU036
3167	0174	Chi-Chi, Taiwan-05	6.2	99999	TCU038
3168	0174	Chi-Chi, Taiwan-05	6.2	99999	TCU039
3169	0174	Chi-Chi, Taiwan-05	6.2	99999	TCU040
3170	0174	Chi-Chi, Taiwan-05	6.2	99999	TCU042
3171	0174	Chi-Chi, Taiwan-05	6.2	99999	TCU044
3172	0174	Chi-Chi, Taiwan-05	6.2	99999	TCU045
3173	0174	Chi-Chi, Taiwan-05	6.2	99999	TCU046
3174	0174	Chi-Chi, Taiwan-05	6.2	99999	TCU048
3175	0174	Chi-Chi, Taiwan-05	6.2	99999	TCU049
3176	0174	Chi-Chi, Taiwan-05	6.2	99999	TCU050
3177	0174	Chi-Chi, Taiwan-05	6.2	99999	TCU051
3178	0174	Chi-Chi, Taiwan-05	6.2	99999	TCU052
3179	0174	Chi-Chi, Taiwan-05	6.2	99999	TCU053
3180	0174	Chi-Chi, Taiwan-05	6.2	99999	TCU054
3181	0174	Chi-Chi, Taiwan-05	6.2	99999	TCU055
3182	0174	Chi-Chi, Taiwan-05	6.2	99999	TCU056
3183	0174	Chi-Chi, Taiwan-05	6.2	99999	TCU057
3184	0174	Chi-Chi, Taiwan-05	6.2	99999	TCU059
3185	0174	Chi-Chi, Taiwan-05	6.2	99999	TCU060
3186	0174	Chi-Chi, Taiwan-05	6.2	99999	TCU061
3187	0174	Chi-Chi, Taiwan-05	6.2	99999	TCU064
3188	0174	Chi-Chi, Taiwan-05	6.2	99999	TCU067
3189	0174	Chi-Chi, Taiwan-05	6.2	99999	TCU068
3190	0174	Chi-Chi, Taiwan-05	6.2	99999	TCU070
3192	0174	Chi-Chi, Taiwan-05	6.2	99999	TCU082
3193	0174	Chi-Chi, Taiwan-05	6.2	99999	TCU083
3194	0174	Chi-Chi, Taiwan-05	6.2	99999	TCU085
3195	0174	Chi-Chi, Taiwan-05	6.2	99999	TCU087
3196	0174	Chi-Chi, Taiwan-05	6.2	99999	TCU092
3197	0174	Chi-Chi, Taiwan-05	6.2	99999	TCU094
3198	0174	Chi-Chi, Taiwan-05	6.2	99999	TCU095
3199	0174	Chi-Chi, Taiwan-05	6.2	99999	TCU096
3200	0174	Chi-Chi, Taiwan-05	6.2	99999	TCU098
3201	0174	Chi-Chi, Taiwan-05	6.2	99999	TCU101
3202	0174	Chi-Chi, Taiwan-05	6.2	99999	TCU102
3203	0174	Chi-Chi, Taiwan-05	6.2	99999	TCU103
3204	0174	Chi-Chi, Taiwan-05	6.2	99999	TCU104

RSN	EQID	Earthquake	M	Station No,	Station
3205	0174	Chi-Chi, Taiwan-05	6.2	99999	TCU105
3206	0174	Chi-Chi, Taiwan-05	6.2	99999	TCU106
3207	0174	Chi-Chi, Taiwan-05	6.2	99999	TCU107
3208	0174	Chi-Chi, Taiwan-05	6.2	99999	TCU109
3209	0174	Chi-Chi, Taiwan-05	6.2	99999	TCU112
3210	0174	Chi-Chi, Taiwan-05	6.2	99999	TCU113
3211	0174	Chi-Chi, Taiwan-05	6.2	99999	TCU115
3212	0174	Chi-Chi, Taiwan-05	6.2	99999	TCU117
3213	0174	Chi-Chi, Taiwan-05	6.2	99999	TCU118
3214	0174	Chi-Chi, Taiwan-05	6.2	99999	TCU119
3215	0174	Chi-Chi, Taiwan-05	6.2	99999	TCU123
3216	0174	Chi-Chi, Taiwan-05	6.2	99999	TCU128
3217	0174	Chi-Chi, Taiwan-05	6.2	9999936	TCU129
3218	0174	Chi-Chi, Taiwan-05	6.2	99999	TCU131
3219	0174	Chi-Chi, Taiwan-05	6.2	99999	TCU136
3220	0174	Chi-Chi, Taiwan-05	6.2	99999	TCU138
3221	0174	Chi-Chi, Taiwan-05	6.2	99999	TCU140
3222	0174	Chi-Chi, Taiwan-05	6.2	99999	TCU141
3223	0174	Chi-Chi, Taiwan-05	6.2	99999	TCU145
3224	0174	Chi-Chi, Taiwan-05	6.2	99999	TTN001
3225	0174	Chi-Chi, Taiwan-05	6.2	99999	TTN002
3226	0174	Chi-Chi, Taiwan-05	6.2	99999	TTN003
3227	0174	Chi-Chi, Taiwan-05	6.2	99999	TTN004
3228	0174	Chi-Chi, Taiwan-05	6.2	99999	TTN005
3229	0174	Chi-Chi, Taiwan-05	6.2	99999	TTN007
3230	0174	Chi-Chi, Taiwan-05	6.2	99999	TTN008
3231	0174	Chi-Chi, Taiwan-05	6.2	99999	TTN009
3232	0174	Chi-Chi, Taiwan-05	6.2	99999	TTN010
3233	0174	Chi-Chi, Taiwan-05	6.2	99999	TTN012
3234	0174	Chi-Chi, Taiwan-05	6.2	99999	TTN013
3235	0174	Chi-Chi, Taiwan-05	6.2	99999	TTN014
3236	0174	Chi-Chi, Taiwan-05	6.2	99999	TTN015
3237	0174	Chi-Chi, Taiwan-05	6.2	99999	TTN018
3238	0174	Chi-Chi, Taiwan-05	6.2	99999	TTN020
3239	0174	Chi-Chi, Taiwan-05	6.2	99999	TTN022
3240	0174	Chi-Chi, Taiwan-05	6.2	99999	TTN023
3241	0174	Chi-Chi, Taiwan-05	6.2	99999	TTN025
3242	0174	Chi-Chi, Taiwan-05	6.2	99999	TTN026
3243	0174	Chi-Chi, Taiwan-05	6.2	99999	TTN027
3244	0174	Chi-Chi, Taiwan-05	6.2	99999	TTN028
3245	0174	Chi-Chi, Taiwan-05	6.2	99999	TTN031
3246	0174	Chi-Chi, Taiwan-05	6.2	99999	TTN032
3247	0174	Chi-Chi, Taiwan-05	6.2	99999	TTN033
3248	0174	Chi-Chi, Taiwan-05	6.2	99999	TTN036
3249	0174	Chi-Chi, Taiwan-05	6.2	99999	TTN040
3250	0174	Chi-Chi, Taiwan-05	6.2	99999	TTN041
3251	0174	Chi-Chi, Taiwan-05	6.2	99999	TTN042
3252	0174	Chi-Chi, Taiwan-05	6.2	99999	TTN044
3253	0174	Chi-Chi, Taiwan-05	6.2	99999	TTN045
3254	0174	Chi-Chi, Taiwan-05	6.2	99999	TTN046
3255	0174	Chi-Chi, Taiwan-05	6.2	99999	TTN048
3256	0174	Chi-Chi, Taiwan-05	6.2	99999	TTN050
3257	0174	Chi-Chi, Taiwan-05	6.2	99999	TTN051
3258	0175	Chi-Chi, Taiwan-06	6.3	99999	CHY014
3259	0175	Chi-Chi, Taiwan-06	6.3	99999	CHY015
3260	0175	Chi-Chi, Taiwan-06	6.3	99999	CHY016
3261	0175	Chi-Chi, Taiwan-06	6.3	99999	CHY017
3262	0175	Chi-Chi, Taiwan-06	6.3	99999	CHY019
3263	0175	Chi-Chi, Taiwan-06	6.3	99999	CHY022
3264	0175	Chi-Chi, Taiwan-06	6.3	99999	CHY024
3265	0175	Chi-Chi, Taiwan-06	6.3	99999	CHY025
3266	0175	Chi-Chi, Taiwan-06	6.3	99999	CHY026
3267	0175	Chi-Chi, Taiwan-06	6.3	99999	CHY027
3268	0175	Chi-Chi, Taiwan-06	6.3	99999	CHY028
3269	0175	Chi-Chi, Taiwan-06	6.3	99999	CHY029
3270	0175	Chi-Chi, Taiwan-06	6.3	99999	CHY030
3271	0175	Chi-Chi, Taiwan-06	6.3	99999	CHY032
3272	0175	Chi-Chi, Taiwan-06	6.3	99999	CHY033
3273	0175	Chi-Chi, Taiwan-06	6.3	99999	CHY034

RSN	EQID	Earthquake	M	Station No,	Station
3274	0175	Chi-Chi, Taiwan-06	6.3	99999	CHY035
3275	0175	Chi-Chi, Taiwan-06	6.3	99999	CHY036
3276	0175	Chi-Chi, Taiwan-06	6.3	99999	CHY037
3277	0175	Chi-Chi, Taiwan-06	6.3	99999	CHY039
3278	0175	Chi-Chi, Taiwan-06	6.3	99999	CHY041
3279	0175	Chi-Chi, Taiwan-06	6.3	99999	CHY042
3280	0175	Chi-Chi, Taiwan-06	6.3	99999	CHY044
3281	0175	Chi-Chi, Taiwan-06	6.3	99999	CHY046
3282	0175	Chi-Chi, Taiwan-06	6.3	99999	CHY047
3283	0175	Chi-Chi, Taiwan-06	6.3	99999	CHY050
3284	0175	Chi-Chi, Taiwan-06	6.3	99999	CHY052
3285	0175	Chi-Chi, Taiwan-06	6.3	99999	CHY054
3286	0175	Chi-Chi, Taiwan-06	6.3	99999	CHY055
3287	0175	Chi-Chi, Taiwan-06	6.3	99999	CHY057
3288	0175	Chi-Chi, Taiwan-06	6.3	99999	CHY058
3289	0175	Chi-Chi, Taiwan-06	6.3	99999	CHY059
3290	0175	Chi-Chi, Taiwan-06	6.3	99999	CHY060
3291	0175	Chi-Chi, Taiwan-06	6.3	99999	CHY061
3292	0175	Chi-Chi, Taiwan-06	6.3	99999	CHY062
3293	0175	Chi-Chi, Taiwan-06	6.3	99999	CHY063
3294	0175	Chi-Chi, Taiwan-06	6.3	99999	CHY065
3295	0175	Chi-Chi, Taiwan-06	6.3	99999	CHY066
3296	0175	Chi-Chi, Taiwan-06	6.3	99999	CHY067
3297	0175	Chi-Chi, Taiwan-06	6.3	99999	CHY069
3298	0175	Chi-Chi, Taiwan-06	6.3	99999	CHY070
3299	0175	Chi-Chi, Taiwan-06	6.3	99999	CHY071
3300	0175	Chi-Chi, Taiwan-06	6.3	99999	CHY074
3301	0175	Chi-Chi, Taiwan-06	6.3	99999	CHY075
3302	0175	Chi-Chi, Taiwan-06	6.3	99999	CHY076
3303	0175	Chi-Chi, Taiwan-06	6.3	99999	CHY078
3304	0175	Chi-Chi, Taiwan-06	6.3	99999	CHY079
3305	0175	Chi-Chi, Taiwan-06	6.3	99999	CHY081
3306	0175	Chi-Chi, Taiwan-06	6.3	99999	CHY082
3307	0175	Chi-Chi, Taiwan-06	6.3	99999	CHY086
3308	0175	Chi-Chi, Taiwan-06	6.3	99999	CHY087
3309	0175	Chi-Chi, Taiwan-06	6.3	99999	CHY088
3310	0175	Chi-Chi, Taiwan-06	6.3	99999	CHY090
3311	0175	Chi-Chi, Taiwan-06	6.3	99999	CHY092
3312	0175	Chi-Chi, Taiwan-06	6.3	99999	CHY093
3313	0175	Chi-Chi, Taiwan-06	6.3	99999	CHY094
3314	0175	Chi-Chi, Taiwan-06	6.3	99999	CHY096
3315	0175	Chi-Chi, Taiwan-06	6.3	99999	CHY099
3316	0175	Chi-Chi, Taiwan-06	6.3	99999	CHY100
3317	0175	Chi-Chi, Taiwan-06	6.3	99999	CHY101
3318	0175	Chi-Chi, Taiwan-06	6.3	99999	CHY102
3319	0175	Chi-Chi, Taiwan-06	6.3	99999	CHY107
3320	0175	Chi-Chi, Taiwan-06	6.3	99999	CHY111
3321	0175	Chi-Chi, Taiwan-06	6.3	99999	CHY114
3322	0175	Chi-Chi, Taiwan-06	6.3	99999	CHY115
3323	0175	Chi-Chi, Taiwan-06	6.3	99999	CHY116
3324	0175	Chi-Chi, Taiwan-06	6.3	99999	HWA002
3325	0175	Chi-Chi, Taiwan-06	6.3	99999	HWA003
3326	0175	Chi-Chi, Taiwan-06	6.3	99999	HWA007
3327	0175	Chi-Chi, Taiwan-06	6.3	99999	HWA009
3328	0175	Chi-Chi, Taiwan-06	6.3	99999	HWA011
3329	0175	Chi-Chi, Taiwan-06	6.3	99999	HWA012
3330	0175	Chi-Chi, Taiwan-06	6.3	99999	HWA014
3331	0175	Chi-Chi, Taiwan-06	6.3	99999	HWA015
3332	0175	Chi-Chi, Taiwan-06	6.3	99999	HWA016
3333	0175	Chi-Chi, Taiwan-06	6.3	99999	HWA019
3334	0175	Chi-Chi, Taiwan-06	6.3	99999	HWA020
3335	0175	Chi-Chi, Taiwan-06	6.3	99999	HWA022
3336	0175	Chi-Chi, Taiwan-06	6.3	99999	HWA023
3337	0175	Chi-Chi, Taiwan-06	6.3	99999	HWA024
3338	0175	Chi-Chi, Taiwan-06	6.3	99999	HWA025
3339	0175	Chi-Chi, Taiwan-06	6.3	99999	HWA026
3340	0175	Chi-Chi, Taiwan-06	6.3	99999	HWA027
3341	0175	Chi-Chi, Taiwan-06	6.3	99999	HWA028
3342	0175	Chi-Chi, Taiwan-06	6.3	99999	HWA029

RSN	EQID	Earthquake	M	Station No,	Station
3343	0175	Chi-Chi, Taiwan-06	6.3	99999	HWA030
3344	0175	Chi-Chi, Taiwan-06	6.3	99999	HWA031
3345	0175	Chi-Chi, Taiwan-06	6.3	99999	HWA033
3346	0175	Chi-Chi, Taiwan-06	6.3	99999	HWA034
3347	0175	Chi-Chi, Taiwan-06	6.3	99999	HWA035
3348	0175	Chi-Chi, Taiwan-06	6.3	99999	HWA036
3349	0175	Chi-Chi, Taiwan-06	6.3	99999	HWA037
3350	0175	Chi-Chi, Taiwan-06	6.3	99999	HWA038
3351	0175	Chi-Chi, Taiwan-06	6.3	99999	HWA041
3352	0175	Chi-Chi, Taiwan-06	6.3	99999	HWA043
3353	0175	Chi-Chi, Taiwan-06	6.3	99999	HWA044
3354	0175	Chi-Chi, Taiwan-06	6.3	99999	HWA045
3355	0175	Chi-Chi, Taiwan-06	6.3	99999	HWA046
3356	0175	Chi-Chi, Taiwan-06	6.3	99999	HWA050
3357	0175	Chi-Chi, Taiwan-06	6.3	99999	HWA051
3358	0175	Chi-Chi, Taiwan-06	6.3	99999	HWA055
3359	0175	Chi-Chi, Taiwan-06	6.3	99999	HWA056
3360	0175	Chi-Chi, Taiwan-06	6.3	99999	HWA057
3361	0175	Chi-Chi, Taiwan-06	6.3	99999	HWA058
3362	0175	Chi-Chi, Taiwan-06	6.3	99999	HWA059
3363	0175	Chi-Chi, Taiwan-06	6.3	99999	HWA060
3365	0175	Chi-Chi, Taiwan-06	6.3	99999	ILA002
3366	0175	Chi-Chi, Taiwan-06	6.3	99999	ILA003
3367	0175	Chi-Chi, Taiwan-06	6.3	99999	ILA006
3368	0175	Chi-Chi, Taiwan-06	6.3	99999	ILA007
3369	0175	Chi-Chi, Taiwan-06	6.3	99999	ILA008
3370	0175	Chi-Chi, Taiwan-06	6.3	99999	ILA010
3371	0175	Chi-Chi, Taiwan-06	6.3	99999	ILA012
3372	0175	Chi-Chi, Taiwan-06	6.3	99999	ILA013
3373	0175	Chi-Chi, Taiwan-06	6.3	99999	ILA014
3374	0175	Chi-Chi, Taiwan-06	6.3	99999	ILA015
3375	0175	Chi-Chi, Taiwan-06	6.3	99999	ILA016
3376	0175	Chi-Chi, Taiwan-06	6.3	99999	ILA019
3377	0175	Chi-Chi, Taiwan-06	6.3	99999	ILA021
3378	0175	Chi-Chi, Taiwan-06	6.3	99999	ILA024
3379	0175	Chi-Chi, Taiwan-06	6.3	99999	ILA028
3380	0175	Chi-Chi, Taiwan-06	6.3	99999	ILA030
3381	0175	Chi-Chi, Taiwan-06	6.3	99999	ILA041
3382	0175	Chi-Chi, Taiwan-06	6.3	99999	ILA048
3383	0175	Chi-Chi, Taiwan-06	6.3	99999	ILA051
3384	0175	Chi-Chi, Taiwan-06	6.3	99999	ILA052
3385	0175	Chi-Chi, Taiwan-06	6.3	99999	ILA055
3386	0175	Chi-Chi, Taiwan-06	6.3	99999	ILA056
3387	0175	Chi-Chi, Taiwan-06	6.3	99999	ILA059
3388	0175	Chi-Chi, Taiwan-06	6.3	99999	ILA061
3389	0175	Chi-Chi, Taiwan-06	6.3	99999	ILA062
3390	0175	Chi-Chi, Taiwan-06	6.3	99999	ILA063
3391	0175	Chi-Chi, Taiwan-06	6.3	99999	ILA064
3392	0175	Chi-Chi, Taiwan-06	6.3	99999	ILA066
3393	0175	Chi-Chi, Taiwan-06	6.3	99999	KAU001
3394	0175	Chi-Chi, Taiwan-06	6.3	99999	KAU006
3395	0175	Chi-Chi, Taiwan-06	6.3	99999	KAU007
3396	0175	Chi-Chi, Taiwan-06	6.3	99999	KAU008
3397	0175	Chi-Chi, Taiwan-06	6.3	99999	KAU012
3398	0175	Chi-Chi, Taiwan-06	6.3	99999	KAU018
3399	0175	Chi-Chi, Taiwan-06	6.3	99999	KAU020
3400	0175	Chi-Chi, Taiwan-06	6.3	99999	KAU022
3401	0175	Chi-Chi, Taiwan-06	6.3	99999	KAU030
3402	0175	Chi-Chi, Taiwan-06	6.3	99999	KAU036
3403	0175	Chi-Chi, Taiwan-06	6.3	99999	KAU045
3404	0175	Chi-Chi, Taiwan-06	6.3	99999	KAU054
3405	0175	Chi-Chi, Taiwan-06	6.3	99999	KAU057
3406	0175	Chi-Chi, Taiwan-06	6.3	99999	KAU058
3407	0175	Chi-Chi, Taiwan-06	6.3	99999	KAU063
3408	0175	Chi-Chi, Taiwan-06	6.3	99999	KAU064
3409	0175	Chi-Chi, Taiwan-06	6.3	99999	KAU066
3410	0175	Chi-Chi, Taiwan-06	6.3	99999	KAU069
3411	0175	Chi-Chi, Taiwan-06	6.3	99999	KAU073
3412	0175	Chi-Chi, Taiwan-06	6.3	99999	KAU074

RSN	EQID	Earthquake	M	Station No,	Station
3413	0175	Chi-Chi, Taiwan-06	6.3	99999	KAU075
3414	0175	Chi-Chi, Taiwan-06	6.3	99999	KAU077
3415	0175	Chi-Chi, Taiwan-06	6.3	99999	KAU078
3416	0175	Chi-Chi, Taiwan-06	6.3	99999	KAU085
3417	0175	Chi-Chi, Taiwan-06	6.3	99999	KAU088
3418	0175	Chi-Chi, Taiwan-06	6.3	99999	TAP010
3419	0175	Chi-Chi, Taiwan-06	6.3	99999	TAP013
3420	0175	Chi-Chi, Taiwan-06	6.3	99999	TAP021
3421	0175	Chi-Chi, Taiwan-06	6.3	99999	TAP026
3422	0175	Chi-Chi, Taiwan-06	6.3	99999	TAP028
3423	0175	Chi-Chi, Taiwan-06	6.3	99999	TAP035
3424	0175	Chi-Chi, Taiwan-06	6.3	99999	TAP040
3425	0175	Chi-Chi, Taiwan-06	6.3	99999	TAP042
3426	0175	Chi-Chi, Taiwan-06	6.3	99999	TAP047
3427	0175	Chi-Chi, Taiwan-06	6.3	99999	TAP050
3428	0175	Chi-Chi, Taiwan-06	6.3	99999	TAP052
3429	0175	Chi-Chi, Taiwan-06	6.3	99999	TAP067
3430	0175	Chi-Chi, Taiwan-06	6.3	99999	TAP086
3431	0175	Chi-Chi, Taiwan-06	6.3	99999	TAP088
3432	0175	Chi-Chi, Taiwan-06	6.3	99999	TAP090
3433	0175	Chi-Chi, Taiwan-06	6.3	99999	TAP094
3434	0175	Chi-Chi, Taiwan-06	6.3	99999	TAP095
3435	0175	Chi-Chi, Taiwan-06	6.3	99999	TAP097
3436	0175	Chi-Chi, Taiwan-06	6.3	99999	TAP098
3437	0175	Chi-Chi, Taiwan-06	6.3	99999	TAP100
3439	0175	Chi-Chi, Taiwan-06	6.3	99999	TCU003
3440	0175	Chi-Chi, Taiwan-06	6.3	99999	TCU006
3441	0175	Chi-Chi, Taiwan-06	6.3	99999	TCU007
3442	0175	Chi-Chi, Taiwan-06	6.3	99999	TCU008
3443	0175	Chi-Chi, Taiwan-06	6.3	99999	TCU010
3444	0175	Chi-Chi, Taiwan-06	6.3	99999	TCU014
3445	0175	Chi-Chi, Taiwan-06	6.3	99999	TCU029
3446	0175	Chi-Chi, Taiwan-06	6.3	99999	TCU031
3447	0175	Chi-Chi, Taiwan-06	6.3	99999	TCU032
3448	0175	Chi-Chi, Taiwan-06	6.3	99999	TCU036
3449	0175	Chi-Chi, Taiwan-06	6.3	99999	TCU038
3450	0175	Chi-Chi, Taiwan-06	6.3	99999	TCU039
3451	0175	Chi-Chi, Taiwan-06	6.3	99999	TCU040
3452	0175	Chi-Chi, Taiwan-06	6.3	99999	TCU042
3453	0175	Chi-Chi, Taiwan-06	6.3	99999	TCU044
3454	0175	Chi-Chi, Taiwan-06	6.3	99999	TCU046
3455	0175	Chi-Chi, Taiwan-06	6.3	99999	TCU048
3456	0175	Chi-Chi, Taiwan-06	6.3	99999	TCU049
3457	0175	Chi-Chi, Taiwan-06	6.3	99999	TCU050
3458	0175	Chi-Chi, Taiwan-06	6.3	99999	TCU051
3459	0175	Chi-Chi, Taiwan-06	6.3	99999	TCU052
3460	0175	Chi-Chi, Taiwan-06	6.3	99999	TCU053
3461	0175	Chi-Chi, Taiwan-06	6.3	99999	TCU056
3462	0175	Chi-Chi, Taiwan-06	6.3	99999	TCU057
3463	0175	Chi-Chi, Taiwan-06	6.3	99999	TCU059
3464	0175	Chi-Chi, Taiwan-06	6.3	99999	TCU060
3465	0175	Chi-Chi, Taiwan-06	6.3	99999	TCU061
3466	0175	Chi-Chi, Taiwan-06	6.3	99999	TCU064
3467	0175	Chi-Chi, Taiwan-06	6.3	99999	TCU065
3468	0175	Chi-Chi, Taiwan-06	6.3	99999	TCU067
3469	0175	Chi-Chi, Taiwan-06	6.3	99999	TCU068
3470	0175	Chi-Chi, Taiwan-06	6.3	99999	TCU072
3471	0175	Chi-Chi, Taiwan-06	6.3	99999	TCU075
3472	0175	Chi-Chi, Taiwan-06	6.3	99999	TCU076
3473	0175	Chi-Chi, Taiwan-06	6.3	99999	TCU078
3474	0175	Chi-Chi, Taiwan-06	6.3	99999	TCU079
3475	0175	Chi-Chi, Taiwan-06	6.3	99999	TCU080
3477	0175	Chi-Chi, Taiwan-06	6.3	99999	TCU082
3478	0175	Chi-Chi, Taiwan-06	6.3	99999	TCU083
3479	0175	Chi-Chi, Taiwan-06	6.3	99999	TCU085
3480	0175	Chi-Chi, Taiwan-06	6.3	99999	TCU086
3481	0175	Chi-Chi, Taiwan-06	6.3	99999	TCU087
3482	0175	Chi-Chi, Taiwan-06	6.3	99999	TCU091
3483	0175	Chi-Chi, Taiwan-06	6.3	99999	TCU092

RSN	EQID	Earthquake	M	Station No,	Station
3484	0175	Chi-Chi, Taiwan-06	6.3	99999	TCU094
3485	0175	Chi-Chi, Taiwan-06	6.3	99999	TCU095
3486	0175	Chi-Chi, Taiwan-06	6.3	99999	TCU096
3487	0175	Chi-Chi, Taiwan-06	6.3	99999	TCU098
3488	0175	Chi-Chi, Taiwan-06	6.3	99999	TCU100
3489	0175	Chi-Chi, Taiwan-06	6.3	99999	TCU102
3490	0175	Chi-Chi, Taiwan-06	6.3	99999	TCU103
3491	0175	Chi-Chi, Taiwan-06	6.3	99999	TCU104
3492	0175	Chi-Chi, Taiwan-06	6.3	99999	TCU105
3493	0175	Chi-Chi, Taiwan-06	6.3	99999	TCU107
3494	0175	Chi-Chi, Taiwan-06	6.3	99999	TCU108
3495	0175	Chi-Chi, Taiwan-06	6.3	99999	TCU109
3496	0175	Chi-Chi, Taiwan-06	6.3	99999	TCU110
3497	0175	Chi-Chi, Taiwan-06	6.3	99999	TCU112
3498	0175	Chi-Chi, Taiwan-06	6.3	99999	TCU113
3499	0175	Chi-Chi, Taiwan-06	6.3	99999	TCU115
3500	0175	Chi-Chi, Taiwan-06	6.3	99999	TCU118
3501	0175	Chi-Chi, Taiwan-06	6.3	99999	TCU119
3502	0175	Chi-Chi, Taiwan-06	6.3	99999	TCU120
3503	0175	Chi-Chi, Taiwan-06	6.3	99999	TCU122
3504	0175	Chi-Chi, Taiwan-06	6.3	99999	TCU123
3505	0175	Chi-Chi, Taiwan-06	6.3	99999	TCU125
3506	0175	Chi-Chi, Taiwan-06	6.3	99999	TCU128
3507	0175	Chi-Chi, Taiwan-06	6.3	9999936	TCU129
3508	0175	Chi-Chi, Taiwan-06	6.3	99999	TCU136
3509	0175	Chi-Chi, Taiwan-06	6.3	99999	TCU138
3510	0175	Chi-Chi, Taiwan-06	6.3	99999	TCU139
3511	0175	Chi-Chi, Taiwan-06	6.3	99999	TCU140
3512	0175	Chi-Chi, Taiwan-06	6.3	99999	TCU141
3513	0175	Chi-Chi, Taiwan-06	6.3	99999	TCU145
3514	0175	Chi-Chi, Taiwan-06	6.3	99999	TCU147
3515	0175	Chi-Chi, Taiwan-06	6.3	99999	TTN001
3516	0175	Chi-Chi, Taiwan-06	6.3	99999	TTN002
3517	0175	Chi-Chi, Taiwan-06	6.3	99999	TTN003
3518	0175	Chi-Chi, Taiwan-06	6.3	99999	TTN004
3519	0175	Chi-Chi, Taiwan-06	6.3	99999	TTN005
3520	0175	Chi-Chi, Taiwan-06	6.3	99999	TTN006
3521	0175	Chi-Chi, Taiwan-06	6.3	99999	TTN007
3522	0175	Chi-Chi, Taiwan-06	6.3	99999	TTN008
3523	0175	Chi-Chi, Taiwan-06	6.3	99999	TTN009
3524	0175	Chi-Chi, Taiwan-06	6.3	99999	TTN012
3525	0175	Chi-Chi, Taiwan-06	6.3	99999	TTN014
3526	0175	Chi-Chi, Taiwan-06	6.3	99999	TTN015
3527	0175	Chi-Chi, Taiwan-06	6.3	99999	TTN018
3528	0175	Chi-Chi, Taiwan-06	6.3	99999	TTN020
3529	0175	Chi-Chi, Taiwan-06	6.3	99999	TTN022
3530	0175	Chi-Chi, Taiwan-06	6.3	99999	TTN023
3531	0175	Chi-Chi, Taiwan-06	6.3	99999	TTN024
3532	0175	Chi-Chi, Taiwan-06	6.3	99999	TTN025
3533	0175	Chi-Chi, Taiwan-06	6.3	99999	TTN026
3534	0175	Chi-Chi, Taiwan-06	6.3	99999	TTN027
3535	0175	Chi-Chi, Taiwan-06	6.3	99999	TTN028
3536	0175	Chi-Chi, Taiwan-06	6.3	99999	TTN031
3537	0175	Chi-Chi, Taiwan-06	6.3	99999	TTN032
3538	0175	Chi-Chi, Taiwan-06	6.3	99999	TTN033
3539	0175	Chi-Chi, Taiwan-06	6.3	99999	TTN036
3540	0175	Chi-Chi, Taiwan-06	6.3	99999	TTN040
3541	0175	Chi-Chi, Taiwan-06	6.3	99999	TTN041
3542	0175	Chi-Chi, Taiwan-06	6.3	99999	TTN042
3543	0175	Chi-Chi, Taiwan-06	6.3	99999	TTN044
3544	0175	Chi-Chi, Taiwan-06	6.3	99999	TTN045
3545	0175	Chi-Chi, Taiwan-06	6.3	99999	TTN046

Appendix B
Estimation of Distance and Geometry Measures for Earthquakes without Finite Rupture Models

Approach

There are 110 earthquakes in the NGA data set that do not have finite fault models, and therefore have only epicentral and hypocentral distances listed in the flat file. Rupture distances and source-site geometry parameters were estimated for the recordings from these earthquakes by simulating 101 possible rupture planes for each earthquake, computing the distance measures for each site for each simulation, and then taking the median of these values for use in completing the metadata in the PEER-NGA data base. The estimated parameters include R_{RUP}, R_{JB}, R_{SEIS}, R_{RMS}, the source=site angle θ_{SITE}, the hanging wall and foot wall indicators F_{HW} and F_{FW}, and the fault rupture width W and depth to top of rupture, Z_{TOR}.

Simulation Process

The first step was to simulate the fault rupture dimensions. The rupture area, A, was simulated using the Wells and Coppersmith (1994) relationship for all fault types:

$$\log(A) = -3.49 + 0.91\mathbf{M} \quad \sigma_{\log(Area)} = 0.24 \qquad \textbf{(B-1)}$$

Figure B-1 shows the data for rupture area versus **M** for the finite rupture models in the PEER-NGA database. The black lines show a linear fit to the data (solid = mean, dashed = 90% confidence on mean). The blue line is Wells and Coppersmith (1994), which falls within the 90% confidence interval and provides a closer fit to the data for smaller magnitude earthquakes of primary interest in the simulation, as those earthquakes without finite fault models are principally of magnitude < **M** 6.

The aspect ratio of the rupture was then simulated using the relationship:

$$\log(AR) = (0.01752 - 0.00472F_{NM} - 0.01099F_{RV}) * (\mathbf{M} - 4)^{3.097} \quad \sigma_{\log(AR)} = 0.16 \qquad \textbf{(B-2)}$$

where F_{NM} and F_{RV} are (0,1) dummy variables for normal and revere earthquakes, respectively. This relationship was defined by fitting the aspect ratio data for the PEER-NGA finite fault model data set (Figure B-2). Correlation in the residuals between rupture area and aspect ratio was low (<0.3) and it was assumed that they were independent in the simulation.

Using the simulated values of A and AR, the rupture width W and rupture length L were computed assuming a rectangular fault rupture.

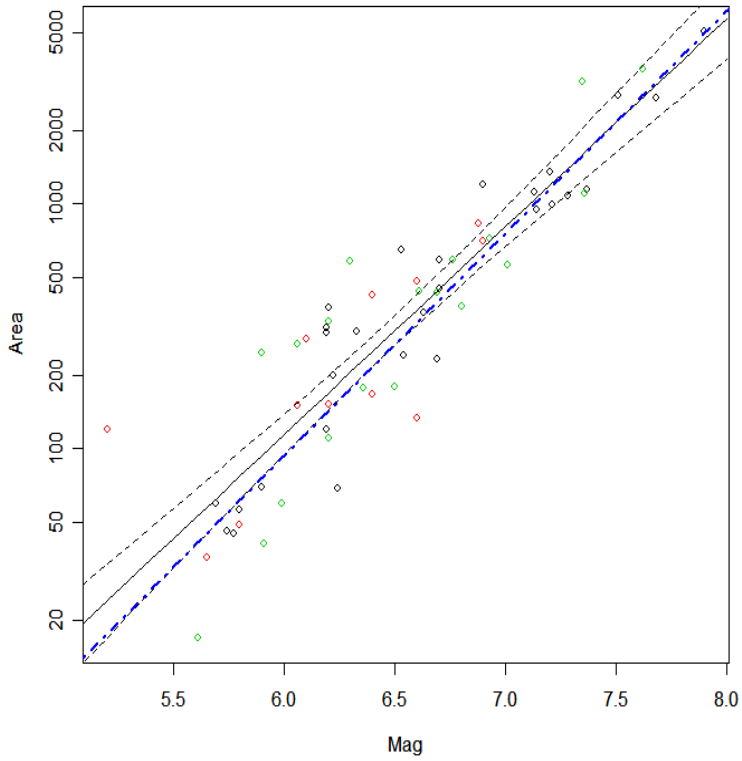

Figure B-1: Data for rupture area versus **M** from PEER-NGA finite fault model set. Symbol color denotes faulting style (black SS, red NM, and green RV). Black lines show fit and 90% confidence interval for fit to data. Blue dash-dot line shows Wells and Coppersmith (1994) relationship for all slip types.

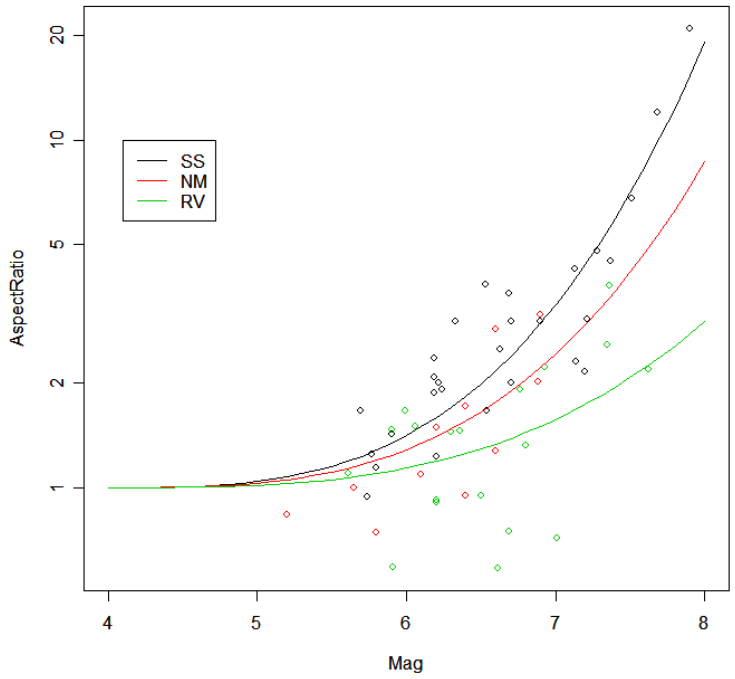

Figure B-2: Data for aspect ratio versus **M** from PEER-NGA finite fault model set. Symbol color denotes faulting style (black SS, red NM, and green RV).

The next step was to locate the rupture plane in space. The vertical location of the simulated rupture with respect to the hypocenter was simulated using empirical distributions for hypocenter location derived from the PEER-NGA set of rupture models. The observed and smoothed empirical distributions are shown in Figure B-3. If the top of the simulated rupture plane extended above 0 depth, it was placed at 0 depth. The rupture plane dip was fixed at the value assigned to the earthquake.

The location of the hypocenter along strike was simulated using data from Mai et al. (2005) for earthquakes $\leq$ **M** 6.5. This distribution is shown in Figure B-4.

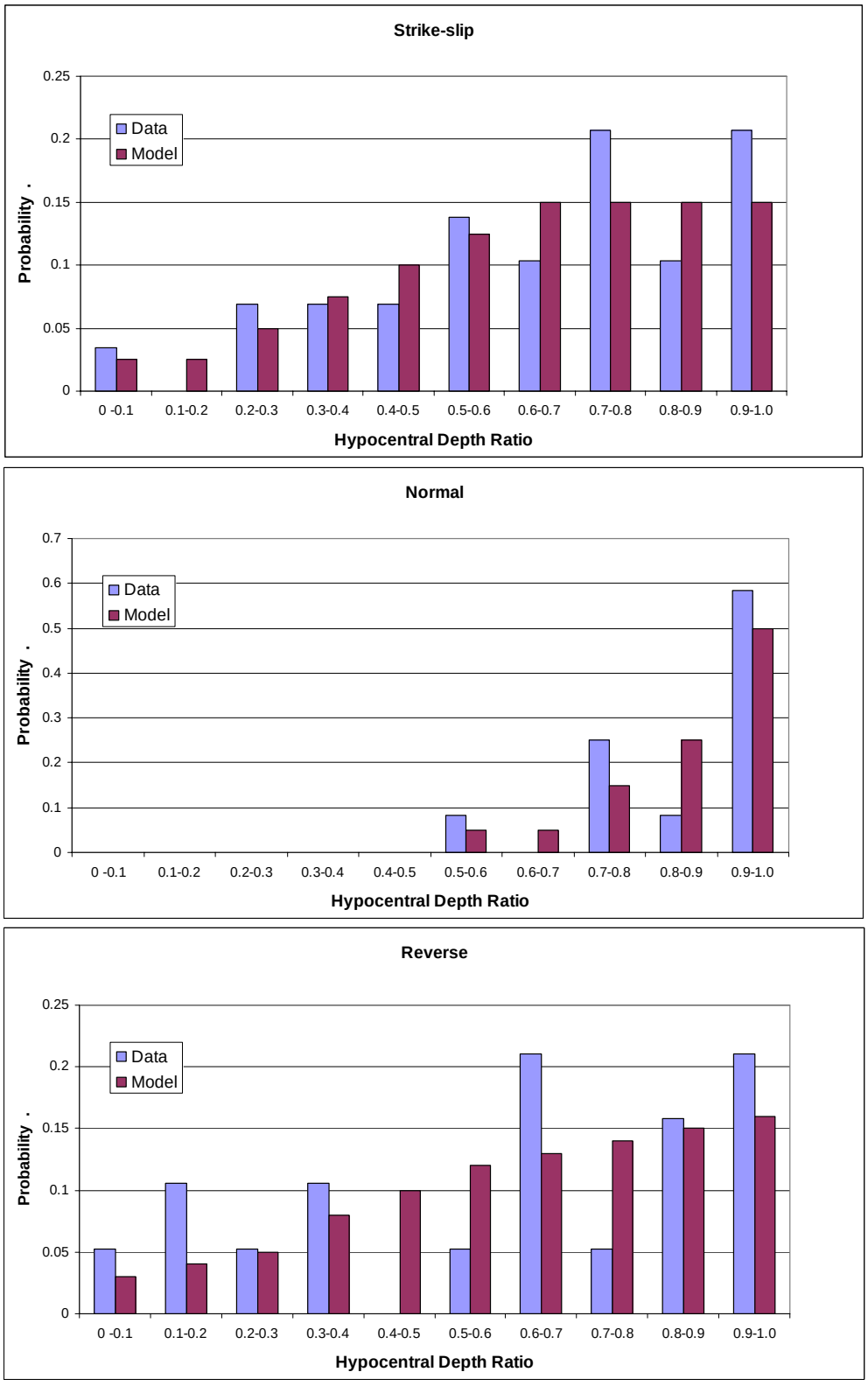

Figure B-3: Empirical distributions for vertical location of hypocenter in rupture plane derived from the PEER-NGA rupture model data set ("Data") and smoothed for use in simulations ("Model").

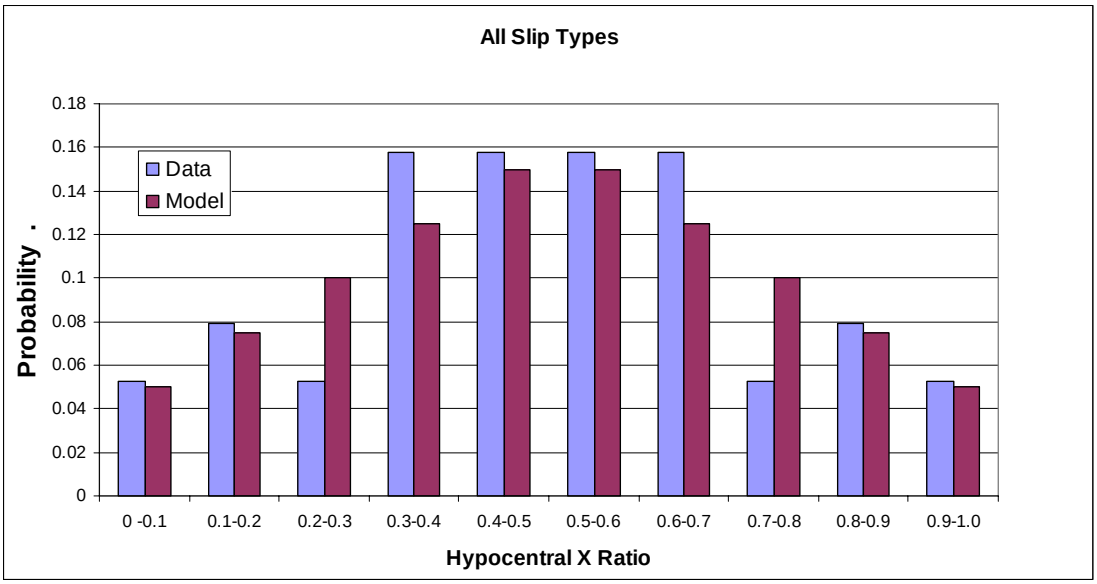

Figure B-4: Distributions for horizontal location of hypocenter in rupture plane derived from data for **M** ≤ 6.5 earthquakes presented in Mai et al. (2005) ("Data") and smoothed for use in simulations ("Model").

For each simulated rupture plane, the distance to all sites was computed in terms of R_{JB}, R_{SEIS} (assuming a minimum seismogenic depth of 3 km), R_{RMS} distance, and closest distance to rupture, R_{RUP}. The depth to top of rupture, Z_{TOR} and the source-site angle were also computed.

The values selected for use were the median values for each site from the 101 simulations. The median was chosen because most of the values enter regressions as logs.

Figure 3 in the main text shows the ratio of the estimated values of Joyner-Boore distance to the epicentral distance and the ratio of the estimated rupture distance to hypocentral distance for the 702 sites associated with the 110 earthquakes analyzed.

Ken Campbell provided the distances he obtained for the 1992 Big Bear **M** 6.46 earthquake based on a rupture model he developed for that event. Figure B-5 compares his estimates of R_{JB} and R_{RUP} to those obtained from this exercise. The values are close, indicating that the process provides reasonable estimates of rupture distance measures

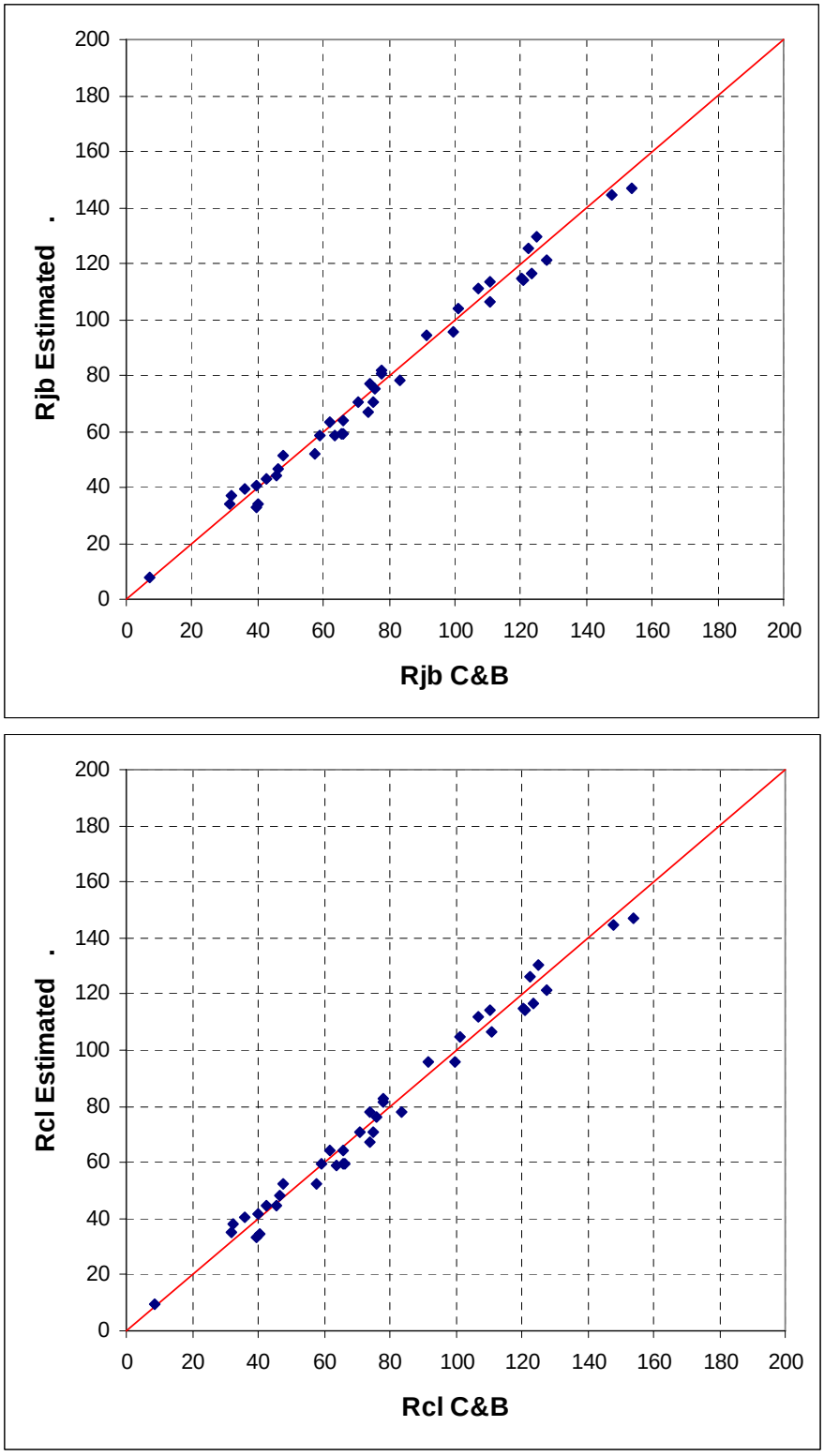

Figure B-5: Comparison of estimated Joyner-Boore distances (R_{JB}) closest distance to rupture (R_{RUP}) obtained in this analysis to those obtained by Ken Campbell and used in Campbell and Bozorgnia (2003).

Appendix C
Estimation of Vs_{30} *at* CWB's Free-Field Sites

Brian Chiou and K.L. Wen

(June 08, 2006)

Introduction

When Vs_{30} measurement is missing, an estimate is typically calculated using an empirical relationship between Vs_{30} and other site data, such as surface geology or Geomatrix's 3rd letter (C_3). This approach is used in the PEER-NGA project and has also been widely used in California (Wills and Silva, 1998; Wills and others, 2000; Wills and Clahan, 2004) and other regions. This short note reports our efforts to establish empirical Vs_{30} - C_3 relationships for strong-motion sites in Taiwan. The Taiwan-specific relationship uses C_3 as the main predictor. It also uses station elevation to capture the within-category variation of Vs_{30}. The use of elevation as a predictor leads to a significant improvement of mapping accuracy within a site category, particularly within Geomatrix's category D.

Data

Vs_{30} data used in this study are derived from the P-S logging provided to the PEER-NGA project by NCREE, who manage the site investigation of strong-motion stations operated by CWB in Taiwan[1]. During the period of 2000 - 2004 a total of 231 holes were drilled and logged. The site investigation project is still on going and more P-S logging data will become available in the next several years.

Dr. Walt Silva (PE&A) reviewed the P-S logging data from each of the 231 holes, smoothed the velocity profile, and computed Vs_{30} from the smoothed profile. We selected 165 sites for use in our study. The remaining 66 strong-motion sites were not used because either the drill hole is less than 20 m deep or a Geomatrix C_3 classification has not been assigned yet.

Other site data are also collected. They include: (1). Geomatrix's 2nd and 3rd letters (D. Wells, pers. comm., 2004); (2) The site classification (PSC) by Lee et al. (2001); and (3) Station elevation (Lee et al., 2001).

Variation of Vs_{30} within a Site Category

Histogram of the 165 Vs_{30} data, grouped by C_3, is shown in Figure C-1. This figure highlights two difficulties in using C_3 to map Vs_{30} in Taiwan. First, categories A, B, and C are not distinguishable by Vs_{30}. Secondly, the most populous category (D) is bimodal with a large Vs_{30} variation within that category. The active tectonic in Taiwan leads to a strong correlation between elevation and geology (Lee et al., 2001). The higher the elevation the stiffer the surface material tends to be. This unique feature prompts us to explore if elevation could be used to explain the large Vs_{30} variation in category D. Vs_{30}

[1] Plots of the drilling logs can be viewed on CWB website at http://www.cwb.gov.tw/V4/index.htm.

data are plotted as a function of station elevation in Figure C-2. Except for a few outliers, the correlation of Vs_{30} with elevation is clearly shown, particularly within Geomatrix-D category. The bimodal distribution observed in Figures 1 can be adequately modeled by the station elevation.

Mapping Vs_{30} by C_3 and Elevation

Based on the trend noted in Figure C-2, the following functional form is selected to model Vs_{30} as a function of station elevation (*Elv*, in meters),

$$ln(Vs_{30}) = ln(\phi_1) + \frac{ln(\phi_2) - ln(\phi_1)}{1 + e^{(ln(\phi_3) - ln(Elv))/\phi_4}}.$$

Interpretations of the unknown coefficients are as followed: ϕ_1 and ϕ_2 are the asymptotic Vs_{30} as the elevation approaches 0 and ∞, respectively; at the elevation of ϕ_3 meters, Vs_{30} is the (geometric) average of the two asymptotes.

The above model was used to fit Vs_{30} data in each of the five Geomatrix categories. The estimated coefficients (ϕ_i, *i=1, 4*) are listed in Table C-1 and the fitted curves are shown on the left hand plot in Figure C-3.

To show the difference between this mapping scheme and that used in California, Vs_{30} estimates of the non-measurement sites are plotted in the right panel of Figure C-3. The solid lines are Vs_{30} mapped by the new model; circles are Vs_{30} mapped by California's model (Silva, 2004; see Note #34 in the site file NGA_Site_V017.XLS). In most cases the difference is not large. The larger difference occurs in Geomatrix-D category at elevation higher than 70m, as expected.

REFERENCES:

Lee, C.T., Cheng, C.T., Liao, C.W., and Tsai, T.B., 2001, Site classfication of Taiwan free-field strong-motion stations: *Bulletin of the Seismological Society of America*, v. 91, no. 5, p 1283-1297.

Wills, C.J., Petersen, M.D., Bryant, W.A., Reichle, M.S., Saucedo, G.J., Tan, S.S, Taylor, G.C, and Treiman J.A., 2000, A site conditions map for California based on geology and shear wave velocity: *Bulletin of the Seismological Society of America*, v. 90, no. 6b, p S187-S208.

Wills, C.J. and Silva, W., 1998, Shear wave velocity characteristics of geologic units in California: *Earthquake Spectra*, v. 14, p. 533-556.

Wills C.J. and Clahan K., 2005, NGA site condition metadata from geology, report to PEER-LL, 2005.

Table C-1. Estimated Coefficients.

Geomatrix 3rd Letter	ϕ_1	ϕ_2	ϕ_3	ϕ_4	σ	Number of Data Points
A	552	680[1]	244	0.1154	0.3174	15
B	418	579	107.1	0.3850	0.2294	35
C	-	-	-	-	-	4[2]
D	228	509	39.4	0.373	0.2953	91
E	201	405	38.2	0.087	0.1810	18
					Total = 163 [3]	

1: This parameter is fixed by judgment.
2: There is insufficient number of data to derive a relationship. To estimate Vs30 of category C site, one could use the relationship for category D.
3: Two data points in Geomtrix-B category were removed.

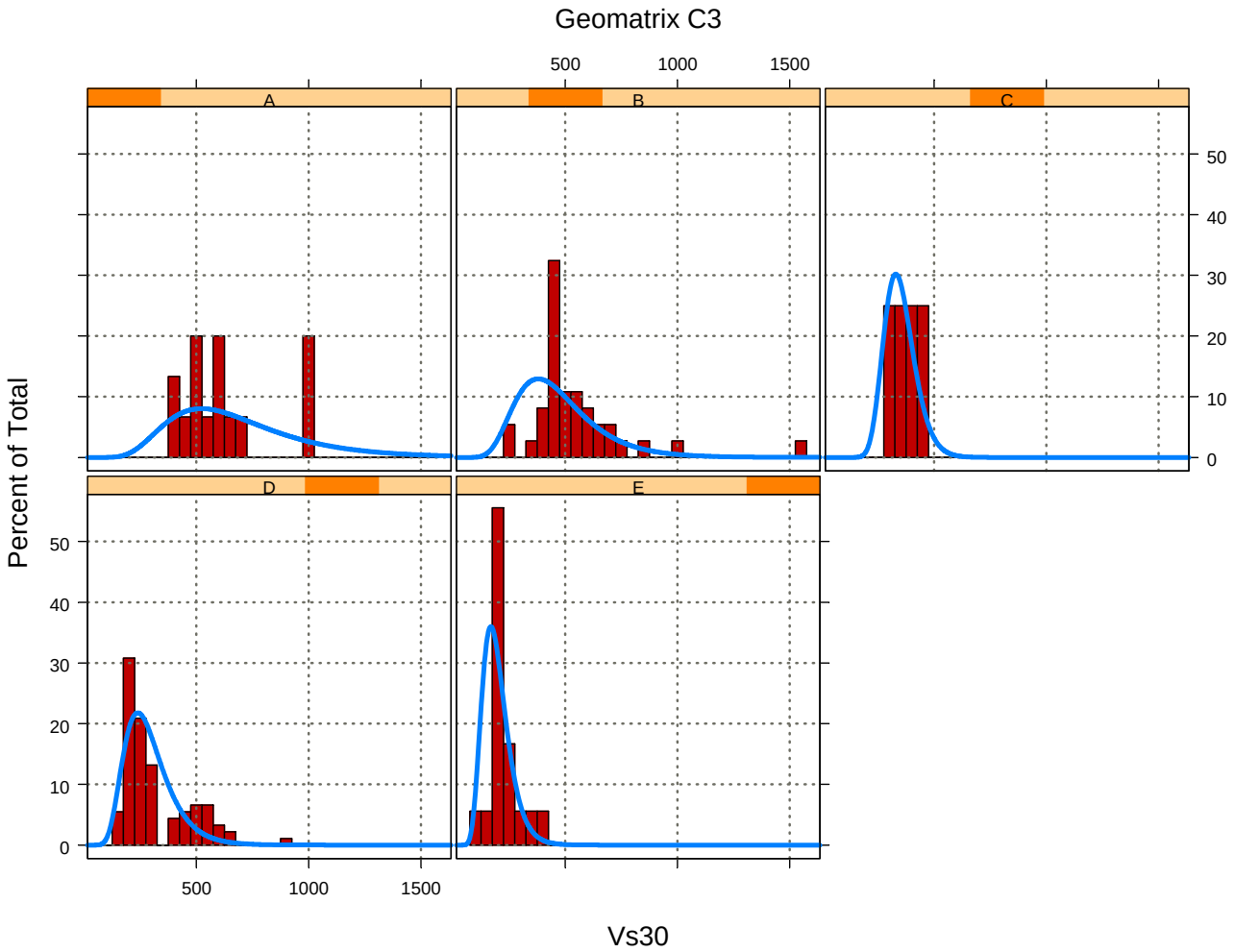

Figure C-1. Histogram of measured Vs_{30} grouped by Geomatrix's 3rd letter C_3. The thick blue line is the Vs_{30} distribution model of California data (Silva, 2004)

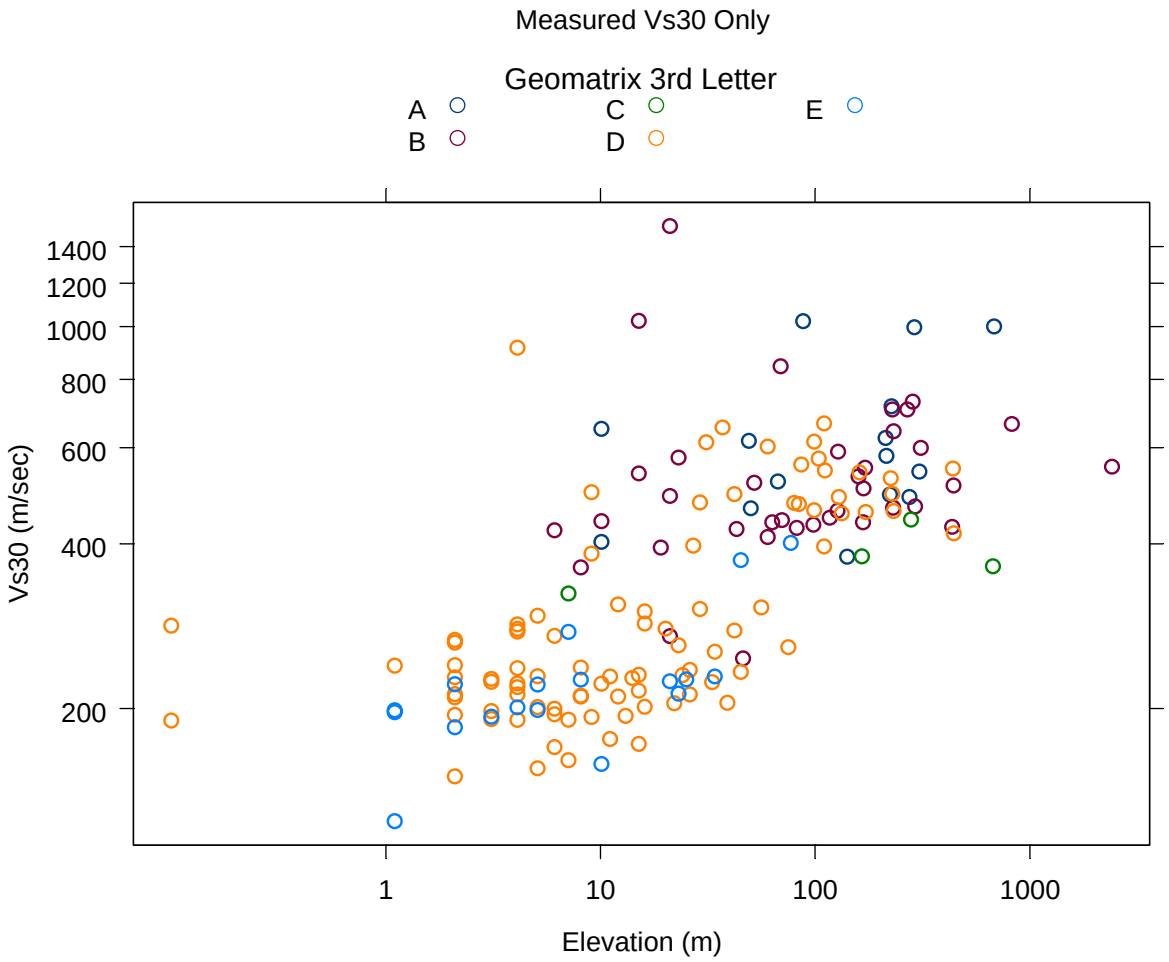

Figure C-2. Measured Vs_{30} as a function of station elevation (in meters).

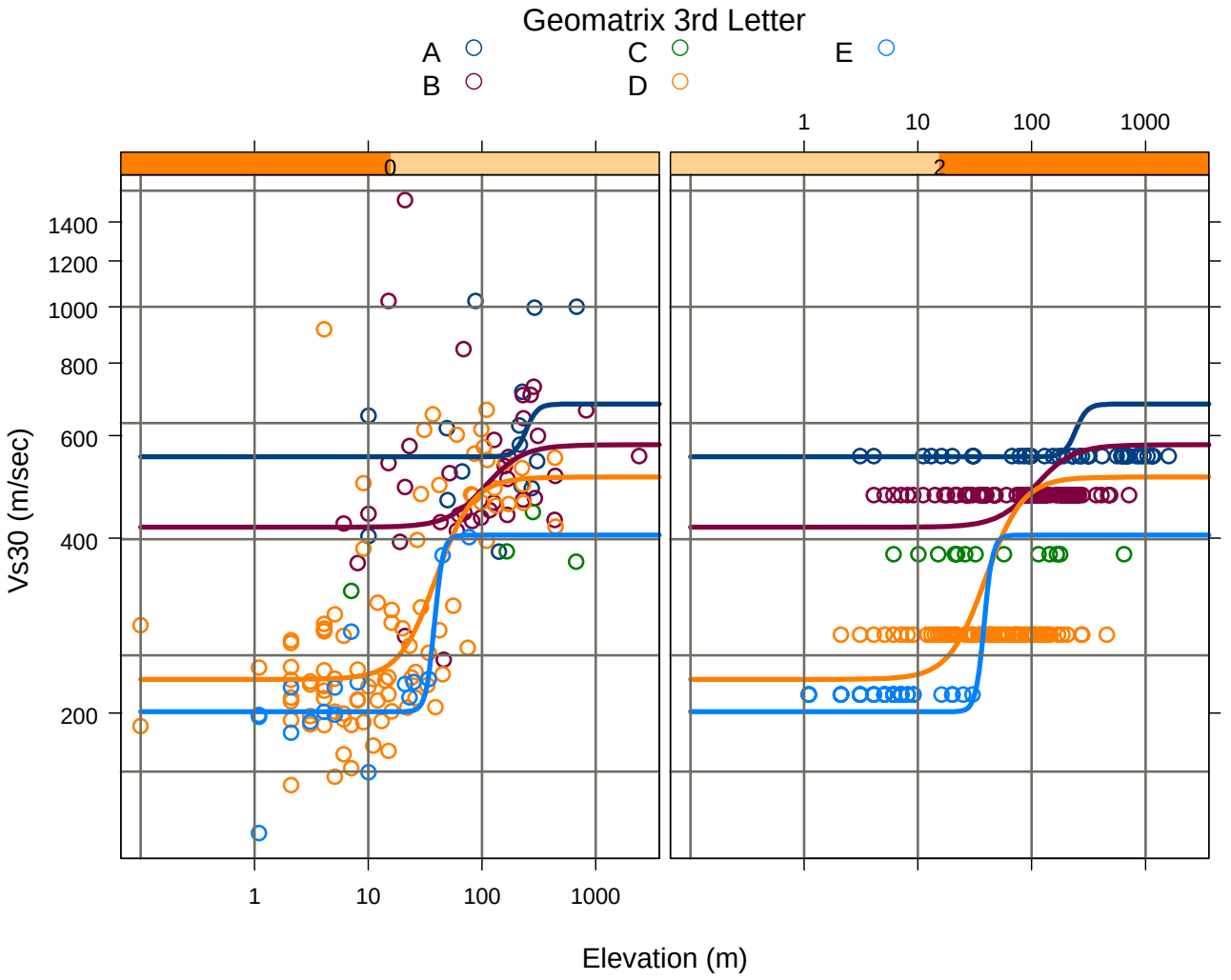

Figure C-3. (Left) Measured Vs_{30} data and the fits to them. (Right) Comparison of Vs_{30} mapped by two different approaches. Solid lines are Vs_{30} mapped by the model developed in this study; circles are Vs_{30} mapped by California model.

Appendix D
Processing and Model Fits to TriNet/ShakeMap Data
(Incomplete)

Dataset

Ground-motion dataset used in this analysis was compiled by USGS (Boatwright, per. communication) from the TriNet. It includes PGA (in units of %g) and PGV (in units of cm/sec) from 252 earthquakes (Figure D-1). Since only the larger of the tow horizontal components is provided, we divide the listed PGA value by 1.13 to adjust the value down to the expected level of average horizontal component. A subset of 102 events are selected and used in the analysis; see below for description of selection criteria. Epicenter location, focal depth, and local magnitude M_L of each earthquake are from the SCSN catalog. Moment magnitude (M_w) is based on the moment tensor solution catalog, also from SCSN.

Since most earthquakes are small in size and therefore without a finite source model, rupture distance is imputed using the same procedure as documented in Appedix ?. For site conditions, we used the Vs_{30} value in the NGA database or estimated it using the same correlation between Vs_{30} and geological unit as was used in NGA. The geological unit at the station coordinate is provided by Chris Wills using the recently refined CGS site-conditions map (Wills et al., 2005). For stations without geological unit and NGA Vs_{30}, we used the site category given in the USGS data file (column 'C') to estimate Vs_{30} using Table ? in Wills et al. (2001?):

C=1, Vs_{30} = 674 (m/sec)
C=2, Vs_{30} = 423 (m/sec)
C=3, Vs_{30} = 281 (m/sec)
C=4, Vs_{30} = 165 (m/sec).

Selection of Data Subset

When earthquake epicenter is outside or near the boundary of the strong-motion station network the majority of the recording stations often lie in a limited distance range. Such earthquakes are removed because they are not very useful to the characterization of distance attenuation. The removed earthquakes are plotted as blue circles in Figure 1.

Furthermore, the quality of PGA data degrades as distance increases. Because of the large number of records a full quality control is not feasible. Instead, we removed PGA from beyond the cutoff distance of 130 * (M-2) (km), slightly more generous than the cutoff distance of 100 * (M-2) (km) recommended by Boatwright et al. (2003) for northern California earthquakes. We also removed data that are obviously in errors. The final subset includes 102 earthquakes, ranging in magnitude from 3.39 to 5.17, and 9060 PGA data, with values ranging from 0.0007 to 24.5 (%g).

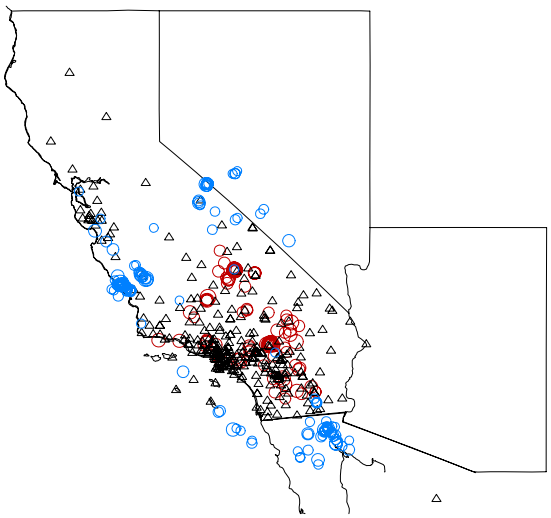

Figure D-1. Epicenter distribution of the TriNet data.

Following this figure are plots of the *pga* values for the individual earthquakes. The dashed line on each figure is the global model developed in this study and the solid line is the event-specific fit.

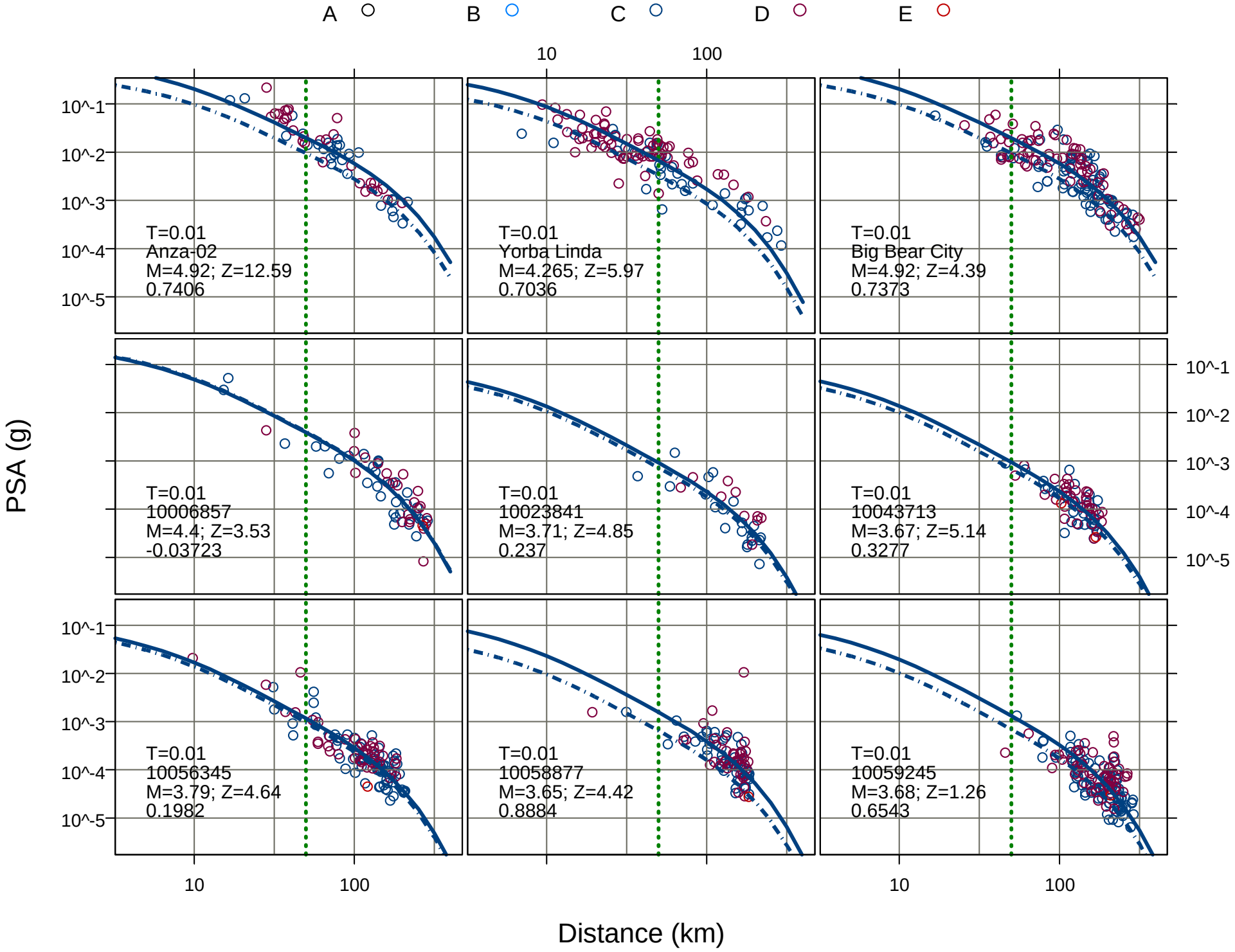
A
B
C
D
E
10
100
10^-1
10^-2
10^-3
10^-4
10^-5
T=0.01
Anza-02
M=4.92; Z=12.59
0.7406
T=0.01
Yorba Linda
M=4.265; Z=5.97
0.7036
T=0.01
Big Bear City
M=4.92; Z=4.39
0.7373
T=0.01
10006857
M=4.4; Z=3.53
-0.03723
T=0.01
10023841
M=3.71; Z=4.85
0.237
T=0.01
10043713
M=3.67; Z=5.14
0.3277
T=0.01
10056345
M=3.79; Z=4.64
0.1982
T=0.01
10058877
M=3.65; Z=4.42
0.8884
T=0.01
10059245
M=3.68; Z=1.26
0.6543
PSA (g)
Distance (km)

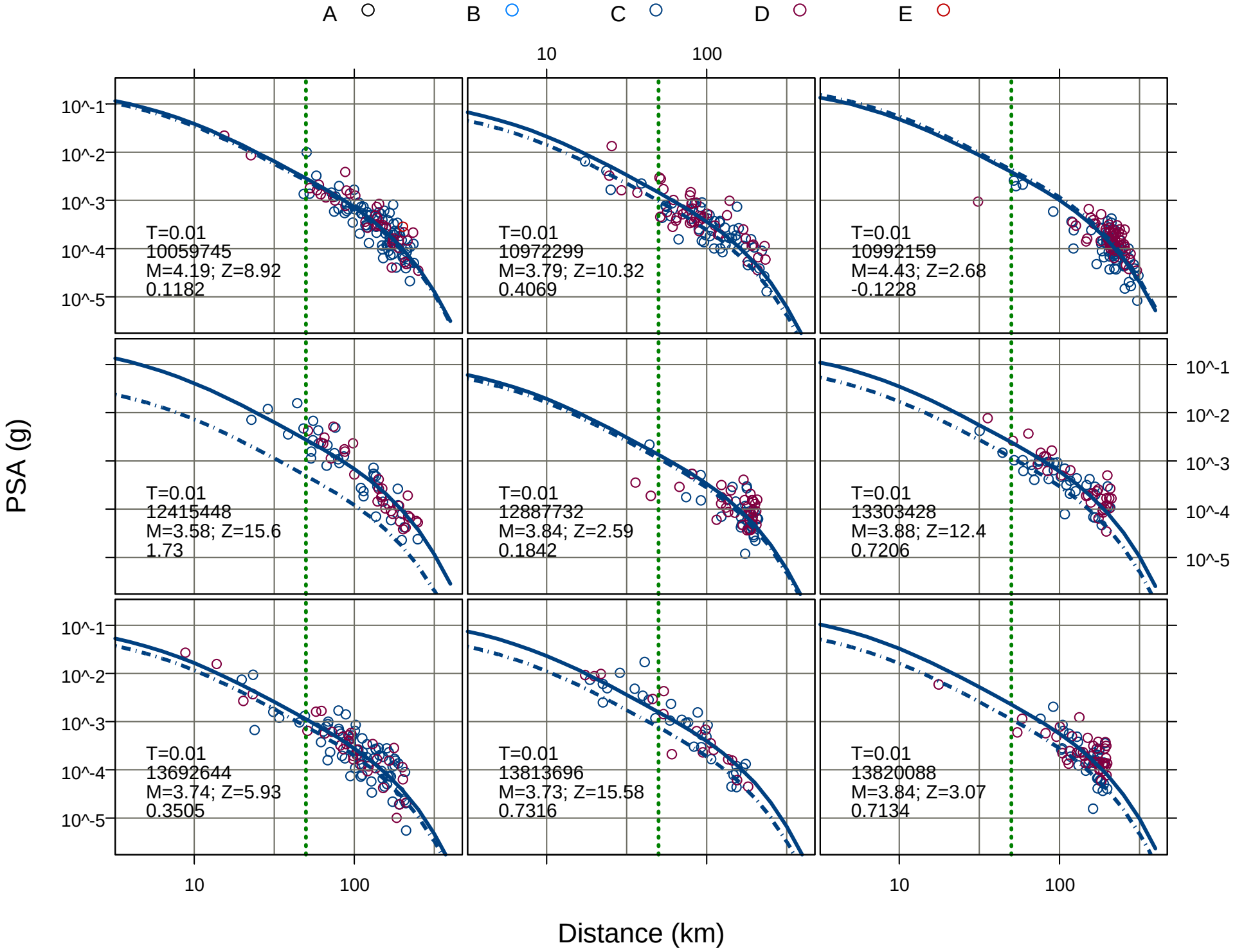
A
B
C
D
E
10
100
10^-1
10^-2
10^-3
10^-4
10^-5
T=0.01
10059745
M=4.19; Z=8.92
0.1182
T=0.01
10972299
M=3.79; Z=10.32
0.4069
T=0.01
10992159
M=4.43; Z=2.68
-0.1228
T=0.01
12415448
M=3.58; Z=15.6
1.73
T=0.01
12887732
M=3.84; Z=2.59
0.1842
T=0.01
13303428
M=3.88; Z=12.4
0.7206
T=0.01
13692644
M=3.74; Z=5.93
0.3505
T=0.01
13813696
M=3.73; Z=15.58
0.7316
T=0.01
13820088
M=3.84; Z=3.07
0.7134
PSA (g)
Distance (km)

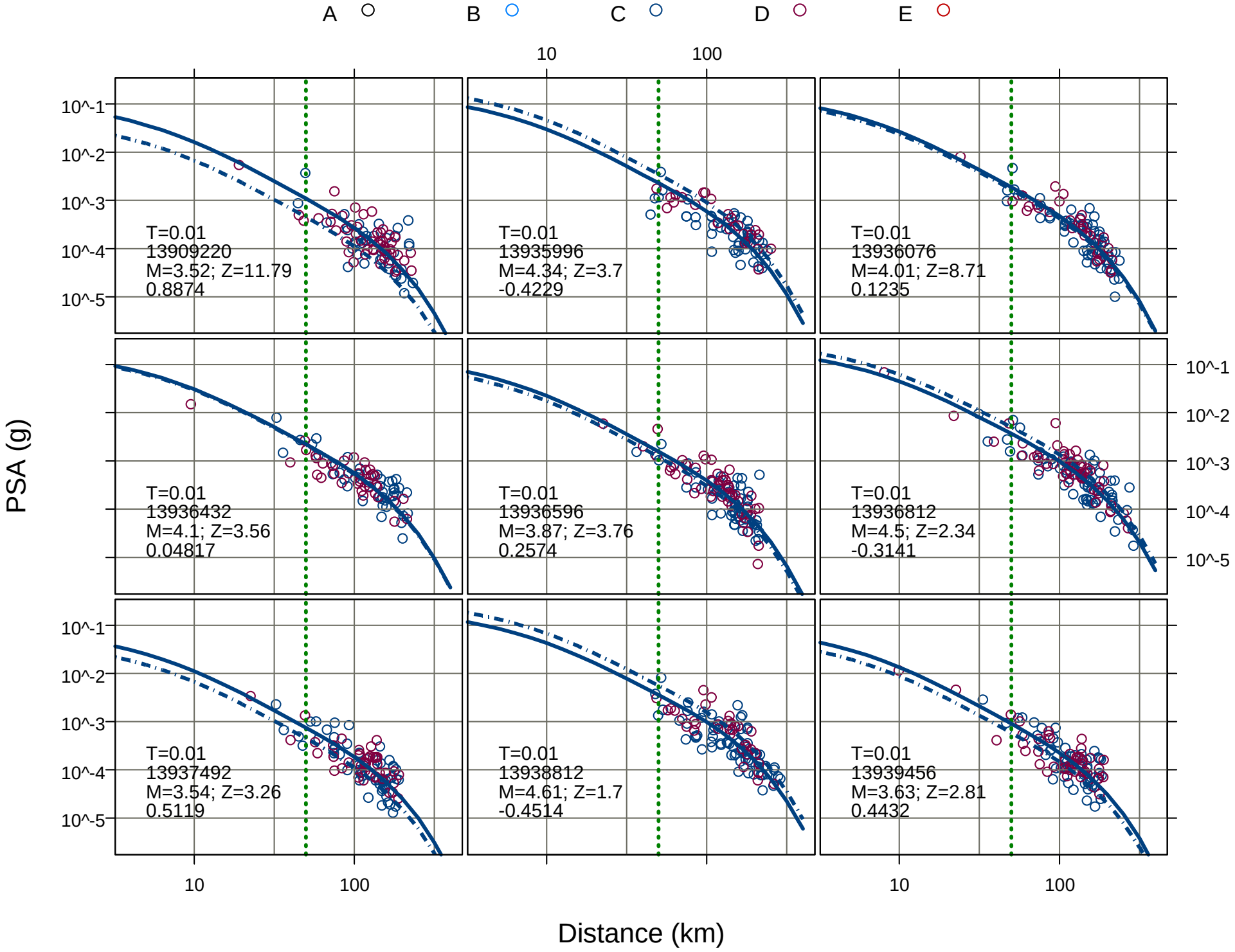
A
B
C
D
E
10
100
10^-1
10^-2
10^-3
10^-4
10^-5
T=0.01
13909220
M=3.52; Z=11.79
0.8874
T=0.01
13935996
M=4.34; Z=3.7
-0.4229
T=0.01
13936076
M=4.01; Z=8.71
0.1235
T=0.01
13936432
M=4.1; Z=3.56
0.04817
T=0.01
13936596
M=3.87; Z=3.76
0.2574
T=0.01
13936812
M=4.5; Z=2.34
-0.3141
T=0.01
13937492
M=3.54; Z=3.26
0.5119
T=0.01
13938812
M=4.61; Z=1.7
-0.4514
T=0.01
13939456
M=3.63; Z=2.81
0.4432
PSA (g)
Distance (km)

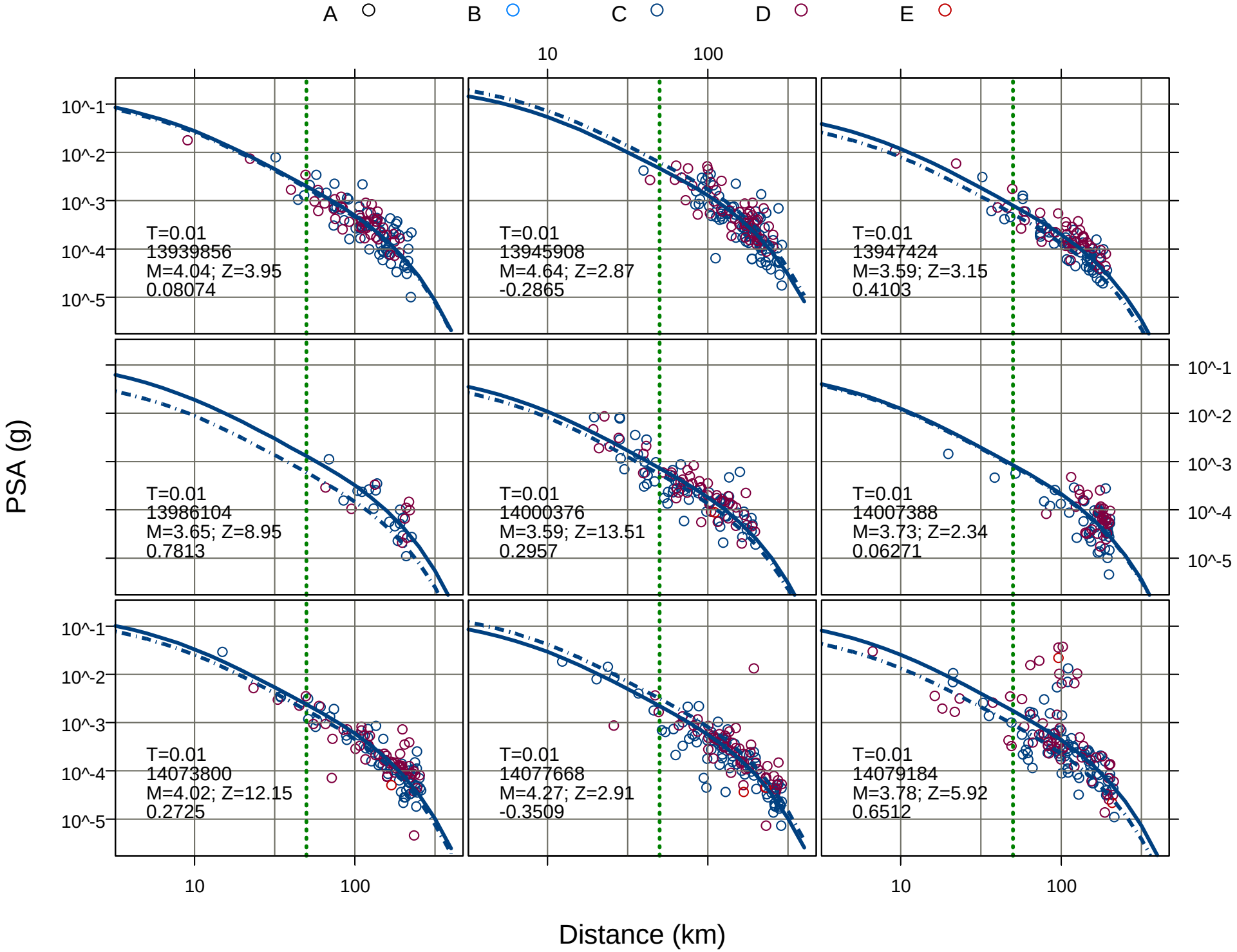
A
B
C
D
E
10
100
10^-1
10^-2
10^-3
10^-4
10^-5
T=0.01
13939856
M=4.04; Z=3.95
0.08074
T=0.01
13945908
M=4.64; Z=2.87
-0.2865
T=0.01
13947424
M=3.59; Z=3.15
0.4103
T=0.01
13986104
M=3.65; Z=8.95
0.7813
T=0.01
14000376
M=3.59; Z=13.51
0.2957
T=0.01
14007388
M=3.73; Z=2.34
0.06271
T=0.01
14073800
M=4.02; Z=12.15
0.2725
T=0.01
14077668
M=4.27; Z=2.91
-0.3509
T=0.01
14079184
M=3.78; Z=5.92
0.6512
PSA (g)
Distance (km)

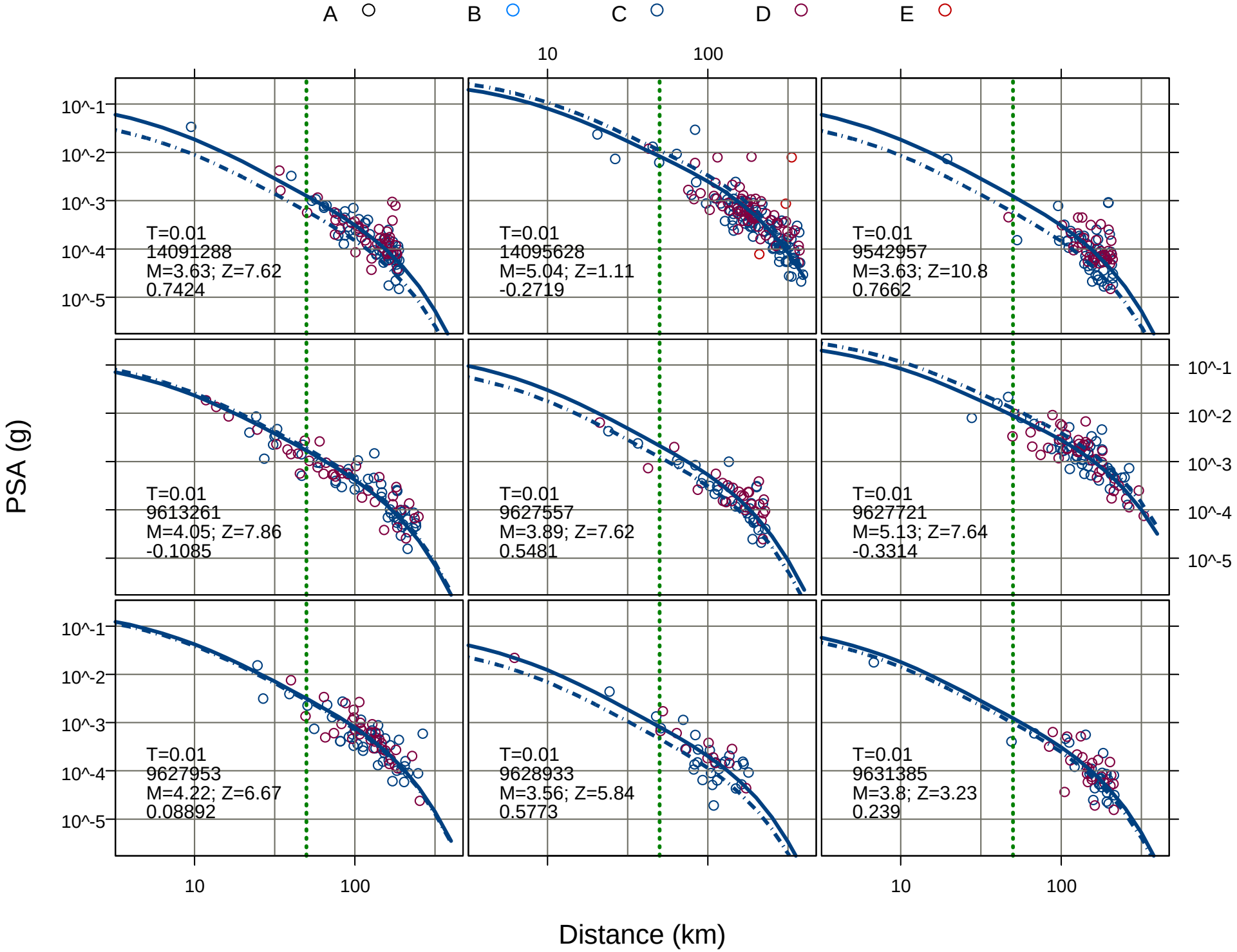
A
B
C
D
E
10
100
10^-1
10^-2
10^-3
10^-4
10^-5
T=0.01
14091288
M=3.63; Z=7.62
0.7424
T=0.01
14095628
M=5.04; Z=1.11
-0.2719
T=0.01
9542957
M=3.63; Z=10.8
0.7662
T=0.01
9613261
M=4.05; Z=7.86
-0.1085
T=0.01
9627557
M=3.89; Z=7.62
0.5481
T=0.01
9627721
M=5.13; Z=7.64
-0.3314
T=0.01
9627953
M=4.22; Z=6.67
0.08892
T=0.01
9628933
M=3.56; Z=5.84
0.5773
T=0.01
9631385
M=3.8; Z=3.23
0.239
PSA (g)
Distance (km)

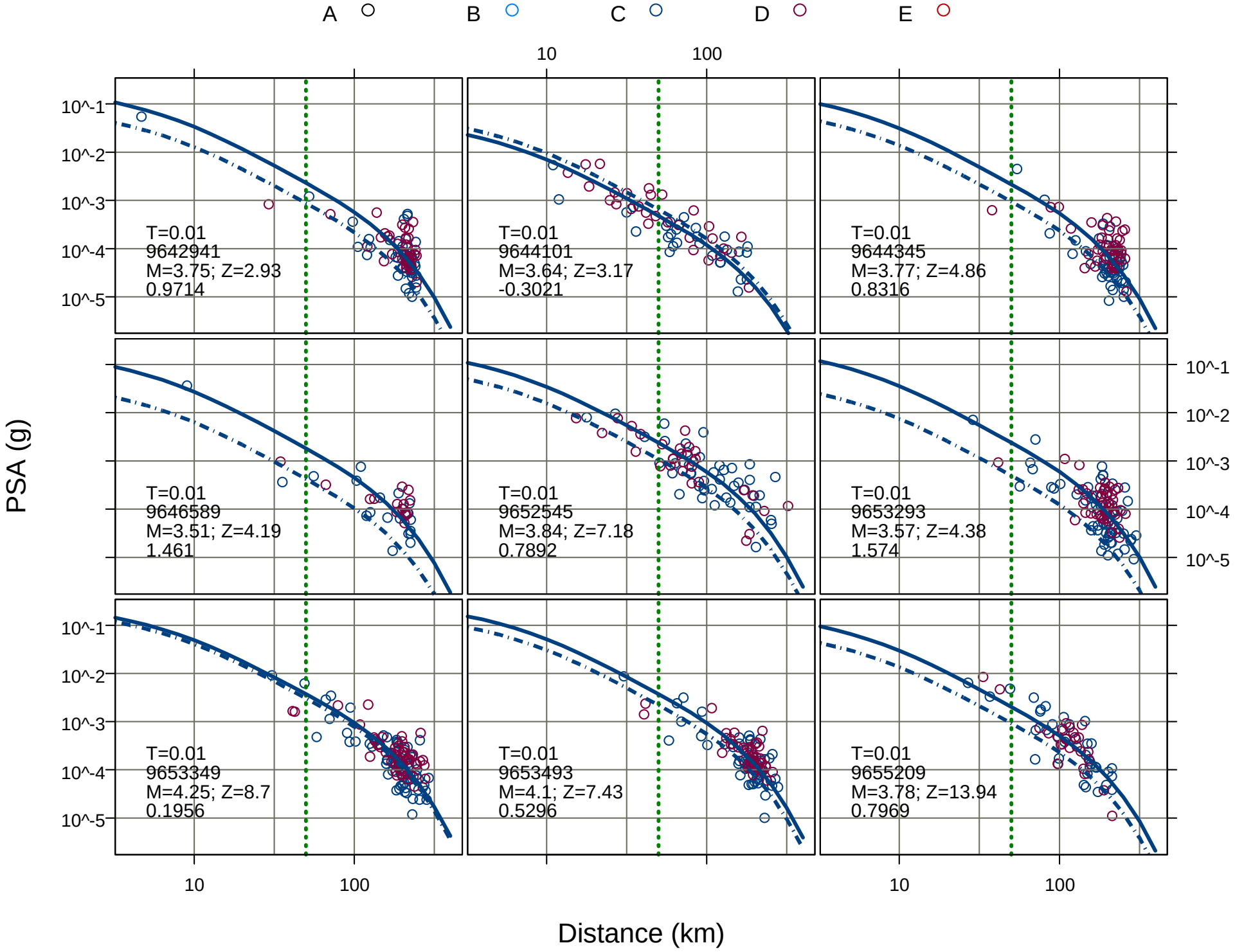
A
B
C
D
E
10
100
10^-1
10^-2
10^-3
10^-4
10^-5
T=0.01
9642941
M=3.75; Z=2.93
0.9714
T=0.01
9644101
M=3.64; Z=3.17
-0.3021
T=0.01
9644345
M=3.77; Z=4.86
0.8316
T=0.01
9646589
M=3.51; Z=4.19
1.461
T=0.01
9652545
M=3.84; Z=7.18
0.7892
T=0.01
9653293
M=3.57; Z=4.38
1.574
T=0.01
9653349
M=4.25; Z=8.7
0.1956
T=0.01
9653493
M=4.1; Z=7.43
0.5296
T=0.01
9655209
M=3.78; Z=13.94
0.7969
PSA (g)
Distance (km)

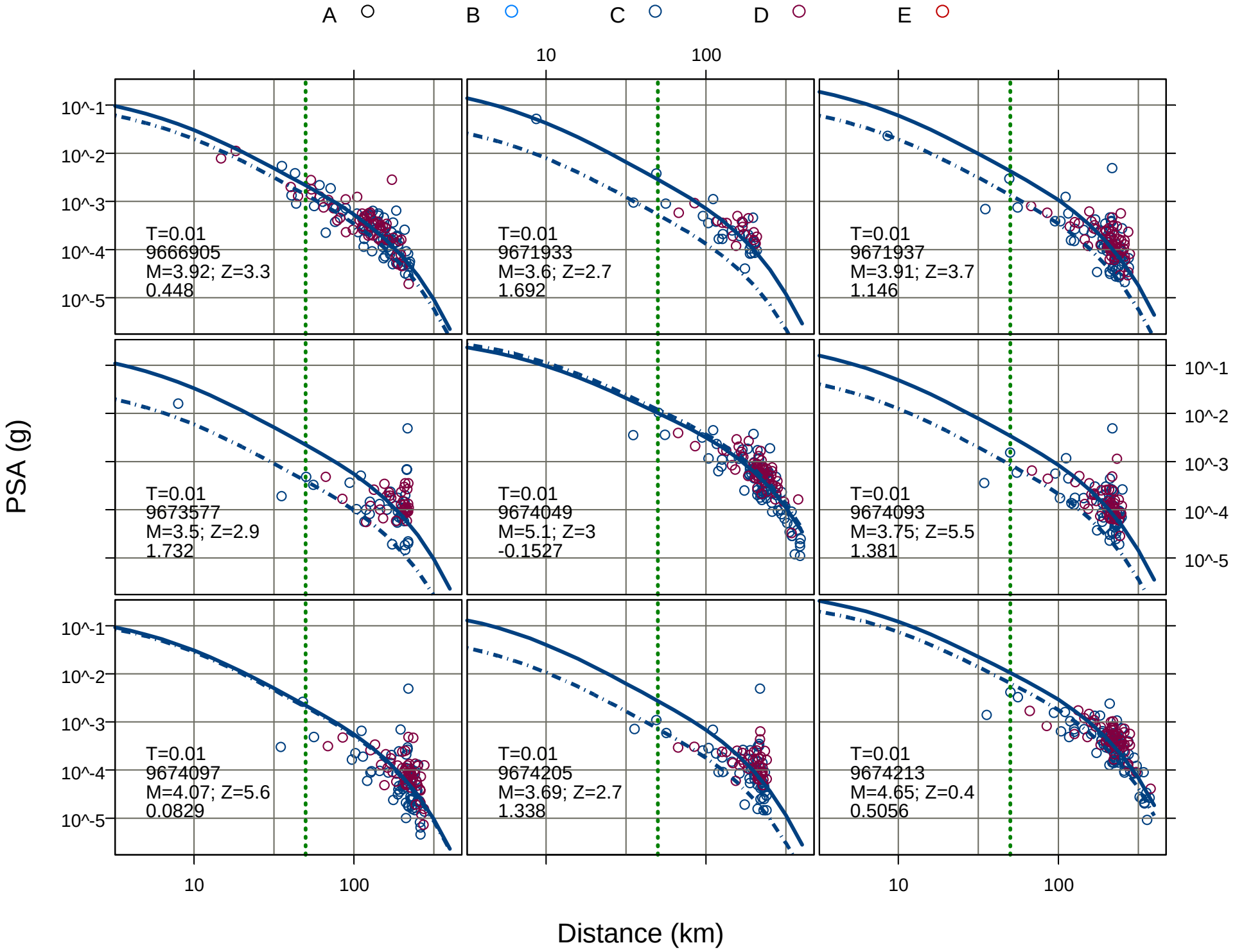
A
B
C
D
E
10
100
10^-1
10^-2
10^-3
10^-4
10^-5
T=0.01
9666905
M=3.92; Z=3.3
0.448
T=0.01
9671933
M=3.6; Z=2.7
1.692
T=0.01
9671937
M=3.91; Z=3.7
1.146
T=0.01
9673577
M=3.5; Z=2.9
1.732
T=0.01
9674049
M=5.1; Z=3
-0.1527
T=0.01
9674093
M=3.75; Z=5.5
1.381
T=0.01
9674097
M=4.07; Z=5.6
0.0829
T=0.01
9674205
M=3.69; Z=2.7
1.338
T=0.01
9674213
M=4.65; Z=0.4
0.5056
PSA (g)
Distance (km)

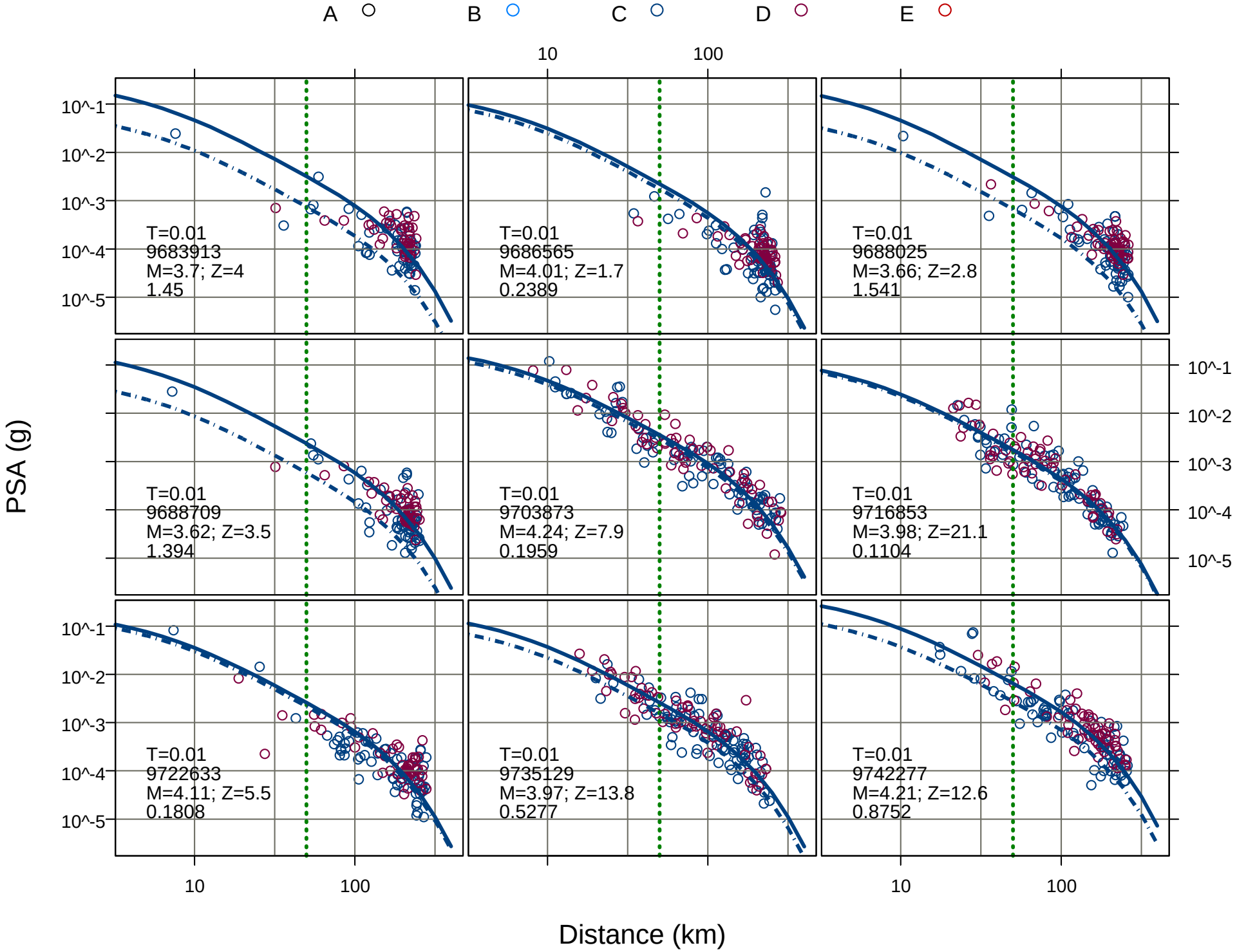
A
B
C
D
E
10
100
10^-1
10^-2
10^-3
10^-4
10^-5
T=0.01
9683913
M=3.7; Z=4
1.45
T=0.01
9686565
M=4.01; Z=1.7
0.2389
T=0.01
9688025
M=3.66; Z=2.8
1.541
T=0.01
9688709
M=3.62; Z=3.5
1.394
T=0.01
9703873
M=4.24; Z=7.9
0.1959
T=0.01
9716853
M=3.98; Z=21.1
0.1104
T=0.01
9722633
M=4.11; Z=5.5
0.1808
T=0.01
9735129
M=3.97; Z=13.8
0.5277
T=0.01
9742277
M=4.21; Z=12.6
0.8752
PSA (g)
Distance (km)

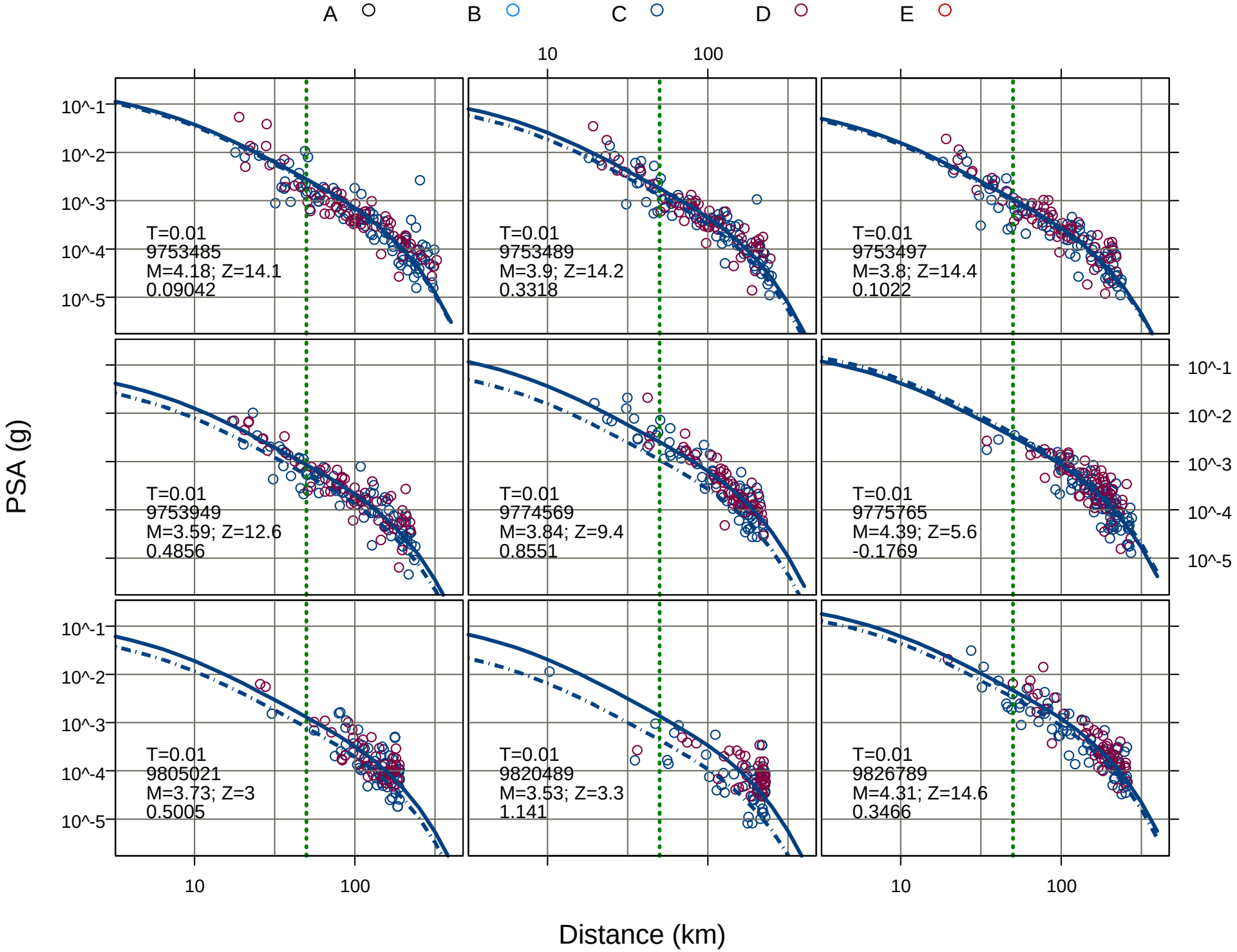
A
B
C
D
E
10
100
10^-1
10^-2
10^-3
10^-4
10^-5
T=0.01
9753485
M=4.18; Z=14.1
0.09042
T=0.01
9753489
M=3.9; Z=14.2
0.3318
T=0.01
9753497
M=3.8; Z=14.4
0.1022
T=0.01
9753949
M=3.59; Z=12.6
0.4856
T=0.01
9774569
M=3.84; Z=9.4
0.8551
T=0.01
9775765
M=4.39; Z=5.6
-0.1769
T=0.01
9805021
M=3.73; Z=3
0.5005
T=0.01
9820489
M=3.53; Z=3.3
1.141
T=0.01
9826789
M=4.31; Z=14.6
0.3466
PSA (g)
Distance (km)

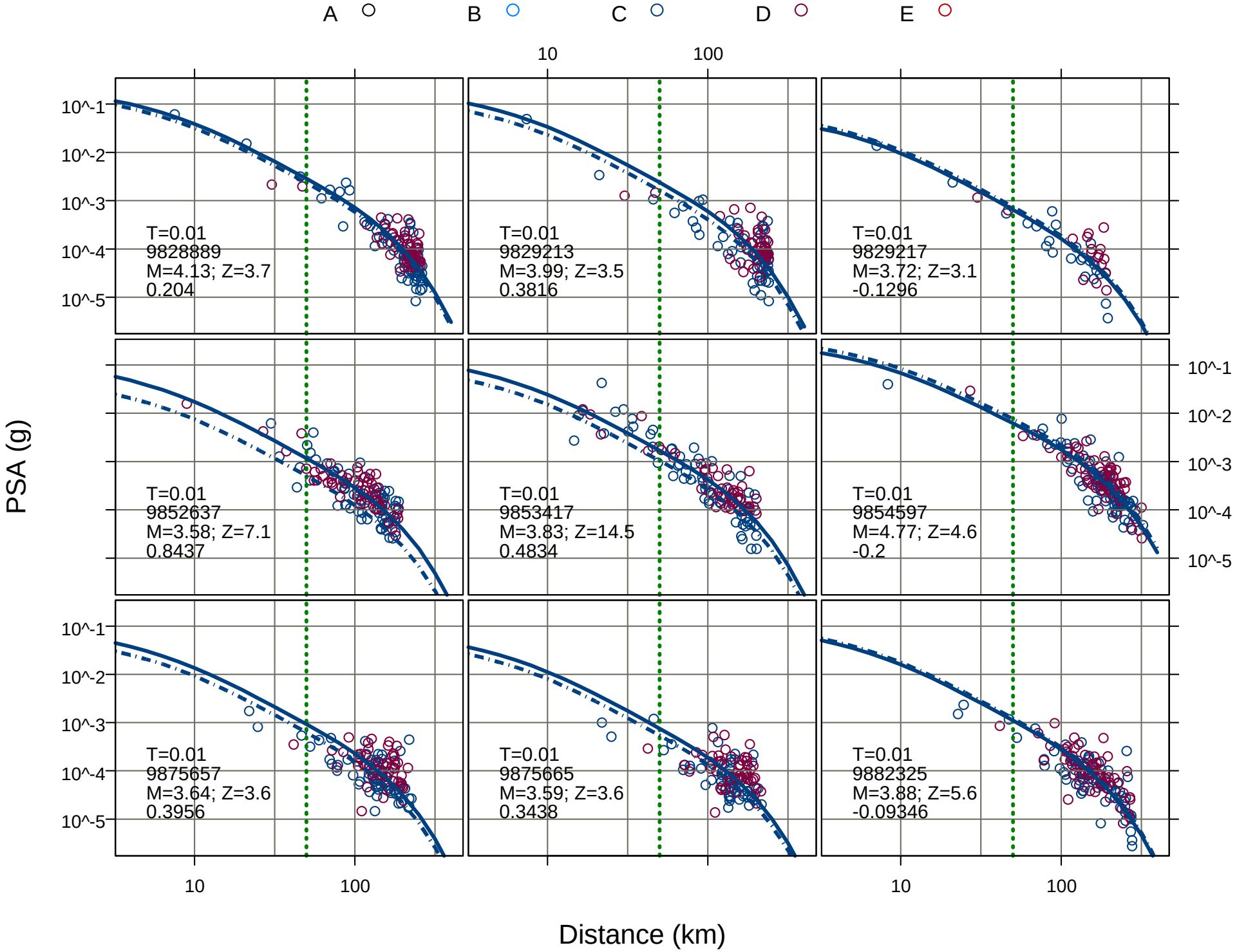
A
B
C
D
E
10
100
10^-1
10^-2
10^-3
10^-4
10^-5
T=0.01
9828889
M=4.13; Z=3.7
0.204
T=0.01
9829213
M=3.99; Z=3.5
0.3816
T=0.01
9829217
M=3.72; Z=3.1
-0.1296
T=0.01
9852637
M=3.58; Z=7.1
0.8437
T=0.01
9853417
M=3.83; Z=14.5
0.4834
T=0.01
9854597
M=4.77; Z=4.6
-0.2
T=0.01
9875657
M=3.64; Z=3.6
0.3956
T=0.01
9875665
M=3.59; Z=3.6
0.3438
T=0.01
9882325
M=3.88; Z=5.6
-0.09346
PSA (g)
Distance (km)

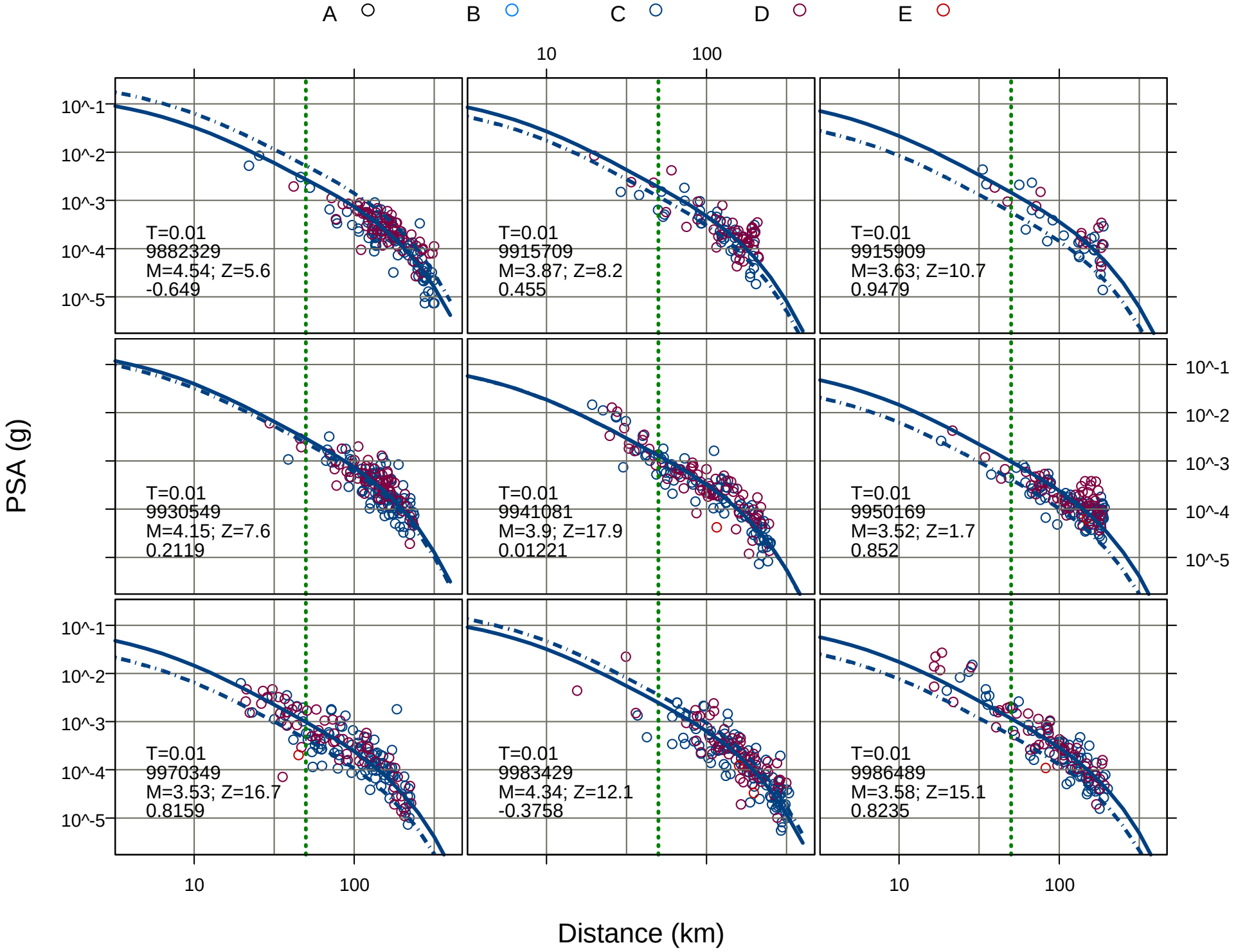
A
B
C
D
E
10
100
10^-1
10^-2
10^-3
10^-4
10^-5
T=0.01
9882329
M=4.54; Z=5.6
-0.649
T=0.01
9915709
M=3.87; Z=8.2
0.455
T=0.01
9915909
M=3.63; Z=10.7
0.9479
T=0.01
9930549
M=4.15; Z=7.6
0.2119
T=0.01
9941081
M=3.9; Z=17.9
0.01221
T=0.01
9950169
M=3.52; Z=1.7
0.852
T=0.01
9970349
M=3.53; Z=16.7
0.8159
T=0.01
9983429
M=4.34; Z=12.1
-0.3758
T=0.01
9986489
M=3.58; Z=15.1
0.8235
PSA (g)
Distance (km)

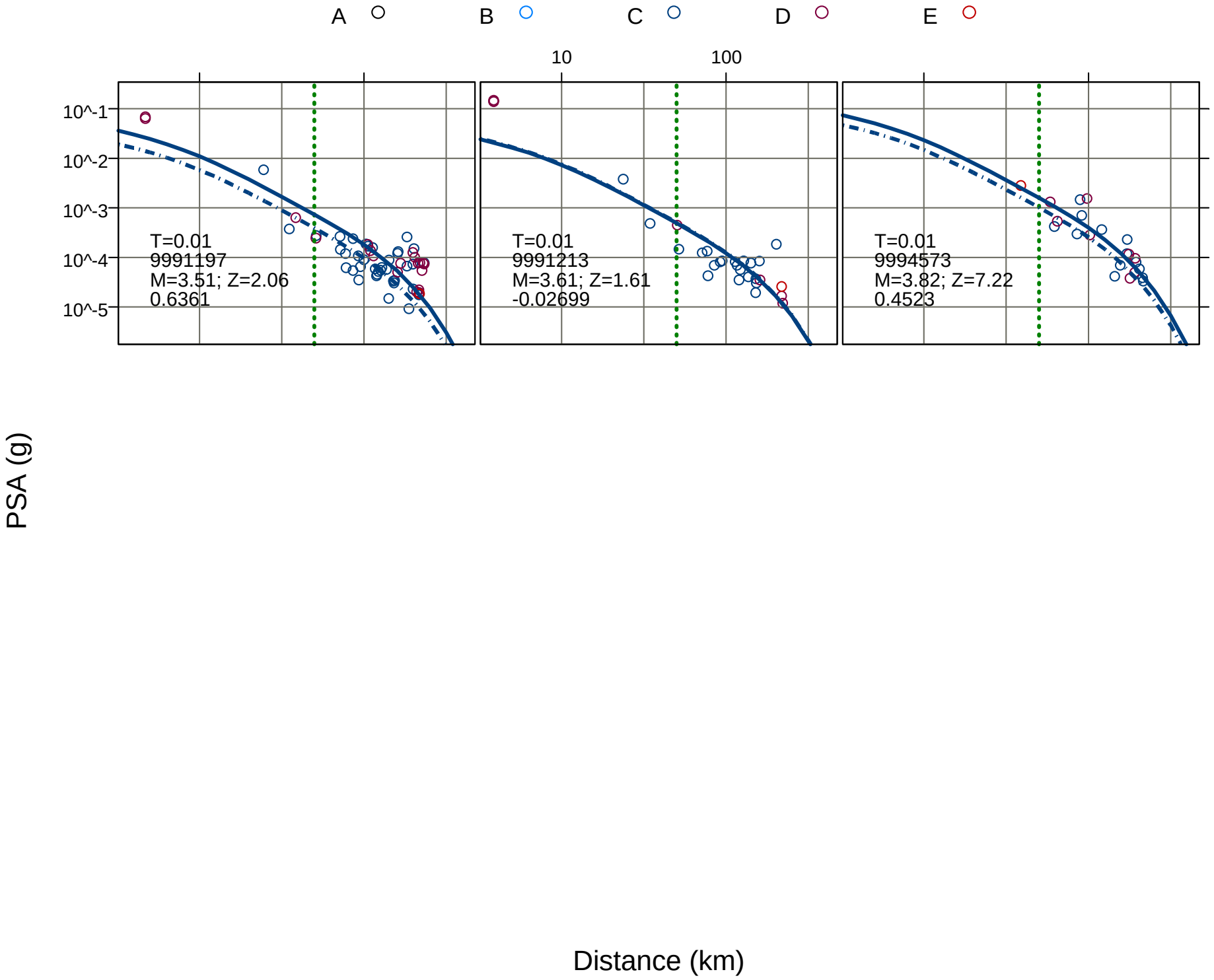
A
B
C
D
E
10
100
10^-1
10^-2
10^-3
10^-4
10^-5
T=0.01
9991197
M=3.51; Z=2.06
0.6361
T=0.01
9991213
M=3.61; Z=1.61
-0.02699
T=0.01
9994573
M=3.82; Z=7.22
0.4523
PSA (g)
Distance (km)

Appendix E
Individual Earthquake Fits for the Chiou and Youngs (2006) Ground Motion Model

The plots in this appendix show the fits to the individual earthquakes obtained as part of the overall regressions conducted to develop the ground motion model. The curves are color coded to indicate the value of V_{S30} used to make the ground motion estimates and the site data are color coded by NEHRP site class. Results are shown for pseudo spectral acceleration at spectral periods of 0.01, 0.2, 1.0 and 3.0 seconds.

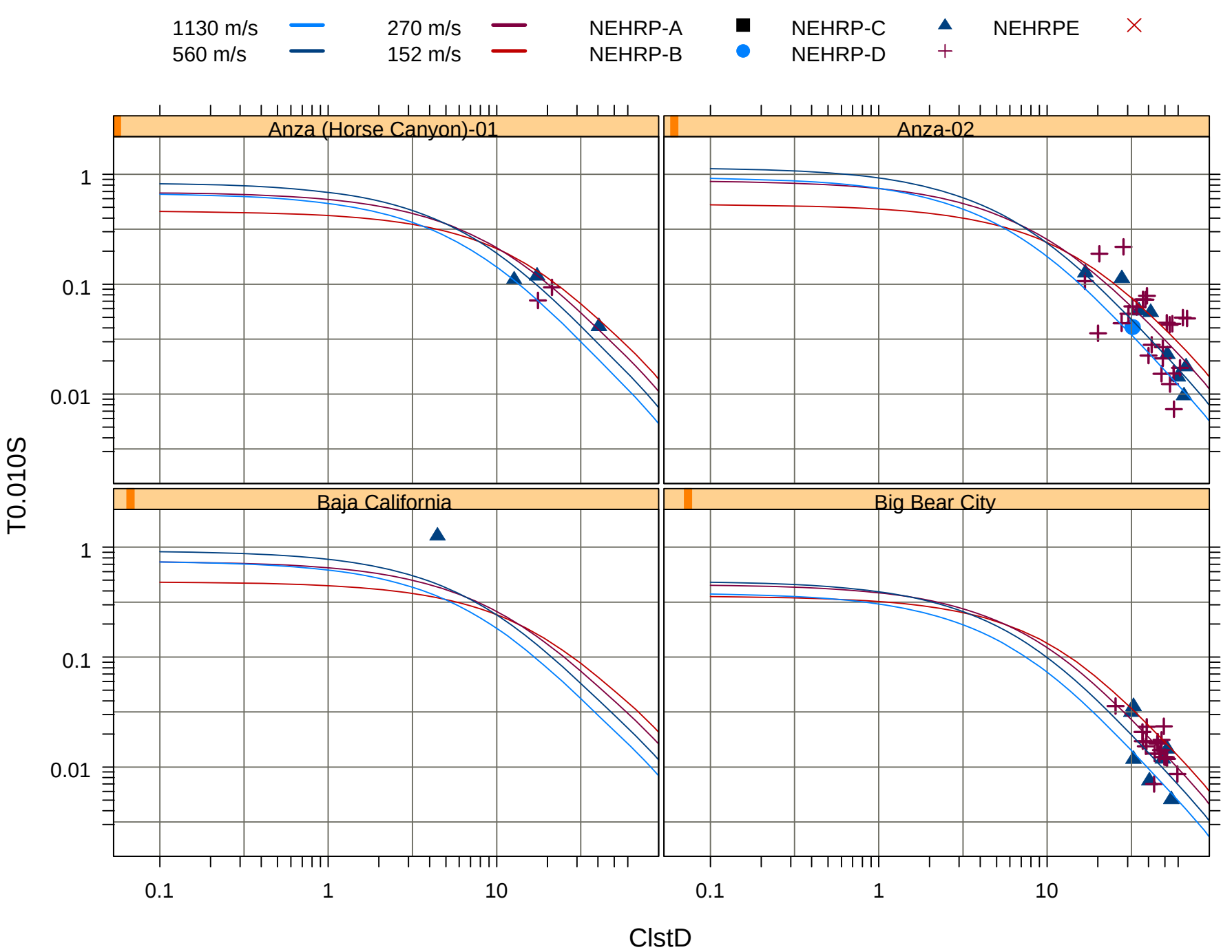
1130 m/s
560 m/s
270 m/s
152 m/s
NEHRP-A
NEHRP-B
NEHRP-C
NEHRP-D
NEHRPE
Anza (Horse Canyon)-01
Anza-02
Baja California
Big Bear City
T0.010S
ClstD
1
0.1
0.01
0.1
1
10

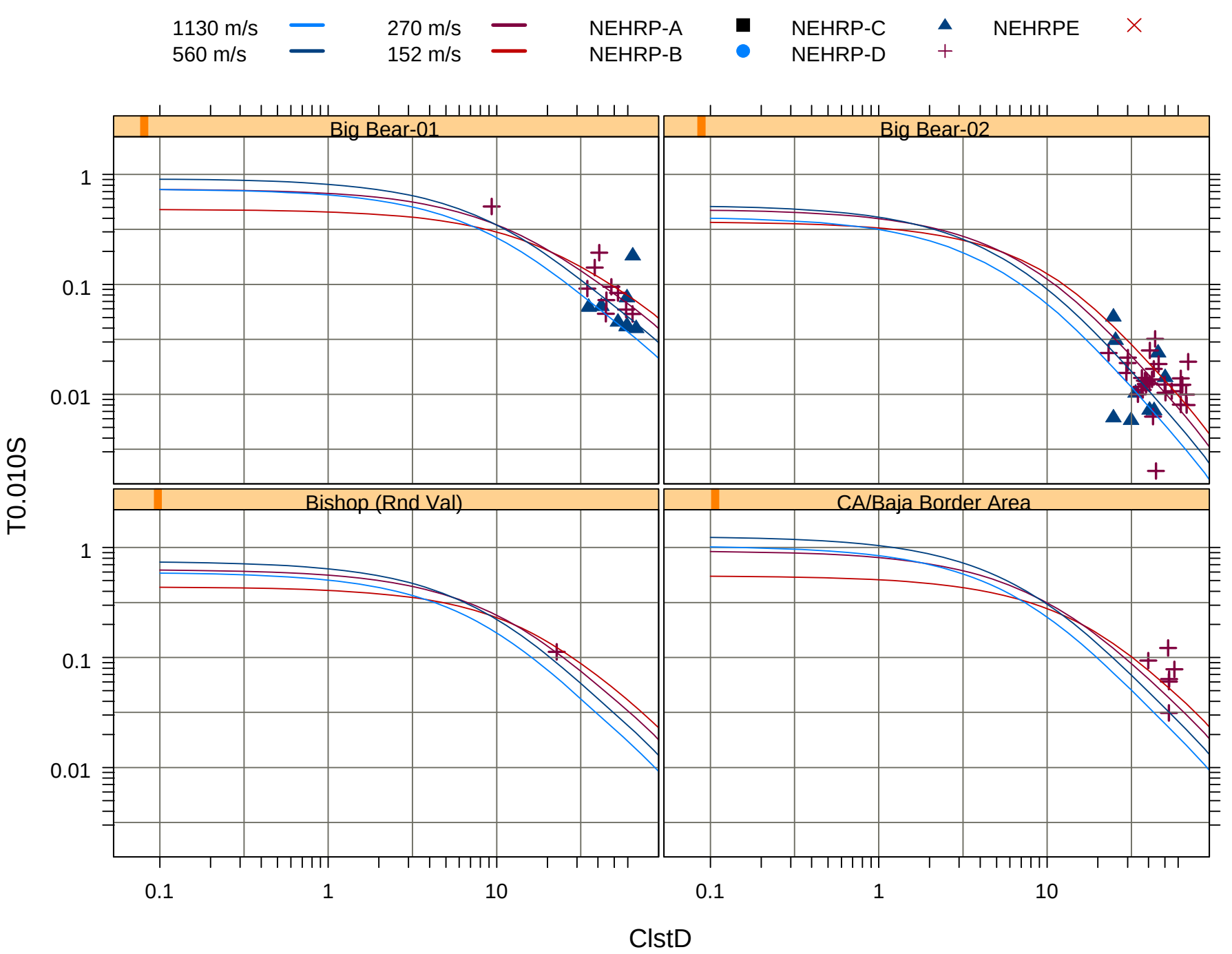
1130 m/s
560 m/s
270 m/s
152 m/s
NEHRP-A
NEHRP-B
NEHRP-C
NEHRP-D
NEHRPE
Big Bear-01
Big Bear-02
Bishop (Rnd Val)
CA/Baja Border Area
T0.010S
ClstD
1
0.1
0.01
0.1
1
10

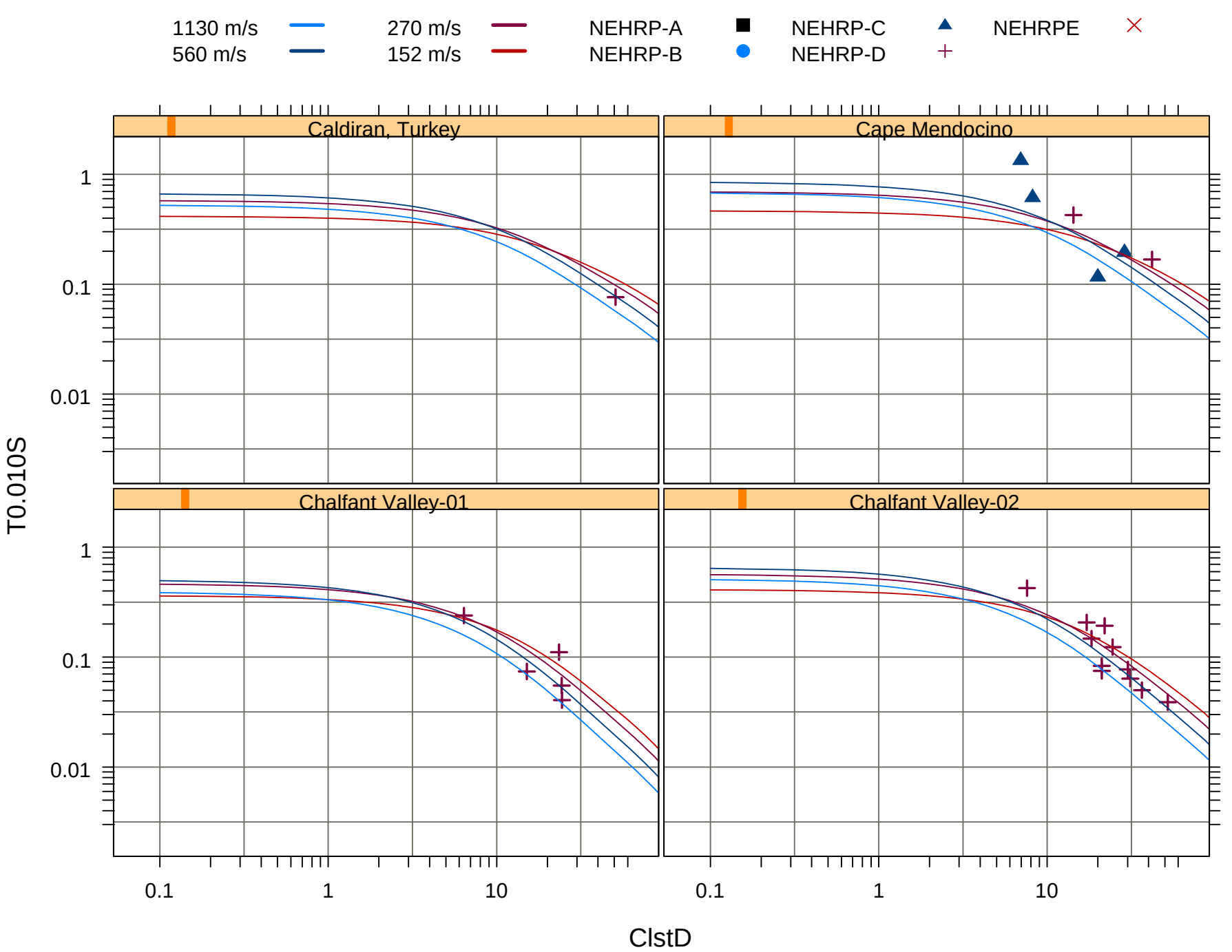
1130 m/s
560 m/s
270 m/s
152 m/s
NEHRP-A
NEHRP-B
NEHRP-C
NEHRP-D
NEHRPE
Caldiran, Turkey
Cape Mendocino
Chalfant Valley-01
Chalfant Valley-02
T0.010S
ClstD
1
0.1
0.01
0.1
1
10

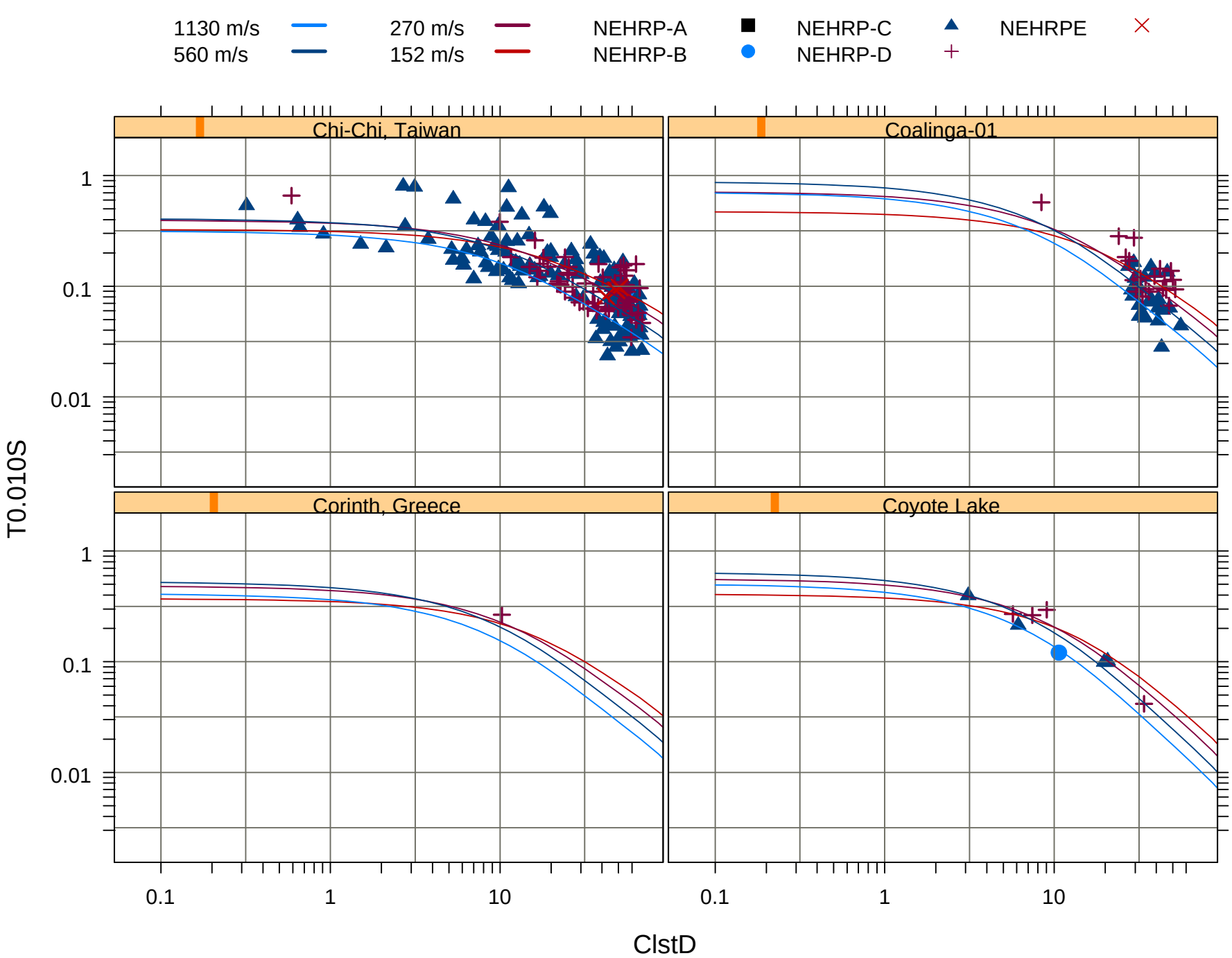
1130 m/s
560 m/s
270 m/s
152 m/s
NEHRP-A
NEHRP-B
NEHRP-C
NEHRP-D
NEHRPE
Chi-Chi, Taiwan
Coalinga-01
Corinth, Greece
Coyote Lake
T0.010S
ClstD
1
0.1
0.01
0.1
1
10

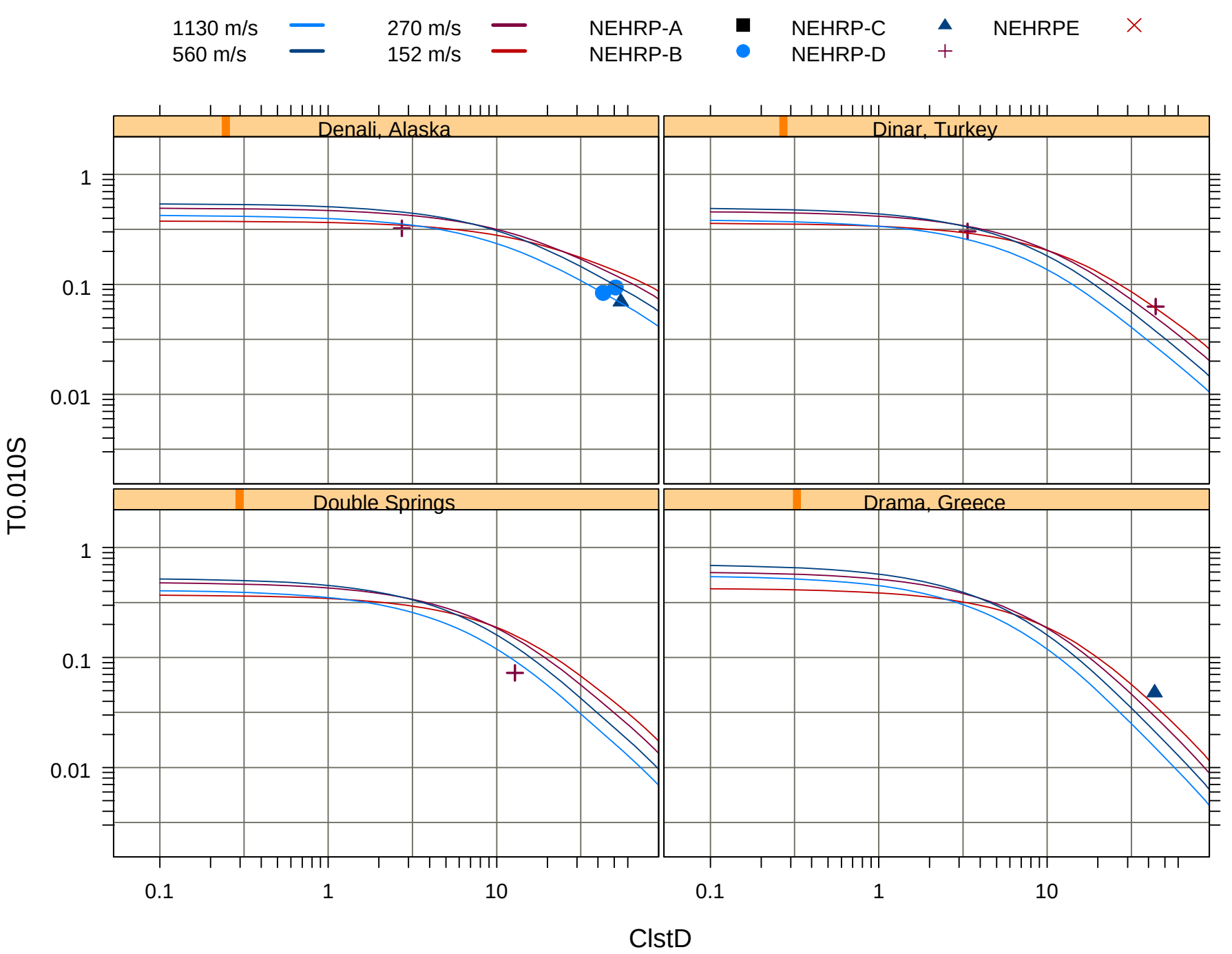
1130 m/s
560 m/s
270 m/s
152 m/s
NEHRP-A
NEHRP-B
NEHRP-C
NEHRP-D
NEHRPE
Denali, Alaska
Dinar, Turkey
Double Springs
Drama, Greece
T0.010S
ClstD
1
0.1
0.01
0.1
1
10

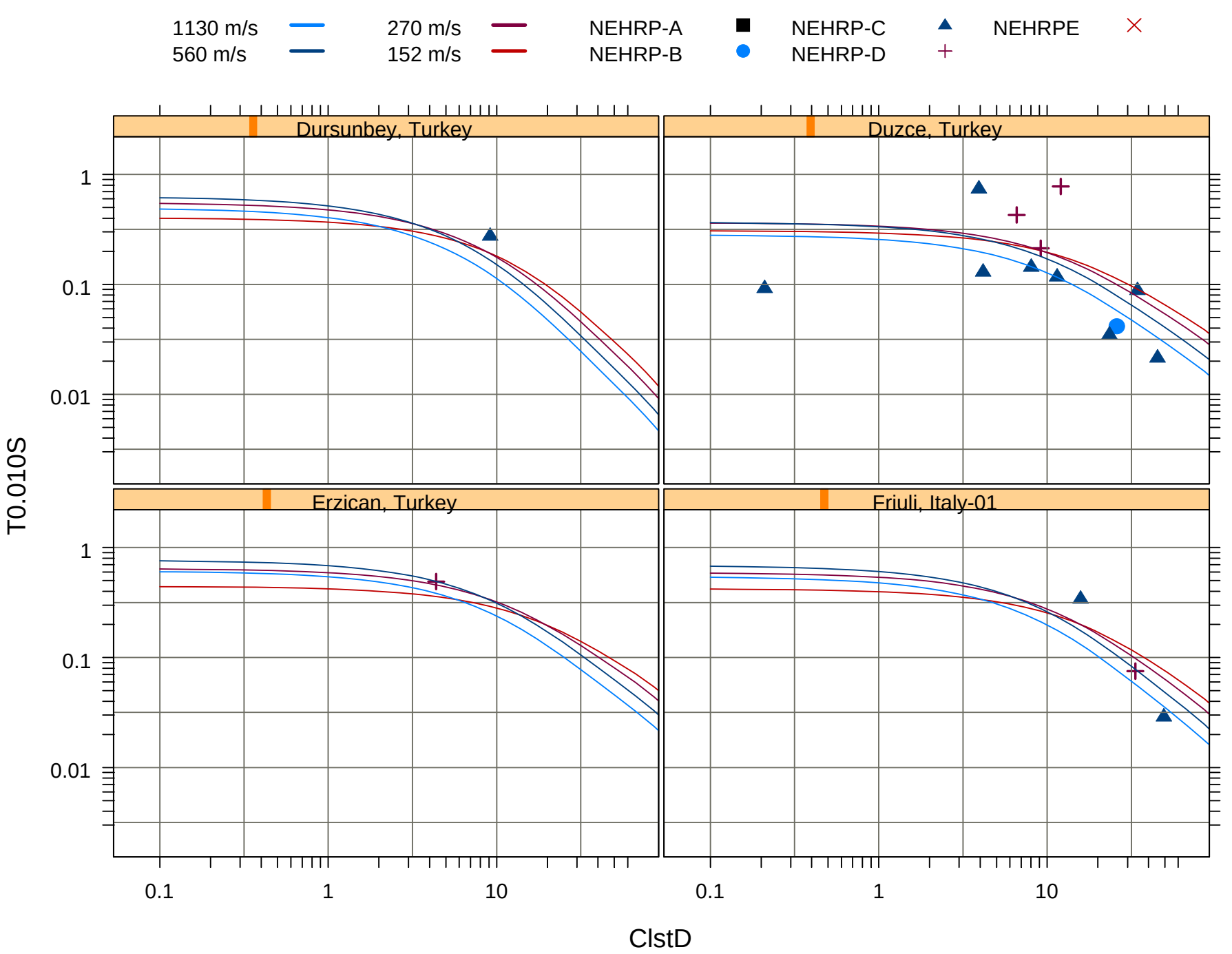
1130 m/s
560 m/s
270 m/s
152 m/s
NEHRP-A
NEHRP-B
NEHRP-C
NEHRP-D
NEHRPE
Dursunbey, Turkey
Duzce, Turkey
Erzican, Turkey
Friuli, Italy-01
T0.010S
ClstD
1
0.1
0.01
0.1
1
10

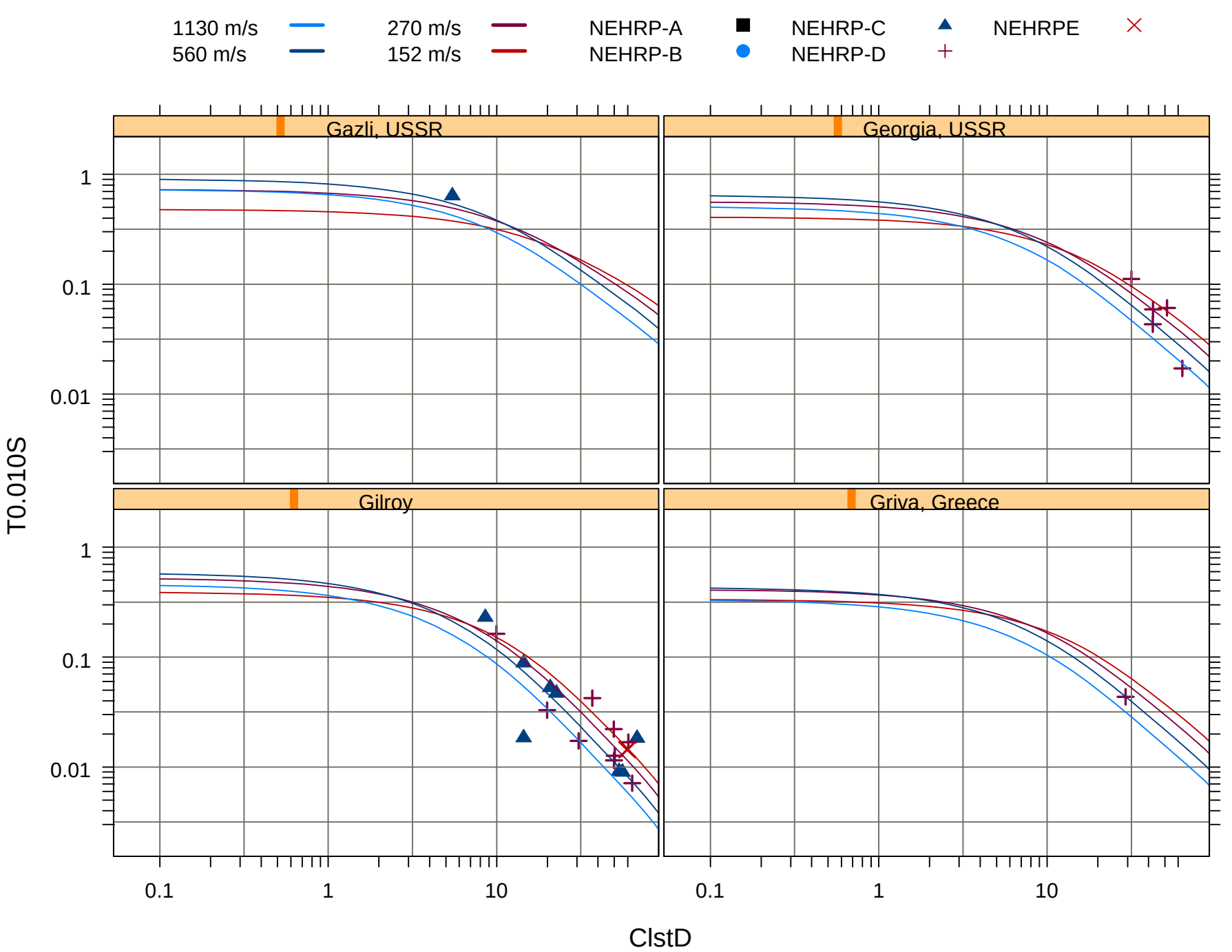
1130 m/s
560 m/s
270 m/s
152 m/s
NEHRP-A
NEHRP-B
NEHRP-C
NEHRP-D
NEHRPE
Gazli, USSR
Georgia, USSR
Gilroy
Griva, Greece
T0.010S
ClstD
1
0.1
0.01
0.1
1
10

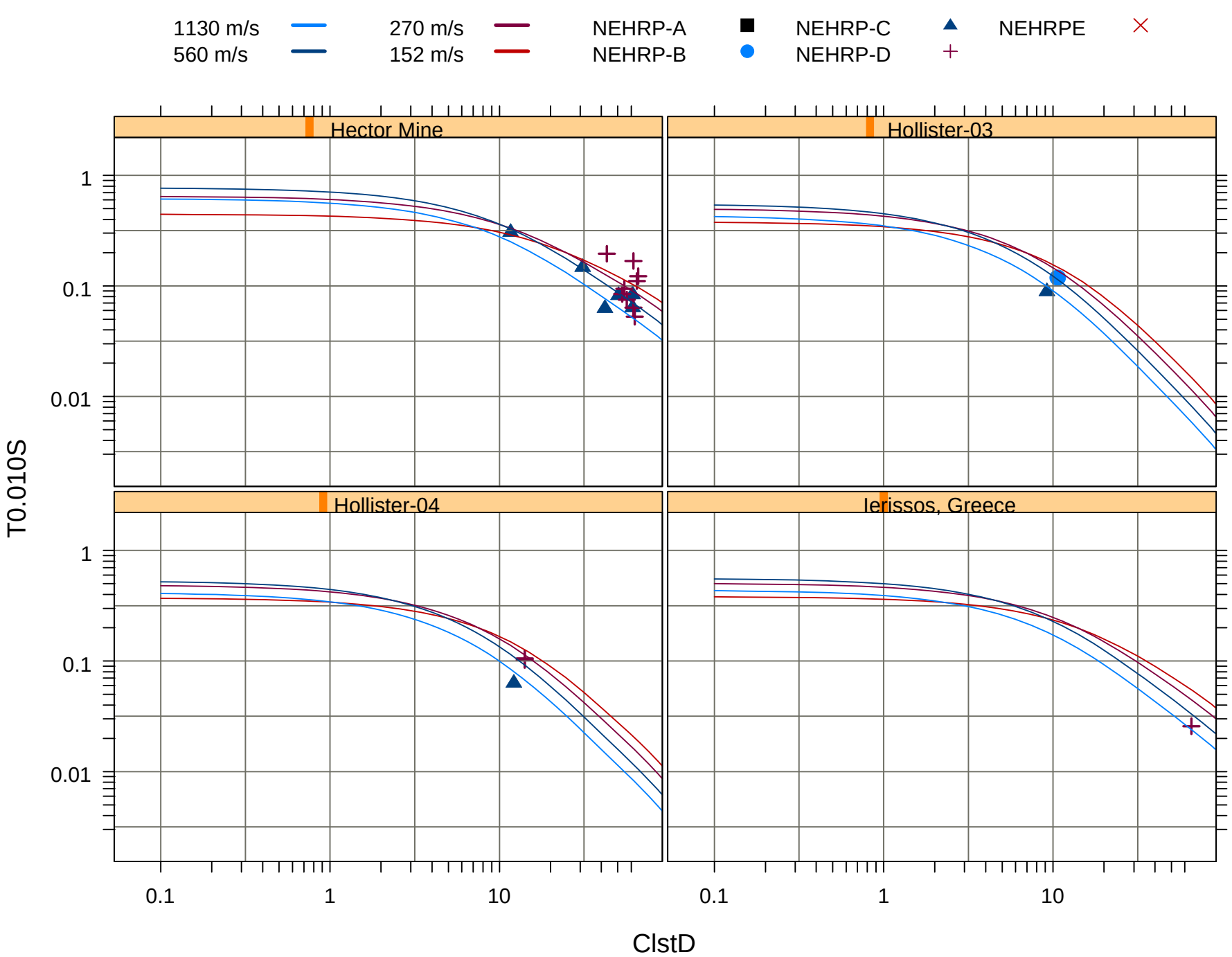
1130 m/s
560 m/s
270 m/s
152 m/s
NEHRP-A
NEHRP-B
NEHRP-C
NEHRP-D
NEHRPE
Hector Mine
Hollister-03
Hollister-04
Ierissos, Greece
T0.010S
ClstD
1
0.1
0.01
0.1
1
10

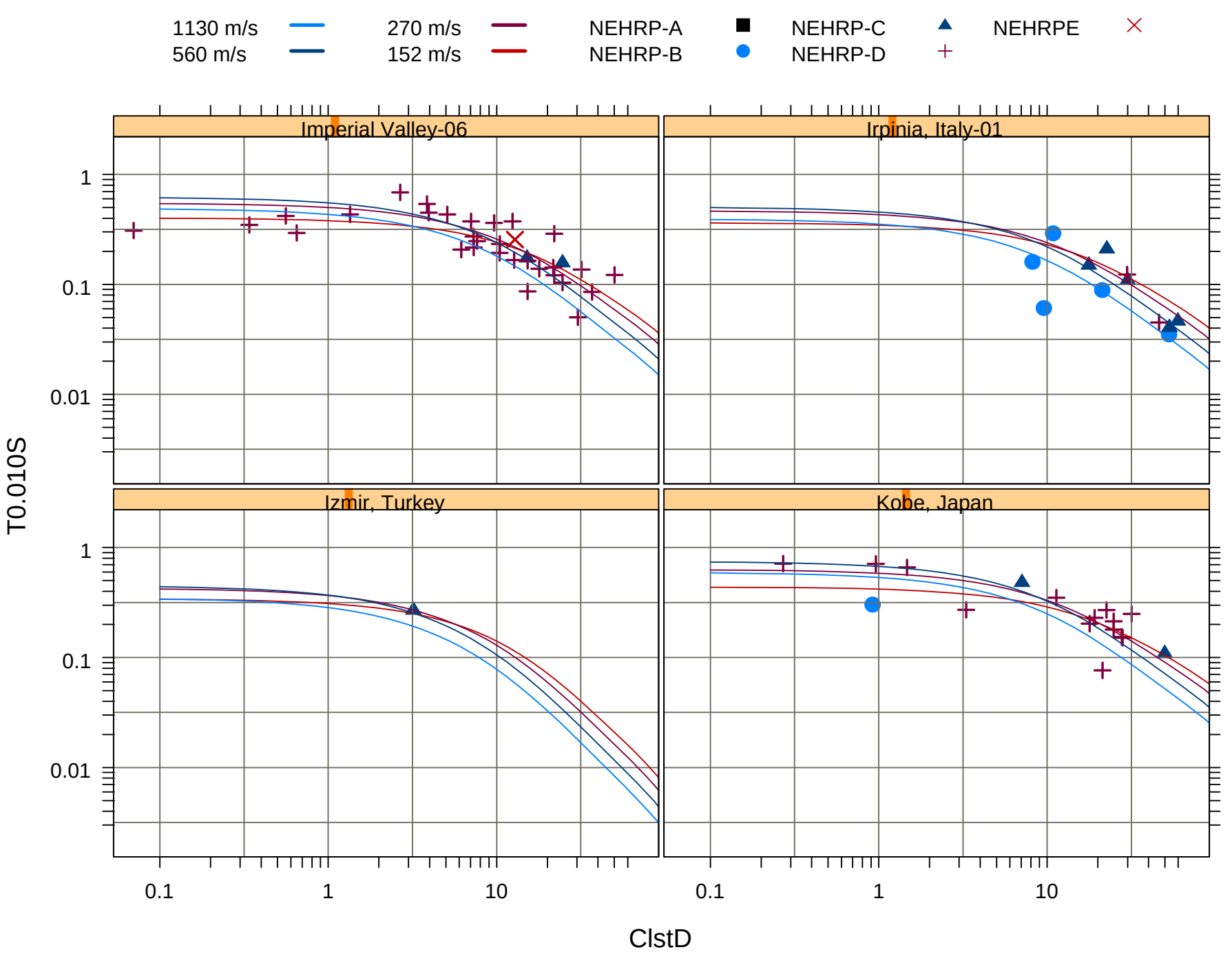
1130 m/s
560 m/s
270 m/s
152 m/s
NEHRP-A
NEHRP-B
NEHRP-C
NEHRP-D
NEHRPE
Imperial Valley-06
Irpinia, Italy-01
Izmir, Turkey
Kobe, Japan
T0.010S
ClstD
1
0.1
0.01
0.1
1
10

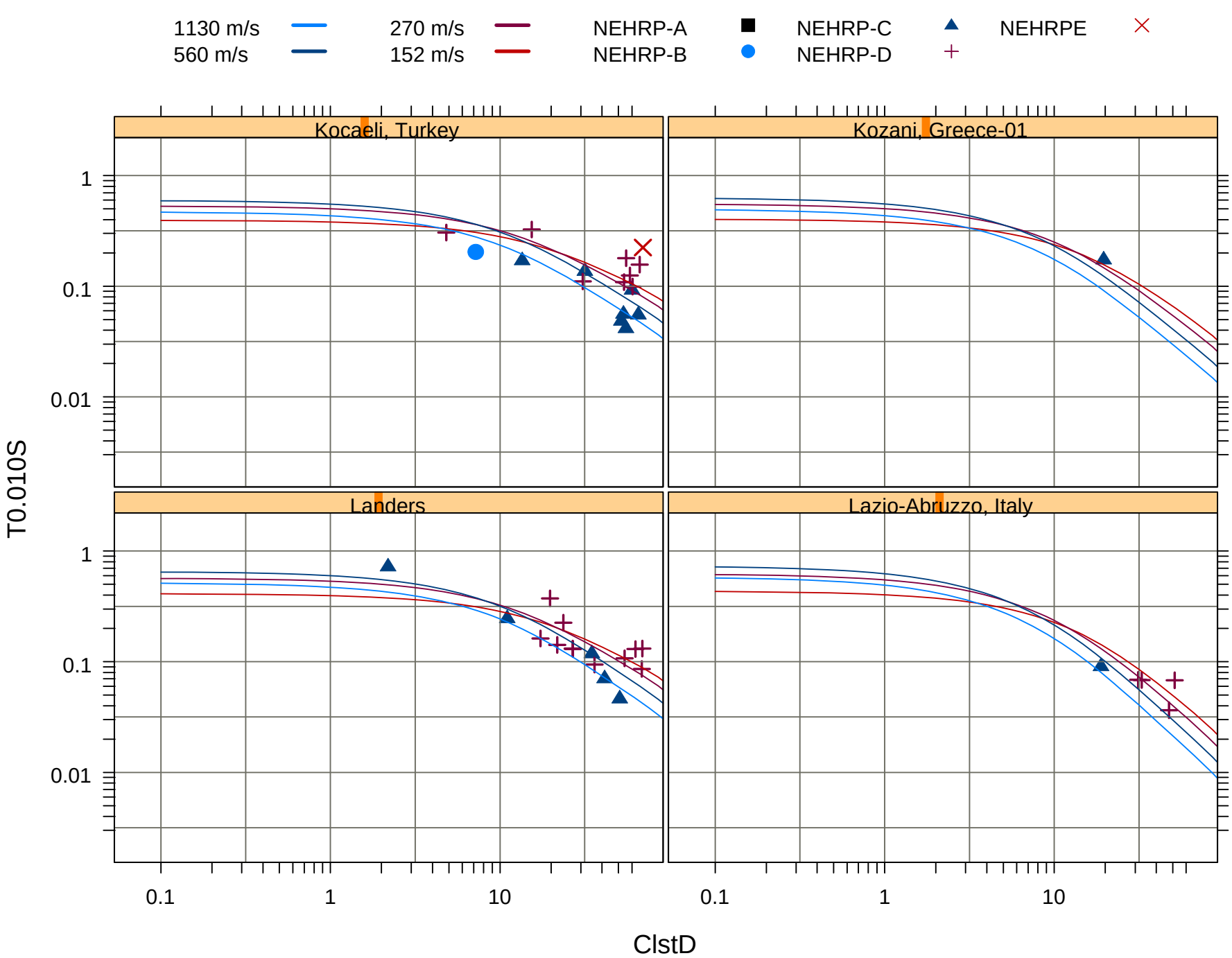
1130 m/s
560 m/s
270 m/s
152 m/s
NEHRP-A
NEHRP-B
NEHRP-C
NEHRP-D
NEHRPE
Kocaeli, Turkey
Kozani, Greece-01
Landers
Lazio-Abruzzo, Italy
T0.010S
ClstD
1
0.1
0.01
0.1
1
10

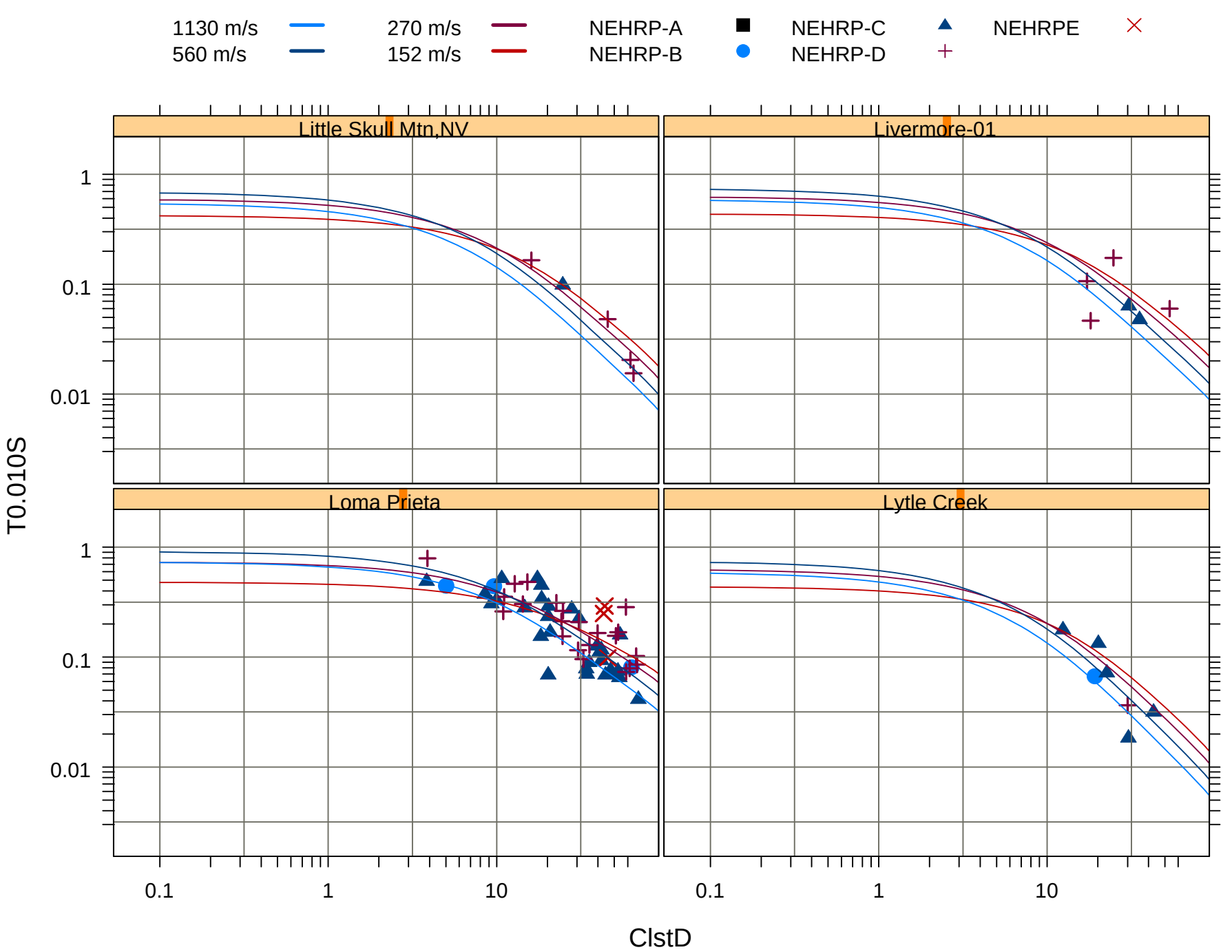
1130 m/s
560 m/s
270 m/s
152 m/s
NEHRP-A
NEHRP-B
NEHRP-C
NEHRP-D
NEHRPE
Little Skull Mtn,NV
Livermore-01
Loma Prieta
Lytle Creek
T0.010S
ClstD
1
0.1
0.01
0.1
1
10

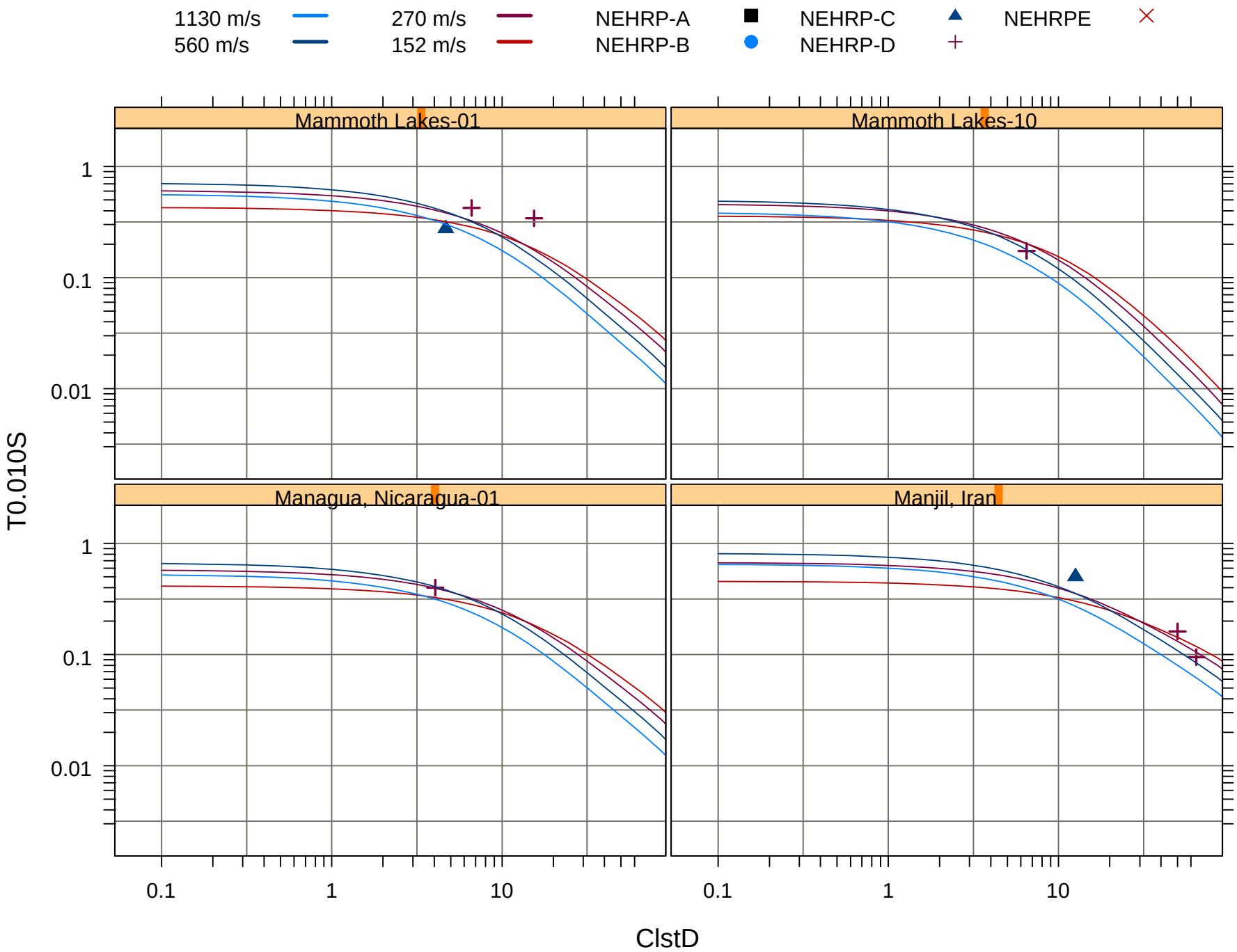
1130 m/s
560 m/s
270 m/s
152 m/s
NEHRP-A
NEHRP-B
NEHRP-C
NEHRP-D
NEHRPE
Mammoth Lakes-01
Mammoth Lakes-10
Managua, Nicaragua-01
Manjil, Iran
T0.010S
ClstD
1
0.1
0.01
0.1
1
10

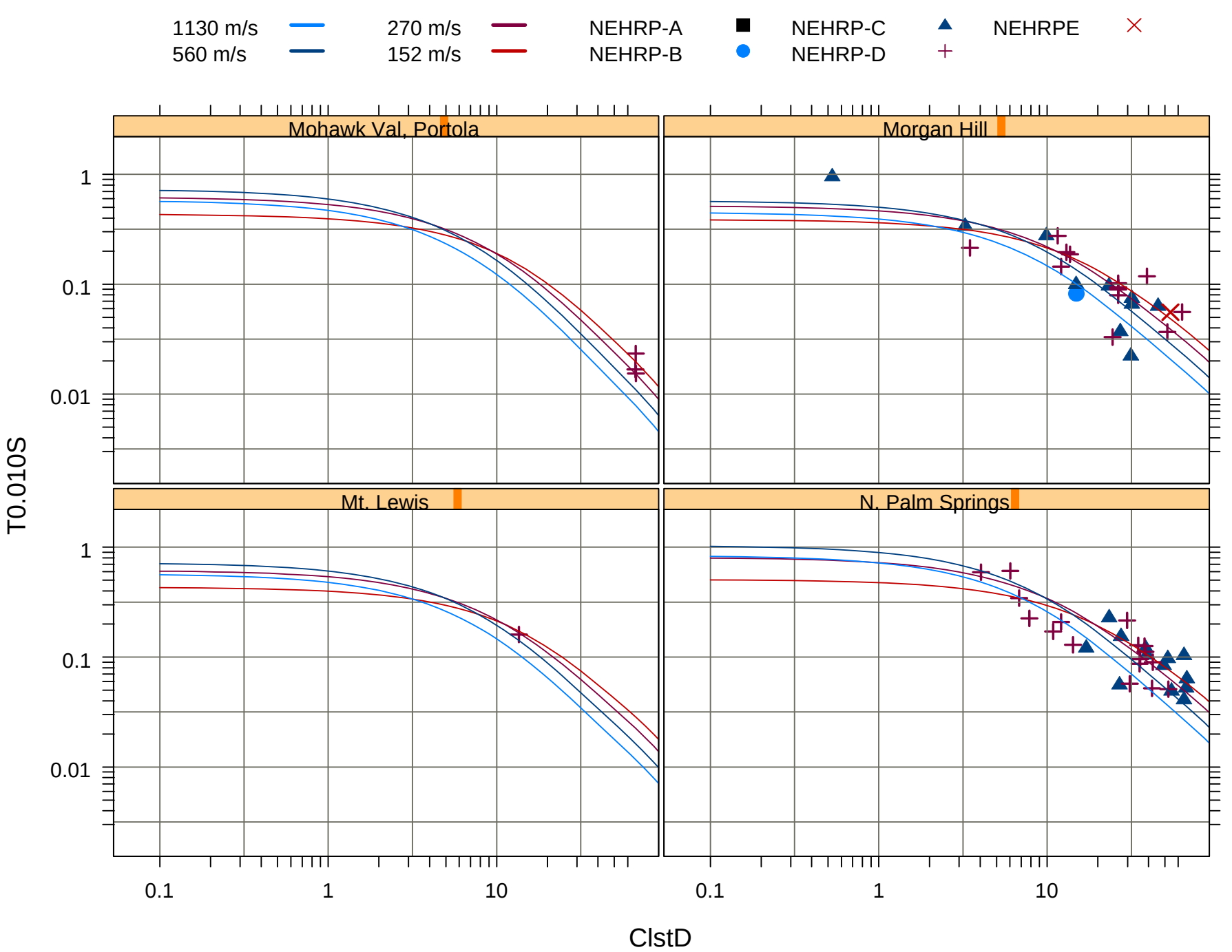
1130 m/s
560 m/s
270 m/s
152 m/s
NEHRP-A
NEHRP-B
NEHRP-C
NEHRP-D
NEHRPE
Mohawk Val, Portola
Morgan Hill
Mt. Lewis
N. Palm Springs
T0.010S
ClstD
1
0.1
0.01
0.1
1
10

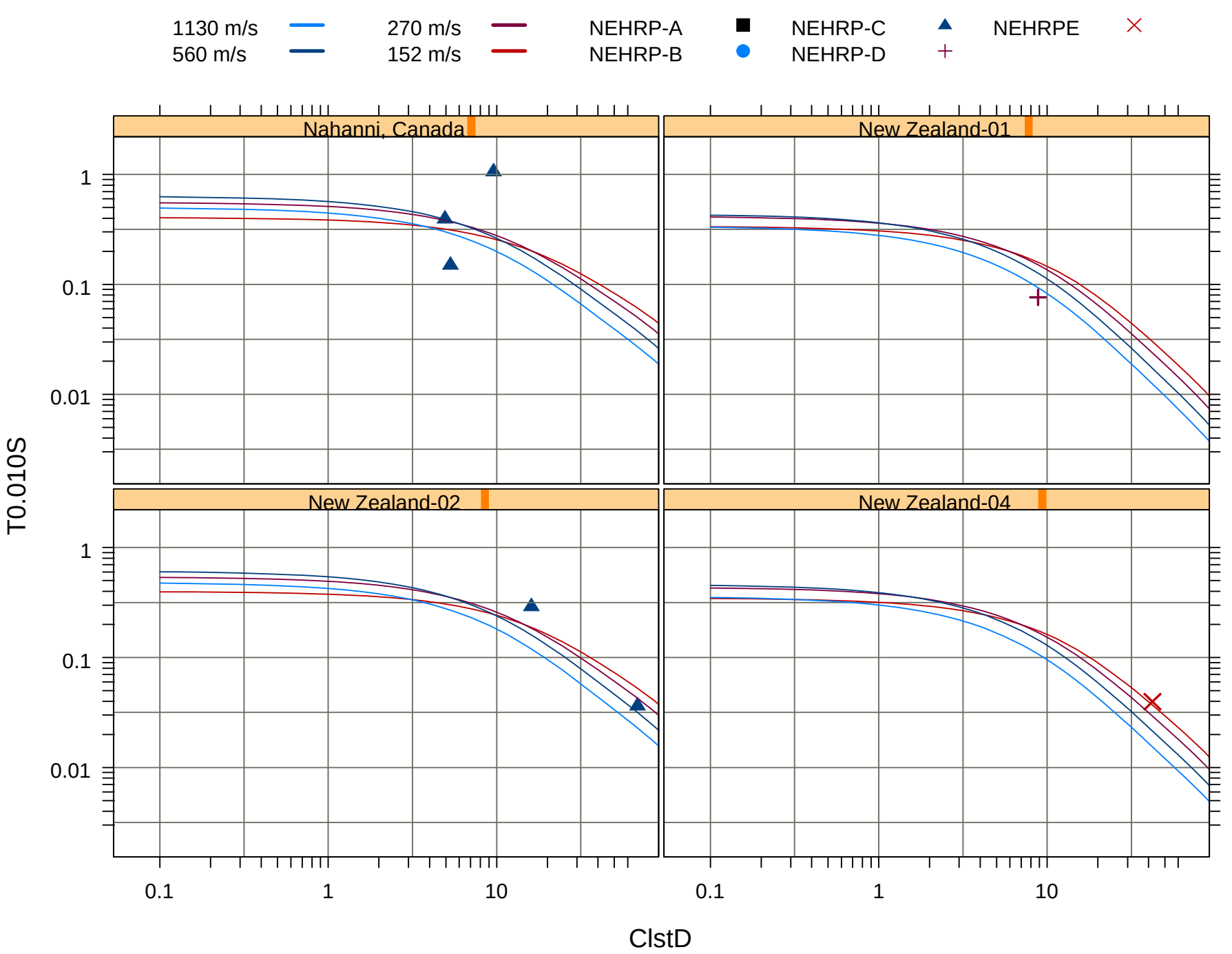
1130 m/s
560 m/s
270 m/s
152 m/s
NEHRP-A
NEHRP-B
NEHRP-C
NEHRP-D
NEHRPE
Nahanni, Canada
New Zealand-01
New Zealand-02
New Zealand-04
T0.010S
ClstD
1
0.1
0.01
0.1
1
10

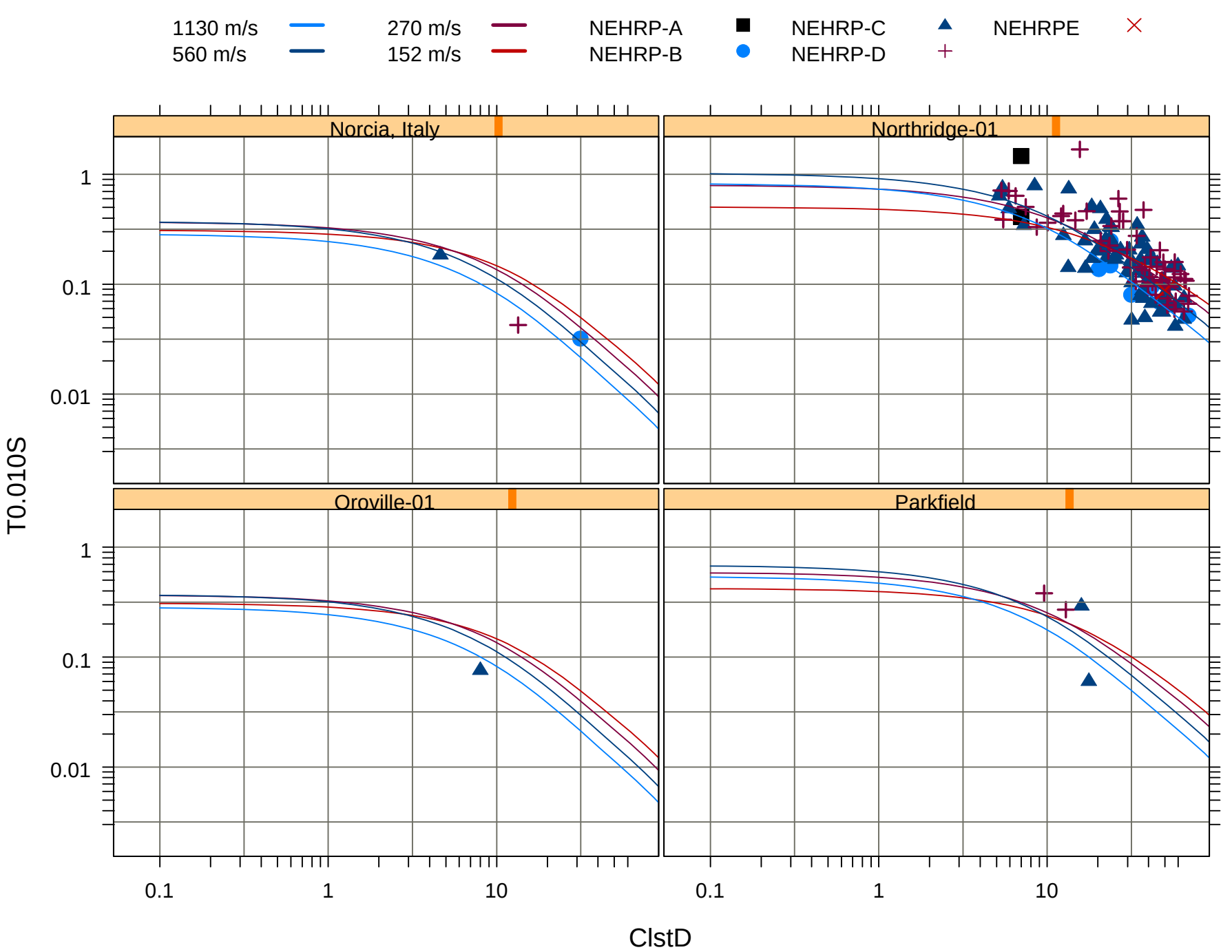
1130 m/s
560 m/s
270 m/s
152 m/s
NEHRP-A
NEHRP-B
NEHRP-C
NEHRP-D
NEHRPE
Norcia, Italy
Northridge-01
Oroville-01
Parkfield
T0.010S
ClstD
1
0.1
0.01
0.1
1
10

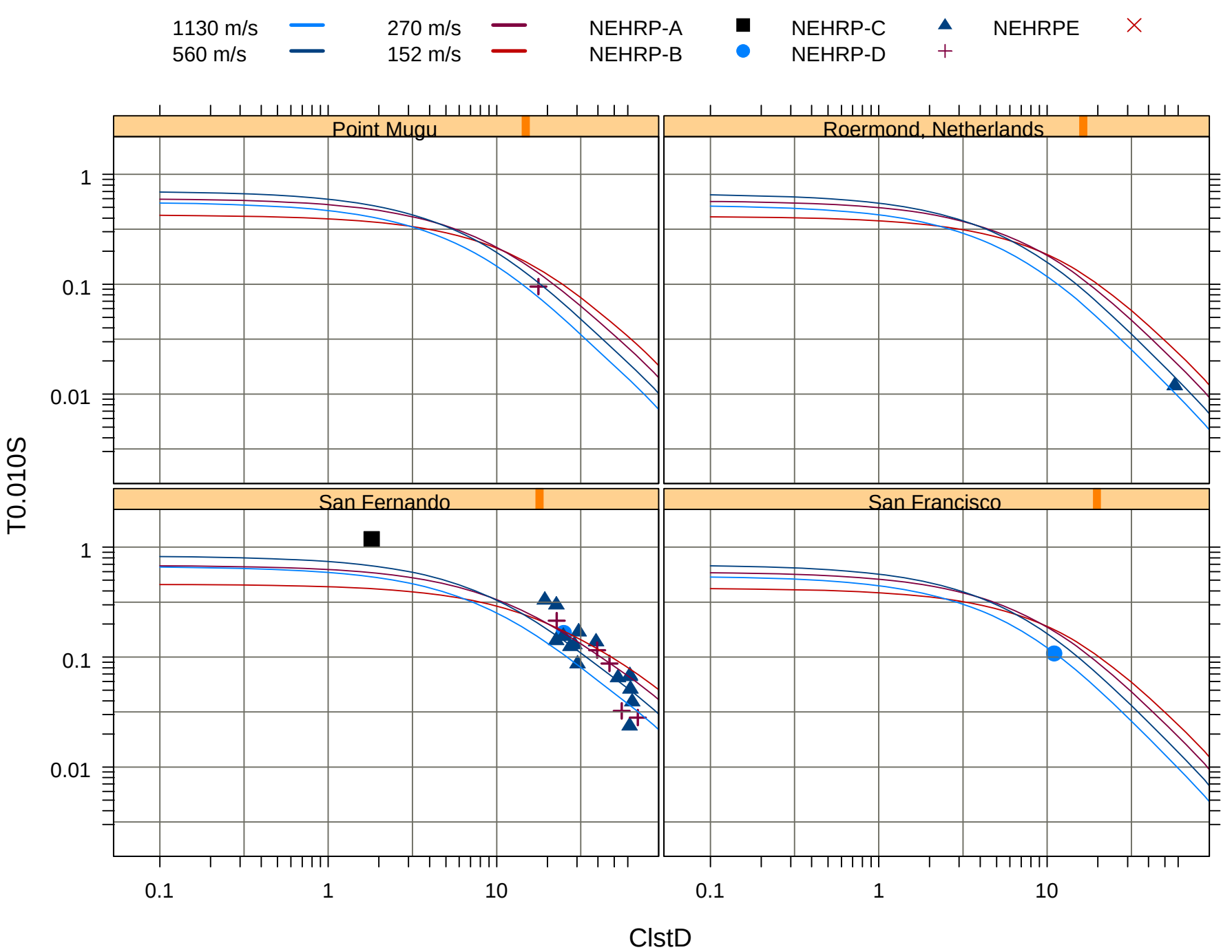
1130 m/s
560 m/s
270 m/s
152 m/s
NEHRP-A
NEHRP-B
NEHRP-C
NEHRP-D
NEHRPE
Point Mugu
Roermond, Netherlands
San Fernando
San Francisco
T0.010S
ClstD
1
0.1
0.01
0.1
1
10

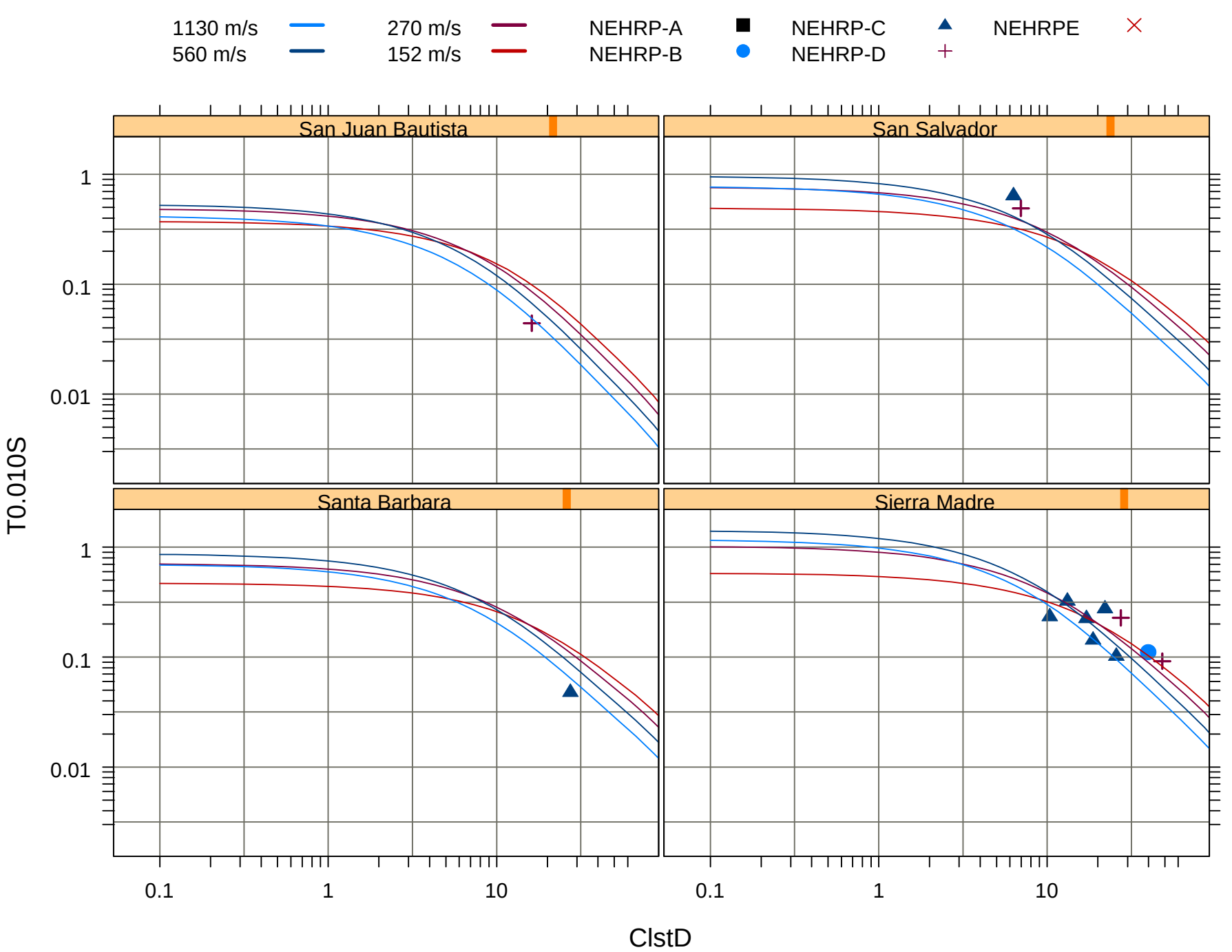
1130 m/s
560 m/s
270 m/s
152 m/s
NEHRP-A
NEHRP-B
NEHRP-C
NEHRP-D
NEHRPE
San Juan Bautista
San Salvador
Santa Barbara
Sierra Madre
T0.010S
ClstD
1
0.1
0.01
0.1
1
10

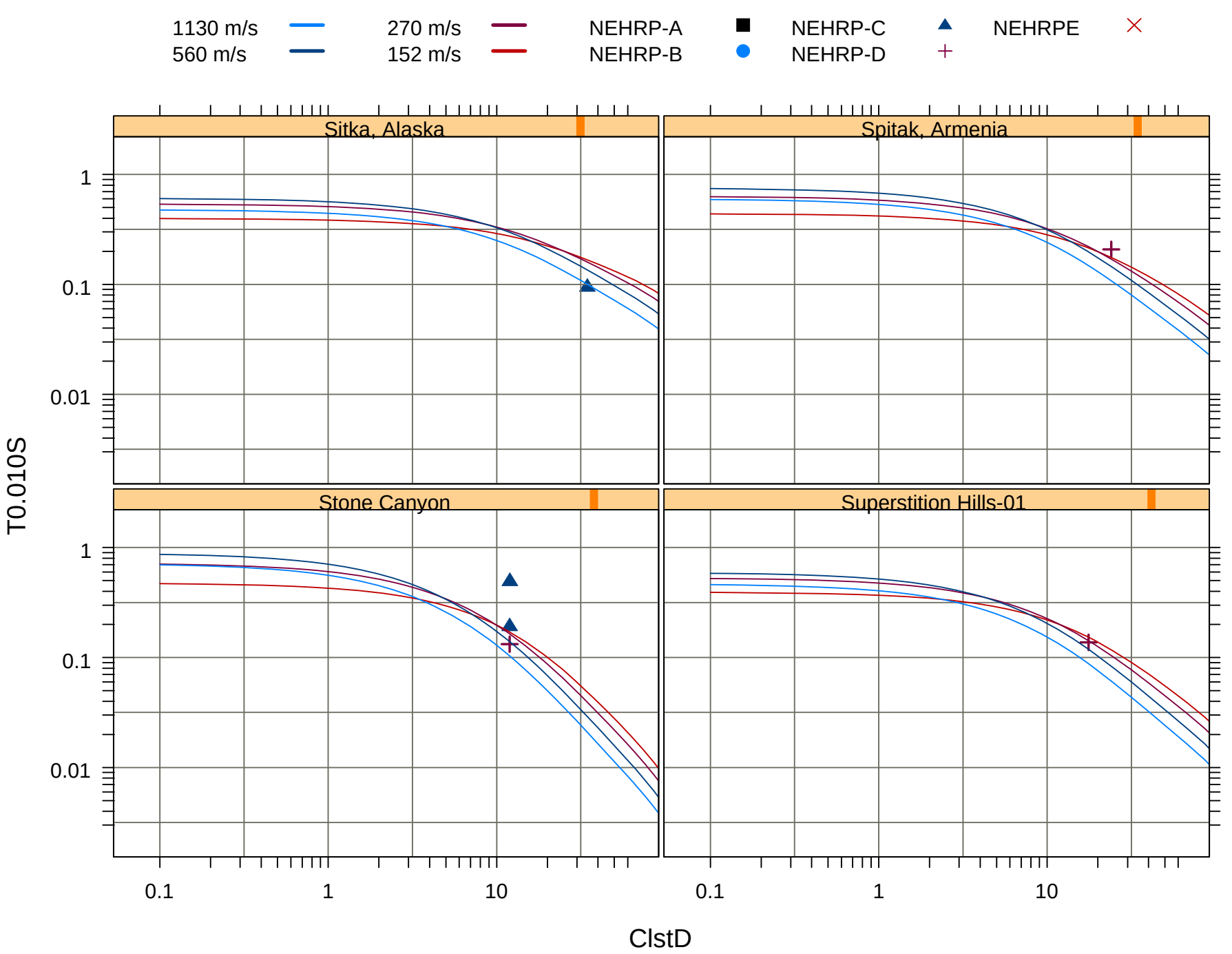
1130 m/s
560 m/s
270 m/s
152 m/s
NEHRP-A
NEHRP-B
NEHRP-C
NEHRP-D
NEHRPE
Sitka, Alaska
Spitak, Armenia
Stone Canyon
Superstition Hills-01
T0.010S
ClstD
1
0.1
0.01
0.1
1
10

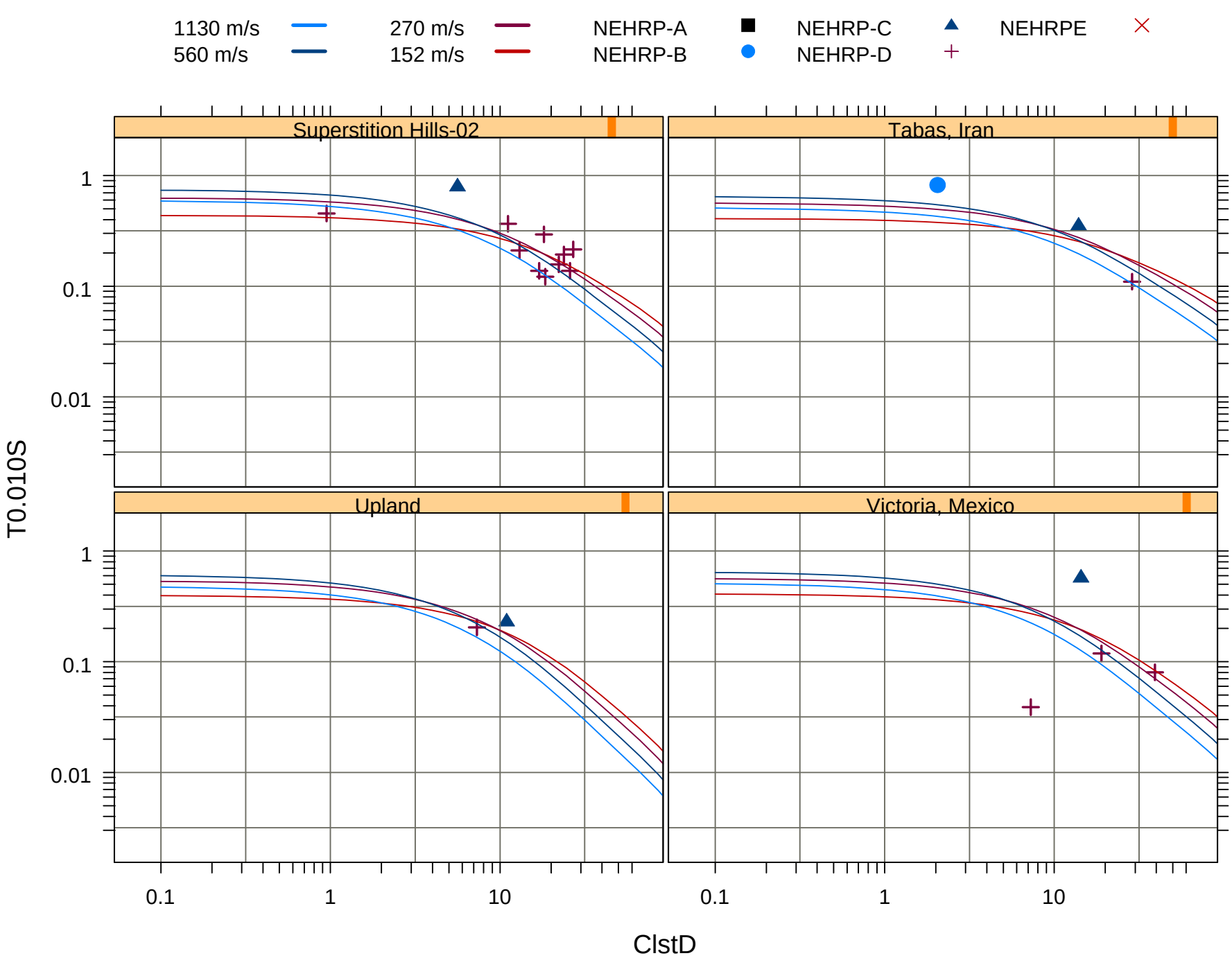
1130 m/s
560 m/s
270 m/s
152 m/s
NEHRP-A
NEHRP-B
NEHRP-C
NEHRP-D
NEHRPE
Superstition Hills-02
Tabas, Iran
Upland
Victoria, Mexico
T0.010S
ClstD
1
0.1
0.01
0.1
1
10

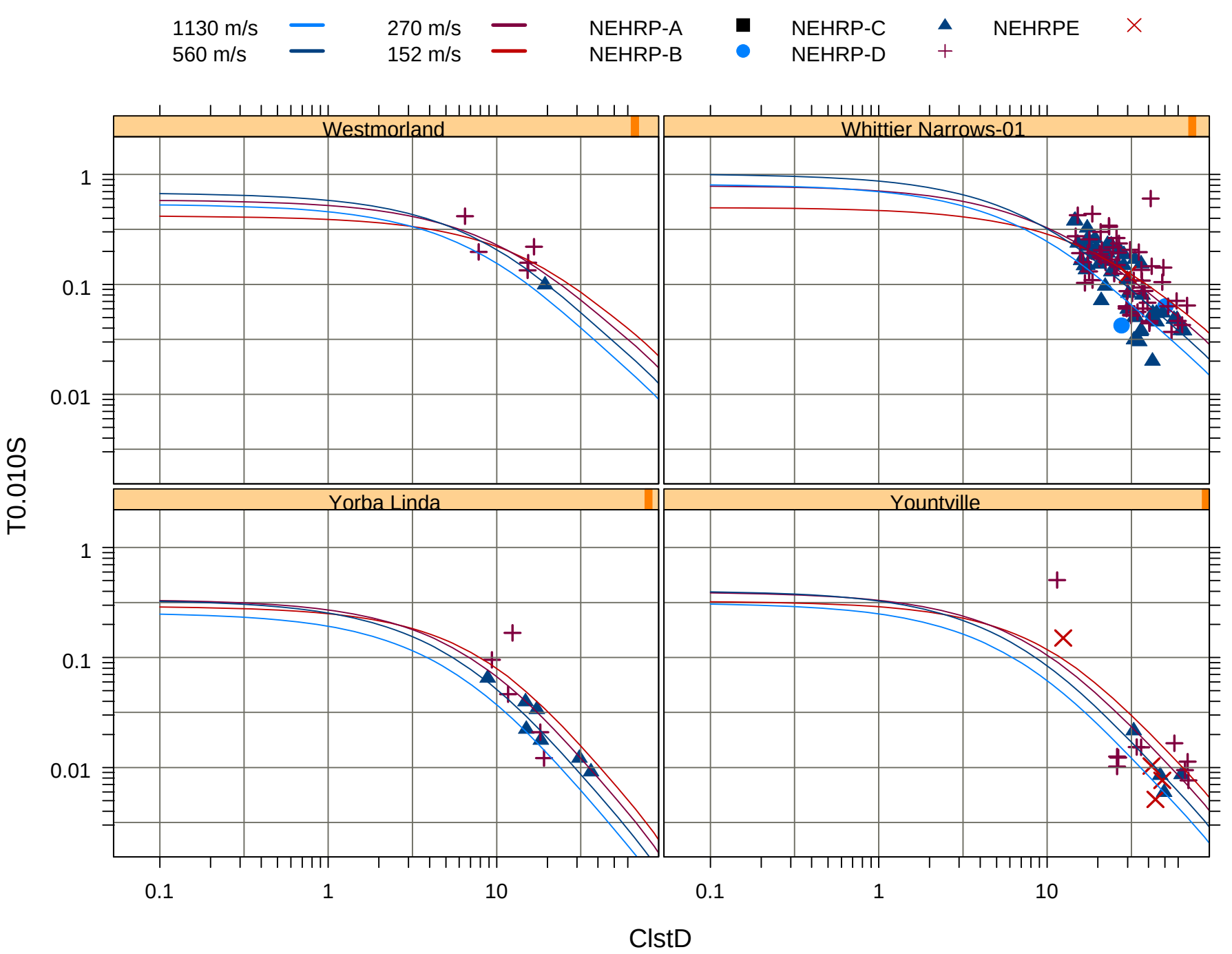
1130 m/s
560 m/s
270 m/s
152 m/s
NEHRP-A
NEHRP-B
NEHRP-C
NEHRP-D
NEHRPE
Westmorland
Whittier Narrows-01
Yorba Linda
Yountville
T0.010S
ClstD
1
0.1
0.01
0.1
1
10

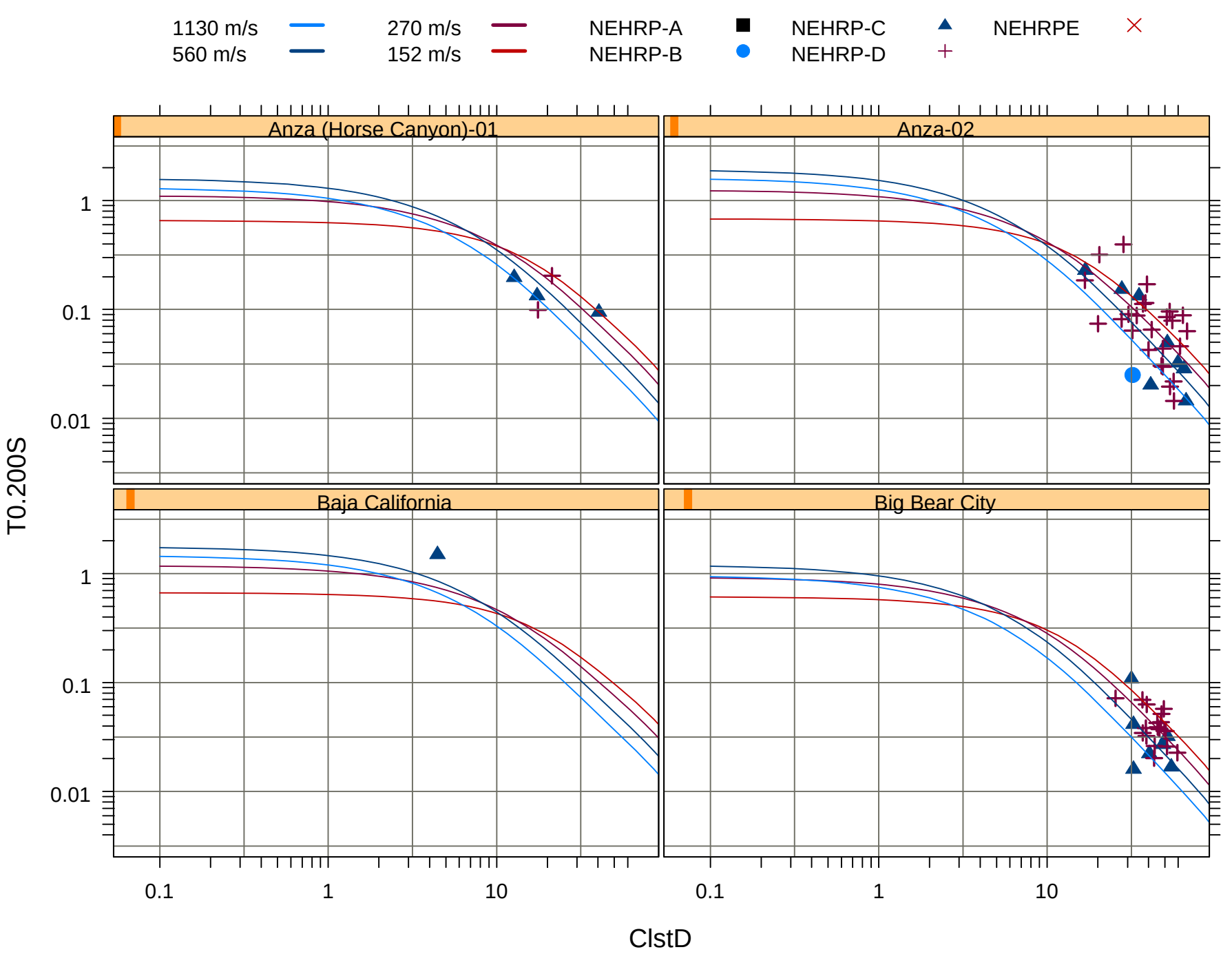
1130 m/s
560 m/s
270 m/s
152 m/s
NEHRP-A
NEHRP-B
NEHRP-C
NEHRP-D
NEHRPE
Anza (Horse Canyon)-01
Anza-02
Baja California
Big Bear City
T0.200S
ClstD
1
0.1
0.01
0.1
1
10

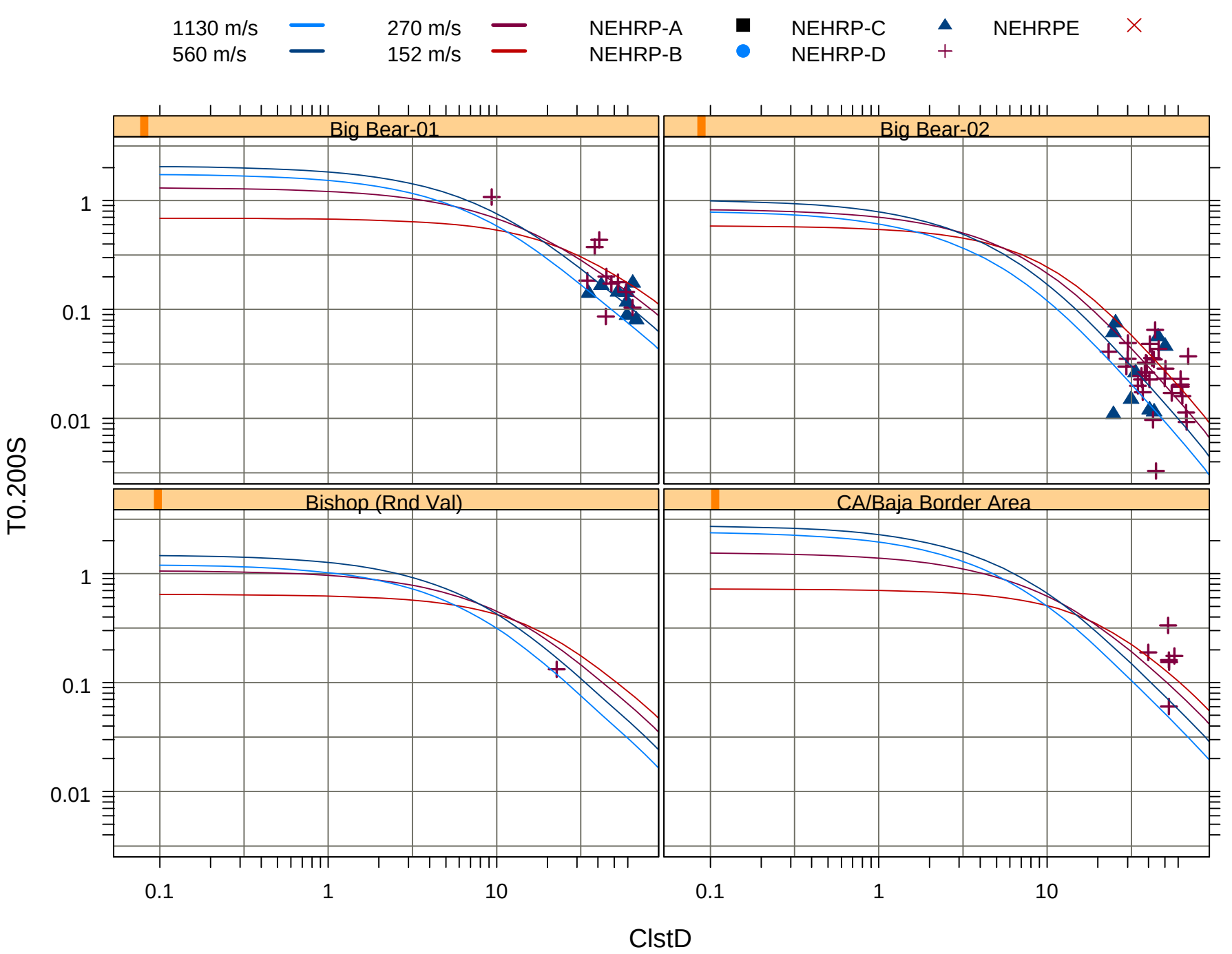
1130 m/s
560 m/s
270 m/s
152 m/s
NEHRP-A
NEHRP-B
NEHRP-C
NEHRP-D
NEHRPE
Big Bear-01
Big Bear-02
Bishop (Rnd Val)
CA/Baja Border Area
T0.200S
ClstD
1
0.1
0.01
0.1
1
10

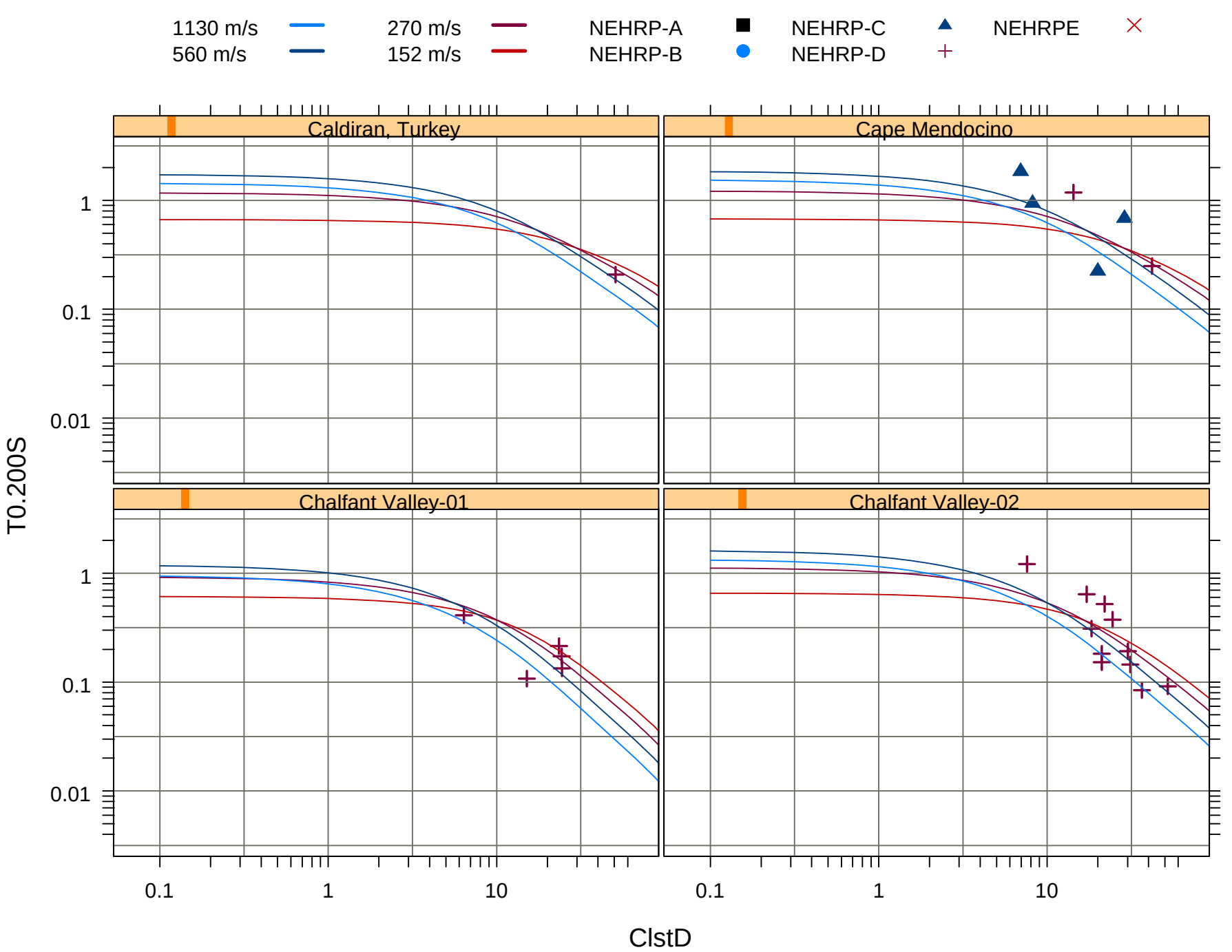
1130 m/s
560 m/s
270 m/s
152 m/s
NEHRP-A
NEHRP-B
NEHRP-C
NEHRP-D
NEHRPE
Caldiran, Turkey
Cape Mendocino
Chalfant Valley-01
Chalfant Valley-02
T0.200S
ClstD
1
0.1
0.01
0.1
1
10

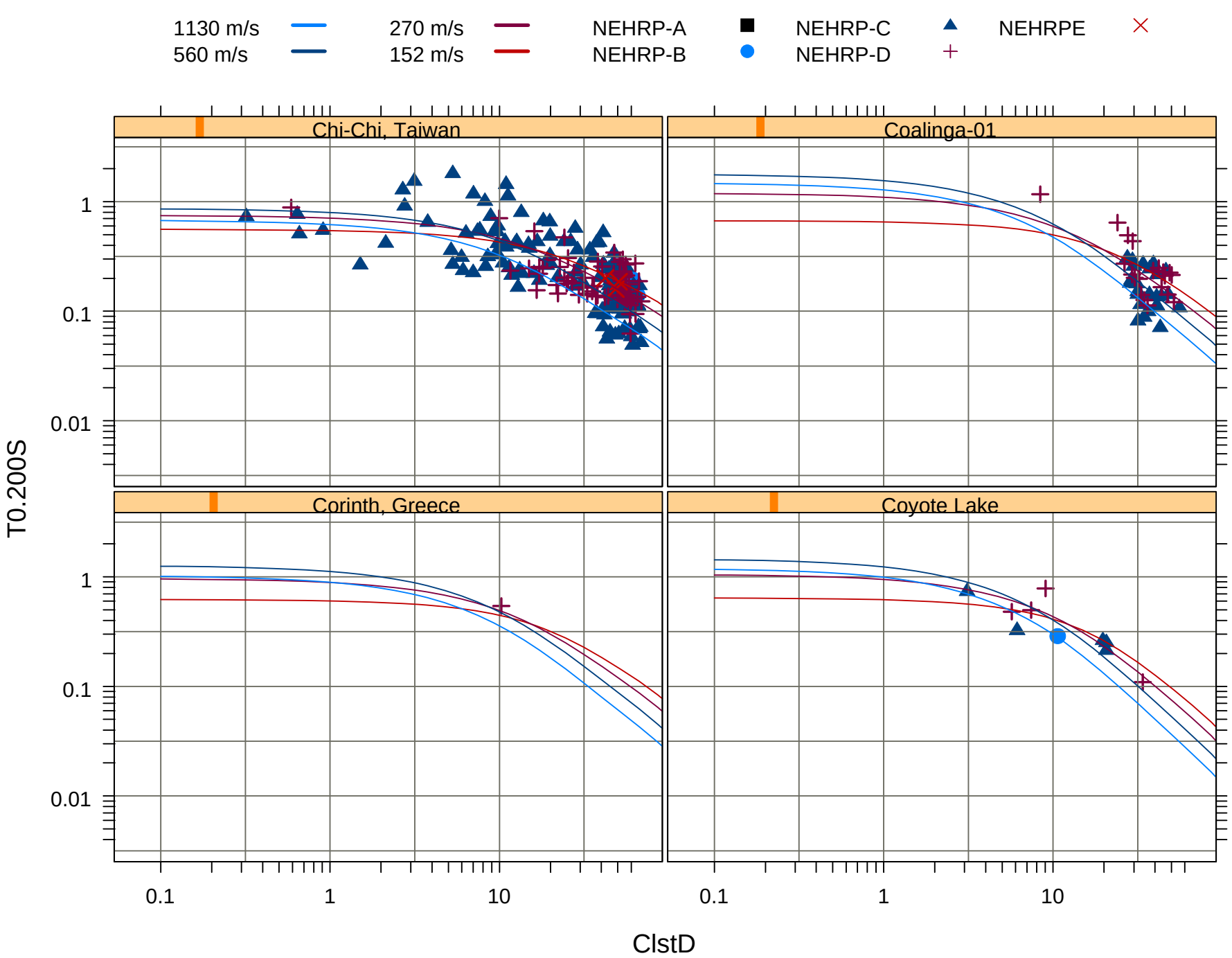
1130 m/s
560 m/s
270 m/s
152 m/s
NEHRP-A
NEHRP-B
NEHRP-C
NEHRP-D
NEHRPE
Chi-Chi, Taiwan
Coalinga-01
Corinth, Greece
Coyote Lake
T0.200S
ClstD
1
0.1
0.01
0.1
1
10

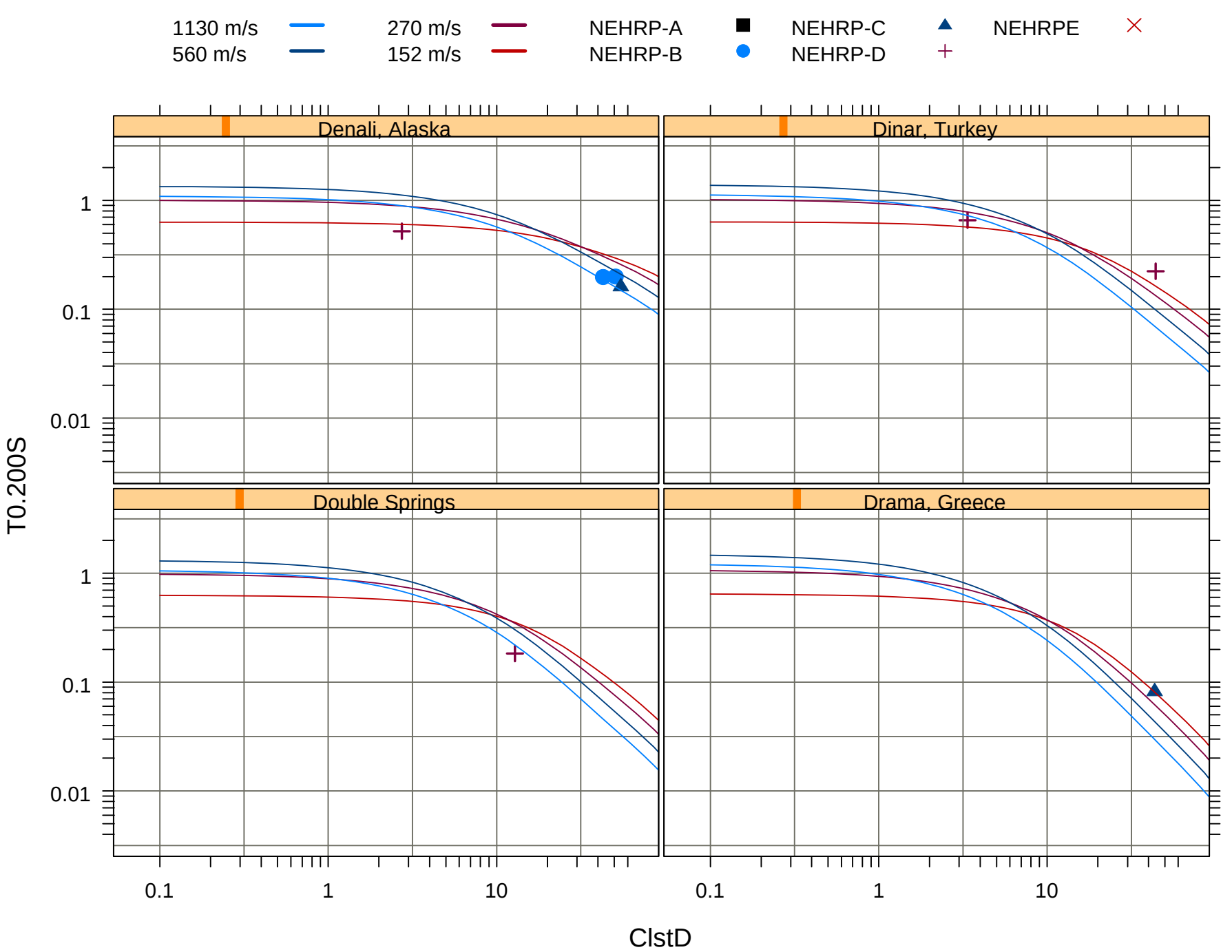
1130 m/s
560 m/s
270 m/s
152 m/s
NEHRP-A
NEHRP-B
NEHRP-C
NEHRP-D
NEHRPE
Denali, Alaska
Dinar, Turkey
Double Springs
Drama, Greece
T0.200S
ClstD
1
0.1
0.01
0.1
1
10

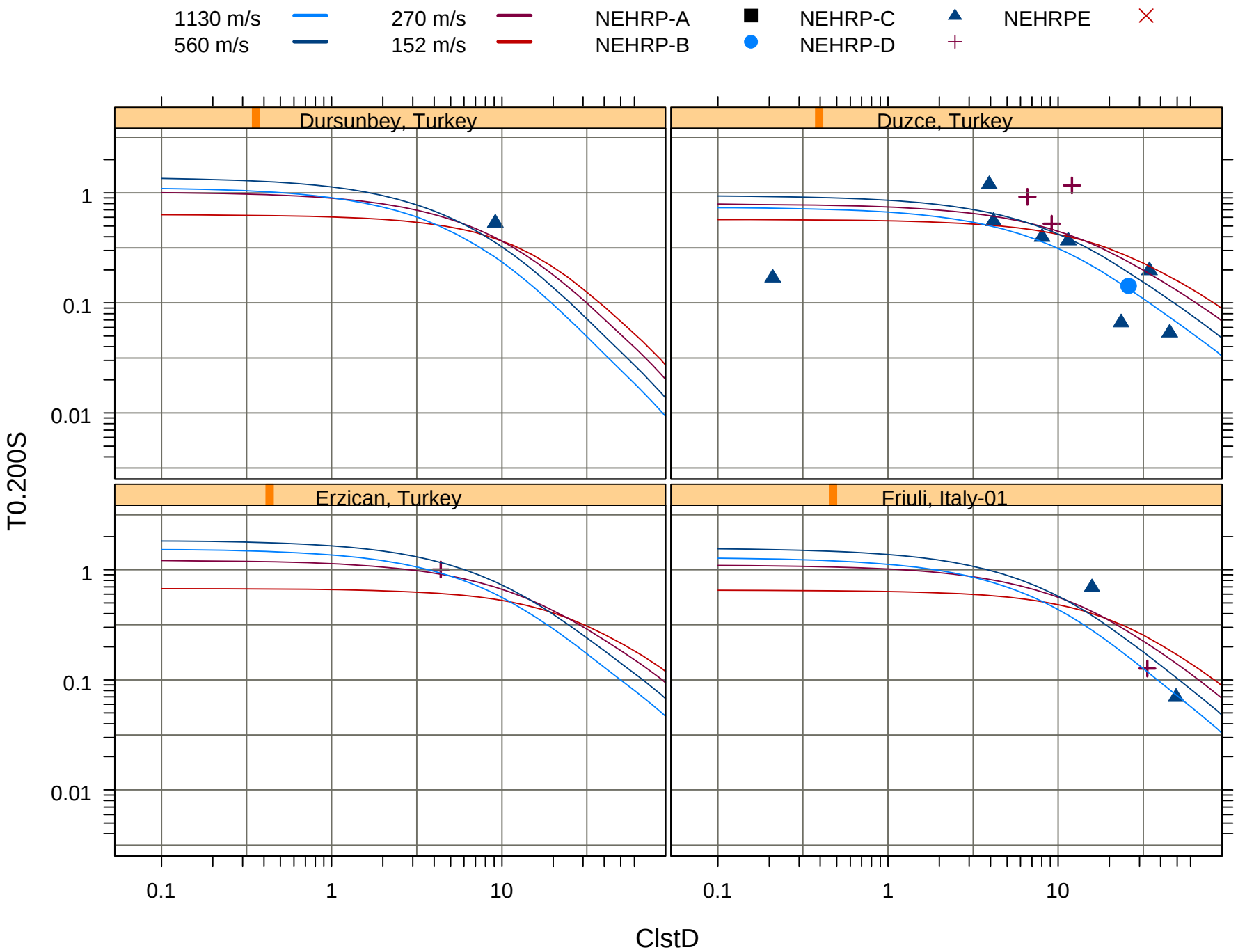
1130 m/s
560 m/s
270 m/s
152 m/s
NEHRP-A
NEHRP-B
NEHRP-C
NEHRP-D
NEHRPE
Dursunbey, Turkey
Duzce, Turkey
Erzican, Turkey
Friuli, Italy-01
T0.200S
ClstD
1
0.1
0.01
0.1
1
10

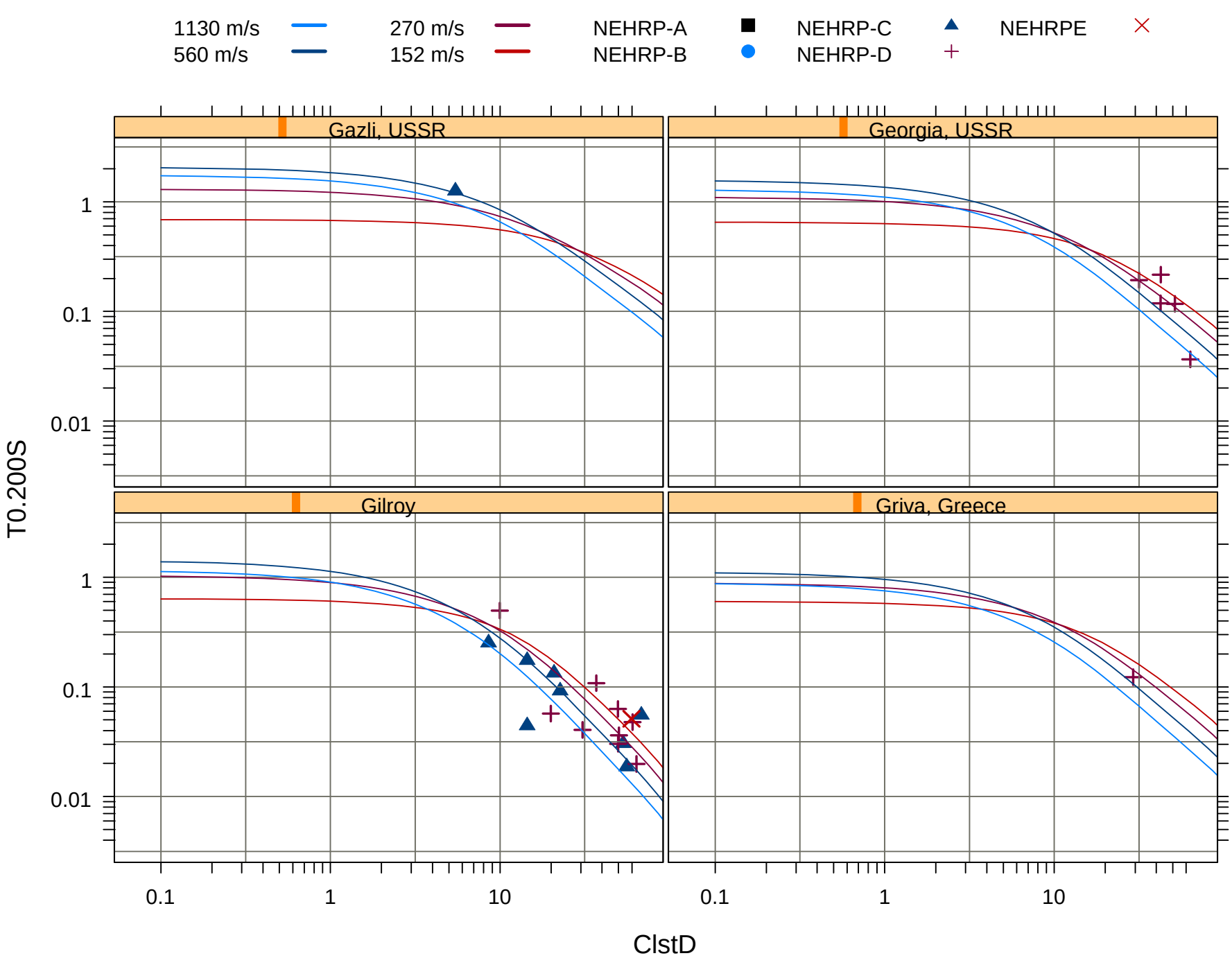
1130 m/s
560 m/s
270 m/s
152 m/s
NEHRP-A
NEHRP-B
NEHRP-C
NEHRP-D
NEHRPE
Gazli, USSR
Georgia, USSR
Gilroy
Griva, Greece
T0.200S
ClstD
1
0.1
0.01
0.1
1
10

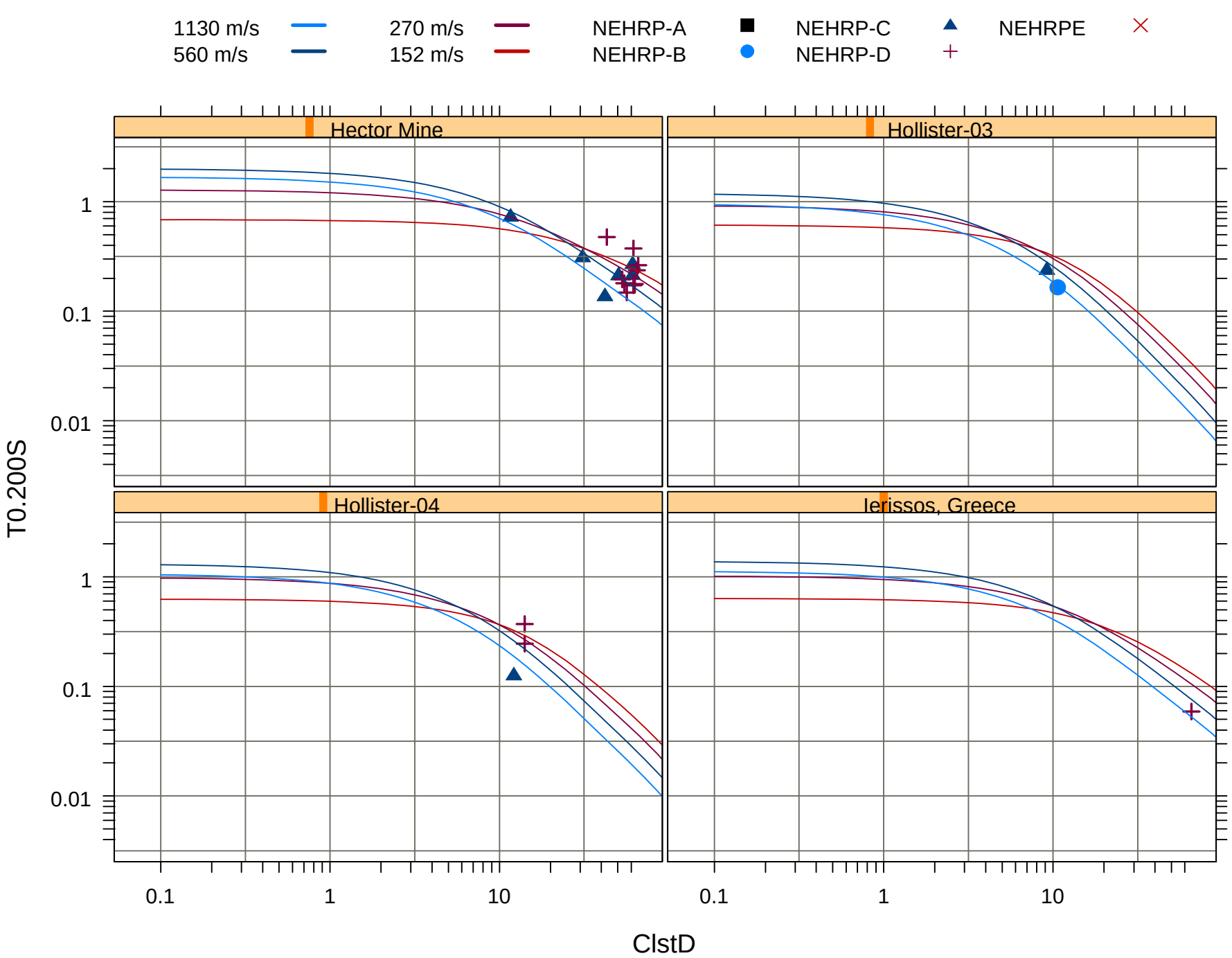
1130 m/s
560 m/s
270 m/s
152 m/s
NEHRP-A
NEHRP-B
NEHRP-C
NEHRP-D
NEHRPE
Hector Mine
Hollister-03
Hollister-04
Ierissos, Greece
T0.200S
ClstD
1
0.1
0.01
0.1
1
10

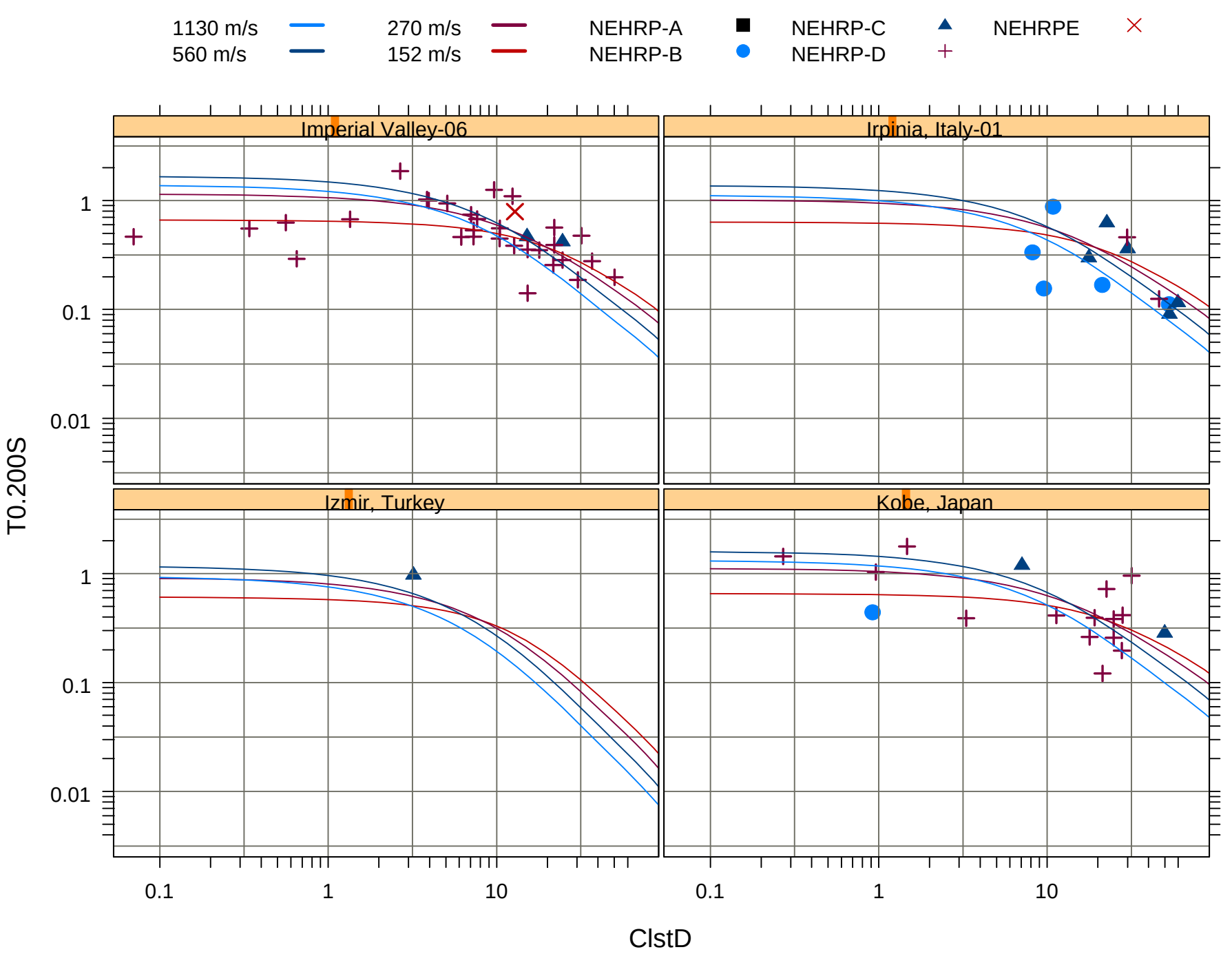
1130 m/s
560 m/s
270 m/s
152 m/s
NEHRP-A
NEHRP-B
NEHRP-C
NEHRP-D
NEHRPE
Imperial Valley-06
Irpinia, Italy-01
Izmir, Turkey
Kobe, Japan
T0.200S
ClstD
1
0.1
0.01
0.1
1
10

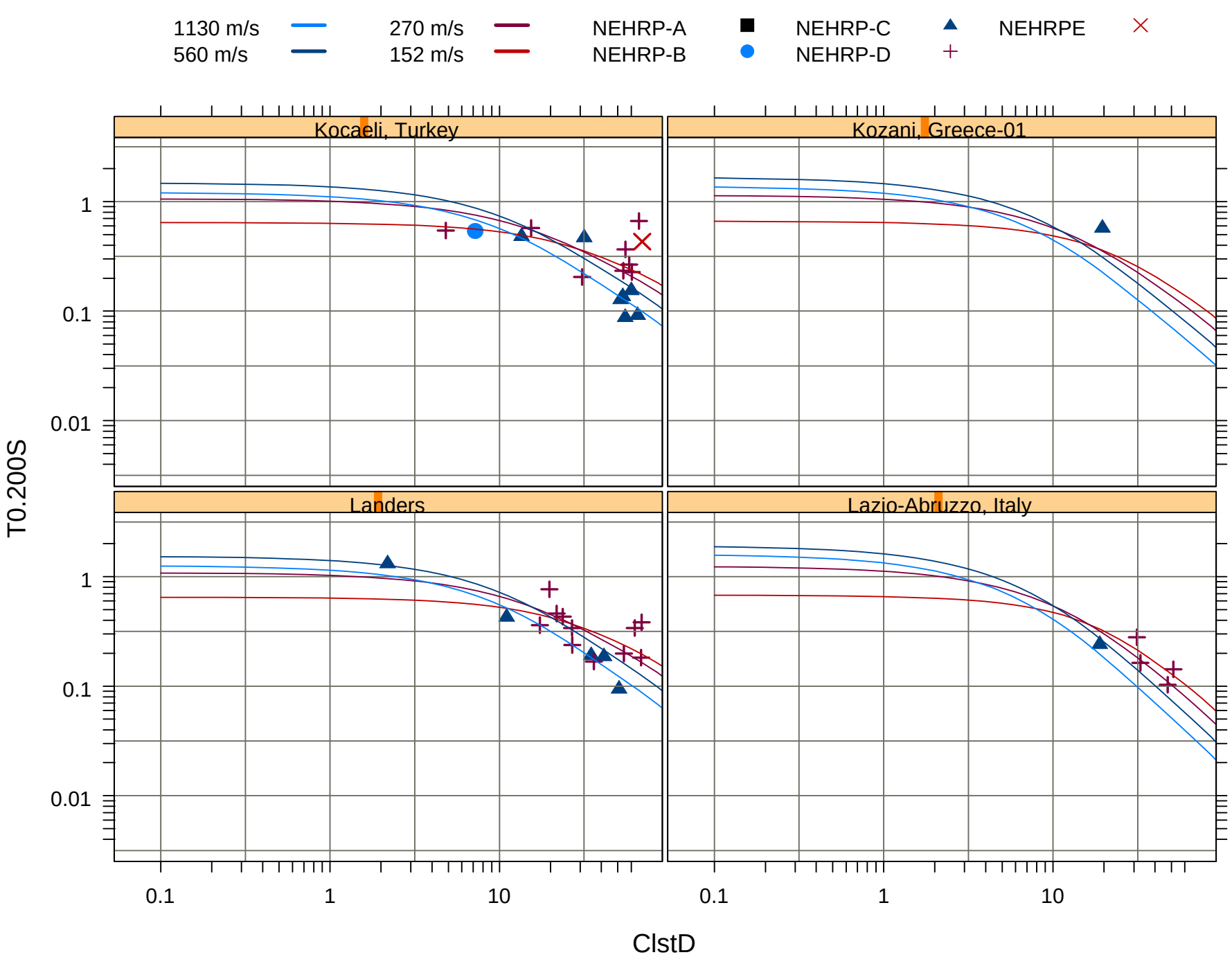
1130 m/s
560 m/s
270 m/s
152 m/s
NEHRP-A
NEHRP-B
NEHRP-C
NEHRP-D
NEHRPE
Kocaeli, Turkey
Kozani, Greece-01
Landers
Lazio-Abruzzo, Italy
T0.200S
ClstD
1
0.1
0.01
0.1
1
10

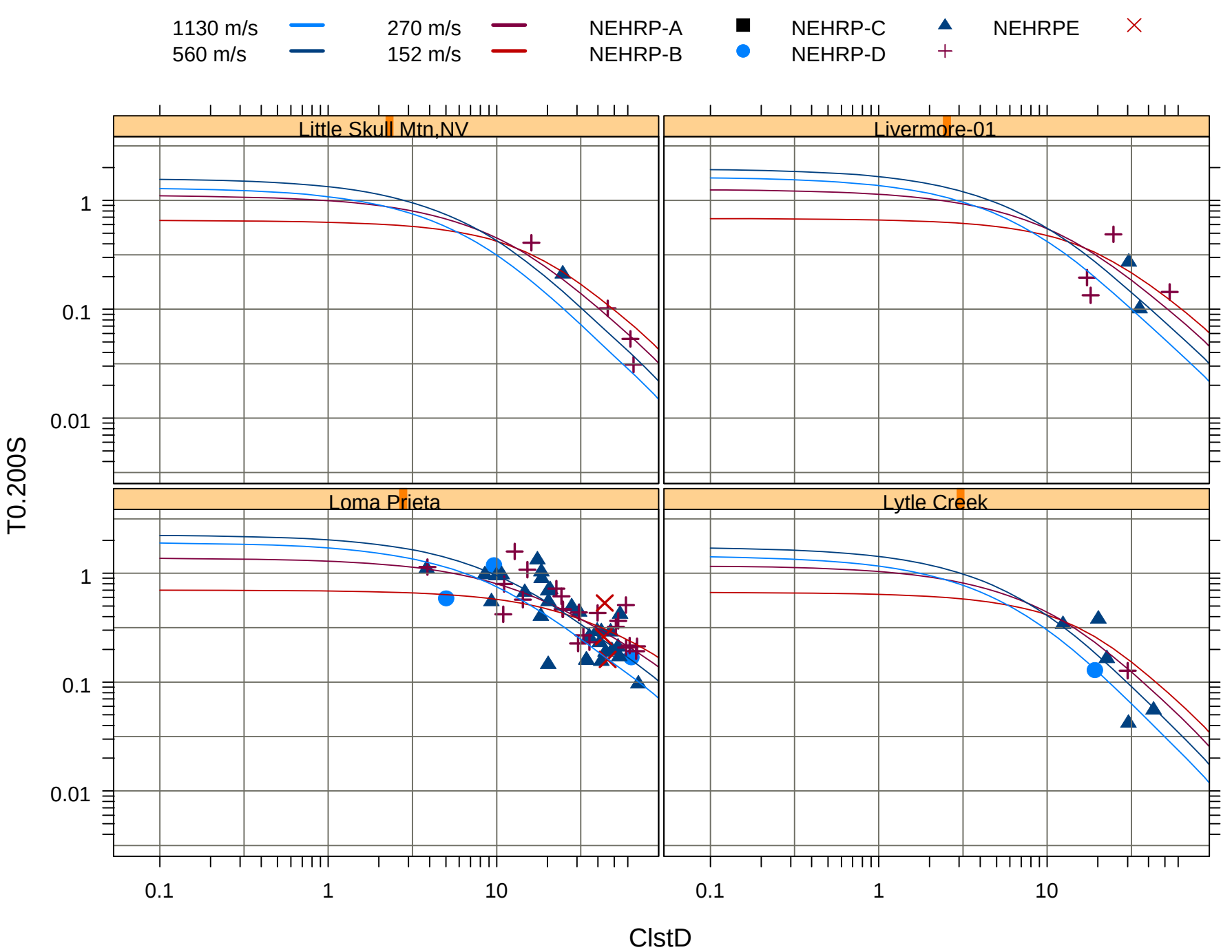
1130 m/s
560 m/s
270 m/s
152 m/s
NEHRP-A
NEHRP-B
NEHRP-C
NEHRP-D
NEHRPE
Little Skull Mtn,NV
Livermore-01
Loma Prieta
Lytle Creek
T0.200S
ClstD
1
0.1
0.01
0.1
1
10

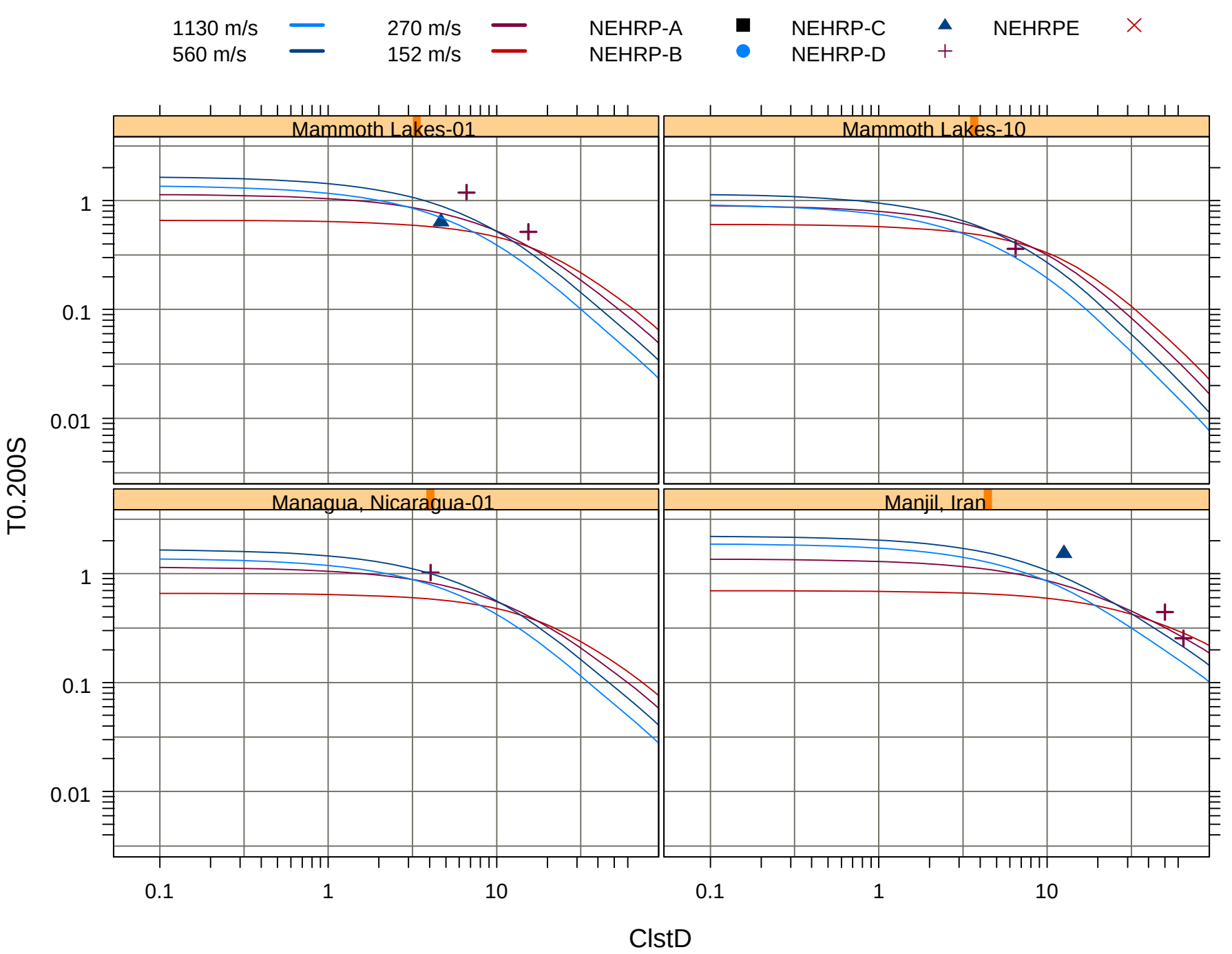
1130 m/s
560 m/s
270 m/s
152 m/s
NEHRP-A
NEHRP-B
NEHRP-C
NEHRP-D
NEHRPE
Mammoth Lakes-01
Mammoth Lakes-10
Managua, Nicaragua-01
Manjil, Iran
T0.200S
ClstD
1
0.1
0.01
0.1
1
10

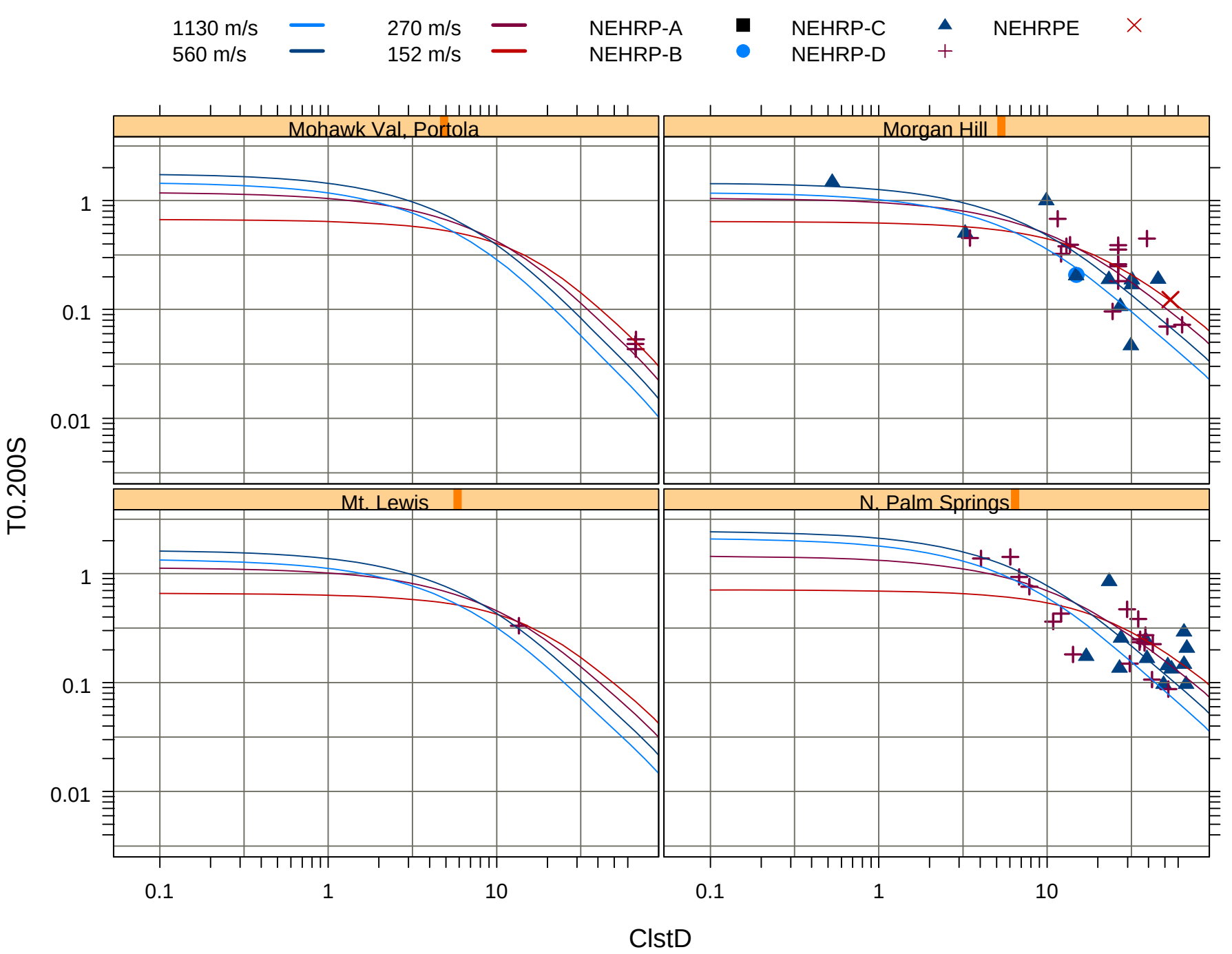
1130 m/s
560 m/s
270 m/s
152 m/s
NEHRP-A
NEHRP-B
NEHRP-C
NEHRP-D
NEHRPE
Mohawk Val, Portola
Morgan Hill
Mt. Lewis
N. Palm Springs
T0.200S
ClstD
1
0.1
0.01
0.1
1
10

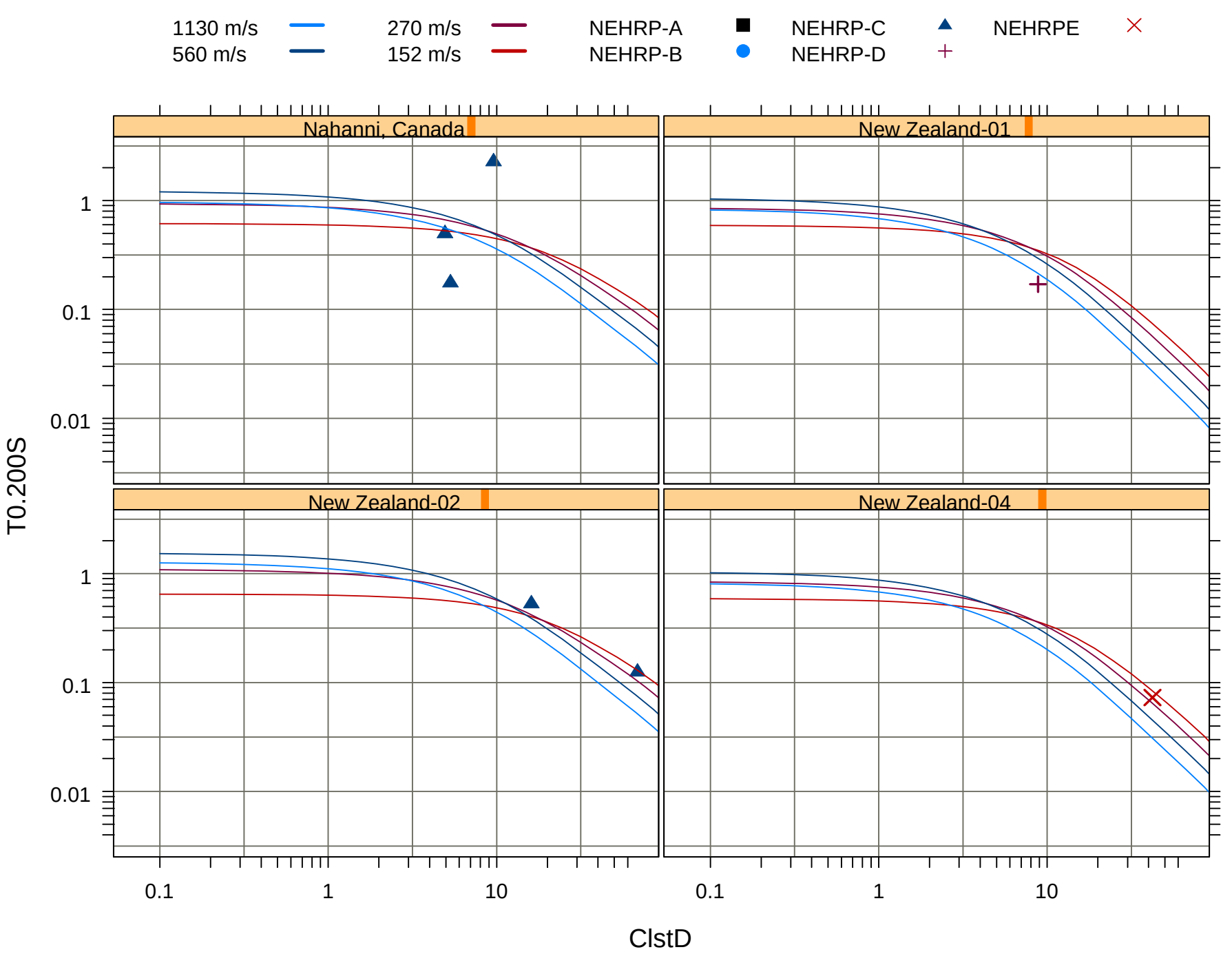
1130 m/s
560 m/s
270 m/s
152 m/s
NEHRP-A
NEHRP-B
NEHRP-C
NEHRP-D
NEHRPE
Nahanni, Canada
New Zealand-01
New Zealand-02
New Zealand-04
T0.200S
ClstD
1
0.1
0.01
0.1
1
10

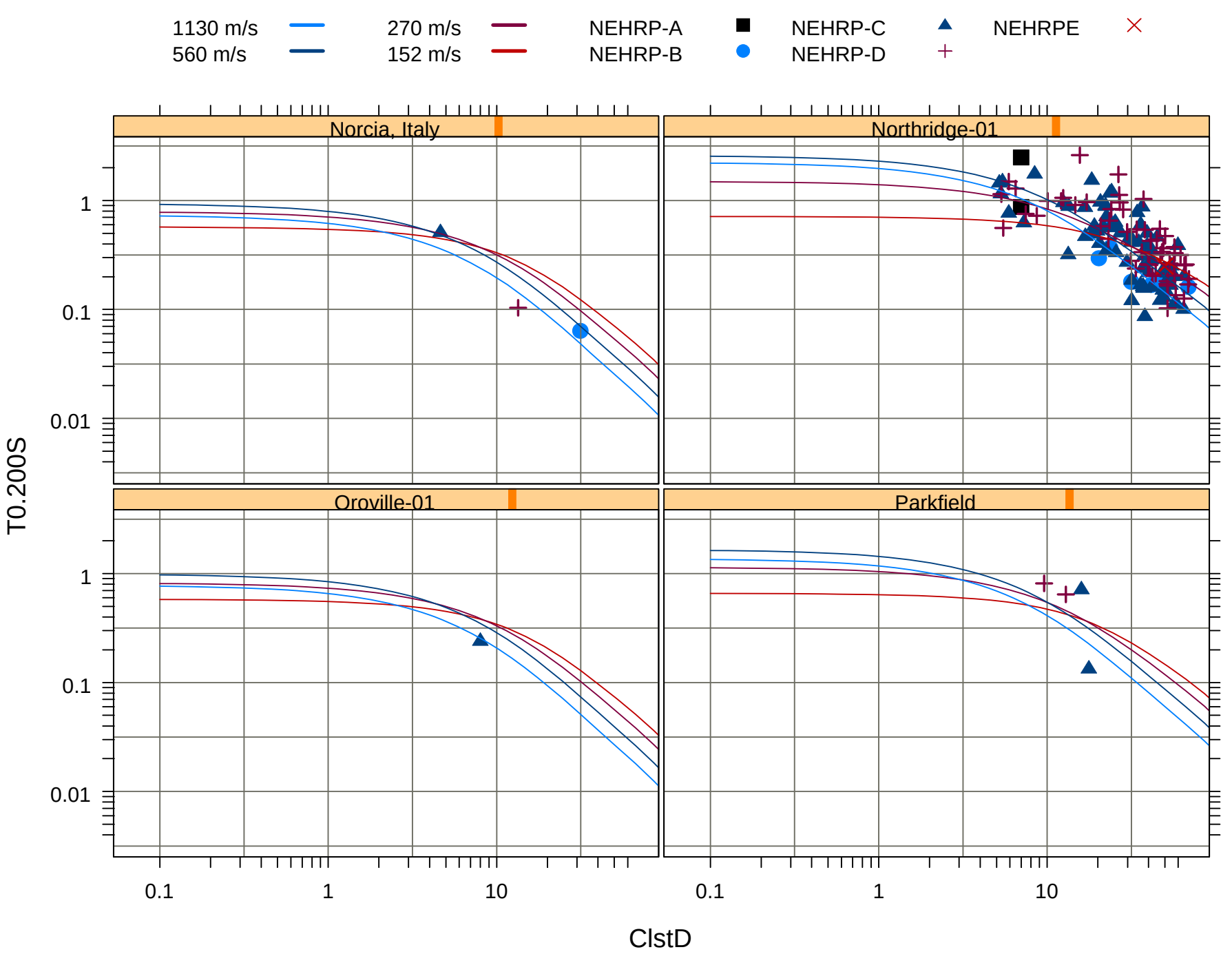
1130 m/s
560 m/s
270 m/s
152 m/s
NEHRP-A
NEHRP-B
NEHRP-C
NEHRP-D
NEHRPE
Norcia, Italy
Northridge-01
Oroville-01
Parkfield
T0.200S
ClstD
1
0.1
0.01
0.1
1
10

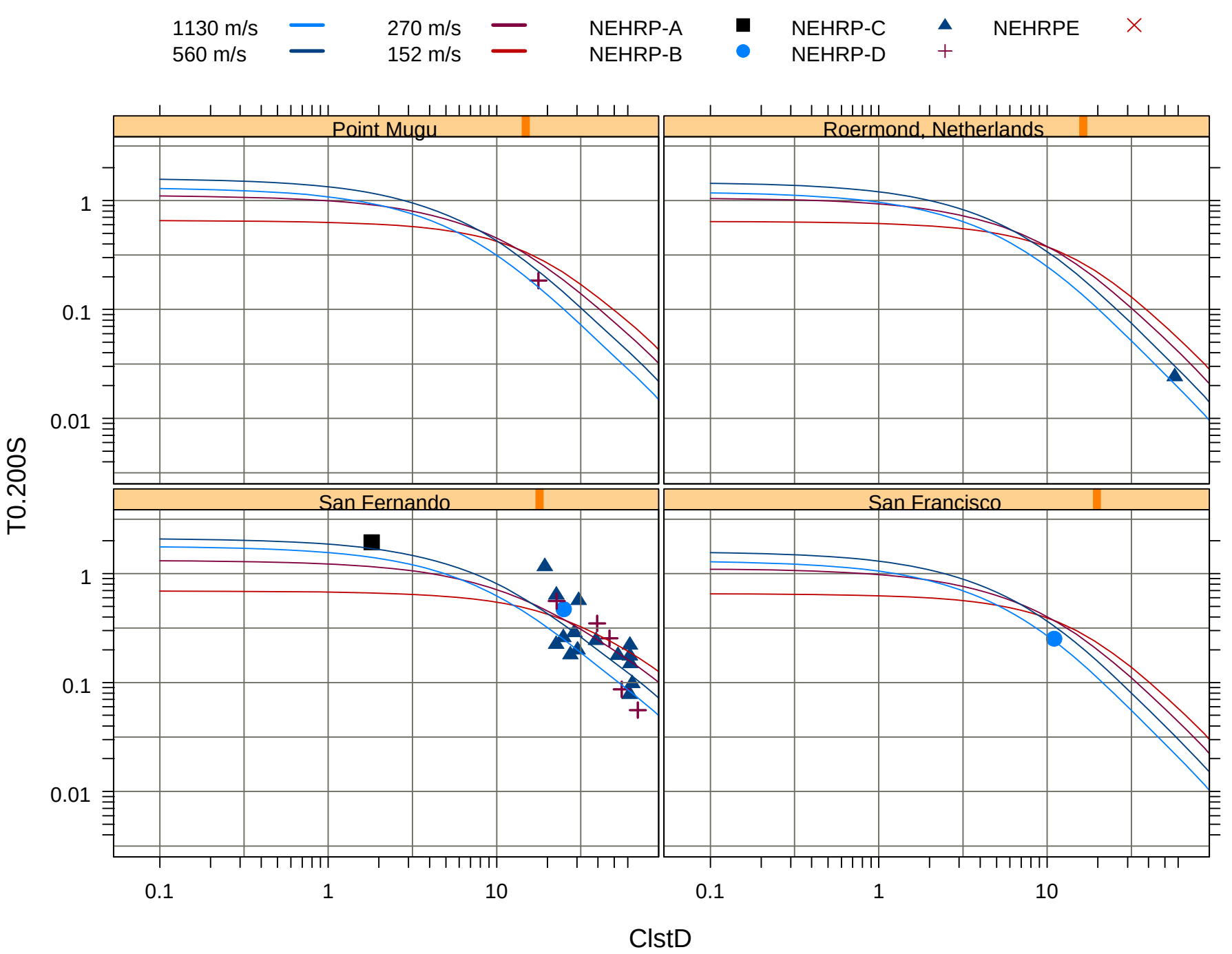
1130 m/s
560 m/s
270 m/s
152 m/s
NEHRP-A
NEHRP-B
NEHRP-C
NEHRP-D
NEHRPE
Point Mugu
Roermond, Netherlands
San Fernando
San Francisco
T0.200S
ClstD
1
0.1
0.01
0.1
1
10

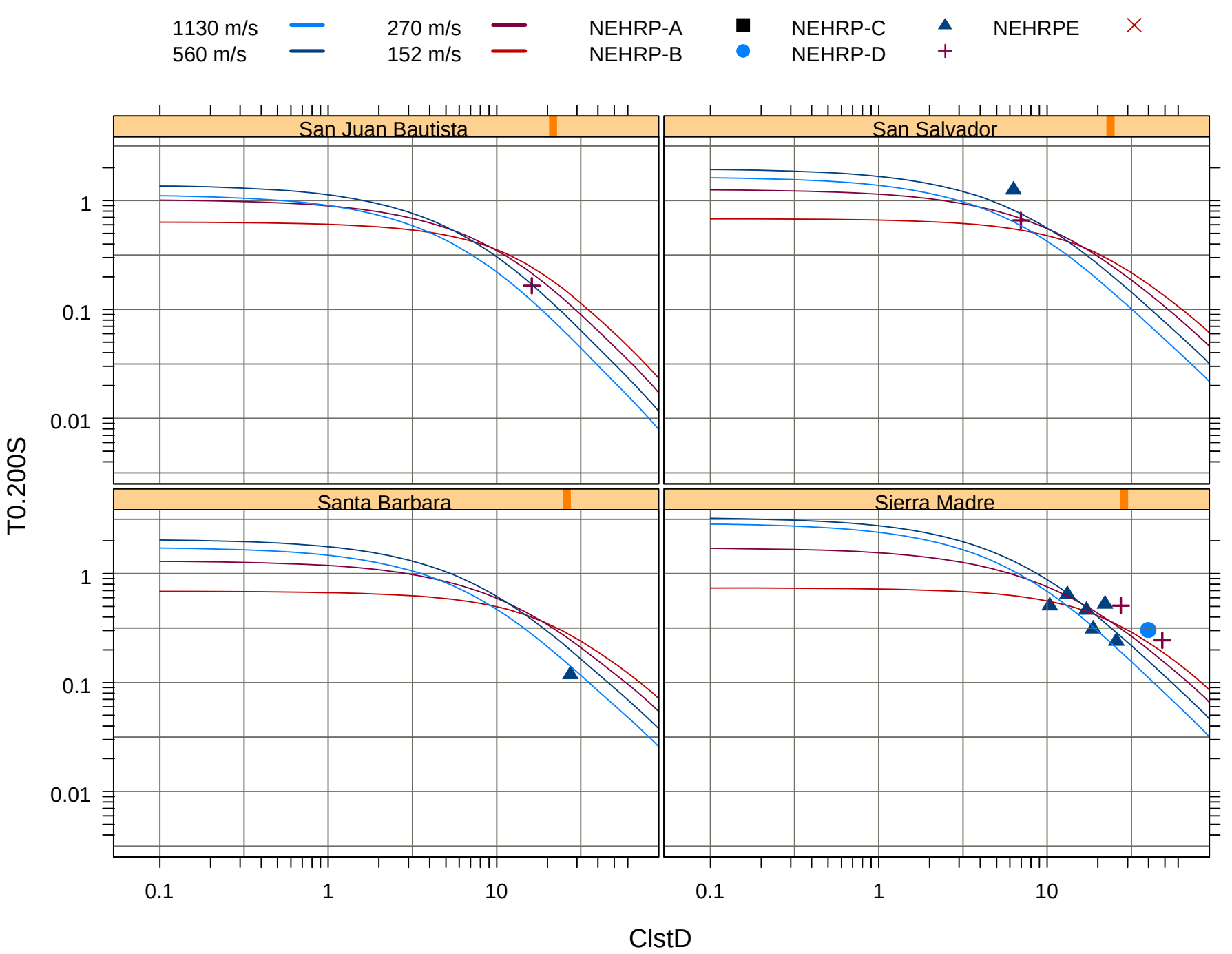
1130 m/s
560 m/s
270 m/s
152 m/s
NEHRP-A
NEHRP-B
NEHRP-C
NEHRP-D
NEHRPE
San Juan Bautista
San Salvador
Santa Barbara
Sierra Madre
T0.200S
ClstD
1
0.1
0.01
0.1
1
10

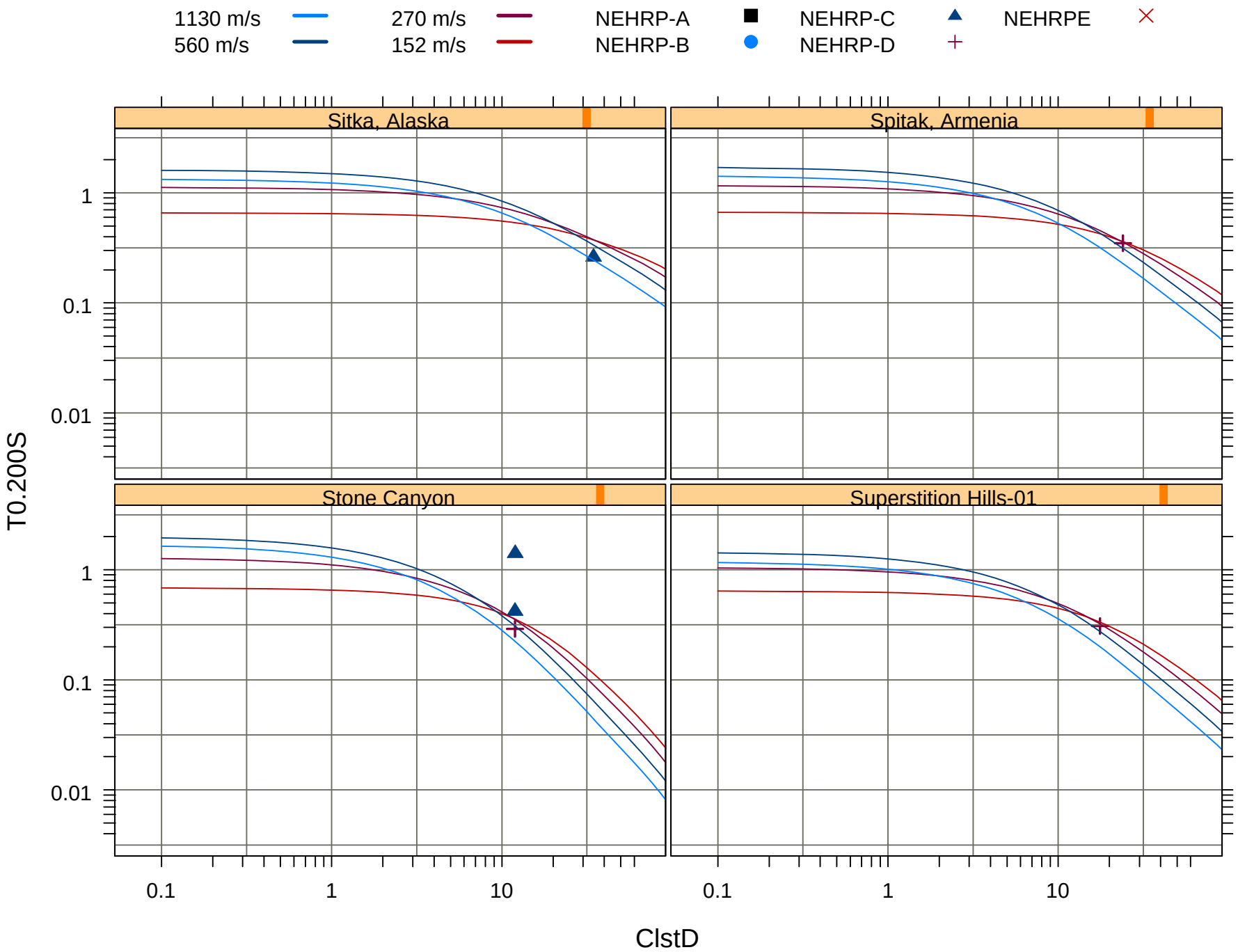
1130 m/s
560 m/s
270 m/s
152 m/s
NEHRP-A
NEHRP-B
NEHRP-C
NEHRP-D
NEHRPE
Sitka, Alaska
Spitak, Armenia
Stone Canyon
Superstition Hills-01
T0.200S
ClstD
1
0.1
0.01
0.1
1
10

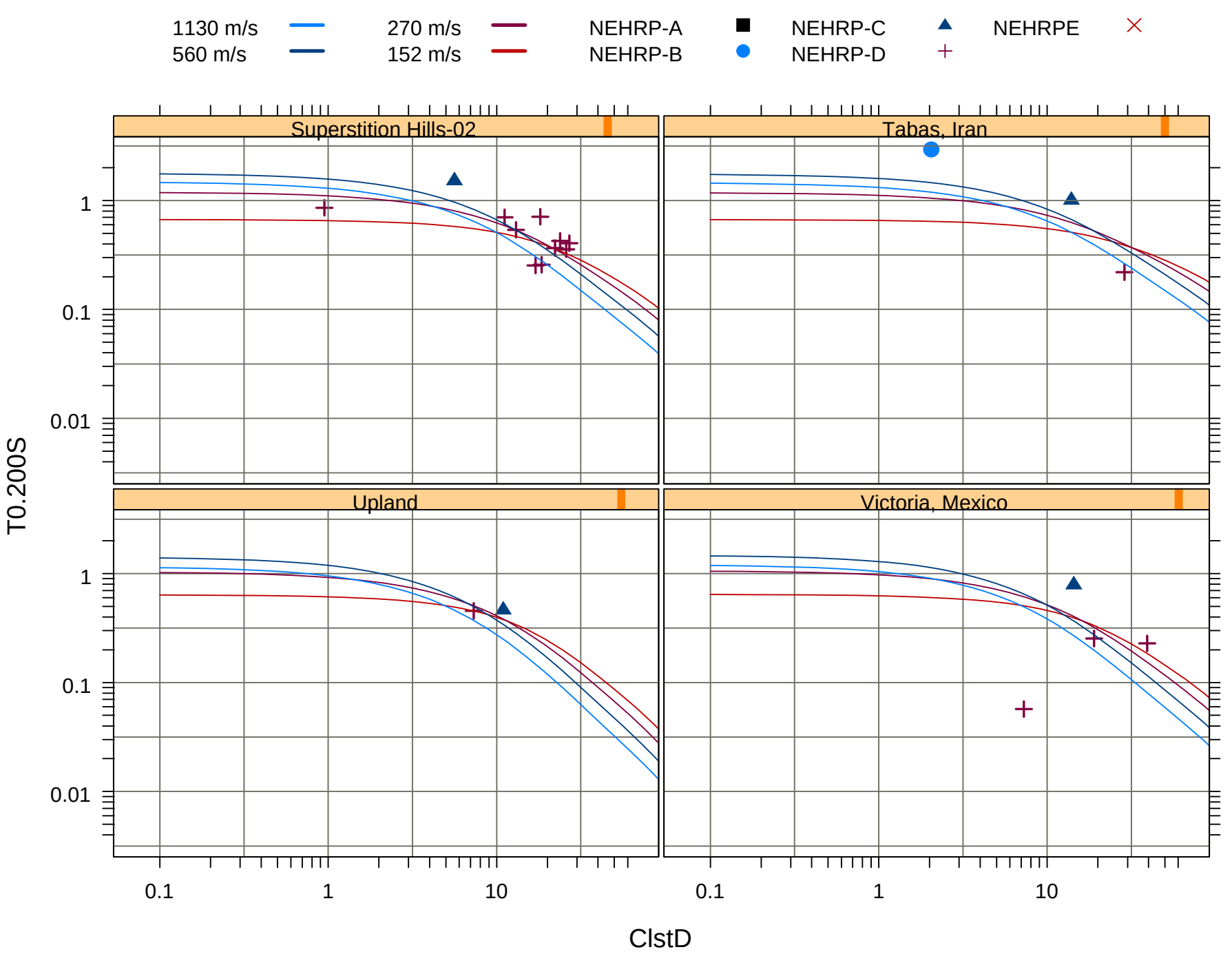
1130 m/s
560 m/s
270 m/s
152 m/s
NEHRP-A
NEHRP-B
NEHRP-C
NEHRP-D
NEHRPE
Superstition Hills-02
Tabas, Iran
Upland
Victoria, Mexico
T0.200S
ClstD
0.01
0.1
1
10

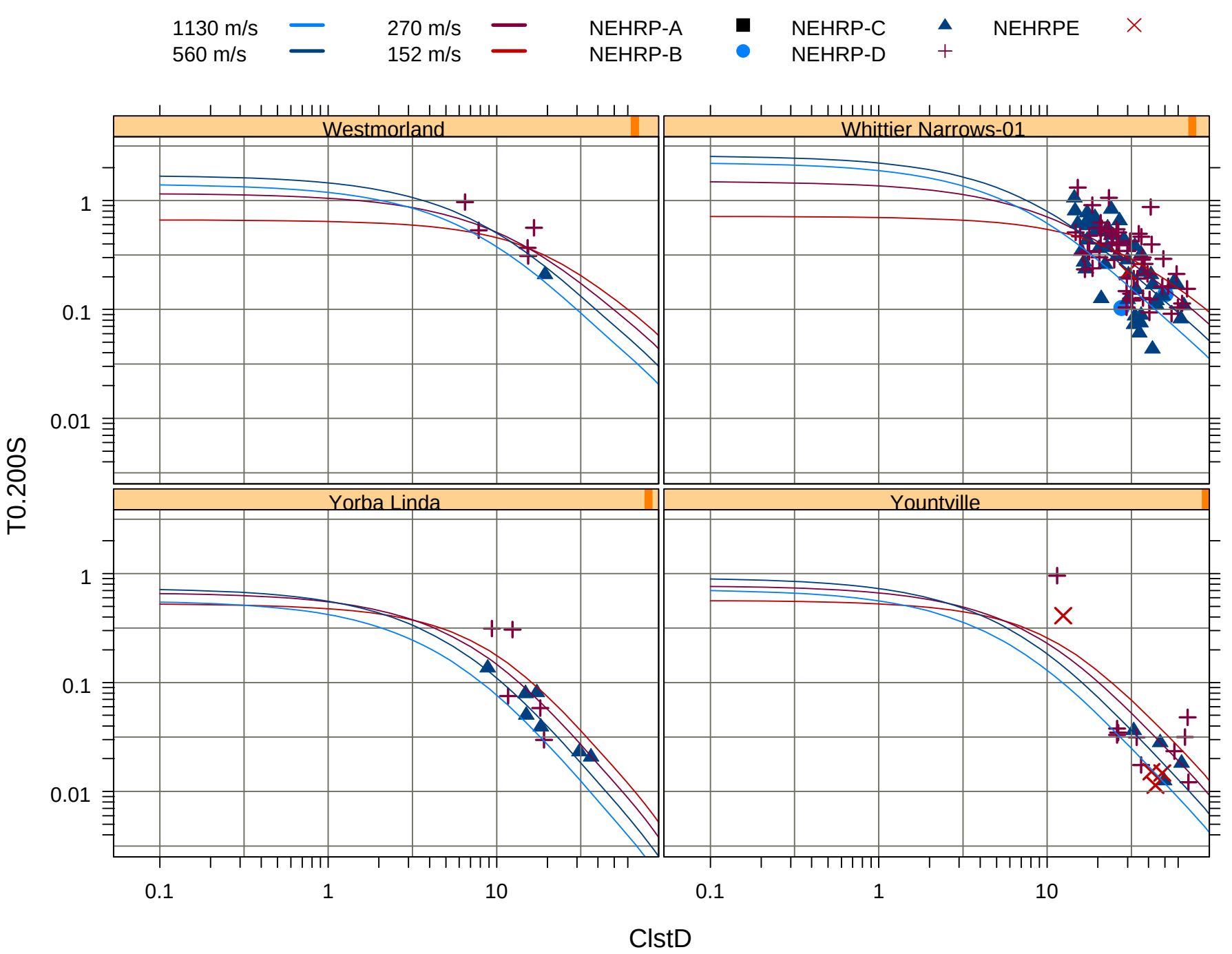
1130 m/s
560 m/s
270 m/s
152 m/s
NEHRP-A
NEHRP-B
NEHRP-C
NEHRP-D
NEHRPE
Westmorland
Whittier Narrows-01
Yorba Linda
Yountville
T0.200S
ClstD
1
0.1
0.01
0.1
1
10

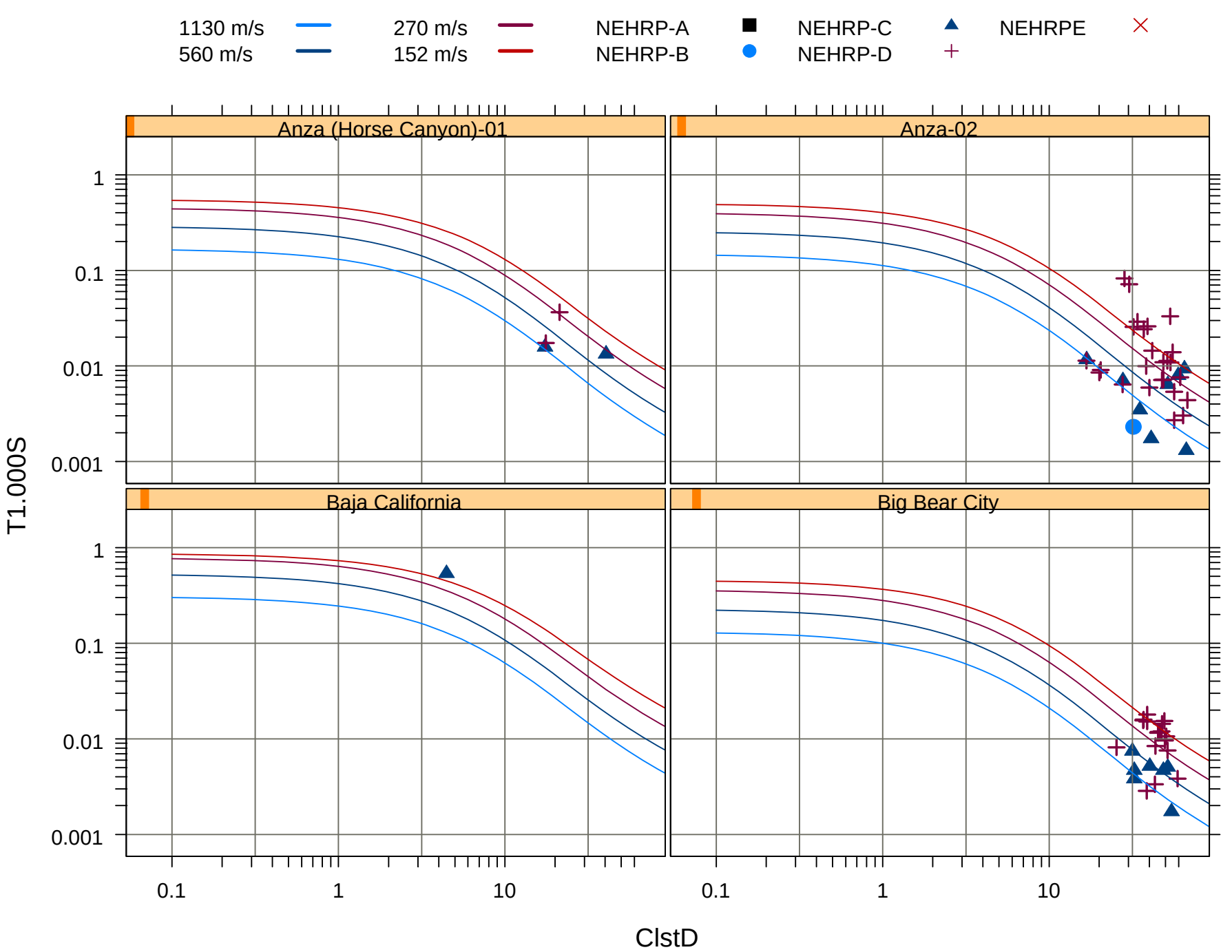
1130 m/s
560 m/s
270 m/s
152 m/s
NEHRP-A
NEHRP-B
NEHRP-C
NEHRP-D
NEHRPE
Anza (Horse Canyon)-01
Anza-02
Baja California
Big Bear City
T1.000S
ClstD
1
0.1
0.01
0.001
0.1
1
10

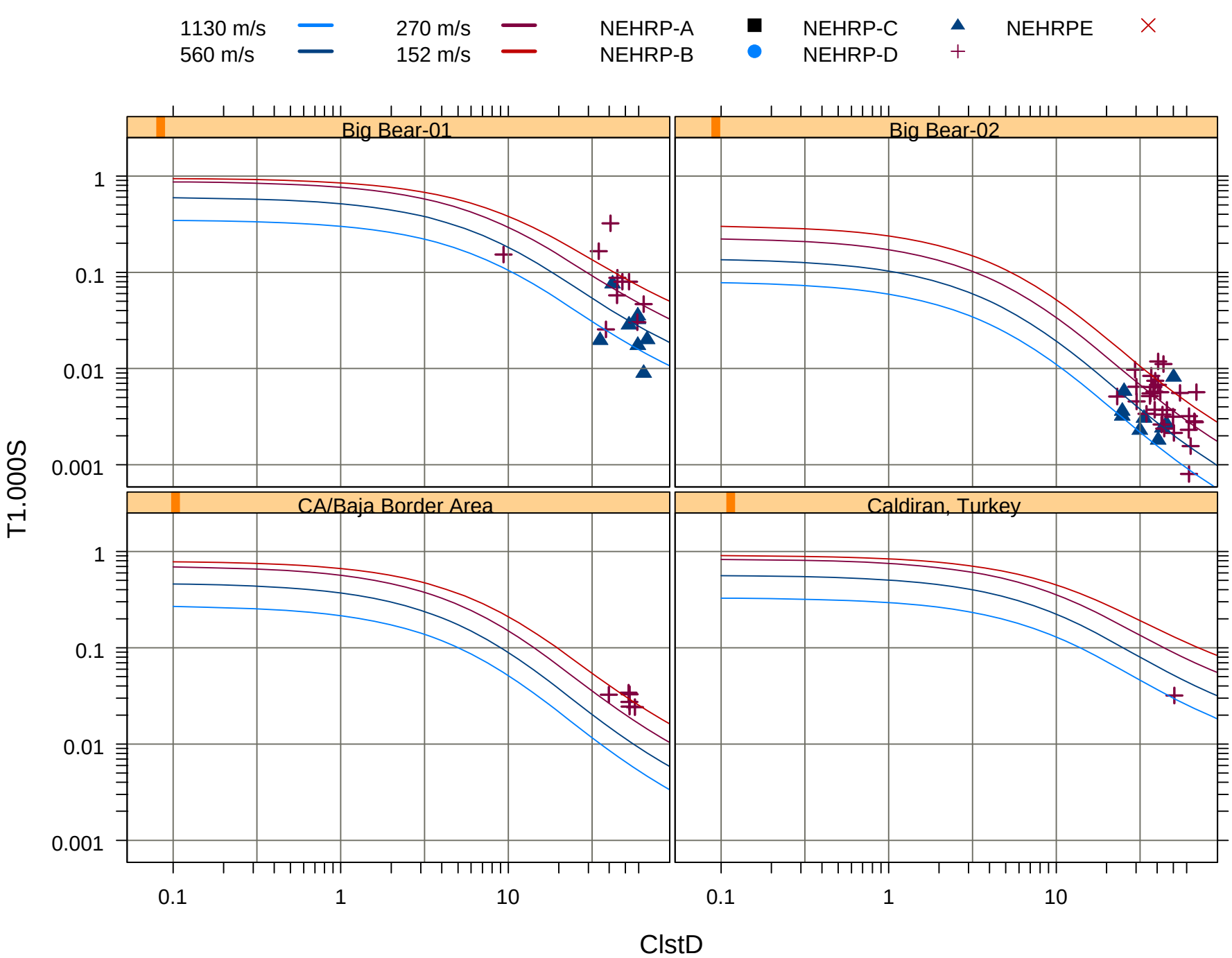
1130 m/s
560 m/s
270 m/s
152 m/s
NEHRP-A
NEHRP-B
NEHRP-C
NEHRP-D
NEHRPE
Big Bear-01
Big Bear-02
CA/Baja Border Area
Caldiran, Turkey
T1.000S
ClstD
1
0.1
0.01
0.001
0.1
1
10

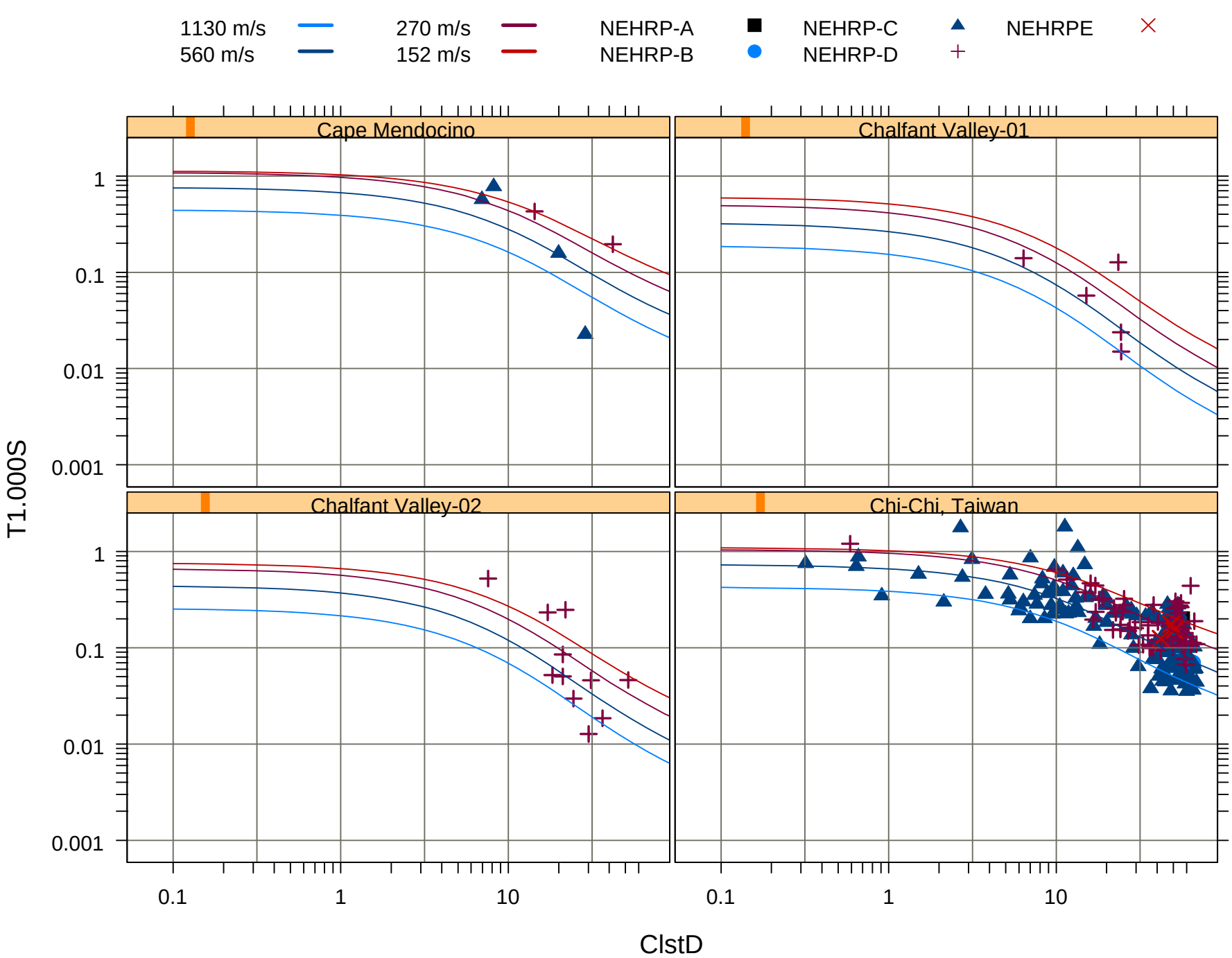
1130 m/s
560 m/s
270 m/s
152 m/s
NEHRP-A
NEHRP-B
NEHRP-C
NEHRP-D
NEHRPE
Cape Mendocino
Chalfant Valley-01
Chalfant Valley-02
Chi-Chi, Taiwan
T1.000S
ClstD
1
0.1
0.01
0.001
0.1
1
10

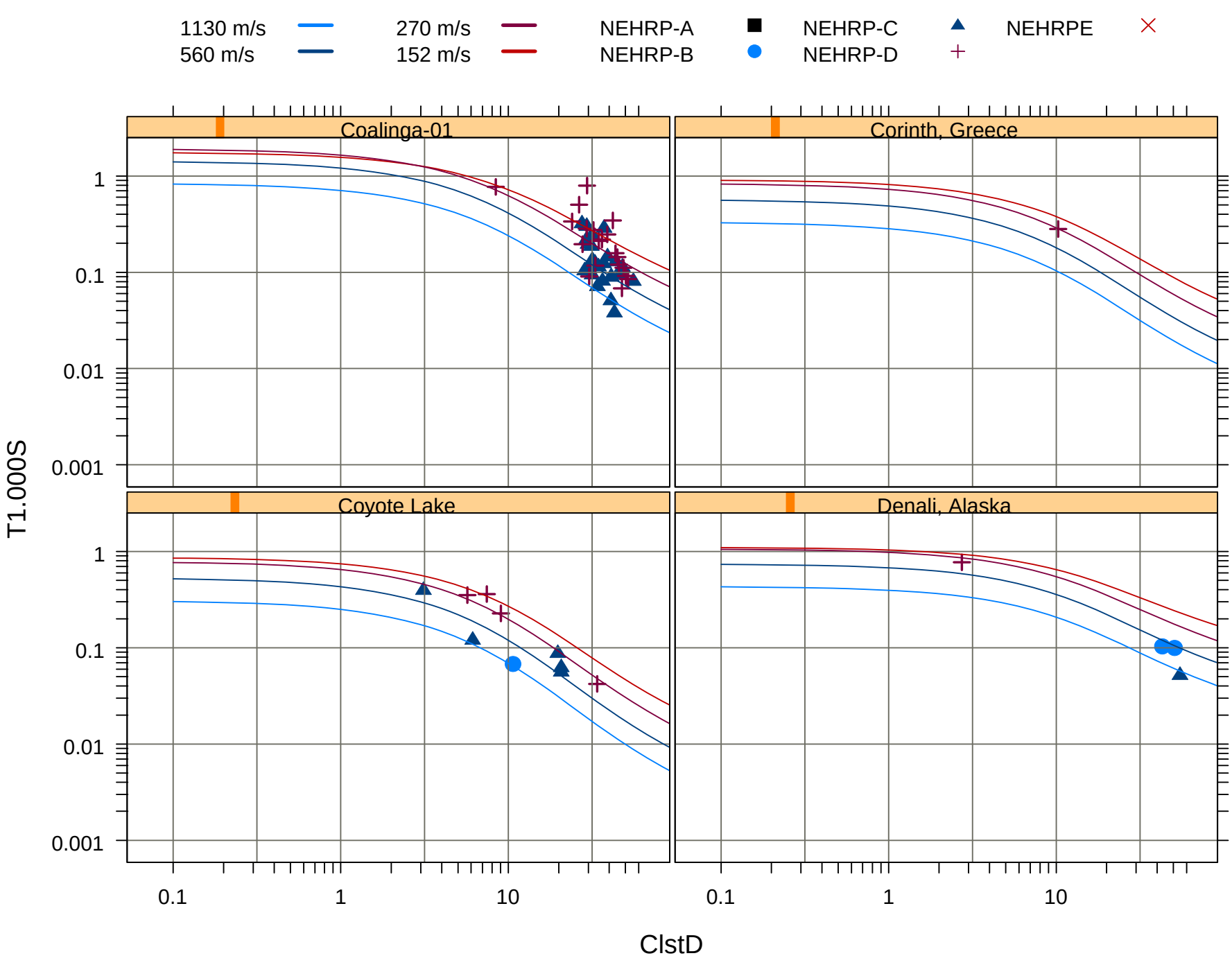
1130 m/s
560 m/s
270 m/s
152 m/s
NEHRP-A
NEHRP-B
NEHRP-C
NEHRP-D
NEHRPE
Coalinga-01
Corinth, Greece
Coyote Lake
Denali, Alaska
T1.000S
ClstD
1
0.1
0.01
0.001
0.1
1
10

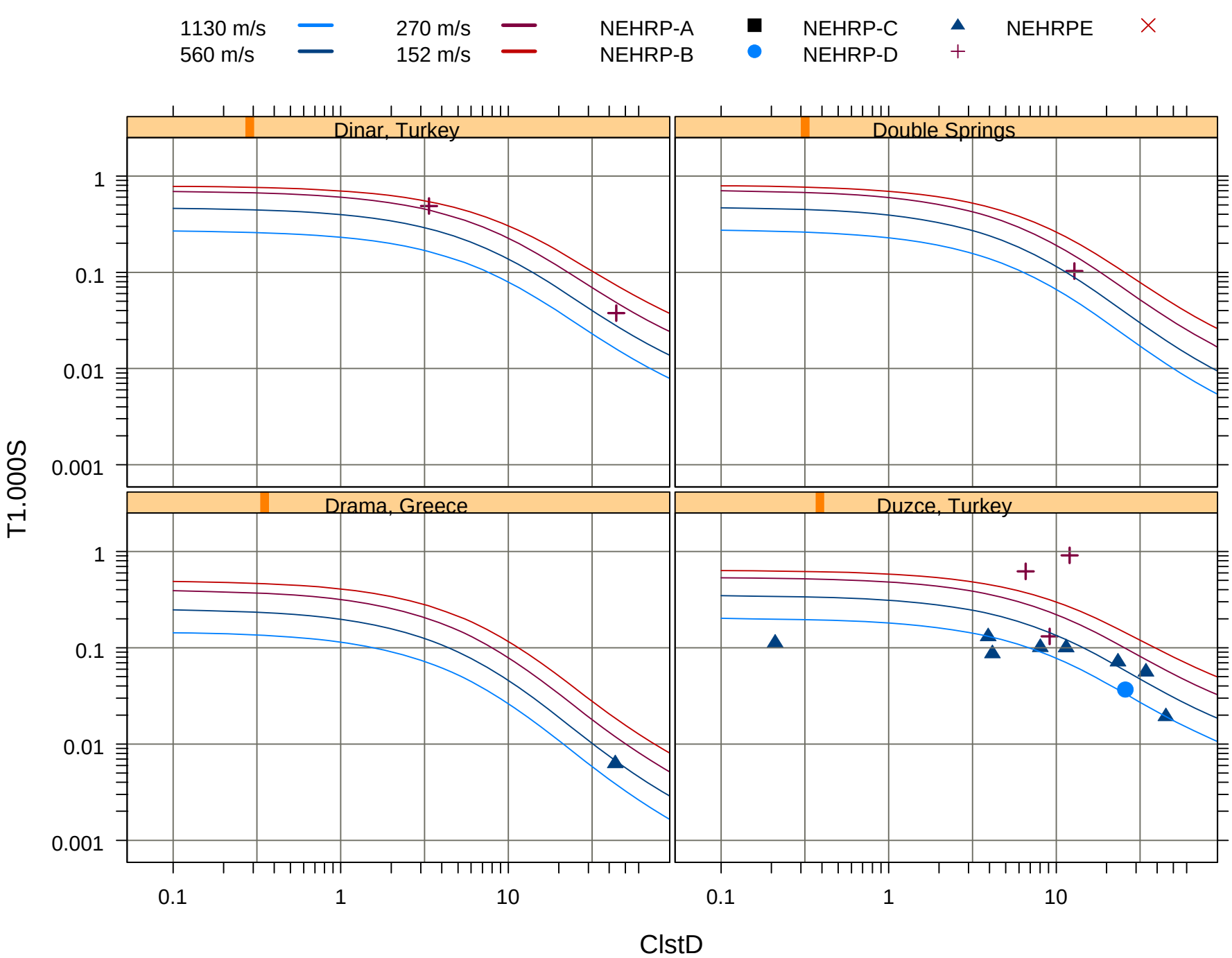
1130 m/s
560 m/s
270 m/s
152 m/s
NEHRP-A
NEHRP-B
NEHRP-C
NEHRP-D
NEHRPE
Dinar, Turkey
Double Springs
Drama, Greece
Duzce, Turkey
T1.000S
ClstD
1
0.1
0.01
0.001
0.1
1
10

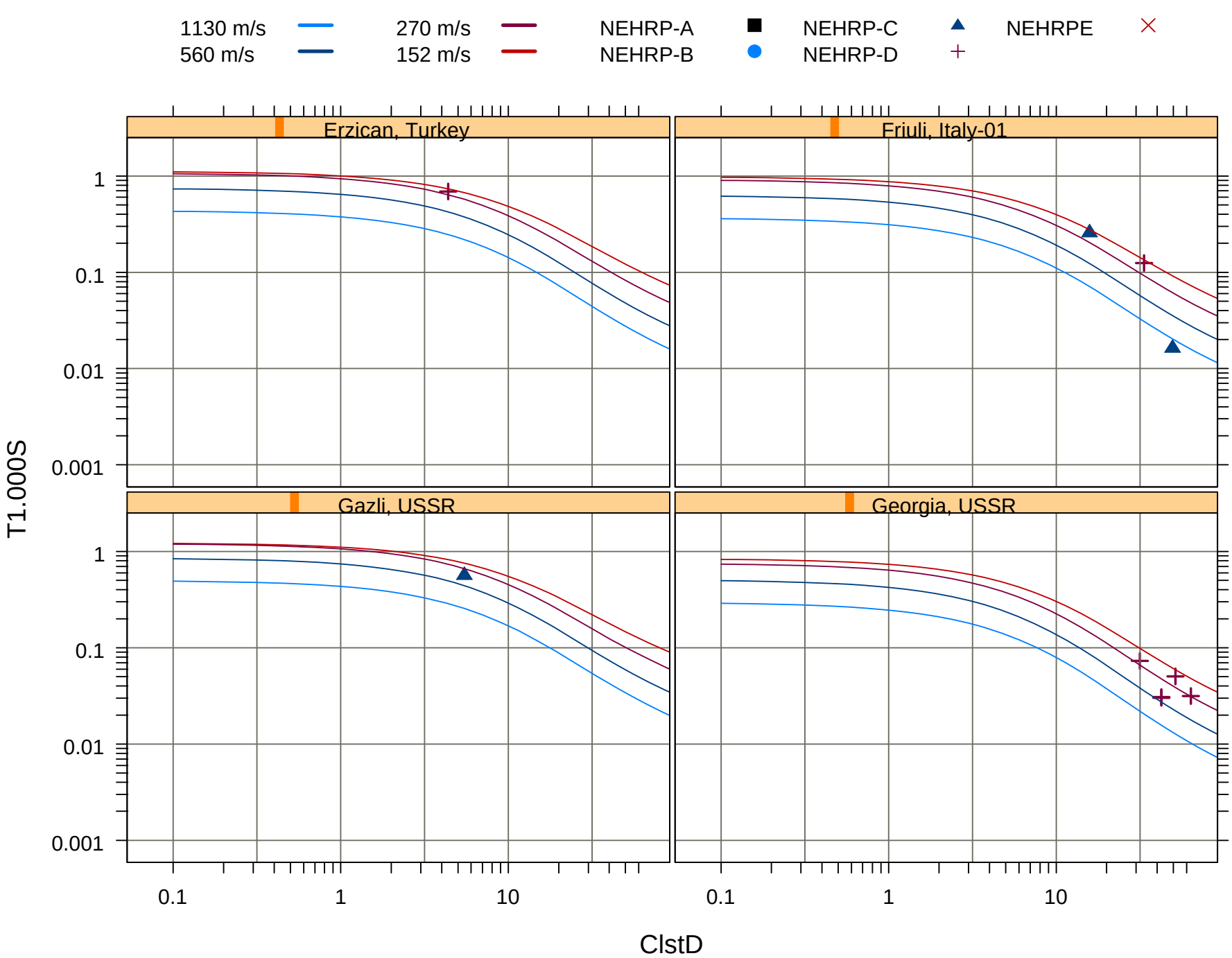
1130 m/s
560 m/s
270 m/s
152 m/s
NEHRP-A
NEHRP-B
NEHRP-C
NEHRP-D
NEHRPE
Erzican, Turkey
Friuli, Italy-01
Gazli, USSR
Georgia, USSR
T1.000S
ClstD
1
0.1
0.01
0.001
0.1
1
10

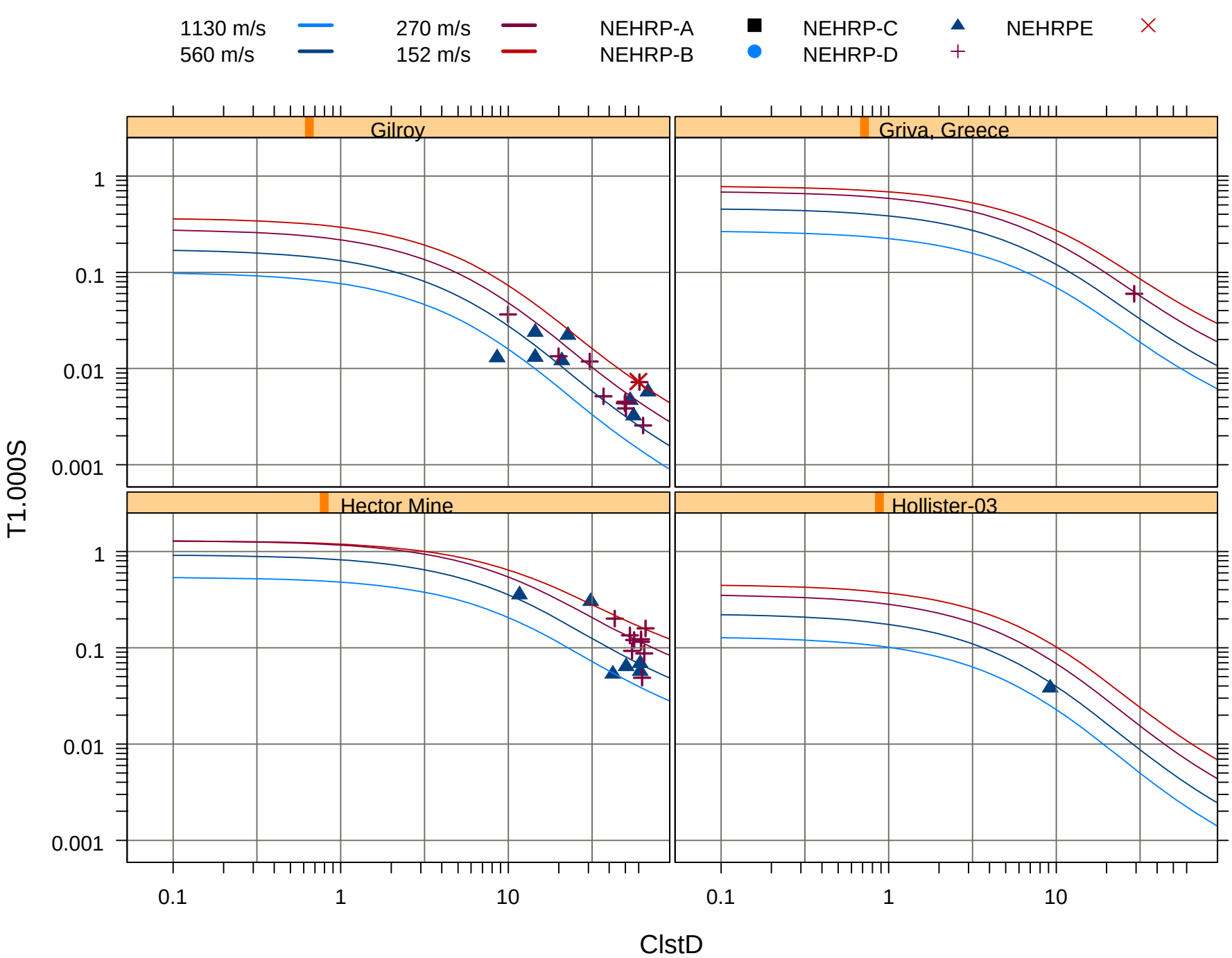
1130 m/s
560 m/s
270 m/s
152 m/s
NEHRP-A
NEHRP-B
NEHRP-C
NEHRP-D
NEHRPE
Gilroy
Griva, Greece
Hector Mine
Hollister-03
T1.000S
ClstD
1
0.1
0.01
0.001
0.1
1
10

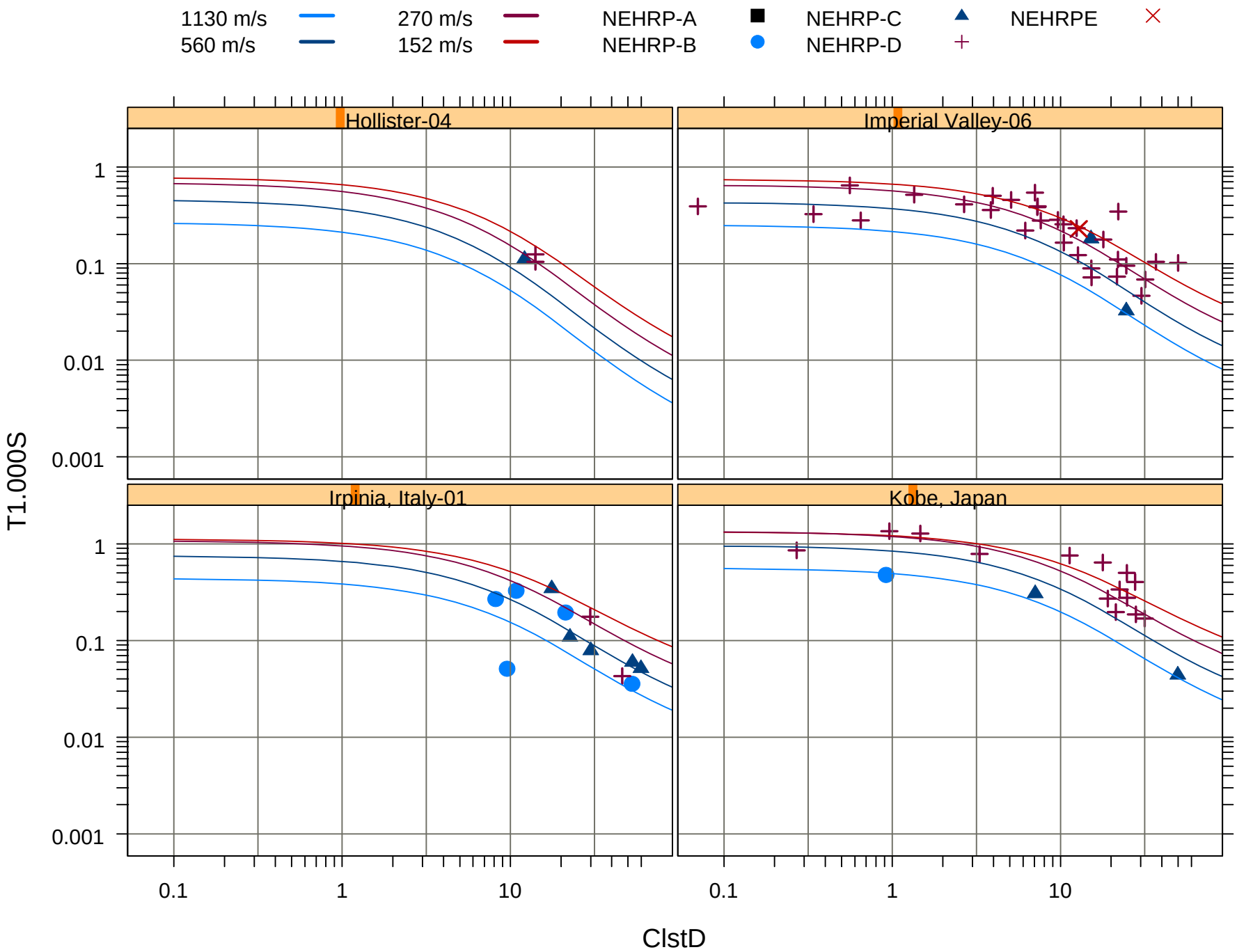
1130 m/s
560 m/s
270 m/s
152 m/s
NEHRP-A
NEHRP-B
NEHRP-C
NEHRP-D
NEHRPE
Hollister-04
Imperial Valley-06
Irpinia, Italy-01
Kobe, Japan
T1.000S
ClstD
1
0.1
0.01
0.001
0.1
1
10

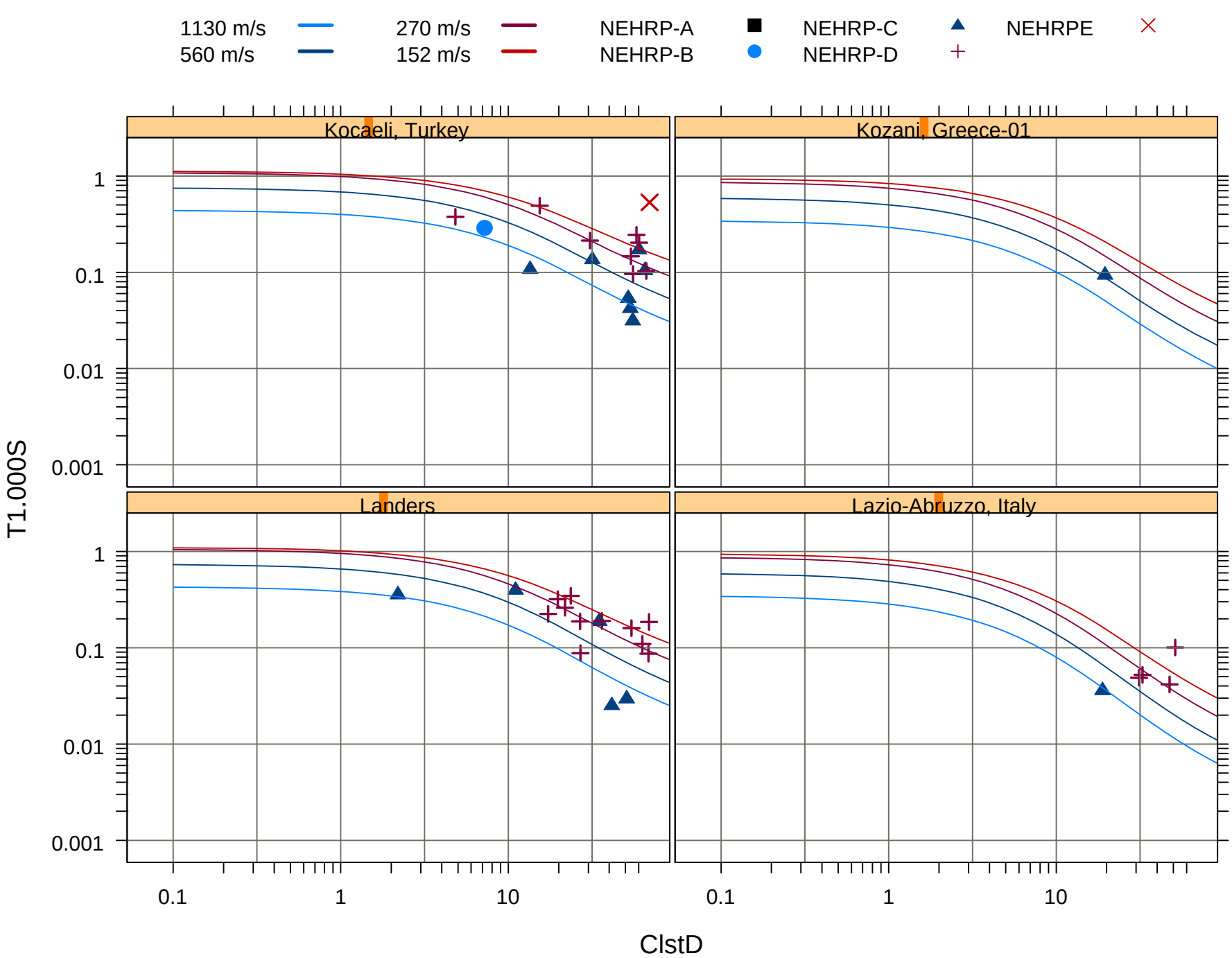
1130 m/s
560 m/s
270 m/s
152 m/s
NEHRP-A
NEHRP-B
NEHRP-C
NEHRP-D
NEHRPE
Kocaeli, Turkey
Kozani, Greece-01
Landers
Lazio-Abruzzo, Italy
T1.000S
ClstD
1
0.1
0.01
0.001
0.1
1
10

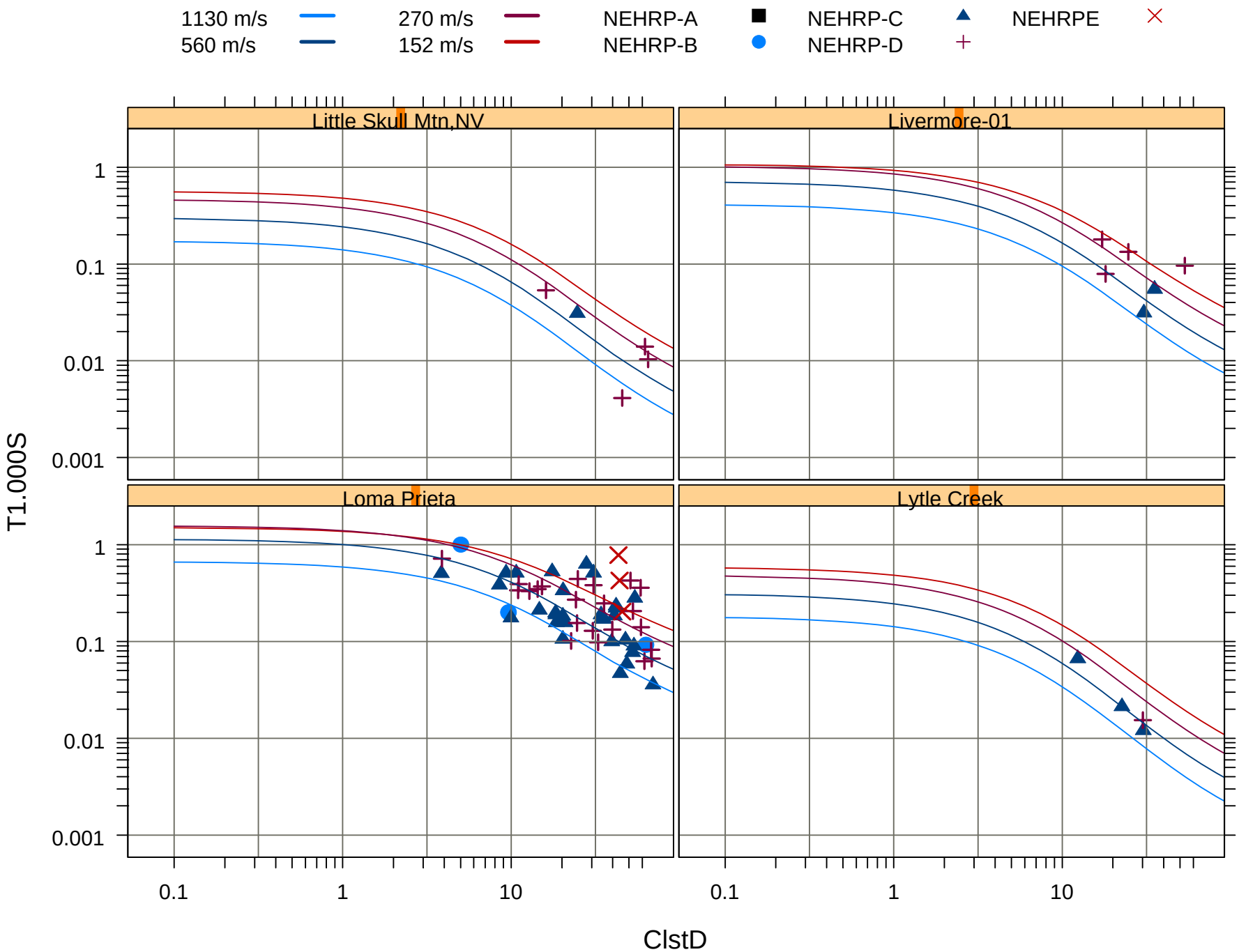
1130 m/s
560 m/s
270 m/s
152 m/s
NEHRP-A
NEHRP-B
NEHRP-C
NEHRP-D
NEHRPE
Little Skull Mtn,NV
Livermore-01
Loma Prieta
Lytle Creek
T1.000S
ClstD
1
0.1
0.01
0.001
0.1
1
10

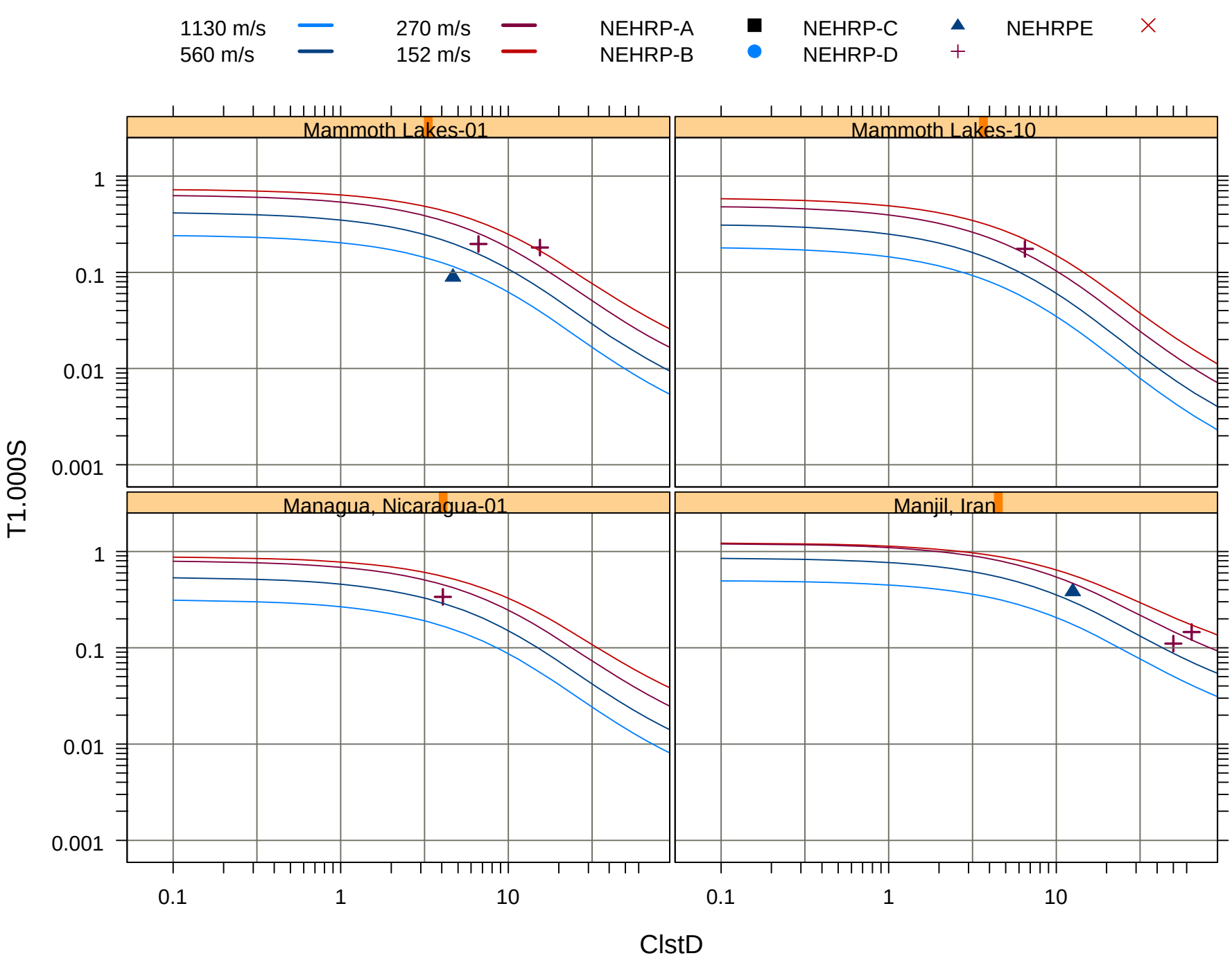
1130 m/s
560 m/s
270 m/s
152 m/s
NEHRP-A
NEHRP-B
NEHRP-C
NEHRP-D
NEHRPE
Mammoth Lakes-01
Mammoth Lakes-10
Managua, Nicaragua-01
Manjil, Iran
T1.000S
ClstD
1
0.1
0.01
0.001
0.1
1
10

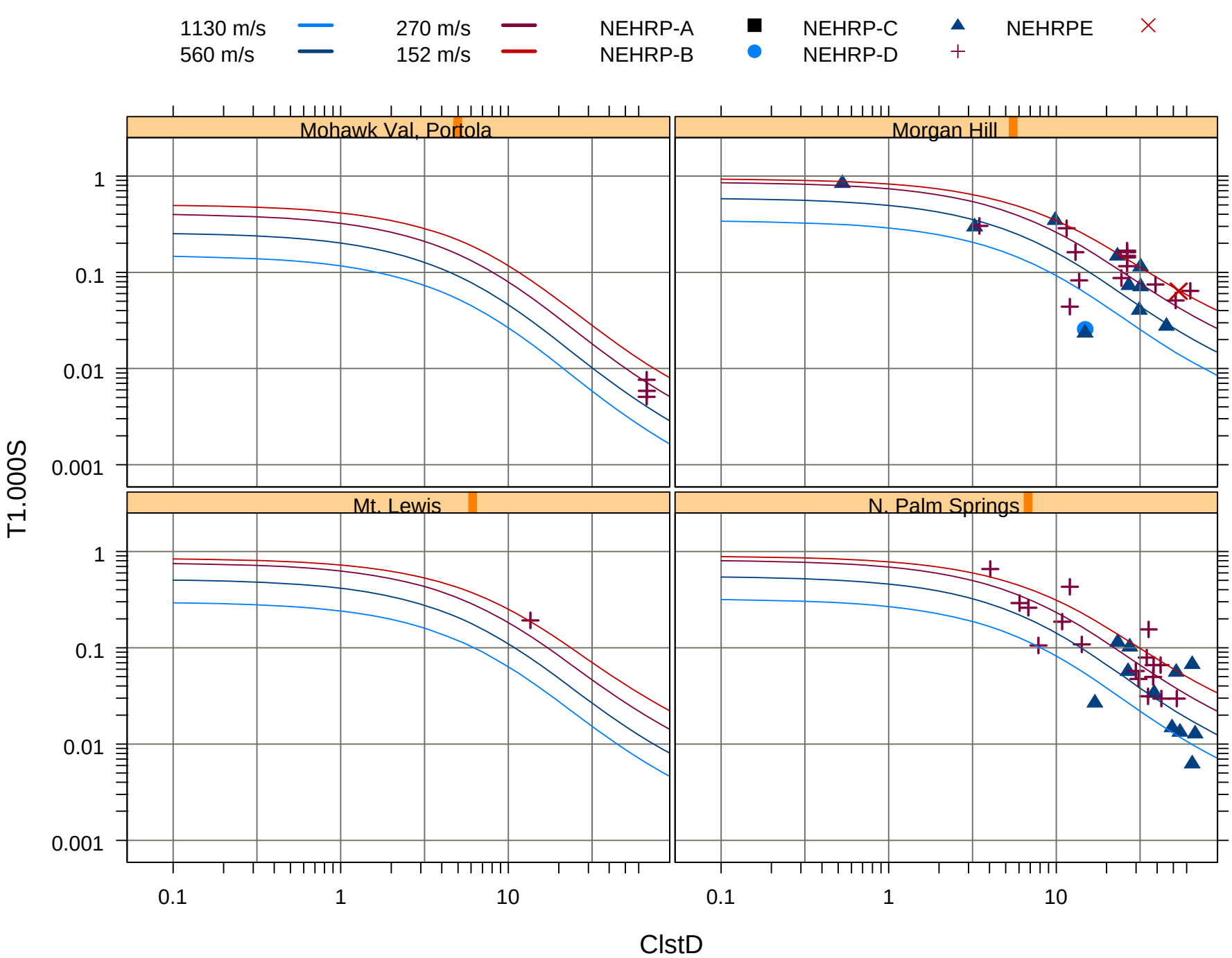
1130 m/s
560 m/s
270 m/s
152 m/s
NEHRP-A
NEHRP-B
NEHRP-C
NEHRP-D
NEHRPE
Mohawk Val, Portola
Morgan Hill
Mt. Lewis
N. Palm Springs
T1.000S
ClstD
1
0.1
0.01
0.001
0.1
1
10

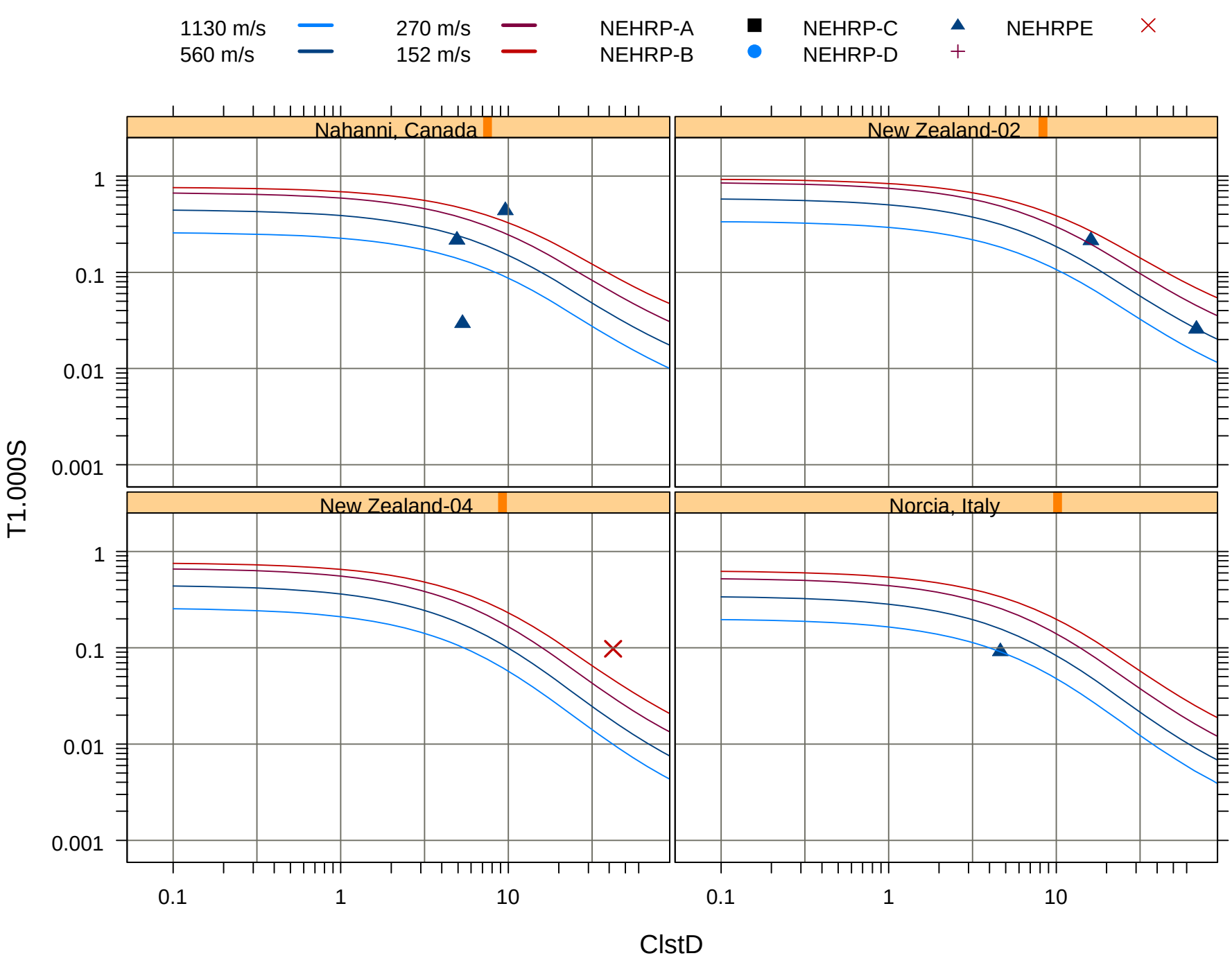
1130 m/s
560 m/s
270 m/s
152 m/s
NEHRP-A
NEHRP-B
NEHRP-C
NEHRP-D
NEHRPE
Nahanni, Canada
New Zealand-02
New Zealand-04
Norcia, Italy
T1.000S
ClstD
1
0.1
0.01
0.001
0.1
1
10

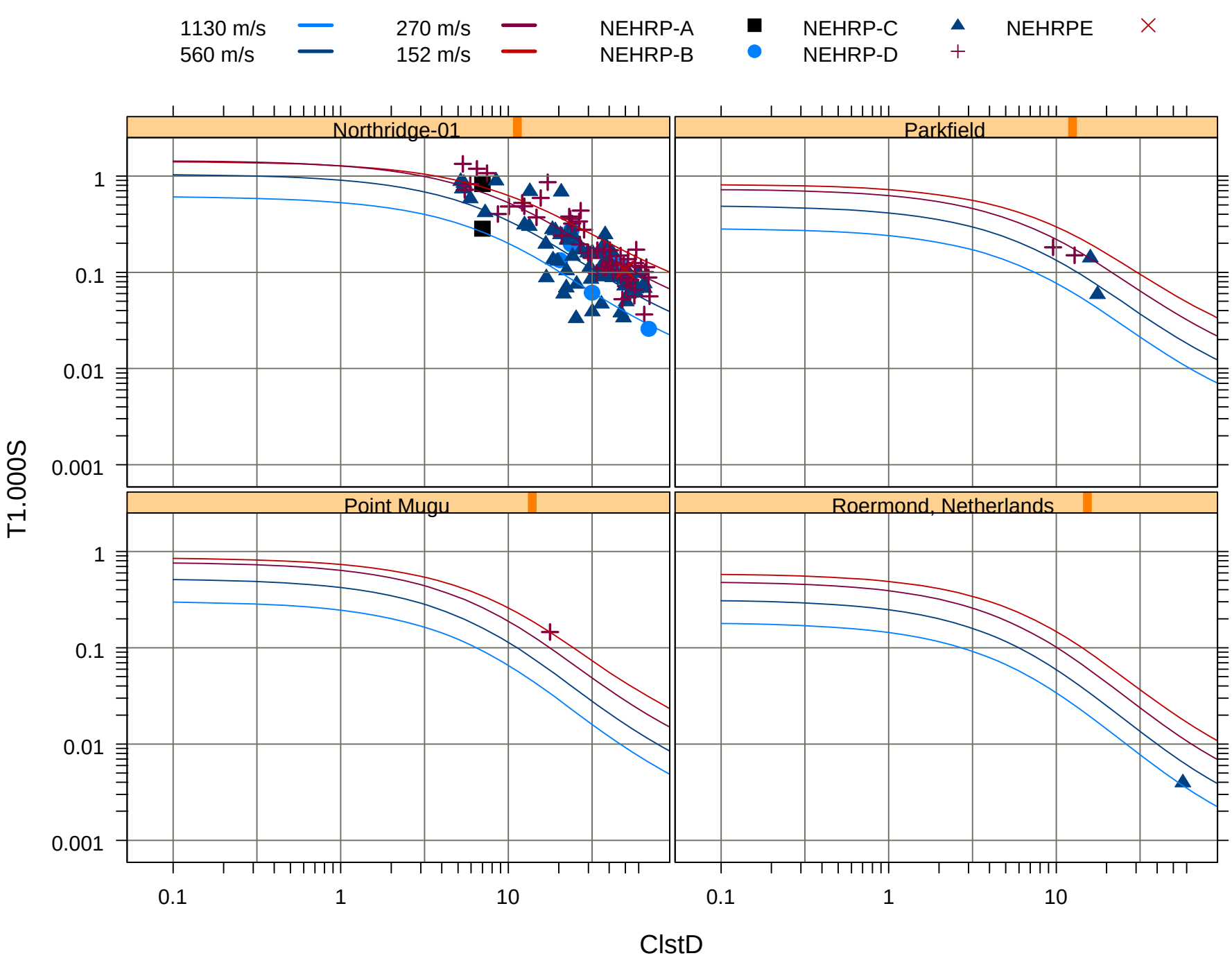
1130 m/s
560 m/s
270 m/s
152 m/s
NEHRP-A
NEHRP-B
NEHRP-C
NEHRP-D
NEHRPE
Northridge-01
Parkfield
Point Mugu
Roermond, Netherlands
T1.000S
ClstD
1
0.1
0.01
0.001
0.1
1
10

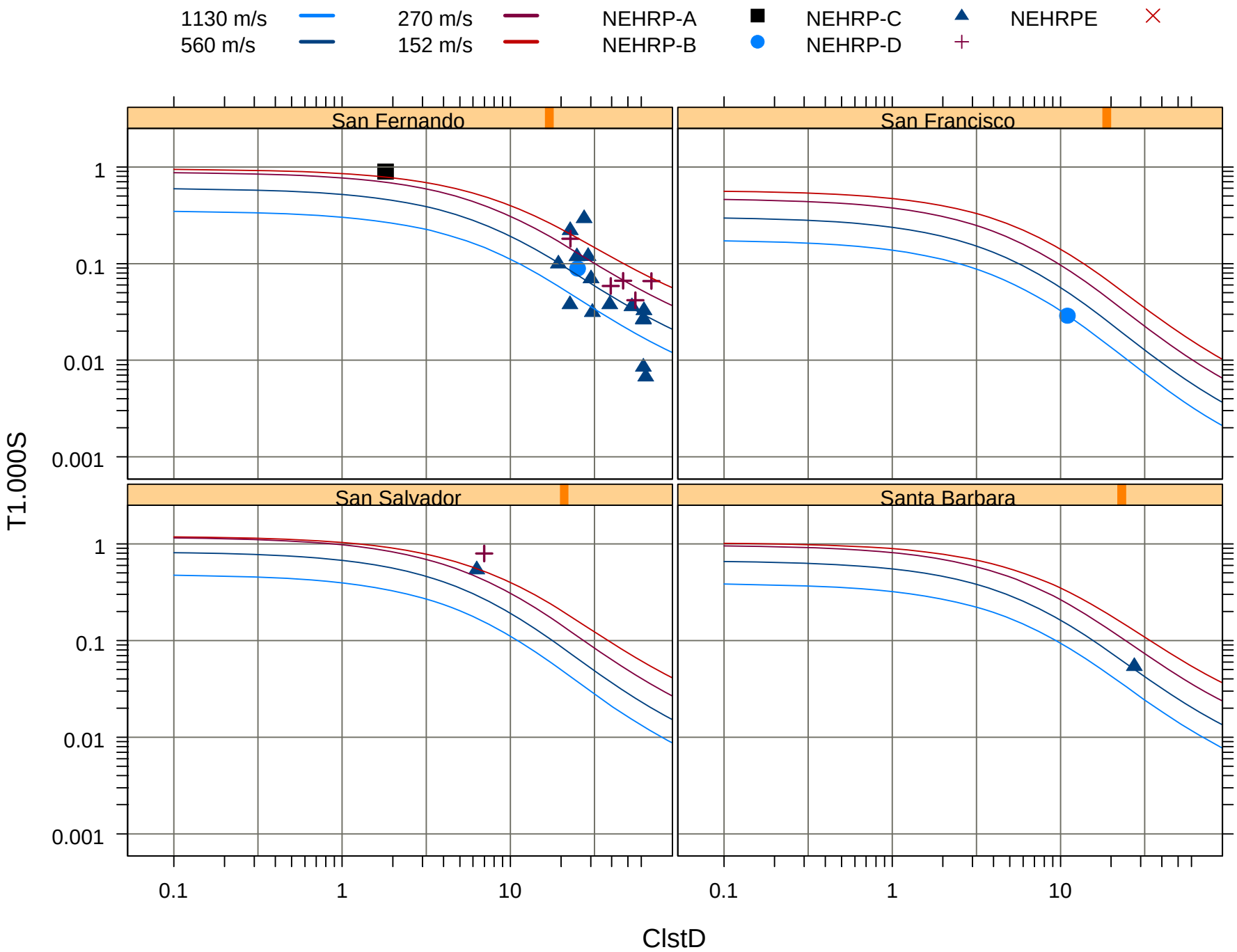
1130 m/s
560 m/s
270 m/s
152 m/s
NEHRP-A
NEHRP-B
NEHRP-C
NEHRP-D
NEHRPE
San Fernando
San Francisco
San Salvador
Santa Barbara
T1.000S
ClstD
1
0.1
0.01
0.001
0.1
1
10

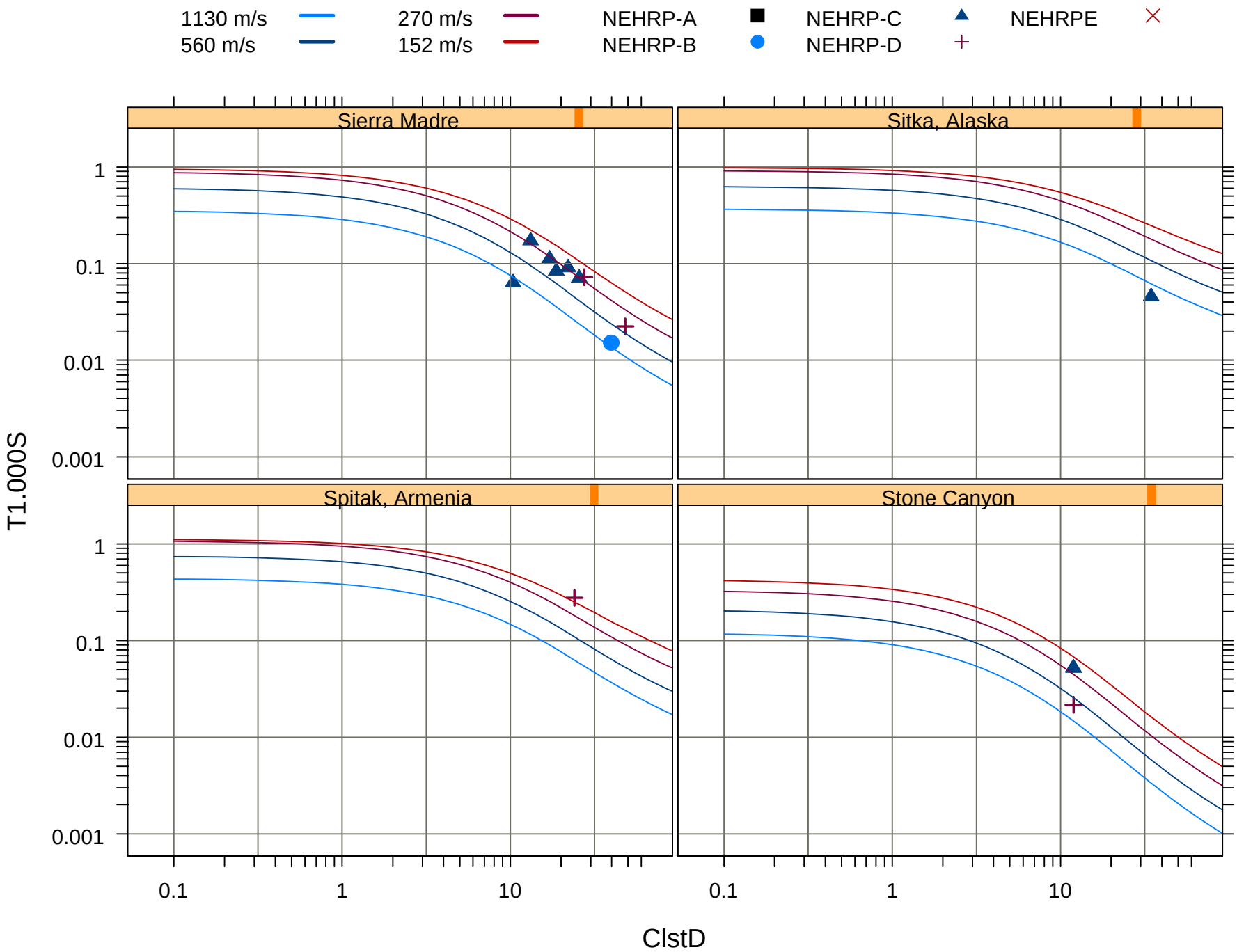
1130 m/s
560 m/s
270 m/s
152 m/s
NEHRP-A
NEHRP-B
NEHRP-C
NEHRP-D
NEHRPE
Sierra Madre
Sitka, Alaska
Spitak, Armenia
Stone Canyon
T1.000S
ClstD
1
0.1
0.01
0.001
0.1
1
10

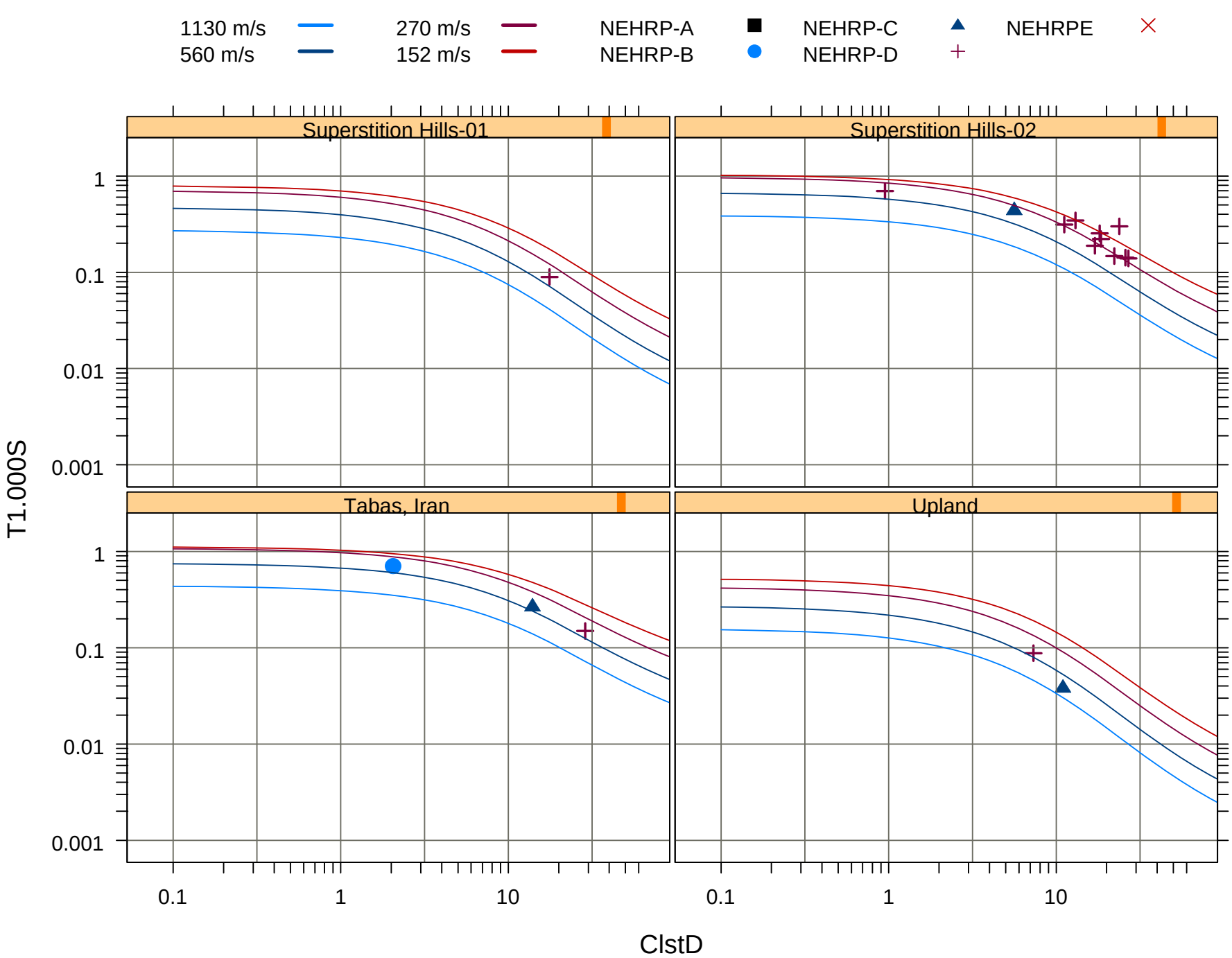
1130 m/s
560 m/s
270 m/s
152 m/s
NEHRP-A
NEHRP-B
NEHRP-C
NEHRP-D
NEHRPE
Superstition Hills-01
Superstition Hills-02
Tabas, Iran
Upland
T1.000S
ClstD
1
0.1
0.01
0.001
0.1
1
10

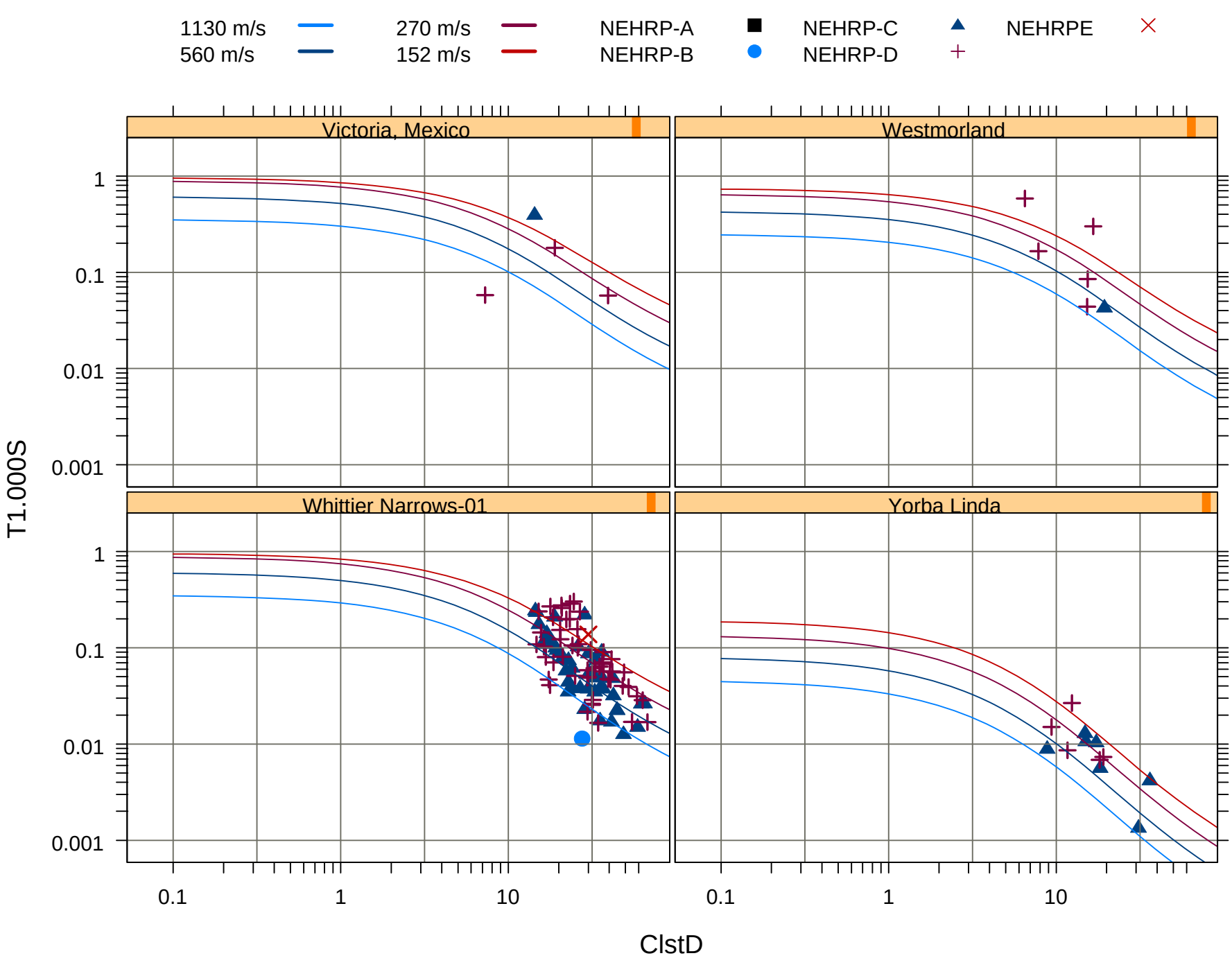
1130 m/s
560 m/s
270 m/s
152 m/s
NEHRP-A
NEHRP-B
NEHRP-C
NEHRP-D
NEHRPE
Victoria, Mexico
Westmorland
Whittier Narrows-01
Yorba Linda
T1.000S
ClstD
1
0.1
0.01
0.001
0.1
1
10

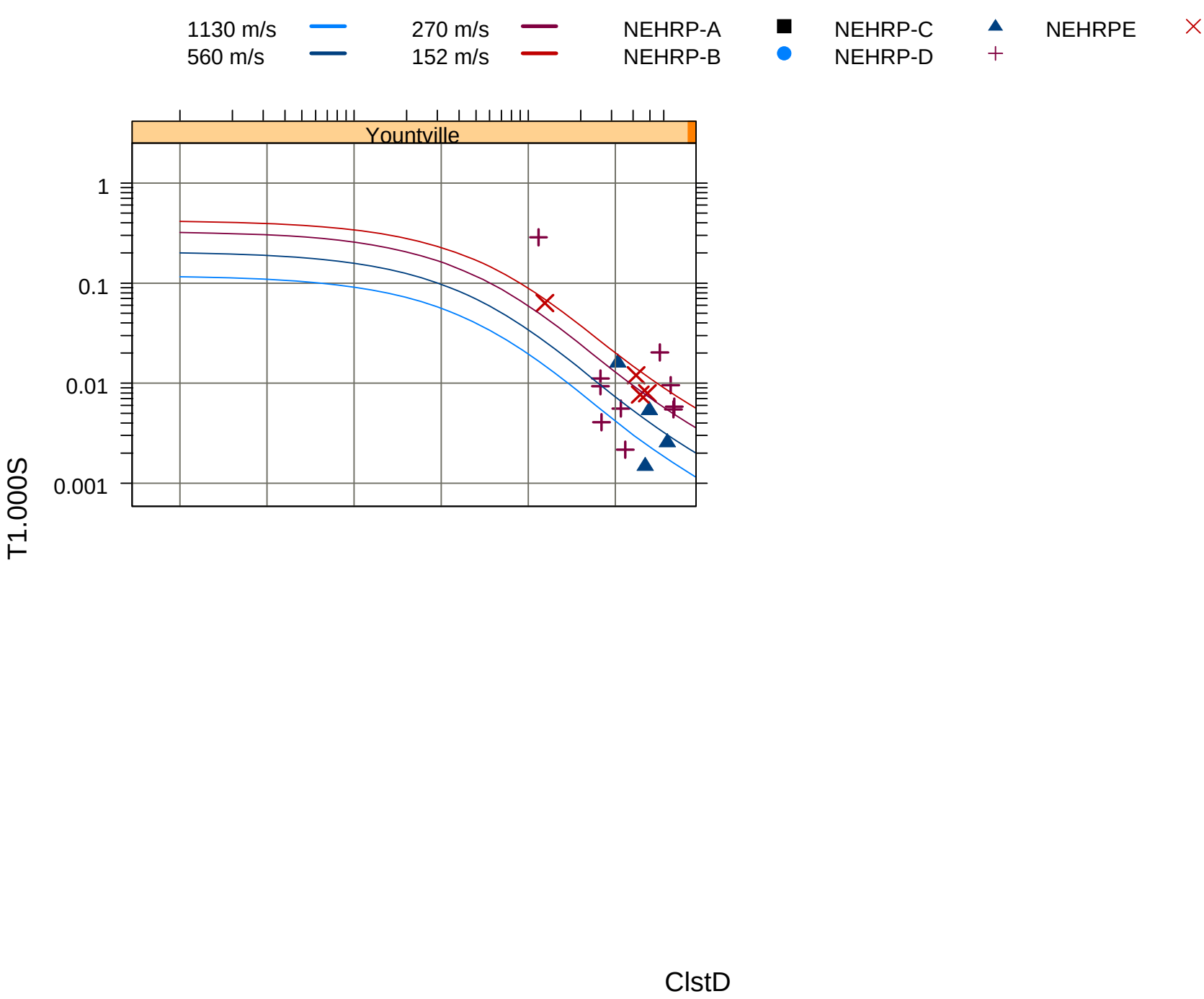
1130 m/s
560 m/s
270 m/s
152 m/s
NEHRP-A
NEHRP-B
NEHRP-C
NEHRP-D
NEHRPE
Yountville
1
0.1
0.01
0.001
T1.000S
ClstD

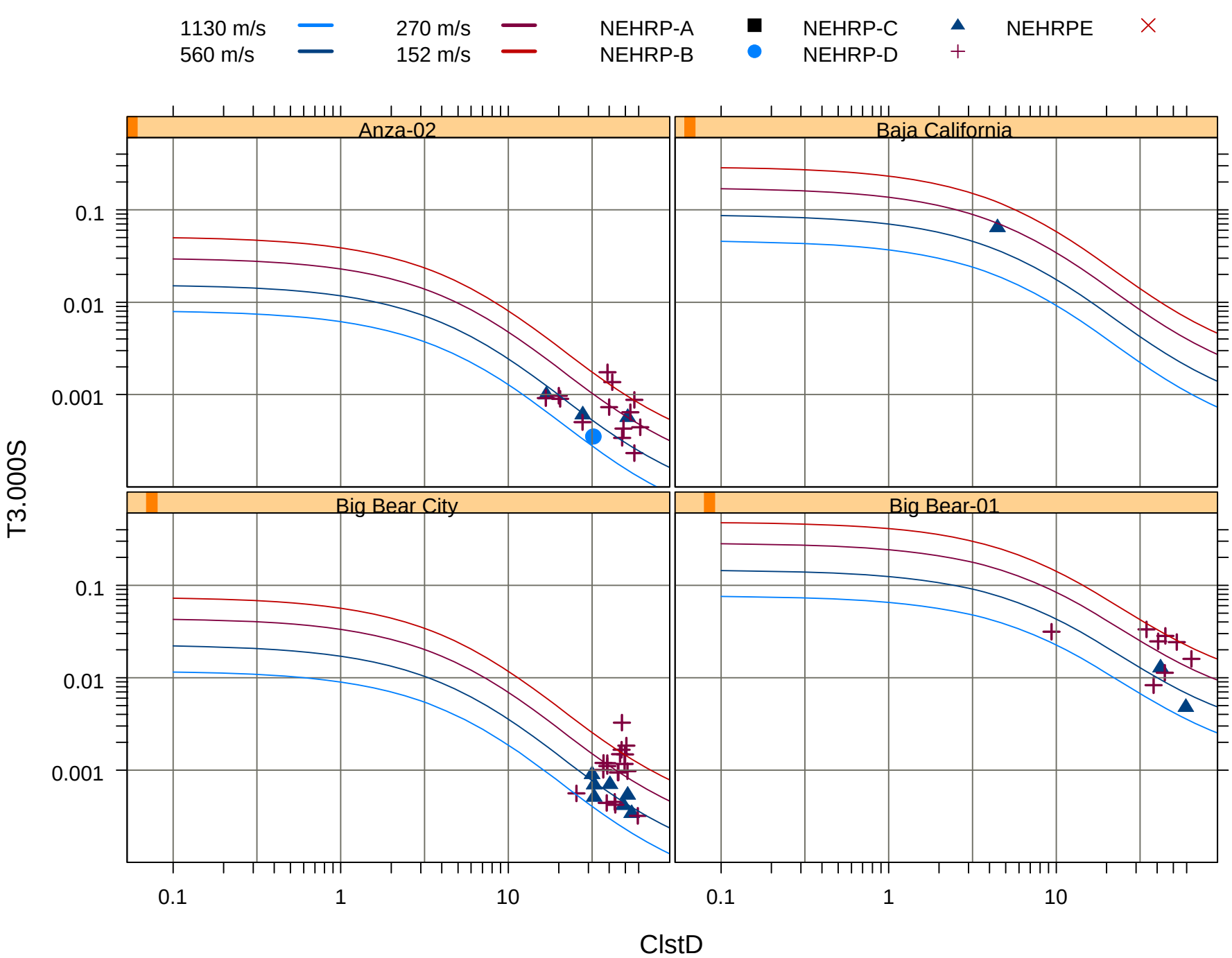
1130 m/s
560 m/s
270 m/s
152 m/s
NEHRP-A
NEHRP-B
NEHRP-C
NEHRP-D
NEHRPE
Anza-02
Baja California
Big Bear City
Big Bear-01
T3.000S
ClstD
0.1
0.01
0.001
0.1
1
10

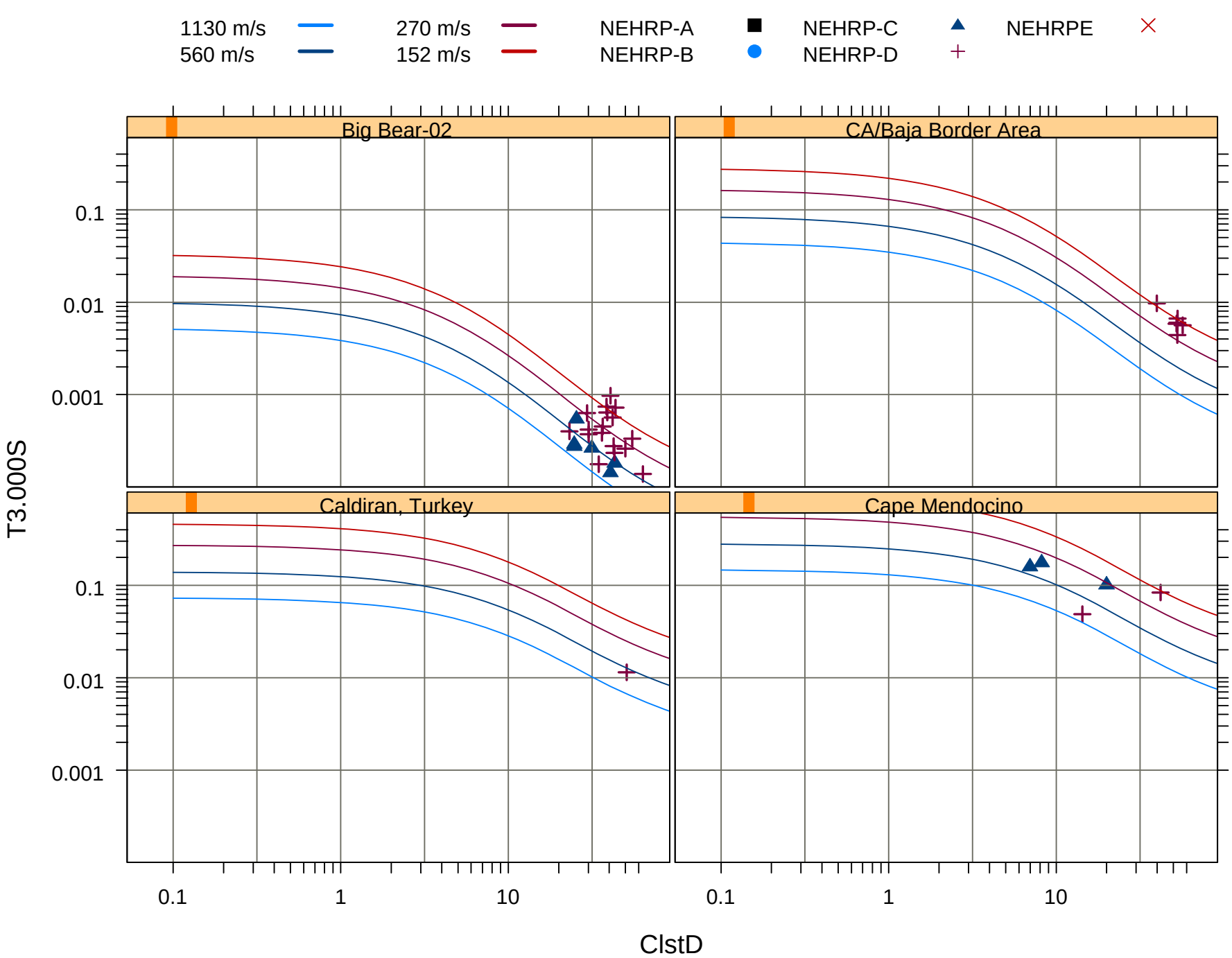
1130 m/s
560 m/s
270 m/s
152 m/s
NEHRP-A
NEHRP-B
NEHRP-C
NEHRP-D
NEHRPE
Big Bear-02
CA/Baja Border Area
Caldiran, Turkey
Cape Mendocino
T3.000S
ClstD
0.1
0.01
0.001
1
10

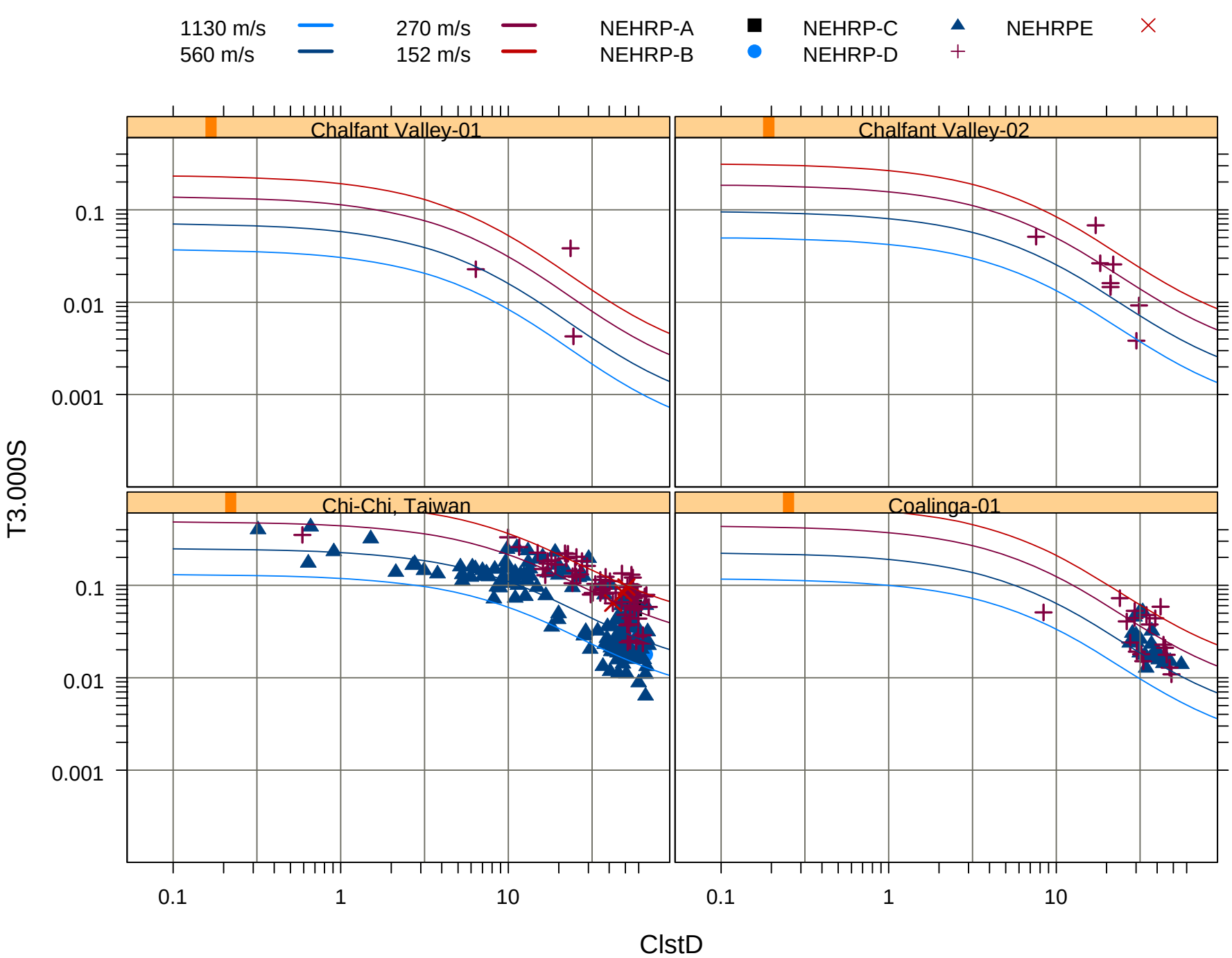
1130 m/s
560 m/s
270 m/s
152 m/s
NEHRP-A
NEHRP-B
NEHRP-C
NEHRP-D
NEHRPE
Chalfant Valley-01
Chalfant Valley-02
Chi-Chi, Taiwan
Coalinga-01
T3.000S
ClstD
0.1
0.01
0.001
1
10

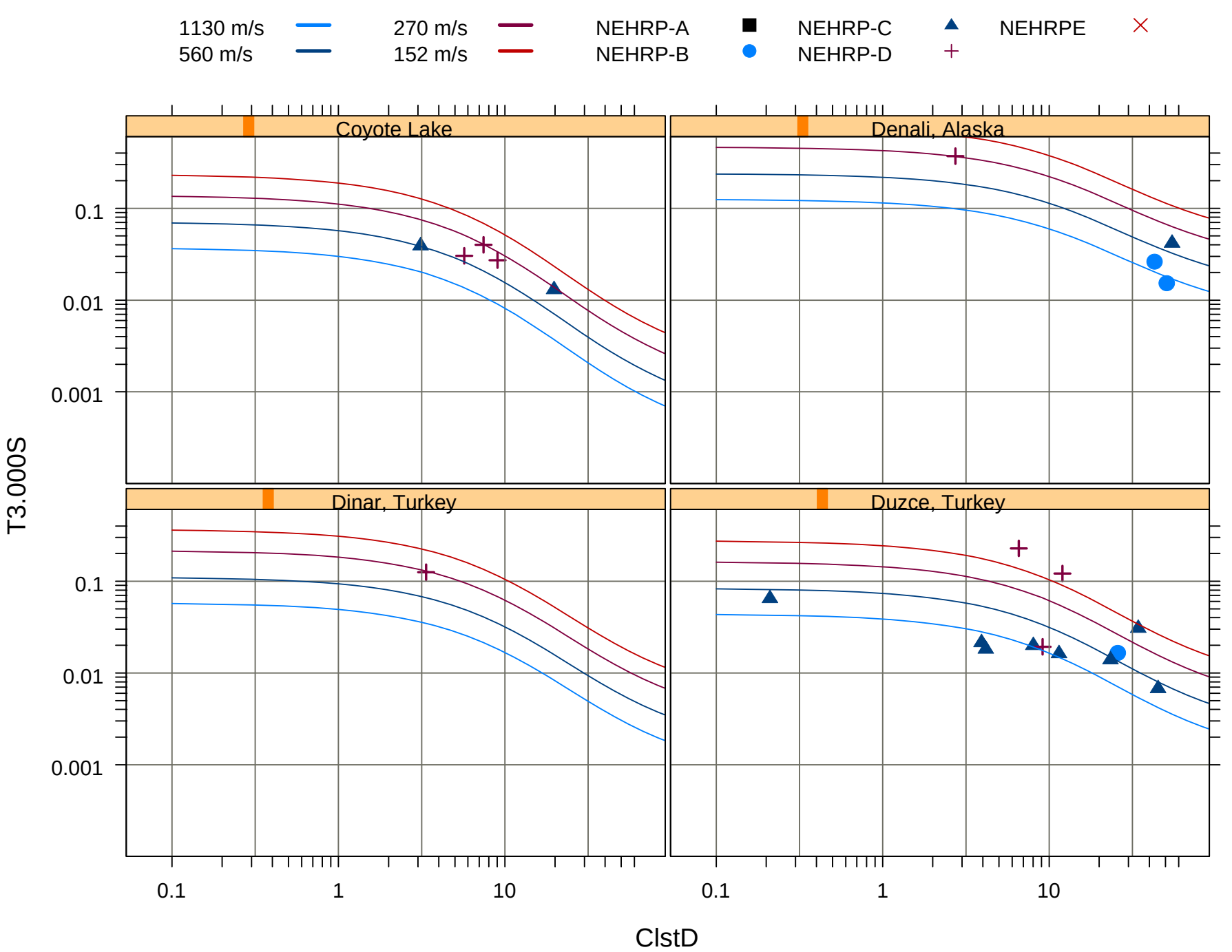
1130 m/s
560 m/s
270 m/s
152 m/s
NEHRP-A
NEHRP-B
NEHRP-C
NEHRP-D
NEHRPE
Coyote Lake
Denali, Alaska
Dinar, Turkey
Duzce, Turkey
T3.000S
ClstD
0.1
0.01
0.001
0.1
1
10

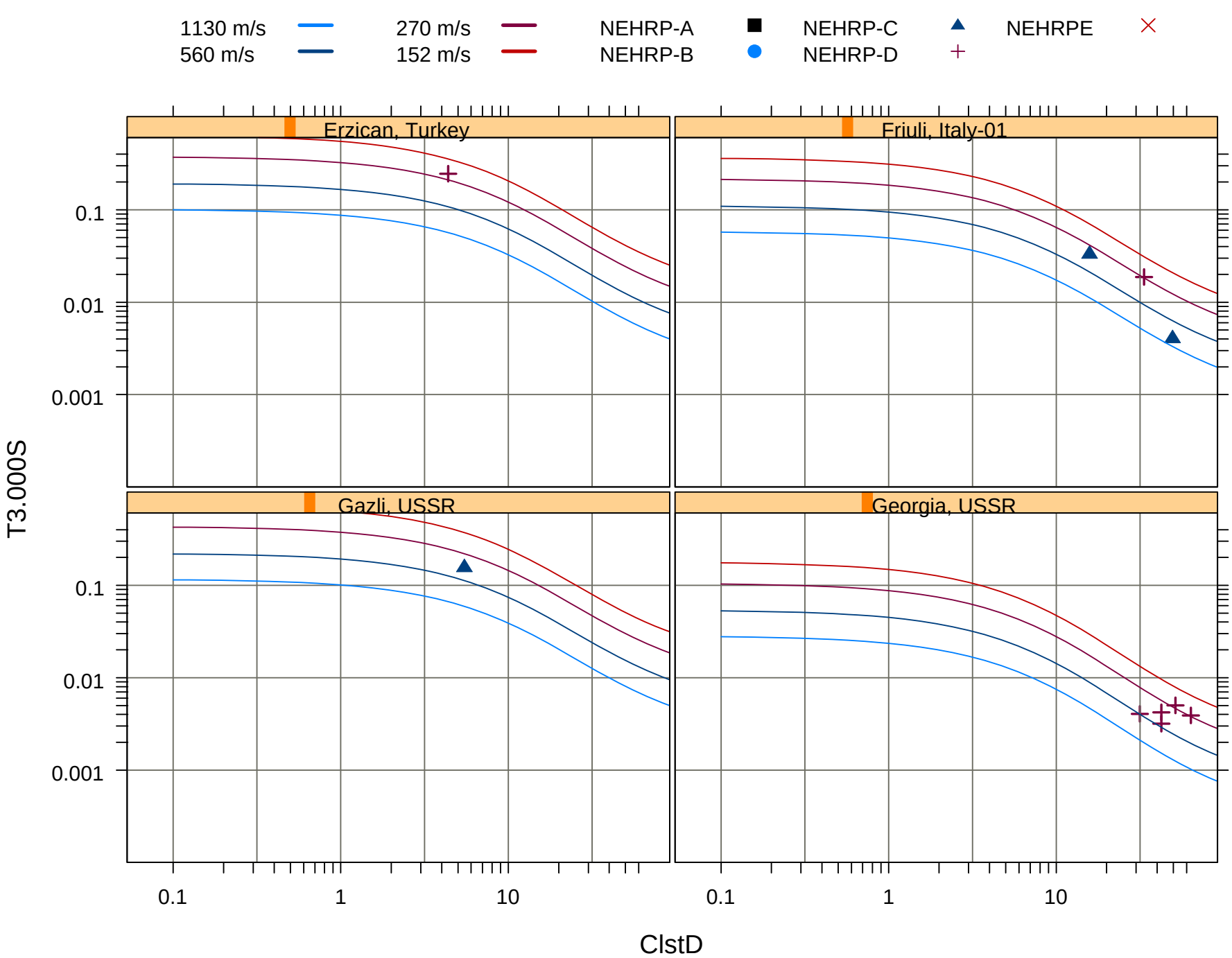
1130 m/s
560 m/s
270 m/s
152 m/s
NEHRP-A
NEHRP-B
NEHRP-C
NEHRP-D
NEHRPE
Erzican, Turkey
Friuli, Italy-01
Gazli, USSR
Georgia, USSR
T3.000S
0.1
0.01
0.001
0.1
1
10
ClstD

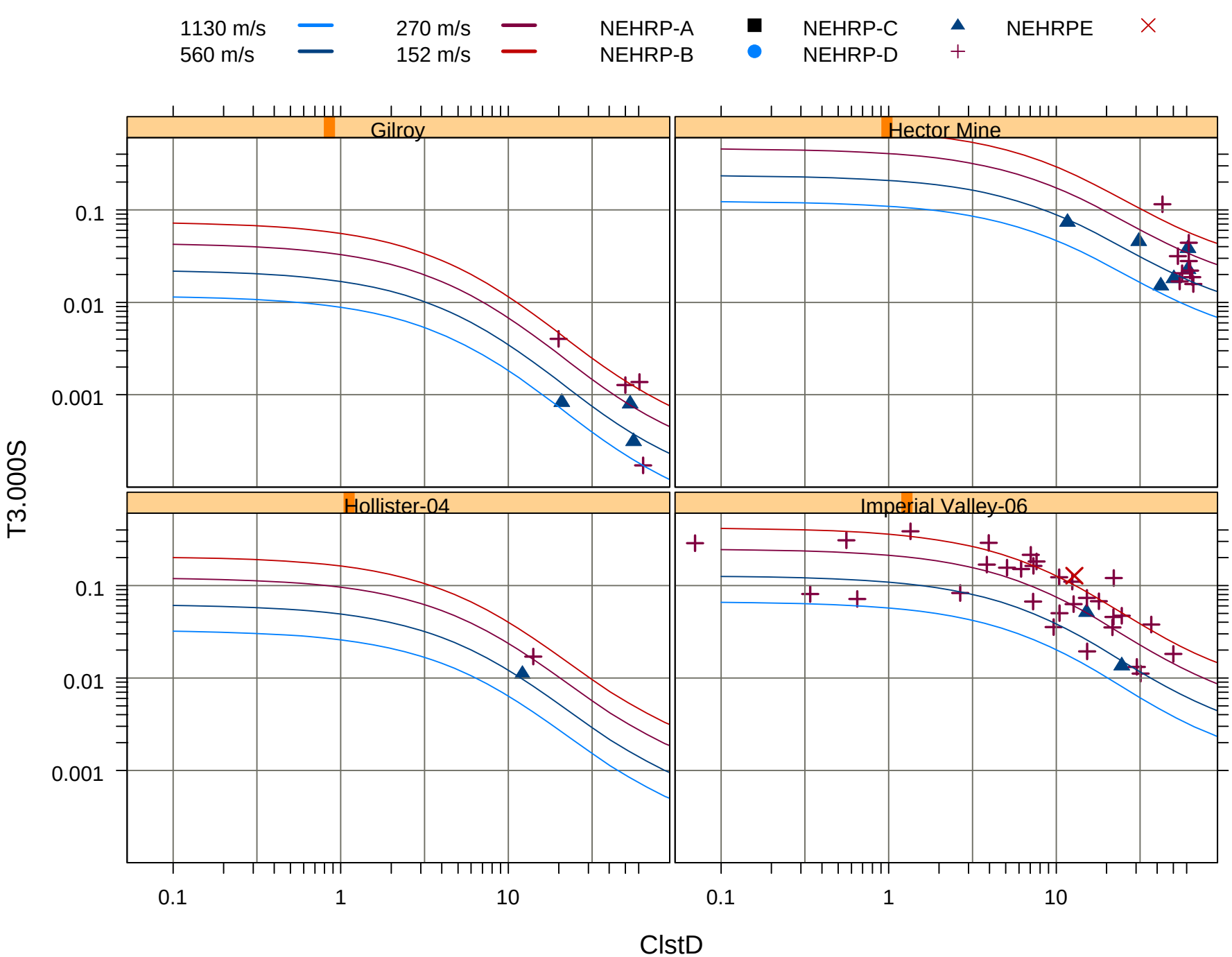
1130 m/s
560 m/s
270 m/s
152 m/s
NEHRP-A
NEHRP-B
NEHRP-C
NEHRP-D
NEHRPE
Gilroy
Hector Mine
Hollister-04
Imperial Valley-06
T3.000S
ClstD
0.1
0.01
0.001
0.1
1
10

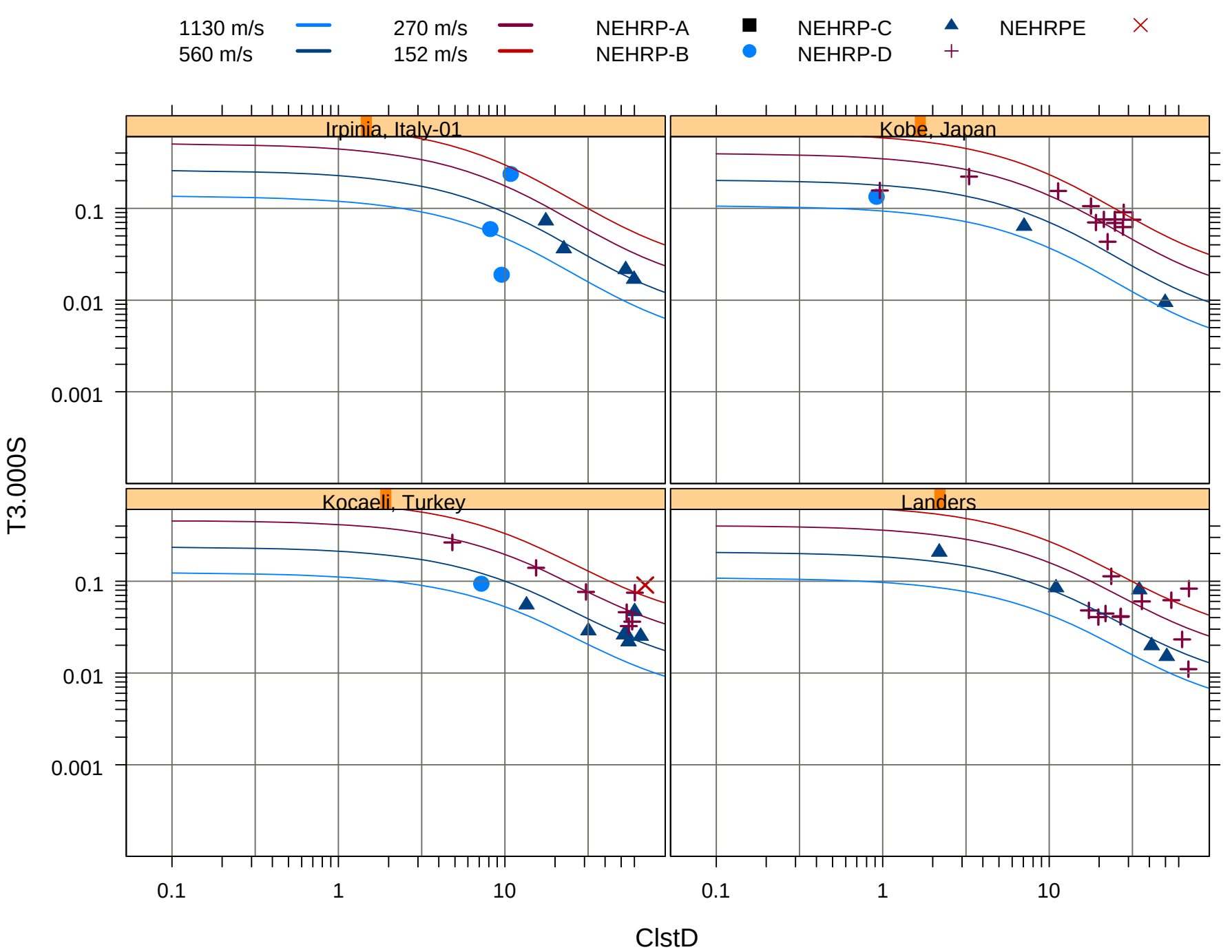
1130 m/s
560 m/s
270 m/s
152 m/s
NEHRP-A
NEHRP-B
NEHRP-C
NEHRP-D
NEHRPE
Irpinia, Italy-01
Kobe, Japan
Kocaeli, Turkey
Landers
T3.000S
ClstD
0.1
0.01
0.001
0.1
1
10

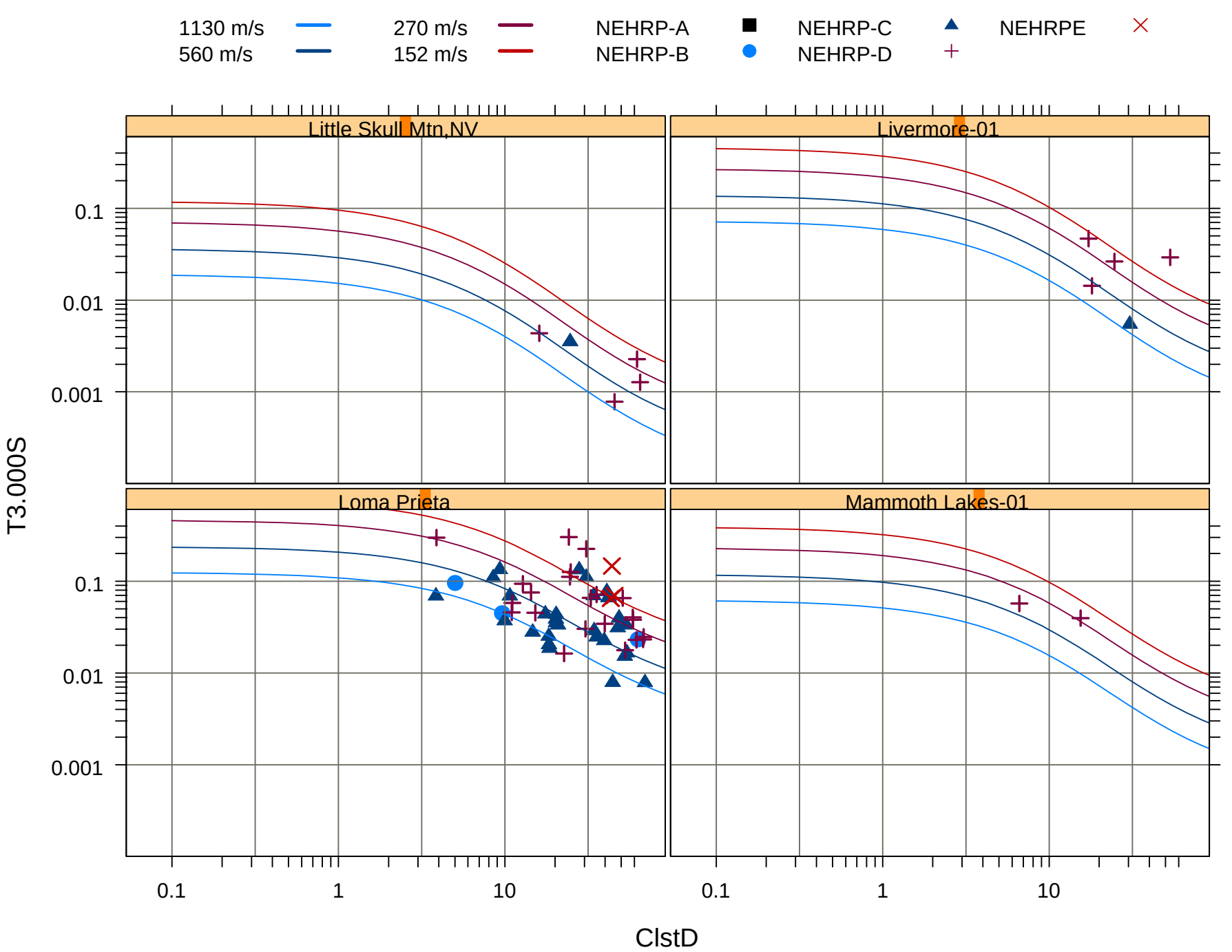
1130 m/s
560 m/s
270 m/s
152 m/s
NEHRP-A
NEHRP-B
NEHRP-C
NEHRP-D
NEHRPE
Little Skull Mtn,NV
Livermore-01
Loma Prieta
Mammoth Lakes-01
T3.000S
ClstD
0.1
0.01
0.001
1
10

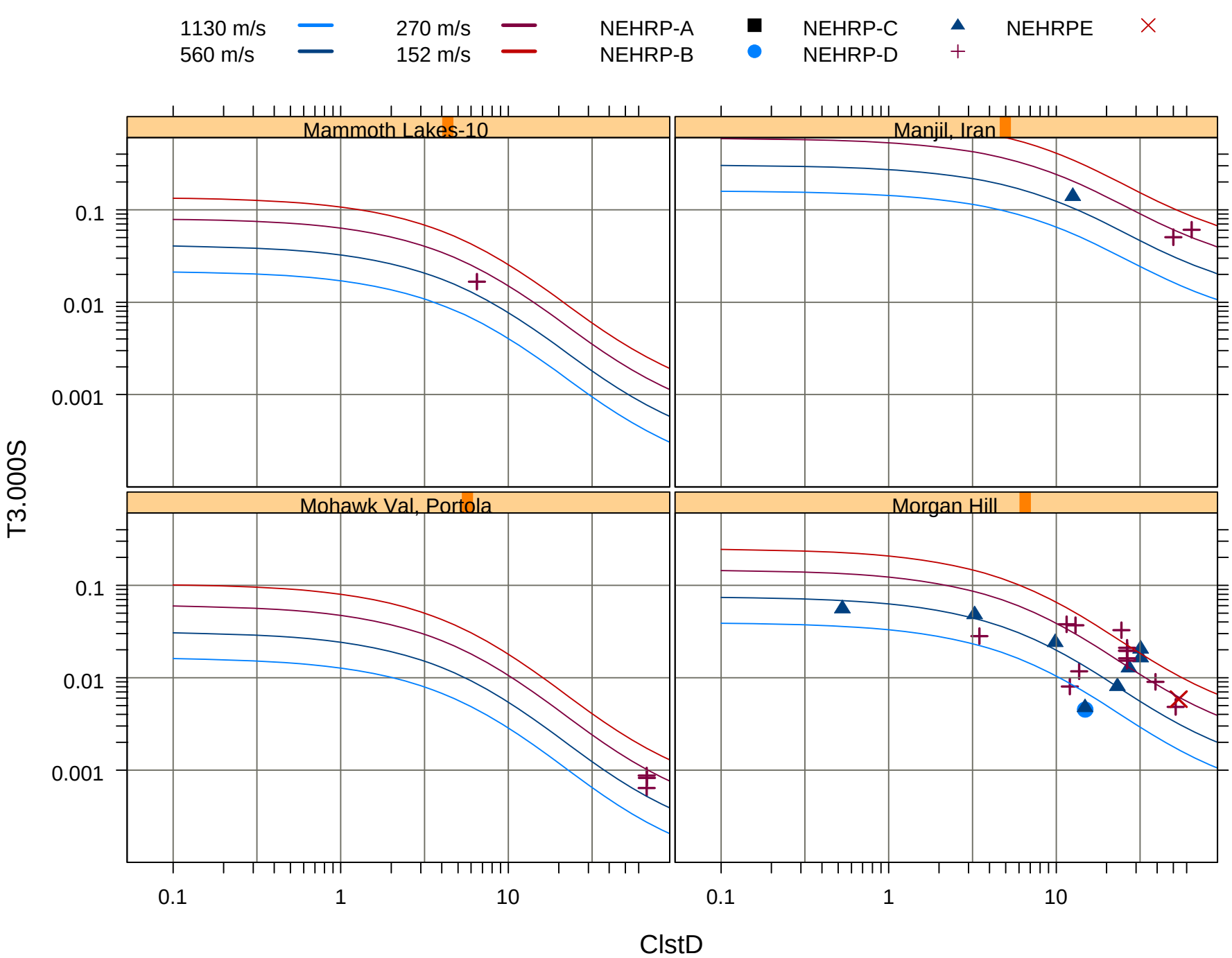
1130 m/s
560 m/s
270 m/s
152 m/s
NEHRP-A
NEHRP-B
NEHRP-C
NEHRP-D
NEHRPE
Mammoth Lakes-10
Manjil, Iran
Mohawk Val, Portola
Morgan Hill
T3.000S
ClstD
0.1
0.01
0.001
0.1
1
10

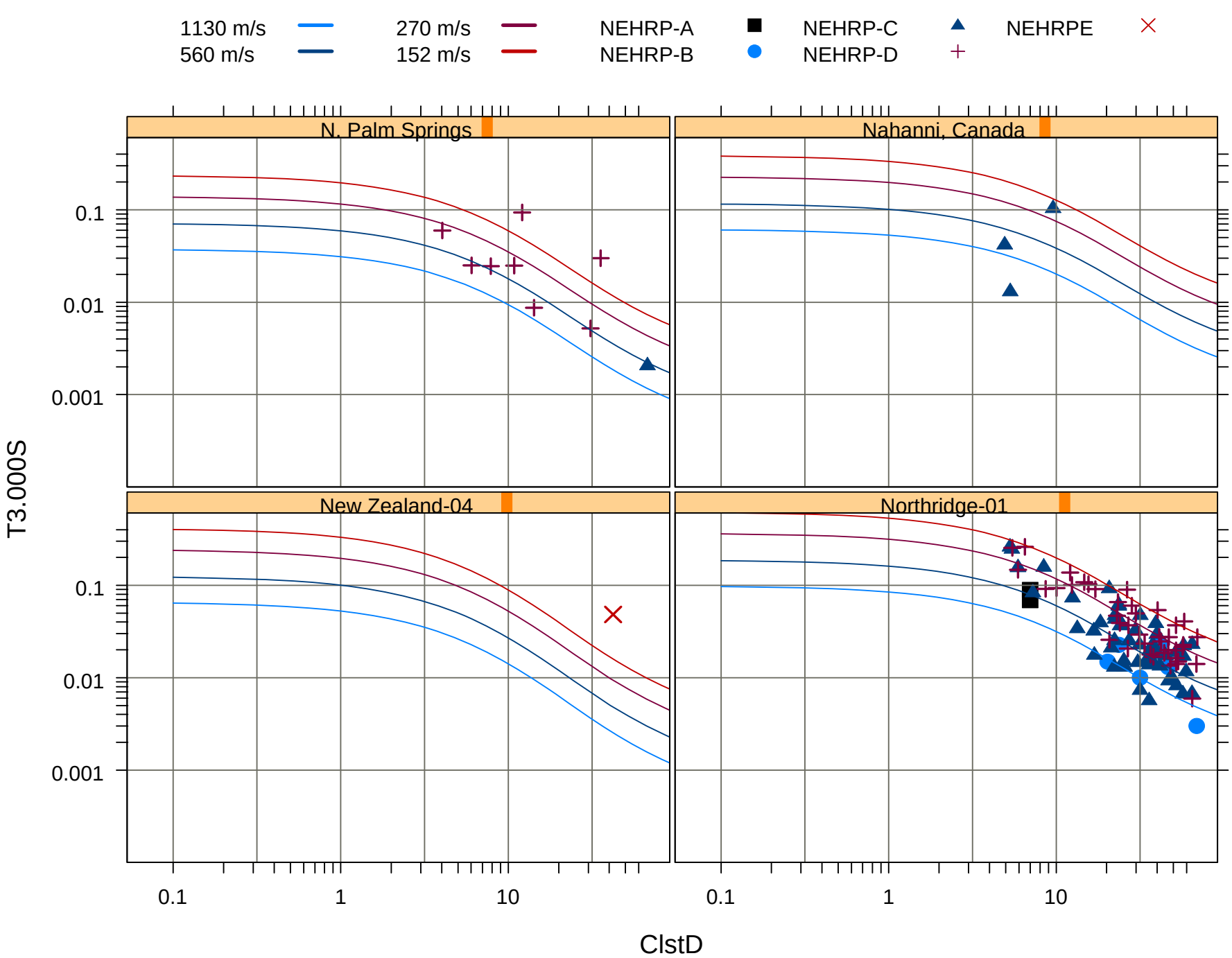
1130 m/s
560 m/s
270 m/s
152 m/s
NEHRP-A
NEHRP-B
NEHRP-C
NEHRP-D
NEHRPE
N. Palm Springs
Nahanni, Canada
New Zealand-04
Northridge-01
T3.000S
ClstD
0.1
0.01
0.001
0.1
1
10

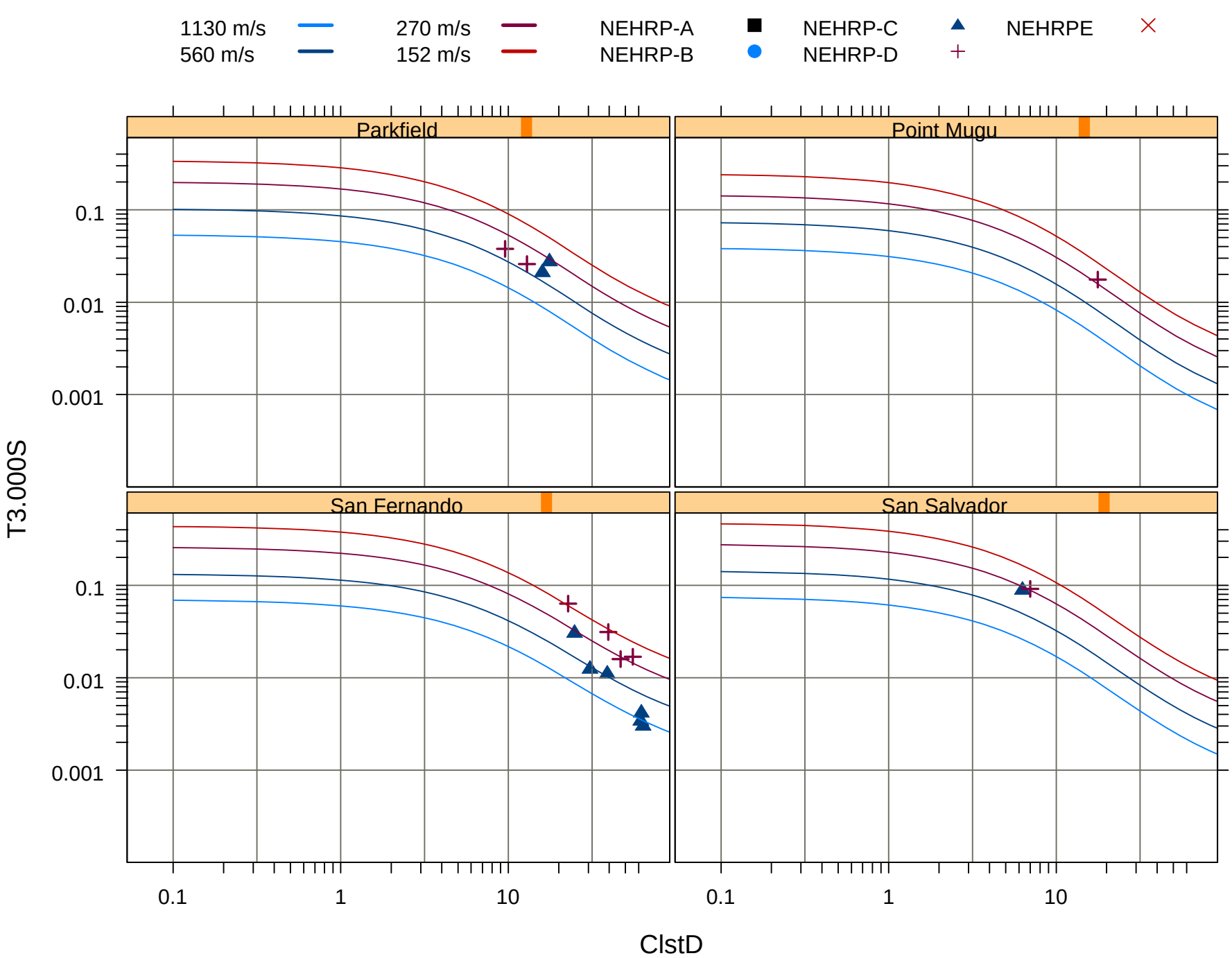
1130 m/s
560 m/s
270 m/s
152 m/s
NEHRP-A
NEHRP-B
NEHRP-C
NEHRP-D
NEHRPE
Parkfield
Point Mugu
San Fernando
San Salvador
T3.000S
ClstD
0.1
0.01
0.001
0.1
1
10

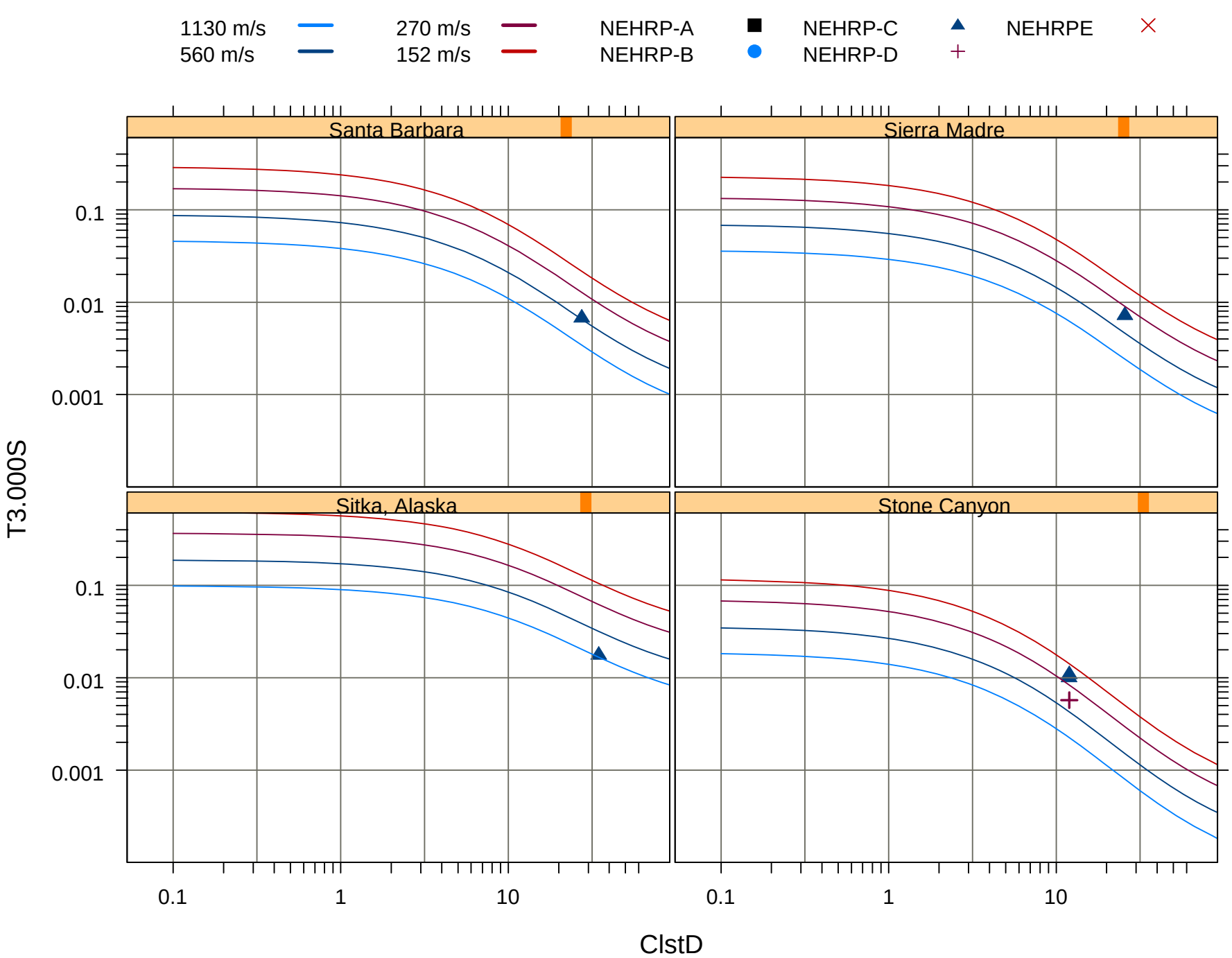
1130 m/s
560 m/s
270 m/s
152 m/s
NEHRP-A
NEHRP-B
NEHRP-C
NEHRP-D
NEHRPE
Santa Barbara
Sierra Madre
Sitka, Alaska
Stone Canyon
T3.000S
ClstD
0.1
0.01
0.001
0.1
1
10

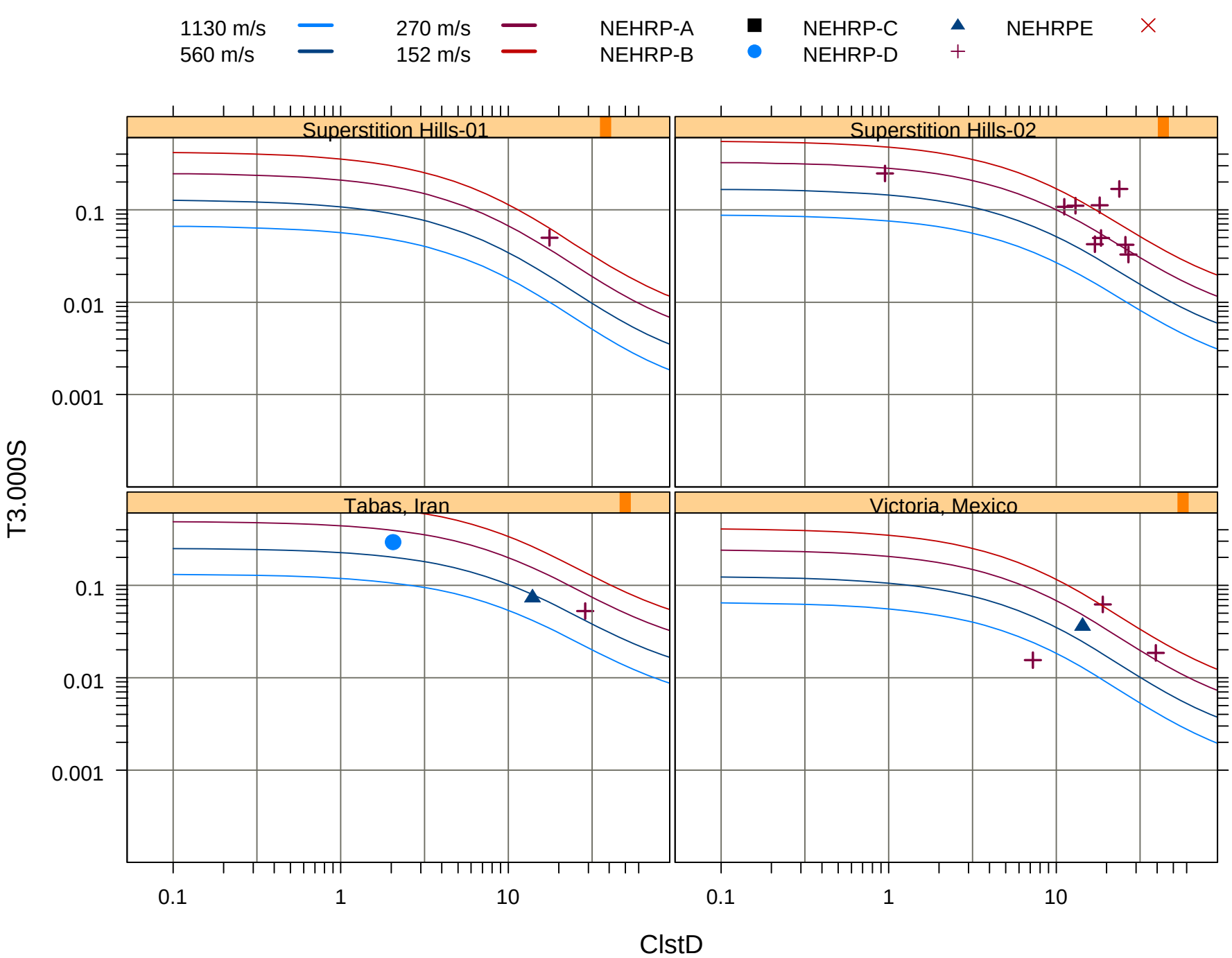
1130 m/s
560 m/s
270 m/s
152 m/s
NEHRP-A
NEHRP-B
NEHRP-C
NEHRP-D
NEHRPE
Superstition Hills-01
Superstition Hills-02
Tabas, Iran
Victoria, Mexico
T3.000S
ClstD
0.1
0.01
0.001
0.1
1
10

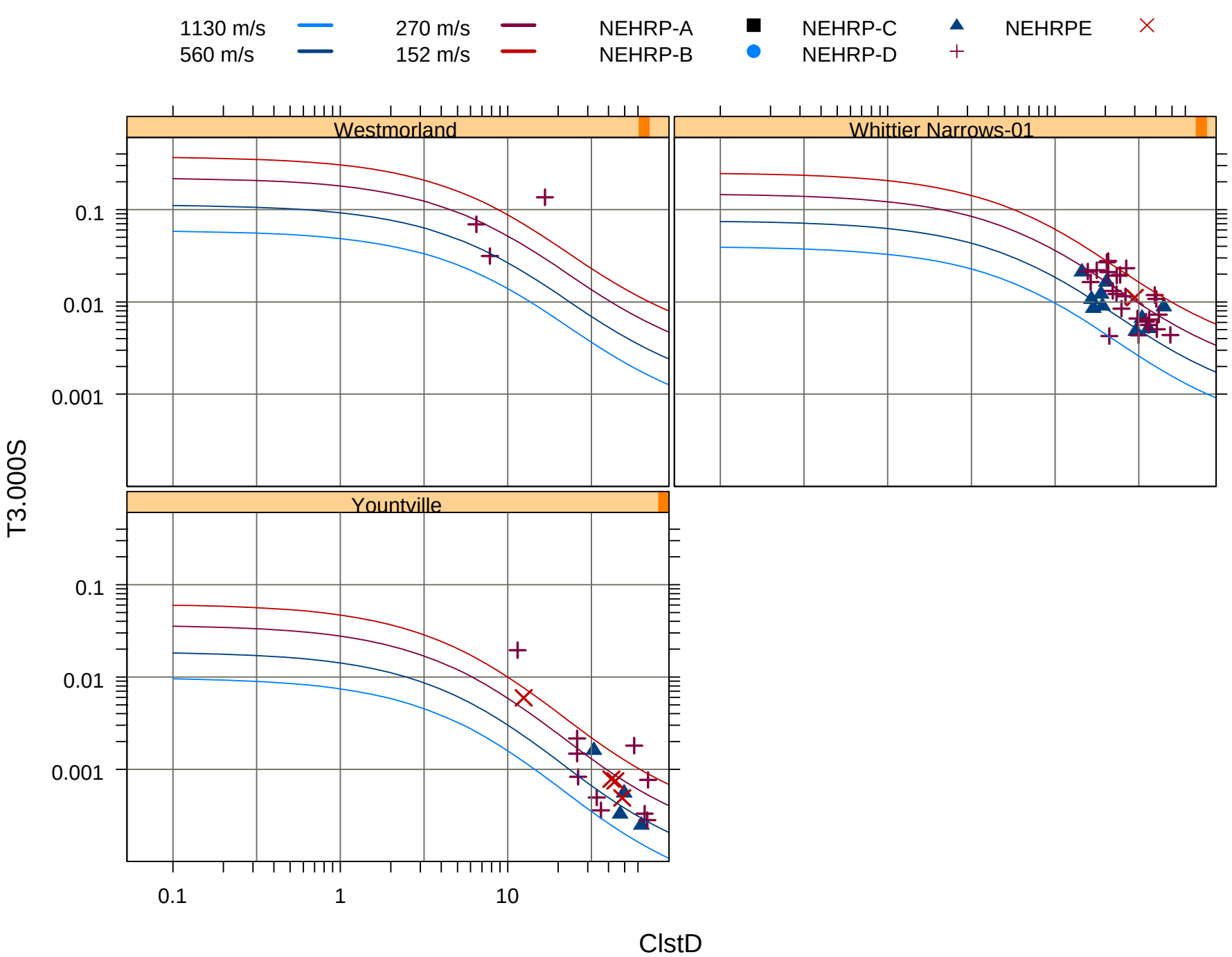
1130 m/s
560 m/s
270 m/s
152 m/s
NEHRP-A
NEHRP-B
NEHRP-C
NEHRP-D
NEHRPE
Westmorland
Whittier Narrows-01
Yountville
T3.000S
ClstD
0.1
0.01
0.001
1
10